



PROCEEDINGS OF THE

25th International Symposium

on Analytical and Environmental Problems

Szeged, Hungary
October 7-8, 2019



University of Szeged

Edited by:
Tünde Alapi
István Ilisz

Publisher:
University of Szeged, H-6720 Szeged, Dugonics tér 13,
Hungary

ISBN 978-963-306-702-4

2019.
Szeged, Hungary

***The 25th International Symposium
on Analytical and Environmental Problems***

Organized by:

SZAB Kémiai Szakbizottság Analitikai és Környezetvédelmi Munkabizottsága

Supporting Organizations

*Institute of Pharmaceutical Analysis, University of Szeged
Department of Inorganic and Analytical Chemistry, University of Szeged
Institute of Environmental Science and Technology, University of Szeged
Hungarian Academy of Sciences*

Symposium Chairman:

István Ilisz, DSc

Honorary Chairman:

Zoltán Galbács, PhD

Organizing Committee:

István Ilisz, DSc

associate professor

University of Szeged, Institute of Pharmaceutical Analysis

ilisz@pharm.u-szeged.hu

Tünde Alapi, PhD

assistant professor

University of Szeged, Department of Inorganic and Analytical Chemistry

alapi@chem.u-szeged.hu

Lecture Proceedings

THE STUDY OF PHOTOCATALYTIC DEGRADATION OF ANIONIC DYES BY 1D COORDINATION POLYMERS BASED ON CADMIUM(II)

Ildiko Mariana Bută, Maria Andreea Nistor, Simona Gabriela Muntean, Otilia Costișor

„Coriolan Drăgulescu” Institute of Chemistry Romania, 24 Mihai Viteazu, Timisoara
e-mail: ildiko_buta@acad-icht.tm.edu.ro

Abstract

Organic dyes resulted from industries such as textile, food, printing, and pharmaceuticals are the main contamination in wastewater. [1] In the last years, several physical, biological and chemical methods have been investigated for the treatment of industrial colored wastewaters. Among them, photocatalysis proved to be a useful method due to the degradation of colored pollutants into smaller, non-toxic compounds. [2] Coordination polymers may exhibit photocatalytic properties under UV or visible light irradiation due to their nature and structure properties [3].

Three new cadmium(II) coordination polymers $[\text{Cd}_3\text{L}(\text{CH}_3\text{COO})_4] \cdot \text{H}_2\text{O}$ (CP-1), $[\text{Cd}_5\text{L}_2(\text{CH}_3\text{COO})_6]$ (CP-2) and $[\text{Cd}_2\text{L}(\text{NO}_3)_2] \cdot \text{CHCl}_3$ (CP-3), where H_2L stands for $\text{N,N}'$ -bis[(2-hydroxybenzylideneamino)-propyl]-piperazine were synthesized by direct metal-ligand reaction of the respective ligand with the corresponding cadmium(II) salts. The nature of the compounds was established based on elemental analysis, and structural information were obtained by IR and UV–Vis spectroscopy and single-crystal X-ray diffraction.

The photocatalytic activity of the CPs 1 - 3 was investigated on the degradation of two anionic: Congo Red (CR), and Methyl Orange (MO). Photocatalytic studies were carried out, at room temperature, in a visible chamber with 500 W Hg lamp providing 546 nm irradiation, and the dye concentrations were determined by a UV/VIS spectrophotometry.

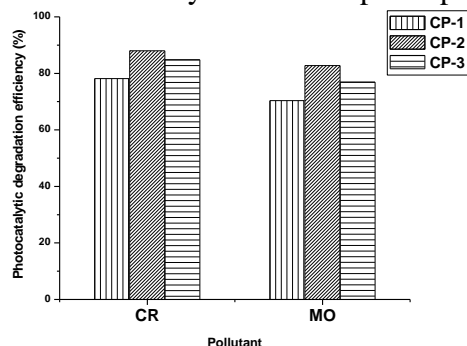


Figure 1. Photodegradation efficiency of CPs for colored pollutants, under visible irradiation (50 mg/L dye, 1 g/L CP, 25°C, solution pH)

For all investigated dyes the photocatalytic degradation efficiency increased in order: $\text{CP-1} < \text{CP-2} < \text{CP-3}$. The CPs were capable of photodegradation of anionic dyes, as evidenced by their decomposition efficiency up to: 88% for CR and 83% for MO.

Acknowledgements

This work was supported by Project 2.4 and Project 4.1 of the “Coriolan Drăgulescu” Institute of Chemistry.

References

- [1] M. Li, X. Wang, C.J. Porter, W. Cheng, X. Zhang, L. Wang, M. Elimelech, *Environ. Sci. Technol.* 53 (2019) 3078.
- [2] A. Kumar, G. Pandey, *Mater. Sci. Eng. C* 1 (2017) 18.
- [3] Gaur, R. *Inorg. Chem. Front.* 6 (2019) 278.

CARBONATION OF SOME CONCRETE MIXTURES USING RECYCLED CONCRETE AGGREGATES

**Remus Chendes¹, Corneliu Bob¹, Liana Iures¹, Sorin Dan¹,
Catalin Badea¹, Dan-Cristian Tănăsie^{*2}**

¹ Politehnica University Timisoara, Faculty of Construction, 2nd Traian Lalescu, 300223, Timisoara, Romania

² National Institute of Research & Development for Electrochemistry and Condensed Matter, 144th Dr. Aurel Paunescu Podeanu, 300569, Timisoara, Romania
e-mail: remus.chendes@upt.com , * tase@incemc.ro

Abstract

Typical C16/20 concrete class has been studied in an accelerated carbonation experiments carried out under high CO₂ concentration. The 100x100x100 mm cube specimens, prepared with natural aggregates and recycled aggregates, were stored for 28 days in water and have been tested (physical-mechanical characteristics). After 60 days of accelerated carbonation conditions test, in a protected environment - 50% carbon dioxide concentration, temperature 25 ° C and humidity 75-80%, the specimens were cleaved to determine the carbonation depth by phenolphthalein test on the faces in the splitting zone, measuring the minimum and maximum carbon dioxide penetration values. Correlation was made between the compressive strengths obtained for the studied specimens and the carbonation depth after the accelerated carbonation experiments in the protected environment.

Introduction

The construction industry plays an important role in the social and economic development. According to Eurostat, in July 2019, the construction sector in Romania registered an increase of 39.5%, being the first in the European Union. Only Hungary is approaching, with an increase of almost 33%, while in Bulgaria or Poland the increases are only a few percent and the average increase of the European Union is only 1.7%. [1]

But, the construction sector has a negative impact on the environment, by large CO₂ emissions (contributing to global warming), by large amount of construction and demolition processes wastes generated (uncontrolled disposal), also leading to the depletion of natural resources by over-exploiting them. The only ways to reduce this negative impact of this sector is reuse, recycling and waste reduction [2].

An option, for the concrete resulted from the demolition process is to be used as aggregates into a new concrete, instead of using as coarse aggregate and filler in road construction industry. [3].

By recycling the materials are changed into new products, preventing this way, the waste of potentially useful materials, reducing the consumption of fresh raw materials, the energy usage and the air and water pollution. [4].

Results and discussions

The study on the durability of recycled concrete was carried out in accelerated carbonation experiments, continuing the previous work on topic of RCA influence on carbonation depth, due to higher porosity (20-30%) of the concretes than those cast with natural aggregates in the mix. ([7],[8]).

The usual concrete class C16 / 20 cast with natural aggregate in the mixture, replaced by the recycled aggregate concrete (different granulometric fractions), obtained after an industrial building demolition has been studied into the experimental program (Table 1.) [8].

Table 1. Experimental mixture

Concrete Class	Mixture				Water/cement ratio
	CEM I 42,5R [kg/m ³]	Mixture water [kg/m ³]	Admixture [kg/m ³]	Aggregate [kg/m ³]	
C16/20	292	205	1,46	1694	0,7

The concrete mixtures belong to the class of consistency S3, the maximum size of the aggregate of 16 mm and a super-plasticizing additive was used.

It was proposed to replace 100% of the natural aggregate (NAT) with RCA (R1). The other mixtures R2, R3, R4 and R5 replace only certain granulometric fractions in the natural aggregate with the RCA, keeping the others granulometric fractions unchanged (Table 2).

Table 2. Granulometric fractions

	(100% NAT)	(100% RCA)	(NAT + RCA)			
	M1	R1	R2	R3	R4	R5
NAT:	0,0-16,0 mm	-	0,0-0,5 mm 1,0-16,0 mm	0,0-1,0 mm 2,0-16,0 mm	0,0-4,0 mm 8,0-16,0 mm	0,0- 8,0 mm
RCA:	-	0,0-16,0 mm	0,5-1,0 mm	1,0-2,0 mm	4,0-8,0 mm	8,0-16,0 mm

As the previous experimental work, the 100x100x100mm cube specimens were stored for 28 days in water, tested (physical-mechanical characteristics) and subjected to accelerated carbonation experiments (fig.1) in a protected environment - carbon dioxide concentration (50%), temperature (25 °C) and relative humidity (75-80%) (figure 3).

The three parameters - carbon dioxide concentration, relative humidity and temperature - were measured with the Testo 350XL analyzer (Fig. 2). [8]



Figure 1. Experimental setup



Figure 2. Testo 350XL analyzer

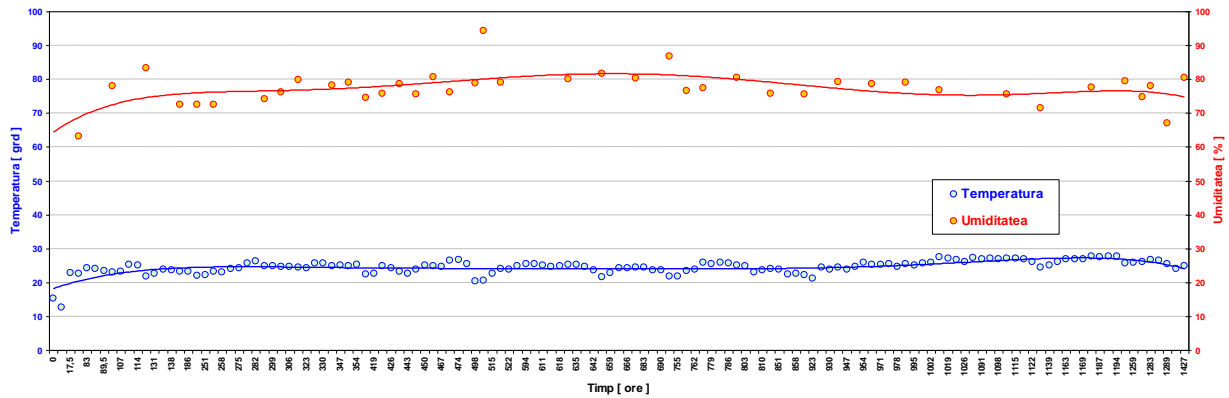


Figure 3. Temperature and relative humidity evolution

After being stored for 60 days under accelerated carbonation conditions, the specimens were cleaved to determine the carbonation depth after phenolphthalein test of the faces in the splitting zone, drawing the carbonated surface and measuring the minimum and maximum carbon dioxide penetration values (figure 4 and table 3).

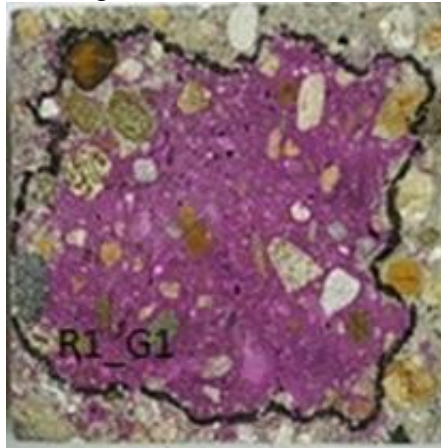


Figure 4. Phenolphthalein test - Carbonated surface [8]

In the calculation of the average depth of theoretical carbonation, the developed C.Bob formula presented below [6] was used:

$\bar{x}_{teoretic} = \frac{150 \cdot c \cdot k \cdot d}{f_c} \cdot \sqrt{t}$	\bar{x} - average carbonation depth [mm] f_c - concrete compression strength [MPa] t - time [years] c, k, d - coefficients
---	---

Table 3. Experimental results

Samples	Compression strength f_c [Mpa]	c	k	d	Time [years]	x theoretic [mm]	x-min exp. [mm]	x-max exp. [mm]
M1 (100% natural)	29	1	0,7	2,7	0,164	3,96	4,0	11,0
R1 (100% RCA)	32,0	1	0,7	2,7	0,164	3,59	4,0	13,0
R2 (natural+RCA)	23,0	1	0,7	2,7	0,164	4,60	8,0	13,0
R3 (natural+RCA)	25,0	1	0,7	2,7	0,164	4,26	12,5	16,0
R4 (natural+RCA)	26,7	1	0,7	2,7	0,164	4,15	11,0	16,0
R5 (natural+RCA)	27,7	1	0,7	2,7	0,164	4,12	9,3	17,2

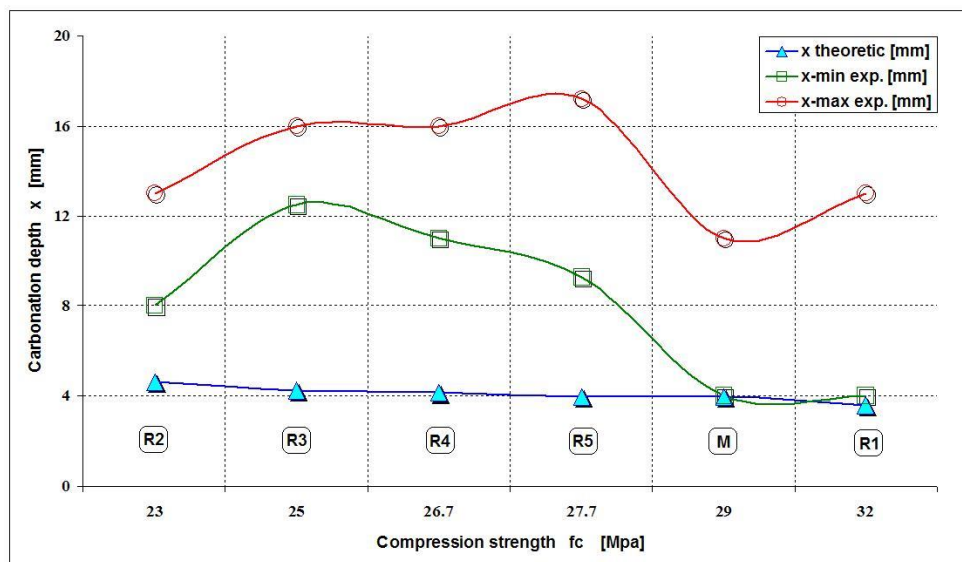


Figure 5. Carbonation depth vs. compression strength evolution

Conclusions

The additive added additionally in the case of studied mixtures, positively influences the carbonation depth.

As the grain size fraction replaced by RCA is larger, the compression strength is higher, but also the carbonation depth is greater.

Due to a quality control, difficult to manage, the results obtained for compression strength correlated with the carbonation depth, exhibit a different behavior from the results obtained in other studied cases.

References

- [1] <https://stirileprotv.ro/stiri/actualitate/constructiile-din-romania-cea-mai-mare-crestere-din-ue-ce-sun-economistii.html>
- [2] *Evaluations of existing waste recycling methods: A Hong Kong study*. Vivian W.Y. Tam, C.M. Tam. s.l. : Building and Environment, 2006, Vol. 41.
- [3] C.Badea, *The Time Behaviour of Self Compacting Concrete With Fly Ash*, 17th International Multidisciplinary Scientific GeoConference SGEM 2017, Energy and Clean

- Technologies, Issue 43, 27-29 November, pp. 259-265, Vienna, Austria, 2017
- [4] M. F. Prada, S. Brata, D. F. Tudor, D. E. Popescu, *Energy Saving in Europe and in the World – a Desideratum at the Beginning of the Millenium Case Study for Existing Buildings in Romania*, Proceedings of the 11th WSEAS International Conference on Sustainability in Science Engineering, p.246 – 251, ISBN: 978-960-474-080-2, Timisoara, Romania, 2009.
- [5] F.T. Olorusongo, *Early Age Properties of Recycled Aggregate Concrete.*, Proceeding of the International Seminar on Exploiting Wastes in Concrete, University of Dundee, 1999.
- [6] Bob, C., Verificarea calității siguranței și durabilității construcțiilor, s.l.Facla, 1989.
- [7] Chendes R., Iures L., Popa R., Bob C., Dan S., Tănasie C. – Comparison between recycled concrete aggregates and natural aggregates density and water absorption, The national technical-scientific conference (international participation) „Modern technologies for the 3rd millennium” - the 17th edition, Oradea, Romania, 2018
- [8] Chendes R., Iures L., Bob C., Dan S., Badea C., Tănasie C. - *Experimental determination of recycled aggregates concrete carbonation*, 24th International Symposium on Analytical and Environmental Problems, Szeged, Hungary, 2018

SELF-ASSEMBLY IN WATER OF BULKY OCTAHEDRAL COORDINATION
COMPLEXES BASED ON RH(III) METAL CENTER

Carmen Cretu¹, Maria A. Spirache¹, Adél Len^{2,3}, Zoltán Dudás⁴, Alessandra Crispini⁵,
Elisabeta I. Szerb¹

¹“Coriolan Dragulescu” Institute of Chemistry, Romanian Academy, 24 Mihai Viteazu Bvd.
300223 – Timisoara, Romania, e-mail: cretucami@yahoo.com

²Nuclear Analysis and Radiography Department/Centre for Energy Research,
Konkoly-Thege 29-33, 1121 Budapest, Hungary

³Faculty of Engineering and Information Technology/University of Pécs, Boszorkány út 2,
7624 Pécs, Hungary

⁴Neutron Spectroscopy Department/Wigner Research Centre for Physics, Konkoly-Thege 29-
33, 1121 Budapest, Hungary

⁵Università della Calabria, Dipartimento di Chimica e Tecnologie Chimiche, 87030
Arcavacata di Rende, Italy

Abstract

Metal complexes able to self-assembly in water into chromonic-type liquid-crystalline phases are progressively attracting attention because of their unique features consisting in the combination of properties deriving from liquid crystals (self-ordering, ease of alignment, sensitivity to changing conditions and additives) coupled with the optical and electro-optical properties brought by the metal centre. [1,2]

In the last decade, rhodium (III) cyclometallated complexes were researched for their electrocatalytic activity, fluorescent properties and especially for medicinal applications as drug delivery and therapeutic agents. [3(a-d)] Therefore, supramolecular organized aqueous systems built up with these compounds should bring important developments in bio-related fields. Herein we report new Rh(III) cyclometallated complexes that show the ability to self-assemble into chromonic-like phases at relatively low concentration in water. Their supramolecular arrangements in mesophase will be proposed based on optical polarization microscopy (POM), X-ray diffraction studies on single crystals and Small Angle Neutron Scattering (SANS) measurements in the mesophase. The role of different molecular moieties will be discussed in the self-assembling with respect to previous reported structurally analogues Ir(III) complexes [1,2].

Acknowledgements: The Romanian authors acknowledge the support of the “Coriolan Dragulescu” Institute of Chemistry, Project 4.1.

References

- [1] Y.J. Yadav, B. Heinrich, G. De Luca, A.M. Talarico, T.F. Mastropietro, M. Ghedini, B. Donnio, E.I. Szerb, *Adv. Optical Mater.* 1 (2013) 844.
- [2] L. Ricciardi, T.F. Mastropietro, M. Ghedini, M. La Deda, E.I. Szerb, *J. Organomet. Chem.* 772-773 (2014) 307.
- [3] a) J. Kima, E. Rajkumara, S. Kima, Y.M. Parka, Y. Kima, S.-J. Kima, H.J. Leeb, *Catal. Today* 295 (2017) 75; b) A. Nano, A.N. Boynton, J.K. Barton, *J. Am. Chem. Soc.* 139(48) (2017) 17301; c) J. Markham, J. Liang, A. Levina, R. Mak, B. Johannessen, P. Kappen, C.J. Glover, B. Lai, S. Vogt, P.A. Lay, *Eur. J. Inorg. Chem.* 12 (2017) 1812; d) C.-H. Leung, H.-J. Zhong, D.S.-H. Chan, M. Dik-Lung, *Coord. Chem. Rev.* 257 (2013) 1764.

LIQUID CRYSTAL PHASES BASED ON FLUORENONE CORE

Daniela Haidu^a, Ya-Xin Li^b, Xiang-Bing Zeng^b, Goran Ungar^{a,c} and Liliana Cseh^a

^a "Coriolan Dragulescu" Institute of Chemistry, 300223-Timisoara, Romania
lilianacseh@gmail.com

^b Department of Materials Science and Engineering, University of Sheffield, Sheffield S1 3JD, U.K.

^c School of Materials, Xi'an Jiaotong University, Xi'an 710049, P.R. China

Dynamic chirality synchronization of supramolecular aggregates in liquids and liquid crystals is a new mode of mirror symmetry breaking, providing chiral fluids of non-chiral compounds with long-term stability even at high temperatures [1]. Formation of networks and, particularly, network junctions seems to be the key to the long-range propagation of homochirality [2, 3]. Depending on the lattice symmetry the cubic phases of rod-like and polycatenar molecules are achiral (double gyroid phase - Ia3d) or chiral triple network - Im3m); therefore, the molecular design play an important role for the achievements of new supramolecular structures with specific required properties. Here, we present the design, synthesis and characterization of first examples of fluorenone derivatives displaying bicontinuous cubic phases. The synthesized compounds show columnar, double gyroid and the triple network phase. The Ia3d seems to be preferred at higher, and Im3m at lower temperatures.

These fluorescent compounds also have the potential to be used as electro- or photoluminescent materials in devices that may emit circularly polarized light.

Acknowledgements: This work was supported by a grant of Ministry of Research and Innovation, CNCS-UEFISCDI, project number PN-III-P4-ID-PCE-20160720, within PNCDI III.

[1] Tschierske C., Ungar G., Chem. Phys. Chem., 17 (2016), 9-26.

[2] Dressel C., Liu F., Prehm M., Zeng X.B., Ungar G., Tschierske C., Angew. Chem. Int. Ed., 53 (2014), 13115-20.

[3] Lu H., Zeng X.B., Ungar G., Dressel C., Tschierske C., Angew. Chem. Int. Ed., 57 (2018), 2835-2840.

DEVELOPMENT OF BAKERY PRODUCT WITH SEA BUCKTHORN POMACE (*HIPPOPHAE RHAMNOIDES* L.)

Zsuzsanna Kiss¹, Beatrix Szabó-Nóti¹, Rentsendavaa Chaagnadorj¹, Mónika Stéger-Máté¹, Éva Stefanovits-Bányai², Diána Furulyás¹

¹Department of Food Preservation, Szent István University, H-1118 Budapest, Villányi Street 29-43, Hungary

²Department of Applied Chemistry, Szent István University, H-1118 Budapest, Villányi Street 29-43, Hungary

e-mail: furulyas.diana@etk.szie.hu

Abstract

In our modern world, avoid wasting or keep it at low level is important for the food industry too. After the fruits pressing stay a lot of pomace, which is rich in vitamins, antioxidant, and polyphenols. It has a few further usages, like pectin commodity or soil conditioners. After drying and grinding, it becomes seed meal.

In our experiment we try out the buckthorn (*Hippophae rhamnoides* L.) pomace further usage, in our case, we mixed with flour and baked cookie. We tested the level of polyphenol and antioxidants in the cookies. Furthermore, the whole polyphenol capacity (TPC), ferric reducing antioxidant power assay (FRAP) and the texture of biscuits have been tested.

The results are favorable in case of TPC and FRAP. The buckthorn pomace has a positive impact regard to substance.

Introduction

There more and more proof confirm the theory of the oxidative progress by radicals are contribute to arteriosclerosis, additionally, it was reported that antioxidant nutrients influence cell response and gene expression, which gives a new perspective to the mechanism of biological antioxidant activity [1-3]. Due to the modern way of life the consumption of the right quantity and quality antioxidant are essential to mitigate the harmful impact of radicals. In our busy world, there is increasing demand to fast food. As a result, the food industry tends to develop and produce such foods, which are good choice for health-conscious customer [4-6].

The sea buckthorn (*Hippophae rhamnoides* L.) is a rich source of antioxidant, polyunsaturated fatty acids, vitamins and minerals [7-10]. It is consumed in many forms in the food industry such as raw, syrup, canned, soda, jam and vitamin-rich processed concentrate. After squeezing the crop of sea buckthorn, the 75-85% of the weight of the berry is juice, other remaining after the press, like seed and peel in the most cases are used for forage or soil conditioner. However only a little percentage of total pomace mass is used in the food industry [11-14]. The sea buckthorn pomace in form of grist can be suitable for the mix with flour. While harvest the favorable physiological effect, it can be made a pleasant taste product. In today's world, the usage of the higher and higher rate of material became very important, while mitigating the weight of waste.

For this reason, the aim of our research is to successfully use the byproduct of buckthorn in the biscuits in order to make antioxidant-rich product.

Experimental

The „Ascola” sea buckthorn was collected from agricultural plots of Hungary in 2018. Chemicals were purchased from Sigma-Aldrich Chemie Ltd. All reagents used were of analytical grade.

Sea buckthorn was destemmed and then heated to 80°C, to inactivate enzymes. The material was squeezed, resulting in juice and pomace. Drying the pomace was the next step by an atmospheric dryer (LMIM, Hungary) at 80°C [15] until moisture content became lesser than 10%. After this step, the pomace was grinded.

In this experiment, three recipes were made with increasing sea buckthorn content (Fig. 1.)

	sugar (g)	coconut oil (g)	flour BL 55 (g)	sea buckthorn (g)	baking powder (g)	water (ml)
control	100	100	250	0	12	100
2.5% pomace	100	100	243.75	6,25	12	100
5% pomace	100	100	237.5	12.5	12	100

The biscuits were baked for the same time (10 min, 190°C).

Samples were stored at room temperature for 2 weeks in a sealed package, during which the following were examined at 3 sampling times:

- Water content was determined by drying until constant weight at 121 °C using a MAC-50 moisture analyzer (Radwag Waagen GMBH, Hilden, Germany).
- Various spectrophotometric measurements were carried out. All spectrophotometry measurements were performed in triplicate:
 - TPC: Total Polyphenol Content was evaluated using a method by Singleton and Rossi [16]. The absorbance was measured at 765 nm. Results were specified in mg Gallic acid equivalent/ 100 g biscuit (mg GAE/100g).
 - FRAP: The ferric reducing antioxidant power method of the samples was determined by Benzie and Strain [17]. The reduction is followed by the measurement of absorption change at 593 nm. FRAP value was defined in ascorbic acid equivalent (mg Ascorbic acid equivalent/ 100g biscuit; mg AA/100g).
- Texture was investigated by Brookfield, LFRA 4500 Texture Analyser. In the course of texture examination, hardness, adhesion, and elasticity were measured, because in the evaluation of the quality of biscuits these parameters are important aspects.

Results and discussion

Water content results during the two weeks storage period show on the Figure 1.

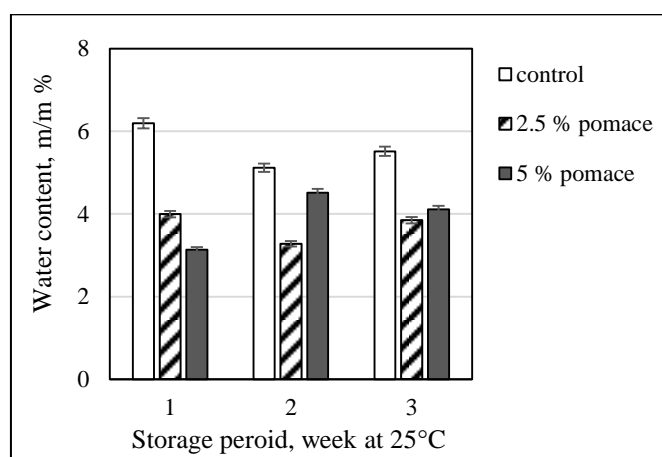


Figure 1. Water content of the biscuits during the storage period

At the beginning the control sample showed the highest level of water content, the 2.5 % pomace had lower and the 5% pomace had the lowest level of water content. After the one-week storage, the control and the 2.5 % pomace content sample had the same water content rate loss, while the water content of the 5% pomace was higher. In two weeks storage period,

water content of the 5% pomace showed a decrease and water content of the other two samples grew a little bit.

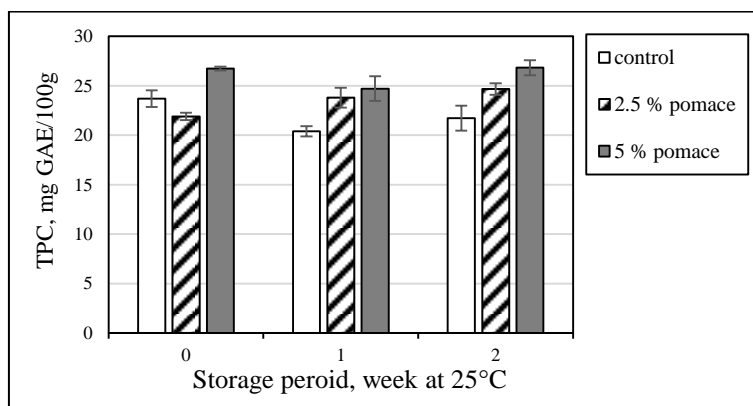


Figure 2. Results of total polyphenol content from biscuits during the storage period

The figure 2 shows the changes of total polyphenol content of biscuits during the storage period. At the first measurement, the 2.5% pomace sample had the lowest level of polyphenol out of the three sample (21.90 mg GAE/100g). In the case of control sample had a little higher value (23.70 mg GAE/100g), the 5% pomace sample had even higher value (26.75 mg GAE /100g). After one week the control sample had the lowest polyphenol content, the 5% pomace sample had a little higher value, while the 5% pomace sample had the highest measured value. At the next week, the measurement the ratio of the samples remained the same as before, but the values were raised a little bit.

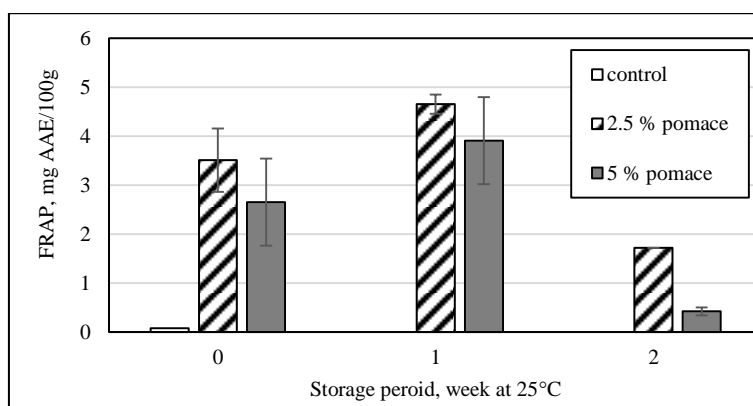


Figure 3. Results of antioxidant capacity (FRAP) from biscuits during the storage period

On the figure 3. the results of antioxidant capacity can see. The control sample barely contained antioxidants and those were completely decomposed during the weeks of storage. The initial sample, which contained 2.5% pomace, had the highest measured value (3,512mg AAE/100g), the 5% sample had less FRAP value (2,654mg AAE/100g). After one week storage, the antioxidant level was raised in both of the samples meanwhile there ratio stayed the same.

At the second week measurement, we experienced decreasing level in the 2.5% sample as well as in the 5% sample. Measured value of the 2.5% pomace sample was (1.720mg AAE/100g), while the 5% pomace had very low level FRAP (0.423mg AAE/100g).

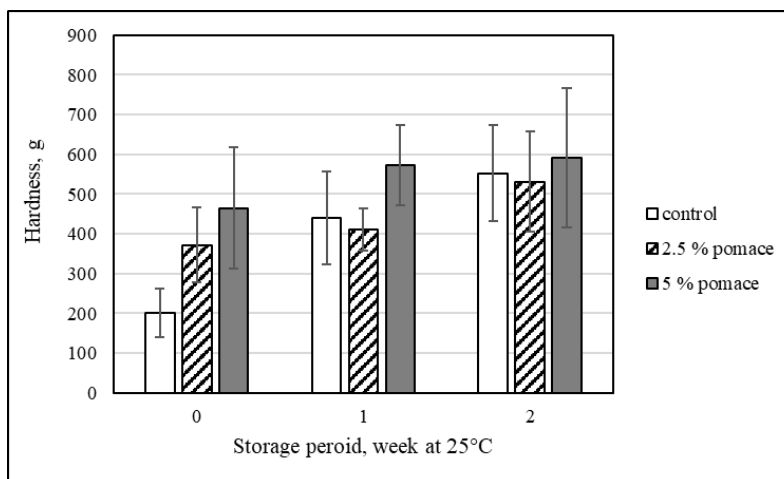


Figure 4. Hardness values of samples during the storage period

The results of texture examination are on the Figure 4. The hardness of the control sample had grown more during the storage, than the other two samples hardness. After one-week the value of hardness had double and after that, it continued to rise. In the beginning, we measured higher value in the case of 2.5% sample, unlike the control sample. A little growing could be observed after the first and second week. We measured double value in the 5% sample than in the beginning status of the control, the 2.5% sample had a little higher value as well. As the time moved forward, the hardness had grown a little bit of this sample.

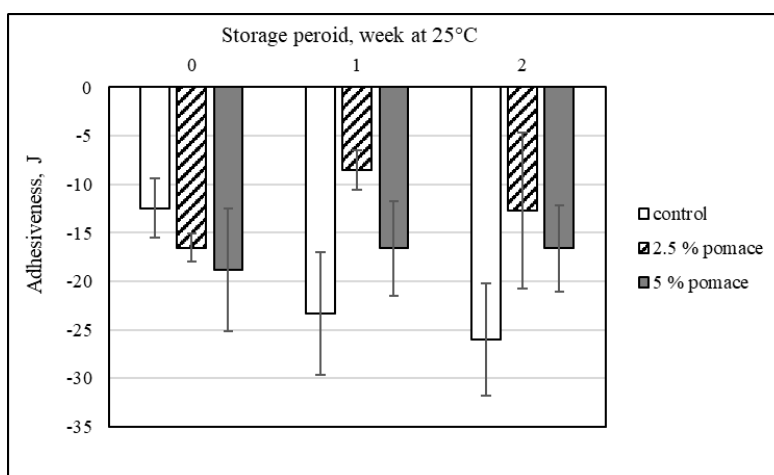


Figure 5. Adhesiveness values of sample during the storage period

The adhesion had decreased as the time has passed in the control sample. In the 2.5% pomace sample this value doubled after the first week and after the second week, it has started to decrease.

In the 2.5% pomace sample first got higher the adhesion level and after the second week, it has started to decrease. The adhesion level of 5% sample had moved just a little and mostly decreased a little.

Conclusion

One possible usage of the buckthorn pomace is to mix in products of the bakery.

Whit that the antioxidant content is enriching and this antioxidant level can be preserved at a high level during one-week store in 25°C as we observed in the research.

The polyphenol concentration of the cookies was almost the same after two weeks at 25°C.

For those who follow health-conscious nutrition, the favorable physiological effect from the buckthorn is available by the cookies. It easily could become an enjoyable but healthy everyday snack for families with children.

Acknowledgements

The authors thank Gábor Juhász for help and support. This work was supported by the Hungarian Government through project No. EFOP-3.6.3-VEKOP-16-2017-00005.

References

- [1] C. Eccleston, Y. Baoru, R. Tahvonen, H. Kallio, G.H. Rimbach, A.M. Minihaane, The Journal of nutritional biochemistry, 13(6) (2002) 346-354.
- [2] M.G. Hertog, D. Kromhout, C. Aravanis, H. Blackburn, R. Buzina, F. Fidanza, M. Pekkarinen, Archives of internal medicine, 155(4) (1995) 381-386.
- [3] R. Puupponen-Pimiä, L. Nohynek, C. Meier, M. Kähkönen, M. Heinonen, A. Hopia, K.M. Oksman-Caldentey, Journal of applied microbiology, 90(4) (2001) 494-507.
- [4] M. Sayegh, C. Miglio, S. Ray, Intl. J. Food Sci. Nutr. 65 (2014) 521–528.
- [5] A.A.M. Botterweck, H. Verhagen, R.A. Goldbohm, J. Kleinjans, P.A. Van den Brandt Food and Chemical Toxicology, 38(7) (2000) 599-605
- [6] Haminiuk, C.W.I., Maciel, G.M., Plata-Oviedo, M.S.V., Peralta, R.M. 2012. Phenolic compounds in fruits –an overview. Int. J. Food Science and Technology, 47:2023–2044.
- [7] J. Bernáth (Eds.) Gyógy és aromanövények. Budapestp, Mezőgazda Kiadó, 2000, pp. 350-354.
- [8] X.Y. Xu, B.J. Xie, S.Y. Pan, L. Liu, Y.D. Wang, C.D. Chen, Asia Pac. J. Clin. 16, (2007) 234–238.
- [9] N.K. Upadhyay, R. Kumar, S.K. Mandotra, R.N. Meena, M.S. Siddiqui, R.C. Sawhney, A. Gupta, Food Chem. Toxicol. 47 (2009) 1146–1153.
- [10] G. Ficzek, G. Matravolgyi, D. Furulyas, C. Rentsendavaa, I. Jocsak, D. Papp, M. Steger-Mate, European Journal of Horticultural Science, 84(1) (2019) 31-38.
- [11] T. Beveridge, J.E. Harrison, J. Drover, J. Agric. Food Chem, 50 (2002) 113-116
- [12] T. Beveridge, T.S.C. Li, B.D. Oomah, A. Smith, J. Agric. Food Chem., 47 (1999) 3480-3488
- [13] J. Krisch, L. Galgóczy, T. Papp, Cs. Vágvolgyi, Journal of engineering. (2009) 1584 – 2665
- [14] A. Mirzaei-Aghsaghali, N. Maheri-Sis, World J. Zool, 3(2) (2008) 40-46.
- [15] D. Furulyás, R. Chagnaadorj, F. Kis, K. Bíró, M. Stéger-Máté, É. Stefanovits-Bányai, Proceedings of the International Symposium on Analytical and Environmental Problems, 23 (2017) 392-396.
- [16] V.L. Singleton, J.A. Rossi, American journal of Enology and Viticulture, 16(3) (1965) 144-158.
- [17] I.I.F. Benzie, J.J. Strain, Annalitical Biochemistry, 239. (1966) 70-76

RECOVERY OF PLATINUM FROM LEACHING SOLUTIONS BY INTERACTION WITH PORPHYRINS

Anca Lascu^{1*}¹*Institute of Chemistry "Coriolan Dragulescu", M. Viteazul Ave. 24, 300223-Timisoara, Romania, Tel: +40256/491818; Fax: +40256/491824*^{*}*email: ancalascu@yahoo.com***Abstract**

Two differently substituted base porphyrins, one containing aliphatic unsaturated groups and one functionalized with basic effect at the periphery: 5,10,15,20-tetrakis-(4-allyloxyphenyl)-porphyrin and 5,10,15,20-tetrakis-(4-aminophenyl)-porphyrin, were investigated for their capacity to complex with hexachloroplatinic acid from leaching solutions. Their different nature makes them interact differently with the hexachloroplatinic acid in solution, as aminophenylporphyrin is more capable to form more stable complexes, therefore it is suitable for the recovery of platinum from diluted solutions (removal capacity is large 86.6 %) whereas the amount of platinum that can be recovered by allyloxyphenylporphyrin is lower, only 74.07 %.

Introduction

The automotive industry uses large amounts of platinum salts as catalysts. As platinum is a rare metal and the natural resources are scarce, the recovery of platinum from leaching solutions has to be taken into serious consideration. This can be achieved based on the capacity of some materials to generate complexes with hexachloroplatinic acid. Some of the compounds capable to perform this task are base porphyrins, properly substituted at the periphery with functional basic groups, or metalloporphyrins, due to their capacity to coordinate ligands at the metal centers [1]. The following step is to obtain platinum colloid, by reducing the already coordinated systems.

A couple of aliphatic- and amino-substituted porphyrin bases were investigated for their capacity of platinum absorption.

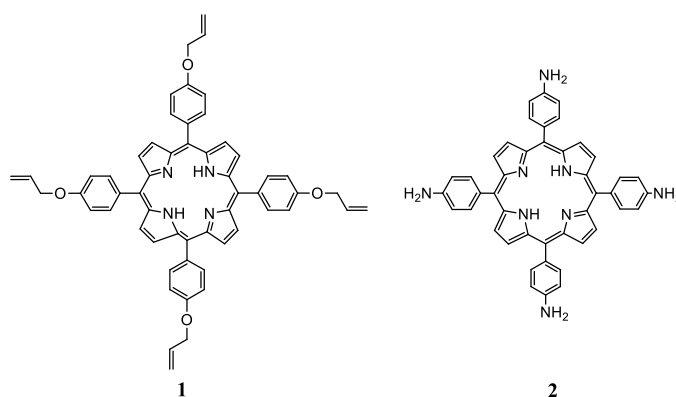


Figure 1. Structure of the investigated compounds: 5,10,15,20-tetrakis-(4-allyloxyphenyl)-porphyrin (1); 5,10,15,20-tetrakis-(4-aminophenyl)-porphyrin (2)

Experimental

Materials and methods. N,N-Dimethylformamide was purchased from Merck (Darmstadt, Germany), chloroplatinic acid hexahydrate was acquired from Sigma-Aldrich (St. Louis, USA). The porphyrins 5,10,15,20-tetrakis-(4-allyloxyphenyl)-porphyrin (1); 5,10,15,20-

tetrakis-(4-aminophenyl)-porphyrin (2) were synthesized and characterized as published in previous papers [2].

The experiments were performed in 5 mL porphyrin solutions in DMF, to which increasing amounts of hexachloroplatinic acid solution in water ($c = 1.03 \times 10^{-3}$ M) were added. The mixtures were stirred for 30 seconds and then the UV-vis spectrum was recorded for each step.

Apparatus. For recording UV-visible spectra, standard 1 cm pass quartz cells were used on a JASCO UV- V-650 spectrometer (Japan).

Results and Discussions

In order to have a precise measurement, without the effect of volatile solvents, the porphyrins were solved in DMF, a polar, nonvolatile solvent compatible with water. The platinum-containing agent of use in the experiment was hexachloroplatinic acid solution in water ($c=1.03 \times 10^{-3}$ M).

The absorption domain of the chloroplatinic acid solution does not interfere with the absorption wavelengths of the investigated porphyrins, as can be observed in Figure 2.

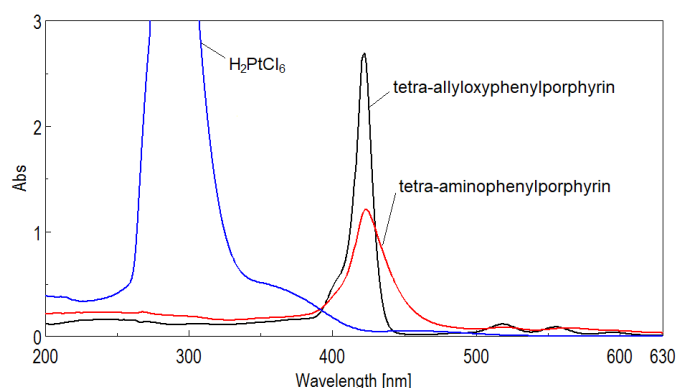


Figure 2. Comparative UV-vis spectra of the investigated compounds

The overlapped spectra for the successive adding of chloroplatinic acid to the solutions of the two porphyrin-base compounds of interest are presented in Figure 3.

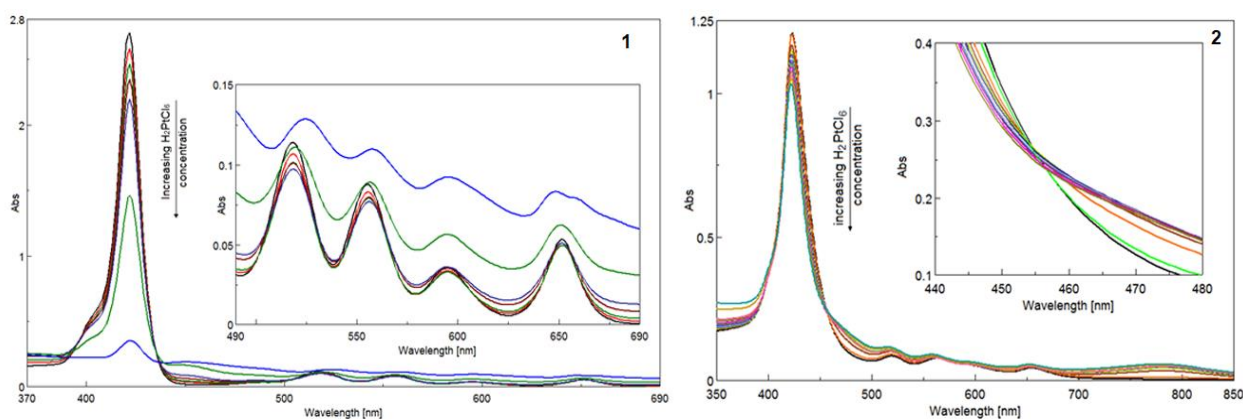


Figure 3. Comparison of the UV-vis spectra after adding chloroplatinic acid to 5,10,15,20-tetrakis-(4-allyloxyphenyl)-porphyrin (1) and 5,10,15,20-tetrakis-(4-aminophenyl)-porphyrin (2). Details present magnification of Q bands and of isosbestic points.

It can be noticed that the allyloxyphenyl porphyrin can only interact with small amounts of platinum from the solution, the intensity of the Soret band decreases drastically after adding 2.2 mL chloroplatinic solution (Figure 3(1)). Nevertheless, some interaction between the

porphyrin molecule and the platinum ions takes place, as isosbestic points show: one on the descending branch of the Soret band, at 435 nm and one at 564 nm, on the Q3 band.

The aminophenylporphyrin is able to better interact with platinum ions in solution, many intermediate species are present, as proven by the presence of numerous isosbestic points: one at 458 nm, on the Soret band, then on the Q bands, in increasing wavelength: 528 nm, 570 nm and 665 nm respectively (Figure 3(2)). The isosbestic point at 570 nm corresponds to the H_2PtCl_6 concentration interval of $2.023 \times 10^{-5} \text{ M}$ to $7.644 \times 10^{-5} \text{ M}$. Also, a new peak appears at 784 nm, probably due to self- aggregation phenomena [3]. Besides, these isosbestic points, together with the appearance of the new peak, indicate a possible acid-base complexation between the weak hexachloroplatinic acid and the four amino groups at the periphery of the porphyrin molecule, that can be protonated. The presumed final complex can have the structure presented in Figure 4.

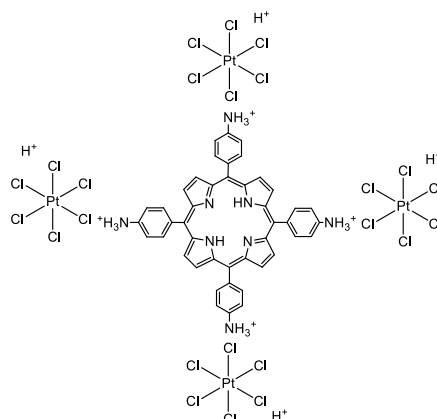


Figure 4. The presumed structure for the complex formed between the tetra-aminophenylporphyrin and the hexachloroplatinic acid

The linear dependence between the intensity of absorption read at the Soret wavelength maxima and the H_2PtCl_6 concentration for the two porphyrins under investigation are presented in Figure 5.

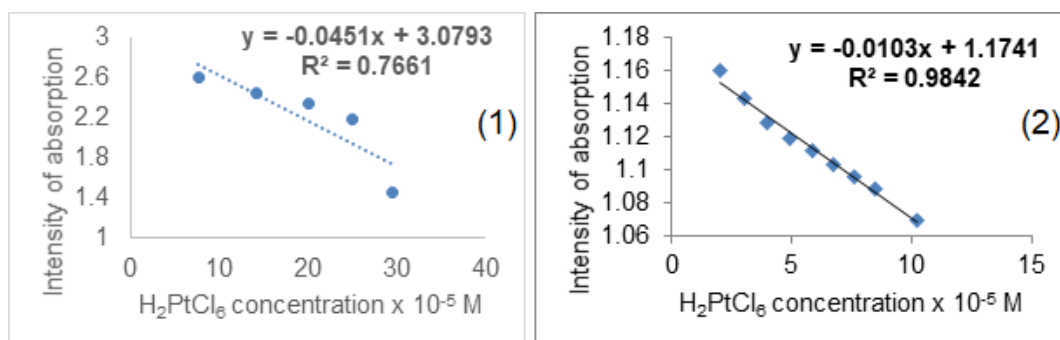


Figure 5. Linear dependence between the intensity of absorption read at Soret maximum wavelength and the H_2PtCl_6 concentration for allyloxyphenylporphyrin (1) and for aminophenylporphyrin (2)

It can be observed that the capacity to recognize platinum ions is very poor in the case of allyloxyphenylporphyrin, as the intensity of absorption read at 422 nm is linear with the concentration of chloroplatinic acid only in the concentration domain of $7.6 \times 10^{-5} \text{ M}$ to $29.5 \times 10^{-5} \text{ M}$, with a poor correlation coefficient of 76.61% and with low sensitivity. In comparison, the chloroplatinic acid concentration interval ($2.023 \times 10^{-5} \text{ M}$ to $10.227 \times 10^{-5} \text{ M}$) for which

the dependence between the intensity of absorption of aminophenylporphyrin and platinum acid concentration is linear, is represented by a high correlation coefficient of 98.42%.

The capacity to remove platinum ions from a solution, with the aid of porphyrin molecules, was the purpose of this study. Therefore, according to [1] the quantity of platinum that can be retrieved by the porphyrins can be evaluated according to the equation:

$$Q_e = \frac{(C_0 - C_e) V}{m} \text{ (mg/g)}$$

Where, adapting the formula for our specific case and taking into consideration the variation of platinum acid:

C_0 is the concentration of Pt in the porphyrin solution at the end of the experiment expressed in ppm

C_e is the concentration of the Pt in the porphyrin solution at the beginning of the experiment expressed in ppm

V is the volume of the solution in L

m is the quantity of porphyrin in the solution expressed in g

The distribution coefficient (K_D) shows the affinity of the porphyrin solution toward Pt colloidal particles and can be calculated according to the equation:

$$K_D = \frac{Q_e}{C_e} \text{ (L/g)}$$

The removal capacity of Pt colloidal particles from solution can be calculated according to the formula:

$$\text{Removal capacity (\%)} = \frac{(C_0 - C_e)}{C_0} \times 100$$

Table 1 presents the results obtained for the two porphyrins investigated.

Porphyrin	Q_e [mg Pt/g porphyrin]	K_D [L/g]	R_c [%]
5,10,15,20-tetrakis-(4-allyloxyphenyl)-porphyrin	1175.208	78.809	74.07
5,10,15,20-tetrakis-(4-aminophenyl)-porphyrin	581.75	293.8	86.6

If the capacity to remove platinum from dilute solutions is the desired target, then the 5,10,15,20-tetrakis-(4-aminophenyl)-porphyrin is the better material as given in Table 1, each NH_2 base unit being capable to interact with the hexachloroplatinic acid.

The platinum can be recovered as colloid or as platinum particles by reducing the novel generated complexes either with sodium citrate or with excess NaBH_4 , a more potent reducing agent and subsequent centrifugation of the solution.

Conclusion

Two differently substituted porphyrin-base compounds, one containing aliphatic unsaturated groups and one containing basic groups at the periphery: 5,10,15,20-tetrakis-(4-allyloxyphenyl)-porphyrin and 5,10,15,20-tetrakis-(4-aminophenyl)-porphyrin, were investigated for their capacity to complex hexachloroplatinic acid from leaching solutions. Their different nature makes them interact differently with the platinum ions in solution. So, aminophenylporphyrin is more capable to bind hexachloroplatinic acid, therefore it is suitable for the recovery of platinum from diluted solutions.

Acknowledgements

The authors are acknowledging UEFISCDI PN-III-P1-1.2-PCCDI-2017-1-Project ECOTECH-GMP 76PCCDI/2018 and the Romanian Academy for financial support in the frame of Programme 3/2019 from ICT.

References

- [1] D. Vlascici, I. Popa, V.A. Chiriac, G. Fagadar-Cosma, H. Popovici, E. Fagadar-Cosma, Chem. Cent. J.7 (2013) 111-118.
- [2] B.O. Taranu, I. Popa Sebarchievici, I. Taranu, M.I. Birdeanu, E. Fagadar-Cosma, Rev. Chim. -Bucharest 67(5) (2016) 892-896.
- [3] E. Tarabukina, E. Fagadar-Cosma, C. Enache, N. Zakharova, M. Birdeanu, J. Macromol. Sci. B 52(8) (2013) 1092–1106.

DETERMINATION OF HYDROXYL RADICALS USING COUMARIN AND COUMARIN-3-CARBOXYLIC ACID DURING GAMMA RADIOLYSIS AND HETEROGENEOUS PHOTOCATALYSIS

Máté Náfrádi¹, László Wojnárovits², Erzsébet Takács², Tünde Alapi¹

¹*Department of Inorganic and Analytical Chemistry, University of Szeged, H-6720 Szeged, Dóm tér 7, Hungary*

²*Institute for Energy Security and Environmental Safety, Centre for Energy Research, Hungarian Academy of Sciences, Budapest, Hungary
e-mail: nafradim@chem.u-szeged.hu*

Abstract

Coumarin and 3-carboxycoumarinic acid, two fluorescent probes commonly used for HO• detection has been used during gamma radiolysis and heterogeneous photocatalysis. The O₂ dependency and the radiation yield of their hydroxylated fluorescent products (7-hydroxycoumarin and 7-hydroxy-3-carboxycoumarinic acid) has been investigated during gamma radiolysis. The radiation yields were found to be 1.2(±0.2) % in O₂-free solutions, while it was 2.9 (±0.06) % in the presence of O₂, proving the importance of peroxy radicals in the formation of these products. The results obtained from radiolysis experiments, were employed during heterogeneous photocatalysis performed with commercial TiO₂ catalyst. The effect of dissolved O₂ was also investigated, as its electron scavenging role during photocatalysis is also important. The formation rate of HO• during photocatalysis was calculated from the formation rate of the fluorescent products, and were found to be 1.8×10⁻⁷ mol dm⁻³ s⁻¹, while the quantum efficiency for its formation is 0.0038.

Introduction

Advanced oxidation processes (AOPs) have been investigated in the last few decades for their possible use as an additional wastewater purification method. During AOPs different reactive species form, the most important one is the hydroxyl radical (HO•), due to its high reaction rate with most organic pollutants. However several methods can be employed, like time-resolved spectroscopy, ESR, the determination of HO• formation rates is a complicated task. Fluorescent probes, like terephthalic acid or coumarines, have also been applied during heterogeneous photocatalysis to evaluate the formation rate of HO•. [1-5]

In this study coumarin (COU) and coumarin-3-carboxylic acid (3-CCA) have been used as a fluorescent probe for determination of the HO• formation rate. They are reported to form highly fluorescent hydroxylated products in their reaction with HO•, 7-hydroxycoumarin (7-HO-COU) and 7-hydroxy-3-carboxycoumarinic acid (7-HO-3-CCA), respectively. The formation rate of both hydroxylated products are reported to be dependant on dissolved O₂. In the presence of O₂ they form via peroxy type radicals, while in the absence of O₂ they form via dismutation, significantly reducing their formation rate. [1-3]

The application of COU and 3-CCA for HO• detection was investigated during two, different AOPs. In the case of gamma radiolysis the formation rate of all reactive species (HO•, e_{aq}⁻, H•) is well determined, since the values of their radiation yields (G value) are well known. Heterogeneous photocatalysis is also a highly researched field of AOPs, but the reaction mechanisms are often not clear. The transformation of organic compounds is mostly related to the reactions with HO•. In addition, the reactions initiated directly by the photogenerated charges (h_{vb}⁺ and e_{cb}⁻) has to be taken into consideration too. The reactions take place on the surface or close to the surface of photocatalyst, and consequently the interactions between the photocatalyst and substrate may have an important role.

The aim of this study is to determine the radiation yields of 7-HO-COU and 7HO-3-CCA, and investigate the effect of dissolved O_2 during gamma radiolysis. Based on these result, the formation rate of $HO\bullet$ and the quantum yield of the $HO\bullet$ formation ($\Phi_{HO\bullet}$) may be determined during the heterogeneous photocatalysis. By comparing the transformation of the non-adsorbed COU, and the well adsorbed 3-CCA, we may investigate the importance of adsorption on the reactions of these substrates with $HO\bullet$.

Experimental

In the gamma-radiolysis experiments a ^{60}Co gamma source was used in a panoramic type irradiator, the dose rate was 1.48 Gy min^{-1} . The solutions of COU and 3-CCA were irradiated in sealed ampulles, which were saturated with either O_2 , N_2O or N_2 . All experiments were performed in $10^{-4}\text{ mol dm}^{-3}$ solutions of COU and 3-CCA in $pH = 7.0$ (in 0.01 mol dm^{-3} phosphate buffer).

Photocatalysis experiments were performed in a glass reactor. 1.0 g dm^{-3} TiO_2 Aeroxide P25 (Acros Organics) was added to the 250 cm^3 solutions, and irradiated using a fluorescent UV light source (GCL303T5/UVA, Lighttech) emitting in the 300-400 nm range. The photon flux of the lamp was $1.20 \times 10^{-5}\text{ mol}_{\text{photon}}\text{ min}^{-1}$, determined by ferrioxalate actinometry. Since 3-CCA adsorbed on the photocatalyst surface ($\approx 30\%$ adsorbed on TiO_2), NaF was added to the samples, for the desorption of the analytes. All samples were centrifuged at 15000 RPM, and filtered using $0.22\text{ }\mu\text{m}$ syringe filters (FilterBio PVDF-L).

The transformation of COU and 3-CCA ($\lambda_{\text{max}}^{\text{COU}} = 277\text{ nm}$, $\lambda_{\text{max}}^{3\text{-CCA}} = 291\text{ nm}$, $\epsilon^{\text{COU}} = 10300\text{ dm}^3\text{ mol}^{-1}\text{ cm}^{-1}$, $\epsilon^{3\text{-CCA}} = 12170\text{ dm}^3\text{ mol}^{-1}\text{ cm}^{-1}$) has been followed using UV-Vis spectrophotometry (Agilent 8453). The formation of 7-HO-COU and 7-HO-3-CCA were followed using fluorescence spectroscopy (Hitachi F4500) at 455 and 447 nm, respectively. The initial transformation rates of COU and 3-CCA were determined from linear regression fits to the actual concentration versus the duration of irradiation, up to 15 % conversion. The initial formation rates of 7-HO-COU and 7-HO-3-CCA were obtained from the linear regression fits to the actual concentration versus the duration of irradiation.

Results and discussion

First the effect of O_2 on the formation of 7-HO-COU and 7-HO-3-CCA was investigated. In the case of radiolysis mainly $HO\bullet$ and e_{aq}^- forms from water. In the presence of O_2 e_{aq}^- transforms into $O_2^{\bullet-}$. Since both $O_2^{\bullet-}$ and its protonated form, HO_2^{\bullet} have a low reactivity towards organic compounds, mainly $HO\bullet$ is responsible for the transformation of COU in this case. Moreover, from carbon centered radicals peroxy radicals form immediately. The formation of peroxy radicals opens a new pathway for the formation of hydroxilated products via unimolecular HO_2^{\bullet} elimination. In O_2 -free solutions both the $HO\bullet$ and the e_{aq}^- are able to initiate the transformation of COU. Without O_2 , the formation of 7-HO-COU happens via bimolecular dismutation. The formation rate of $HO\bullet$ in the presence of O_2 , air or N_2 can be calculated ($r_0^{HO\bullet} = 6.91 \times 10^{-9}\text{ mol dm}^{-3}\text{ s}^{-1}$). In N_2O saturated solutions e_{aq}^- transforms into $HO\bullet$, and doubling the $HO\bullet$ yield ($r_0^{HO\bullet} = 1.33 \times 10^{-8}\text{ mol dm}^{-3}\text{ s}^{-1}$).

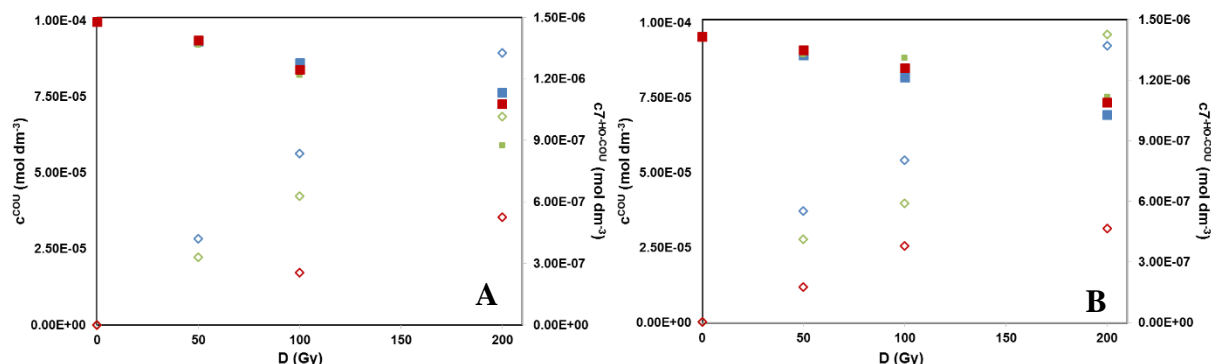


Figure 1. Concentration of COU (A) and 3-CCA (B) as a function of dose in O₂ (■), N₂O (■) and N₂ (■) saturated solutions, and the formation of 7-HO-COU during gamma radiolysis in O₂ (◇), N₂O (◇) and N₂ (◇) saturated solutions.

The effect of the different gases on the transformation rate of COU and 3-CCA were negligible. Despite the similar transformation rates, the formation rate of the hydroxylated products show significant differences. The lowest formation rate can be observed in O₂-free solution, due to the lack of the possibility of peroxy radical formation, and probably because of the significant contribution of e_{aq}^- to the transformation of COU/3-CCA, which do not result in hydroxylated products. The formation rates in N₂O saturated solutions are greatly increased, due to the increased HO• formation rate. The formation rates are even higher in the presence of O₂, despite the lower HO• formation, proving the importance of peroxy radicals in the formation of the hydroxylated products. (Figure 1. and Table 1)

From the formation rates of the hydroxylated products and the formation rate of HO•, the radiation yield for both fluorescent product can be calculated. In N₂ saturated solutions 0.94 and 1.35 %, in N₂O saturated solutions 1.16 and 1.29 %, while in O₂ saturated solutions 2.99 and 2.86% of HO• produces 7-HO-COU from COU and 7-HO-3-CCA from 3-CCA, respectively.

Table 1. Initial transformation rates of COU and 3-CCA and initial formation rates of 7-HO-COU and 7-HO-3-CCA during gamma radiolysis

	r_0^{COU} ($\times 10^{-9} \text{ mol dm}^{-3} \text{ s}^{-1}$)	$r_0^{7\text{-HO-COU}}$ ($\times 10^{-10} \text{ mol dm}^{-3} \text{ s}^{-1}$)	$r_0^{3\text{-CCA}}$ ($\times 10^{-9} \text{ mol dm}^{-3} \text{ s}^{-1}$)	$r_0^{7\text{-HO-3-CCA}}$ ($\times 10^{-10} \text{ mol dm}^{-3} \text{ s}^{-1}$)
O ₂	3.35	2.06	3.23	1.98
Air	4.33	1.55	2.40	1.71
N ₂	3.38	0.64	2.73	0.93

During heterogeneous photocatalysis the main reactive species is the HO•. The photogenerated h_{ν}^+ and e_{cb}^- pair may also react with organic compounds, especially when there is special interaction between the substrate and the catalyst surface. COU and 3-CCA have different adsorption properties, as COU do not adsorb on the catalyst surface, as opposed to 3-CCA, due to the strong interaction between its carboxyl groups and Ti=OH surface groups of photocatalyst.

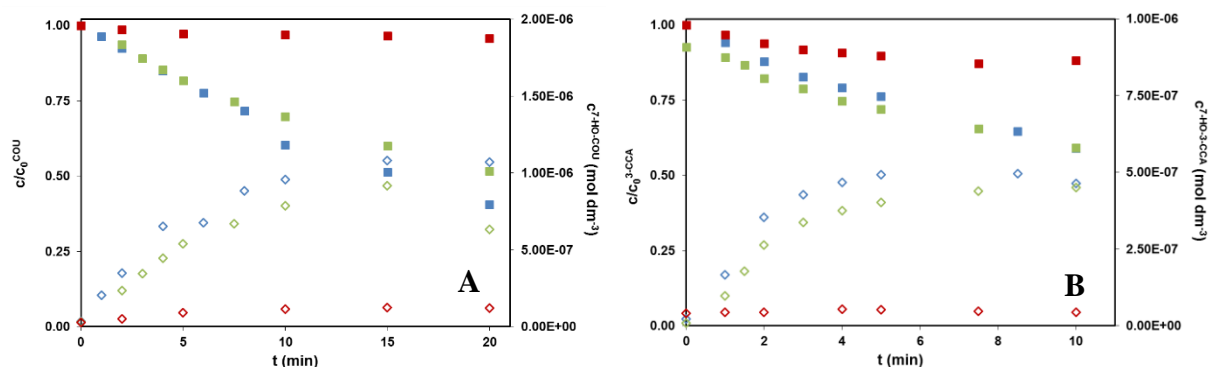


Figure 2. Transformation of COU (A) and 3-CCA (B) as a function of time, in O₂ (■), air (■) and N₂ (■) saturated suspensions, and the formation of 7-HO-COU during heterogeneous photocatalysis in O₂ (◇), air (◇) and N₂ (◇) saturated suspensions.

O₂ plays a crucial role as an electron scavenger, hindering charge recombination, and helping HO• formation via O₂•⁻. In the case of COU there was no difference in the transformation rates determined in O₂ saturated and airted suspensions. At the same time, the formation rate of 7-HO-COU is nearly 1.5 times greater in the case of higher dissolved O₂ concentration. In the case of 3-CCA the transformation rate is also higher with 25% in the case of O₂ saturated suspension, while the formation rate of 7-HO-3-CCA increased with 33 %. In N₂ saturated suspensions the transformation of COU and the formation of 7-HO-COU is negligible. This suggests, that direct charge transfer reactions have a low probability, and HO• formation is negligible. The transformation rate of the well adsorbed 3-CCA is 47 % of the value measured in O₂ saturated suspension, and there is no 7-HO-3-CCA formation. This suggest that, 3-CCA transformation can happen via direct charge transfer, but this way does not results in hydroxilated products.

Table 2. Initial transformation rates of COU and 3-CCA and initial formation rates of 7-HO-COU and 7-HO-3-CCA during heterogeneous photocatalysis

	$r_0^{\text{COU}} \times 10^{-8}$ (mol dm ⁻³ s ⁻¹)	$r_0^{7\text{-HO COU}} \times 10^{-9}$ (mol dm ⁻³ s ⁻¹)	$r_0^{3\text{-CCA}} \times 10^{-8}$ (mol dm ⁻³ s ⁻¹)	$r_0^{7\text{-HO-3-CCA}} \times 10^{-9}$ (mol dm ⁻³ s ⁻¹)
O₂	6.15	2.55	8.98	2.77
Air	6.08	1.73	7.10	2.08
N₂	0.29	-	4.23	-

Using the results obtained from gamma radiolysis, the formation rate of HO• in the case of O₂ saturated TiO₂ suspension was found to be 1.78×10^{-7} and 1.86×10^{-7} mol dm⁻³ in the case of COU and 3-CCA respectively. Assuming that, TiO₂ absorbs completely the emitted photons from the light source, the quantum yield for the formation of HO• is 0.0037 and 0.0039, respectively.

Conclusion

- The formation of 7-HO-COU from COU and 7-HO-3-CCA from 3-CCA requires HO•, while dissolved O₂ highly enhances their formation rate.
- The radiation yield of 7-HO-COU from COU and 7-HO-3-CCA from 3-CCA were determined in the case of gamma-radiolysis
- Based on radiation yields of the hydroxylated products, and the photon flux of the light source, the formation rate of HO• and its quantum efficiency has been determined during heterogeneous photocatalysis, using TiO₂ as photocatalyst

Acknowledgements

This work was financially supported by Industrial Research and development Projects of Hungarian-Indian cooperation (TÉT_15_IN-1-2016-0013). This publication was supported by the János Bolyai Research Scholarship of the Hungarian Academy of Sciences, ÚNKP-19-3-SZTE-207 and UNKP-19-4-SZTE-115, new national excellence programs of the Ministry for Innovation and Technology.

References

- [1] Louit, G., Foley, S., Cabillic, J., Coffigny, H., Taran, F., Valleix, A., Renault, J.P., Pina, S., Radiation Physics and Chemistry 72 (2005) 119–124.
- [2] Manevich, Y., Held, K., Biaglow, J.E., Radiation Research 148 (1997) 580–591.
- [3] Yamashita, S., Baldacchino, G., Maeyama, T., Taguchi, M., Muroya, Y., Lin, M., Kimura, A., Murakami, T., Katsumura, Y., Free Radical Research 46 (2011) 861–871.
- [4] Zhang, J., Nosaka, J., Applied Catalysis B: Environmental 166–167 (2015) 32–36.
- [5] Nosaka Y., Nishikawa, M., Nosaka, A.Y., Molecules 19 (2014) 18248–18267.

SYNTHESIS AND CHARACTERIZATION OF MAGNETIC NANOPARTICLES BY THE COMBUSTION METHOD USED AS ADSORBENT FOR REMOVAL OF DYES FROM COLORED WASTEWATER

Maria-Andreea Nistor¹, Simona Gabriela Muntean¹, Robert Ianos²

¹ *Institute of Chemistry „Coriolan Drăgulescu”, Romania, 24 Mihai Viteazu, Timisoara*

² *Faculty of Industrial Chemistry and Environmental Engineering, Politehnica University Timisoara, Romania, 6 Parvan Blv., Timisoara
email: anistor@acad-icht.tm.edu.ro*

Abstract

The textile industry plays a role as the largest sources of the presence of dyestuffs in the environment, in which most of the dyes have toxic, mutagenic and carcinogenic properties [1]. About 10–15% of commercial dyes produced from the textile industries are discharged into the environment every year [2]. The direct discharge of colored and toxic wastewater into the environment affects its ecological status by causing various undesirable changes [1,3]. Dyes usually have complex aromatic molecular structures which make them more stable and more difficult to biodegrade [3]. Therefore, the removal of colored components from wastewater is one of the biggest issues of concern [4]. Adsorption is verified to be one of the most promising alternative techniques to remove the nonbiodegradable dyes from wastewater due to its simple

operation, superior adsorption effectiveness, relatively low cost, almost harmless byproducts, and the possibility of reusing the spent adsorbent via regeneration [5,6].

Recently, magnetic nanocomposites are widely used as adsorbent in polluted water treatment. Such types of adsorbents have high adsorption capacity and selectivity as compared to traditional adsorbents, and shows a magnetic character which makes their separation easier after wastewater treatment [4,5].

In this study we set out to obtain nanoparticles which combine very good adsorption ability of the carbon-based materials with magnetic properties of the iron oxides, and to test them as potential adsorbents for the removal of, anionic: Acid Orange 7 (AO7), Chromazurol S (Ch-S) and cationic: Methylene Blue (MB), Basic Red 1 (RB1) dyes from aqueous solutions.

The synthesis of magnetic nanocomposites (CAN) was performed by the combustion method. This method is environmentally friendly and has many advantages such as simplicity, short reaction time, and low energy consumption.

For the synthesis of nanocomposites, sample of activated carbon was impregnated with the precursor solution of iron nitrate nonahydrate and with arginine used as a fuel.

The effect of experimental conditions, such as the specific surface of active carbon, reaction time and magnetite/carbon ratio, on the nanoparticles characteristics was investigated. The resulted powders were characterized by X-Ray diffraction (XRD), FT-IR, energy-dispersive X-ray spectroscopy (EDS), specific surface area (BET), N₂ adsorption-desorption isotherms and thermal analysis (TG/DSC).

The resulting nanocomposites had a magnetite/carbon ratio varying between 2/3 and 1/9. As the magnetite/carbon ratio decreased, the BET surface area increased from 485 m²/g to 1095 m²/g.

In order to evaluate the potential application in dye wastewater treatment, the obtained nanocomposites are employed as the adsorbent for the removal of both anionic and cationic dyes from wastewater.

The adsorption process was optimized by studying the influence of solution pH (2÷12), magnetite/carbon ratio, adsorbent dose (0.25 ÷ 3 g/L), initial dye concentration (10÷300 mg/L), and temperature (298, 318, 328 K) on the dye removal.

The increase of the carbon content increases the removal efficiency. It is also evident that the removal efficiency increases with increasing dose of CAN, and temperature, and by decreasing the initial dye concentration for investigated dyes.

Using an adsorbent mass of 1 g/L, and working at the natural solution pH, the synthesized compounds showed removal efficiency higher than 90.00% for all investigated dyes

The first-order and pseudo-second-order kinetic models were used for the kinetic interpretations, and adsorption isotherm analysis was used to elucidate the adsorption mechanism.

Adsorbents regeneration were performed using ethanol solution (1:1). Even after four adsorption-desorption cycles the nanocomposite presents a good efficiency (greater than 65%) for dyes removal from aqueous solution, indicating the possible industrial application.

The experimental results suggest that the as-prepared nanocomposite with high adsorption capacity, excellent separation capability and short equilibrium time has a potential application in the water purification management.

Acknowledgements

This work was supported by program no 2, Project no. 2.4 from Coriolan Drăgulescu” Institute of Chemistry Timisoara of Romanian

References

1. S. Gao, W. Zhang, Z. An, S. Kong, D. Chen, *Adsorption Science & Technology*, (2019), Vol. 37(3–4), 185–204.
2. H. Li, X. Cao, C. Zhang, Q. Yu, Z. Zhao, X. Niu, X. Sun, Y. Liu, L. Ma, Z. Li, *RSC Adv.*, (2017), 7, 16273.
3. Y. Liu, Y. Huang, A. Xiao, H. Qiu, L. Liu, *Nanomaterials*, (2019), 9, 51.
4. M. Kumar, H. S. Dosanjh, *Fibers and Polymers*, (2019), Vol.20, 739-751.
5. S. G. Muntean, M. A. Nistora, R. Ianos, C. Păcurariu, A. Căpraru, V.A. Surdu, *Applied Surface Science* 481, (2019) 825–837
6. A. Allafchian, Z.S. Mousavi and S.S. Hosseini, *International Journal of Biological Macromolecules*, <https://doi.org/10.1016/j.ijbiomac.2019.06.083>

POLYANILINE/POLY (3-AMINOPHENYLBORONIC ACID) FILM AND ITS SENSING PROPERTIES

Nicoleta Plesu¹, Andrea Kellenberger², Milica Tara-Lunga Mihali¹, Nicolae Vaszilcsin²

¹Romanian Academy, Institute of Chemistry, Bd.Mihai Viteazul 24, 300223 Timisoara,

²Romania bUniversity Politehnica Timisoara, Faculty of Industrial Chemistry and Environmental Engineering, P-ta Victoriei 2, 300006 Timisoara, Romania

e-mail: plesu_nicole@yahoo.com

Biologically compounds can be detected using conducting polymers, compound capable to offer some practical advantages. Well-known conducting polymer is polyaniline (PANI) due to its stability electronic properties and strong interactions with analytes [1]. Various sensors and biosensors, such as enzyme sensors, DNA sensors and immunosensors based on PANI are reported in the literature. Most applications of PANI require good mechanical properties and proper workability. The basic polymers have the highest conductivities, but in return, they are difficult to process. To ensure proper workability most known ways are synthesis of mixtures, composite materials (with other polymers having the desired mechanical properties) or derivatization of the base polymers. These methods make a compromise between solubility and fusibility on the one hand and conductivity and stability on the other. In order to increase the processability of polyaniline, other methods have been proposed which involve either substituting aniline at the nucleus or a hydrogen at nitrogen with different groups such as alkyl, alkoxy, aryl or halogen, or copolymerizing it with other suitable momomers. However, the obtained polymers have the disadvantage of lower conductivity and small molar masses. The functionalization of aniline boronic grups generated poly(aniline boronic acid) PABA [2] a polymer which exhibits redox activity also in solutions with neutral pH. The polyaniline(PANI)/poly(3-aminophenyl boronic acid) (PABA)-film was obtained for the detection of diols. The study involved the electrochemical polymerization of 3-aminophenylboronic acid (3-APBA) in the absence or presence of fluoride on the surface of non-noble electrodes. The PANI/ PABA films were tested for detection of dopamine (DA). The electropolymerization conditions were optimized in order to enhance the sensing performance. Cyclic voltammetry was used for deposition and characterization of the PANI/PABA. The electrochemical impedance spectra describe the different phenomena occurring at the interfaces and were presented by Nyquist and Bode representations. The changes in the PANI/PABA capacitance and resistance properties was monitored by EIS. The film thickness was adjusted from the amount of charge that passes during the potentiostatic deposition process. After electrochemical deposition the polymer modified electrodes was washed with distilled water and with phosphate buffer pH 7.4. The gradual change in impedance due to the effect of boronic acid complexation on resistance of polymer film was correlated with de DA concentration and the response was found to be linear between 10^{-1} to 10^{-10} mol L⁻¹.

Acknowledgements

The authors are acknowledging the Romanian Academy for financial support in the frame of Programme 2/2019 from ICT.

References

- [1] A.G. MacDiarmid, A. J. Epstein, Faraday Discuss. Chem. Soc. 88 (1989) 317.
- [2] B. Fabre, L.Taillebois, Chem. Commun. 24 (2003) 2982.

ADVANCED MASS SPECTROMETRY TECHNIQUES FOR DETERMINATION OF BRAIN GANGLIOSIDE EXPRESSION AND THEIR FUNCTIONAL INTERACTIONS IN HEALTHY AND DISEASED CENTRAL NERVOUS SYSTEM

Mirela Sarbu¹, Raluca Ica¹, Alina Petrut¹, Cristian V.A. Munteanu²,
David E. Clemmer³, Alina D. Zamfir^{1,2}

¹National Institute for Research and Development in Electrochemistry and Condensed Matter, Timisoara, Romania; ²Biochemistry Institute of the Romanian Academy, Bucharest, Romania; ³Indiana University, Bloomington, Indiana, USA; ⁴“Aurel Vlaicu” University of Arad, Arad, Romania
e-mail: mirela.sarbu86@yahoo.co.uk

Abstract

A pivotal role in the brain development is played by the cellular membrane. Since glycolipids (GLs) are the predominant components of plasma membrane, a direct correlation of GLs with crucial processes and neurological disorders exists [1]. Therefore, GLs, formed by a ceramide moiety attached to an oligosaccharide chain, possibly mono- to polysialylated, are important biomarkers in early diagnosis of central nervous system (CNS) pathologies, being in the focus of our research as potential therapeutic targets [2]. Here, we have developed here an approach based on nanoelectrospray (nanoESI) Orbitrap mass spectrometry (MS) in combination with ion fragmentation by collision induced dissociations (CID) for profile comparison and structural characterization of native GL mixtures extracted and purified from histopathologically-defined anencephalic brain remnants originating from fetuses in different intrauterine developmental stages [3]. The native GL extracts dissolved in pure methanol up to a concentration of 5 pmol/μl were infused at 2 μL/min flow rate on a LTQ Orbitrap MS. Based on high resolution mass spectrometry capability for a reliable determination of glycopatterns, changes in diversity and number of GLs with age were observed. Over 150 distinct GL structures were identified in the three samples of anencephalic fetal brain remnants. The high resolution of the instrument and the newly developed methodology allowed not just the ionization and detection of low-abundance species, such as polysialylated GLs, but also revealed the presence of different components modified by fucosylation, acetylation and *N*-acetyl galactosamine attachment. Tandem MS (MS/MS) experiments carried out in the LTQ by CID in the manual mode of ion selection and fragmentation using variable collision energy within 25-30 eV confirmed the incidence of potential biomarker species in the investigated anencephalic fetal brain remnants.

Acknowledgements

This project was supported by the Romanian National Authority for Scientific Research, UEFISCDI through projects PN-III-P4-ID-PCE-2016-0073, PN-III-P1-1.2-PCCDI-2017-0046 granted to ADZ and PN-III-P1-1.1-PD-2016-0256 granted to MS.

References

- [1] R.L. Schnaar, R. Gerardy-Schahn, H. Hildebrandt, *Physiol. Rev.* 94 (2014) 461.
- [2] M. Sarbu, A.C. Robu, R.M. Ghiulai, Ž. Vukelić, D.E. Clemmer, A.D. Zamfir, *Anal. Chem.* 88, (2016) 5166.
- [3] M. Sarbu, Ž. Vukelić, D.E. Clemmer, A.D. Zamfir, *Biochimie* 139 (2017) 81.

NOVEL NICKEL COMPLEXES WITH SCHIFF BASES AND α -GLYOXIMES, SYNTHESIS AND PHYSICAL-CHEMICAL STUDY

Csaba Várhelyi jr.¹, Roland Szalay², György Pokol^{3,4}, Firuța Goga¹, Péter Huszthy³, Melinda Várhelyi¹, Ligia-Mirabela Golban¹, Alexandra Bogdan¹, Lóránd Demeter¹

¹ Faculty of Chemistry and Chemical Engineering, "Babeş-Bolyai" University, RO-400 028 Cluj-N., Arany János str. 11, Romania

² Institute of Chemistry, "Eötvös Loránd" University, H-1117 Budapest, Pázmány Péter str. 1/a, Hungary

³ Faculty of Chemical Technology and Biotechnology, Budapest University of Technology and Economics, H-1111 Budapest, Műegyetem rkp. 3, Hungary

⁴ Research Centre for Natural Sciences, H-1117 Budapest, Magyar tudósok körútja 2, Hungary

e-mail: vcaba@chem.ubbcluj.ro

Abstract

Nickel complexes, especially with Schiff bases gain potential interest in various areas such as catalysis, luminescent probes in analytical chemistry, dye and polymer industry, food industry, magneto-structural chemistry, agrochemistry, biological fields and several miscellaneous applications. There are numerous reports on the biological activities of Schiff base ligands and their metal complexes, including their use for DNA cleavage, enzyme modeling, and as antimicrobial, antifungal and antitumor agents [1].

In our research, new nickel complexes were synthesized with α -glyoximes, such as $[\text{Ni}(\text{Me-propyl-GlyoxH})_2(\text{imidazole})_2]$, $[\text{Ni}(\text{Me-pentyl-GlyoxH})_2(\text{diisopropyl-amine})_2]$, $[\text{Ni}((4\text{-benzyl-2-hydroxy-phenyl})\text{-Me-GlyoxH})_2]$, where GlyoxH = mono deprotonated glyoxime, and with Schiff bases, such as $[\text{Ni}(3\text{-heptanone})_2\text{A}]$, $[\text{Ni}(\text{propiophenone})_2\text{A}]$, A = ethylenediamine (en), 1,2-, 1,3-propylenediamine (1,2-pn, 1,3-pn), o-phenylene-diamine (o-fen). The Schiff bases were obtained with a simple condensation reaction between 3-heptanone or propiophenone and the corresponding diamines.

The molecular structure of our products was investigated by IR, UV–VIS spectroscopy, mass spectrometry (MS), thermoanalytical measurements (TG-DTG-DTA), and powder XRD. The biological activity was studied for a few bacteria, however, these complexes have shown no antibacterial activity so far.

Introduction

Nickel (Ni) is a naturally occurring element existing in various forms, and it is present in all compartments of the environment and, furthermore, is ubiquitous in the biosphere as its compounds and complexes. It is a silvery-white lustrous metal with a slight golden tinge. Nickel is a hard and ductile transition metal belonging to the 3d group. Nickel is one of the five ferromagnetic elements. Nickel is used in a wide variety of metallurgical processes such as electroplating and alloy production as well as in nickel cadmium batteries. Besides it plays a well defined role in the biological system and plants. It is also essential for the biosynthesis of hydrogenase, carbon monoxide dehydrogenase, and, moreover, it can be found in a number of genera of bacteria [2].

The Schiff bases are widely used as N-donor ligands in the field of coordination chemistry. Due to the attractive physicochemical properties of metal complexes, extensive studies have been carried out on complexation of Schiff bases with different metal ions, resulting broad range of utilization in various areas of science. The toxicity of Schiff base

derivatives of sulfane thiadiazole, 2-thiophene aldehydes, and salicylaldehyde, together with their some metal complexes, has been tested against insects as well [3]. In general, the C=N linkage in azomethine derivatives is an essential structural requirement for biological activity. Several azomethines have been reported to possess remarkable antibacterial, antifungal, anticancer and diuretic activities [4].

In the present paper we report the synthesis, characterization and biological evaluation of some Ni(II) complexes with Schiff bases and α -glyoximes.

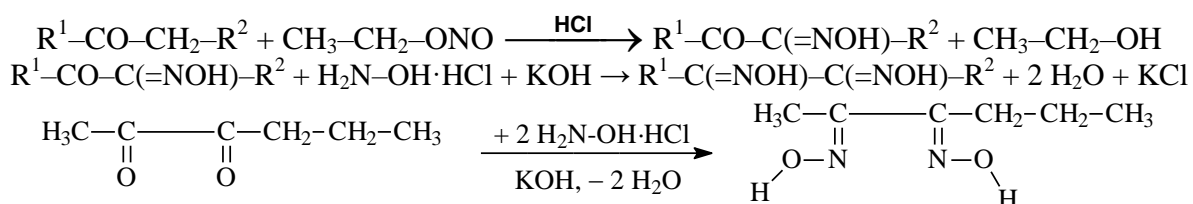
Experimental

Used materials: NiSO₄, EtOH, EtONO, 2,3-hexanedione, 4-benzyl-2-hydroxy-propionophenone, 2-octanone, hydroxylamine hydrochloride, KOH, imidazole, diisopropylamine, 3-heptanone, propionophenone, ethylenediamine, 1,2-propylene-diamine, 1,3-propylene-diamine, *ortho*-phenylene-diamine, sodium acetate.

Methods:

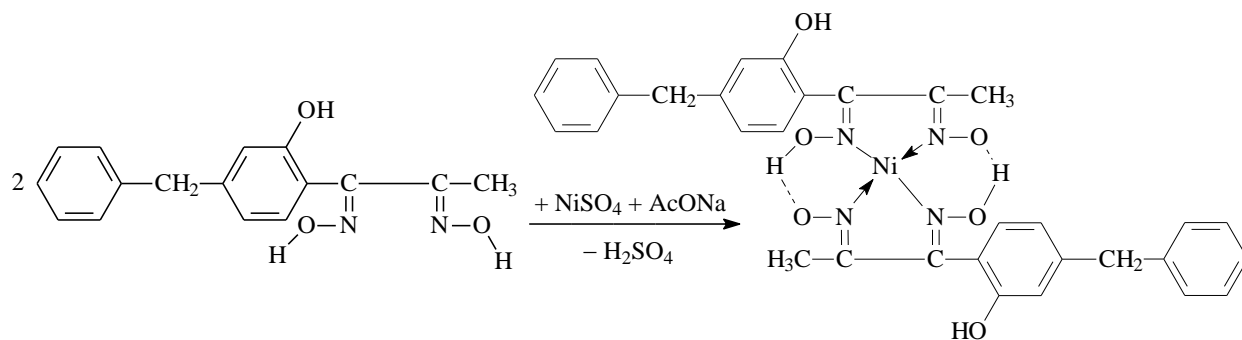
- Preparation of (4-benzyl-2-hydroxyphenyl)-Me-GlyoxH₂, Me-propyl-GlyoxH₂ and Me-pentyl-GlyoxH₂

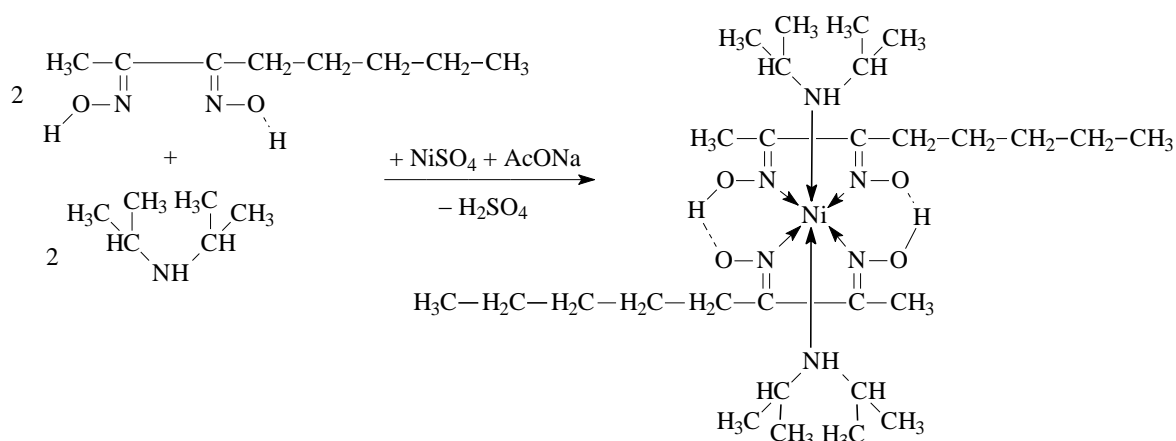
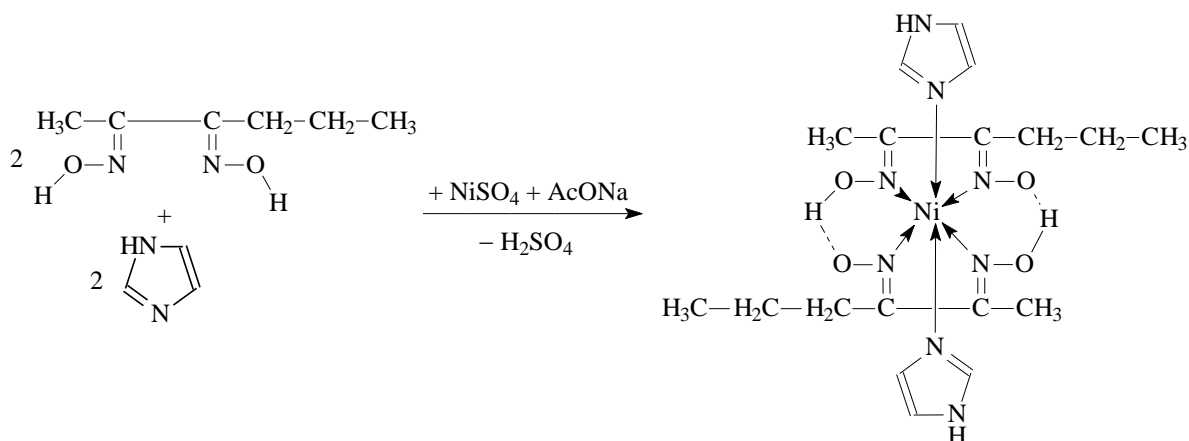
First, the (4-benzyl-2-hydroxyphenyl)-Me-dione-monoxime and Me-pentyl-dione-monoxime were prepared from 4-benzyl-2-hydroxypropionophenone and 2-octanone, respectively. The keton reactants were acidified with HCl, and, according to the isonitroso method, gaseous ethyl nitrite was bubbled into the cooled mixture. Then the obtained monoximes, and, furthermore, the 2,3-hexanedione, were reacted with hydroxylamine generated from the aqueous solution of the corresponding hydrochloride salt by addition of equimolar amount of KOH. The reaction mixture was heated for 2–3 hours, and then the precipitated product was filtered off. After recrystallization from EtOH or MeOH, it was dried on air. The reactions:



- Synthesis of [Ni(GlyoxH)₂(amine)₂] type complexes

(4-benzyl-2-hydroxyphenyl)-Me-GlyoxH₂ or Me-propyl-GlyoxH₂ or Me-pentyl-GlyoxH₂ was dissolved in EtOH, then added to the aqueous solution of NiSO₄ containing spatula tip amount of sodium acetate. In the latter case of Me-propyl-GlyoxH₂ and Me-pentyl-GlyoxH₂, imidazole and diisopropylamine, resp., were added. The mixtures were heated for 2–3 hours. After cooling the crystalline complexes were filtered, washed with EtOH–water mixture (1:1), and then dried on air. The reactions are shown below:

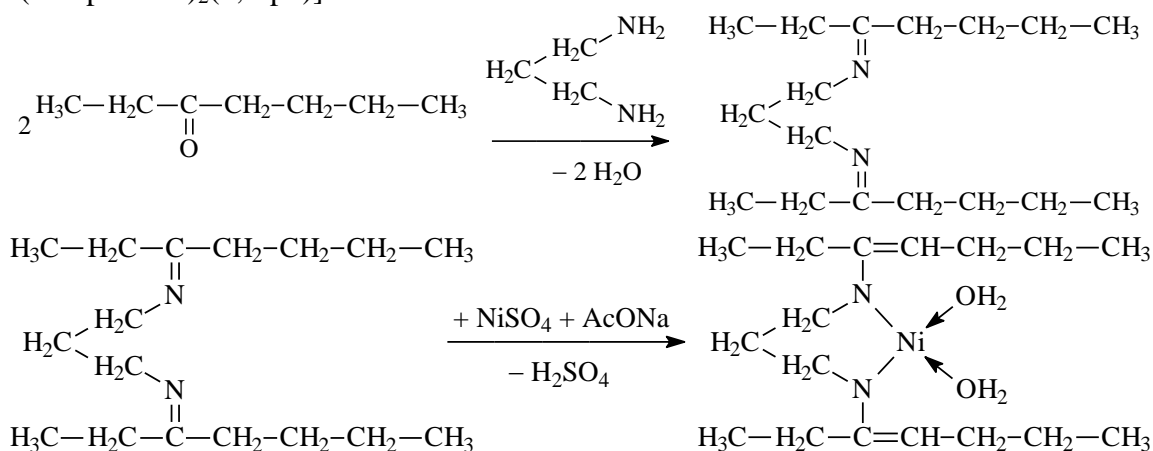




- Synthesis of $[\text{Ni}(\text{3-heptanone})_2(\text{diamine})]$, $[\text{Ni}(\text{propiophenone})_2(\text{diamine})]$ complexes

The Schiff bases were prepared by the condensation reaction between 3-heptanone or propiophenone, and the corresponding diamine (ethylenediamine, 1,2-, 1,3-propylenediamine, o-phenylenediamine) in EtOH solution. The mixture was heated at 70–80 °C for 2–3 hours. The solution obtained was directly used for the synthesis of complexes by adding the aqueous solution of NiSO_4 containing slight amount of sodium-acetate. The product was filtered off, washed with EtOH–water mixture (1:1), and then dried on air.

For example, the reactions below were performed for the synthesis of $[\text{Ni}(\text{3-heptanone})_2(1,3\text{-pn})]$:



Results and discussion

Microscopic characterization and the yield of prepared complexes are presented in Table 1.

Table 1. Microscopic characterization, calculated molecular weight and the yield of prepared complexes.

Nr.	Compound	Calc. mol. weight	Yield (%)	Microscopic characterization
1.	[Ni((4-benzyl-2-HO-phenyl)-Me-GlyoxH) ₂]	625.30	63	Light brown discs
2.	[Ni(Me-propyl-GlyoxH) ₂ (imidazole) ₂]	481.17	63	Red triangle-based prisms
3.	[Ni(Me-pentyl-GlyoxH) ₂ (diisopropyl-amine) ₂]	603.51	32	Orange-red discs and triangle-based prisms
4.	[Ni(3-heptanone) ₂ (en)]	309.11	25	Greenish-blue triangle-based prisms
5.	[Ni(3-heptanone) ₂ (1,2-pn)]	323.14	15	Greenish-blue irregular microcrystals
6.	[Ni(3-heptanone) ₂ (1,3-pn)]	323.14	65	Green irregular microcrystals
7.	[Ni(3-heptanone) ₂ (o-fen)]	357.16	28	Brown triangle-based prisms
8.	[Ni(propionophenone) ₂ en]	349.09	44	Light purple triangle-based prisms
9.	[Ni(propionophenone) ₂ (1,2-pn)]	363.12	10	Light blue triangle-based prisms
10.	[Ni(propionophenone) ₂ (o-fen)]	397.14	45	Dark brown triangle-based prisms

Infrared spectroscopic study

The mid-IR spectra were recorded with a Bruker Alpha FTIR spectrometer (Platinum single reflection diamond ATR), at room temperature, in the wavenumber range of 4000–400 cm⁻¹, and the far-IR range of 650–150 cm⁻¹, respectively, on a Perkin–Elmer System 2000 FTIR spectrometer, operating with a resolution of 4 cm⁻¹. The samples were measured in solid state (in powder form) and in polyethylene pellets, respectively. The data of the most characteristic IR bands for the selected complexes are presented in Table 2.

Table 2. IR data of the selected complexes.

Comp. cm ⁻¹	1	2	3	4	5	6	7	8	9	10
ν_{O-H}	3648 w	-	3648 w	-	-	-	-	-	-	-
ν_{C-H}	2940 m	2961 m	2926 s	2970 m	2971 s	2971w	2970 s	2970 w	2970 w	2970 w
$\nu_{C=N}$	1609 s	1560vs	1560vs	1739vs	1739vs	1541vs	1738vs	1739vs	1739 s	1739 s
δ_{CH_2}	1456 m	1454 m	1458 s	1425 s	1425vs	1417vs	1457vs	1456 m	1420 s	1436 s
δ_{CH_3}	1366vs	1364 w	1366 s	1373 s	1374 m	1216 w	1374vs	1373 s	1374 m	1374 s
ν_{N-O}	1217vs	1239vs	1229vs	-	-	-	-	-	-	-
ν_{N-OH}	1191vs	1117vs	1119vs	-	-	-	-	-	-	-
τ_{O-H}	1098vs	1049 s	1049 s	1068vs	1066vs	1057vs	1092 m	1063vs	1066vs	1078vs
γ_{C-H}	616 vs	709 vs	731 vs	612 vs	612 vs	608 vs	755 s	610 vs	611 vs	743 vs
ν_{Ni-N}	488 s	516 vs	514 s	528 s	543 s	476 m	527 m	528 s	548 m	518 s

(Abbreviations: vs = very strong, s = strong, m = medium, w = weak)

Mass spectrometry

Mass spectra of the samples were recorded using electrospray ionization (ESI). In the spectra we could detect the molecular ions and some decomposition fragments.

Thermoanalytical measurements (TG-DTG-DTA)

Thermal measurements were performed with a 951 TG and 910 DSC calorimeter (DuPont Instruments), in Ar or N₂ at a heating rate of 10 Kmin⁻¹ (sample mass of 4–10 mg).

In the case of [Ni(GlyoxH)₂(amine)₂] type complexes the first decomposition steps are belonging to the leaving amine groups up to 300 °C. Subsequently, the decomposition of glyoxime groups takes place which is accompanied by big exothermic peaks. This behavior

can be explained with the presence of oxygen in the molecule. In the case of Schiff bases, first heptanone and propiophenone parts, respectively, are leaving, afterwards the diamine moieties eliminate. Two examples are presented in the figure. The general decomposition mechanisms:

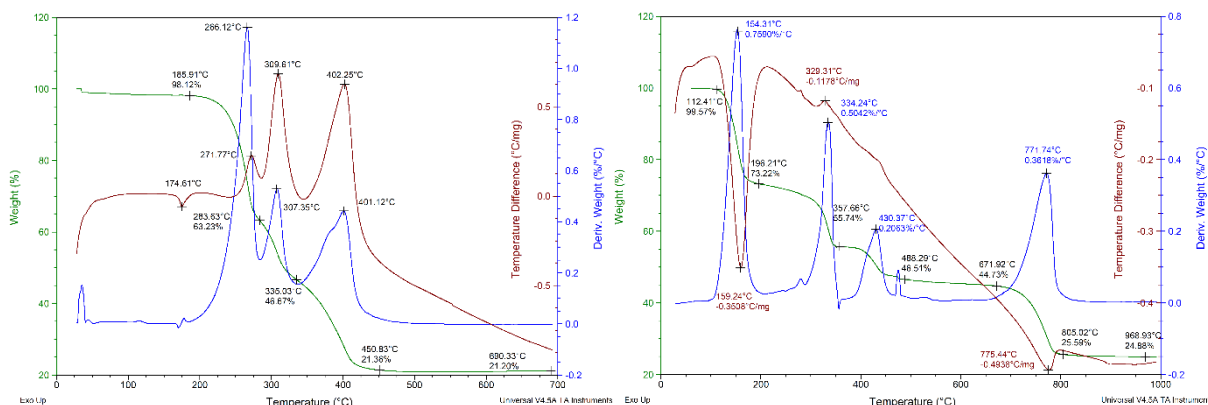
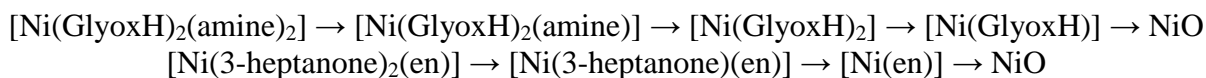


Figure. Thermal decomposition of [Ni(Me-propyl-GlyoxH)₂(imidazole)₂] and [Ni(3-heptanone)₂(en)]

Powder X-ray diffraction measurements

The crystal structure of the complexes was studied with powder XRD measurements, carried out on a PANalytical X'pert Pro MPD X-ray diffractometer. As being new compounds their diffractograms are not deposited in the Cambridge database.

UV–VIS spectroscopy

The electronic spectra were recorded with Jasco V-670 Spectrophotometer in 10% EtOH/water solutions containing substrate in 10^{-4} mol/dm³ concentration. Using Sørensen buffer solutions the electronic spectra were also recorded as a function of pH, and then the acidity constants were calculated too.

Conclusion

In this work new nickel complexes were synthesized and their physico-chemical properties were studied. Decomposition mechanism was determined with the thermoanalytical method.

Acknowledgement

The authors wish to express their thankfulness to the “Domus Hungarica Foundation” of Hungary for the several fellowships provided to Csaba Várhelyi jr.

References

- [1] M. Salehi, F. Rahimifar, M. Kubicki, A. Asadi, *Inorganica Chimica Acta* 443 (2016) 28
- [2] S. Kumar, A.V. Trivedi, *Int. J. Curr. Microbiol. App. Sci* 5(3) (2016) 719
- [3] S.M. El-Megharbel, A.S. Megahed, M.S. Refat, *J. of Molecular Liquids* 216 (2016) 608
- [4] O.E. Sherif, N.S. Abdel-Kader, *Spectrochimica Acta Part A: Molecular and Biomolecular Spectroscopy* 117 (2014) 519

POTENTIAL DEVELOPMENT METHODS OF MEMBRANE FILTRATION TO PURIFY OIL-CONTAMINATED WATERS

Erika Nascimben Santos^{1,2,3,*}, Gábor Veréb^{1,*}, Szabolcs Kertész¹, Cecilia Hodúr^{1,3}, Zsuzsanna László¹

¹ *Institute of Process Engineering, Faculty of Engineering, University of Szeged, HU-6725, Moszkvai Blvd. 9., Szeged, Hungary*

² *Doctoral School of Environmental Sciences, University of Szeged, H-6701, P.O.B. 440, Szeged, Hungary*

³ *Institute of Environmental Science and Technology, University of Szeged, H-6720, Tisza Lajos Blvd. 103, Szeged, Hungary*

* *e-mail address: erikans123@gmail.com, verebg@mk.u-szeged.hu*

Introduction

It is important to treat effectively the oil-contaminated waters, since they are produced in high amounts by several industrial activities [1], and their toxic compounds can significantly affect negatively the environment [2, 3]. To achieve excellent efficiency, the conventional techniques (such as flotation, centrifugation, skimming, *etc.*) are not enough because of the small emulsified oil droplets that cannot be removed by these methods [4]. The complementation of these techniques with membrane filtration can be a good solution to this problem, since, over the high achievable efficiency, it has other additional advantages, like the easy operation and integration. However, the generation of a hydrophobic cake layer – and the fouling of the pores – that reduce quickly and significantly the flux can make the utilization of this technology not feasible [5]. Thinking about this, many studies target to fix this problem by developing different promising solutions. One of them is the membrane modification, which can be achieved, for example, by using hydrophilic and photocatalytic nanomaterials. The present work shows a brief overview about the utilization of membrane filtration for treating oily wastewaters – explains the difficulties, the main problems and discusses promising solutions to improve this treatment method and to find feasible technologies, focusing on membrane modifications, mainly with hydrophilic and photocatalytic nanomaterials that can result in self-cleaning and antifouling properties.

Main pollutants of oil-contaminated waters and their harmful effects

Oils contain several harmful compounds: saturated straight and branched-chain hydrocarbons, cyclic hydrocarbons, olefins, aromatic hydrocarbons and others, such as sulfur compounds, nitrogen-oxygen compounds, and heavy metals. The harmfulness of the oil-contaminated waters depends on the type, volume, and quality of the polluting oil, but also on the place and conditions of the discharge. The oily wastewaters can cause harmful effects on organisms by coating, asphyxiation, poisoning or causing sublethal and stress effects, reducing the abundance and diversity of the fauna and flora [2]. The soils also can be affected by oil contaminations, reducing the bacteria activity, the life of earthworms and plant growth, by affecting the root elongation and germination [6]. In relation to animals and human beings, oil contaminations can be accumulated in the food chain, can damage the DNA, and can produce genotoxic, carcinogenic, mutagenic effects, and immune-suppression as well [3, 7].

Membrane technology to treat oil-contaminated waters

Membrane filtration technique became a promising purification method to treat oily wastewaters due to its' several advantages, *i.e.* no chemical addition, easy handling, low energy requirement, and high efficiency. The separation method consists of using a physical

barrier (membrane) that allows the water to flow by the action of a driving force while the contaminants are retained by the barrier [8]. Both micro- and ultrafiltration can be used to remove efficiently the oils, however, ultrafiltration shows higher efficiency to remove smaller droplets and to reduce the total organic carbon (TOC) content and chemical organic demand (COD) [9, 10]. The technology faces several challenges *e.g.* the reduction of fouling, which is the major limitation in several cases [5]. During the filtration, various compounds can be deposited or adsorbed on the membrane surface, such as salts, hydroxides, surfactants and oil droplets [11], causing the fouling of the pores and the formation of hydrophobic cake layer. These problems cause significantly reduced flux, permeability, productivity, decreased life span, and increased energy consumption and treatment costs. The fouling layer can be affected by different reasons [5]:

- i. characteristics of the feed water, *e.g.* concentrations and physicochemical properties;
- ii. characteristics of the membrane, *e.g.*, surface roughness, charge properties, hydrophobicity;
- iii. operational conditions, *e.g.* cross-flow velocity, applied pressure difference, recovery and temperature.

It is necessary to solve the major limitation and make the use of this technology feasible for treating oil-in-water emulsions.

Potential solutions for fouling problems

It is necessary to minimize the interaction between the wastewater's contaminants and the membrane surface to reduce fouling and, for this, there are some possible solutions, *i.e.*:

- i. utilization of backflushing with air, water or permeate, to increase the efficiency and hydrophilicity [12];
- ii. application of biological, physical or chemical pre-treatment for example, degasification, chemical softening, media filtration, ion-exchange softening, ozonation, *etc.* [13]–[15];
- iii. Utilization of membrane modification by blending [16], by coating or by the deposition of nanomaterials onto the membrane surface [17].

The use of nanomaterials to modify the membrane has a huge potential to improve membrane efficiency due to its high surface area and high surface-active groups [8].

Membrane modification with photocatalytic nanomaterials

Photocatalytic nanomaterials can also be used to modify the membrane, since they have the ability to decompose several organic pollutants via their light-induced activation [18]. These UV and/or solar-light activated semiconductor materials can generate electron/hole pairs that can oxidize directly or indirectly the organic contaminants. Therefore, these photocatalytic nanoparticles can be used to prepare self-cleaning membrane, that can be activated and purified by photons regaining the permeability without shutdown the filtration, increasing costs or reducing the membrane life [19]. There are several well-known photocatalytic materials such as zinc oxide (ZnO), zinc sulfide (ZnS), tin oxide (SnO₂), copper oxide (CuO₂), cadmium sulfide (CdS), tungsten trioxide (WO₃), and the most investigated, titanium dioxide (TiO₂) due to its low cost, high chemical stability and photocatalytic activity, availability, *etc.* [18]. TiO₂ can improve hydrophilicity, stability and anti-fouling properties of membranes, however, it can be activated mostly with ultraviolet light, which is a small fraction of the solar spectrum – 3 to 8%. Therefore, efforts have to be done to develop visible-light sensitive photocatalytic material [20], [21], to form solar-light activable photocatalytic membrane. The addition of other nanomaterials to TiO₂ to modify the membrane has gaining attention because of the enhanced properties of the coupled materials. The use of WO₃, ZnO, BiVO₄ and noble metals such as Ag, Au, Pt, and Pd are showing good results in relation with visible-light-driven activities [20, 22–25], but their effects on filtration properties are also

important, and not well investigated until now. It is possible to recognize the effort on research to find efficient photocatalytic composites that can be used to modify membrane used to the treatment of oily wastewater with higher efficiency and better anti-fouling properties, however, further investigations are necessary to be carried out for industrial utilization.

Conclusions

It is difficult, but necessary to find an excellent purification technology to treat oily wastewaters with high efficiency and economically friendly. Membrane filtration has been developed intensely in the last years, nevertheless, membrane fouling and flux reduction are still serious limiting factors in the case of oily contaminants. Membrane modification methods show good potential to further enhances because they can improve the hydrophilicity and anti-fouling properties of the membranes. Photocatalytic nanocomposites can be used to reduce the adhesion of these kinds of pollutants on the membrane surface and to decompose photocatalytically the yet adhered organic pollutants. TiO_2 has been widely investigated for membrane modification, but further investigations are necessary to be done in order to find photocatalytic nanocomposites that are able to combine the good filtration properties and high visible-light and solar-light activities to make the system more economical and efficient.

Acknowledgments

The authors are grateful for the financial support provided by the Hungarian Science and Research Foundation (2017-2.3.7-TÉT-IN-2017-00016) and by the Hungarian State and the European Union (EFOP-3.6.2-16-2017-00010 – RING 2017). E.N.S thanks for the support of the Stipendium Hungaricum Scholarship Program.

References

- [1] S. G. Pouloupoulos, E. C. Voutsas, H. P. Grigoropoulou, and C. J. Philippopoulos, "Stripping as a pretreatment process of industrial oily wastewater," *J. Hazard. Mater.*, vol. 117, no. 2–3, pp. 135–139, 2005.
- [2] R. P. Cote, "The effects of petroleum refinery liquid wastes on aquatic life, with special emphasis on the Canadian environment," *Natl. Res. Counc. Canada*, vol. K1A 0R6, no. NRC Associate Committee on Scientific Criteria for Environmental Quality, p. 77, 1976.
- [3] H. I. Abdel-Shafy and M. S. M. Mansour, "A review on polycyclic aromatic hydrocarbons: Source, environmental impact, effect on human health and remediation," *Egypt. J. Pet.*, vol. 25, no. 1, pp. 107–123, 2016.
- [4] L. Yu, M. Han, and F. He, "A review of treating oily wastewater," *Arab. J. Chem.*, vol. 10, pp. S1913–S1922, 2017.
- [5] C. Y. Tang, T. H. Chong, and A. G. Fane, "Colloidal interactions and fouling of NF and RO membranes: A review," *Adv. Colloid Interface Sci.*, vol. 164, no. 1–2, pp. 126–143, 2011.
- [6] J. Tang, M. Wang, F. Wang, Q. Sun, and Q. Zhou, "Eco-toxicity of petroleum hydrocarbon contaminated soil," *J. Environ. Sci.*, vol. 23, no. 5, pp. 845–851, 2011.
- [7] T. L. Tasker *et al.*, "Environmental and Human Health Impacts of Spreading Oil and Gas Wastewater on Roads," *Environ. Sci. Technol.*, vol. 52, no. 12, pp. 7081–7091, 2018.
- [8] Y. Zhu, D. Wang, L. Jiang, and J. Jin, "Recent progress in developing advanced membranes for emulsified oil/water separation," *NPG Asia Mater.*, vol. 6, no. 5, pp. e101-11, 2014.
- [9] S. S. Chin, K. Chiang, and A. G. Fane, "The stability of polymeric membranes in a

- TiO₂ photocatalysis process,” *J. Memb. Sci.*, vol. 275, no. 1–2, pp. 202–211, 2006.
- [10] S. Nazirah, W. Ikhsan, N. Yusof, and F. Aziz, “a Review of Oilfield Wastewater Treatment Using Membrane Filtration Over Conventional Technology,” *Malaysian J. Anal. Sci.*, vol. 21, no. 3, 2018.
 - [11] S. Alzahrani and A. W. Mohammad, “Challenges and trends in membrane technology implementation for produced water treatment: A review,” *J. Water Process Eng.*, vol. 4, no. C, pp. 107–133, 2014.
 - [12] P. Srijaroonrat, E. Julien, and Y. Aurelle, “Unstable secondary oil/water emulsion treatment using ultrafiltration: Fouling control by backflushing,” *J. Memb. Sci.*, vol. 159, no. 1–2, pp. 11–20, 1999.
 - [13] I. Kovács, G. Veréb, S. Kertész, C. Hodúr, and Z. László, “Fouling mitigation and cleanability of TiO₂ photocatalyst-modified PVDF membranes during ultrafiltration of model oily wastewater with different salt contents,” *Environ. Sci. Pollut. Res.*, vol. 25, no. 35, pp. 34912–34921, 2018.
 - [14] G. Doran, F. Carini, and D. Fruth, “Evaluation of Technologies to Treat oil Field Produced Water or Reuse Quality.” 1997.
 - [15] R. J. W. Brooijmans, M. I. Pastink, and R. J. Siezen, “Hydrocarbon-degrading bacteria: the oil-spill clean-up crew,” *Microb. Biotechnol.*, vol. 2, no. 6, pp. 587–594, 2009.
 - [16] G. Arthanareeswaran, T. K. Sriyamuna Devi, and M. Raajenthiren, “Effect of silica particles on cellulose acetate blend ultrafiltration membranes: Part I,” *Sep. Purif. Technol.*, vol. 64, no. 1, pp. 38–47, 2008.
 - [17] W. Chan, H. Chen, A. Surapathi, and M. Taylor, “Zwitterion Functionalized Carbon Nanotube / Polyamide Nanocomposite Membranes for Water Desalination,” *ACS Nano*, no. Xx, 2013.
 - [18] J. Saien and H. Nejati, “Enhanced photocatalytic degradation of pollutants in petroleum refinery wastewater under mild conditions,” *J. Hazard. Mater.*, vol. 148, no. 1–2, pp. 491–495, 2007.
 - [19] S. S. Madaeni and N. Ghaemi, “Characterization of self-cleaning RO membranes coated with TiO₂ particles under UV irradiation,” *J. Memb. Sci.*, vol. 303, no. 1–2, pp. 221–233, 2007.
 - [20] H. Jiang *et al.*, “Hydrothermal fabrication and visible-light-driven photocatalytic properties of bismuth vanadate with multiple morphologies and/or porous structures for Methyl Orange degradation,” *J. Environ. Sci.*, vol. 24, no. 3, pp. 449–457, 2012.
 - [21] R. Molinari, C. Lavorato, and P. Argurio, “Recent progress of photocatalytic membrane reactors in water treatment and in synthesis of organic compounds. A review,” *Catal. Today*, vol. 281, pp. 144–164, 2017.
 - [22] L. Baia *et al.*, “Preparation of TiO₂/WO₃ composite photocatalysts by the adjustment of the semiconductors’ surface charge,” *Mater. Sci. Semicond. Process.*, vol. 42, pp. 66–71, 2016.
 - [23] G. Kovács *et al.*, “TiO₂/WO₃/Au nanoarchitectures’ photocatalytic activity, ‘from degradation intermediates to catalysts’ structural peculiarities”, Part I: Aeroxide P25 based composites,” *Appl. Catal. B Environ.*, vol. 147, pp. 508–517, 2014.
 - [24] A. Mishra, A. Mehta, M. Sharma, and S. Basu, “Impact of Ag nanoparticles on photomineralization of chlorobenzene by TiO₂/bentonite nanocomposite,” *J. Environ. Chem. Eng.*, vol. 5, no. 1, pp. 644–651, 2017.
 - [25] X. Yu, Q. Ji, J. Zhang, Z. Nie, and H. Yang, “Photocatalytic degradation of diesel pollutants in seawater under visible light,” *Reg. Stud. Mar. Sci.*, vol. 18, pp. 139–144, 2018.

INVESTIGATION OF PRIORITY POLLUTANTS IN THE SEDIMENT PHASE – PROJECT SIMONA

Mária Mörtl¹, Zsófia Kovács², Győző Jordán³, András Székács¹

¹*Department of Environmental Analysis, Agro-Environmental Research Institute, National Agricultural Research and Innovation Centre,
H-1022 Budapest, Herman Ottó u. 15, Hungary.*

²*Institute of Environmental Engineering, University of Pannonia,
H-8200 Veszprém, Egyetem u. 10, Hungary*

³*Department of Applied Chemistry, Faculty of Food Science, Szent István University,
H-1118 Budapest, Villányi út 29-43, Hungary
e-mail: mortl.maria@akk.naik.hu*

Abstract

The Framework Directive (WFD) of the European Union (EU) aims to achieve good status for water bodies in EU, but there occurs a delay in its implementation related to priority pollutant substances. A key issue in water protection and management is that priority pollutants should be monitored not only in the water bodies, but also in sediments and the biota. Distribution between the water and sediment phases is strongly affected by numerous factors, including the polarity of the analytes, as well as amorphous organic matter and suspended matter content in the water body, and are often affected by methodological parameters. As a result, certain pollutants will be detected in the water phase, others in the sediment, again others in both, as indicated by reported cases in the scientific literature. This challenge is illustrated in the case of project “Sediment-quality Information, Monitoring and Assessment System” (SIMONA) (2018-2021) within the Danube Transnational Program.

Introduction

Water protection is one of the priorities of the European Commission. The European Water Policy aims to protect clean water in the European Union (EU) by preventing water pollution and to restore clean water from polluted sites. Thus, the EU Water Framework Directive (WFD), as one of the key EU policy measures, aims to reach a good status both chemical and ecological, for water bodies in Europe [1]. Water pollutants that jeopardize such good status represent a threat to the aquatic environment, and the WFD specified the most hazardous substances of these to be phased out. For this purpose, priority substances (PSs) presenting a significant risk to or via the aquatic environment were listed in 2008 [2]. The first watch list for European Union-wide monitoring of water bodies was published in 2015 [3] containing ten substances or groups of components, that was further extended in 2018 [4].

Nonetheless, the original goals of the EU water protection policy have not yet been achieved, and there appears a delay in the implementation of the objectives set in the WFD [5]. Previously monitoring at the point of discharge was typical to control the emission of specific pollutants (end-of-pipe). In turn, regulation has shifted lately towards systematic (integrated) thinking that focuses on sustainability, flexible water governance, determination of indicators, complex understanding of drivers, pressures, state impacts and responses in catchments. In addition to the determination of emissions and maximum limits, environmental quality standards (EQSs) have been set for certain substances, and management actions must account for the effects of multiple stressors. Monitoring and assessment need to better reflect improvement in the ecological status and long-term tendencies [6].

Affecting factors that influence distribution of pollutants

The current list of 20 PSs, 13 priority hazardous substances (PHSs) [2], 11 substances subject to review for possible identification as PSs or PHSs, and 8 substances on watch list [3] includes, among other groups of toxic compounds, pesticide active ingredients and their metabolites or contaminants. In addition, chemical intermediates, by-product polyaromatic hydrocarbons (PAHs), polybrominated biphenylethers (PBDEs), biocides, metals, as well as hormones and antibiotics are also found on the lists.

These compounds are regularly measured in water bodies, their EQSs are intended also for sediment and biota, yet far less information is available about their substantive concentration in the sediment. Partition of the components depends on their polarity characterized by their octanol/water partition coefficient (K_{ow}). On the other hand, higher organic matter content in the sediment bind more non-polar components compared to those with lower organic content. Therefore, the equilibrium constant is often given to organic matter content of soils (K_{oc}). Distribution between the two phases results in different mobilities, which is strongly influenced by other factors e.g., suspended matter content. Worthy of note, that there is no equilibrium in the rivers between water body and the sediment. Based on the K_{ow} , compounds having $K_{ow} < 3$ are water pollutants, while components characterized by $K_{ow} > 5$ are sediment pollutants. Other components ($3 \leq K_{ow} \leq 5$) are present in both phases. Partition influences the analytical results and contamination levels determined in water. Analysis of the entire water body often fails as the water sample is filtered prior to sample preparation (solid phase extraction) or instrumental analysis (liquid chromatography) in numerous analytical protocols. Certain pollutants, however, are partially or completely removed by filtration. Faludi et al. [8] determined substituted phenols in both the Danube river and its suspended matter. Yet e.g., priority substance pentachlorophenol was detected only in the suspended phase, which is rarely analyzed.

Temporal variation of the analytes is high in the water phase, but less variable in the sediment. If a spot sample is taken, only the concentration currently present in water can be measured. Nowadays, pollutant levels on a longer time-scale can be determined in surface water by the use of passive samplers. These keep collecting pollutants for one or two weeks, but the derived information differ from the results obtained for spot samples. Both information are important as not only the maximum, but also the average concentrations are often regulated for certain pollutants. Grab sampling and collection by polar organic chemical integrative sampler (POCIS) for organic compounds with a $0 \leq \log K_{ow} \leq 5$ were simultaneously applied, and the results were compared [9]. Pollution patterns reflect the land use and loads, but also the presence of persistent components. For example, herbicide active ingredient atrazine is still detected, despite of its ban in the EU in 2004. A partial cause of this water polluting characteristics is accumulation and practically no decomposition of the compound in the anaerobic soil zones, and subsequent leaching to surface water. Unfortunately, illegal use of this prohibited pesticide active ingredient also occurs: fresh loads of atrazine were confirmed by its high concentration together with its low metabolite levels (desethyl atrazine). Atrazine was detected by us in Hungarian water and soil samples as well at around 2010, after its ban in 2007, but it did not appear any further during monitoring of the Danube river in 2015, indicating that its level decreased below the detection limit of our method [10].

Comparison of pollution patterns and contamination levels of sediment and water samples [11] showed significant spatial variations in water and sediment. Seasonality in concentration was observed in water, but not in sediment, although sediment concentrations varied substantially among different years. Average measured non-equilibrium distribution coefficients exceeded equilibrium hydrophobic partitioning-based predictions for 5 of the 7 detected contaminants by at least an order of magnitude. Agreement increased with

hydrophobicity and persistence. These observations indicate non-equilibrium conditions between water and sediment phases and slow rate of adsorption. Among detected compounds, the distribution of more polar and degradable components showed greater variability, probably due to their degradation. On the other hand, non-sorptive components (based on their $\log K_{ow}$ values) were found also in the sediment indicating the importance of other processes (e.g. complex formation).

Inorganic components of the sediment may occasionally be equally important, as it was observed for example in the case of glyphosate and iron-oxide. Gama et al. [12] studied the distribution of different herbicides. Non-polar compounds with high $\log K_{ow}$ and K_{oc} values were more likely to be found in the inorganic fraction of the sediment, whereas more polar herbicides with high solubility and low K_{oc} values were dispersed between both the organic and inorganic fractions. The interaction between chemicals and amorphous organic matter (e.g., humic and fulvic acids, proteins, lignin, polysaccharides) might also modify the partition process.

Partition among the water-dissolved phase (DP), suspended particulate matter (SPM) and sediment may also become characteristic. Montuori et al. [13] measured pollution by organophosphate pesticides (OPP) in the Sarno river (Italy), and detected these compounds in DP, SPM and sediment samples simultaneously. Total OPP concentrations ranged from 5.58 to 39.25 ng L⁻¹ in the water phase as the sum of the DP and SPM, and from 0.19 to 3.98 ng g⁻¹ in the sediment samples. Their conclusion has been that chlorpyrifos is a pseudo-persistent pollutant, and that higher levels of chlorpyrifos found in DP than in SPM samples and sediment samples indicate fresh inputs.

The SIMONA project

Sediment quality is an existing problem in the Danube River Basin (DRB), and countries in the region lack sufficient institutional capacity, including information, guidelines and methods, to build a transnational sediment monitoring network for trend assessment of hazardous substances. The international project SIMONA (Sediment-quality Information, Monitoring and Assessment System) was launched in 2018, as a part of the Danube Transnational Program (DTP), to support transnational cooperation for joint DRB water management by harmonized sediment monitoring [14]. The main objective of project SIMONA, carried out by the participation of 17 full consortium partners and 12 strategic associated partners from 12 DRB countries, is to respond to the current demand for effective and comparable measurements and assessments of sediment quality in surface waters in the DRB by delivering a ready-to-deploy sediment quality information, monitoring and assessment system to support transnational cooperation for joint DRB water management. For this purpose, project SIMONA aims to develop an improved, harmonized and coordinated sediment quality monitoring system of the water body status in the DRB. Together with experts trained in sediment quality management by SIMONA, the project will also generate international cooperation between stakeholders concerning the monitoring of PHS concentrations in water, in sediments and in biota. The immediate and middle term benefit of the project will be a transparent method supported by an online platform information technology tool (SIMONA-tool) for sediment quality monitoring that will encourage the cooperation in transnational water management, as well as the sediment quality assessment.

Working groups in the project collect currently existing protocols and develop transnationally harmonized guidance in the field of sediment sampling, laboratory measurement of PSs and data evaluation, including quality assessment and quality control procedures. Outputs of the project will be integrated into the SIMONA-tool developed, containing a sediment quality evaluation protocol for PHSs, three harmonized protocols (sampling, laboratory and

evaluation), as well as earlier monitoring data for sediment. Evaluation of data will be based on predefined formula and display of the information (e.g. for decision-making authorities).

Conclusion

As demonstrated by the scientific results reported, equilibrium between the water and sediment phases is a complex issue, and actual distribution of pollutants depends on numerous factors. More accurate assessments of exposure and risk to surface water ecosystems can be performed by improving the prediction of fate and transport processes. This requires a dual solution. On the one hand, there is a knowledge gap in exploring the affecting factors related to the partition of PHSs in the sediment that requires further investigations. On the other hand, a harmonized protocol is necessary to compare the monitoring results and to determine the background levels in the DRB.

Acknowledgements

This work was supported by project DTP2-093-2.1 “Sediment-quality Information, Monitoring and Assessment System” (SIMONA) 2018-2021.

References

- [1] European Council, Directive 2000/60/EC of the European Parliament and of the Council, establishing a framework for community action in the field of water policy. Off. J. L327 (2000) 1-73.
- [2] European Council, Priority substances and certain other pollutants according to Annex II of Directive 2008/105/EC. Off. J. L348 (2008) 1-84.
- [3] European Commission, Implementing Decision 2015/495 establishing a watch list of substances for Union-wide monitoring in the field of water policy pursuant to Directive 2008/105/EC of the European Parliament and of the Council. Off. J. L78 (2015) 40-42.
- [4] European Commission, Implementing Decision (EU) 2018/840 establishing a watch list of substances for Union-wide monitoring in the field of water policy pursuant to Directive 2008/105/EC of the European Parliament and of the Council and repealing Commission Implementing Decision (EU) 2015/495. Off. J. L141 (2018) 9-12.
- [5] N. Voulvoulis, K.D. Arpon, T. Giakoumis, Sci. Total Environ. 575 (2017) 358-366.
- [6] L. Carvalho, E.B. Mackay, A.C. Cardoso et al., Sci. Total Environ. 658 (2019) 1228-1238.
- [7] M. Mörtl, O. Kereki, B. Darvas, et al., J. Chem. 2016 (2016) Article ID 4546584.
- [8] T. Faludi, A. Vasanits-Zsigrai, Gy. Záray et al., Microchem. J. 118 (2015) 45-54.
- [9] R. Guibal, S. Lissaide, J. Leblanc et al., Environ Sci Pollut Res 25 (2018) 14280-14293.
- [10] A. Székács, M. Mörtl, B. Darvas et al., J. Chem. 2015 (2015) Article ID 717948.
- [11] D.J. Fairbairn, M.E. Karpuzcu, W.A. Arnold et al., Sci. Total Environ. 505 (2015) 896-904.
- [12] A.F. Gama, R.M. Cavalcante, W.C. Duaví et al., J. Soils Sedim. 17 (2017) 1160–1169.
- [13] P. Montuori, S. Aurino, A. Nardone et al., Environ. Sci. Pollut. Res. 22 (2015) 8629-8642.
- [14] <http://www.interreg-danube.eu/approved-projects/simona>

BiOI/MWCNT COMPOSITES FOR PHENOL DEGRADATION UNDER VISIBLE LIGHT

Nikita Sharma¹, Pap Zsolt^{2,3}, Seema Garg⁴, Klára Hernádi¹

¹ *Department of Applied and Environmental Chemistry, University of Szeged, H-6720 Rerrich Béla 1, Szeged, Hungary*

² *Institute of Environmental Science and Technology, University of Szeged, H-6725, Tisza Lajos 103, Szeged, Hungary*

³ *Nanostructured Materials and Bio-Nano-Interfaces Centre, Institute for Interdisciplinary Research on Bio-Nano-Sciences, Babeş-Bolyai University, RO400271, Treboniu Laurian 42, Cluj-Napoca, Romania*

⁴ *Department of Chemistry, Amity Institute of Applied Sciences, Amity University, Sector-125, NOIDA, U.P. 201313, India
email: nikita_sh18@yahoo.co.in*

Abstract

In the present work, composites of BiOI with multi-walled carbon nanotubes (MWCNTs) of different compositions (0.5%, 1%, and 2% in weight percentage) were synthesized via hydrothermal synthesis at different time and temperature conditions (4:30 and 6:30 hours at 120°C and 150°C each). The composites were characterized by X-Ray diffraction (XRD), Scanning Electron Microscopy (SEM) and Diffuse Reflectance Spectroscopy (DRS) for their structural, morphological and optical properties. The morphology of the composites varied with different temperature conditions. The nano-plates/sheets-like structure was observed at 120°C while microflowers were observed at 150°C. However, no significant results were observed in overall photocatalytic efficiency of the composites with change in morphology. BiOI/MWCNT showed enhanced photocatalytic degradation of phenol under visible light as compared to BiOI.

Introduction

In recent past, enormous energy crises and water pollution instances have risen and has threatened the sustainable development of human beings. Wastewaters containing organic pollutants are of major environmental concern. Apart from being toxic and carcinogenic in nature, they persist in the environment for a long time and therefore, adversely affects the human health. Heterogeneous photocatalysis have now emerged as one of the most effective and “greener” technique to eliminate such organic pollutants by complete mineralization [1-2]. Bismuth oxyhalides (BiOX) are among one of the efficient photocatalysts in addition to TiO₂, to decompose pollutants into non-toxic molecules for environmental remediation [3-4]. Several classes of visible light photocatalyst are being investigated and modified, but bismuth oxyhalides, (BiOX, X= Cl, Br, I), due to their unique layered structure, suitable band gap values, and stability has shown promising visible light response. They have relative stability under UV/visible light irradiation, show visible light active response and superior performance compared to Evonik Aeroxide P25 (titania) under UV irradiation [5-6].

Among BiOX, BiOI is known to have narrow band gap (1.72-1.9 eV), therefore shows a high rate of utilization of visible light. However, BiOI suffers from drawbacks such as easy recombination of e⁻/h⁺ pairs, weak photo-oxidation ability and low quantum yield. Different methodologies have been adopted to improve the photocatalytic response: building a hierarchical structure, composite formation, heterojunctions, dye sensitization etc. In the past BiOI/carbon composites (BiOI/g-C₃N₄, BiOI/activated carbon, BiOI/graphene) have been reported to show enhanced photocatalytic response [7-8]. Carbon nanotubes composites due

to their hollow structure, excellent electronic properties and good adsorbent properties, are one of the promising nanomaterials effective in improving the charge transfer between the nanostructure interfaces and they also exhibit high catalytic activity.

Experimental

Materials

Bismuth nitrate pentahydrate [$\text{Bi}(\text{NO}_3)_3 \cdot 5\text{H}_2\text{O}$] purchased from Sigma–Aldrich, 98.0%, glacial acetic acid, 100% purchased from Molar Chemicals Kft. and potassium bromide [KBr], 99.0 % purchased from Reanal, Phenol (VWR extra pure, 100%) was purchased from VWR. Deionized water was used for the entire study. All the reagents were of analytical grade and were used without further purification.

Synthesis of BiOI

For the synthesis of BiOI, bismuth nitrate pentahydrate (1 mM in the final synthesis mixture, 3.0 g) was dissolved in 3 mL glacial acetic acid with slight heating (40 - 45 °C) to decrease the dissolution time. This solution was added to 25 mL deionized water (marked as solution A) and was stirred until it was well dispersed. For solution B, potassium iodide (1 mM in the final synthesis mixture, 0.78 g) was dissolved in 25 mL deionized water under magnetic stirring until it was completely dissolved. Further, solution A was added to solution B dropwise and the mixture was stirred for 20 minutes to ensure completion of the reaction. A yellow precipitate appeared which was transferred to a stainless-steel, Teflon lined autoclave and subsequently heated at two different time and temperature conditions (120 °C & 150 °C for 4:30 hours and 6:30 hours each.). It was then cooled down to room temperature (naturally) and the product was collected and washed with ethanol and deionized water three times each using centrifugation at 4400 rpm for 5 minutes. The final product was dried at 60-80 °C in a vacuum furnace overnight.

Synthesis of BiOI/MWCNT composite

BiOI/MWCNTs composites were prepared in a similar manner, except the MWCNTs were added to solution A prior mixing of the two solutions (A and B). Therefore, after adding desired % content of MWCNTs (0.5%, 1%, 2% - values in weight percentage), solution A was sonicated for 2 hours, during which a black colored suspension was formed. This was now solution A with MWCNTs, while solution B was prepared similarly as mentioned before and the same procedure follows.

Results and discussion

X-Ray diffraction: The composites were characterized by X-Ray diffractometer for their structural analysis. All the peaks corresponds to the tetragonal phase (JCPDS Card No. 10-0445) and no additional characteristic peaks were observed which implies pure BiOI. The diffraction peaks for MWCNTs were not visible due to their low content. Fig. 1 shows the X-Ray diffraction of composites prepared at different time and temperature conditions with 0.5% and 1% MWCNTs content (by weight). In some of the cases, diffraction peaks of (001) and (101) facets were appearing. This suggests some structural changes have occurred.

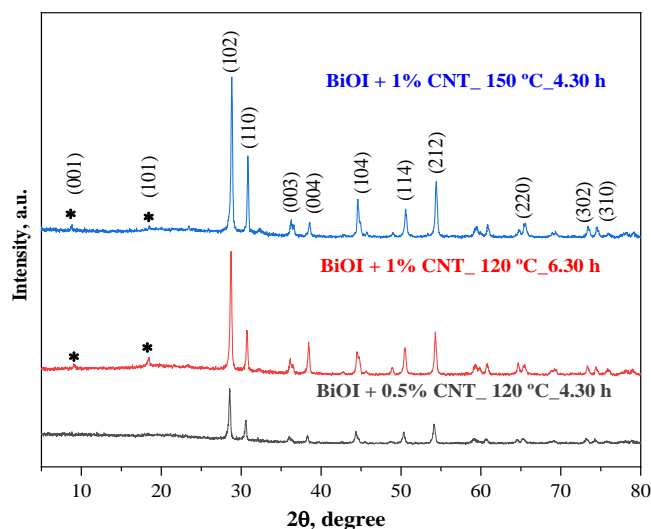


Figure 1. XRD patterns of BiOI/MWCNT composites with different amount of CNTs, prepared at different hydrothermal time and temperature conditions

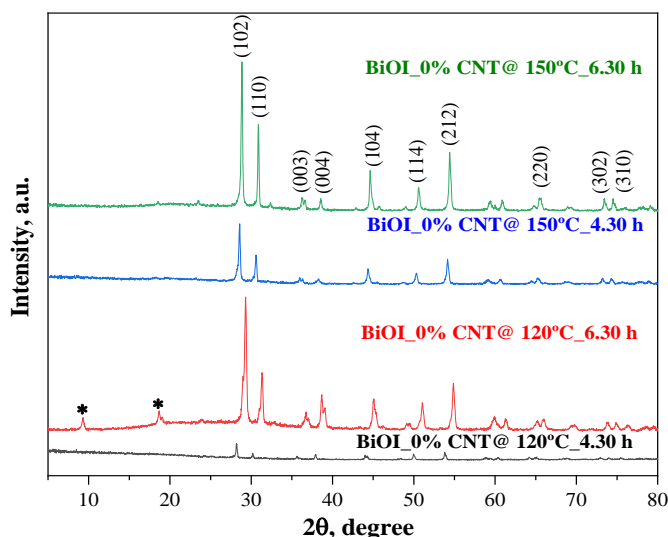


Figure 2. XRD patterns of BiOI prepared at 120 °C and 150 °C at 4:30 and 6:30 hours

N₂ adsorption: The BET calculated specific surface areas of the samples varied with changes in hydrothermal synthesis parameters (time and temperature). These measurements confirmed that all the samples have low surface area in agreement with the higher crystallite size as calculated from XRD data. The specific surface area ranges from 2.6 m²/g to 9.2 m²/g.

Scanning Electron Microscopy (SEM): The morphology of the composites varied with different hydrothermal temperature conditions. The nano-plates/sheets-like structure was observed in case of 120 °C (Fig. 3 (a),(b)) while microflowers in case of 150 °C as shown in Fig. 3 (c), (d).

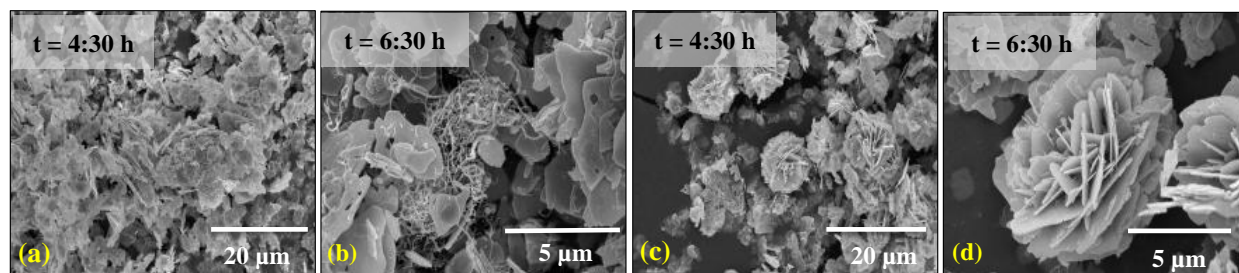


Figure 3. SEM micrographs of samples prepared at two different hydrothermal temperature conditions (120°C and 150°C) depicting two different morphologies

Diffuse Reflectance Spectroscopy (DRS): The optical properties of the prepared samples were studied via UV-vis absorption spectra in the wavelength range of 200-800 nm. The band gap energy value of the BiOI/CNT composites fall in the range 1.62-1.89 eV. The color of the samples gradually changed from red to brick-red to brown with the increasing carbon content. The darker the sample is, the more light it will absorb. Therefore, the BiOI/CNT composites may exhibit enhancement in absorbing visible light compared to pure BiOI.

Photocatalytic Test: Photocatalytic activity of BiOI and BiOI/CNT were evaluated by photodegradation of phenol under visible light. The experimental results were shown in Fig. 4. BiOI/CNT composites showed enhanced photocatalytic activity as compared to pure BiOI.

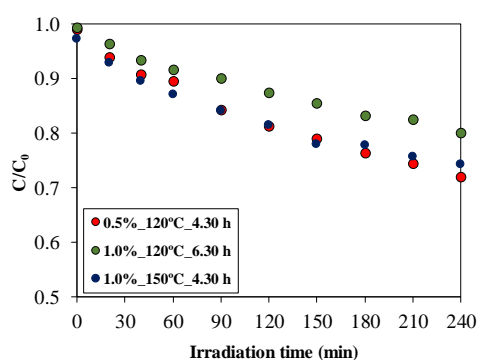


Figure 4. Photocatalytic degradation of phenol under visible light by BiOI/CNT composite

Conclusion

Composites of BiOI/CNTs were prepared at various hydrothermal time and temperature conditions. Different morphologies were observed. Nanoplates were derived at 120°C and microflowers were obtained at 150°C. However, no significant effects were observed on the overall photocatalytic efficiency of the composites. BiOI/CNT composites resulted in the photodegradation of phenol under visible light. Pure BiOI showed the least photocatalytic activity. Therefore, to some extent CNTs played a role of charge separation in the photocatalytic process.

Acknowledgement

This work was supported by the Indo-Hungarian TÉT project (TÉT_15_IN-1-2016-0013 and Department of Science and Technology, Delhi, India (INT/HUN/P-06/2016).

References

- [1] J. Wang, Y. Zhang, L. Tian, F. Liu, Q. Xia, Ultrathin BiOBr nanocrystals with dominant {001} facets and their high photocatalytic activity, J. Nanoparticle Res. 16 (2014). doi:10.1007/s11051-014-2691-9.

- [2] P. Chowdhury, A. Elkamel, A.K. Ray, CHAPTER 2. Photocatalytic Processes for the Removal of Toxic Metal Ions, in: Heavy Met. Water, Royal Society of Chemistry, Cambridge, (2014): 25–43. doi:10.1039/9781782620174-00025.
- [3] X. Chen, W. Shanguan, Hydrogen production from water splitting on CdS-based photocatalysts using solar light, *Front. Energy*. 7 (2013) 111–118. doi:10.1007/s11708-012-0228-4.
- [4] S. Nahar, M.F.M. Zain, A.A.H. Kadhum, H.A. Hasan, M.R. Hasan, Advances in photocatalytic CO₂ reduction with water: A review, *Materials (Basel)*. 10 (2017). doi:10.3390/ma10060629.
- [5] L. Chen, J. He, Y. Liu, P. Chen, C.T. Au, S.F. Yin, Recent advances in bismuth-containing photocatalysts with heterojunctions, *Cuihua Xuebao/Chinese J. Catal.* 37 (2016) 780–791. doi:10.1016/S1872-2067(15)61061-0.
- [6] Fujishima, X. Zhang, Titanium dioxide photocatalysis: present situation and future approaches, *Comptes Rendus Chim.* 9 (2006) 750–760. doi:10.1016/j.crci.2005.02.055.
- [7] X. Xiong, L. Ding, Q. Wang, Y. Li, Q. Jiang, J. Hu, Synthesis and photocatalytic activity of BiOBr nanosheets with tunable exposed (010) facets, *Appl. Catal. B Environ.* 188 (2016) 283–291. doi:10.1016/j.apcatb.2016.02.018.
- [8] E.F. Pérez-Ramírez, M. de la Luz-Asunción, A.L. Martínez-Hernández, C. Velasco-Santos, Graphene Materials to Remove Organic Pollutants and Heavy Metals from Water: Photocatalysis and Adsorption, *Semicond. Photocatal. - Mater. Mech. Appl.* (2016). doi:10.5772/62777

STUDY TO EVALUATE THE EFFECT OF ULTRA-SONICATION PRIOR TO MICROWAVE DISINTEGRATION ON ANAEROBIC DIGESTION OF DAIRY SLUDGE

Mahmood Al Ramahi¹, Sándor Beszédes², Gábor Keszthelyi-Szabó²

¹*Doctoral School of Environmental Sciences, University of Szeged, H-6724 Szeged, Dugonics ter 13, Hungary*

²*Department of Process Engineering, University of Szeged Faculty of Engineering, H-6725 Szeged, Moszkvai krt. 9, Hungary
e-mail: m7mod-rm7i@hotmail.com*

Abstract

The aim of this work is to study the effect of ultra-sonic pretreatment efficiency prior to microwave (MW) irradiation on dairy sludge characterization and biogas yield. Pretreatment experiments were performed as batch process with 250 mL of sludge placed in ultra-sonication and followed by MW irradiation. Results revealed in higher trend of soluble chemical oxygen demand (SCOD) and dissolved organic carbon (DOC), both, are considered as index for evaluating the efficiency of sludge solubilization. However, further investigation is needed to determine the potential enhancement of methane production after this combined process.

1. Introduction

Unlike conventional heating, heating via Microwave irradiation is delivered directly into the material through a molecular interaction with electromagnetic field and converted into thermal energy. Therefore, emerging research has focused on the effect of MW irradiation on sludge dewaterability, solubility and biogas production. Microwave irradiation is expected to increase the surface area of the biomass and decrease the polymerization and crystallinity of the cellulose and therefore, improve the enzymatic degradation of the organic matter and consequently the digestion itself (Sapci, 2013). The effect of microwave occurs as a result of the interaction between the electrical field with dipolar molecules such as water, proteins, fats and other organic complexes. Hence, changing dipole orientation in the polarized side chains of the cell membrane macromolecules, and results in a breakage of hydrogen bonds and subsequently leading to the disintegration of floc matrix and changes the protein structures of the microorganisms (Appels et al., 2013). Therefore, MW irradiation is expected to enhance the solubility of proteins and volatile fatty acids, while reduce the solubility of sugars (Qiao et al., 2008). Kavitha et al. (2016) evaluated the effect of MW irradiation on COD solubilization and SS reduction and reported a significant enhancement of 22% and 17%, respectively. Other studies have evaluated the effect of MW treatment as a function of temperature such as Toreci et al. (2009) which reported high degrees of sludge solubilization after microwave irradiation when sludge temperature exceeds 175 °C. On the other hand, the study of Eskicioglu et al., (2007) investigated the effect of MW irradiation on waste activated sludge (WAS) in low temperatures (50–96) °C and claimed an enhancement of biogas production up to 16%. Other studies such as Apples et al., (2013) has reported an enhancement of biogas production up 50% in low temperatures by energy input of 336 (KJ/Kg). An interesting findings of the latter study stated that while MW irradiation significantly enhanced the solubilization of the organic materials to the aqueous phase; it did not affect the degradation of the major organic component at temperatures below 80 °C. Therefore, microwave irradiation is expected to increase the conversion of organic into easily accessible compounds (Kovács et al., 2018). Destruction of microorganisms occurs generally due the thermal effects

of microwave exposure, however, several studies have investigated whether such irradiation has athermal effect (Tyagi & Lo, 2013).

The prime effect of MW irradiation leverages dielectric parameters such as temperature, radiation time, and penetration depth (Kavitha et al., 2016). The major disadvantage of MW pretreatment is the energy consumption during the pretreatment process. However, the high energy requirement of microwave can be downsized by combining with other disintegration methods to disrupt the flocs such as ultra-sonication (Pilli et al., 2011). Sludge exposure to ultra-sonication is expected to cause higher rate of Extracellular Polymeric Substances (EPS) release. As a result, disrupting the flocs through the release of EPS will enhance the disintegration efficiency. Hence, the main objective of the present study was to disrupt the flocs with ultra-sonication, then evaluate its disintegration through subsequent microwave pretreatment.

2. Experimental

2.1 Ultrasonic pretreatment

Ultrasonic pretreatment was carried out using Hielscher UP200S ultrasonic homogenizer (Germany) with operating frequency of 50-60 kHz, rated voltage of 200-240 V, and rated current of 2 A. 250 mL of sludge were placed in a glass beaker without temperature adjustment and an ultrasonic probe was submerged in the sludge to a depth of 2 cm. The effect of this pretreatment, which mainly depends on the treatment time, was evaluated by taking samples at different times (10 s, 20 s, 30 s, 40 s, 50 s, 1 min, 2 min, 3 min) to study the effect of sludge disintegration. Specific energy was considered as a main variable parameter for evaluation of disintegration performance of the sludge. It is determined by using ultrasonic power (P), ultrasonic time (t), sample volume (V) according to the following Eq. (1):

$$E = P(W) \times t(s) / V(L) \quad (1)$$

2.2 Microwave pretreatment

Pretreatment experiment was performed as batch process with 250 mL of sludge in a microwave oven (2450 MHz frequency). The experiments were carried out in Polytetrafluoroethylene (PTFE) vessels for effective microwave diffusion and a cover was employed to evade sludge losses caused by hot spot formation during the disintegration process.

2.3 Analytical methods

COD, SCOD, Volatile Fatty Acids (VFA) were estimated as per standard methods (APHA, 2005).

2.4 Statistical analysis

Statistical analysis was performed to determine differences between each parameter on the investigated characteristics. First-way ANOVA was performed in Excel 2016 at 95% confidence level; when a significant difference was detected post hoc pairwise multiple comparisons were calculated.

3. Results and discussion

3.1 COD solubilization and SCOD release

Ultra sonication pretreatment was done to improve the bioavailability of sludge particulate material by increasing the rate of Extracellular Polymeric Substances (EPS) release. As the ultra-sonic treatment increased from 10 s to 3 min, an increase in COD solubilization was observed. COD solubilization increased by 21.87% to the value of 2500 mg/L after 3 min (data not shown). COD solubilization increased rapidly with the increase in sonic treatment time up to 1 min, after that, the increment in COD solubilization was in a slower rate. The rapid disintegration obtained at the beginning of the study was attributed to the availability of biomass for the action of cavitation forces. In the period between 1-3 min, and even though

cavitation effect remains the same, it releases less amount of SCOD. This attributed to the depletion of easily disintegratable organics and the presence of more recalcitrant organics after the initial period of 1 min treatment (Gayathri et al., 2015).

The behaviour of COD solubilization and SCOD release after microwave pretreatment followed a simple role; when higher specific energy was performed, the increment of COD solubilization to the aqueous phase occurs in higher rates. This increase can be explained by the hydrolysis of the large organic molecules, the lysis of the cell walls and the disintegration of sludge floc, which was intensified by the applied microwave irradiation. Interestingly, ultrasonic pretreatment resulted in higher SCOD initial values, and higher trend of SCOD release when higher MW intensities and/or longer contact times were applied.

Soluble COD of the raw sludge was found to be about 2005 mg/L and it went up to 7040 mg/L prior to the boiling point that occurred at specific energy of 1250 KJ/L. However, for the ultrasound followed by MW; the initial value of SCOD started at 2360 mg/L and raised to 8000 mg/L prior to the boiling point performing same MW energy; suggesting higher SCOD release caused by the ultra-sonication. The increase of SCOD concentration after microwave pretreatment of dairy sludge is attributed to the transfer of organic substances from non-soluble materials into soluble materials. Nonetheless, the intracellular organic materials may have been released into the medium as a result of cell wall disintegration, indicating that; the effect of microwave irradiation was significant in disintegrating sludge floc.

Table 1 SCOD, DOC and Volatile fatty acids concentrations for dairy sludge after MW irradiation and ultra-sonic pretreatment at 700 KJ/L input energy. Statistical differences are indicated by different superscript letters.

Parameter	Raw sludge	MW irradiation	Ultrasonic+MW
SCOD	2005±100 ^a	7042±340 ^b	8000±160 ^c
DOC	2000±200 ^a	7321±520 ^a	8918±211 ^b
Volatile Fatty Acids (VFA)			
Acetic acid (ppm)	370±21 ^a	790±43 ^b	810±16 ^b
Propionic acid (ppm)	5±0.1 ^a	23.0±0.1 ^b	29.3±0.1 ^c
Butyric acid (ppm)	61±7.8 ^a	306±6.8 ^b	308±1.8 ^b
Butyric acid (ppm)	32±4.2 ^a	50±8.3 ^b	91±5.1 ^c
Caproic acid (ppm)	14±0.8 ^a	44±5.4 ^b	33±9 ^b

Conclusion

This study explored the upshot of ultra-sonication as a pretreatment an addition of microwave pretreatment for waste activated dairy sludge on the basis of COD solubilization. The effective floc disruption was achieved at a specific energy input 52.8 kJ/L. This novel pretreatment process reduces the energy consumption significantly with enhanced COD and DOC solubilization. However, a follow up biodegradability studies are needed to determine the potential methane production relatively to MW irradiation alone. Conclusively, this novel process may possibly be entitled as a plausible pretreatment process.

Acknowledgements

The support of European Union and Hungarian State (grant agreement no. EFOP-3.6.2-16-2017-00010) is gratefully appreciated.

References

- [1] Appels, L., Houtmeyers, S., Degève, J., Van Impe, J., & Dewil, R. (2013). Influence of microwave pre-treatment on sludge solubilization and pilot scale semi-continuous anaerobic digestion. *Bioresource technology*, 128, 598-603
- [2] Eskicioglu, C., Terzian, N., Kennedy, K. J., Droste, R. L., & Hamoda, M. (2007). Athermal microwave effects for enhancing digestibility of waste activated sludge. *Water Research*, 41(11), 2457-2466.
- [3] Gayathri, T., Kavitha, S., Kumar, S. A., Kaliappan, S., Yeom, I. T., & Banu, J. R. (2015). Effect of citric acid induced deflocculation on the ultrasonic pretreatment efficiency of dairy waste activated sludge. *Ultrasonics sonochemistry*, 22, 333-340.
- [4] Kavitha, S., Banu, J. R., Kumar, J. V., & Rajkumar, M. (2016). Improving the biogas production performance of municipal waste activated sludge via disperser induced microwave disintegration. *Bioresource technology*, 217, 21-27.
- [5] Kovács, P. V., Lemmer, B., Keszthelyi-Szabó, G., Hodúr, C., & Beszédes, S. (2018). Application of dielectric constant measurement in microwave sludge disintegration and wastewater purification processes. *Water Science and Technology*, 77(9), 2284-2291.
- [6] Qiao, W., Wang, W., Xun, R., Lu, W., & Yin, K. (2008). Sewage sludge hydrothermal treatment by microwave irradiation combined with alkali addition. *Journal of Materials Science*, 43(7), 2431-2436.
- [7] Pilli, S., Bhunia, P., Yan, S., LeBlanc, R. J., Tyagi, R. D., & Surampalli, R. Y. (2011). Ultrasonic pretreatment of sludge: a review. *Ultrasonics sonochemistry*, 18(1), 1-18.
- [8] Sapci, Z. (2013). The effect of microwave pretreatment on biogas production from agricultural straws. *Bioresource technology*, 128, 487-494
- [9] Toreci, I., Kennedy, K. J., & Droste, R. L. (2009). Evaluation of continuous mesophilic anaerobic sludge digestion after high temperature microwave pretreatment. *Water Research*, 43(5), 1273-1284.
- [10] Tyagi, V. K., & Lo, S. L. (2013). Microwave irradiation: A sustainable way for sludge treatment and resource recovery. *Renewable and Sustainable Energy Reviews*, 18, 288-305.

CARBAMATE INSECTICIDES EXTRACTION DEPENDING ON THE SOIL PROPERTIES

Milica Baloš^{1*}, Vojislava Bursić¹, Vuković Gorica², Rada Đurović-Pejčev², Tijana Zeremski³, Aleksanda Petrović¹, Sonja Gvozdenac³, Tijana Stojanović¹

¹University of Novi Sad, Faculty of Agriculture, Trg Dositeja Obradovića 8, Novi Sad, Serbia

²Institute of Public Health, Bulevar despota Stefana 54a, Belgrade, Serbia

³University of Belgrade, Faculty of Agriculture, Nemanjina 6, Zemun, Serbia

*Corresponding author: e-mail: cucuzm@yahoo.com

Abstract

The influence of physic-chemical properties of soils on retention of insecticides belonging to carbamate pesticides was studied. The recoveries determination was done in three soils for all pesticides applying QuEChERS method. Identification and quantification were done by LC-MS/MS. Except methiocarb, recovery values for multiple analysis of different soil samples spiked at 1.0 and 10.0 mg/kg of each of the pesticides ranged from 70.2 to 109.1%. The statistical analyses emphasized high statistical differences among pesticides and obtained recoveries.

Introduction

Carbamate consists of a wide spectrum of biologically active pesticides used worldwide to control insects and nematodes [1]. Carbamate insecticides are derivatives of carbamic acids and the first carbamate insecticide, carbaryl, was introduced in 1956 [2]. They inhibit the AChE enzyme and cause overstimulation of nervous system. Carbaryl (1-naphthyl *N*-methylcarbamate), broad spectrum carbamate insecticide is extensively used worldwide in more than 120 different crops and ornamental plants [3]. Because of its very low mammalian toxicity together with the short half-life carbaryl is the most popular insecticide and it effectively acts against 160 harmful insects. Carbaryl is the second most widely detected insecticide in surface waters in the United States [4].

Carbamate pesticides usage in agriculture is increasing significantly compared with other organohalogen pesticides, due to the fact that carbamate compounds have been considered stable in the environment in term of their application for preventing disease attack in case of plants' leaves and fruits [5]. Soil acts as one type of a "filter", providing sufficient time for biological or chemical degradation of pesticides before they reach groundwater. Carbamate pesticides have a low persistence in soil. When they are applied to crops or directly to the soil as systemic insecticides, carbamates generally persist from only a few hours to several months. However, they have been fatal to large numbers of birds on turf and in agriculture; the negative effect is seen on decreased breeding of the birds who have been consumed the treated seeds or plants [6].

In general, measurement of trace compounds such as pesticide residues is highly difficult due to time consumption, while the long procedure causes losses of the analytes [7]. The aim of this study was to determine the recoveries of investigated carbamates depending on the physic-chemical properties of three different soils. For the extraction of the aldicarb sulfone, aldicarb sulfoxide, carbaryl, methiocarb, methomyl, fenoxycarb, propoxur and thiodicarb the QuEChERS method was used, followed by liquid chromatography tandem mass spectrometry (LC-MS/MS).

Material and method

Chemicals and apparatus - The analytical standards of aldicarb sulfone, aldicarb sulfoxide, carbaryl, methiocarb, methomyl, fenoxycarb, propoxur and thiodicarb were purchased from Dr. Ehrenstorfer. The stock (≈ 1.0 mg/mL) and working solutions ($10 \mu\text{g/mL}$) were prepared in acetonitrile (HPLC purity, J.T. Baker). As an internal standards ($10 \mu\text{g/mL}$) carbofuran-D3, atrazine-D5 and isoproturon-D6 were used. Three soil types with different physical-chemical characteristics (Table 1) were used.

Table 1 Soil characteristics

Soil	pH (H ₂ O)	CaCO ₃ %	Organic matter %	Sand 2-0.2 mm, %	Sand 0.2-0.02 mm, %	Powder 0.02-0.002 mm, %	Clay <0.002 mm, %
1.	8.71	30.66	0.11	1.58	91.7	3.4	3.32
2.	8.16	7.45	3.76	10.25	22.45	25.03	42.27
3.	7.65	1.02	0.88	0.53	21.39	29.04	49.04

LC-MS/MS analysis. LC-MS/MS with electrospray ionization. 6410 Agilent Technologies. The separation was performed using a Zorbax Eclipse XDBC18 column (50 mmx4.6mm id 1.8 μm .) at 25 °C. The mobile phase (0.4 mL/min): methanol with 0.1% formic acid and 0.1% formic acid in water in the gradient mode. Total run was 30 min. The injection volume was 5 μL . The target ion transition with highest intensity (primary ion transition) was used for quantitation, whereas the second target ion transition was used for confirmation. The instrument uses MassHunter software version B.06.00 for the quantitation and confirmation.

Method validation - recovery was determined according to SANTE/11813/2017. Recovery was obtained by spiking soil samples in the concentrations 1.0 and 10.0 mg/kg. Limit of detection (LOD) was estimated in the MRM mode analysis as the lowest concentration level that yielded S/N ratio of five.

Pesticides extraction from spiked soil samples was carried out using a modified QuEChERS method [8].

Statistical analyses. In order to determine the statistical differences among obtained recovery values as the dependent variables and the pesticides and soil types as independent variables the factorial and one-way factor analysis of variance (ANOVA) were applied using Statistica 13.2 (TIBCO Software Inc. University license). The calculated differences were tested by Fisher's LSD post-hoc test.

Results and Discussion

Before accessing qualitative analysis or quantification of pesticides it is necessary to set the acquisition parameters of the mass spectrometer - to set the multiple reaction monitoring mode (MRM). MRM-MS sensitivity is dependent upon the appropriate tuning of instrument parameters such as collision energy (CE) and energy of fragmentation (Frag) in order to generate maximal transmission of the pesticide product ions (Table 1).

Table 1. MRM transitions with retention times of the tested pesticides

Pesticide	Formula	Rt (min)	Precursor ion (m/z)	Product ion (m/z)	Frag (V)	CE (V)
Aldicarb sulfone	$C_9H_{10}Cl_2N_2O_2$	16.01	249	182.3	100	8
			249	160.1	100	20
Aldicarb sulfoxide	$C_{12}H_{12}D_3NO_3$	13.28	225.1	165	94	10
			225.1	123.1	94	22
Carbaryl	$C_{12}H_{11}NO_2$	19.38	202.1	145	100	20
			202.1	127	100	35
Methiocarb	$C_{11}H_{15}NO_2S$	23.86	226.1	169	62	6
			226.1	121	62	18
Methomyl	$C_5H_{10}N_2O_2S$	5.75	163.1	106	80	5
			163.1	88	80	5
Fenoxycarb	$C_{17}H_{19}NO_4$	25.93	302.1	116.1	100	5
			302.1	88	100	20
Propoxur	$C_{11}H_{15}NO_3$	17.00	210.1	168.1	60	5
			210.1	111	60	10
Thiodicarb	$C_{10}H_{18}N_4O_4S_3$	20.87	355.1	108	80	10
			355.1	88	80	15

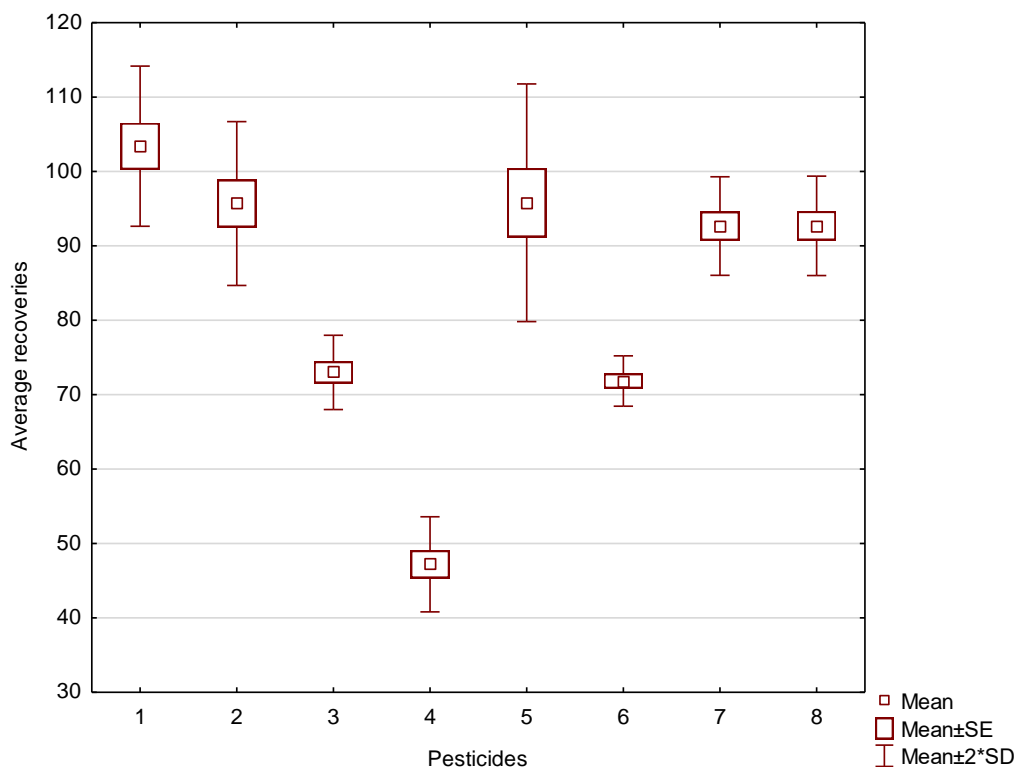
The obtained recoveries with RSD (%) values are given in the table 2. The obtained RSD values represent the precision of the method.

Table 2. Average recoveries of investigated pesticides (%)

Pesticide	Soil 1	Soil 2	Soil 3
Aldicarb sulfone	109.1 (16.33)	102.7 (17.96)	98.4 (12.04)
Aldicarb sulfoxide	101.6 (12.72)	94.8 (19.02)	90.7 (14.25)
Carbaryl	75.0 (9.43)	73.8 (6.23)	70.2 (10.32)
Methiocarb	50.8 (15.1)	46.1 (8.64)	44.7 (10.51)
Methomyl	104.2 (16.65)	94.9 (12.46)	88.3 (10.46)
Fenoxycarb	73.7 (9.57)	70.4 (8.92)	71.4 (5.98)
Propoxur	96.4 (10.16)	91.5 (4.78)	90.1 (7.49)
Thiodicarb	96.4 (9.93)	91.8 (4.55)	89.9 (8.69)

*RSD, % were given in brackets

The factorial ANOVA did not show any statistical significances regarding the influence of the paired values of different pesticides and soil types. The same result was obtained by one-way ANOVA calculated for different soil types and the values of average recoveries ($p_s=0.694684$ for $p<0.05$). However, the applied statistical analyses emphasized high statistical differences among pesticides and obtained recoveries ($p_p=0.000000$ for $p<0.01$). Fisher's LSD test distinguished aldicarb sulfone, aldicarb sulfoxide and methomyl as the pesticides with the highest values of average recovery values and high statistical significances compared to the other prospected pesticides (Graph 1).



Graph 1. Statistical analyses

Conclusion

The influence of main physico-chemical properties of three soils on carbamate insecticides recoveries in this matrix were studied applying QuEChERS soil sample preparation followed by LC-MS/MS determination.

The organic matter and clay content affected the recovery of studied pesticides. The obtained dependence indicates that with increasing organic matter and clay content (soil 2 and 3), the recoveries were lower than in soil 1.

The applied statistical analyses emphasized high statistical differences among pesticides and obtained recoveries ($p_p=0.000000$ for $p<0.01$). Fisher's LSD test distinguished aldicarb sulfone, aldicarb sulfoxide and methomyl as the pesticides with the highest values of average recovery values and high statistical significances compared to the other prospected pesticides.

Acknowledgements

The authors acknowledge the financial support of the Ministry of Education and Science, Republic of Serbia. Project Ref. III43005.

References

- [1] M.U Mustapha, N. Halimoon, W.L. Johar, M.Y.A. Shukor, J. Pertanika, J. Sci. & Technol. (2019) 547.
- [2] P.A. Thacker, S. Qiao, V.J. Racz, J. Sci. Food Agric. 82 (2002) 1312.
- [3] Ware. J., Kosinski. M. and Dewey. J. (2000) How to score version two of the sf-36 health survey. Quality Metric. Incorporated. Lincoln. RI.
- [4] B. Tiwari, S. Kharwar, D.N. Tiwari, Pesticide and rice agriculture. Cyanobacteria (2019).
- [5] R.T. Rosmalina, A.E. Persulesy, 3rd International Symposium on Green Technology for Value Chains (2018).
- [6] K.T. Osman, Soil Degradation. Conservation and Remediation (2014).

- [7] M. Čučuz, V. Bursić, G. Vuković, V. Ćirić, T. Zeremski, R. Đurović-Pejčev, *Annals of Agronomy* (2016) 61.
- [8] R. Đurović-Pejčev, V. Bursić, Zeremski T., *J. AOAC Int.* 102 (2019) 46.
- [9] SANTE/11813/2017: Method validation and quality control procedures for pesticide residues analysis in food and feed.

LIPOXYGENASE INHIBITORY ACTIVITY OF OXIDIZED RESVERATROL METABOLITE MIXTURES

Orinamhe Godwin Agbadua¹, Attila Hunyadi^{1,2,*}

¹ *Institute of Pharmacognosy, University of Szeged, Eötvös str. 6, 6720 Szeged, Hungary*

² *Interdisciplinary Centre for Natural Products, University of Szeged, Eötvös str. 6, H-6720 Szeged, Hungary*

**e-mail: hunyadi.a@pharmacognosy.hu*

Abstract

Resveratrol, a natural polyphenol, has numerous biological activities such as anticancer, antioxidant, anti-inflammatory. Resveratrol is highly oxidisable due to its chemical structure, and reacts with reactive oxygen species or free radicals resulting in new metabolites that are also potentially bioactive. Oxidation of resveratrol in various conditions resulted in mixtures that exhibited greater lipoxygenase inhibitory activities compared to the parent compound. This, together with the complex chromatographic fingerprints of the mixtures suggests that several oxidized metabolites of resveratrol may exert greater biological activity than their parent compound.

Introduction

Resveratrol is a well-known polyphenol with plethora of pharmacological activities such as anticancer, antioxidant, anti-inflammatory, cardio-protective and neuroprotective [1,2]. Most polyphenols are not stable, especially under oxidative conditions and often lead to the accumulation of new metabolites in living systems [3]. These new metabolites have been suggested to mediate at least some biological effects of the parent compound [4]. One of such studies showed a greater lipoxygenase (LOX) inhibitory activity of Fe-catalyzed oxidation of resveratrol and led to the identification of some active metabolites that, however, did not fully explain the increase in bioactivity [5].

LOX accelerates lipid oxidation by converting arachidonic, linoleic and other polyunsaturated fatty acids into biologically active metabolites, which are implicated in the pathogenesis of a variety of human diseases. Therefore, it is a promising therapeutic target for the prevention and/or treatment of a wide spectrum of human diseases [6].

Thus, we aimed at preparing oxidized resveratrol metabolites through various chemical reactions including biomimetic approaches, and to study the lipoxygenase inhibitory activity of the mixtures obtained.

Experimental

Resveratrol with a purity 97%, was purchased from Career Henan Chemical Co., China. Several oxidative reactions were carried out on resveratrol as shown in Table 1. The reactions were monitored by TLC at regular intervals. At the end of each reaction, the mixtures were evaporated, extracted with ethyl acetate and evaporated. As a prepurification step, each residue was filtrated through silica with hexane – acetone (1:1, v/v). A ten microliters aliquot of each mixture dissolved in CH₃CN was analyzed by HPLC (PU-2080 pumps; AS-2055 Plus autosampler; MD-2010 Plus PDA detector, Jasco Co., Tokyo, Japan) under the following conditions: column, Kinetex XB-C18 (250 x 4.6mm, 5_μ); solvent system, water (solvent A) and CH₃CN (solvent B): elution, linear gradient from 25% solvent B to 75% solvent B for 25 min and then isocratic mode for 75% solvent B for 2 min; flow rate, 1mlmin⁻¹; detection, 199nm – 650nm.

Table 1: Oxidative conditions applied on resveratrol.

ID	Oxidants	Experimental conditions ^a
Rox1	2 eq. (Diacetoxyiodo)benzene (PIDA)	EtOH, r.t., 2h
Rox2	2 eq. (Diacetoxyiodo)benzene (PIDA)	CH ₃ CN, r.t., 5h
Rox3	1 eq. (Bis(trifluoroacetoxy)iodo)benzene (PIFA)	EtOH, r.t., 2h
Rox4	1 eq. (Bis(trifluoroacetoxy)iodo)benzene (PIFA)	CH ₃ CN, r.t., 5h
Rox5	1.5eq. (Diacetoxyiodo)benzene (PIDA)	CH ₃ CN, r.t., 2h
Rox6	1 eq. 2,2'-Azobis(2-amidinopropane) dihydrochloride	EtOH, 65°C, 72h ^c
Rox7	1.5 eq. 2,2'-Azobis(2-amidinopropane) dihydrochloride, 1 eq sodium periodate	EtOH/H ₂ O (3:1), 65°C, 24h ^c
Rox8	1.5eq. 2,2'-Azobis(2-amidinopropane) dihydrochloride, 10eq hydrogen peroxide	EtOH/H ₂ O (2:1), 65°C, 24h ^c
Rox9	1 eq. Iodine	EtOH/H ₂ O (1:1), r.t, 24h ^b
Rox10	2 eq. Iodine	EtOH/H ₂ O (1:1), r.t. 24h ^b
Rox11	1 eq. periodic acid	EtOH/H ₂ O (3:1), r.t, 24h ^b
Rox12	2 eq. 2,2-diphenyl-1-picrylhydrazyl (DPPH)	EtOH, dark/r.t., 0.5h
Rox13	2 eq. 2,2-diphenyl-1-picrylhydrazyl (DPPH)	CH ₃ CN, dark/r.t., 0.5h
Rox14	2 eq. 2,2-diphenyl-1-picrylhydrazyl (DPPH)	MeOH, dark/r.t., 0.5h
Rox15	0.001 eq. FeCl ₃	EtOH, r.t., 20 days
Rox16	0.01 eq. FeCl ₃	EtOH, r.t., 20 days
Rox17	0.31eq. iron (III) meso-tetra (p-hydroxyphenyl) porphine chloride, 10eq, hydrogen peroxide	MeOH/Acetate buffer (4:1) r.t., 48h

^aExperimental conditions are given as solvent, temperature, time, respectively.

^breactions were stopped using aq. sodium thiosulfate

^creactions were stopped using ice-bath.

Lipoxygenase inhibition of the reaction mixtures was determined using the Lipoxygenase Inhibition Screening Assay Kit (760700, Cayman Chemical, USA) according to the leaflet instructions, with absorbance measured using a plate reader (BMG Lambtech GmbH, Germany)

Percentage inhibition was calculated as;

$$\% \text{ inhibition} = (\text{IA} - \text{inhibitor})/\text{IA} \times 100$$

IA = absorbance of the 100% initial activity wells (containing LOX and solvent used to dissolve the reaction mixtures).

Inhibitor = absorbance of the inhibitor wells (containing LOX and reaction mixture).

Results and discussion

Results show resveratrol had little or no inhibitory activity on 15-LOX, which corroborates several reports [5]. Lipoxygenase is a key pro-inflammatory enzyme with a central role in various diseases; therefore, lipoxygenase inhibitors have attracted much interest in medical science [7]. Our data indicated that various oxidized resveratrol mixtures exhibited significant activities while resveratrol itself was inactive. Similar increase in the increased LOX inhibitory following Fe-catalysed oxidation was found as previously reported [5]. In our case, mixtures obtained with periodic acid and iodine exerted the greatest LOX inhibitory activities that were ca. 50% at 4mM concentration; chromatographic fingerprints of these samples are shown in Figure 1.

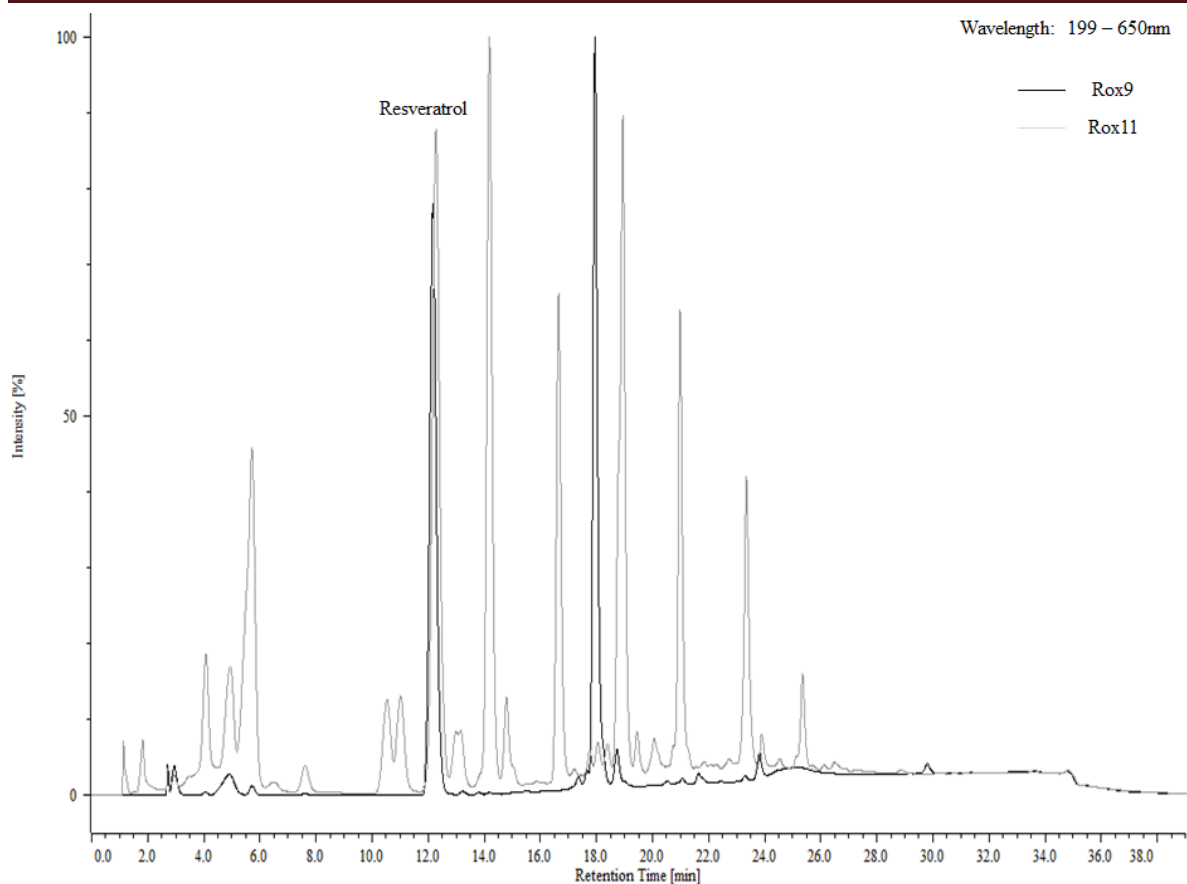


Figure 1. HPLC fingerprint of samples ROX9 and ROX11 that exerted near 50% inhibition of LOX in our experimental setup, while their parent compound resveratrol was inactive at the same concentration.

We plan to perform metabolomic studies of the reaction mixtures in the near future to assist the identification of compounds with a high LOX inhibitory potential.

Previously, resveratrol was found to moderately inhibit cell proliferation and viability in MCF-7 and MDA-MB-231 cancer cell lines [8,9]. Evaluation of the anti-proliferative activities of the oxidized resveratrol mixtures is currently ongoing.

Conclusion

The oxidation of resveratrol led to the accumulation of metabolites that showed favorable LOX inhibitory as compared to the parent compound. Isolation and purification of the individual metabolites in these complex oxidized mixtures could result in the discovery of compounds with potentially greater pharmacological activity.

Acknowledgements

This work was supported by the National Research, Development and Innovation Office, Hungary (NKFIH; K119770). The EU-funded Hungarian grant EFOP-3.6.1-16-2016-00008 is acknowledged. A.H. was supported by the János Bolyai Fellowship of the Hungarian Academy of Sciences and by the Kálmán Szász Prize. I would also like to acknowledge the contributions from members of the Natural Product Chemical Space Research Group, Institute of Pharmacognosy, University of Szeged, Szeged, Hungary.

References

- [1] P. Fan, A. Marston, A.E. Hay, K. Hostettmann, J. Sep. Sci. (2009) 32:2979–2984.

- [2] A. Duarte, A. Martinho, A. Luís, A. Figueiras, M. Oleastro, F.C. Domingues, F. Silva, *Food Sci. Technol.* (2015) 63:1254–1260.
- [3] T. Masuda, J. Akiyama, A. Fujimoto, S. Yamauchi, T. Maekawa, Y. Sone, *Food Chem.* (2010) 123:442–450.
- [4] A. Hunyadi, *Med. Res. Rev.* (2019) 1-29.
- [5] Y. Shingai, A. Fujimoto, M. Nakamura, T. Masuda, *J. Agric. Food Chem.* (2011) 59:8180-8186.
- [6] A.D. Dobrain, D.C. Lieb, B.K. Cole, D.A. Taylor-Fischwick, S.K. Chakrabarti, J.L. Nadler, *Prog. Lipid. Res.* 50 (2011) 115-131.
- [7] C. Menna, F. Olivieri, A. Catalano, A. Procopio, *Curr. Pharm. Des.* (2010) 16:725–733.
- [8] Y. Gao, C. He, *Oncol. Letter* (2017) 13:4371-4377.
- [9] S. Poschner, A. Maier-Salamon, M. Zehl, J. Wackerlig, D. Dobusch, A. Meshcheryakova, D. Mechtcheriakova, T. Thakhammer, B. Pachmann, W. Jäger, *Front. Pharmacol.* (2018) 9, Article 742.

PHYTOCHEMICAL AND PHARMACOLOGICAL ANALYSIS OF TWO IRANIAN PLANTS, *DUCROSIA ANETHIFOLIA* AND *EREMURUS PERSICUS*

Javad Mottaghipisheh¹, Márta Nové², Gabriella Spengler², Norbert Kúsz^{1,3}, Judit Hohmann^{1,3} and Dezső Csupor^{1,3}

¹ Department of Pharmacognosy, Faculty of Pharmacy, University of Szeged, Szeged, Hungary; ² Department of Medical Microbiology and Immunobiology, Faculty of Medicine, University of Szeged, Szeged, Hungary; ³ Interdisciplinary Centre for Natural Products, University of Szeged, Szeged, Hungary
e-mail: imanmottaghipisheh@pharmacognosy.hu

Context: *Ducrosia anethifolia* (DC.) Boiss. (Apiaceae), is an Iranian medicinal plant and traditionally used as analgesic and remedy of anxiety and insomnia in Iranian folk medicine. *Eremurus persicus* (Jaub. & Spach) Boiss. (Xanthorrhoeaceae) is widely grown in diverse regions of Iran. The leaves have been traditionally used for treatment of constipation and diabetes, and to remedy of different disorders of liver, stomach and the genitourinary system [1,2].

Objective: This study was aimed at the isolation and identification of the secondary metabolites of *E. persicus* and *D. anethifolia* and the evaluation of the antitumor and anti-multidrug resistance activities of some of the pure compounds.

Materials and methods: Diverse chromatographic methods were applied to isolate the pure phytoconstituents from plant materials. Bioactivities were tested on multidrug resistant and sensitive mouse T-lymphoma cell lines. The inhibition of the cancer MDR efflux pump ABCB1 was investigated by flow cytometry (at 2 and 20 mM). A checkerboard microplate method was also utilized to study the interactions of furocoumarins and doxorubicin. Besides, toxicity was studied using normal murine NIH/3T3 fibroblasts.

Results: From *D. anethifolia*, thirteen isolated pure compounds were isolated, nine furocoumarins including pabulenol (**1**), (+)-oxypeucedanin hydrate (**2**), oxypeucedanin (**3**), oxypeucedanin methanolate (**4**), (-)-oxypeucedanin hydrate (**5**), imperatorin (**6**), isogospherol (**7**), heraclenin (**8**), heraclenol (**9**), along with vanillic aldehyde (**10**), harmine (**11**), 3-hydroxy-a-ionone (**12**) and 2-C-methyl-erythrytol (**13**) were identified [3]. From *E. persicus*, corchoionoside A (**14**), isoorientin (**15**), auraptene (**16**), and imperatorin (**6**) were isolated.

Oxypeucedanin showed the highest *in vitro* antiproliferative and cytotoxic activity against parent (IC₅₀: 25.98 ± 1.27, 40.33 ± 0.63 mM) and multidrug resistant cells (IC₅₀: 28.89 ± 0.73, 66.68 ± 0.00 mM), respectively, and exhibited slight toxicity on normal murine fibroblasts (IC₅₀: 57.18 ± 3.91 mM).

Discussion and conclusions: Compounds **2**, **3**, **5**, **7**, **10–13** were identified for the first time from the *Ducrosia* genus. All the compound isolated from *E. persicus* are reported for the first time from this taxon. From the tested furocoumarins, oxypeucedanin is a promising compound for its anticancer effects.

References

[1] S.R. Shahrokhi, M. Ghanimatdan, M. Akbari-Bazm, I. Karimi. Bull. Env. Pharmacol. Life Sci. 3 (2014) 45–49.

- [2] M. H. Vala, J. Asgarpanah, M. H. Hedayati, J. Shirali, F. B. Bejestani. Afr. J. Microbiol. Res. 5 (2011) 2349–2352.
- [3] J. Mottaghipisheh, M. Nové, G. Spengler, N. Kúsz, J. Hohmann, D. Csupor. Pharm. Biol 56 (2018) 658-664.

CHARACTERIZATION OF SOIL AMENDED WITH SEWAGE SLUDGE AND GROWTH OF RYE PLANT

Hosam Bayoumi Hamuda

*Environmental Engineering Institute, Óbuda University, H-1034 Budapest Doberdo Út 6,
Hungary*

e-mail: bayoumi.hosam@rkk.uni-obuda.hu

Abstract

There is an increasing issue in the agricultural application of sewage sludge obtained from wastewater treatment plants, due to the possibility of recycling valuable components; organic matter, and plant nutrients. The objectives of the pot experiment were to determine the effects of sewage sludge treatment on rye plant growth and the physicochemical soil properties of rye rhizosphere for 9 weeks. Kovárvány brown forest soil from Nyíregyháza was used and treated with various rates of sewage sludge (Control soil (0), 20, 40, 60, 100 (sludge) %). Different soil parameters were studied such as pH, soil moisture, fluorescein diacetate (FDA) activity, carbon dioxide release and rye plant growth. The results indicated that after the application of sewage sludge, the soil retained its moisture content for a longer period than the control. Also, soil pH was maintained to be favourable for plant growth. In addition to exhibiting healthy growth and development, the plants also produced the greatest dry matter mass on soils with the largest proportion of sewage sludge (60–100%). The enzymatic activities in the soil samples treated with sewage sludge were increased in soil with higher sludge doses. Finally, soil treatment with sewage sludge stimulated rye plant growth, improved the biochemical and microbial properties of the rye plant rhizosphere, promoted the retention of soil moisture and raised the soil pH, which also had a favourable effect on rye plant growth.

Introduction

Demographic growth and western economic model seriously menace these vital resources: soil scarcity, soil losses through erosion, natural disasters and contamination; water scarcity and contamination; and limitation and exhaustion of mineral resources and fossil energies. One of the most pressing environmental and environmental problems of our day is the increasing volume of waste, including waste water treatment, sewage sludge treatment, utilization and disposal. Sewage sludge is used as possible way of organic fertilization and also of the utmost importance because it is not only nutrient input into the soil, but it also improves soil structure and induces useful microbiological processes. Nowadays, it is vital to ensure that all kinds of organic matter can be preserved. Sewage sludge is, on the one hand, environmentally polluting and, on the other hand, is suitable for organic farming as fertilizer. From an environmental and soil protection point of view, it is important that the sewage sludge used does not restrict the production of safe food raw materials. Biodegradation of organic matter in soil is basically the result of microbial and biochemical processes, therefore all factors that have an effect on the structure, function and enzymatic activity of microorganisms affect the rate of degradation.

In the case of agricultural utilization it contributes to increasing the content of organic matter of the soil and has a favourable effect on the physical and chemical properties of the soils. Sewage sludge increases the water absorbing ability of soils, promote aggregation of the medium on sandy soils and increase the cation exchange ability. During the present work, we investigated the effects of sewage sludge on the some soil properties such as soil pH, moisture content, CO₂-release, FDA activity and the rye plant growth at different levels of sewage sludge treated in two soil types.

Experimental

The origin of soil samples was Kovárvány brown forest soil (KBET) collected from the Center for Agricultural and Technical Sciences at the Nyíregyháza Research Institute of the University of Debrecen. Soil samples were collected from the upper layer of 0-25 cm. Some chemical properties of communal sewage sludge from the municipal wastewater treatment plants (Nyíregyháza) and soil samples are presented in Table 1.

Table 1
Properties of the soils and sludge used in the model experiment

Parameters	Soil type: KBET	Wastewater sludge: NySzv
pH _(KCl)	5.78	6.71
a) Dry matter content, %	na	53
b) Organic matter, %	na	21.7
c) Humus content, %	2.54	na
d) Total-N, mg·kg ⁻¹	na	7470
NO ₃ -N, mg·kg ⁻¹	23	na
NH ₄ -N, mg·kg ⁻¹	5.6	na
Mg, mg·kg ⁻¹	214	2507
Na, mg·kg ⁻¹	64	994
P ₂ O ₅ , mg·kg ⁻¹	318	28720
K ₂ O, mg·kg ⁻¹	412	3171
Zn, mg·kg ⁻¹	1.7	537
Cu, mg·kg ⁻¹	1.4	110.4
Mn, mg·kg ⁻¹	55	421
Fe, mg·kg ⁻¹	945	11308
Cd, mg·kg ⁻¹	1.7	2.3
Pb, mg·kg ⁻¹	1.3	66.9

na: no data available

The air dry soil was thoroughly mixed with sewage sludge so that the final mixture contained sewage sludge in the soil sample was as following percentages: 0% (sewage-free control soil), 20, 40, 60 and 100% (sewage sludge only, without soil). Rye (*Secale cereale* L.) seeds were sterilized and planted in plastic containers of 3 kg of tested soil as prepared above. After ten days of germination, young plants were reduced for 10 plant densities/pot.

Soils pH was measured by Pérez De Mora et al. [1] at various sewage sludge doses. The pH of the untreated and treated soil was tested in a 1: 2.5 (soil: 1 mole KCl) g ml⁻¹ ratio after shaking for 60 minutes. The moisture content (%) of the treated and untreated soil samples was modified by the method of Brzezinska et al. [2] (measured at 48 hours at 28°C, incubation). The relative dry weight of the rye plants samples was determined after 9 weeks of cultivation at 75°C, drying cabinet, to constant weight. For the measurement of CO₂ emissions, 0.5 kg of sewage sludge treated soil was poured into 2 l glass containers and in the middle of the soil were placed a plastic tube containing 50 mL of 1.0 mol of NaOH solution to bind the developing CO₂, then the containers are tightly closed. The NaOH solution was titrated with 1 mol of HCl solution and calculated the volume of CO₂ released during the soil respiration [3, 4]. Enzyme Activity: Measurement of FDA activity was performed by the method developed by Zelles et al. [5], modified by Schnürer and Rosswall [6]. Fluorescein concentration (µg hydrolyzing fluorescein/g⁻¹ dry soil/h⁻¹), in all samples was determined using spectrophotometer at 490 nm. The experimental work was done in triplicates.

Results and discussion

The results in Figure (1) showed that application of sewage sludge increased the pH values as well as the soil moisture content (%). These increases reach the significant level high doses in comparison with control values, although, it was found that the high applied

dose extend the moisture time in sewage treated samples and the moisture content remained for longer than in the controls.

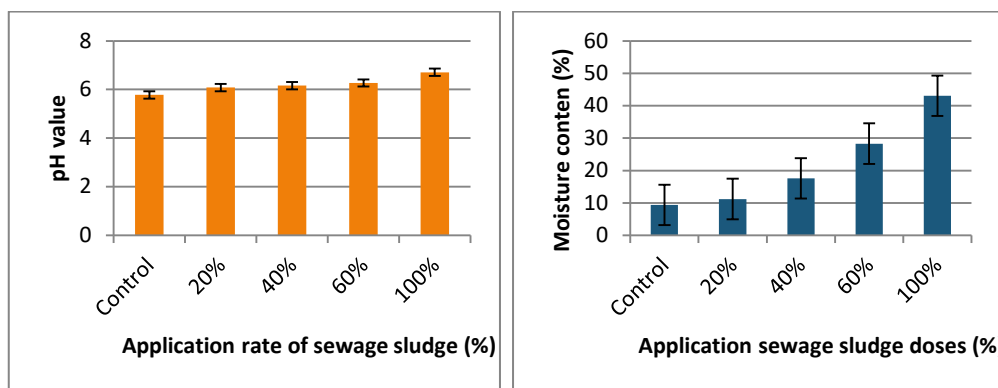


Figure 1. Effect of sewage sludge application on pH and moisture content in soil samples

The addition of sludge to soil significantly increased rye plant dry matter content (Figure 2) for each soil sample. Growth and development of plants were faster and healthier. The total biomass mass of the plants increased proportionally with the increase in the amount of sewage sludge added to soil. Growth and nutritional needs were uniform on the basis of morphological characteristics during the vegetation period. Adverse symptoms were not observed on either control plants or plants derived from sewage sludge treated soil. The morphological characters of all plants (leaves, shape, color and size) were normal and healthy.

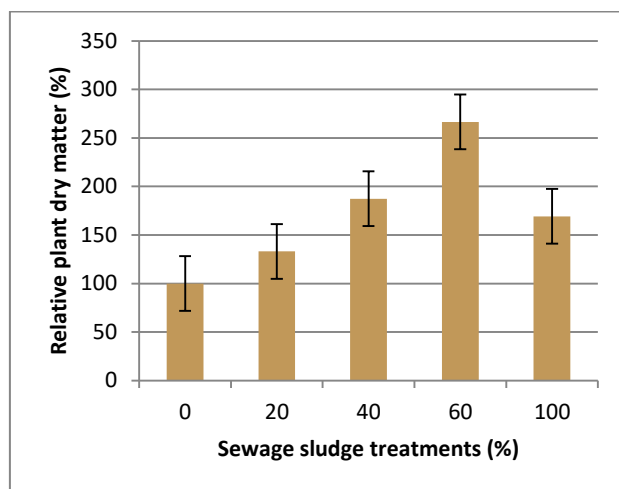


Figure 2. Effect of sewage sludge application on rye plant dry weight in two soil samples

The maximum dry matter of rye plants was obtained at sewage sludge 60. According to the results, the increases in pH values were favors for the growth of rye plants and reduce or inhibit the harmful effects of heavy metals. The degree of microbial activity can be determined by the amount of CO₂ released from the soil samples. It was found that the value of soil respiration compared to the control increased significantly by increasing the sewage sludge dose. Figure 3 shows that the amount of CO₂ released in the soil of brown forest soil from Nyíregyháza amended with different sludge doses.

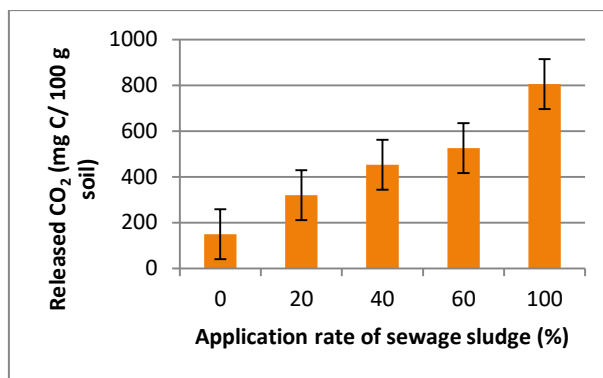


Figure 3. Effect of sewage sludge application on the amount of CO₂ released in soil samples

Such rate of respiration can provide valuable information on the increased metabolism activity of the soil biotas. The enzyme activity of FDA hydrolysis is shown in Figure 4. In soil samples amended with sewage sludge had high FDA activities and these activities are directly proportional with the rate of sewage sludge applied to the soil. The results show that the amount of fluorescein produced by FDA hydrolysis is in direct proportion with microbial growth, and the hydrolytic activity of FDA shows a close correlation with soil respiration.

The equilibrium effects of sewage sludge did not only significantly increase the soil microbial population, but also the activity of the soil enzymes investigated, soil respiration and FDA activity.

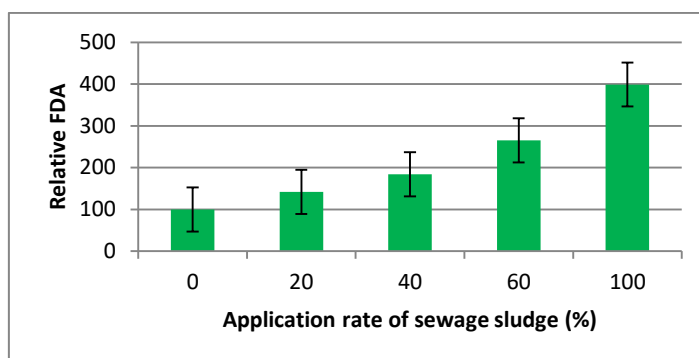


Figure 4. Effect of sewage sludge application on the activity of FDA enzyme in soil samples

Evaluation of results:

Eid et al. [7] mentioned that the application of sewage sludge significantly increased the soil organic matter content and most plant growth parameters, as well as the biomass of treated wheat, were significantly increased with the amendment of sewage sludge. The use of sewage sludge in agriculture will make the land in the inadequate regions more efficient in terms of organic matter for the soil [8]. Sewage sludge application in forest plantations is an interesting complementary alternative practice to sewage sludge reutilization and recycling, with a significant and sustainable net effect in climate change mitigation [9]. The study demonstrated the possibility of sludge application as a soil fertilizer in urban areas. In most of cases city landscapes are covered with poor soils, sludge application provides soil amendment and additional nutrient supply for planted trees, as it had been shown in the study of Soudani [10]. Chu et al. [11] suggested that a reasonable rate of sewage sludge compost addition can enhance *M. persiciforma* growth without causing the contamination of landscaping soil by heavy metals. When proper sludge products quality attained and recycling is feasible many objectives connected with sustainability of the soil. In pot experiment we

found that beside rye growth, the plant health was better than control. So the plant utilized the micro and macro nutrients necessary and easy to apply from the immediate environment. Our results are in agreement with the Pierzynski et al. [12] that soil quality is determined mainly by physical, chemical properties which can strongly affect fertility, biological activity, or other important soil factor. The degradation of the organic material of the sewage sludge can be monitored well in the soil based on the measured amounts of the releasing of CO₂. Previous studies [13] have shown that soil respiration has increased due to addition of sewage sludge. In summary, the treatment of soil samples with sewage sludge stimulates the development of plants, improves the physical, biochemical and microbial properties of the rhizosphere, helps to maintain soil moisture and increases soil pH, which is favorable for plant development.

Conclusion

The present study is considered as a short-term study, so the selected variables are indicative for future long-term studies, which will allow technical definitions to create specific legislation for the use of this effluent in agricultural production. The results of pot experiments support the above mentioned works that the plant dry matter is related to the amount of sewage sludge mixed with the soil samples, increases the fertility rate, the crop production and soil biological activity by increasing the proportion of sewage sludge mixed with soil. At the same time, due to the aspects of food safety, the use of continuous state monitoring methods is recommended. We consider it important to continue the research, and to study the process with other long-term observations in addition to other soil conditions.

References

- [1] A. Perez de Mora, P. Burgos, E. Madejón, F. Cabrera, P. Jaeckel, M. Schlöter, *Soil Biol. Biochem.*, 38 (2006) 327-341.
- [2] M. Brzezinska, C.S. Tiwari, Z. Stepniewska, M. Nosalewicz, P.R. Bennicelli, A. Samborska, *Biol. Fertil. Soils*, 43 (2006) 131-135.
- [3] A.D. Wardle, D. Parkinson, *Mycol. Res.*, 95 (1991) 504-507.
- [4] P.A.S. Fernandes, W. Bettiol, C.C. Cerri, *Appl. Soil Ecol.*, 30 (2005) 65-77.
- [5] L. Zelles, P. Adrian, Y.Q. Bai, K. Stepper, V.M., Adrian M.V., K. Fischer, A. Maier, A. Ziegler, *Soil Biol. Biochem.*, 191 (1991) 955-962.
- [6] J. Schnürer, T. Rosswall, *Appl. Environ. Microbiol.*, 43 (1982) 1256-1261.
- [7] M.E. Eid, A.S. Alrumman, A.F. El-Bebany, K. Fawy, A.M. Taher, H. Abd El-Latif, A.G. El-Shaboury, T.M. Ahmed, *Environ. Sci. Pollut. Res.*, 26 (2019) 392-401.
- [8] U. Gunay, S. Dursun, *Int. J. Environ. Pollut. Environ. Model.*, 1(2018)103-109
- [9] M. Bouriou, O Girardclos, F. Gillet, L. Alaoui-Sehmer, B. Pascale, B. Alaoui-Sossé, L. Aleya, *Science of the Total Environment* 621 (2018) 291-301.
- [10] L. Soudani, M. Maatoug, H. Heilmeyer, M. Kharytonov, O. Wiche, C. Moschner, E. Onyshchenko, N. Bouchenafa, *Biotechnology Reports* 13 (2017) 8–12.
- [11] S. Chu, D. Wu, L.L. Liang, F. Zhong, Y. Hu, X. Hu, C. Lai, S. Zeng, *Scientific Reports*, 7 (2017) 13408.
- [12] M.G. Pierzynski, T.J. Sims, F.G. Vance, CRC Press, Inc., (1990)
- [13] X. Stadelmann, J.O. Furrer, In: G. Catroux, P. L'hermite, E. Suess, D. Reidel Publ. Co. Dordrecht, 1983, pp. 141-166.

EVAPORATION OF LIQUIDS FROM POROUS FILMS – METHODOLOGY AND ANALYTICAL POSSIBILITIES

Ildikó Y. Tóth¹

¹*Department of Applied and Environmental Chemistry, University of Szeged, Interdisciplinary Excellence Centre, H-6720, Szeged, Rerrich Béla tér 1, Hungary
e-mail: ildiko.toth@chem.u-szeged.hu*

Abstract

The evaporation of liquids from porous films is a very complex phenomenon, which can be followed by simultaneous weight monitoring, electric resistance measurement and infrared imaging. The appropriate evaluation of these measurement results can carry both quantitative and qualitative analytical information. The aim of our recent work is to demonstrate this opportunity through the example of the evaporation of simple solvents from the porous buckypaper prepared from carbon nanotubes.

Introduction

Recent developments in nanotechnology have highlighted the importance of the classical topics of wetting, droplet spreading and evaporation due to their pronounced effect in technological applications (*e.g.*, air/fuel premixing, micro-fluidics, oil recovery, etc.) [1,2]. Multiple phenomena take place simultaneously when a liquid droplet contacts a porous surface: wetting, spreading, capillary filling, gravity induced convective flow, adsorption, evaporation from the surface, evaporation from the pores, etc. The evaporation of a sessile droplet can be studied by several experimental methods: transmission electron microscopy, environmental scanning electron microscopy, contact angle measurement, high speed camera recordings, thermal imaging, just to name a few. The evaporation of sessile droplets can be followed by an equipment assembled at the Department of Applied and Environmental Chemistry, University of Szeged: this equipment can guide simultaneous weight monitoring, electric resistance measurement and infrared imaging at a controlled temperature (typically at 50 °C). There are several experimental results characteristic for the evaporation process, the most important ones being the total evaporation time, time of evaporation only from the surface, full width at half maximum of the time-dependent mass and resistance curves, evaporation rate, initial area of the droplet, and the wetted area at the moment of total evaporation from the surface, etc. [3-5].

The main goal of this work was to demonstrate the analytical possibilities of this method through the example of sessile droplet evaporation (water, 1-propanol, ethanol, heptane, acetonitrile) from porous buckypapers prepared from pristine non-functionalized carbon nanotubes (*nf*-CNT) and –COOH functionalized CNT (*f*-CNT).

Experimental

Materials: The multiwall carbon nanotubes were synthesized by 2 h of catalytic chemical vapor deposition from a C₂H₄:N₂ (30:300 cm³/min) gas mixture at 650 °C over Fe,Co/Al₂O₃ catalyst (metal loading: 2.5-2.5 m/m%). The synthesized materials were purified by repeating 4 h of refluxing in 10 mol/dm³ aqueous NaOH, then 4 h in cc. HCl solution four times. Some pristine non-functionalized carbon nanotubes (*nf*-CNT) were subjected to oxidative chemical functionalization (8 h reflux of 4 g CNT in 500 cm³ cc. HNO₃ solution) to facilitate surface carboxyl group formation and improve their hydrophilicity to get so called functionalized carbon nanotubes (*f*-CNT). The typical length of CNTs was over 10 μm and their outer diameter fell in the 15-25 nm range as determined from TEM image analysis. CNTs were

converted into buckypaper (BP) by filtering 70 cm³ of their 0.1 g/dm³ suspensions through a 0.45 mm nominal pore diameter Whatmann nylon membrane filter. The *nf*-CNTs and *f*-CNTs were suspended by 40 min ultrasonication in N,N-dimethylformamide and water, respectively [3,4].

Methods: Liquid droplet evaporation (1-propanol, distilled water, ethanol, acetonitrile, heptane) was studied from both *nf*-CNT and *f*-CNT buckypaper films. The droplets (3-10 μ L, 25 °C) were instilled with an Eppendorf Xplorer electronic pipette on the heated surface of the porous films (50 °C). The temperature, the electric resistance and weight variations were simultaneously monitored.

Buckypaper was placed onto a purpose-built sample holder and kept in place by a top piece that had a 0.7 cm diameter circular opening in it for placing the liquid droplet. The setup included a type K thermocouple in contact with the non-wetted part of the BP. The distance between the porous film and the heater was 1 cm. Data from the thermocouple was fed back to the temperature controller that maintained a base BP temperature of 50 ± 0.5 °C by continuously adjusting the heater power using fuzzy logic control.

The sample holder was placed on a Sartorius Cubis microbalance with 0.01 mg readability and the weigh variation during droplet evaporation was recorded.

For thermal imaging a FLIR A655sc infrared (IR) camera was used. This unit has a thermal sensitivity of 30 mK, an accuracy of ± 2 °C for temperatures up to 650 °C at 640x480 resolution. Its uncooled microbolometer detector has a spectral range of 7.5-14.0 μ m. The IR camera is equipped with a 2.9x (50 μ m) IR close-up lens, with 32x24 mm field of view and 50 μ m spatial resolution. The recorded images are transferred to a PC with FLIR ResearchIR Max software. Sessile droplet evaporation movies were acquired at maximum resolution with 50 Hz frame rate. Each CNT film's emissivity (ϵ_{film}) was determined by calibration at the initial film temperature (50 °C) with a black electrical tape ($\epsilon = 0.95$). During liquid surface evaporation the temperature was determined by taking into account the emissivity of the liquid ($\epsilon_L = 0.95$); after surface evaporation, the emissivity of the wetted film was calculated as the average between the emissivities of the studied liquid and the porous film.

The sample holder plastic plate with the 0.7 cm radius gap in the center was equipped with two copper electrical connections at the opposite edges of the gap on the bottom of the sheet. The BP was fixed to the bottom of the plastic section with magnetic clips. The copper electrodes were contacted to the source meter by 0.3 mm diameter copper wires. The rigidity of these wires did not affect the balance because of the large inertia of the whole assembly mounted on the balance plate. This was confirmed by independent experiments before the evaporation profile (electrical resistance variation as a function of time) measurements. The computer recorded the electrical resistance of the buckypaper as measured by a Keithley 2612A Source Meter.

Before the measurements, the BP film was mounted in the assembly and heating at initial temperature was applied until the electrical resistance and the sample weight both stabilized. Then all three recordings (resistivity, IR imaging and sample weight) were started a few seconds before dropping. The evaporation was studied by dropping a single droplet of a selected solvent to the center of the BP film and simultaneously recording the IR video, the mass and electrical resistance until they returned to their original values.

The schematics of the equipment is presented in Fig. 1. The ambient air temperature and the relative humidity of the ambient atmosphere were kept constant (at 25 °C and 55 RH%, respectively) [3-5].

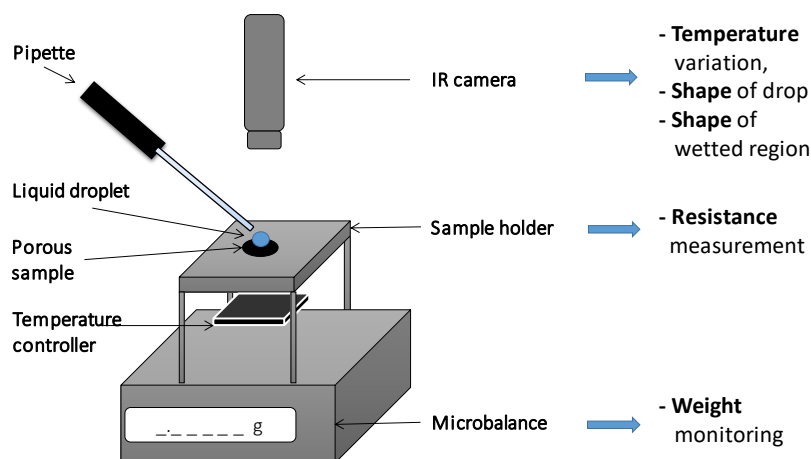


Figure 1. Evaporation monitoring equipment schematic.

Results and discussion

In general at the moment we drop the liquid on the buckypaper film (t_0), the liquid starts to diffuse immediately into the pores of the BP, but a part of it remains spread on the surface of the film. The evaporation of this liquid from the surface takes place together with the diffusion. Once all liquid evaporates from the surface, namely the primary surface evaporation is complete (t_s), liquid is left only in the pores. The solvent gradually evaporates from the pores as well because of the continuous heating. The complete evaporation of the solvent (t_t) was confirmed by the fact that the electrical resistance and mass of the buckypaper returned to the baseline.

One typical mass variation is illustrated in Fig. 2. where t_0 marks the time when the drop was instilled. The mass of the BP increased as soon as the solvent was dropped to the film and this is followed by a quasi-linear weight decrease. Once the primary surface evaporation is complete (t_s), the mass of the buckypaper decreases as linear (within experimental error) functions of time due to the continuous evaporation of the solvent. The total evaporation time (t_t) was at the moment when the mass of the BP returned to the baseline. At the linear weight decreasing ranges, the rate of evaporation (dm/dt) is constant. The change of dm/dt value suggests the change of the dominant evaporation process, *e.g.*, evaporation of the droplet sitting on the surface of the BP, evaporation of the condensed water from the porous system or the evaporation of the adsorbed water from the microscopical surface of the porous system (see the linear ranges in Fig.2.). From this type of measurement, the typical experimentally determined data are the shape of the curve: m_{max} , area, FWHM; the t_s and t_t , the evaporation rate dm/dt and its change. These data are characteristic for the measured system and can be used to identify them [3-5].

The electrical resistance of the BP increased as soon as the solvent was dropped to the film. One typical resistance variation is illustrated in Fig. 2 where t_0 marks the time when the drop was instilled and t_s marks the time needed to surface evaporation. In case of typical organic solvents (*e.g.*, 1-propanol, acetone, ethanol, etc.) the electrical resistance increases continuously between t_0 and t_s , because in this interval the solvent fills the pores of the BP film and the resistance of its solvent occupied section is higher than the liquid-free one. Once the primary surface evaporation is complete, the electrical resistance of the BP decreases as linear (within experimental error) functions of time due to the continuous evaporation of the organic solvent. Evaporation takes place both within the BP pores (resulting in vapor diffusing to the atmosphere) and from the surface where capillary forces continue to deliver liquid from the inside of the BP (secondary surface evaporation). Summarizing, when a droplet of solvent contacts a heated porous film, the electrical resistance of the film exhibits a very characteristic change as a function of time, which can be named as evaporation profile.

The shape of this curve is slightly different for every solvent and the fine details of the curve's shape can be described by the R_{\max} , area, FWHM, t_s and t_t , etc. These data are characteristic for the measured system, too. For example, the shape of the evaporation profile depends strongly on the solvent in case of fixed solid, temperature and liquid volume (see Fig. 3.) or it depends strongly on the porous solid in case of fixed solvent, temperature and liquid volume (see Fig. 4.) [3-5].

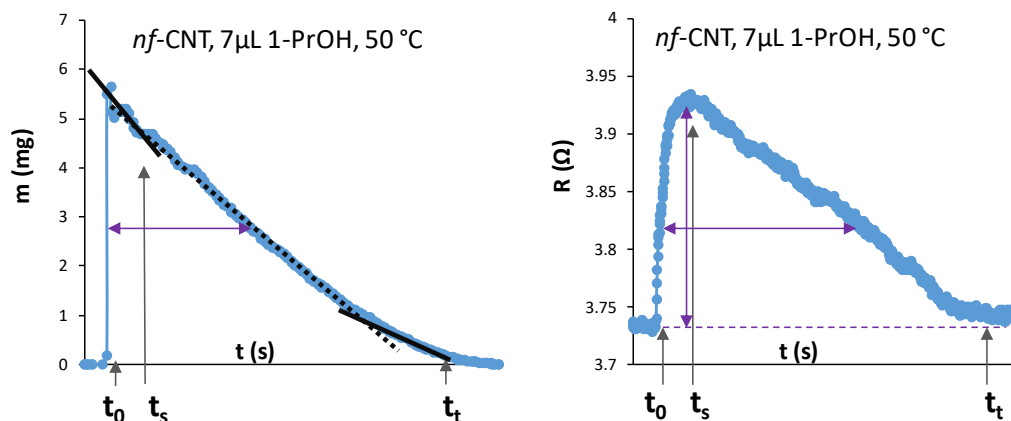


Figure 2. Weight and electrical resistance variation of the buckypaper as functions of time.

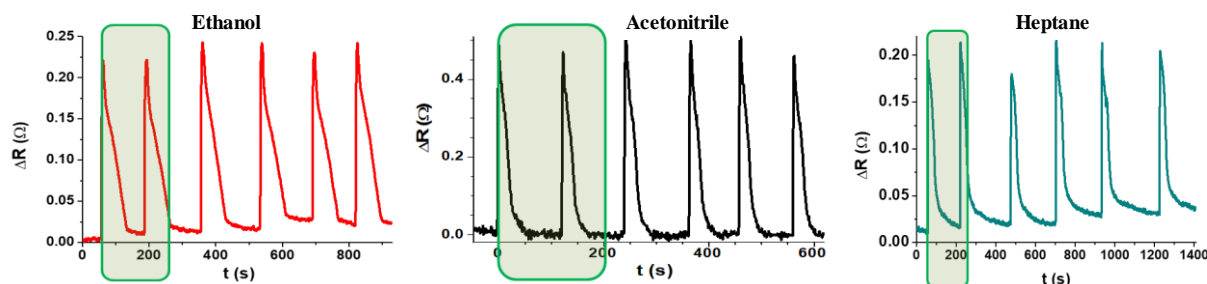


Figure 3. Evaporation profiles: solvent dependence. Evaporation of different organic solvents from *nf*-CNT buckypapers (5 μ L, 50°C).

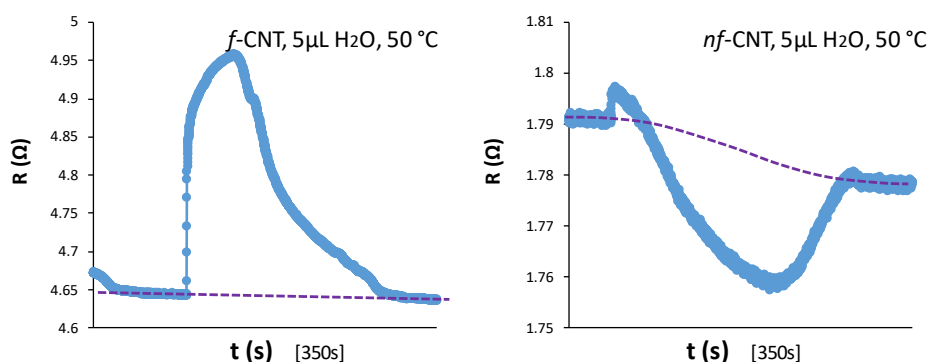


Figure 4. Evaporation profiles: solid dependence. Evaporation of distilled water from *nf*-CNT and *f*-CNT buckypapers (5 μ L, 50°C).

Infrared imaging is suitable to monitor the evaporation of the solvent from the porous film in our case from a vertical perspective. To improve the infrared contrast, solvents were kept at room temperature before the experiments. Therefore, there was a temperature difference between the initial 5 μ L drops and the porous film kept at 50 °C. The temperature of the liquid and the solid is changed continuously during the experiment because of the initial difference,

the heating of the solid layer, the endotherm evaporation process, etc. The videos were evaluated at selected representative moments, such a typical series of images is shown in Fig. 5. [3-5]. The temperature change profile is characteristic for each measured solvent. It is possible to determine the spot area and average temperature of the drop (S_d , T_d) and of the wetted region (S_w , T_w) as a function of time. Usually, we use relative timescale ($t_{rel} = t/t_s$) for comparable representation. Some data extracted from infrared videos are characteristic for the evaporation of a selected liquid/solid system: surface evaporation time (t_s), total evaporation time (t_t), initial area of the drops ($S_{d(t_0)}$), area of the wetted region at the end of the surface evaporation ($S_{w(t_s)}$). The change of S_d as a function of time can give information about the mechanism of the evaporation (*e.g.*, constant contact radius mode - CCR) and the relationship between S_d and S_w can describe the wetting degree of the porous system.

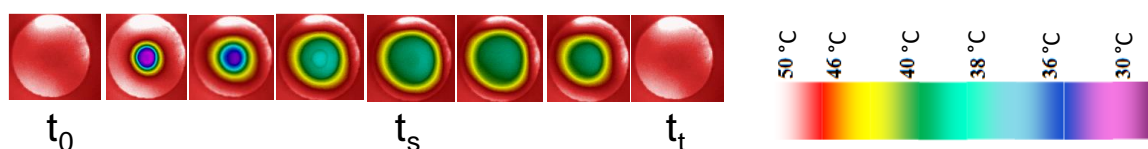


Figure 5. Images exported pro rata from the IR video correspond to t_0 , t_s , t_t and several representative intermediate times (*nf*-CNT, 5 μ L H₂O, 50°C).

Conclusion

The simultaneous weight monitoring, electric resistance measurement and infrared imaging of the evaporation of liquids from porous films can provide information about the mechanism of wetting and vaporization which is a significant area of the basic researches. Furthermore, it can be proved by using appropriate statistical methods (*e.g.*, matrix of Pearson correlation coefficients, hierarchical cluster analysis, functional analysis, etc.), that the experimentally determined characteristic values are specific for the physical properties of the solvents, and they are also dependent on the quality of the solid materials, therefore, they can be used for qualitative chemical analysis via the estimation of physical properties. The results allow us to presume the possibility of this experimental setup and theoretical approach for a potential future application in the field of analytics.

Acknowledgements

Financial support from the Hungarian National Research, Development and Innovation Office through the GINOP-2.3.2-15-2016-00013 “Intelligent materials based on functional surfaces—from syntheses to applications” project, the Ministry of Human Capacities, Hungary, grant 20391-3/2018/FEKUSTRAT and the János Bolyai Research Fellowship of the Hungarian Academy of Sciences is acknowledged.

References

- [1] D. Bonn, J. Eggers, J. Indekeu, J. Meunier, E. Rolley, *Mod. Phys.* 81(2) (2009) 739–804.
- [2] H.Y. Erbil, *Adv. Colloid Interface Sci.* 170(1-2) (2012) 67–86.
- [3] G. Schusztér, E.S. Bogya, D. Horváth, Á. Tóth, H. Haspel, Á. Kukovecz, *Mic. Mes. Mat.* 209 (2015) 105–112.
- [4] E.S. Bogya, B. Szilagyi, Á. Kukovecz, *Carbon* 100 (2016) 27–35.
- [5] Á. Kukovecz, *Egydimenziós nanoszerkezetek és hálózataik létrehozása, módosítása és néhány felhasználási lehetősége*, MTA értekezés, Szeged, 2018

CHANGE IN ATTITUDES TO CORPORATE SOCIAL RESPONSIBILITY

László Berényi¹

¹*Institute of Management Science, University of Miskolc, H-3515 Miskolc-Egyetemváros,
Hungary
e-mail: szvblaci@uni-miskolc.hu*

Abstract

In addition to decades of efforts on making the word sustainable, the achievements are often powerless. Attitudes to business and its social responsibility are continuously evolving. Changing personal attitudes is a key issue in the field. The research question of this paper is whether a change in attitudes is to find among higher education students in recent years in Hungary. The sample consists of 150-150 students from the academic years 2014/2015, 2016/2017 and 2018/2019. The survey asked to rate statements about the characteristics of corporate social responsibility (CSR). However, the results suggest a remarkable change, the statistical analysis confirms only a few of them. General experience of the survey is that the proportion of uncertain respondent (who gave middle-value ratings) has increased. These results show that the change has started, and it proposes that the efforts must be continued.

Introduction

Defining the responsibility of a corporation is an interesting issue. The stakeholder theory [1] interweaves management concepts even nowadays. Endeavors to achieve and sustain the satisfaction of various corporate stakeholder groups is generally accepted. However, there may be a conflict of interests between the stakeholders because they need to share both the available resources and the outcomes of the corporation. A famous concept of social responsibility by Friedman [2] limits the responsibility of corporations in making money to the shareholders. Any actions are only acceptable if those strengthen the future or wider abilities for making money. An early concept of corporate social responsibility (CSR) by Bowen [3] stated it “refers to the obligations of businessmen to pursue those policies, to make those decisions, or to follow those lines of action which are desirable in terms of the objectives and values of our society”. The development of the concept clearly shows that the key focus has moved from the businessman to the business and the organization. E.g. the International Organization for Standardization defines social responsibility as “responsibility of an organization for the impacts of its decisions and activities on society and the environment, through transparent and ethical behavior...” [4]. Braun [5] highlights that CSR initiations seem to give the answer on a corporate level since it incorporates stakeholder values and interests in the business.

However, we cannot neglect that the staff of organizations is made up of persons. Dealing with personal competencies is popular recently [6] [7] [8]. According to higher education students, even though their knowledge and opinion may be different from the professional approach, it is essential to explore their characteristics since they are the future employees and managers. Both organizations and higher education programs can learn from the experience.

The conceptual diversity in the field proves that there is a continuous improvement in line with the development of society. Several factors influence the impact of attitudes on behavior (see [9] [10]). The model of Doob [11] suggests that learning is inevitable. Attitudes are learned predispositions to responses and related actions. Based on this idea, changing the attitude needs the breakdown of the old one and build up the new. Since sustainability is a complex challenge, changing related attitudes requires much effort and time.

Experimental

I launched a survey to explore the attitudes towards sustainability and corporate social responsibility (CSR) among higher education students in 2013. The continuous data collection allows a follow-up on the changes in these attitudes. Data collection uses a voluntary survey with an online questionnaire. Data collection is supported by Evasys Survey management system, statistical analysis is executed in IBM SPSS.

The present study focuses on the question ‘How much do you agree with the following statements about CSR?’. The respondents are asked to evaluate 7 statements from strongly disagree to strongly agree (Figure 1). Since the evaluation scale was modified from 6-point to a 5-point one, the results are denominated to a 0 to 100 scale.

The research sample consists of 450 randomly selected respondents of the survey, uniformly from the three data collection periods. The respondents are business students of various Hungarian higher education institutions. Gender, level of studies or type of studies is not filtered. However, the limitations due to the sampling method do not allow the general interpretation of the results, the random methods may suggest wider experience.

The research question is whether the attitudes have changed during the examination period to CSR. According to the Introduction, the hypothesis says that the changes are not relevant.

Results and discussion

The mean values of the responses by years is presented in Figure 1.

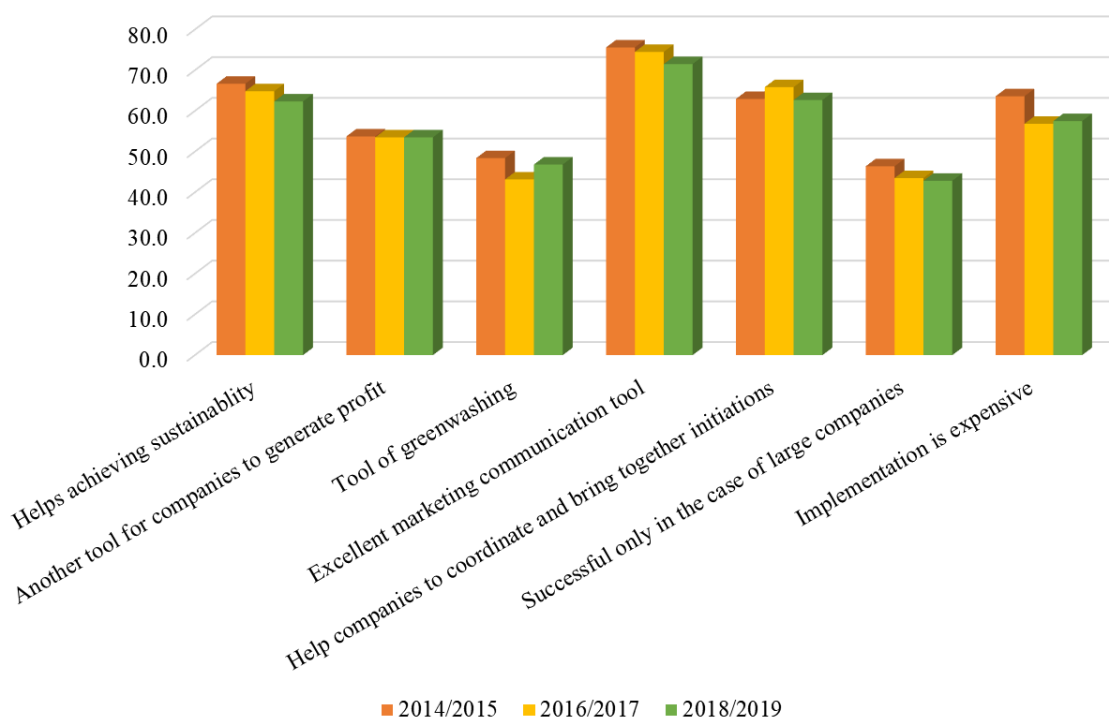


Figure 1. Mean values of rating by academic years, measured on 0-100 scale (own edition)

The respondents feel CSR an excellent marketing communication tool. Based on the mean values, CSR is moderately evaluated as a tool of profit generation or the tool of greenwashing. The belief that it helps to achieve a more sustainable world shows a higher mean value than previously mentioned statements but the value is decreasing. At the same time, statements about feasibility show similarly declining values. However, the respondents still consider the implementation expensive, the results are lower in later periods than in 2014/2015.

Beyond the mean values, it is expressive to compare the ratio of agreeing (over the value 60 in the 100-point scale) and disagreeing (under 40 in the 100-point scale) answers. Figure 2 presents the relationships. The results support the experience shown in Figure 1.

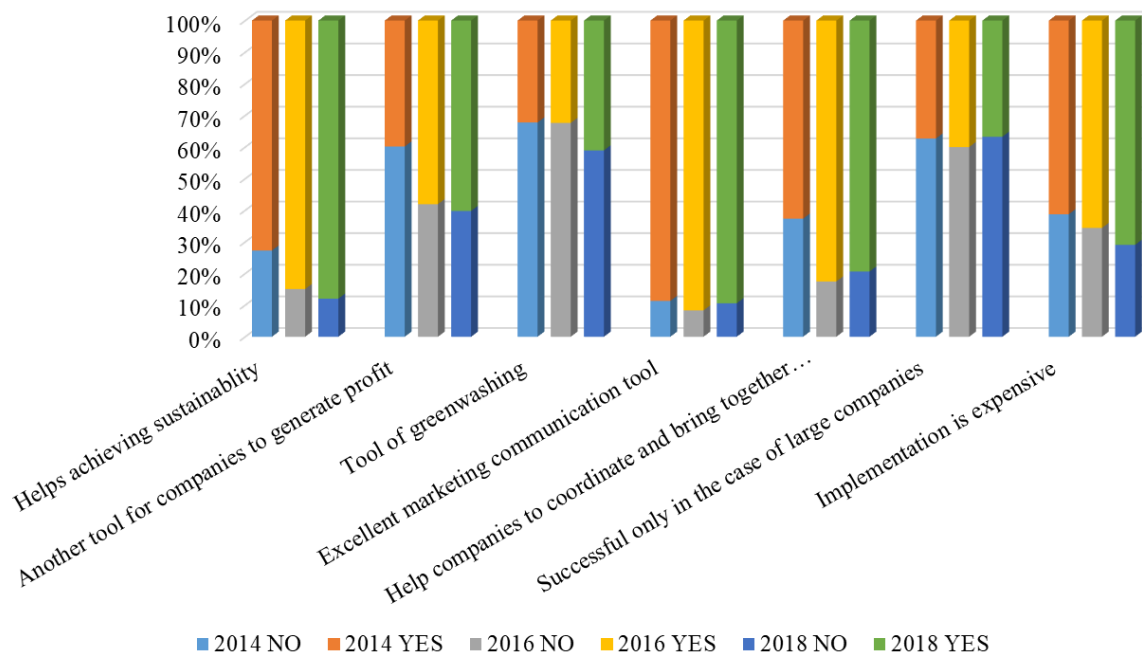


Figure 2. The relative proportion of agreeing and disagreeing responses (own edition)

Years	2014/2016			2016/2018			2014/2018		
Indicator	Chi-Square	d _f	Asymp. Sig.	Chi-Square	d _f	Asymp. Sig.	Chi-Square	d _f	Asymp. Sig.
Helps achieving sustainability	6.478	1	0.011	2.255	1	0.133	16.567	2	0.000
Another tool for companies to generate profit	0.162	1	0.687	0.047	1	0.829	0.200	2	0.905
Tool of greenwashing	1.156	1	0.282	1.922	1	0.166	1.969	2	0.374
Excellent marketing communication tool	1.969	1	0.161	1.229	1	0.268	6.072	2	0.048
Help companies to coordinate and bring together various initiations	0.001	1	0.977	1.445	1	0.229	1.986	2	0.370
Successful only in the case of large companies	0.413	1	0.521	0.008	1	0.930	0.723	2	0.696
Implementation is expensive	9.350	1	0.002	0.102	1	0.750	12.312	2	0.002

Table 1. Results of significance test (Kruskal-Wallis H test, based on SPSS output)

Comparing the mean values between the years can confirm the research hypothesis. Since the responses fail the normality test (significance level of Kolmogorov-Smirnov test is 0.000 in

each case), the non-parametric Kruskal-Wallis H-test is conducted for the analysis of variance. Significant differences in Table 1 are marked bold.

Figure 2 shows a remarkable change in attitudes in case of some statements, but the mean values and the analysis do not confirm if significant. The role of CSR in achieving sustainability is an increasingly and significantly popular idea. Similarly, the expanding cost commitment shows significantly more agreeing respondents. The results related to the role of CSR as a profit-generator and greenwashing tool are not significant.

Moreover, a surprising experience is that the most visible difference between the years is to find related to the statement ‘CSR help companies to coordinate and bring together various initiations’. Due to the high share of the middle-value ratings (44.6% in 2014; 31.3% in 2016 and 35.3% in 2018), the difference of mean values is not significant (see Figure 3).

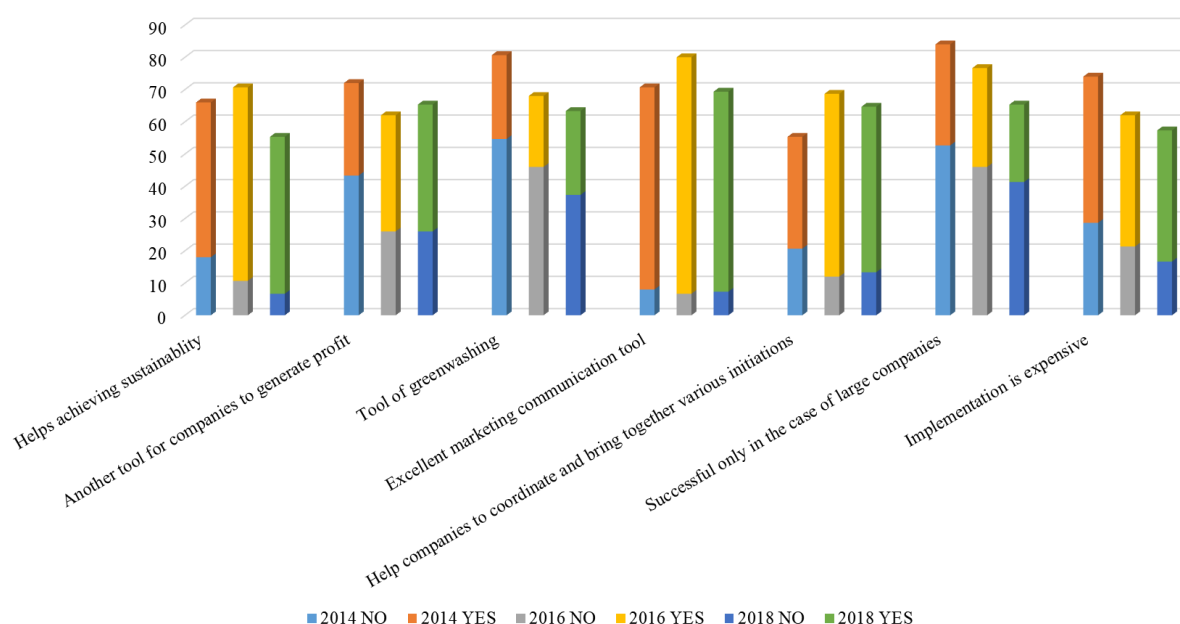


Figure 3. The proportion of agreeing and disagreeing responses (% of all responses, own edition)

Conclusion

The research question asked whether the attitudes have changed during the examination period to CSR. Since changing the attitudes require much effort and time, the hypothesis is formulated in a negative form. Statistical analysis confirmed only a few significant differences between the samples taken from different years. Based on these results I have to find that the attitudes have not been changed fundamentally.

Ignoring the strict statistical approach, it can be concluded that there are remarkable changes in attitudes towards CSR among higher education students in recent years. This permissible approach can be justified by the need that education and training actions are required in the present, based on the available information.

The experience of the survey includes both favorable and distressing elements. There is rising trust in CSR considered. Even more students think that it is achievable (cost and opportunities for non-large companies). Nevertheless, a growing proportion of the respondents think that CSR is about money and greenwashing. The increase in the occurrence of middle-value ratings is typical in the survey; it shows uncertainty. These results suggest that the change has started, and the efforts must be continued.

References

- [1] R.E. Freeman, Strategic management: A stakeholder approach. Boston: Pitman, 1984.
- [2] M. Friedman, The Social Responsibility of Business Is to Increase Its Profits, New York Times Magazine, September 13, 1970.
- [3] H.R. Bowen, Social Responsibility of the Businessman, New York: New York University Press, 1953.
- [4] ISO 26000:2010 -- Guidance on social responsibility
- [5] R. Braun, A vállalatok politikája: Vállalati társadalmi felelősségvállalás, vállalati közösségek és a vállalati stratégia jövője, Vezetéstudomány. 44(1) (2013) 18-28.
- [6] A.M. Lämsä, M. Vehkaperä, T. Puttonen, H.L. Pesonen, Effect of business education on women and men students' attitudes on corporate responsibility in society, Journal of Business Ethics. 82(1) (2008) 45-58.
- [7] N. Deutsch, L. Berényi, Personal approach to sustainability of future decision makers: a Hungarian case, Environment Development and Sustainability. 20(1) (2018) 271-303.
- [8] B. Gallei, F. Hourneaux, L. Munck, Sustainability and human competences: a systematic literature review, Benchmarking: An International Journal. 2019. doi: 10.1108/BIJ-12-2018-0433.
- [9] P. Isaias, T. Issa, High level models and methodologies for information systems. New York: Springer, 2015.
- [10] T. Keszey, J. Zsukk, Az új technológiák fogyasztói elfogadása: A magyar és nemzetközi szakirodalom áttekintése és kritikai értékelése, Vezetéstudomány. 48(10) (2017) 38-47.
- [11] L.W. Doob, L.W. The behavior of attitudes. Psychological Review 54(3) (1947) 135-156.

ANALYSIS OF DESIGNER DRUGS AND THEIR METABOLITES IN BLOOD AND URINE SAMPLES

Tímea Körmöczi¹, Orsolya Kovács², Éva Sija³, Ákos Hunya⁴, Reza Samavati², Róbert Gáspár², László Institóris³, István Ilisz¹, Róbert Berkecz¹

¹*Institute of Pharmaceutical Analysis, University of Szeged, H-6720 Szeged, Somogyi utca 4, Hungary*

²*Department of Pharmacology and Pharmacotherapy, University of Szeged, H-6721 Szeged, Dóm tér 12, Hungary*

³*Department of Forensic Medicine, University of Szeged, H-6724 Szeged, Kossuth Lajos sgt. 40, Hungary*

⁴*Institute of Biochemistry, Biological Research Centre, Hungarian Academy of Sciences, H-6726 Szeged, Temesvári krt. 62, Hungary
e-mail: kormoczi.timea@pharm.u-szeged.hu*

Abstract

Synthetic cannabinoids (SCs) has hundreds of street names for instance “Spice”, “Spice Gold”, “K2”, “Black Mamba”, “Feek Weed,” “Genie”. SCs are group of designer drugs that mimic the natural cannabinoid effects. However, SCs have significantly higher binding affinities to the CB1 and CB2 cannabinoid receptors than the well-known Δ^9 -tetrahydrocannabinol (THC) thanks to their special pharmacodynamic properties. In clinical and forensic practices only detecting the mother compound of SCs cannot provide reliable confirmation of their consumption due to their rapid metabolism. The aims of this study were in vitro (human liver microsome, immortalized human hepatocytes), in vivo (human urine and blood) and ex vivo (isolated rat liver perfusion) analysis of metabolites of the newest designer drugs in 2019. After optimizing the sample preparation (liquid-liquid extraction), new targeted LC-MS/MS method was developed for detecting the parent molecule and its phase I metabolites. Currently, the most commonly used SC is the 5F-MDMB-PICA. The importance of identifying metabolites can be well demonstrated by extracted ion chromatogram of positive urine sample (**Figure 1**), which shows that the ester hydrolysis metabolite of 5F-MDMB-PICA (363.2082 m/z, t_R : 1.86 min) has 150 times higher intensity than the parent molecule.

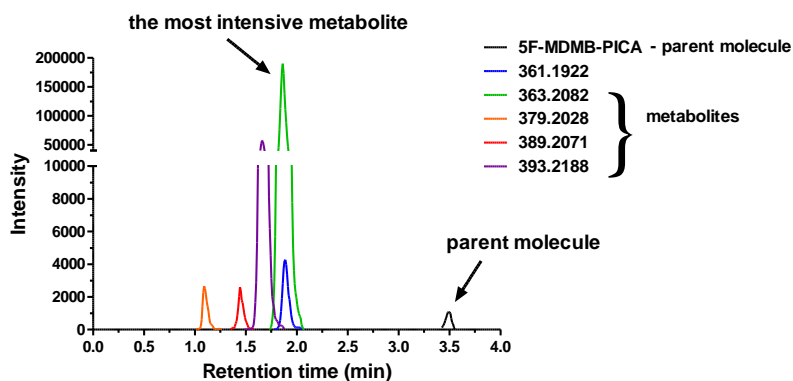


Figure 2. Positive urine sample

Acknowledgements

This research was supported by the EU-funded Hungarian grant EFOP 3.6.1-16-2016-00008.

SWAP BETWEEN NORMAL PHASE AND POLAR ORGANIC MODE ON ADMPC CHIRAL STATIONARY PHASES

Horváth, S.^{1,2}, Eke, Zs.^{3,4}, Péter, A.⁵, Ilisz, I.⁵, Németh, G.¹

¹Egis Pharmaceuticals PLC, Drug Substance Development Division, H-1475 Budapest, Keresztúri út 30-38, Hungary

²Eötvös Loránd University, György Hevesy Doctoral School of Chemistry, H-1117 Budapest, Pázmány Péter sétány 1/A, Hungary

³Eötvös Loránd University, Joint Research and Training Laboratory on Separation Science, H-1117 Budapest, Pázmány Péter sétány 1/A, Hungary

⁴Wessling International Research and Educational Center, H-1045 Budapest, Anonymus u. 6, Hungary

⁵Institute of Pharmaceutical Analysis, University of Szeged, H-6720 Szeged, Eötvös u. 6, Hungary

e-mail: horvath.simon@egis.hu

Abstract

Investigation of enantiomers is a common and important task in the pharmaceutical industry. In vast majority of the cases direct HPLC methods are used with polysaccharide-based chiral stationary phases [1-3]. The reason behind their versatility is the fact that many different chiral environments are accessible on them, due among others to their multimodal nature.

In continuation to our studies about the characterization [4] and the practical assessment of some history dependent chiral chromatographic systems in the polar organic (PO) mode, we extended our investigations to normal phase (NP).

We found that an amylose tris(3,5-dimethylphenylcarbamate) (ADMPC) based column in the alkane-IPA systems exhibited hysteresis phenomenon. The effect can be observed both in heptane-IPA and hexane-IPA systems, and it is in close alignment with the known cost-increasing issue in chiral HPLC, namely that the reproduction of the retentions after swapping the modes is often problematic with polysaccharide-based columns. To avoid this undesirable consequence, column manufacturers advise to dedicate polysaccharide-based chiral columns to eluent modes.

However, we discovered that by a quick rinse with a particular alcohol mixture the normal phase column test of the manufacturer can be reproduced after using the column in polar organic mode. We also found that heptane/IPA mixtures can be used indefinitely, without losing the purchased selectivity, if the IPA content does not exceed 70%.

References

- [1] J. Shen, Y. Okamoto, Chem. Rev. 116 (2016) 1094-1138.
- [2] B. Chankvetadze, J. Chromatogr. A 1269 (2012) 26-51.
- [3] E. Francotte, LCGC Europe 29 (suppl) (2016) 31-37.
- [4] S. Horváth, G. Németh, J. Chromatogr. A 1568 (2018) 149-159.

ARSENIC UPTAKE IN TOMATO AND POTATO PLANTS GROWN IN SILT AND SAND SOIL AND IRRIGATED WITH WATER CONTAINING ARSENIC

Sirat Sandil¹, Peter Dobosy², Victoria Vetesi¹, Kriszta Kröpfl², Anna Füzy³, Mihály Óvári², Gyula Záray^{1,2}

¹Cooperative Research Centre of Environmental Sciences, Eötvös Loránd University, Pázmány Péter sétány 1/A, H-1117 Budapest, Hungary

²MTA Centre for Ecological Research, Danube Research Institute, Karolina út 29-31, H-1113 Budapest, Hungary

³MTA Centre for Agricultural Research, Institute for Soil Sciences and Agricultural Chemistry, Herman Ottó út 15, H-1022 Budapest, Hungary

e-mail: sirat29@gmail.com

Abstract

Arsenic uptake by tomato (*Solanum lycopersicum* L.) and potato (*Solanum tuberosum* L.) plants was studied by cultivating the plants in silt and sand soil and irrigating them with water containing arsenic at concentrations of 0.05 and 0.2 mg As L⁻¹.

Introduction

Aquifers in the Pannonian basin contain naturally occurring arsenic (1-174 µg L⁻¹), and the water from these aquifers is utilized for drinking and irrigation purpose, which affects a million people at levels greater than the recommended 10 µg L⁻¹ WHO standard (Varsanyi et al., 2006). The transfer of arsenic in soil-plant systems represents one of the principal pathways for human exposure to arsenic (Lu et al., 2010). As uptake by vegetables depends on its availability in soil and the ability of the crop to take up and translocate As (Huang et al., 2006).

Experimental

Arsenic uptake by tomato and potato was studied in sand and silt soil by applying irrigation water containing As, mimicking the groundwater As concentration. Arsenic was supplied in the form of sodium arsenate, at concentrations 0.05 and 0.2 mg L⁻¹. Arsenic accumulation in root, shoot, and fruit was analyzed at the fruiting stage. Plants were grown in a pot-soil system in open greenhouse, supplied with Hoagland's nutrient solution and irrigated once a week.

Upon harvest plant samples were thoroughly washed with Milli-Q water and oven dried at 40°C for 48hrs. The dry homogenized samples were digested in a microwave-assisted acidic digestion system using 7 cm³ 67 % nitric acid and 3 cm³ 30 % hydrogen-peroxide. The resultant solutions were diluted with deionized water up to 25 cm³. Concentration of As and certain nutrients (P, K, Mg, Fe, Mn, Cu, Zn) were determined by inductively-coupled plasma mass spectrometer.

Results and discussion

- The As content of the sand and silt soil was 4.32 mg kg⁻¹ and 9.02 mg kg⁻¹, respectively.
- Increase in As concentration of the irrigation water caused an increase in the As accumulation in the plant, and in both plants maximum As concentration was found in the roots and minimum in the fruit.
- Vegetables grown in sandy soil had the maximum As concentration and minimum biomass productivity.

- At 0.05 mg As L⁻¹ potato displayed a positive biomass production in silt soil. At 0.2 mg As L⁻¹ treatment, both plants displayed a negative biomass production in both soil types.
- As accumulation in edible part was higher in potato.
- Arsenic intake for a person consuming 450g (FW) of tomato would be 0.99 µg (sand) and 0.54 µg (silt). In case of potato the As intake would be 2.79 µg (sand) and 1.26 µg (silt).

Conclusion

Considering the FAO-WHO recommended maximum tolerable daily intake limit of 2 µg kg⁻¹ body weight, and the biomass production, both plants grown in irrigation water containing up to 0.2 mg As L⁻¹ are safe for consumption. But considering the biomass production it is advised to cultivate plants at 0.05 mg As L⁻¹ treatment and in silt soil.

This work was supported by the Hungarian Scientific Research Foundation (NVKP_16-1-2016-0044) granted to GZ and the Stipendium Hungaricum scholarship to SS.

References

- [1] Varsanyi, I. Kovacs, L.O. (2006), Arsenic, iron and organic matter in sediments and groundwater in the Pannonian Basin, Hungary, Appl. Geochem. 21(6), 949-962.
- [2] Lu Y., Dong F., Deacon C., Chen H., Raab A. and Meharg A.A. (2010), Arsenic accumulation and phosphorus status in two rice (*Oryza sativa* L.) cultivars surveyed from fields in South China, Environmental Pollution 158, 1536–1541.
- [3] Huang R., Gao S., Wang W., Staunton S. and Wang G. (2006), Soil arsenic availability and the transfer of soil arsenic to crops in suburban areas in Fujian Province, southeast China, Science of the Total Environment, 368, 531–54.
- [4] FAO-WHO Joint FAO/WHO Expert Committee on Food Additives. Food and Agriculture Organization of the United Nations, Rome, Italy / World Health Organization, Geneva, Switzerland, (1988).

MEMBRANE SEPARATION PROCESS FOR DAIRY WASTEWATER TREATMENT

Elias Jigar Sisay^{1,2*}, Zsuzsanna László^{2,3}, Ákos Fazekas²

¹ *Doctoral School of Environmental Sciences, University of Szeged, Hungary. H-6720, Rerrich B. tér 1.*

² *Department of Process Engineering, Faculty of Engineering, University of Szeged, H-6725 Szeged, Moszkvai krt. 9.*

³ *Institute of Environmental Science and Technology, University of Szeged, H-6720, Tisza Lajos Blvd. 103, Szeged, Hungary
eliasjig@gmail.com, zsizsu@mk.u-szeged.hu*

Abstract

In recent years, membrane separation processes in dairy industrial wastewater treatment offers several advantages: it runs with much less ecological footprint, more economical, more energy efficient, ease of operation and better possibilities of integration with other processes. Moreover it gives the possibility of water reuse. However, these processes suffer from concentration polarization and membrane fouling which limit the membrane flux during filtration and negatively impact production efficiency with corresponding increases in energy consumption and is a major factor in determining the practical application of these techniques in water purification, wastewater treatment and desalination. Solving the problem of fouling through membrane modification by nano-materials has been attracting the attention of scientists. The aim of this work is to identify the factors affecting the membrane fouling during treatment of dairy wastewaters and present the recent development of research in this field.

Keywords: Membrane separation processes, dairy wastewater, fouling, nano-materials, membrane modification

Acknowledgements

This study was supported by the János Bolyai Research Scholarship of the Hungarian Academy of Sciences and by the New National Excellence Program of the Ministry of Human Capacities (UNKP-18-4-SZTE-78). The authors are grateful for the financial support of the Hungarian Science and Research Foundation (2017-2.3.7-TÉT-IN-2017-00016), the Hungarian State and the European Union (EFOP-3.6.2-16-2017-00010).

References

1. Y.R.Chang; Y.J.Lee; D.J.Lee; J. Taiwan Inst. Chem. Eng. (2018), doi:10.1016/j.jtice.2017.12.019
2. Y. W. Gong; H. X. Zhang; & X. N. Cheng; Water Science and Technology (2012), 915,919.
3. H. Lu; J. Wang; M. Stoller; T. Wang; Y. Bao; & H. Hao; Advances in Materials Science and Engineering (2016), 1,10.

EX-SITU XPS STUDY OF THE ROLE AND BEHAVIOUR OF COBALT-OXIDE SUPPORT SURFACES IN CO₂ HYDROGENATION

Ákos Szamosvölgyi¹, András Sági¹, Ákos Kukovecz¹, Zoltán Kónya^{1,2}

¹*University of Szeged, Interdisciplinary Excellence Centre, Department of Applied and Environmental Chemistry, H-6720 Szeged, Rerrich Béla tér 1, Hungary*

²*MTA-SZTE Reaction Kinetics and Surface Chemistry Research Group, University of Szeged, H-6720 Szeged, Rerrich Béla tér 1, Szeged, Hungary*

e-mail: szamosvolgyi@chem.u-szeged.hu

Abstract

While noble metals' excellent catalytic properties are undeniable, they are scarce and expensive materials, hence the research for new options is of great interest. One fairly appropriate solution is to use as little noble metals as possible while maintaining or improving catalytic performance. This approach emphasises the role of support materials greatly. In this study the role and mechanism of mesoporous support materials were examined by conducting ex situ x-ray photoelectron spectroscopy on the pretreated and the spent catalysts.

In this study our catalysts' were cobalt-oxide samples with different structures. The catalytic reactions were carried out in the modified pre-chamber of our XPS instrument. The standard pre-chamber was expanded with a quartz tube, a thermocouple, a heating element which provided uniform heating and a programmable control unit. During the pretreatment of the sample and during the reaction continuous gas flow was provided.

The reaction of CO₂ hydrogenation may take many reaction paths and these paths may yield different products and by-products, depending on what type of catalyst was used. And depending on reaction conditions the surface of the catalyst undergoes changes. The main purpose of my research was to track these changes by acquiring the spectra for the Co 2p and O 1s regions and evaluate the results.

The gathered and processed data helps to evaluate the role of different surfaces in the given catalytic process. Furthermore, studying their behaviour enables the design of new catalytic systems, reducing the trial-and-error nature of these experiments.

Acknowledgements

Financial support from the Hungarian National Research, Development and Innovation Office through the GINOP-2.3.2-15-2016-00013 "Intelligent materials based on functional surfaces—from syntheses to applications" project and the Ministry of Human Capacities, Hungary, grant 20391-3/2018/FEKUSTRAT is acknowledged.

MAKE IT CIRCULAR – CIRCE2020 PROJECT: RATING METHOD FOR A PROBLEMATIC PLASTIC COMPOSITE TO CHOSE THE BEST CIRCULAR ECONOMY SOLUTION

Eszter Tanka¹, Enikő Csoma¹, Zsolt István²

¹*Green Economy Unit, IFKA Public Benefit Nonprofit Ltd. for the Development of Industry, H-1062 Budapest, Andrásy str. 100., Hungary*

²*Division of Intelligent Systems, Bay Zoltán Nonprofit Ltd. for Applied Research, H-3519 Miskolc, Iglói str. 2, Hungary
e-mail: tanka@ifka.hu*

Abstract

The European Union's ambitious legislative package was accepted in May 2018 setting many challenges to the member states. One of the potential tools to foster the needed transition in this respect is to applying circular economy solutions. Some material is only just a waste to the company, but another company can utilize it as a secondary raw material. We have to track down these possibilities and need to promote the industrial symbiosis connections in favor also of our environment. Many barriers exist from feasibility to economical interest, but the strongest key factor is the commitment to protecting the environment. CE is not only a waste management law, but it requires new product development methodologies and new business models.

Introduction

The CIRCE2020 – Expansion of the CIRcular Economy concept in the Central Europe local productive districts – Interreg Central Europe project aims to facilitate a larger uptake of integrated environmental management approach in five specific Central European industrial areas by changing patterns from single and sporadic company recycling interventions to an integrated redesign of industrial interactions based on the concept of circular economy (CE). The goal is to introduce innovative cross-value chain waste governance models and transnational analytic tools to improve capacities of concerned waste public-private sector to reduce dependencies from primary natural resources within industrial processing. The project should also provide robust evidences about environmental and economic benefits from shifting to enhanced industrial symbiosis. That is why the main objective of the project is to test and work out a decision supporting tool analyzing the alternative options from different perspectives.

Results and discussion

In the Hungarian pilot area, two relevant waste flows and their amounts were identified by using material flow analysis to target two critical material flows. One of them is a plastic composite from a medical tool producing company containing several types of ingredients, such as polyethylene (PE), polypropylene (PP), polyethylene terephthalate (PET), polyvinylchloride (PVC), polyamide (PA), ethylene vinyl acetate (EVA) and some starch. The currently applied waste management technology of the critical amount (yearly 5000 tonnes) of plastic waste is incineration with energy and steam recovery.

The following phase was a detailed research about the possible alternative solutions, technologies and recipient companies. The aim was to change the present waste management system and develop the present treatment choice to a higher and more efficient level or - being a critical material- to produce valuable products from these waste plastics as a

secondary raw material. Due to the complexity of the composition and because of the quantity it is quite a challenge to identify producers who can deal with this material. Continuous, long-term and sustainable relation is needed.

During the project a rating system has been developed for identifying the impacts of the currently used and the circular economy based solutions. The following figure shows the essence of the methodology.

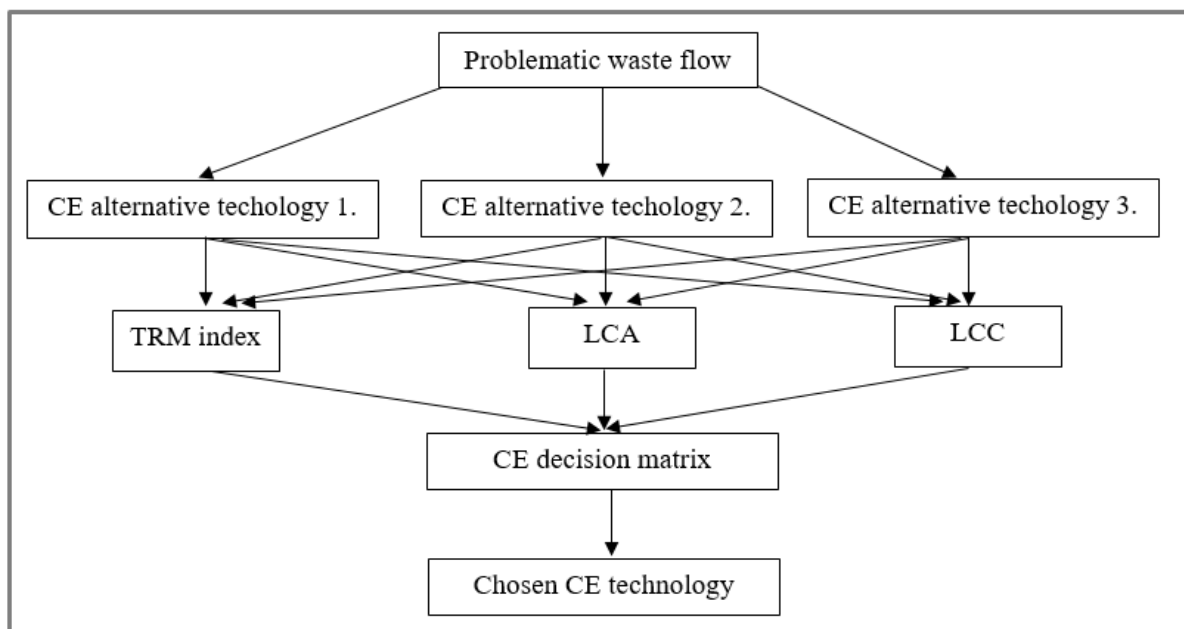


Figure 1. Methodology of the developed rating system

Experts of Bay Zoltán Nonprofit Ltd. for Applied Research developed a special process. Technological Rating Methodology (TRM index) represent an instrument which allows to user to assess the identified circular solution considering the three most significant driver for a circular business: technology, environment and economy.

In the process a weighted evaluation of the following factors was required:

- technology readiness level index;
- references in the market;
- reliability of technology provider;
- circularity level of the technology;
- operational experience;
- technical limitations;
- others.

In the following definition can be seen the calculation of the TRM, where TRM_i is i^{th} specific TRM aspect and W_i is the i^{th} specific weighting factor.

$$TRM = \sum_{i=0}^n TRM_i * W_i$$

After the rating method a life cycle assessment (LCA) and life-cycle cost analysis (LCC) were followed. The purpose to applying the tools was to:

1. support decisions among different choices;
2. measure the environmental and economic impact of the changes.

In order to test the environmental sustainability of the pre-selected circular economy cases and quantify the relevant environmental impacts of products, a life cycle assessment was performed based on the latest Environmental Footprint (PEF) methodological requirement. LCA required a detailed and strict rules in connection with the quality and documentation of the collected data, modelling of transportation processes, applied allocation rules and methods of environmental impact assessment. Environmental evaluation focused on the main environmental aspects (soil, air, water) and considering for impact assessment robustness, inventory cover completeness and inventory robustness. Because of that Climate change, Particular matter, Acidification, Eutrophication (terrestrial) and Resource use (minerals and metals) categories had been selected during the process.

General patent or detailed regulated reference are not exist in case of LCC, but it has to be comparable with the LCA-PEF assessment within same system boundaries and functional units.

At the end the CE decision matrix summarizes the main weighted results of the TRM, LCA-PEF and LCC with respect to each circular economy based solutions. According to the TRM, environmental and economical index a qualitative evaluation and a final score were given where we can see that the analyzed technology is „not recommended“, „partly not recommended“, „recommended“ or „highly recommended“.

In the final section the user can summaries the evidences deriving from the analysis of the three main drivers for CE. The last assessment would synthetize all the information, leading to the choise of adopting or discarding the identified solution for the selected flow. It is significant to see the whole picture which contains all the information about advantages, disadvantages and feasibility before chosing the best alternative technology.

Conclusion

In case of plastic composite waste, the chosen technology was to make granulate and after that produce valuable product. It was a big challenge to find partners for that.

According to the preliminary researches the team defined the TRM numbers in each above mentioned category and performed the weighting. The final number belonged to the limited recommended category – since we face many challenges in this respect.

Environmental driver was given by LCA-PEF assessment in the 5 categories. In the present scenario there were some impact categories where the energy recovery had the biggest environment impact, but in case of the other categories the CE stage had bigger effect. Overall it can reach environmental benefit with another/better waste disposal or recycling alternative, because the qualitative evaluation result was highly recommended in case of CE scenario.

Regarding the LCC final score, both scenario produced almost the same result. However, we need to acknowledge that the system boundary of the analysis is only the production of granulates. This could then be transformed into new, more value added products in the market. With this and with long term contracts regarding transportation and treatment, these costs could be decreased. Getting back to the rationale behind the qualitative scores, since with the new CE solution the environmental sustainability could be increased plus the dependency hence the risk of the company could be decreased.

References

- [1] CIRCE2020: Shared technology rating methodology (TRM) to check out readiness of new techs and processes
- [2] CIRCE2020: Guidelines for adaptation of LCA methodology to estimate environmental impact
- [3] Zs. István, B. Sára: Technological, environmental and economical evaluation of circular economy solutions with life cycle approach

Poster Proceedings

ASSOCIATIONS BETWEEN ENVIRONMENTAL NON-ESSENTIAL HEAVY METALS, ECOBIOCHEMISTRY AND HEALTH

**Mirela Ahmadi¹, Ioan Pet², Lavinia Stef², Narcisa Mederle¹, Cornelia Milovanov¹,
Gabi Dumitrescu², Marioara Nicula², Laura Iosefina Smuleac³, Raul Pascalau⁴,
Adrian Smuleac³, Dorel Dronca²**

¹*Faculty of Veterinary Medicine, Banat's University of Agricultural Sciences and Veterinary Medicine „King Michael Ist of Romania“ from Timisoara (BUASVM), Timisoara – 300645, Calea Aradului, no. 119, Romania*

²*Faculty of Bioengineering of Animal Resources, BUASVM Timisoara*

³*Faculty of Agriculture, BUASVM Timisoara*

⁴*International Relations Office, BUASVM Timisoara
e-mail: ddronca@animalsci-tm.ro*

Abstract

Environmental heavy metals should be a concern of the entire world due to its impact on the animal and human population. "Heavy metals" is a generic name used for metals characterized by relatively high atomic weight, density, and atomic number. Some of the heavy metals are essential nutrients for animals and humans, but when their ingested concentration exceeds the needs, their homeostasis is unbalanced and health status is impaired. Non-essential heavy metals are minerals that are harmful to the environment and living organisms. The environment is the main source of minerals provided by soil, water and air. Any deficiency or excess of minerals in the environment will be transferred to the living organisms. Plants, meat and water – are ingredients of humans' diet, and because of that, any overload affects the minerals' homeostasis that could lead to accumulation in target organs – mainly in the liver and kidney, also in the brain, heart, lungs, and other organs. Ecobiochemistry and xenobiochemistry are two complex sciences that are trying to find correlations between the biochemical processes related to the minerals' needs, intake, and excretion to assure a good health status.

Key words: environment, heavy metals, health

Introduction

Health status for animals and humans is a very complex subject that involves the environment, lifestyle, and biochemical characteristics. Lately, more and more concerns are related to the environment and pollution, in order to ensure a healthy environment for all living organisms. Thus, one major concern is focused on heavy metals, which are much spread and could suffer risk assessment due to the trophic transfer and/or biomagnification. "Heavy metals" is a generic name that characterizes natural chemical elements with high atomic mass (usually higher than 23) and high density (higher than 5g/cm³) [1]. Heavy metals are found wild spread, but their concentration in environment and organisms is relatively low. Ecobiochemistry as a term, was mention in a research experiment that studied the adenine nucleotides in the deep-water pelagic community as an estimator of energetic metabolism, and also it was mentioned in a USPA Program – which has studied sub-Antarctic habitats [2]. It's a science that evaluates the organisms' metabolic processes related to the quality of the living environment – which most of the time is assessed in order to found out if there is any contamination of air, water or soil. Thus, the main chemical reactions from animal and human organism are evaluated in terms of efficacy in the presence of excessive amounts of organic chemicals (ex. pesticides, insecticides) or inorganic chemicals (such as metals with toxicogenic potential), finally referring to the quality of soil, water and air.

Xenobiochemistry studies the foreign compounds in plants, animals or human organism, or studies the chemical compounds that are essential for the living organisms but are found in too high concentrations. Specialized functions in the body identify the presence of toxic substances or

essential substances in concentrations that exceed the tolerance of the body, block their absorption, and are transported to the liver to be annihilated. For example, heavy metals bind to various chelators which make them impossible to be absorbed, and thus their action is blocked, after which they are transferred to the renal function in order to be excreted through the urine [3].

The chelation process in the body is a very easy process and is often used by enzymes that have metal cofactors. These chelators have two or more chemical bonds between metal and the organic molecule, which are coordination bonds formed between metal ion and chelator. The strength of the coordination bond and the accessibility of chelation process are depending on various characteristics, such as: accessibility of the chelators and metal ions in the tissues; the metal ion and chelator concentration; the strength of the metal ion already bound to other chemicals; and the strength of the bond formed between the chelator and the metal ion. The most important chelators are metallothioneins and glutathione – enzymes that play the role of biomarkers, being involved in the cellular response of the presence of toxic heavy metals, in mobilization, transport and renal excretion (in urine). Dietary fibers can also help in detoxification processes, playing an alternative role in reducing the quantity of toxic metals in the body, absorbing chemicals and excreting them via digestive tract (in feces). USA (US Environmental Protection Agency, World Health Organization) and Canada (Environment Canada, Canadian Institute of Health Research, Canadian Poison Control Centers) developed and funded different divisions that are specialized in treatments using chelators regarding the most heavy metals exposure, such as: arsenic, cadmium, mercury, and lead among their population, especially for the children [4,5].

If we talk about the possibility of eliminating the heavy metals from the organism through chelation we must remember that along with the main elimination pathways (the renal and digestive pathways) it is necessary to take in consideration the excretion of these chelated substances also by sweat. But having in view that for any organism there are tolerance limits to concentrations of certain substances, we must emphasize that living organisms are capable of evolving over time and tolerating increasing amounts of pollutants [4].

Heavy metals in environment

The environment is a very important source for heavy metals, in which water plays a key role in translocation. Humans' activities could be also important factors that can influence the quantity of heavy metals from the environment. The heavy metals released in the eco-biosphere come from agriculture, industries, technologies, automotive and medical uses and applications. Proper use of these chemicals does not harm the environment, but we are increasingly witnessing disasters caused by improper use (quantitative and qualitative), uncontrolled discharges and pollution, that have serious consequences on the environment in the very long term.

Biomagnification is a process that occurs when some chemicals (such as heavy metals or organic pollutants) accumulate in the internal organs and tissues of plants, animals and/or humans. The biomagnification processes are characterized by bioaccumulation, biodilution and bioconcentration. Bioaccumulation is referring to accumulation on some chemicals along the trophic chain that lead to increased concentration in specific organs and tissues. Biodilution is the process in which the chemicals concentration is diluted due to an increase in trophic level [6].

Humans and animals are at the top of the trophic chain and from this point of view biomagnification has become a subject extensively studied in recent years. Biomagnification of toxic, polluting substances - such as heavy metals, increases the risk of serious diseases such as various types of cancer; liver, kidney and heart failure; birth disorders; and brain irreversible damage [7,8].

Environmental decontamination and de-pollution are the main target of environmental researchers, biologists, and biochemists, who are trying to find new solutions to reduce the degree of environmental contamination. Thus, recent studies have shown that a system that combines

functional bacteria with absorbent materials (sponge, cotton treatment) has a direct effect of removing copper, cadmium, and chromium; and indirectly on lead and chromium [9].

For decontamination of water polluted by heavy metals, there are more options to take into consideration, such as physical, chemical or thermal treatment, but the best and effective traditional solution remains the alkaline lime precipitation. This method is effective for treatment of contaminated wastewater where the heavy metals exceed 1g/L [10].

Phytoremediation is another method very useful for biodilution of the heavy metals. There are some specific plants that have the ability to chemically transform the heavy metals into chemically bioavailable form for the plant, with the final effect of decreasing the concentration of metal pollutants or high concentrations of essential metals, in the soil. This method is a recent technology, being a cost-effective, efficient, safety ecologic method, and available for decontamination of soils and waters. The phytoremediation is a very good option to “clean” the environment of different chemical hazardous substances, with the help of some plants that are capable to upload thousands of ppm of heavy metals [11,12].

Ecobiochemistry and heavy metals

For living organisms, there are different essential minerals and even heavy metals – which are important for metabolic processes. Between the heavy metals, arsenic, cadmium, lead, mercury, and chromium have the highest toxicity, chromium being essential for carbohydrates metabolism – but in very small amounts. Regarding the quantitative needs of heavy metals in living organisms, they are necessary in trace amounts, less than 10ppm or even ppb. The quantity of heavy metals is significant for environmental pollution characterization, but it has to be taken in account their bioavailability that it is influenced by physical factors (such as temperature, absorption, sequestration, phase association) and chemical factors (water or lipid solubility, the chemical form, concentration, pH) [13].

The classification of minerals into heavy metals with toxic effect must be done careful because there are recent studies that have shown the beneficial effect of toxicogenic metals in the treatment of serious diseases, such arsenic used as cancer cell apoptosis in the case of leukemia.

In the following we will make some references to toxic effects of some minerals with essential role in the human and animal organism.

Chromium is an essential trace element directly involved in carbohydrates and cholesterol metabolism. Lately, due to the technological food and feed processes, nutritional chromium intake is lower and thus become a very popular dietary supplement. The key role of chromium in the organism is to facilitate the intracellular access of glucose, involved in the processes of energogenesis. Also, chromium is taking part in lipid metabolism, and influence the cholesterol level into the bloodstream. Due to its implication in energy metabolism, chromium has become an important nutrient in the weight loss programs, and also in diabetic patients. From chemically point of view, chromium occurring in environment and organism in different valence states, as $\text{Cr}^{(2+)}$ to $\text{Cr}^{(6+)}$, but $\text{Cr}^{(3+)}$ compounds are the most stable, followed by $\text{Cr}^{(6+)}$. Hexavalent chromium is known as industrial pollutant, classified as carcinogenic. $\text{Cr}^{(3+)}$ naturally occurs in soil, water, air and other biological sources. Ingesting or inhalation of chromium leads to reproduction damages, gastrointestinal irritation, anemia, liver and kidney failure, neurological and hematological damages [14].

Lead is a naturally mineral in the environment. Lately the industrial used of lead was significant reduced, but the largest source of lead contamination is contaminated soil, dust and chips of old paint from deteriorated houses – especially for children [15]. In children there are many studies that demonstrated that lead exposure diminish the intelligence; leads to growth retardation; brain, kidney, and heart damages; gastrointestinal diseases, and disturb the central nervous system [16].

Cadmium has essential role in the metabolism of various microalgae from Diatomophyceae class [17]. Sedimentary rocks and marine phosphates accumulate the highest level of environmental

cadmium, in concentration of about 15mg/Kg [18]. Also some dietary products can be important sources of cadmium for human organism, such as crustaceans, mollusks, leafy vegetables, mushrooms, potatoes, seeds, grains, cacao powder, and organs like liver and kidney [19,20]. The metabolic pathways of cadmium toxicity is poorly known and understood, but researchers speculate that the main damage of cadmium is generation of reactive oxygen species inside the cells that lead to single-strain DNA, disrupting the DNA and proteins synthesis [21]. Cadmium quantitative determination from different biological samples can reflect the acute or chronic exposure. Thus, cadmium determination from blood reflects acute or recent exposure, while cadmium from urine reflects the chronic or accumulation of cadmium (usually the rate between cadmium/creatinine is calculated). Lately, due to the industrial applications, cadmium environmental contamination has dramatically increased.

In humans arsenic exposure is associated with carcinogenic and systemic health effects, and the main exposure source is the diet and drinking water, and much less important the soil and air. Arsenic contamination is associated with pesticides use, wood preserving technologies, semiconductor manufacturing, glass and ceramic factories and smelting [21]. The toxicogenic effects of arsenic are difficult to estimate because it is highly influenced by exposure dose, frequency and duration, by organism characteristics, by solubility, by its oxidation state, and by nutritional factors. Experimental studies demonstrated that exposure of trivalent arsenite (As^{3+}) is 2-10 times more toxic compared to pentavalent arsenate (As^{5+}) [22]. Experimental studies demonstrated that arsenic can also be used in the treatment of promyelocytic leukemia, which can be achieved by the administration of arsenic trioxide – compound approved for pharmaceutical use by the Food and Drug Administration which provide cancer cell apoptosis [23].

But the quantity and the chemical form of some heavy metals are the major characteristics in being necessary or harmful for organism. Most of these minerals have been demonstrated that have carcinogenic (antimony, arsenic, hexavalent chromium, cobalt, mercury, nickel, vanadium), teratogenic (arsenic), and mutagenic (arsenic, vanadium), allergenic (nickel), and/or endocrine-disrupting (copper, selenium, silver, zinc) effect. Other less known heavy metals, such as thallium – are harmful to the nervous system – especially in children. Mercury, lead, tin, and thallium are toxic to the body, affecting the central nervous system, the bone marrow, the immune system, and also the heart, liver and kidney – organs that are involving in detoxification and excretion of excess or toxic chemicals [23].

Conclusions

Heavy metals are chemicals naturally present into the environment, and some of them are even essential for metabolic pathways.

Ecobiochemistry and xenobiochemistry are sciences that evaluate the metabolic processes from animal or human organisms, regarding the contamination from diet, soil, air, water. Biomagnification is the accumulation of some chemicals in internal organs, and could be characterized by bioaccumulation and biodilution.

Body chelation process and phytoremediation are the best methods to decontaminate the environment and the living organism.

Arsenic, cadmium, chromium, lead, magnesium, manganese, mercury, molybdenum – are considered heavy metals, but some of these are essential nutrients for animal and human organism, being involved in metabolic processes. The toxic effect of heavy minerals has to be evaluated related to other minerals, to the environment concentration, chemical form, bioavailability, temperature, pH, and also to the environmental type: water, soil or air.

References

[1] M. Koller, H.M. Saleh, Introductory Chapter: Introducing Heavy Metals, in Heavy metals, editors: H.M. Saleh, R.F.Aglan, Intechopen, 2018

- [2] U.S. Antarctic Program, 2003-2004 USAP Field Season, Biology & Medicine, International collaborative expedition to collect and study fish indigenous to sub-antarctic habitats, 2003
- [3] M.E. Sears, Chelation: Harnessing and Enhancing Heavy Metal Detoxification – A review, *Scientific World Journal* 2013 (2013) 219840.
- [4] M.E. Sears, K.J. Kerr, R.I. Bray, Arsenic, cadmium, lead and mercury in sweat: a systemic review, *J. Environ. Public Health* 2012 (2012) 184745.
- [5] Agency for Toxic Substances and Disease Registry, Toxicological Profile: Arsenic, 2007.
- [6] K. Watanabe, M.T. Monaghan, Y. Takemon, T. Omura, Biodilution of heavy metals in a stream macroinvertebrate food web: Evidence from stable isotope analysis, *Sci. Environ.* 394 (2008) 57.
- [7] J. Liu, L. Cao, S. Dou, Trophic transfer, biomagnification and risk assessments for four common heavy metals in the food web of Laizhou Bay, the Bohai Sea, *Sci. Total Environ.* 670 (2019) 508.
- [8] I.G. David, M.L. Matache, A. Tudorache, G. Chisamera, L. Rozyłowicz, G.L. Radu, Food chain biomagnification of heavy metals in samples from the lower Prut Floodplain Natural Park, *Environmental Engineering and Management Journal* 11 (2012) 69.
- [9] K. Yang, L. Zhu, Y. Zhao, Z. Wei, X. Chen, C. Yao, Q. Meng, R. Zhao, A novel method for removing heavy metals from composting system: The combination of functional bacteria and absorbent materials, *Bioresource Technology* 293 (2019) 122095.
- [10] M.A. Barakat, New trends in removing heavy metals from industrial wastewater, *Arabian Journal of Chemistry* 4 (2011) 361.
- [11] H. Ali, E. Khan, M.A. Sajad, Phytoremediation of heavy metals – Concepts and applications, *Chemosphere* 91 (2013) 869.
- [12] N. Sarwar, M. Imran, M.R. Shaheen, W. Ishaque, M. Asif, M.A. Kamran, A. Matloob, A. Rehman, S. Hussain, Phytoremediation strategies for soils contaminated with heavy metals: Modifications and future perspectives, *Chemosphere*, 171 (2017) 710.
- [13] Kabata-Pendias, Trace elements in soil and plants, 3rd edition, FL: CRC Press, 2001.
- [14] Agency for Toxic Substances and Disease Registry (ATSDR), US Department of Health and Human Services, Atlanta, GA: Public Health Service, 2008.
- [15] Agency for Toxic Substances and Disease Registry (ATSDR), Public Health Service, Atlanta, US Department of Health and Human Services, Toxicological profile of lead, 1999.
- [16] S.J.S. Flora, G.J.S. Flora, G. Saxena, Environmental occurrence, health effects and management of lead poisoning, in *Lead: Chemistry, analytical aspects, environmental impacts and health effects* (S.B. Casca, J. Sordo – Eds.), Netherlands: Elsevier Publication, 2006, pp. 158-228.
- [17] T.W. Lane, M.A. Saito, G.N. George, I.J. Pickering, R.C. Prince, F.M. Morel, Biochemistry: A cadmium enzyme from a marine diatom, *Nature* 435 (2005) 7038.
- [18] P.B. Tchounwou, C.G. Yedjou, A.K. Patlolla, D.J. Sutton, Heavy metals toxicity and the environment, *Molecular, Clinical and Environmental Toxicology* 101 (2012) 133.
- [19] S. Satarug, J.R. Baker, S. Urbenjapol, M. Haswell-Elkins, P.E. Reilly, A global perspective on Cd pollution and toxicity in non-occupationally exposed population, *Toxicol. Lett.*, 137 (2003) 65.
- [20] C.M. Gallagher, J.S. Kovach, J.R. Meliker, Urinary cadmium and osteoporosis in US women \geq 50 years of age: NHANES 1988-1994 and 1999-2004, *Environ. Health Perspect.* 126 (2008) 1338.
- [21] P. Bhattacharya, A.H. Welch, K.G. Stollenwerk, M.J. McLaughlin, J. Bundschuh, G. Panaullah, Arsenic in the environment: biology and chemistry, *Sci. Total Environ.* 379 (2007) 109.
- [22] M.P. Pothier, A.J. Hinz, A.J. Poulain, Insights into arsenite and arsenate uptake pathways using a whole cell biosensor, *Front. Microbiol.*, 9 (2018)
- [23] P.B. Tchounwou, A.K. Patlolla, J.A. Centeno, Carcinogenic and systemic health effects associated with arsenic exposure – a critical review, *Toxicol. Pathol.* 31 (2003) 575.

VOCs EMISSION ON THE ALUMINUM SHEETS PAINTING LINE

Snežana Aksentijević¹, Jelena Kiurski², Jelena Golubović¹

¹College of Applied Sciences, Trg Svetog Save 34, 31000 Užice, Serbia,

²University Business Academy in Novi Sad, Faculty of Economics and Engineering Management,
Cvećarska 2, 21000 Novi Sad, Serbia

e-mail: sneza.aksentijevic@gmail.com

Abstract

During technological processes, pollutants are emitted into factories, pollute the working environment and transferred to the environment. Many pollutants emitted do not remain in one segment of the environment, but are transmitted from one medium to another and also affect the quality of air, water and soil. This paper describes the technological process of applying paints and coatings to aluminum rolled sheets and the procedures undertaken to remove and minimize organic volatile compounds - VOCs. Waste gas testing was conducted twice a year, in three individual samples, under the highest workload of stationary sources, over a period of 5 years. Based on the measured concentrations of total organic carbon, it was concluded that all values obtained were within the permitted limits prescribed by the Air Protection Act of the Republic of Serbia.

Key words: Aluminium rolled sheet, painting, pollutants emission, VOCs

Introduction

VOC is any organic compound having an initial boiling point equal to or less than 250°C at a standard pressure of 101.3 kPa. It can be natural or artificial. Emissions of highly volatile organic compounds - VOCs, have a short-term and / or long-term adverse effect on humans and the environment [1]. For this reason, the industry is taking a number of measures to reduce the emissions of these gases. The aluminum rolled sheets dyeing line consists of: degreasing of rolled sheets intended for dyeing, chemical preparation, application of dyes and dyes fired. The Bylaws of the Air Protection Act set the limit values for the emission of harmful and dangerous substances in the air at the place of the source of pollution, the manner and deadlines for measuring and recording data on the performed measurements of emissions. Permissible exposure limit (PEL) is the highest permissible level of pollutant in the air, established on the basis of scientific knowledge, in order to avoid, prevent or reduce harmful effects on human health and / or the environment. The conditions for performing the emission measurements (appropriate sampling points, safe access to sampling points, necessary facility data, etc.) are provided by the operator, and the measurements themselves are carried out by expert organizations authorized to measure emissions [2].

In the degreasing technological operation, the unpainted strip passes through 4 tubs cascaded, so that water from tub 4 is used to replenish tub 3 and from it when 2 and then 1 [3]. At the end of the degreasing process, there is a dryer that serves to completely dry the tape after exiting the squeeze roller. After drying, a defined layer of chemical to passivate the unpainted tape is applied to the horizontal device for chemical preparation in a closed system. After passivation, the tape is dried, cooled and switched to a technological dyeing operation [3]. A primer is applied to one or both surfaces of the tape by rollers with a rubberized coating in a paint application chamber, in the thickness of 5-15 µm. In the coating process, polyester, polyurethane, PVDF and epoxy paints, varnishes, solvents, and thinners are used for the coating process. After application, the primer is fired in furnaces (in four zones) at a

temperature of 216-241 °C [3]. Figure 1 shows a technological diagram of the process of dyeing aluminum sheets.

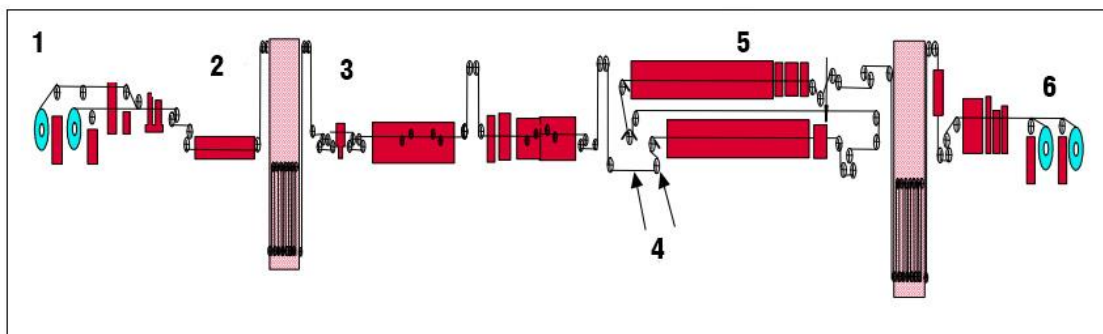


Figure 1. Technological scheme of dyeing aluminum rolled sheets

1 - sheet entry, 2 - degreasing, 3 - chemical preparation, 4 - dyeing chamber, 5 - firing furnaces, 6 - output

The firing temperature is achieved with the help of a natural gas burner. Part of the air used for the operation of the burner is supplied by a ventilation system from the chamber to apply a wet coating. The chamber air contains VOCs compounds that evaporate at ambient temperature as the paint rolls and cleans. Exhaust gases generated during the coating process are routed to the incinerator. The main function of incinerators is to control the process after combustion of waste gases and to reduce VOCs emissions. The temperatures at which incineration is carried out are between 590-1200 °C. Based on the data at a gas holding time of 0.75 seconds, 98% of the VOCs would be combusted and thus the VOC emission level would reach 20 mg / m³, the incineration temperature should be 870 °C. According to the regulations in force in the Republic of Serbia, the limit value for the emission of VOCs into the atmosphere is 50 mg/Nm³. By reducing the incineration temperature, the degree of VOCs conversion of the compound decreases exponentially [4].

Experimental

Measurement of VOCs emission was performed by measuring devices (GLOBUS, Italy) using prescribed and documented methods of measurement and standards - the continuous method of flame ionization detection (SRPS EN 12619: 2013 [5]). The basic goal of any sampling and measurement technique is to provide an air sample that is representative. Comparison of measured pollutant concentrations with emission limit values is a key element in any emission measurement. Accurate and reliable documented results are necessary to accurately determine measures to reduce the adverse environmental impact of the plant or broadcasters [2]. The results of the emission measurements, reduced to dry waste gas, standard conditions and reference oxygen content, are compared with the emission limit values. For comparison with the emission limit values, the measurement results expressed as mass concentrations of pollutants in the flue gas are calculated per unit volume of dry or wet flue gases, normal conditions (273.15 K and 101.3 kPa) and the oxygen reference fraction in the flue gas, unless otherwise specified [2].

Measurements were made twice a year (in the first half of the year - measurement I and in the second half of the year - measurement II), three samples were taken for each measurement.

Table 1. Overview of pollutant limit values [4]

Pollutant	Design value
VOC (organic compound expressed as total carbon)	<30 mg/Nm ³

Pollutants measured in waste gas from the dye line emitter were determined on the basis of the Decree on the list of industrial plants and activities controlling the emission of volatile organic compounds, the emission values of volatile organic compounds at a given solvent consumption and the total allowable emissions, as and emission reduction schemes (Annex 5, Item 7, Coating Solvent Consumption Coils > 25 t/year) [6]. Table 2 shows the results of periodic measurements on the emitter of the dye line from 2013 to 2018 at the Impol Seval plant in Sevojno.

Table 2. Results of periodic measurements of VOC emission at the emitter of the Dye Line [4]

Period of time measurements	Sample 1 (mg/Nm ³)	Sample 2 (mg/Nm ³)	Sample 3 (mg/Nm ³)	GVE [6] (mg/Nm ³)
I period 2013.	9 ± 0,45	11 ± 0,55	14 ± 0,70	50
II period 2013.	6 ± 0,30	10 ± 0,50	16 ± 0,80	
I period 2014.	3,50 ± 0,14	3,90 ± 0,16	4,10 ± 0,16	
II period 2014.	6,10 ± 0,30	6,90 ± 0,35	7,50 ± 0,38	
I period 2015.	1,76 ± 0,09	2,10 ± 0,11	2,60 ± 0,13	
II period 2015.	5,45 ± 0,27	6,10 ± 0,31	6,30 ± 0,32	
I period 2016.	21,5 ± 11,5	21,2 ± 11,5	20,1 ± 11,5	
II period 2016.	7,32 ± 0,37	7,08 ± 0,35	5,76 ± 0,29	
I period 2017.	7,52 ± 0,49	8,86 ± 0,57	7,15 ± 0,46	
II period 2017.	19,1 ± 1,2	10,5 ± 0,7	14,4 ± 0,9	
I period 2018.	38,0 ± 2,5	46,1 ± 3,0	43,6 ± 2,8	

Table 2 shows an increase in the measured values of VOCs emissions since during this period the beginning of the heating season and the increased combustion of furnaces, the operation of car engines and industrial plants contributes to the increase of the values of volatile organic compounds. The air quality assessment is done by the Environmental Protection Agency on the entire territory of Serbia and is done by analyzing the average annual values of pollutants. Along with the average annual values, the exceedances of the daily and hourly limit values of individual pollutants are monitored, and these results are good indicators of cleaner production.

The process of dyeing aluminum sheets carries out the process of cleaner production and with the aim of saving, reducing the environmental impact and fulfilling the legal obligations in the field of environmental protection. Cleaner production in production processes involves the more rational use of raw materials, water and energy, the replacement of hazardous raw materials by more environmentally friendly ones, and the reduction of emissions and toxicity of emissions and waste into water, air and soil. The emission values in the flue gases according to the above regulation for the consumption of solvents greater than 25t/year are 50 mg/Nm³ and from the presented results it has not exceeded the permitted value in any measurement in the period of 5 years. It is observed that the concentrations in the last year of measurements are significantly higher than the previous measurements.

Conclusion

The Law on Air Protection (“Official Gazette of the RS” No. 36/2009 [7] and No. 10/2013 [8]) industrial pollutants in Serbia are obliged to report annually on emissions of harmful gases released into the environment and to pay certain environmental taxes accordingly. In particular, Article 45 of this Law defines the use of organic solvents. A legal entity and an entrepreneur using organic solvents in their production process is obliged to implement measures to reduce the emission value of volatile organic compounds below the prescribed values.

Based on the results of the test of the waste gases on the dyeing line for a period of 5 years, there was no exceeding of the prescribed emission limit value. The techniques used for the removal of volatile organic compounds are sufficient to purify the waste gases and avoid the pollution of atmospheric air at this stage of processing of aluminum and its alloys. Reducing the amount of pollutants released today is a basic form of air protection. The installation of filters and special exhaust and smoke purification plants at factory plants can produce good results. A special group of air protection measures are greening actions in the area where the air pollution occurs.

References

- [1] A. M. Stojić, “Analysis of the Distribution and Dynamics of Volatile Organic Compounds and Aerosols in the Troposphere”, Belgrade (2015) pp. 20-24
- [2] Official Gazette of RS, No. 5/2016 - Regulation on measurements of pollutant emissions into the air from stationary sources of pollution
- [3] Impol Seval a.d. Assessment and Impact Study (2018) Sevojno
- [4] Emission Measurement Reports at Impol Seval a.d. (2018) Sevojno
- [5] SRPS EN 12619: 2013 - Stationary source emissions - Determination of mass concentration of total gaseous organic carbon - Continuous flame ionization detector method
- [6] Official Gazette of RS, No. 100/2011 - Regulation on the list of industrial plants controlling the emission of volatile organic compounds, on the emission values of volatile organic compounds at specified solvent consumption and on the total allowable emissions, as well as emission reduction schemes
- [7] Official Gazette of RS, No. 36/2009
- [8] Official Gazette of RS, No. 10/2013

Zn-METALLOPORPHYRINS CONTAINING PYRIDYL GROUPS AND THEIR COMPARATIVE CAPACITY TO COORDINATE HEXACHLOROPLATINIC ACID

**Diana Anghel^{1*}, Anca Lascu¹, Ion Fratilescu¹, Camelia Epuran¹,
Eugenia Fagadar-Cosma¹**

¹*Institute of Chemistry "Coriolan Dragulescu", M. Viteazul Ave. 24, 300223-Timisoara, Romania, Tel: +40256/491818; Fax: +40256/491824*

^{*}*email: dianaracanel@yahoo.com*

Abstract

Two Zn-metalloporphyrins, both containing at least one-pyridyl group, were studied regarding their capacity to complex hexachloroplatinic acid comprised in leaching solutions and resulted after hydrometallurgical processes on spent automotive catalysts. The number of pyridyl groups and the steric and electronic influences from surrounding groups determine a different type of coordination with the hexachloroplatinic acid from solution, and surprisingly, although containing only one group of basic pyridyl, the unsymmetrical Zn(II)-5-pyridyl-10,15,20-tris-(3,4-di-methoxy-phenyl)-porphyrin had a removal capacity of 98% higher than that of Zn(II)-*meso*-tetrakis-pyridylporphyrin, substituted with four pyridyl groups, but with only a removal capacity of 84 % .

Introduction

The platinum is an expensive and rare element, so that its recovery must be appropriately considered. Several compounds are able to generate complexes with hexachloroplatinic acid. Among them, metalloporphyrins, due to their capacity to coordinate ligands at the metal centers [1], have to be analyzed. In this study, Zn(II)-tetrakis-pyridylporphyrin and Zn(II)-5-pyridyl-10,15,20-tris-(3,4-di-methoxy-phenyl)-porphyrin were investigated for their capacity to form complexes with hexachloroplatinic acid.

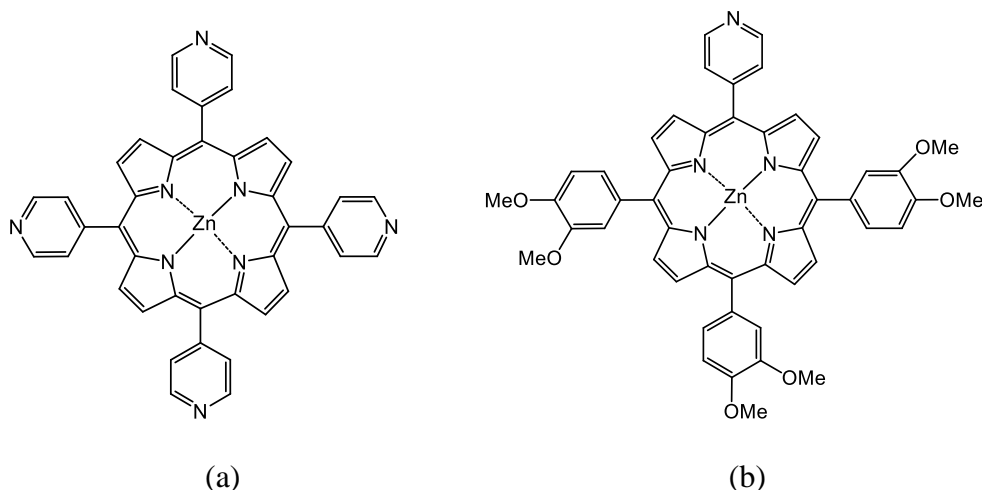


Figure 1. Structure of the investigated compounds: Zn(II)-tetrakis-pyridylporphyrin (a); Zn(II)-5-pyridyl-10,15,20-tris-(3,4-di-methoxy-phenyl)-porphyrin (b)

Materials and methods

Reagents. The Zn(II) metalloporphyrins were obtained in our laboratory and reported previously [2, 3]. N,N-Dimethylformamide was aquired from Merck (Darmstadt, Germany), hexachloroplatinic acid was obtained from Sigma-Aldrich (St. Louis, USA).

Methods. In the first case of Zn(II)-tetrakis-pyridylporphyrin, the experiments were performed by taking 5 mL porphyrin in DMF ($c = 4.49 \times 10^{-6}$ M) and adding at each step 0.05 mL hexachloroplatinic acid solution in water of 1.03×10^{-3} M concentration. Each mixture was stirred for 2 minutes and after, the UV-vis spectrum was recorded.

In the second case regarding Zn(II)-5-pyridyl-10,15,20-tris-(3,4-di-methoxy-phenyl)-porphyrin the method was similar but the porphyrin concentration was 1.192×10^{-5} M in DMF. The hexachloroplatinic acid concentration was the same. The amounts of hexachloroplatinic acid that were added differed from one sample to another.

Apparatus. For recording UV-visible spectra, standard 1 cm pass quartz cells were used on a JASCO UV- V-650 spectrometer (Japan).

Results and Discussions

The superposed spectra for the successive adding of chloroplatinic acid to the solution of the Zn(II)-tetrakis-pyridylporphyrin (Zn-TPyP) are presented in Figure 2, and to the Zn(II)-5-pyridyl-10,15,20-tris-(3,4-di-methoxy-phenyl)-porphyrin (Zn-Py-3,4diMeOPP), respectively in Figure 3.

As can easily be seen, the UV-vis spectrum of Zn-TPyP (figured in black) has the main characteristics of a metalloporphyrin, the Soret band around 425 nm and only two Q bands (due to higher symmetry), located at 575 nm and 625 nm respectively. In the course of increasing the hexachloroplatinic acid concentration, some changes are occurring, as follows: all the absorption bands are blue shifted with around 15 nm, and all the bands are suffering a hyperchromic effect.

Many isobestic points are accompanying these changes (at 412 nm, 545 nm, 605 and 615 nm), proving that a lot of equilibrium processes are taking place and the complex formation can be explained on the pyridyl groups protonation, that are alternatively forming and breaking.

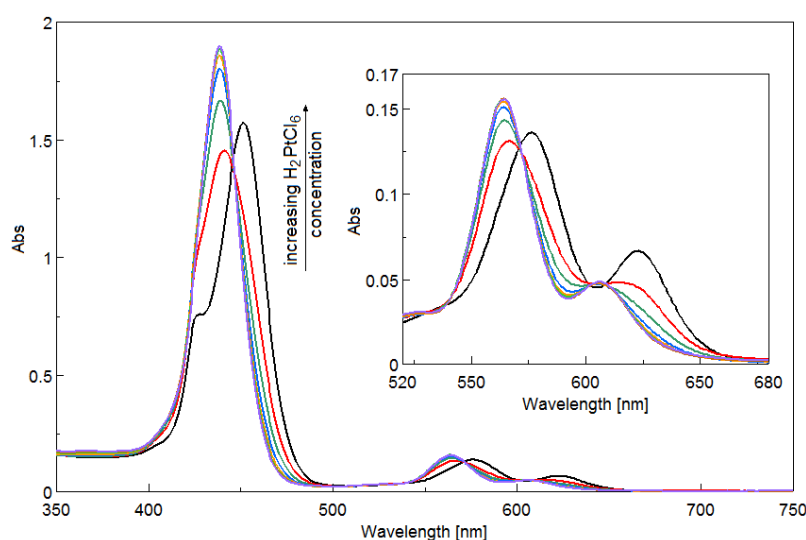


Figure 2. Overlapped UV-vis spectra after adding H_2PtCl_6 solution in water to Zn-TPyP solution in DMF. Details of the Q bands

A completely different phenomenon is produced regarding Zn-Py-3,4diMeOPP. In this case by increasing the hexachloroplatinic acid concentration the Soret band decreases in intensity and also the two Q bands. Only three isobestic points are appearing at 405 nm and around 440 nm, on both branches of Soret and on the Q band at 640 nm (Figure 3).

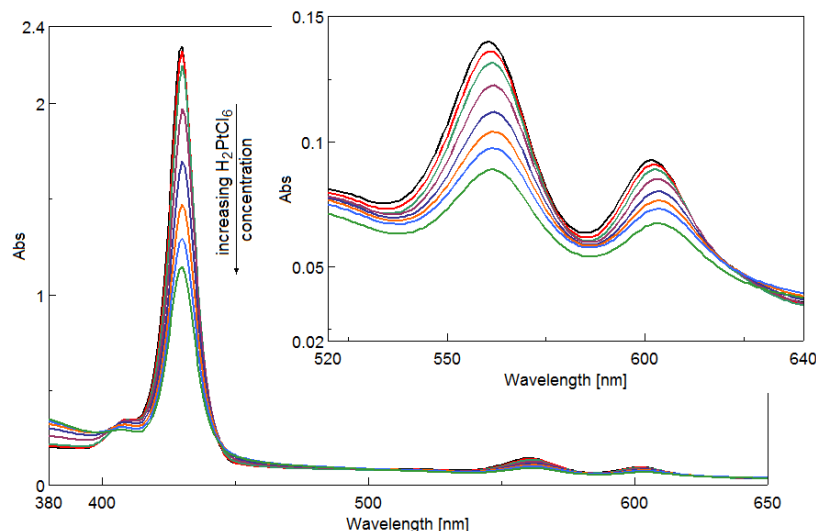


Figure 3. Overlapped UV-vis spectra after adding H_2PtCl_6 solution to a solution of Zn-Py-3,4diMeOPP in DMF. Detail of the isosbestic point at 640 nm

The dependences (polynomial and linear) between the intensity of absorption read at the Soret wavelength maxima and the H_2PtCl_6 concentration for the two Zn-metalloporphyrins porphyrins studied here are shown in Figure 4 a and b.

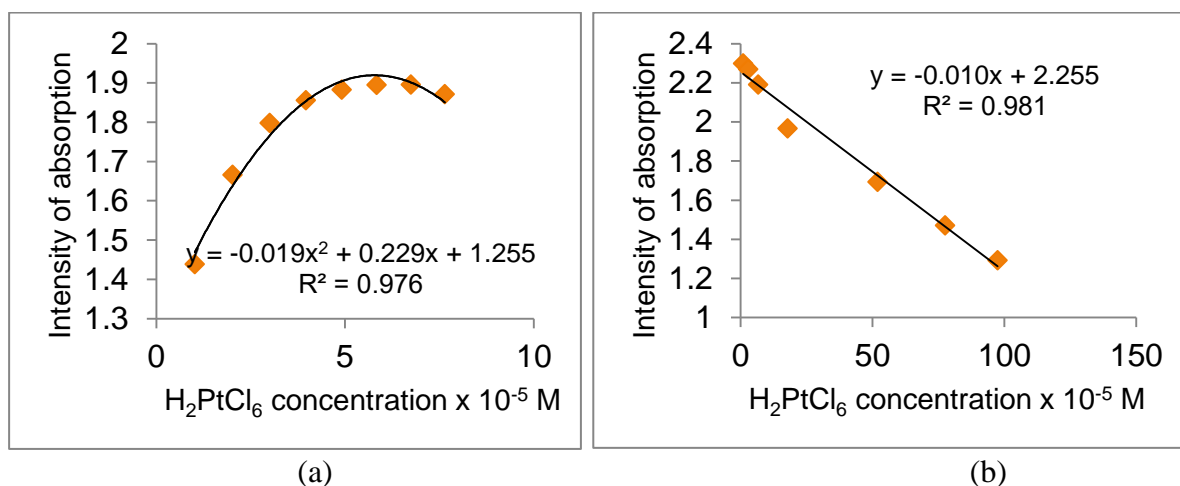


Figure 4. Polynomial a) and linear b) dependence between the intensity of absorption read at Soret maximum wavelength and the H_2PtCl_6 concentration in case of using Zn(II)-tetrakis-pyridylporphyrin (a) and Zn(II)-5-pyridyl-10,15,20-tris-(3,4-di-methoxy-phenyl) porphyrin (b)

It can be observed that the plateau is obtained by Zn(II)-tetrakis-pyridylporphyrin at a very low concentration of hexachloroplatinic acid up to 5×10^{-5} M, but the interference between the unsymmetrical Zn(II)-5-pyridyl-10,15,20-tris-(3,4-di-methoxy-phenyl) porphyrin and H_2PtCl_6 has a twentyfold wider domain up to 100×10^{-5} M.

The removal capacity of Pt colloidal particles from solution can be calculated according to the formula [4]:

$$\text{Removal capacity (\%)} = \frac{(C_0 - C_e)}{C_0} \times 100$$

In our case the removal capacity is 84.867 % for Zn(II)-tetrakis-pyridylporphyrin and 98% for Zn(II)-5-pyridyl-10,15,20-tris-(3,4-di-methoxy-phenyl) porphyrin, result that is surprising, due to the large number of basic molecules of the Zn(II)-tetrakis-pyridylporphyrin.

The obtaining of the desired Pt nanoparticles from the complexes that were formed with Zn-metalloporphyrins, was done in each case, by adding 4.55 mL of NaBH₄ solution in water ($c = 7.077 \times 10^{-3}$ M) (a tenfold more concentrated NaBH₄ solution than the expected concentration of Pt) to 5.5 mL of each complex solution. When NaBH₄ was added under stirring, almost instantly an intense brown colloidal solution was formed. After a few seconds, the particles of Pt were observable with the naked eye.

Conclusion

Two Zn-metalloporphyrins, both containing pyridyl groups, were tested regarding their capacity to complex hexachloroplatinic acid resulted in leaching solutions after hydrometallurgical processes on spent automotive catalysts. Although it was believed that the bigger number of pyridyl groups will be a benefit for complexation, it was surprisingly found that the loss of planarity, the steric and electronic inductive donor influences from the surrounding -OCH₃ groups determine a better coordination with the hexachloroplatinic acid for the unsymmetrical Zn(II)-5-pyridyl-10,15,20-tris-(3,4-di-methoxy-phenyl)-porphyrin that had an excellent removal capacity of 98%, based on axial coordination on Zn atom.

Acknowledgements

The authors are acknowledging UEFISCDI PN-III-P1-1.2-PCCDI-2017-1-Project ECOTECH-GMP 76PCCDI/2018 and the Romanian Academy for financial support in the frame of Programme 3/2019 from ICT.

References

- [1] A. Lascu, M. Birdeanu, B. Taranu, E. Fagadar-Cosma, Journal of Chemistry, (2018) 1-11, DOI:10.1155/2018/5323561
- [2] E. Fagadar-Cosma, C. Enache, I. Armeanu, G. Fagadar-Cosma, Dig. J. Nanomater. Bios., 2 (2007) 175 – 183
- [3] E. Fagadar-Cosma, E. Tarabukina, N. Zakharova, M. Birdeanu, B. Taranu, A. Palade, I. Creanga, A. Lascu, G. Fagadar-Cosma, Polym. Int., 65 (2016) 200–209, DOI: 10.1002/pi.5047
- [4] D. Vlascici, I. Popa, V.A. Chiriac, G. Fagadar-Cosma, H. Popovici, E. Fagadar-Cosma, Chem. Cent. J.7 (2013) 111-118.

SYNTHESIS AND CHARACTERIZATION OF SENSITIVE COMPONENTS: N-TYPE BINARY OXIDES (TiO₂, ZnO) AND P-TYPE CREDNERITE (CuMnO₂) FOR AMPEROMETRIC SENSOR

Cornelia Bandas, Maria Poienar, Paulina Vlazan, Corina Orha, Daniel Ursu, Carmen Lazau

*National Institute for Research and Development in Electrochemistry and Condensed Matter,
Condensed Matter Department, no 144 A. Paunescu Podeanu Street,
Timisoara 300569
e-mail: carmen.lazau@google.com*

Abstract

In the last years, an increasing number of oxides were investigated for detection of low gases concentrations from environment. More binary oxides with energy band gap between 2-4 eV (TiO₂, Nb₂O₅, Ta₂O₅, ZnO, SnO₂ and WO₃), when used with large specific surface area, present an *n-type* behavior like response to introduction of gases in small concentrations in ambient air. Other binary oxides as NiO, CuO, Cr₂O₃, Co₃O₄ and Mn₃O₄, and also the crystalline structures type perovskites (BaTiO₃, SrTiO₃, LaFeO₃₀) or crednerite (ABO₂, ex. CuMnO₂) presents an *p-type* characteristics for detection of gas traces in the environment.

The synthesis methods of heterostructured oxide materials, used in the specialized literature, have sought to obtain perfect structures with a high degree of homogeneity. As the morphology and structure of oxide material play an important role in their functional properties, lately, many efforts have been focused to choose the best synthesis method and the “design” of heterostructures of different architectures. The reason of these researches is mainly to demonstrate the fact that studied materials can be obtained by different methods, so to present interesting properties for proposed application field and to lead to achieving of new devices with new and improved functionality, and also synthesis technologies for sensitive modules.

In this study, we report the synthesis and characterization of *n-type* (TiO₂, ZnO) and *p-type* (CuMnO₂) semiconducting components, by hydrothermal methods at low temperatures and pressures using different precursors soluble in water. For obtaining oxide powders and crednerite materials, with morphology and desired size (nano and micro) for crystallite, will be used different synthesis conditions, varying the precursors, temperatures, pressures, synthesis times and/or solution pH. The obtained materials will be characterized by specific methods: crystalline phase of TiO₂ particles will be identified by X-ray diffraction (XRD), surface morphology and qualitative analysis by atomic force microscopy (AFM) and scanning electron microscopy (SEM), band gap determination with UV-VIS spectroscopy, and thermal stability by TG-DTA analysis. Based on these materials will be obtained some heterostructures *p-n* for development to a sensor with characteristics of diode.

Acknowledgements

This work was supported by a grant of the Roumanian Ministry of Research and Innovation PN 19 22 04 01, Contr. Nr. 40N/2019, “New technologies applied in development of sensor devices for environment monitoring”

TEMPERATURE EFFECT ON CO₂ ADSORPTION-DESORPTION PROCESS OF DIFFERENT FUNCTIONALIZED MESOPOROUS MATERIALS

Silvana Borcanescu, Alexandru Popa, Orsina Verdes, Mariana Suba

*"Coriolan Drăgulescu" Institute of Chemistry, Blvd. Mihai Viteazul no. 24
300223 Timișoara, Romania,
e-mail: silvana.borcănescu@gmail.com*

Abstract

In this paper was studied the adsorption-desorption of CO₂ and the effect of temperature on amino-functionalized mesoporous materials by using temperature programmed desorption – TPD method. The adsorption of CO₂ and its TPD method was investigated using thermogravimetric analysis coupled with a Pfeiffer-Vacuum-Thermo Star mass spectrometer. For this purpose MCM-41, SBA-15 and SSBA-15 functionalized mesoporous materials were prepared and investigated at different adsorption-desorption temperatures: 50, 60, 70 and 80°C. These composites were also characterized from the structural point of view: FT-IR spectroscopy and nitrogen physisorption at 77K.

Introduction

Mesoporous molecular sieves have been used as adsorbents, catalysts support, and heterogeneous catalysts in various applications [1, 2]. MCM-41 has great properties like uniform hexagonal cylindrical pore system, tunable pore size (15-100 Å), high surface area (>700 m²/g), large pore volume (≥0.7 cm³/g), large number of silanol groups (~40–60%), negligible pore blocking effect, high surface reactivity and good hydrothermal, chemical and mechanical stability [3,4]. Due to investigations from previous years SBA-15 like MCM-41, presents also interesting properties like large surface areas (600–1000 m²/g), well-defined pore structure with variable pore diameters (50-300 Å) [5] and a highly ordered hexagonal mesostructure.

Modifying these materials with different organic groups (thiol, vinyl, amine, phenyl, propyl) has attracted much attention in recent years [6, 7]. Supported amine functionalized mesoporous silica presents a very great interest for CO₂ capture process due to very high selectivity towards CO₂ at low partial pressure, wide range of temperature [8, 9], adjustable uniform pore size, and facile surface functionalization schemes available [10, 11].

These materials have recently emerged as a promising class of solid adsorbents that can effectively adsorb CO₂ and regenerated using variety of approaches [12]. The present study was carried out to see how the temperature influences CO₂ adsorption-desorption process on these amino functionalized materials.

Experimental

Preparation of molecular sieves

MCM41 and SBA15 molecular sieves were tested from the adsorption-desorption point of view using TPD method. These molecular sieves were prepared by grafting, using 3-aminopropyl triethoxy silane as functionalization agent. MCM41 and SBA15 were functionalized by 3-aminopropyl-triethoxysilane. In a typical reaction, 1g of MCM41 or SBA15 was added in 50 mL toluene and the mixture was stirred for an hour. After that an excess of 3.39 mmol of (C₂H₅O)₃Si(CH₂)₃NH₂ was added and refluxed overnight. The white solid was removed from solvent by filtration washed with toluene and water and finally dried for 8 h under reduced pressure at 70 °C. A different sample named SSBA15 was prepared by the hydrolysis of tetraethyl orthosilicate using as surfactant a P123 block copolymer and 1-

phenyldecane as swelling agent. The synthesis of SSBA15: 4.6 g of Pluronic P123 was dissolved in 145 mL of HCl solution and stirred at 40 °C until the solution became clear. Then, 9.0 g of 1-phenyl-decane was added to the solution with stirring at 40 °C for 1 h. Finally, 0.05 g of NH_4F was added under stirring, followed by 9.0 g of TEOS. The above mixture was stirred at 40 °C for 24 h and then transferred to an autoclave for further reaction at 100 °C for 48 h.

The difference between the synthesis of SSBA15 and the synthesis of SBA15 is the presence of 1-phenyl-decane used as swelling agent. Modified SSBA15 was functionalized first by a silane coupling agent 3-glycidyl-oxypropyl-trimethoxysilane and finally by an amination reagent: ethylene diamine (N_2). The role of the amine used was to improve the CO_2 adsorption performance.

Methods

The resulted composites were characterized by thermal analysis using TGA/SDTA 851-LF 1100 Mettler apparatus. The thermal analysis system was coupled with a Pfeiffer—Vacuum—Thermo Star mass spectrometer by silica capillary at temperature of 200 °C. Adsorption measurements were carried out using the same thermogravimetric analyzer connected to a gas delivery manifold. High-purity CO_2 and 30% CO_2 in N_2 at 1 atm. was used for the adsorption runs, and N_2 was used as a regenerating purge gas for CO_2 desorption. In a typical adsorption –desorption run, a blank test of the empty sample container was performed at 25 °C in N_2 stream with a flow rate of 50 mL min^{-1} . Afterwards, the sample are weighed and placed in the sample container. The samples with mass of about 20 mg were placed in alumina crucible of 150 μL . The measurements were performed in dynamic air atmosphere with the flow rate of 50 mL min^{-1} , in the temperature range of 25–650 °C with a heating rate of 10 °C min^{-1} . Each sample was first pretreated in flowing N_2 at 150 °C, then cooled to the desired adsorption temperature (50-60-70-80°C), and exposed to 30% CO_2/N_2 (70 mL/min) for 120 min. The CO_2 adsorption capacity of the adsorbent in milligrams of CO_2 per gram of adsorbent was calculated from the mass gain of the sample in the adsorption process.

The FTIR absorption spectra were obtained with: Jasco 430 spectrometer in the 4000 - 400 cm^{-1} range, using KBr pellets.

The results in case of textural characteristics of the outgassed samples were obtained using Nova 2000 Quantachrome instrument series, $\text{N}_2(\text{g})$ adsorption-desorption technique.

Results and discussion

Infrared spectroscopy

The FTIR spectra of each sample were recorded and confirmed that SBA15 sil was successfully functionalized with ethylene diamine (not shown). The typical band of stretching vibration of Si-O-Si group in the silica structure appears at 1080, 800 and 461 cm^{-1} . The broad absorption band centered around 3440 cm^{-1} and a weak absorption band at 1630 cm^{-1} indicates the presence of water due to the absorbed water molecules in the sample, and belongs to the bending vibrations of H-O-H. The present bands at $1636\text{--}1522 \text{ cm}^{-1}$ on the IR spectra of SSBA15sil+N₂ were assigned to N–H stretching vibrations and N–H bending vibrations, respectively, providing evidence of the successful grafting of ethylene diamine onto SSBA15sil.

Specific surface area

The pore parameters of amino-functionalized molecular are listed in Table 1. The data reveal that the surface areas of MCM41 and SBA15 decreased after modification with 3-aminopropyltriethoxy silane (SBA15 sil and MCM41 sil samples). The reductions in surface

areas can be attributed to the increase in agglomeration of silica particles and/or occupation of pores after modification.

Table 1. Textural properties of the studied composites

No.	Sample	Specific surface area (m ² /g)	Pore volume BJH _{Des} (cc/g)	Average pore diameter BJH _{Des} (nm)
1.	SBA15	725.0	1.19	6.64
2.	SBA15 sil	288.8	0.664	6.63
3.	SSBA15	766.5	1.294	6.62
4.	SSBA15 sil +N ₂	224.8	0.337	5.49
5.	MCM41	1299.7	0.695	3.30
6.	MCM41 sil	655.8	0.611	3.25

Thermal analysis

From thermal analysis in case of SSBA15 sil+N₂ the endothermic effect at 64 °C corresponds to the removal of small amounts of physically adsorbed water (Figure 2.). The mass loss represented by the peaks at 248 °C and 301 °C is due to the oxidation and the decomposition of amino propyl functional groups meaning that this material could be used for adsorption of CO₂ at temperatures below 250 °C.

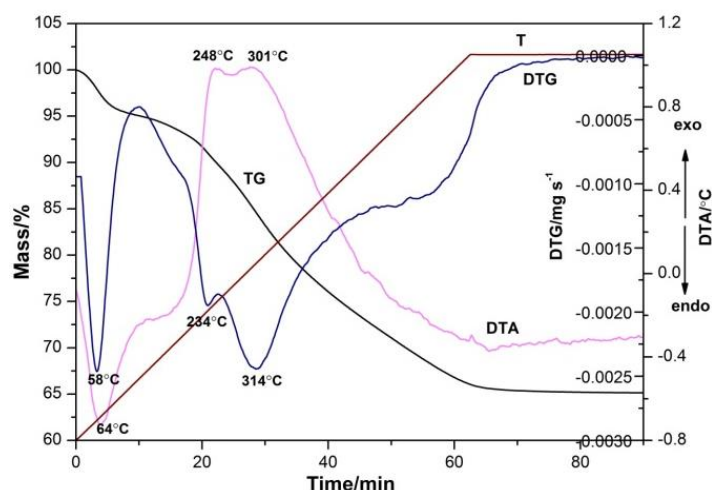


Figure 2. TG-DTG-DTA curves of SSBA15 sil + N₂ composite.

For a possible use of these amino-functionalized molecular sieves as sorbents for CO₂ removal, their adsorption–desorption properties towards CO₂ were also investigated by TPD method. The adsorption-desorption of CO₂ and its TPD method using thermogravimetry were studied for amino-functionalized molecular sieves (Figure 3.)

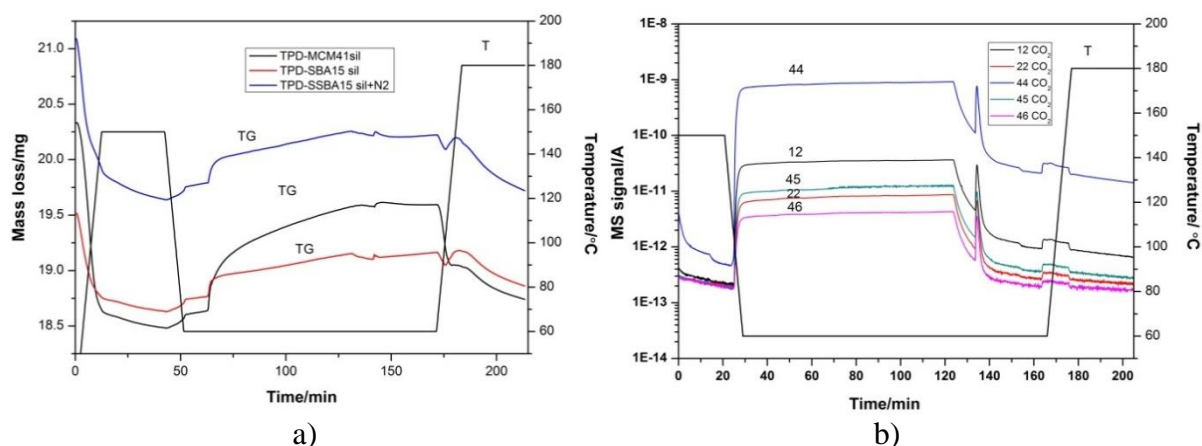


Figure 3. CO₂ adsorption-desorption steps of functionalized composites with isotherms at 60 °C (a) and MS analysis spectra of MCM41 sil at 60 °C(b).

Table 2. The amounts of the captured CO₂ on molecular sieves at different temperatures.

No.	Sample	$n_{CO_2}/g\ SiO_2/mmole/g\ SiO_2$			
		50°C	60°C	70°C	80°C
1.	MCM41sil	3.01	3.32	2.18	2.88
2.	SBA15 sil	0.86	1.23	1.09	0.79
3.	SSBA15 sil+N2	1.77	1.96	1.73	0.16

The CO₂ adsorption capacity of the adsorbent in mmol of CO₂ per gram of adsorbent could be seen from the mass gain of the sample in the adsorption process (Figure 3a) and was calculated more accurate from the mass loss during the desorption step. In Table 2, the amounts of the captured CO₂ on the composites are shown. The best result was obtained with MCM41 sil and SSBA15 sil+N2 samples and the optimal temperature for CO₂ adsorption-desorption by TPD results to be 60 °C.

The evolved gases during the adsorption-desorption of CO₂ on amino-functionalized molecular sieves were identified by online mass spectrometry coupled with thermogravimetry. As expected, the main compound observed in the evolved gases on MS spectra of amino-functionalized molecular sieves is CO₂ (Figure 3b).

Conclusion

In this paper was investigated the temperature influence over adsorption-desorption of CO₂ on amino-functionalized mesoporous materials using TPD method.

CO₂ adsorption-desorption of functionalized samples was studied for samples temperature ranging between 50-80 °C. The best result was obtained with MCM41 sil and SBA15sil+N2 composites and the optimal temperature for CO₂ adsorption-desorption by TPD results to be 60 °C.

The mass loss of SSBA15 sil+N2 above 250 °C is due to the decomposition of amino propyl functional group. This means that these amino-functionalized mesoporous materials are thermally stable below this temperature and can be used as sorbents for CO₂ as resulted from the mass spectroscopy.

References

- [1] J. Abolfazl, A.A.M. Seyed, B. Bahamin, M. Amin, J. Porous. Mater. 19 (2012) 979.

- [2] X. Sheng, J. Kong, Y. Zhou, Y. Zhang, Z. Zhang, S. Zhou, Microporous Mesoporous Mater. 187 (2014) 7.
- [3] J.S. Beck, J.C. Vartuli, W.J. Roth, M.E. Leonowicz, C.T. Kresge, K.D. Schmitt, C.T.W. Chu, D.H. Olson, E.W. Sheppard, J. Am. Chem. Soc. 114 (1992).
- [4] P. Selvam, S.K. Bhatia, C.G. Sonwane, Ind. Eng. Chem. Res. 40 (2001) 3237.
- [5] D. Zhao, J. Feng, Q. Huo, N. Melosh, G.H. Fredrickson, B.F. Chmelka, G.D. Stucky, Science 279 (1998) 548.
- [6] X. Wang, J.C.C. Chen, Y-H. Tseng, S. Cheng, Microporous Mesoporous Mater. 95 (2006) 57.
- [7] Y. Wang, B. Zibrowins, C-M. Yang, B. Spliethoff, F.Schuth, Chem Commun. (2004) 46.
- [8] D. Wang, X. Wang, X. Ma, E. Fillerup, C. Song, Catal. Today, 233 (2014) 100.
- [9] N. Gargiulo, A. Peluso, P. Aprea, F. Pepe, D. Caputo, J.Chem. Eng. Data 59 (2014) 896.
- [10] T. Asefa, Z. Tao, Can. J. Chem. 90 (12) (2012) 1015.
- [11] C. Chen, S. Zhang, H. R. Kyung, W-S. Ahn, 26 (2017) 868.
- [12] P. Bollini, S. A. Didas, C.W Jones, 2011. J. Mater. Chem. 21(2011) 15100.

THE BEHAVIOR OF NITRIFYING MICROORGANISMS FROM A SOIL CULTIVATED WITH *LOTUS CORNICULATUS* L.

Aurica Breica Borozan, Despina-Maria Bordean, Luminița Pîrvulescu, Liana Alda, Dan Raican, Sorina Popescu

Banat University of Agricultural Sciences and Veterinary Medicine “King Michael I of Romania” from Timisoara, Calea Aradului 119, 300645 Timisoara, Romania

Corresponding authors: sorinapopescu@usab-tm.ro; despina.bordean@gmail.com

Abstract

The knowledge of the behavior of the nitrifying microorganisms is of real use, because the microbial activities related to the nitrogen circuit and especially the nitrification determine the results of the agronomic practices. In this paper, the influence of the *Lotus corniculatus* L. (I-IV culture years) on the nitrifying bacteria and the correlation between the growth of these bacteria and soil moisture was studied. The soil samples were taken during the flowering period (summer season), from the rhizosphere of the pottery, but also from the uncultivated plots (control), placed in the western part of the country. Studies have shown that plants and soil moisture have influenced the evolution of nitrifying bacteria.

Key words: nitrifying bacteria, *Lotus corniculatus* L., rhizosphere, *Nitrobacter*, *Nitrosospira*

Introduction

Nitrogen is one of the most important nutrients for plant growth, limiting the primary productivity in many terrestrial ecosystems. For this reason it is applied in large quantities in agricultural systems, in the form of chemical fertilizers. The dynamics of this chemical element depends on some key microbial activities, such as: molecular nitrogen fixation, ammonification, nitrification, denitrification. Through nitrification, the conversion of ammonium to nitrites, is essential for soil microbiota and plant nutrition. Oxidation of ammonia to nitrites is accomplished by bacteria and archaeobacteria, and oxidation of nitrites to nitrates is the result of nitrate-bacterial activity [1]. There are two groups of bacteria involved in the nitrification process (*Nitrobacter* and *Nitrosospira*). The increase of agricultural production by applying chemical fertilizers results in the loss of significant amounts of nitrogen through leaching [6], a process followed by eutrophication of water with an important effect on biodiversity. It also produces emission of nitrogen oxide, greenhouse gas, which contributes to global warming of the Earth [2]. Therefore the knowing of this process provides important information on nitrogen availability, an essential element for agricultural crops and soil livestock. As a result, researchers use alternatives that could reduce these unwanted effects, including growing leguminous plants [15]. The positive effects of legume cultivation lie in the fact that, if nitrogen loss is reduced, the nitrifying microorganisms would not be blocked by the nitrogen introduced through the anthropic pathway and would not affect the availability of nitric nitrogen for large nitrogen-consuming crops. The same researchers point out that the process of nitrification depends on the composition of the nitrifying community. It is also appreciated that the structure of this bacterial segment is influenced by soil moisture, water being an essential factor for the development of enzymatic activity [7,9] appreciate that the thermal and hydrological regime are the main factors responsible for the evolution of the microbiological and biochemical parameters of the soil. The rhizosphere is the soil that surrounds the roots system, through which plants release a large amount of metabolites that act on the one hand as chemoreceptors for microorganisms, and on the other hand they are essential nutrients for plant growth [5,12]. Based on all of this information in an

initial step we evaluated the abundance of nitrifiers from the soil cultivated with pods in relation to the uncultivated soil and followed the effect of soil moisture on the nitrifying bacteria. We consider that these results will provide a viable ecological alternative that will in turn provide the necessary nitrogen for plants, without loss and without affecting the nitrifying microbial flora. It should be mentioned that nitrification is particularly important for soil fertility.

Materials and methods

Our studies were performed on a soil from the perimeter of Arad County, which is located between 20°45'- 22°30' east longitude and 45°0'58'- 46°0'38' north longitude, with a moderate continental temperate climate and soils consisting mostly of sedimentation parental materials [20]. Soil samples were collected from the root growth depth of *Lotus corniculatus* L., from the rhizosphere area (Rh1-Rh4), but also from the uncultivated plots, used as a control (Mt1-Mt4), during the flowering period (the growing season - summer). The soil from 4 years of culture was microbiologically analyzed in the same calendar year.

The soil samples processing and the setting up of experiments was carried out in the Microbiology laboratory, University of Agricultural Sciences and Veterinary Medicine of the Banat "King Michael I of Romania" in Timisoara and was accompanied by the determination of humidity by using the thermo-gravimetric method, with Sartorius scale MA-50 at 105°C, as described by Bordean et al. 2011 [3]. Isolation of nitrifying bacteria from soil samples was performed on liquid mineral nutrient medium, supplemented with color indicator. The principle of the method was according with Saratchandra, taken over by Stefanic (2006) . The growth temperature of the bacteria was 28°C with an incubation time of 8 weeks.

Results and discussions

The availability of nitrogen from the soil influences the abundance and composition of nitrifiers. Nitrifying bacteria occupy different ecological niches and their abundance varies with the amount of ammonium in the soil [14].

Nitrifying bacteria were found in large numbers in the control plots during the first 2 years. The number of nitrifiers decreased with the passage of years; the number of nitrifiers was lower in the years III- IV and the smallest number was highlighted in the control version from year IV. The highest number of nitrifying bacteria was isolated from the rhizosphere of the culture from the year II, compared to the other experimental variants. Depending on the abundance of the nitrifiers the experimental variants follow one another in descending order: Rh2>Rh1>Rh3>Rh4.

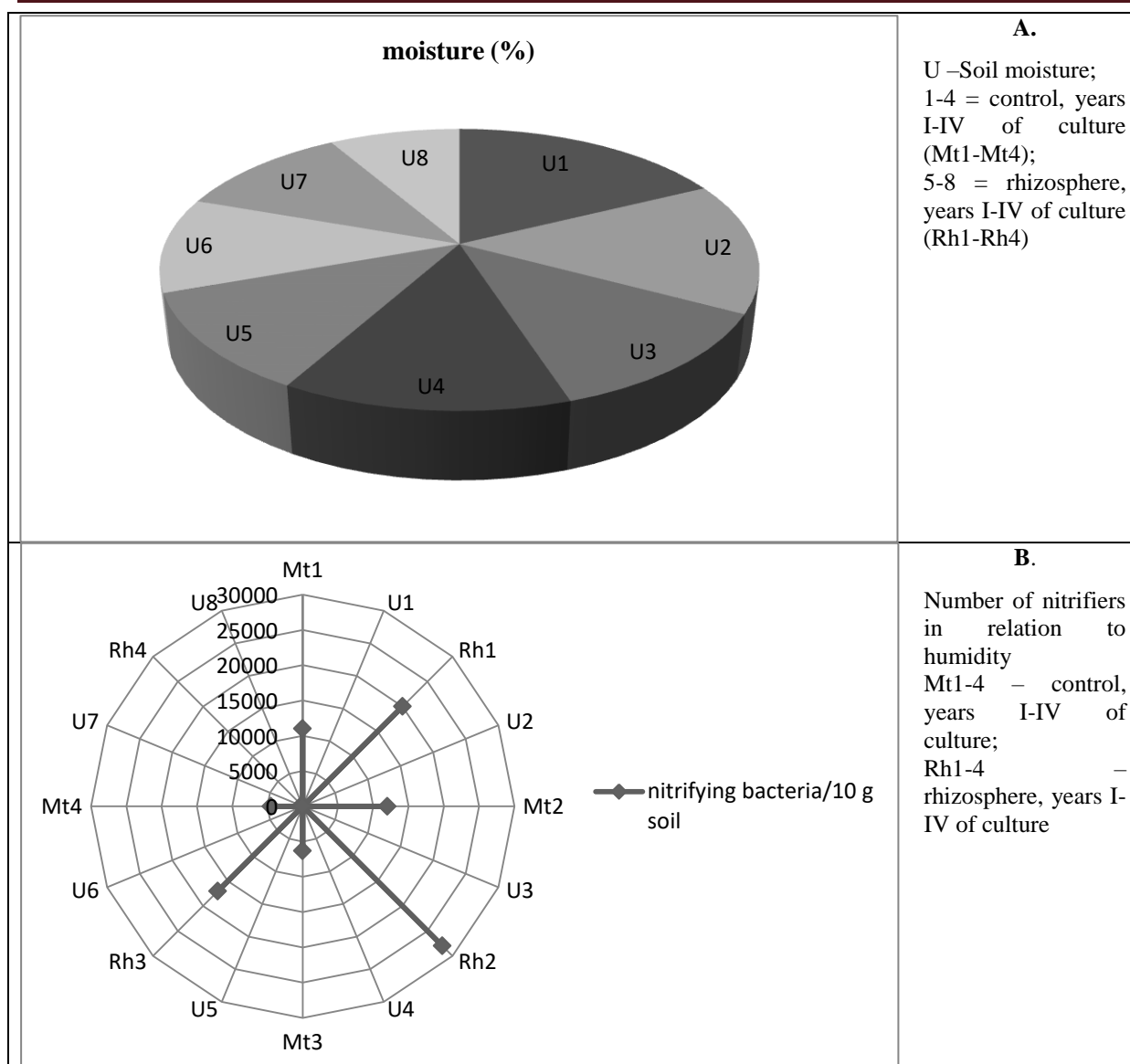


Figure 1 The abundance of nitrifying bacteria from experimental variants depending on soil moisture (%)

Compared to the control variants, it was observed that an increase of the nitrifiers in the rhizosphere of plants, in the I-III years of culture, except for year IV when the number of bacteria in the rhizosphere (Rh4) was lower compared to the control (Mt4). Plants have influenced nitrifying bacteria, as demonstrated by many studies [13, 18]. Another important factor that can determine the variation of the bacterial community is the vegetation type. According to Attard et al., 2010, nitrification depends on the methods of processing and treating the soil [1], but also on the changes in the genera *Nitrosospira* and *Nitrobacter*.

The soil moisture from the experimental variants is high in the Mt1 variant, followed by Rh1, Rh2 and the other experimental variants (Figure 1A). The samples with the lowest water content come from Rh4, where the lowest number of nitrifying bacteria was recorded (Figure 1B).

Humidity influences the evolution of nitrifiers in the soil, but the plant also makes a significant contribution, as the evidence that the largest number of nitrifying bacteria is found in soil samples from the rhizosphere of plants (fig. 3,4B). The results are in concordance with some authors who report that excessive soil moisture causes low microbial biomass [17], and

low water content disrupts soil homeostasis. In contrast, [4] observed that soil moisture influenced soil microbial and biochemical activity to a lesser extent than soil type. Other studies have shown that the microbial and biochemical activity of the soil is closely related to the physical and chemical properties of the soil [10].

Conclusions

Soil microbial activities are determined by a variety of factors, including moisture and the plant. This influence is seen in the evolution of nitrifying bacteria from the rhizosphere of *Lotus corniculatus* L. plants in the first years of culture. The highest number was recorded in the rhizosphere of the plants of the second year followed by the rhizosphere of the first year of the culture. The smallest number of nitrifiers was highlighted in the rhizosphere of plants from the fourth year of cultivation. The number of nitrifiers in the 8 experimental plots decreased simultaneously with the year of culture and the water content.

Acknowledgements

All authors are principal authors and have contributed evenly to this paper. The present paper was funded by the project “*Study of synergic bioactivity of some antioxidant mixes fortifications with the role to fortify patients with Parkinson's disease*”, No 47/12.11.2015, financed by Antiparkinson Association from Romania.

References

- [1] E. Attard, F. Poly, C. Commeaux, F. Laurent, A. Terada, B.F. Smets, S. Recous, X.L. Roux. Shifts between *Nitrospira*- and *Nitrobacter*-like nitrite oxidizers underlie the response of soil nitrite oxidizing enzyme activity to changes in tillage practices. *Environ. Microbiol.* 2010;12:315–326. doi: 10.1111/j.1462-2920.2009.02070.x.
- [2] F. Beeckman, H. Motte, T. Beeckman, Nitrification in agricultural soils: impact, actors and mitigation. *Current Opinion in Biotechnology*, vol. 50, 2018, pages 166-173. <https://doi.org/10.1016/j.copbio.2018.01.014>.
- [3] D.M. Bordean, M. Bărbăscu, A.B. Boroșan, L. Alda, N. Filimon, R. Popescu, et al. Studies regarding speciation and chemical fingerprinting as fruit products quality markers. *Journal of Horticulture, Forestry and Biotechnology*. 2011;15(4):101-105.
- [4] A. Borowik, J. Wyszowska. Soil moisture as a factor affecting the microbiological and biochemical activity of soil. *Plant Soil Environ.* Vol. 62, 2016, No. 6: 250–255. doi: 10.17221/158/2016-PSE.
- [5] A.B. Boroșan, S. Popescu, O.M. Boldura, Plants Root Interference Area, a Benefit to the Microbial Community. *Bulletin UASVM Horticulture* 74(1): 2017, 1-8. DOI:10.15835/buasvmcn-hort:12302.
- [6] H.J. Di, K.C. Cameron. Inhibition of nitrification to mitigate nitrate leaching and nitrous oxide emissions in grazed grassland: a review. *Front. Soils Sed.* 2016;16:1401–1420. doi: 10.1007/s11368-016-1403-8.
- [7] C. Giacometti, M.S. Demyan, L. Cavani, C. Marzadori, C. Ciavatta, E. Kandeler (2013): Chemical and microbiological soil quality indicators and their potential to differentiate fertilization regimes in temperate agroecosystems. *Applied Soil Ecology*, 64: 32–48.
- [8] A. Gigon, I. H. Rorison (1972). The response of some ecologically distinct plant species to nitrate- and to ammonium-nitrogen. *J. Ecol.* 60 93–102. 10.2307/2258043.
- [9] M.G. Jiang, J.H. Zhang (2002): Water stress-induced abscisic acid accumulation triggers the increased generation of reactive oxygen species and up-regulates the activities of antioxidant enzymes in maize leaves. *Journal of Experimental Botany*, 53: 2401–2410.

- [10] A. Lagomarsino, S. Grego, E. Kandeler (2012): Soil organic carbon distribution drives microbial activity and functional diversity in particle and aggregate-size fractions. *Pedobiologia*, 55: 101–110.
- [11] M. Pester, F. Maixner, D. Berry, T. Rattei, H. Koch, S. Lüscher, B. Nowka, A. Richter, E. Spieck, E. Lebedeva, A. Loy, M. Wagner, H. Daims. NxrB encoding the beta subunit of nitrite-oxidoreductase as functional and phylogenetic marker for nitrite-oxidizing *Nitrospira*. *Environ. Microbiol.* 16, 3055–3071 (2014).
- [12] M. Pasca, L. Cojocariu, M. Horablaga, D. Bordean, D. Nica, N. Filimon, I. Gergen, and A.B. Borozan. 2012. “Changes in the Structure of Actinomycete Populations in the Rhizosphere of *Vicia Sativa* Species”. *Review on Agriculture and Rural Development* 1 (1. suppl.), 352–57. <http://www.analecta.hu/index.php/rard/article/view/13232>.
- [13] A.K. Patra, L. Abbadie, A. Clays-Josserand, V. Degrange, S.J. Grayston, N. Guillaumaud, P. Loiseau, F. Louault, S. Mahmood, S. Nazaret et al. Effects of management regime and plant species on the enzyme activity and genetic structure of N-fixing, denitrifying and nitrifying bacterial communities in grassland soils. *Environ. Microbiol.* (2006) 8, 1005–1016.
- [14] M. Simonin, X. Le Roux, F. Poly, C. Lerondelle, B.A. Hungate, N. Nunan, A. Niboyet. Coupling between and among ammonia oxidizers and nitrite oxidizers in grassland mesocosms submitted to elevated CO₂ and nitrogen supply. *Microb. Ecol.* 2015, 70:809–818. doi: 10.1007/s00248-015-0604-9.
- [15] M. Skiba, T. George, E. Baggs, T. Daniell, Plant influence on nitrification. *Biochemical Society Transactions*. 2011, 39.(1)275–278; DOI:10.1042/BST0390275
- [16] G. Stefanic, Probleme de agrofitotehnie teoretica si aplicata. Editia a II-a). In: Probleme de agrofitotehnie teoretica si aplicata, XXVIII, ICDA Fundulea. 2006;28:38–39 (in Romanian).
- [17] I.M. Unger, A.C. Kennedy, R.M. Muzika (2009): Flooding effects on soil microbial communities. *Applied Soil Ecology*, 42: 1–8.
- [18] R. Wheatley, K. Ritz and B. Griffiths, Microbial biomass and mineral N transformations in soil planted with barley, ryegrass, pea or turnip. *Plant Soil* (1990) 127, 157–167.
- [19] X. Q. Zhao, S. W. Guo, F. Shinmachi, M. Sunairi, A. Noguchi, I. Hasegawa, et al. (2013b). Aluminum tolerance in rice is antagonistic with nitrate preference and synergistic with ammonium preference. *Ann. Bot.* 111 69–77. 10.1093/aob/mcs234
- [20] <http://www.ospaarad.ro/cadrul-natural-al-jud-arad>

CHRONOPOTENTIOMETRIC STUDY OF NICOTINAMIDE (VITAMIN B₃)

Tanja Brezo-Borjan¹, Zorica Stojanović¹, Zvonimir Suturović¹, Snežana Kravić¹, Ana Đurović¹

¹*Faculty of Technology, University of Novi Sad, 21000, Novi Sad, Bul. cara Lazara 1, Serbia
e-mail: tanja.brezo@tf.uns.ac.rs*

Abstract

The electrochemical behavior of nicotinamide, a vitamer of vitamin B₃, was studied employing adsorptive stripping chronopotentiometry. Mercury film electrode was used as the working electrode, whereas the Ag/AgCl (3.5 mol/l KCl) and a platinum wire were used as the reference and the auxiliary electrode, respectively. The most important experimental and instrumental parameters were optimized and proposed method was validated. Citrate buffer of pH 6 (0.05 mol/l) was used as the optimal supporting electrolyte. The analytical signal of vitamin B₃ was the highest and sharpest in quiescent solutions, leading to the conclusion that no stirring during the accumulation step was needed. The appropriate experimental conditions were as follows: accumulation potential of -1.405 V, accumulation time of 15 s in a quiescent solution and oxidation current in the range of 1.4 – 15.1 μ A. The thickness of the mercury film was investigated and optimized as well, with the optimal value being 129.82 nm, which corresponded to the deposition time of 240 s from a 0.2 g/l Hg²⁺ ion solution. A well-defined oxidation wave belonging to nicotinamide appeared at about -250 mV. The linearity of the analytical signal was achieved in two concentration ranges: 5 – 25 mg/l and 10 – 100 mg/l. The calculated limit of detection (LOD) and limit of quantitation (LOQ) values were 2.20 mg/l and 6.66 mg/l, respectively. The precision of the developed method was acceptable (relative standard deviation (RSD) < 3.90%). Further study is in progress to apply proposed method to the determination of nicotinamide in pharmaceutical preparations.

Acknowledgements

The financial support of the Ministry of Education, Science and Technological Development of the Republic of Serbia (Project III 46009) is gratefully acknowledged.

IMPROVED PIEZOELECTRIC RESPONSE IN LEAD FREE PIEZOCERAMICS

Bucur Raul Alin, Farkas Iuliana, Bucur Alexandra Ioana

*National Institute for Research and Development in Electrochemistry and Condensed Matter,
Condensed Matter Department, No. 1 Plautius Andronescu, 300224 Timisoara, Romania.
e-mail: raul_alin_bucur@yahoo.com*

Abstract

(K,Na)NbO₃ based perovskites are considered promising materials as alternative environmental friendly piezoelectrics, envisioned to replace current lead based materials Pb(Zr,Ti)O₃ [1, 2]. Sodium and potassium niobate (K_{0.5}Na_{0.5}NbO₃) is a ferroelectric perovskite that crystallizes at room temperature in the orthorhombic symmetry. For this compound, a series of temperature dependent phase transitions are known: rhomboidal → orthorhombic at – 150°C, orthorhombic → tetragonal at 200°C and tetragonal → cubic at 400°C [3]. As some authors pointed out [4], the improvement of the piezoelectric properties can be achieved by shifting the polymorphic phase transition toward room temperature, or by using chemical alteration (doping, substitutions or sintering aids) near a morphologic phase transition. Since the chemical modifications leads to temperature independent piezoelectric properties [5], such techniques are often preferred for piezoelectric devices that operate at different temperature than room temperature.

Lead-free perovskite (K_{0.5}Na_{0.5})_{1-x}Li_xNbO₃ (with x=0.065) doped with 1 mol% (Gd-Sm)BO₃ (B=Co, Mn, Cr, Fe, Al) were prepared by a conventional solid-state method. The research was conducted with interests on the effects of (Gd-Sm)BO₃ content on the crystalline structure (x ray diffraction with PanAnalytical X'Pert Pro MPD diffractometer), dielectric and piezoelectric properties of the ceramics. The dielectric measurements (from room temperature up to 420° C, at 10 kHz, 100 kHz and 1MHz, with an Impedance/LRC meter TEGAM model 3550) reveals shifting of the orthorhombic to tetragonal phase transitions and Curie temperature. A full set of the piezoelectric properties were obtained using the resonance method with an impedance analyzer Agilent E5100A. Owing to the increase of the coupling factor and piezoelectric constants, such ceramics can be considered as viable candidates for piezoelectric devices used for electric energy generation.

References

- [1] M.D. Maeder, D. Damjanovic, N. Setter, J. Electroceram. 13 (2004) 385.
- [2] Saito, H. Takao, I. Tani, T. Nonoyama, K. Takatori, T. Homma et al., Nature 432, 84 (2004).
- [3] R.E. Jaeger and L. Egerton, J. Am. Ceram. Soc. 45, 209 (1962).
- [4] X. Wang, J. Wu, D. Xiao, J. Zhu, X. Cheng, T. Zheng, B. Zhang, X. Lou, X. Wang, J. Am. Chem. Soc. 136, 2905 (2014).
- [5] L.J. Rigoberto, G.V. Virginia, M.P. Cruz, M.E. Villafuerte-Castrejon, J. Electron. Mater. 44, 2862 (2015).

PRELIMINARY STUDIES ON THE HYDROTHERMAL SYNTHESIS OF PROMISING MULTIFERROIC PIEZOCERAMICS FOR THE MEDICAL APPLICATIONS

Cristian Casut^{1,3}, Raul Bucur¹, Daniel Ursu¹, Nicolae Miclau², Paul Barvinschi³, Alina Zamfir^{1,3}, Marinela Miclau¹

¹ National Institute for Research and Development in Electrochemistry and Condensed Matter, 1 Plautius Andronescu Street, 300224 Timisoara, Romania

² Politehnica University Timisoara, Str. PiataVictoriei, nr.2, 300006 Timisoara, Romania

³ West University of Timisoara, Bulevardul Vasile Pârvan 4, Timișoara 300223 Timisoara, Romania

Abstract

Lead-free piezoceramics aiming at replacing the market-dominant lead-based ones have been extensively searched for more than a decade worldwide [1]. From the beginning, the goal was obviously to develop lead-free piezoceramics whose properties are no less than those of the market-dominating lead zirconate titanate (PZT). With the functionality of interconverting mechanical and electrical energy, piezoelectric materials have the versatility to address a wide range of applications, including actuators, sensors, and transducer devices [2]. Multiferroics have been known to have ferromagnetic and ferroelectric properties at the same time, with interesting physical properties as well as the possibility of the practical applications for new memory devices. Multiferroic piezoceramics maintain considerable piezoelectricity, whilst presenting challenges in terms of processing of single-phase material. The synthesis of high-purity of BiFeO_3 (BFO) ceramic using solid-state reaction is known to be very difficult due to inevitable formation of the secondary phases, mostly mullite-type $\text{Bi}_2\text{Fe}_4\text{O}_9$ and sillenite-type $\text{Bi}_{25}\text{FeO}_{39}$ [3].

In this study, we report the synthesis and characterization of BiFeO_3 by hydrothermal methods using $\text{Bi}(\text{NO}_3)_3 \cdot 5\text{H}_2\text{O}$ and $\text{Fe}(\text{NO}_3)_3 \cdot 9\text{H}_2\text{O}$ as precursors with a solution of 2M NaOH as mineralizer at a 200 °C temperature for 48 hours. In typical synthesis process, the precursors were mixed in 30 ml of water. a temperature of 200 °C, 48 hours. The structure of BiFeO_3 was determined by powder X-ray diffraction (XRD) PW 3040/60 X'Pert PRO using Cu-K α radiation with ($\lambda=1.5418\text{\AA}$), in the range $2\theta = 10\text{--}80^\circ$, at room temperature (Fig. 1a). A Scanning Electron Microscope InspectS (SEM) was used to observe the morphology of synthesized nanocrystals (Fig. 1b). The diffuse reflectance spectra (DSR) was obtained using a Lambda 950 UV-Vis-NIR Spectrophotometer with 150 mm integrating sphere in the wavelength range of 300–800 nm.

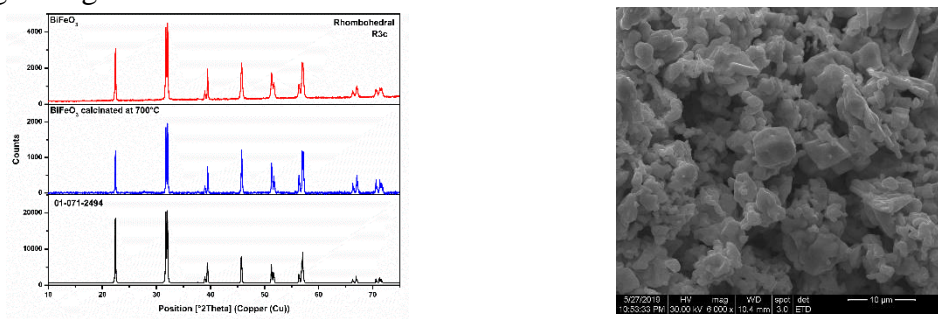


Figure 1. a) X-ray diffraction patterns and b) SEM image of BiFeO_3 obtained from hydrothermal methods using $\text{Bi}(\text{NO}_3)_3 \cdot 5\text{H}_2\text{O}$ and $\text{Fe}(\text{NO}_3)_3 \cdot 9\text{H}_2\text{O}$ as precursors with a solution of 2M NaOH as mineralizer at a 200 °C temperature for 48 hours.

Acknowledgements

This project was supported by the Romanian National Authority for Scientific Research, UEFISCDI, through project PN-III-P1-1.2-PCCDI-2017-0046 and PN 19 22 04 01, no. 40N/2019.

References

- [1] Hong C-H, Kim H-P, Choi B-Y, Han H-S, Son JS, Ahn CW, Jo W, Lead-Free Piezoceramics - Where to Move on?, Journal of Materiomics (2016)
- [2] J. Koruza, A. J. Bell, T.Frömling, K. G. Webber, K. Wang, J. Rödel, Journal of Materiomics, 13-26 (2018).
- [3] H. Han, J. H. Lee, H. M. Jang, Inorganic Chemistry, 56 (19), 11911–11916 (2017).

DETERMINATION OF SALICIN CONTENT IN FOOD SUPPLEMENTS CONTAINING WILLOW BARK

Adina Căta¹, Mariana N. Ștefănuț¹, Ioana M.C. Ienașcu^{1,2}

¹ *National Institute of Research and Development for Electrochemistry and Condensed Matter, Dr. Aurel Păunescu Podeanu 144, 300569, Timișoara, Romania*

² *“Vasile Goldiș” Western University of Arad, Faculty of Pharmacy,
Liviu Rebreanu 86, 310045, Arad, Romania
e-mail: adina.cata@yahoo.com*

Abstract

The medicinal properties of willow bark can be attributed to the presence of salicylic glycosides, mainly salicin and salicortin. Salicin is the metabolic precursor of salicylic acid and has a similar action in the human body. Preparations containing willow bark extract are popular herbal remedies and have been used for anti-inflammatory, anti-rheumatic, antipyretic, antihypertensive, analgesic, antiseptic and astringent properties but many of them are not chemically standardized. The aim of this work was to investigate the presence of salicin in some commercially available food supplements (willow bark for tea, capsules containing willow bark, capsules and tablets containing willow bark extract). Salicin content in six *Salix* supplements, was quantified through HPLC-DAD analysis. According to the information provided by the manufacturer, only for two of the selected food supplements there is specified the content of salicin. The presence of salicin was monitored at 266 nm. Prior to chromatographic analysis, all products were extracted with methanol for 2 hours under heating and stirring. The highest salicin content was identified in capsules of *Salix alba* extract from Rotta Natura.

Acknowledgements

This work is part of the project PN 19 22 03 01 / 2019 “Supramolecular inclusion complexes of some natural and synthetic compounds with applications in health”, carried out under NUCLEU Program funded by National Authority for Scientific Research (Romania).

References

- [1] M. Shara, S.J. Stohs, *Phytotherapy Research*, 29 (2015) 1112.
- [2] J.G. Mahdi, A.J. Mahdi, A.J. Mahdi, I.D. Bowen, *Cell Proliferation*, 39 (2006) 147.
- [3] J.G. Mahdi, *Journal of Saudi Chemical Society*, 14 (2010), 317.

SYNTHESIS OF IRON OXIDE (Fe_2O_3) BY HYDROTHERMAL DECOMPOSITION OF $\text{Fe-Na}_4\text{EDTA}$ COMPLEX AT TEMPERATURES BETWEEN 140 °C AND 200 °C

Marius Chirita^{1,*}, Liviu Mocanu¹

¹National Institute for Research and Development in Electrochemistry and Condensed Matter, Timisoara, PlautiusAndronescu Str. No. 1, RO-300224, Timisoara, Romania

*Corresponding author: chirifz@gmail.com

Continuing our previous studies [1,2], the present experimental procedure is focused on the hydrothermal decomposition of the Fe(II)-EDTA complex in the presence of urea at temperatures between 140°C and 200°C after 4 h of high pressure-temperature treatment time. Fe_2O_3 particles with dimensions between 1 and 2 micrometers were obtained. The experiments were repeated in identical concentrations by progressive decreasing temperature from 200°C to 140°C 20 to 20 degrees. The molar concentrations were identical in all cases. It was found that the lowest temperature at which the hematite synthesis process takes place is 140°C.

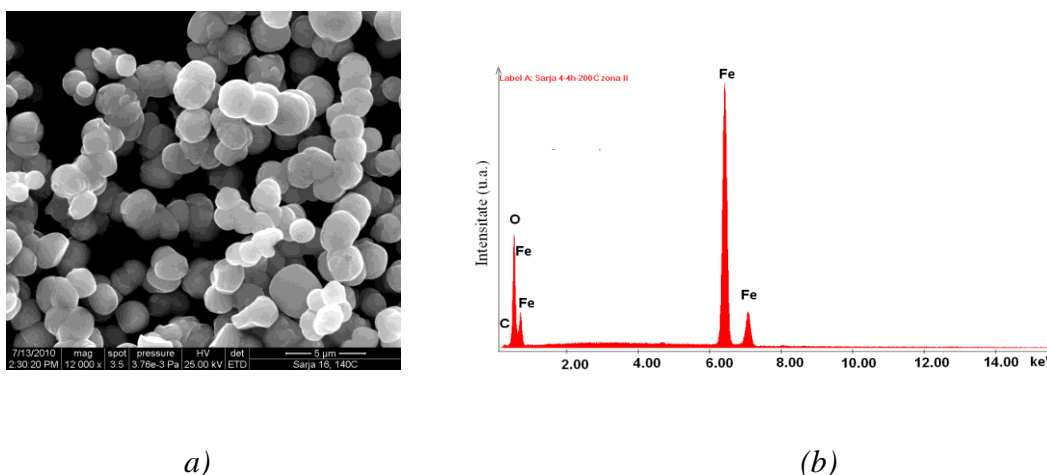


Figure 1: SEM Images of micrometric Fe_2O_3 (a) and EDAX spectrum (b)

In the EDAX spectrum of these samples, only iron and oxygen maxima can be seen, which unequivocally indicates that the final product is pure Fe_2O_3 , without traces of S, Na, C, N which could have resulted from the precursor's decomposition. The diffraction spectrum (not presented here) showed distinct maxima for hematite only.

Keywords: hematite, crystalline, micrometric.

References:

- [1] M. Chirita, R. Banica, A. Ieta, A. Bucur, P. Sfirloaga, D. H. Ursu, and I. Grozescu, "Highly Crystalline FeCO_3 Microparticle Synthesis by Hydrothermal Decomposition of Fe-EDTA Complex." American Institute of Physics Conf Proceedings, vol. 1262/2010: 124.
- [2] M. Chirita, R. Banica, P. Sfarloaga, A. Ieta, I. Grozescu, "A short route of micrometric magnetite synthesis via Fe-EDTA thermal decomposition." IEEE ConfProc 11-13 Oct. 2010, ISBN 978-1-4244-5781-6, pp. 391-394.

HYDROTHERMAL SYNTHESIS OF THE MIXED-PHASES BASED ON Mn FOR LITHIUM ION BATTERY APPLICATION

Dabici Anamaria¹, Ursu Daniel¹, Vajda Melinda¹, Miclau Marinela^{1*}, Casut Cristian¹, Albulescu Daiana¹

¹National Institute for Research and Development in Electrochemistry and Condensed Matter, 1 Plautius Andronescu Street, 300224 Timisoara, Romania
e-mail: marinela.miclau@gmail.com

Abstract

Over the past few years, Li-ion batteries (LIBs) have been widely applied in mobile devices, electronic vehicles (EVs) and energy storage systems in our daily life [1,2]. The cathode material is a critical part in LIBs which determines the electrochemical properties. Among this family, Mn-based layered cathode materials, considered as one of the most promising candidates in next-generation rechargeable batteries, have been attracting significant attention due to their extraordinarily high specific capacity of 280 mA h g⁻¹, potential in improving the working voltage to 4.8 V and relatively high Li-ion diffusivity compared with LiFePO₄ and LiMn₂O₄. Materials such as: Li_{1.2}Ni_{0.13}Co_{0.13}Mn_{0.54}O₂ and Li_{1.2}Mn_{0.56}Ni_{0.16}Co_{0.08}O₂ have been investigated intensively, however, the progress of the commercialization has been slow due to voltage fade, insufficient rate capability and structural degradation during long-time cycling, which are considered as the bottlenecks for further promotion [5].

According to the literature reports, the layered Li₂MnO₃ belongs to the C2/m symmetry where Li and Mn ions occupy the octahedral interstices of a cubic close-packed oxygen lattice [6]. Forming composite phase of Li₂MnO₃ with other polymorphs of lithium metal oxides is also of great interest. For example, Li₂MnO₃–LiMO₂ M = Mn, Co, Ni, Cr, etc. etc. composite electrode materials were reported where the Li₂MnO₃ in the composite can stabilize the monoclinic structure of LiMO₂ upon cycling [7].

In this paper, we report the successful hydrothermal synthesis of LiMnO₂/Li₂MnO₃ obtained from hydrothermal method at 250 °C for 48 hours using 10mL H₂O and Na₂S₂O₈ as oxidant. The structure of products was determined by powder X-ray diffraction (XRD) PW 3040/60 X'Pert PRO using Cu-Kα radiation with (λ=1.5418Å), in the range 2θ = 10–80°, at room temperature (figure 1a). A Scanning Electron Microscope InspectS (SEM) was used to observe the morphology of synthesized nanocrystals (figure 1b). The diffuse reflectance spectra (DSR) was obtained using a Lambda 950 UV-Vis-NIR Spectrophotometer with 150 mm integrating sphere in the wavelength range of 300–800 nm.

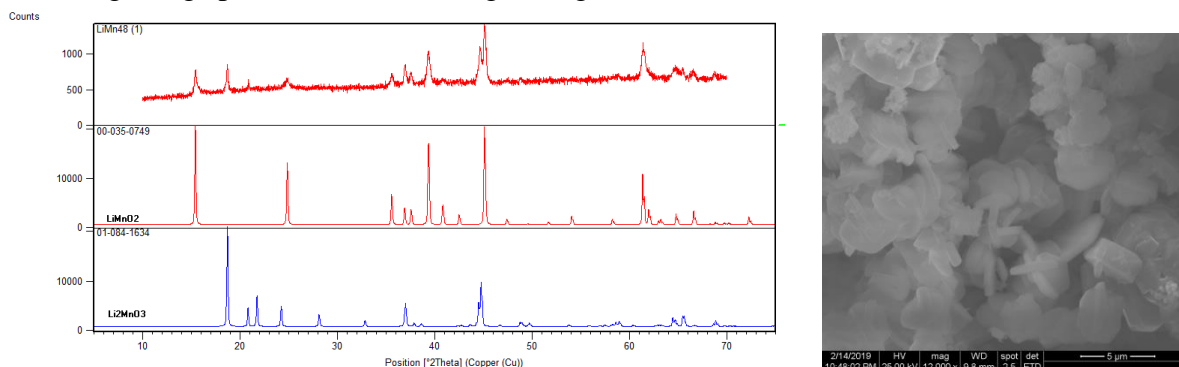


Figure 1. a) X-ray diffraction patterns and b) SEM images of LiMnO₂/Li₂MnO₃ obtained from hydrothermal method at 250 °C for 48 hours.

Acknowledgements

This paper is supported by the Romanian Government under the project PN 19 22 01 03.

References

- [1] B. Dunn and J. M. Tarascon, *Science*, 2011, 334, 928–935.
- [2] B. Luo, B. Wang, X. Li, Y. Jia, M. Liang and L. Zhi, *Adv. Mater.*, 2012, 24, 3538–3543.
- [3] M. M. Thackeray, C. S. Johnson, J. T. Vaughey, N. Li and S. A. Hackney, *J. Mater. Chem.*, 2005, 15, 2257–2267.
- [4] J. B. Goodenough and Y. Kim, *Chem. Mater.*, 2010, 22, 587– 603.
- [5] B. Xu, C. R. Fell, M. Chi and Y. S. Meng, *Energy Environ. Sci.*, 2011, 4, 2223.
- [6] P. J. Phillips, J. Bareno, Y. Li, D. P. Abraham and R. F. Klie, ~ *Adv. Energy Mater.*, 2015, 5, 1501252.
- [7] M. M. Thackeray, C. S. Johnson, J. T. Vaughey, N. Li, and S. A. Hackney, *J. Mater. Chem.*, 2005, 15, 2257

PHOTOCATALYTIC ACTIVITY OF METAL OXIDE NANOPARTICLES FOR REMOVAL OF THE HERBICIDE FLUROXYPYR FROM WATER

Vesna Despotović¹, Paula Sfirloaga², Daniela Šojić Merkulov¹, Biljana Abramović¹

¹*University of Novi Sad Faculty of Sciences, Department of Chemistry, Biochemistry and Environmental Protection, Trg Dositeja Obradovića 3, 21000 Novi Sad, Serbia*

²*National Institute for Research and Development in Electrochemistry and Condensed Matter, Department of Condensed Matter, 1 Plautius Andronescu St., 300224 Timisoara, Romania*

e-mail: vesna.despotovic@dh.uns.ac.rs

Abstract

The photocatalytic materials absorb the photons having energy equals to or more than the band gap energy between the valence and conduction bands of the photocatalyst. The positive holes in the valence band either oxidize the water to produce hydroxyl radical or pollutant, whereas excited electrons reduce the adsorbed oxygen on the photocatalyst in the conduction band [1]. Till date a wide range of metal oxide/semiconductor-based nanomaterials have been explored for the photocatalytic degradation of harmful and toxic organic pollutants into the non-toxic products [2,3]. The aim of this work was to investigate removal of the herbicide fluroxypyr from double distilled water in the presence of novel TiO₂, MgO and ZnO nanoparticles under UV and simulated solar irradiation. It was found that TiO₂ photocatalyst showed higher photocatalytic activity for removal of fluroxypyr from water compared with MgO and ZnO. However, a major drawback of photocatalyst is that it has higher rate of recombination of photogenerated electron-hole pairs, which suppressed its catalytic potential [1,4]. Because of that it was investigated the photodegradation behaviour of fluroxypyr in aquatic systems using UV and simulated solar irradiation in the presence of TiO₂/(NH₄)₂S₂O₈. The efficiency of elimination the herbicide from double distilled water was monitored by UFLC–DAD technique.

Acknowledgments

This work was supported by the Ministry of Education, Science and Technological Development of the Republic of Serbia (Project No. 172042).

References

- [1] R. Gusain, K. Gupta, P. Joshi, O.P. Khatri, Adv. Colloid. Interf. Sci. 272 (2019) 102009.
- [2] S. Ahmed, M.G. Rasul, R. Brown, M.A. Hashib, J. Environ. Manag. 92 (2011) 311.
- [3] U.I. Gaya, A.H. Abdullah, J. Photochem. Photobiol. C Photchem. Rev. 9 (2008) 1.
- [4] S. Ahmed, M.G. Rasul, W.N. Martens, R. Brown, M.A. Hashib, Desalination 261 (2010)

ELECTROCHEMICAL BEHAVIOR OF QUERCETIN ON BORON-DOPED DIAMOND ELECTRODE IN DIFFERENT SUPPORTING ELECTROLYTES

Ana Đurović^{*1}, Zorica Stojanović¹, Snežana Kravić¹, Zvonimir Suturović¹, Lukas Richtera^{2,3}, Tanja Brezo-Borjan¹

¹*University of Novi Sad, Faculty of Technology Novi Sad, Department of Applied and Engineering Chemistry, Bulevar cara Lazara 1, 21000 Novi Sad, Republic of Serbia*

²*Mendel University in Brno, Department of Chemistry and Biochemistry, Zemědělská 1, 613 00 Brno, Czech Republic*

³*Brno University of Technology, Central European Institute of Technology, Purkyňova 123, 612 00 Brno, Czech Republic*
e-mail: djurovic.ana@tf.uns.ac.rs

Abstract

Quercetin is one of the most abundant flavonoid compounds with a broad spectrum of health beneficial properties. In this study electrochemical behavior of quercetin on boron-doped diamond electrode as a working electrode was investigated in different supporting electrolytes. Experiments embraced 0.1 mol/L acetate buffer, citrate buffer, phosphate buffer, 0.04 mol/L Britton-Robinson buffer and 0.05 mol/L solution of HCl, while studied quercetin concentration were in the range from 2 mg/L to 30 mg/L. Voltammograms recorded in different supporting electrolytes revealed one sharp and well-defined oxidation peak of quercetin at the potential of about +0.70 V, and it was chosen for quantification of quercetin, although in some buffers one additional protracted peak was observed. In comparison to differential pulse voltammetry, square-wave voltammetry showed higher sensitivity, so this technique could be more suitable for further development. Even though high values of correlation coefficients (> 0.9900) were obtained for all studied supporting electrolytes, the best results in terms of sensitivity were observed for citrate and Britton-Robinson buffers. These preliminary results demonstrated that boron-doped diamond electrode can be used as a sensitive sensor for precise determination of quercetin in real samples.

Introduction

Polyphenols are naturally occurring compounds produced as plant secondary metabolites that serve as protecting agents from pathogens and UV radiation. Several classes of polyphenols can be found in nature, and flavonoids represent one of the major groups of these substances widely present in many fruit and vegetables species. Quercetin (3,3',4',5,7-pentahydroxyflavone) is one of the most abundant flavonoid compound. A broad spectrum of health beneficial properties are associated with quercetin consumption including: antioxidant, anti-inflammatory, and antimicrobial activity, while it can be used as a protecting agent against cancer, pulmonary, cardiovascular diseases and neurodegenerative disorders as well [1].

Owing to its favorable health effects on human health, quercetin is not used only from its naturally sources, but also as a nutritional food ingredient and dietary supplement. Therefore, development of simple and sensitive analytical methods that can be used for its accurate determination in different matrixes is attracting great attention. A variety of methods for determination of quercetin have been reported including high pressure liquid chromatography (HPLC) [2, 3], gas chromatography (GC) [4, 5], spectrophotometry [6, 7] and capillary electrophoresis [8]. However, most of these methods are lengthy, complicated and require expensive instrumentation and skilled analysts. Due to numerous advantages that are providing electroanalytical methods, such as easy instrumental manipulation, low operating

costs, short analysis time, they can be used as an alternative techniques for quercetin determination. Voltammetric determination of quercetin was performed using different electrode materials: glassy carbon electrode (GCE) [9, 10], platinum electrode [11], but also the use of different modified electrode materials in order to increase sensitivity and selectivity was evident lately [12-14].

Boron-doped diamond is an electrode material with excellent properties including: wide potential window, low background current, exceptional inertness and stability that distinguish it from other electrode materials, and it has been proven as a versatile electrode material for the detection of the numerous analytes with low detection limit, excellent precision and stability [15, 16]. Only few reports describe the electroanalytical analysis of quercetin using boron-doped diamond electrode (BDDE). Permpool et al. [17] characterized the oxidation of quercetin using BDDE by cyclic voltammetry, and compared it to GCE. In the study published by Abdullah et al. [18] square-wave stripping voltammetric method with the presence of cationic surfactant cetyltrimethylammonium bromide in the electrolyte was developed for determination of quercetin in apple juice.

In this study we compared electrochemical behavior of quercetin in different electrolytes on bare BDDE. Cyclic voltammetry (CV), square-wave voltammetry (SWV) and differential pulse voltammetry (DPV) were used as voltammetric techniques. The best performance in terms of linearity, sensitivity, sharpness of oxidation peak was achieved in citrate and Britton-Robinson buffer. These preliminary results are promising and can be used for developing a sensitive voltammetric method for determination of quercetin in real samples.

Experimental

Chemicals

Standard stock solution of quercetin (1 g/L) was prepared by dissolution of the proper mass of standard (Sigma-Aldrich) in the ethanol, and stored in the dark at 4°C. The solutions of lower concentrations were prepared by dilution with the supporting electrolyte. 0.1 mol/L citrate buffer, 0.1 mol/L acetate buffer, 0.1 mol/L phosphate buffer, 0.04 mol/L Britton-Robinson (BR) buffer and 0.05 mol/L HCl were used as the supporting electrolytes. Doubly distilled water was used throughout the experiments.

Instrumentation

For voltammetric measurements PalmSens 4 potentiostat (GA Houten, Netherlands) connected to a personal computer using the PStace 5.4 software and standard three-electrode system were used. A three-electrode system consisted of BDDE diameter 3 mm (Windsor Scientific, Slough, UK), as a working electrode, platinum wire as a counter electrode, and an Ag/AgCl (3.5 mol/L KCl) as a reference electrode.

Voltammetric procedures

A 15.0 mL of the supporting electrolyte was added to the process glass. Before the analysis the working electrode was firstly wiped off with filter paper soaked with acetone, doubly distilled water, and then electrodes were rinsed with doubly distilled water and dried. Voltammograms were recorded in the presence of dissolved oxygen in quiescent solution in the anodic potential range from 0 V to +1.4 V. Cyclic voltammograms were recorded using potential step of 0.05 V and scan rate 0.3 V/s. Square-wave voltammograms were recorded after 10 s of equilibrium time using step potential of 0.01 V, amplitude 0.075 V and frequency of 25 Hz. Equilibrium time of 5 s, step potential 0.05 V, pulse potential 0.1 V, pulse time 0.05 s and scan rate of 0.06 V/s were used for performing DPV.

Results and discussion

In order to develop a sensitive and precise method for voltammetric determination of quercetin, the primary step is the choice of the optimal supporting electrolyte. Apart from having a great influence on the height of the analytical signal, the composition of the supporting electrolyte also affects the electrochemical processes conducting at the working electrode. Therefore, this study was based on the choice of the optimal supporting electrolyte for voltammetric determination of quercetin. According to the studies performed by other authors for voltammetric determination of quercetin by using BDDE as a working electrode, acetate buffer and phosphate buffer were used as the optimal supporting electrolytes [17, 18]. In this study 0.1 mol/L acetate buffer, citrate buffer, phosphate buffer, 0.04 mol/L BR buffer and the 0.05 mol/L solution of HCl were tested as the supporting electrolytes. To study electrochemical behavior of analyte, different voltammetric techniques were applied including CV, SWV and DPV and after recording voltammograms for blank, measurements were done in the presence of quercetin (2-30 mg/L).

Cyclic voltammograms of quercetin in different supporting electrolytes showed one oxidation peak in the potential range from +0.65 V in 0.1 mol/L phosphate buffer pH 7 to +0.80 V in 0.1 mol/L acetate buffer pH 4, with no reduction peaks in reversed scan.

SWV performed in tested electrolytes showed one well-defined oxidation peak in the potential range at similar values as obtained by CV (+0.59 V - +0.73 V), while second protracted oxidation peak (+1.23 V) was observed only in 0.05 mol/L HCl.

Similar behavior of quercetin was observed by applying DPV, with one well-defined oxidation peak (+0.55 - +0.65 V), and one protracted oxidation peak (+1.05 - +1.15 V), whereas in phosphate buffer only the first oxidation peak was notable. Considering that the shape and intensity of the first peak were much better for all studied electrolytes, this peak would be more suitable for quantification of quercetin.

Linear relationships between the current for first oxidation peak and studied concentration range in tested electrolytes for SWV and DPV measurements are showed on Figure 1. Good linearity was obtained for all studied electrolytes with both SWV and DPV techniques with correlation coefficients higher than 0.9900. From Fig.1 it is evident that the values for analytical signal were much higher by applying SWV than DPV, therefore this technique was recommended as more suitable for quantification of quercetin in real samples. Obtained slopes and intercepts for calibration curves indicated the highest sensitivity by using citrate and BR buffers.

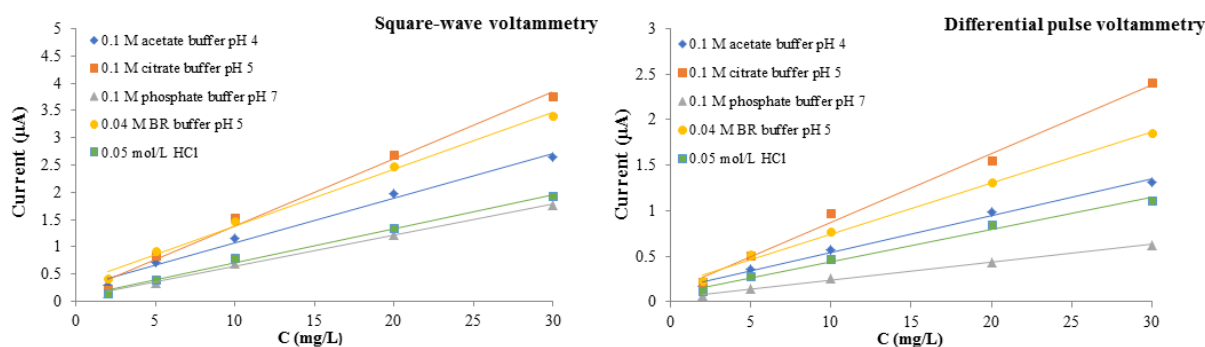


Figure 1. Plots between peak current vs. concentration of quercetin obtained using SWV and DPV.

Conclusion

In this study preliminary results for voltammetric determination of quercetin by using boron-doped diamond electrode as a working electrode were presented. Voltammetric behavior of quercetin was investigated by CV, SWV and DPV in different supporting electrolytes. For

developing a voltammetric method a well-defined oxidation peak at the potential of about +0.70 V was selected. The analytical signal of SWV was much higher than for DPV, therefore this technique would be more suitable for further optimization and validation of analytical method for quercetin determination in real samples. Although good linearity was obtained for all studied supporting electrolytes, the best sensitivity was expected to obtain for citrate and Britton-Robinson buffers. Based on these preliminary results, further experiments will be focused on the optimization of pH value and concentration of the buffer, as well on optimization of the instrumental parameters of the SWV.

Acknowledgements

This study is supported by the Serbian Ministry of Education, Science and Technological Development (Grant III 46009).

References

- [1] A. V. A. David, R. Arulmoli, S. Parasuraman, *Pharmacogn. Rev.* 10 (2016) 84.
- [2] V. Pilařová, K. Plachká, L. Chrenková, I. Najmanová, P. Mladěnkac, F. Švec, O. Novák, L. Nováková, *Talanta* 185 (2018) 71.
- [3] S. Kumar, V. Lather, D. Pandita, *Food Chem.* 197 (2016) 959.
- [4] M. Al-Owaisi, N. Al-Hadiwi, S. A. Khan, *Asian Pac. J. Trop. Biomed.* 4 (2014) 964.
- [5] D. G. Watson, E. J. Oliveira, *J. Chromatogr. B Biomed. Sci. Appl.* 723 (1999) 203.
- [6] G. S. Kanberoglu, E. Yilmaz, M. Soylak, *J. Mol. Liq.* 279 (2019) 571.
- [7] R. Khani, R. Sheykhi, G. Bagherzade, *Food Chem.* 129 (2019) 220.
- [8] Z. Gan, Q. Chen, Y. Fu, G. Chen, *Food Chem.* 130 (2012) 1122.
- [9] B. Pierozynski, D. Zielinska, 651 (2011) 100.
- [10] A. M. O. Brett, M. E. Ghica, *Electroanal.* 15 (2003) 1745.
- [11] A. Masek, M. Zaborski, E. Chrzescijanska, *Food Chem.* 127 (2011) 699.
- [12] D. Saritha, A. R. Koirala, M. Venu, G. D. Reddy, A. V. B. Reddy, B. Sitaram, G. Madhavi, K. Aruna, *Electrochim. Acta* 313 (2019) 523.
- [13] M. Mosleh, S. M. Ghoreishi, S. Masoum, A. Khoobi, *Sensor Actuat. B-Chem.* 272 (2018) 605.
- [14] V. Erady, R. J. Mascarenhas, A. K. Satpati, S. Detriche, Z. Mekhalif, J. Delhalle, A. Dhason, *Mat. Sci. Eng. C-Mater.* 76 (2017) 114.
- [15] J. H. T. Luong, K.B. Male, J.D. Glennon, *Analyst* 134 (2009) 1965.
- [16] M. Hupert, A. Muck, J. Wang, J. Stotter, Z. Cvackova, S. Haymond, Y. Show, G. M. Swain, *Diam. Relat. Mater.* 12 (2003) 1940.
- [17] J. Permpool, T. Tangkuaram, A. Preechaworapun, *NU. Int. J. Sci.* 15 (2018) 69.
- [18] A. A. Abdullah, Y. Yardım, Z. Şentrürk, *Talanta* 187 (2018) 156.

CLASSICAL EXTRACTION OF POLYPHENOLIC COMPOUNDS FROM INDUSTRIAL HEMP (*CANNABIS SATIVA* L.)

Zorica Drinić^{1,2}, Jelena Vladić¹, Anamarija Koren³, Biljana Kiprovska³, Aleksandra Mišan³, Senka Vidović¹

¹*Department of Biotechnology and Pharmaceutical Engineering, Faculty of Technology, University of Novi Sad, 21000 Novi Sad, Serbia*

²*Institute for Medicinal Plants Research "Dr. Josif Pančić", 11000 Belgrade, Serbia*

³*Institute of Field and Vegetable Crops, 21000 Novi Sad, Serbia*

e-mail: drinic_zorica@yahoo.com

Abstract

Hemp (*Cannabis sativa* L.) is an herbaceous annual dioecious plant recognizable for their characteristic spiky leaves from the Cannabaceae family. *C. sativa* L. is a complex plant with more than 480 compounds which can be divided into diverse phytochemical classes such as cannabinoids, terpenoids, flavonoids, noncannabinoid phenols, hydrocarbons, nitrogen-containing compounds, carbohydrates. The most studied class is the cannabinoids, but *C. sativa*

is a significant source of polyphenols, also.

The effect of different water/ethanol mixtures (30, 50, 70, and 90%) and pure water on the polyphenol content and antioxidant activity of *C. sativa* L. extracts obtained by classical extraction at room temperature for 24 h was investigated. Two different samples were used, aerial parts of young hemp and aerial parts of mature hemp. Young hemp present stage of plant growth before the plant has a reproductive organ, and a mature plant is one which is an incomplete stage of growth with flowers as reproductive organs. The extraction yield, qualitative and quantitative phenolic profiles, total phenols content, total flavonoids content, antioxidant activity, and reductive capacity were determinate in the obtained extracts. TP was from 5.76 to 17.05 mg GAE/g dw for aerial parts of young hemp, and from 5.00 to 10.48 mg GAE/g dw for aerial parts of mature hemp. TF content was from 2.37 to 4.82 mg CE/g dw and from 1.67 to 3.58 mg CE/g dw for aerial parts of young hemp and aerial parts of mature hemp, respectively. Sinapic acid, protocatechin acid, vanillic acid, syringic acid, epicatechin acid, ferulic acid, isovitexin, rutin, cinnamic acid, naringenin, and apigenin were detected in hemp extracts. Antioxidant activity in obtained extracts was determined by the DPPH assay. IC₅₀ values were from 0.1600 to 0.6700 mg/mL and from 0.2500 to 1.7900 mg/mL for aerial parts of young and mature hemp, respectively. Reductive capacity was expressed by EC₅₀ values. EC₅₀ were in the range from 0.5800 to 0.9700 mg/mL for young hemp extracts, while for mature hemp extracts were from 0.7200 to 1.5800 mg/mL.

OPTICAL DETECTION OF RHODAMINE B BY Pt(II) TETRA-(4-ALLYLOXY-PHENYL)-PORPHYRIN

Camelia Epuran^{1*}, Diana Anghel¹, Anca Lascu¹, Ion Fratilescu¹, Eugenia Fagadar-Cosma¹

¹*Institute of Chemistry "Coriolan Dragulescu", M. Viteazul Ave. 24, 300223-Timisoara, Romania, Tel: +40256/491818; Fax: +40256/491824*

**email: camy.epuran@yahoo.ro*

Abstract

Rhodamine B is a red, water-soluble synthetic dye with multiple uses in cosmetics, textiles, medicines, food, plastics. Nevertheless, the colorant is toxic causing irritation of the skin, eyes, and airways. For this reason, the control of foods and cosmetics is a must. The present study reports a simple and fast UV-vis spectrophotometric method for the detection of rhodamine B by using as sensitive material Pt(II)-tetra-(4-allyloxy-phenyl)-porphyrin. The method is viable in the range of rhodamine B concentrations from 1.94×10^{-6} M to 4.26×10^{-5} M with very good accuracy.

Introduction

Rhodamine B, represented in Figure 1a, is a red, water-soluble synthetic dye that is part of the xanthine class [1]. Due to its intense color, rhodamine B has been extensively used as a dye in industrial applications such as cosmetics, textiles, medicines, food, plastics [2]. Besides, being a strong fluorescent compound, rhodamine is also used in biotechnological applications such as fluorescence microscopy and flow cytometry [3]. Rhodamine B dyes are generally toxic to humans and animals, causing irritation of the skin, eyes, and airways [4] and is soluble in polar solvents, such as: water, methanol and ethanol. Due to its harmful effects it is of great importance to develop a simple and fast method for recognizing and determining of rhodamine content in different samples.

Various techniques were used in the last years for the specific determination of rhodamine as follows: rhodamine content in tap water by UV-VIS spectroscopy with a limit of detection of $1.47 \mu\text{g/L}$ [3]; rhodamine presence in ballpoint pen inks by high performance liquid spectrophotometry [5] and the presence of unauthorized rhodamine B colorant in foods (curry paste and chili sauce) by capillary chromatography [6]. The purpose of our study was to achieve a simple and efficient method for the detection of Rhodamine B as unauthorized colorant in different foods and tap waters, by using as sensitive material a novel synthesized Pt-porphyrin, namely Pt(II) tetra-(4-allyloxy-phenyl)-porphyrin (**Pt-TAPP**) (structure presented in Figure 1b).

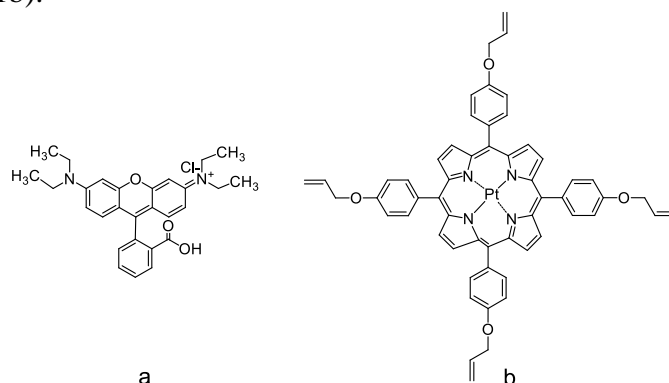


Figure 1. a) The structure of rhodamine B; b) the structure of **Pt-TAPP** metalloporphyrin

Materials and methods

Reagents

Dimethyl sulfoxide (DMSO) was purchased from Merck (Darmstadt, Germany), rhodamine B is provided by Polske Odczynniki Chemiczne (Gliwice, Poland). The platinum metalloporphyrin Pt(II)-5,10,15,20-tetrakis-(4-allyloxyphenyl)-porphyrin was synthesized in our laboratory by classical metallation reaction performed in chlorobenzene [7] using as salt the platinum soluble complex $\text{PtCl}_2(\text{PhCN})_2$ an a molar ratio of 1:1.5 between the porphyrin base and the platinum salt.

Method

The experiments were performed in 5 mL porphyrin solutions in DMSO with concentration of 9.93×10^{-6} M, to which for the first 5 experiments 0.05 mL of rhodamine B solution with concentration of 2.004×10^{-5} M, were added and for the next, the rhodamine B additions were increased to 0.1 mL. The mixtures were stirred for 1 minute and then the UV-vis spectrum was recorded for each step.

Apparatus

For recording of the UV-visible spectra a JASCO UV- V-650 spectrometer (Japan) and standard 1 cm pass quartz cells were used.

Results and Discussions

The UV-vis spectroscopy, presented in Figure 2, displays the porphyrin base electronic spectrum, typical for a metalloporphyrin, having the intense Soret band located at 409 nm and the Q band at 513 nm. Besides, the rhodamine B spectrum is represented having a large absorption band with its main peak located at 560 nm, accompanied by two shoulders the first one at 475 nm and the second at 513 nm.

By increasing the rhodamine B content, the spectra change as follows: a continuous decrease of the intensity of the Soret bands is accompanied by a continuous increasing of a new band located at 550 nm. All these phenomena are associated by the appearance of three isosbestic points, one on Soret band (see Figure 2) and two on the Q band, as represented in Figure 3.

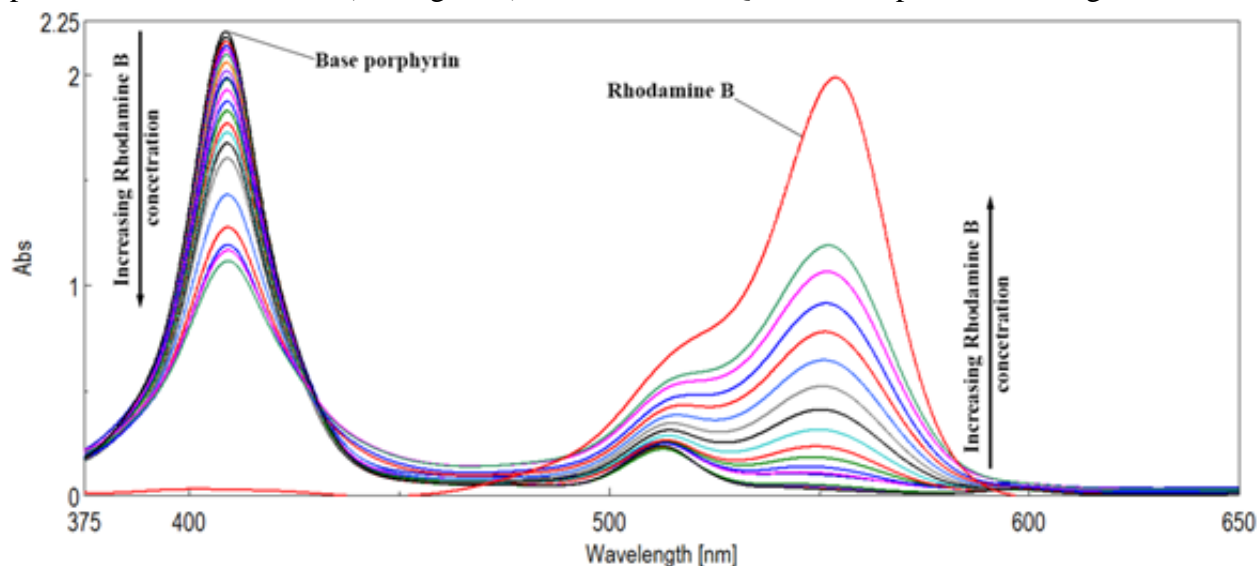


Figure 2. Overlapped UV-vis spectra monitoring the changes during rhodamine B additions

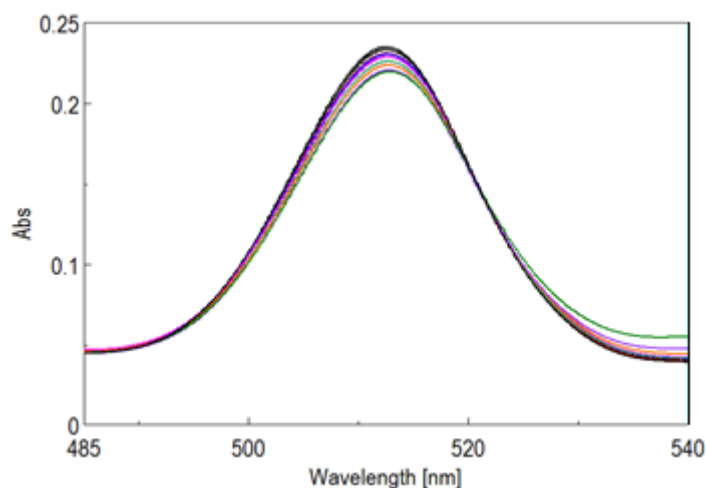


Figure 3: Isosbestic points located on Q band at 493 nm and 521 nm (the first 8 samples)

The dependence between the intensity of the new generated band from 550 nm and the rhodamine B concentration was represented in Figure 4. The dependence is linear in the rhodamine B concentration range from 1.94×10^{-6} M to 4.26×10^{-5} M, that is a large domain relevant for both food content analysis and for cosmetics control and toxicity of released waters after dyeing processes. The correlation coefficient is very good of 98%.

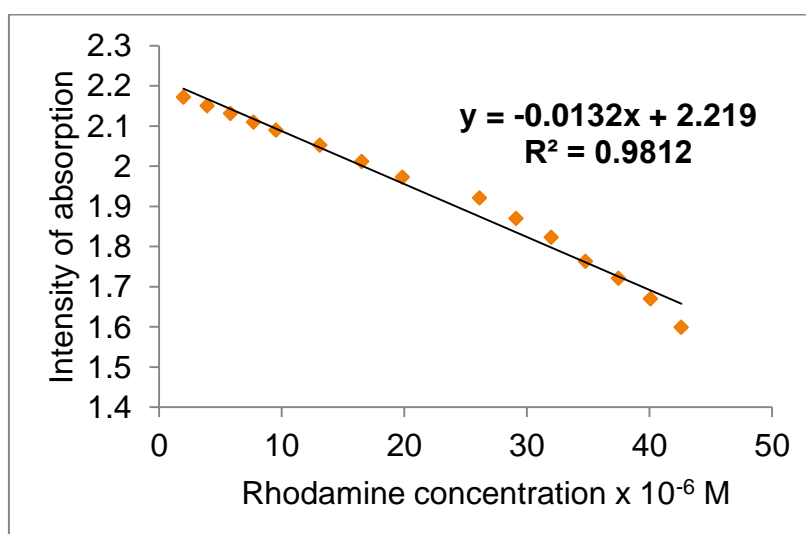


Figure 4. The dependence between the intensity of the new generated band from 550 nm and the rhodamine B concentration

Test on real samples

Tests were performed on two water samples from two different regions (Romania and France) and on a cosmetic sample (lipstick).

Following the analysis, the lack of rhodamine B was recorded in the water samples, but in the sample from cosmetics the presence of rhodamine B was identified.

Conclusion

We obtained a simple and fast UV-vis spectrophotometric method for the detection of rhodamine B applicable in the control of different foods by using as sensitive material Pt(II)-

tetra-(4-allyloxy-phenyl)-porphyrin. The method is viable with very good accuracy in the range of rhodamine B concentrations from 1.94×10^{-6} M to 4.26×10^{-5} M.

Acknowledgements

The authors are acknowledging UEFISCDI PN-III-P1-1.2-PCCDI-2017-1-Project ECOTECH-GMP 76PCCDI/2018 and the Romanian Academy for financial support in the frame of Programme 3/2019 from ICT.

References

- [1] D. Glossman-Mitnik, *Procedia Computer Science* 18 (2013) 816 – 825.
- [2] K. Ravi, B. Deebika, K. Balu, J. Hazard, *Mater*, 122 (2005) 75-83.
- [3] N. Ozkantar, M Soylak, M. Tuuzen, *Turk J. Chem.*, 41(2017) 987 – 994.
- [4] J. Chen, X. Zhu, *Food Chemistry* 200 (2016) 10–15.
- [5] H. Chen, *Forensic Science Journal*, 6 (2007) 21-37.
- [6] C. Tatebe X. Zhong, T. Ohtsuki, H. Kubota, K. Sato, H. Akiyama, *Food Sci. Nutr.*, 2 (2014) 547-56.
- [7] K. Yamashita, N. Katsumat, S. Tomita, M. Fuwa, K. Fujimaki, T. Yoda, D. Hirano, K. Sugiura, *Chem. Lett.*, 44 (2015) 492-494.

PLATINUM-PORPHYRIN INVOLVED IN THE UV-VIS SPECTROPHOTOMETRIC DETECTION OF RHODAMINE B AND OXYGEN PEROXIDE

Ion Fratilescu^{1*}, Diana Anghel¹, Anca Lascu¹, Camelia Epuran¹, Eugenia Fagadar-Cosma¹

¹Institute of Chemistry "Coriolan Dragulescu", M. Viteazul Ave. 24, 300223-Timisoara, Romania, Tel: +40256/491818; Fax: +40256/491824

* email: ion.fratilescu@gmail.com

Abstract

Based on the potential toxicity of rhodamine B, the purpose of this study was to realize a novel UV-vis spectrophotometric method for the rapid and not expensive detection of this dye from water, soft drinks and various foods, using as sensitive material Pt(II) 5,10,15,20-tetra(4-methoxy-phenyl)-porphyrin (Pt(II)-TMeOPP). The method was successful in the detection domain 2×10^{-8} M up to 1.2×10^{-7} M. The second achievement was the application of this complex formed between Pt(II)-TMeOPP and rhodamine B as potential sensitive agent for the sensing of hydrogen peroxide, and it proved to be efficient in the medical field relevance ($5-14 \times 10^{-8}$ M).

Introduction

Rhodamine B is an organic dye having as scaffold the xanthene structure (Figure 1a) and is often used for measuring absolute fluorescence quantum yields [1], as biomarker and tracer for wildlife studies [2,3]. The organic chloride salt rhodamine b with IUPAC name N-[9-(ortho-carboxyphenyl)-6-(diethylamino)-3H-xanthen-3-ylidene] diethyl ammonium chloride is very soluble in water and gives a powerful reddish coloration. The xanthene dye is also used as a colorant in textiles, food industry and as water tracer [4]. Based on the knowledge that Rhodamine B inhibits the proliferation of human lip fibroblasts KD cells that are essential for the maintenance of the healthy lip tissue, so that the application of this compound as coloring agent in cosmetics such as: lipsticks and soaps, has to be strictly monitored. There are also studies that report the toxicity of rhodamine B which leads to liver damage, erythrocyte hemolysis, mutagenicity and carcinogenicity [5].

Based on the potential toxicity of rhodamine B, the purpose of this study is to realize a novel spectrophotometric method for the rapid and not expensive detection of this dye from water, using as sensitive material Pt(II)-5,10,15,20-tetra(4-methoxy-phenyl)-porphyrin (Pt(II)-TMeOPP), with the structure presented in Figure 1b.

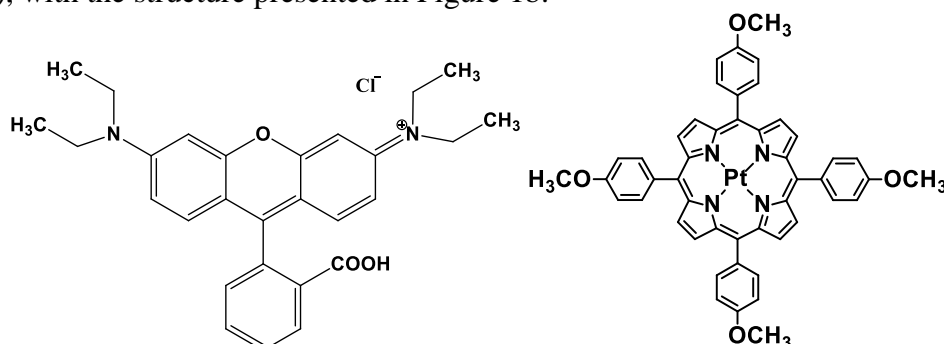


Figure 1. a) The xanthene-type structure of rhodamine B; b) the structure of Pt(II)-TMeOPP. The second aim was to use the complex formed between Pt(II)-TMeOPP and rhodamine B as potential sensitive agent containing two active fluorescent dyes, for the sensing of hydrogen peroxide.

Experimental

Apparatus. For the spectrophotometric determinations we used a UV-visible JASCO V-650 spectrophotometer with Perkin Elmer quartz cuvettes with 1 cm pitch.

Reagents. The Pt(II)-5,10,15,20-tetra(4-methoxy-phenyl)-porphyrin was synthesized and fully characterized, in our laboratory, as previously reported [6].

Tetrahydrofuran (THF) was acquired from Merck GaA (Darmstadt, Germany). The rhodamine B origin is from Polskie Odczynniki Chemiczne (Gliwice, Poland).

Spectrophotometric method for rhodamine B detection. The experiment is based on the UV-vis spectrophotometric titration of 5 mL Pt(II) 5,10,15,20-tetra(4-methoxy-phenyl)-porphyrin solution ($c=1.592 \times 10^{-5}$ M) in THF, with portions of 0.5 mL rhodamine B solution ($c=2.004 \times 10^{-5}$ M). After each addition of rhodamine, the mixture was stirred with electromagnetic stirrer for 30 seconds and the UV-vis spectrum was performed.

The second experiment consisted in stepwise addition of 0.03 mL of H_2O_2 to the sample 7 from the previous experiment, under stirring.

Results and discussions

Figure 2 is showing the overlapped UV-vis spectra after adding rhodamine B to the solution of Pt(II)-5,10,15,20-tetra(4-methoxy-phenyl)-porphyrin. The metalloporphyrin displays the characteristic spectrum for a Pt-porphyrin with the Soret band located at 405 nm and the Q band placed at 511 nm. The rhodamine B has the main characteristic peak at 560 nm. The emergence of a new band blue shifted relative to the bare rhodamine B band at 550 nm, together with the appearance of two isosbestic points on the Soret band at 386 nm, respectively at 421 nm, associated with the decrease of the Soret band and the increase of the new band proves that a new complex was formed.

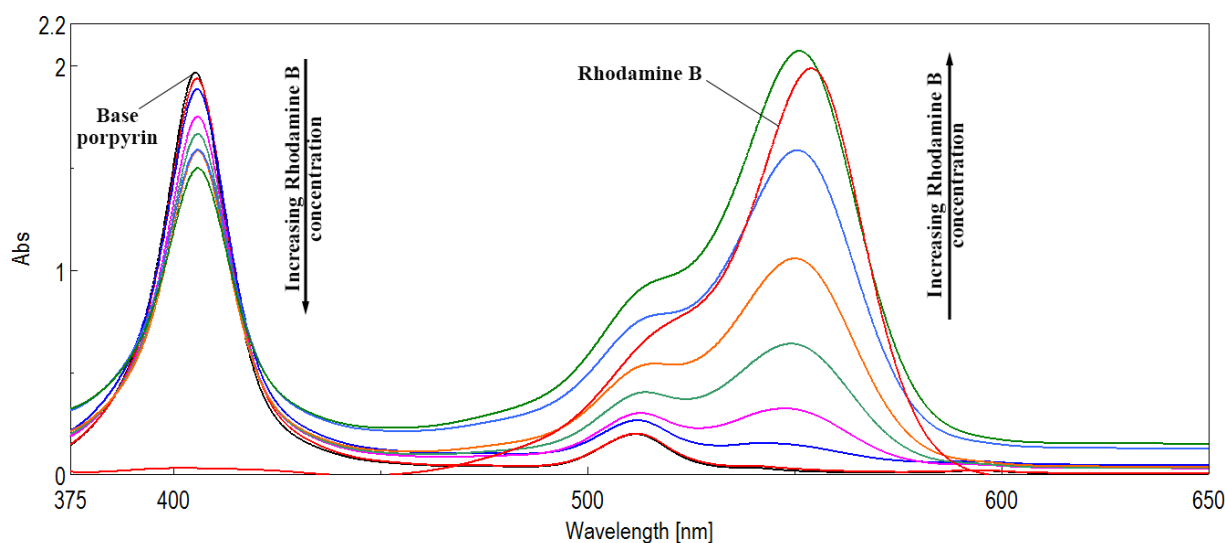


Figure 2. Superposed UV-vis spectra proving the obtaining of the complex between Pt(II)-TMeOPP and rhodamine B.

Besides, the graphical representation between the intensity of absorption measured at Soret band and the concentration of rhodamine B is linear with a fair correlation coefficient of 98.66% (Figure 3), in a domain from 2×10^{-8} M up to 1.2×10^{-7} M, a field that is relevant for the monitoring of soft drinks, red wine grape juice and chili oil [7]. As a conclusion, Pt(II)-TMeOPP can act as sensitive compound for the detection of rhodamine B in several drinks and foods. In order to achieve a real optical sensor, further studies will be performed regarding the effect of different analytes interference.

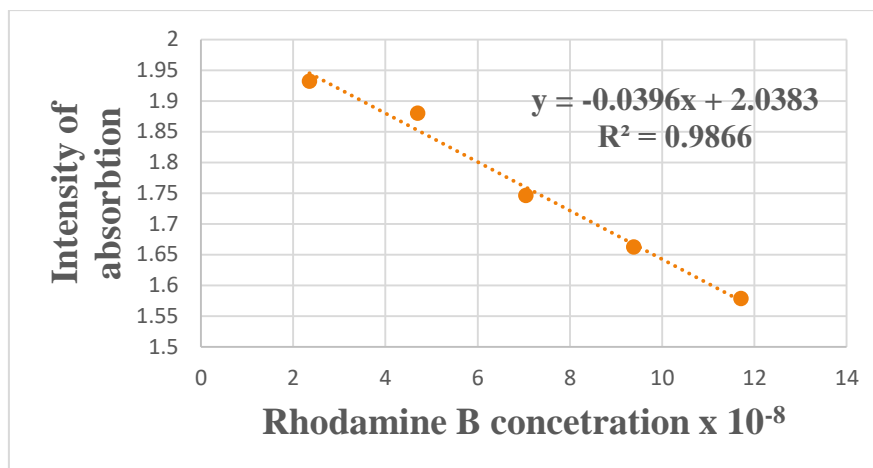


Figure 3. The linear dependence between the intensity of absorption measured at Soret band and the concentration of rhodamine B

The second part of this investigation, was focused on the capacity of the complex formed between the Pt(II)-TMeOPP and rhodamine B to detect hydrogen peroxide. As can be seen from Figure 4, by increasing H_2O_2 concentration, the intensity of the Soret band of the complex is continuously decreasing, while the main band of the complex, located at 550 nm is increasing.

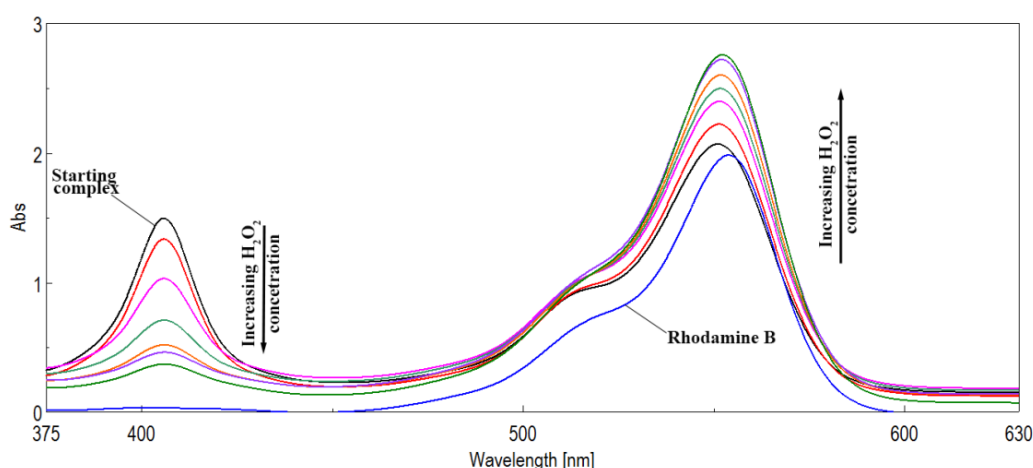


Figure 4. The overlapped UV-vis spectra of the complex Pt(II)-TMeOPP - rhodamine B showing the influence of adding H_2O_2

This phenomenon, going to the complete disappearance of the Soret band and the hyperchromic effect of the band at 551 nm, can be explained by the capacity of the rhodamine B partner to decompose the porphyrin ring in the presence of H_2O_2 . Nevertheless, the dependence between the intensity of absorption measured at 551 nm and the H_2O_2 concentration (Figure 5) is linear in a field ($5\text{--}14 \times 10^{-8}$ M) that is of medical relevance for oxidative stress tests [8].

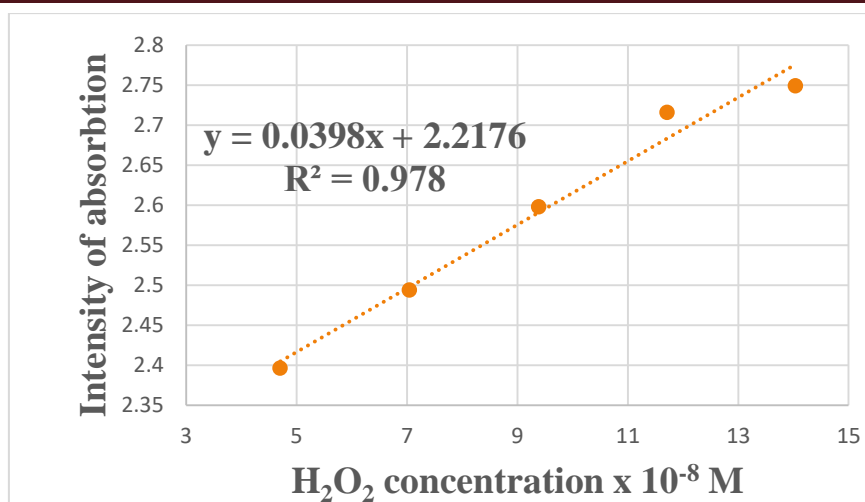


Figure 5. The dependence between the absorption intensity of the complex between Pt(II)-TMeOPP and rhodamine B and the concentration H₂O₂ read at 551 nm

Conclusion

This work comprised many steps: the obtaining of a new complex complex between rhodamine B and Pt(II)-TMeOPP; the potential application on the spectrophotometric detection of rhodamine B from foods and drinks in the field 2×10^{-8} M up to 1.2×10^{-7} M using the Pt-porphyrin as sensitive material; the application of the complex for the detection of minute amounts of hydrogen peroxide with relevance for medical tests. The work has to be continued with the study of different analytes interference in order to set up the real sensors.

Acknowledgements

The authors are acknowledging UEFISCDI PN-III-P1-1.2-PCCDI-2017-1-Project **ECOTECH-GMP 76PCCDI/2018** and the Romanian Academy for financial support in the frame of Programme 3/2018 from ICT.

References

- [1] T. Karstens, K. Kobs, The Journal of Physical Chemistry 84 (1980) 1871.
- [2] P. Fisher, Wildlife Society Bulletin, 27 (1999) 318.
- [3] G. Lindsey, Northwest Science, 57 (1983) 16.
- [4] R. Jain, M. Mathur, S. Sikarwar, A. Mittal, Journal of Environmental Management, 85 (2007) 956.
- [5] T. Kaji, T. Kawashima, C. Yamamoto, M. Sakamoto, Y. Kurashige, F. Koizumi, Toxicology Letters 60 (1992) 69.
- [6] D. Vlascici, N. Plesu, G. Fagadar-Cosma, A. Lascu, M. Petric, M. Crisan, A. Belean, E. Fagadar-Cosma, Sensors, 18 (2018), 2297.
- [7] N. Ozkantar, M. Soylak, M. Tuzen, Turkish Journal of Chemistry, 41 (2017) 987.
- [8] H. Sies, Redox Biology 11, (2017) 613.

EFFECTS OF ETHANOL ON THE HEPATIC DNA IN MATERNO-FETAL COMPLEX AND ON THE SERUM PROTEINS IN PREGNANT FEMALE RATS

Mirela Ahmadi-Vincu^{1,8}, Florin Muselin^{2,8}, Gabriela Gârban³, Adina Avacovici^{4,8}, Robert Ujhelyi^{5,8}, Sorin Marinescu⁶, Zeno Gârban^{7,8}

¹Department of Biochemistry, Faculty of Veterinary Medicine, University of Agricultural Sciences and Veterinary Medicine of Banat "King Michael I of Romania" Timișoara, Calea Aradului No. 119, Romania; ²Department of Toxicology, Faculty of Veterinary Medicine, University of Agricultural Sciences and Veterinary Medicine of Banat "King Michael I of Romania" Timișoara, Romania; ³Laboratory of Environment and Nutrition, National Institute of Public Health-Branch Timișoara, Romania; ⁴Francisc Neuman Vocational School, Arad, Romania; ⁵Medical Department, S.C. CaliVita International, Timișoara, Romania; ⁶Institute of Chemistry of the Romanian Academy, Bd. M. Viteazu Nr.24, Timișoara, Romania; ^{7,8}Department of Biochemistry and Molecular Biology (former), Faculty of Food Products Technology, University of Agricultural Sciences and Veterinary Medicine of Banat "King Michael I of Romania" Timișoara, Romania; ⁸ Working Group for Xenobiochemistry, Romanian Academy-Branch Timișoara, Bd. M. Viteazu No. 24, Timișoara, Romania
e-mail: zeno.garban@yahoo.com

Abstract

Experimental investigations on the action of ethanol were performed on pregnant female rats and their fetuses. The Wistar strain pregnant rats were included into an experimental (E) and a control (C) group. Animals of experimental group received ethanol and the control group consumed tap water. At the end of the experiment blood samples and liver samples were taken for analysis. In the present study there were pursued values of some biochemical parameters, i.e. maternal and fetal hepatic DNA concentration, maternal serum proteins and electrophoretic fractions (albumins as well as α -, β - and γ -globulins). The obtained data revealed a statistically non-significant increase of hepatic DNA both in mothers and fetuses of experimental group. Serum proteins concentration in the pregnant rats showed a significant increase. Regarding the electrophoretic fractions, a decrease of albumins and increase of globulins were observed. As to globulin subfractions a hyper- α -globulinemia, hypo- β - and hypo- γ -globulinemia were revealed.

Key words: ethanol, pregnant rats, biochemical parameters

Introduction

The harmful action of ethanol on mammalian conception products is manifested by morphological and biochemical disorders during prenatal development (embryonic and fetal periods) and also on postnatal development (Kissin, 1971; Sokol, 2003). Clinical observations and experimental research on laboratory animals have led to the circumscription of the concept of fetal alcohol syndrome (FAS), also called alcoholic embryopathy or alcoholic fetopathy (Henderson et al., 1979; Gârban, 1993; Scott, 2014). Our investigations pursued the changes induced by ethanol on the maternal and fetal hepatic DNA as well as on the maternal serum proteins of rats.

Experimental

General design. Investigations were performed on pregnant female rats (Wistar strain) with an average weight of 180-200 g. Rats were included in two groups: one experimental (E) – animals receiving 20% v/v ethanol ad libitum in drinking water and one control (C) - animals consuming only drinking water. Each group comprised 8 animals and had the same feeding and environmental conditions. On day 20th of pregnancy the animals were euthanased by overdosage of an anesthetic agent. By puncture of the vena cava caudalis blood samples were

collected from the pregnant rats and afterwards a hepatic sample was excized for analysis. Liver samples were taken also from fetuses after fetal laparotomy in order to determine the hepatic DNA concentration. Requirements for the protection of animals used in scientific or other experiments were respected (Council Directive 86/609/EEC).

Biochemical investigations. Maternal and fetal hepatic DNA were determined by Spirin's method (1958) adapted to an UV Vis spectrophotometer (C. Zeiss-Jena). Maternal serum proteins were determined spectrophotometrically based on a reaction with copper sulfate (λ 550 nm), while the electrophoretic fractions by using paper electrophoresis (Kaplan and Pesce, 2010).

Statistical evaluation. All the obtained experimental data were statistically processed, mean values (X) and standard deviations (SD) were calculated. For this purpose the ANOVA (Analysis of Variance) test was used.

Results and discussions

Experimental data revealed the effects of ethanol - considered as a xenobiotic - on the hepatic DNA biosynthesis and indirectly the disturbance of proteins biosynthesis (Mandal et al., 2017; Gârban, 2018). These aspects give an image on the subcellular mechanisms disturbing the morphogenesis processes triggered by chronic alcohol intake.

Understanding the effects induced by ethanol and its metabolites involves the knowledge of the mechanism of ethanol biodegradation (fig.1). It occurs in two steps: initially ethanol is

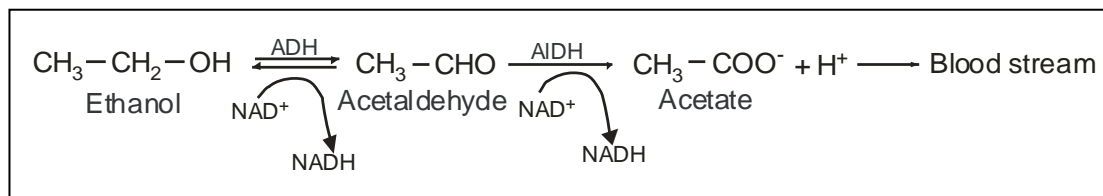


Fig.1. Ethanol biodegradation - general mechanism

transformed to acetaldehyde in cytosol in the presence of the enzyme alcohol dehydrogenase (ADH), afterwards acetaldehyde is converted into acetate in mitochondria under the action of the enzyme aldehyde dehydrogenase (AIDH). The first step of ethanol oxidation, i.e. acetaldehyde formation, can occur in two ways: by the Peroxisomal Ethanol Oxidizing System (PEOS) in which the peroxisomal catalase is involved and by Microsomal Ethanol Oxidizing System (MEOS) in which the CYP2E1 enzyme is acting.

Our experimental data regarding maternal hepatic DNA (Table 1) reveal an increase of the DNA concentration in group E, under the action of ethanol.

Table 1. Concentration of maternal hepatic DNA

Group	Number of gestant females	Hepatic DNA ($\mu\text{g}/\text{mg}$ tissue) $\bar{X} \pm \text{DS}$	$\Delta\bar{X}$ $\bar{X}_C - \bar{X}_E$	Concentration range
C	8	2.95 ± 0.20	-	2.69 – 3.16
E	8	3.01 ± 0.23	+ 0.06	2.73 – 3.19

In literature studies regarding the action of ethanol on fetal and maternal DNA gained more and more extension. Thus, Dreosti et al. (1981) observed the decrease of DNA in rats brain under the action of ethanol. Investigating the DNA content in various organs: brain, liver, heart, Henderson et al. (1978) decelated also, decreases, mentioning the quantitative depresion on the whole organ and augmentation in the determination in $\mu\text{g}/\text{mg}$ hepatic tissue (dosage, possible by lumbar tissue sampling).

Investigations on fetal hepatic DNA – data presented in Table 2 – reveal modifications, i.e. increase (non significant from statistical point of view).

Table 2. Concentration of fetal hepatic DNA

Group	No of gestant females	No of conceptuses	No of living fetuses	Hepatic DNA ($\mu\text{g}/\text{mg}$ tissue) $\bar{X} \pm \text{DS}$	$\Delta\bar{X}$ $\bar{X}_C - \bar{X}_E$
C	8	73	72	3.08 ± 0.38	-
E	8	71	65	3.11 ± 0.46	+ 0.03

Table 3. Serumproteins and electrophoretic fractions in pregnant rats

Specification	Unit	Group C		Group E		$\Delta\bar{X}$ $\bar{X}_C - \bar{X}_E$
		No. anim.	$\bar{X}_C \pm \text{DS}$	No. anim.	$\bar{X}_E \pm \text{DS}$	
Proteins *	g%	8	5.47 ± 0.42	8	5.64 ± 0.59	+ 0.17
Albumins	%	8	56.30 ± 6.12	8	55.20 ± 8.32	- 1.10
Globulins – total			43.70 ± 6.12		44.80 ± 8.32	+ 1.10
α -globulins**			22.70 ± 4.26		25.50 ± 5.63	+ 2.80
β -globulins**			15.20 ± 3.08		14.20 ± 3.96	- 1.00
γ -globulins			5.80 ± 1.60		5.10 ± 1.82	- 0.70

* $0.95 < p < 0.99$ ** $0.90 < p < 0.95$

Results obtained for group C are between characteristic range of species (He et al., 2017). In Group E one can observe the increase of the serum proteins concentration, decrease of albumin fraction and augmentation of globulin fraction, as well as modifications of the globulin subfractions.

Albumins and globulin fractions are involved in the material metabolism. Thus, albumins take part in trophic processes and circulation of diverse inorganic compounds (anions, cations) and small molecule organic compounds. Globulins take also part in trophic and immune processes.

Conclusions

1. Chronic alcohol consumption in case of pregnant rats showed a statistically non-significant increase of their hepatic DNA concentration.
2. Fetuses of the experimental animals revealed also a non-significant increase of the hepatic DNA concentration.
3. A significant increase of serum proteins in pregnant female rats from experimental group was found.

4. Electrophoretic fractions in group E evidenced a decrease of albumins and increase of total globulins. As to globulin subfractions a hyper- α -globulinemia and hypo- β - and hypo- γ -globulinemia were revealed.

References

- [1] Dreosti I.E., Ballard J., Belling G.B., Record J.R., Manuel J.S., Hetzel B.S. – The effect of ethanol and acetaldehyde on DNA synthesis in growing cells and on fetal development in the rat, *Alc. Clin. Exp.Res.*, 1981, 5, 357-362.
- [2] Gârban Z. - Acțiunea alcoolului asupra metabolismului embrio-fetal. pp.139-149, în “*Embrio- și fetopatia alcoolică*”, (Editor Sandor S.), Editura Academiei Române București, 1993.
- [3] Gârban Z. - Quo vadis food xenobiochemistry, 3rd edition, Editura Academiei Române, București, 2018.
- [4] He Q., Su G., Liu K., Zhang F., Jiang Y., Gao J., Liu L., Jiang Z., Jin M., Xie H.- Sex-specific reference intervals of hematologic and biochemical analytes in Sprague-Dawley rats using the nonparametric rank percentile method, *PLoS One*. 2017, 12(12):e0189837. doi: 10.1371
- [5] Henderson G.I., Hoyumpa A.M. Jr., McClain C., Schenker S. – Effects of chronic and acute alcohol administration on fetal development in the rat. *Alcohol Clin. Exp.Res.*, 1979, 33, 99-106
- [6] Kaplan L.A, Pesce A.J. - *Clinical chemistry: theory, analysis and correlation*, 5th edition, Mosby Inc, St. Louis, 2010.
- [2] Kissin, B. (Ed.) - *The Biology of Alcoholism*, Vol. 1: Biochemistry, Plenum Press, New York, London, 1971.
- [7] Mandal C., Halder D., Jung K.H., Chai Y.G.- Gestational Alcohol Exposure Altered DNA Methylation Status in the Developing Fetus, *Int. J. Mol. Sci.*, 2017, 18(7), 1386 doi: 10.3390/ijms18071386
- [8] Scott C.M. - *The SAGE Encyclopedia of Alcohol: Social, Cultural, and Historical Perspectives*. SAGE Publications, New York, 2014.
- [9] Sokol R.J., Delaney-Black V., Nordstrom B. - Fetal alcohol spectrum disorder, *JAMA*, 2003, 290, 2996-2999.
- [10] Spirin A.S. - Spectrophotometric determination of total nucleic acids. *Biochimica*, 1958 23, 656-662.
- [11] *** - Council Directive 86/609/EEC of 24 November 1986 on the approximation of laws, regulations and administrative provisions of the Member States regarding the protection of animals used for experimental and other scientific purposes, Official Journal of the European Union, L 358 , 18/12/1986.

CHARACTERIZATION AND KINETIC STUDY OF MAGENTA PRINTING EFFLUENT AFTER HOMOGENEOUS FENTON TREATMENT

Vesna Gvoić¹, Miljana Prica¹, Đurda Kerkez², Milena Bečelić-Tomin², Aleksandra Kulić², Anita Leovac Maćerak², Božo Dalmacija²

¹*Department of Graphic Engineering and Design, University of Novi Sad, Faculty of Technical Sciences, Trg Dositeja Obradovića 6, 21000 Novi Sad, Serbia*

²*Department of Chemistry, Biochemistry and Environmental Protection, University of Novi Sad, Faculty of Sciences, Trg Dositeja Obradovića 3, 21000 Novi Sad, Serbia
e-mail: kecic@uns.ac.rs*

Abstract

The objectives of this study were to determine the physico-chemical characterization of Magenta printing effluent treated with homogeneous Fenton process, as well as kinetic model that best describes degradation process of organic pollutant. Physico-chemical characterization of printing effluent before and after homogeneous Fenton treatment included measurements of pH, electrical conductivity, temperature, turbidity, chemical oxygen demand, biochemical oxygen demand, total organic carbon and toxicity test. Three kinetic models (first-order, second-order, and Behnajady-Modirshahla-Ghanbary) were evaluated in order to best describe Magenta degradation process. Results indicated that dye degradation process is followed with the increase of conductivity and biological oxygen demand due to the formation of various by-products and release of inorganic ions. The obtained results are in accordance with the established dye mineralization degree on the basis of chemical oxygen demand and total organic carbon content. However, treated printing effluent is characterized as nontoxic due to the *Vibrio fischeri* inhibition of 18.16%.

Introduction

In last two decades, researchers have emphasized the use of advanced oxidation processes (AOPs) as techniques that take prominence among various treatments, in order to reduce the concentration of inorganic and organic pollutants in industrial effluents. The advantages of these processes are reflected in the generation of hydroxyl radicals (HO[•]), powerful oxidizing agents, with a pronounced tendency for degradation of difficult biodegradable compounds, or transformation of pollutants into less toxic products of small molecular weight through rapid and non-selective radical reactions. The most commonly AOPs used in wastewater treatment are ozonization, photocatalysis, electrochemical oxidation, Fenton and Fenton-like processes [1]. In our previous work [2], the homogeneous Fenton process (FeSO₄/H₂O₂ treatment) was applied in order to examine the possibility of Magenta dye removal from flexo printing wastewater. The process was optimized and maximum decolorization efficiency of 95.91% was achieved. The aim of this study was to determine physico-chemical characterization of Magenta printing effluent treated with homogeneous Fenton process. Further more, three kinetic models were used to describe degradation process of Magenta dye in printing effluent.

Experimental

Materials. Experiments were performed on Magenta printing effluent obtained from flexographic printing facility located in Novi Sad, Serbia. Magenta dye (C.I.: PR57:1, CAS number: 5281-4-9, chemical formula: C₁₈H₁₂N₂O₆, molar mass: 352 g/mol; λ_{max} = 573 nm) was produced from Flint Group and belongs to the group of azo dyes.

Physico-chemical analysis of printing effluent before and after Fenton treatment. Physico-chemical characterization of printing effluent before and after homogeneous Fenton treatment included determination of pH, electrical conductivity, temperature (AD110 Adwa instrument), turbidity (Turb 430 IR WTW), chemical oxygen demand (COD), biochemical oxygen demand (BOD), total organic carbon (TOC) (LiquiTOC II - Elemental, Germany), as well as toxicity evaluation. COD measurement was conducted using the potassium dichromate volumetric method - SRPS ISO 6060: 1994 [3]. Determination of BOD after 5 days at 20 °C was carried out by the manometer method - H1.002 (Velp Scientifica Italia, Lowibond and WTW), while the method SRPS ISO 8245:2007 [4] was used to determine the TOC value, which was used to estimate the mineralization degree of treated effluent according to the equation (1):

$$TOC (\%) = \frac{TOC_0 - TOC}{TOC_0} * 100 \quad (1)$$

where: TOC_0 represent total organic carbon content in the printing effluent before the homogeneous Fenton treatment, and TOC is the total organic carbon content in the printing effluent after the homogeneous Fenton treatment.

Determination of anionic surface active substances (dodecylbenzene sulfonate - DBS) was measured by the index of methylene blue spectrophotometric method based on SRPS EN 903:2009 [5]. Chloride content was determined according to ISO 9297/1: 2007 [6], while the phosphorus content was determined with spectrophotometric method with ammonium-molybdate according to the SRPS EN ISO 6878:2008 [7].

Standard ISO 11348-3:2009 method was applied to test the toxicity of printing effluent before and after treatment, in order to evaluate negative impact of printing wastewater on living organisms [8].

Kinetics of homogeneous Fenton process. Numerous mathematical models have been used to describe the degradation kinetics of organic pollutants, based on the equilibrium state approximation. The main assumptions are based on the facts that the concentration of HO^\bullet radicals is correlated with the concentration of hydrogen peroxide, or that the HO^\bullet radicals formation rate is equal to their consumption rate [9, 10]. Since the whole dye degradation process cannot be described by simple kinetic model, the first-order, second-order and Behnajady-Modirshahla-Ghanbary (BMG) models were used to study Magenta degradation kinetics by the homogeneous Fenton oxidation process [11, 12]. The mathematical models of the first and second order reaction kinetics, as well as the BMG model are present in equations 2 - 4 [13]:

$$\frac{dA_t}{dt} = -k_1 A_t \quad (2)$$

$$\frac{dA_t}{dt} = -k_2 (A_t)^2 \quad (3)$$

$$\frac{A_t}{A_0} = 1 - \left(\frac{t}{m+bt} \right) \quad (4)$$

where A_0 and A_t represent the initial dye absorbance over a period of time from zero to t , k_1 and k_2 are the first and second order constants, while b and m are the BMG model constants, related to the reaction kinetics and oxidation capacity, respectively.

The parameters of kinetic models were calculated using linear forms of first- and second-order mathematical models, as well as BMG models (equations 5 - 7):

$$A_t = A_0 * e^{-k_1 t} \quad (5)$$

$$\frac{1}{A_t} = \frac{1}{A_0} + k_2 t \quad (6)$$

$$\frac{t}{1 - \frac{A_t}{A_0}} = m + bt \quad (7)$$

By plotting the dependence graphs $\ln(A_0/A_t)$ in function t for the first-order model, $(1/A_t)$ in function t for second-order model and $t/(1 - (A_t/A_0))$ in function t for BMG model, the kinetic model parameters were calculated and used to interpret the kinetics of the observed reactions.

Results and discussion

The obtained values of physico-chemical parameters (Table 1) indicate that homogeneous Fenton treatment is characterized with the conductivity and BOD increase, pointing to the formation of numerous degradation by-products. The experimental results indicate that the mineralization percentage of Magenta dye of 49.82% is followed with 71.44% of COD reduction (Figure 1). On this basis, Magenta dye degradation resulted within the formation of low molecular weight fragments during the homogeneous Fenton process.

Table 1. Physico-chemical characterization of printing effluent before and after treatment

Parameter	Printing effluent	Treated printing effluent
pH	7.60	7
Conductivity [μScm^{-1}]	403	560
Temperature [$^{\circ}\text{C}$]	22.1	22.6
Turbidity [NTU]	18.81	10.3
COD [$\text{mgO}_2\text{L}^{-1}$]	377.7	107.87
BOD [$\text{mgO}_2\text{L}^{-1}$]	5	27
TOC [mgCL^{-1}]	166.4	83.49
DBS [mgL^{-1}]	0.77	<0.1
Phosphate [mgPL^{-1}]	<0.011	<0.011
Chlorides [mgCIL^{-1}]	21.60	22.30

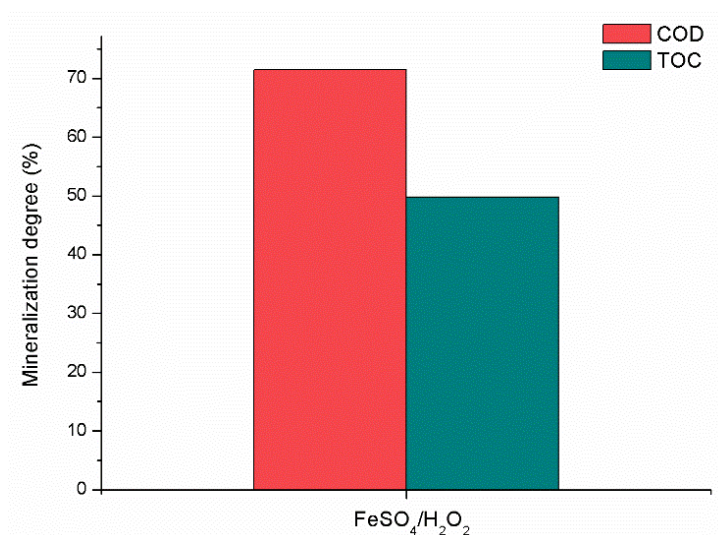


Figure 1. Mineralization degree of printing effluent after homogeneous Fenton treatment. The results of acute toxicity test on *Vibrio fischeri* bacteria (Table 2) indicated slightly increased toxicity of treated printing effluent after homogeneous Fenton process. This percentage of inhibition falls within the range below 50%, confirming that the treated printing effluent is nontoxic.

Table 2. Results of toxicity test by *Vibrio Fischeri* inhibition

Sample	GL	Inhibition (%)
Wastewater before Fenton treatment	4	15.11
FeSO ₄ /H ₂ O ₂ treatment	2	18.16

The results of the kinetic studies used to analyze the Magenta dye degradation in printing effluent are presented in Table 3 and Figure 2. The highest values of correlation coefficient were established using the BMG model, which best describes the dye degradation process.

Table 3. Kinetic parameters of selected models for Magenta dye degradation

Model	First-order		Second-order		^a BMG model			
Process	K ₁ (min ⁻¹)	R ²	K ₂ (l mg ⁻¹ min ⁻¹)	R ²	b	m	1/m	R ²
FeSO ₄ /H ₂ O ₂	0,031	0,649	0,062	0,602	0,905	18,439	0,054	0,986

^aBehnajady-Modirshahla-Ghanbary model

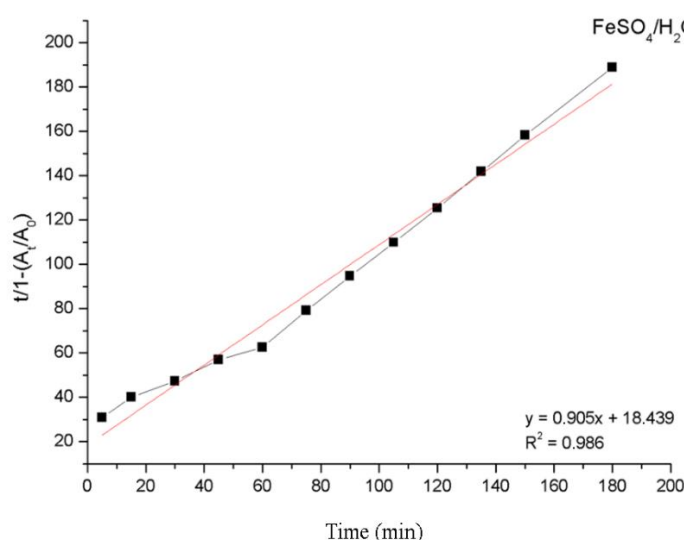


Figure 2. Decolorization kinetics of printing effluent under optimal process conditions - BMG model

Linear plot of $t/(1-A/A_0)$ versus t was used to determine the parameters b and m , which describes the oxidizing capacity and the initial rate of decolorization reaction, respectively. Based on R^2 value, chosen model offers satisfactory interpretation of the kinetic process, while the obtained high value of $1/m$ indicates high initial rate of Magenta dye degradation.

Conclusion

Due to the high homogeneous Fenton efficiency in our previous work a physico-chemical characterization of treated printing effluent was investigated. Conductivity and biological oxygen demand increasment was established, which together with the obtained mineralization degree indicated the formation of numerous low molecular weight fragments during the homogeneous Fenton process. However, the isolated by-products did not contribute to the toxicity increase, confirming that the treated printing effluent is nontoxic. Behnajady-Modirshahla-Ghanbary, as most appropriate kinetic model, indicated high initial rate and oxidation capacity of Magenta dye degradation during the homogeneous Fenton treatment.

Acknowledgements

The authors acknowledge the financial support of the Ministry of Education, Science and Technological Development of the Republic of Serbia within the Projects No. TR 34014 and III43005.

References

- [1] S. Karimifard, M. Moghaddam, *Sci. Total. Environ.* 640-641 (2018) 772.
- [2] V. Kecić, M. Prica, Đ. Kerkez, M. Bečelić-Tomin, A. Kulić, A. Leovac Maćerak, B. Dalmacija (2018) 13th International Scientific Conference “Flexible Technologies“ - MMA, 331.
- [3] Water quality - Determination of the chemical oxygen demand SRPS ISO 6060: 1994.
- [4] Water quality - Guidelines for the determination of total organic carbon (TOC) SRPS ISO 8245:2007.
- [5] Water quality - Determination of anionic surfactants by measurement of the methylene blue index MBAS (ISO 7875-1:1984 modified) SRPS EN 903:2009.
- [6] Water quality - Determination of chloride - Silver nitrate titration with chromate indicator (Mors method) - Amendment 1 SRPS ISO 9297/1:2007
- [7] Water quality - Determination of phosphorus - Ammonium molybdate spectrometric method (ISO 6878:2004) SRPS EN ISO 6878:2008.
- [8] Water quality - Determination of the inhibitory effect of water samples on the light emission of vibrio fischeri (luminescent bacteria test) - part 3, ISO 11348-3:2009
- [9] T. Liu, H. You, *React. Kinet. Mech. Cat.* 109 (2013) 233.
- [10] M. El-Haddad, A. Regti, R. Laamari, R. Mamouni, N. Saffaj, *Journal of Materials and Environmental Science* 5 (2014) 667.
- [11] A. Hassan, M. Rahman, G. Chattopadhyay, R. Naidu *Environmental Technology and Innovation* 15 (2019) 100380.
- [12] M. Behnajady, N. Modirshahla, F. Ghanbary, *J. Hazard. Mater.* 148 (2007) 98
- [13] N. Ertugay, F. Acar, *Arab. J. Chem.* 10 (2017) S1158.

DETERMINATION OF STRUCTURAL-FUNCTIONAL INTERACTIONS OF GANGLIOSIDES WITH PEPTIDES AND PROTEINS BY MICROFLUIDICS –MASS SPECTROMETRY

Raluca Ica¹, Mirela Sarbu¹, Alina Secara², Laurentiu Popescu¹, Alina Petrut¹, Alina D. Zamfir^{1,3}

¹National Institute for Research and Development in Electrochemistry and Condensed Matter, Timisoara, Romania; ²“Victor Babes” University of Medicine and Pharmacy, Timisoara, Romania; ³“Aurel Vlaicu” University of Arad, Arad, Romania
e-mail: raluca.ica@gmail.com

Abstract

Gangliosides (GGs) mediate vital biological processes through non-covalent intermolecular interactions. To understand the structure-function relationship at the molecular level for each GG structural entity involved in a physiological / pathological process and to improve the therapeutic significance, it is necessary to determine their interactions in detail using the most accurate methods of analysis. To address the issues of high biological relevance of GGs, mass spectrometry (MS) has lately become a method of choice due to its capability to detect minor species in complex mixtures with an unsurpassed sensitivity.

The noncovalent interaction between the Amyloid beta (A β) protein and a native complex mixture of gangliosides extracted and purified from normal adult human brain was studied using an analytical platform encompassing fully automated chip-nanoelectrospray ionization (nanoESI) on a NanoMate robot coupled to a high-capacity ion trap (HCT) mass spectrometer (MS). The interaction assay involved the incubation at 37 °C under constant steering of A β and gangliosides dissolved in 10 mM ammonium acetate buffer, pH 6.0, up to a concentration of 1 pmol μL^{-1} and 10 pmol μL^{-1} , respectively. Aliquots of the reaction products were collected directly after 1, 5, 10, 15, 30, 60 and 180 min of incubation in the 96-well plate of the NanoMate robot and immediately submitted to MS analysis.

Chip-nanoESI QTOF MS and CID MS/MS revealed the formation of the A β -GT1 (d18:1/18:0) non-covalent complex formed between the protein and the dihydroxylated sphingoid base of GT1, detected as $[M + 4H]^{4+}$ at m/z 1615.181 and the A β -GT1 complex (t18:1/18:0) of the protein with a trisialylated trihydroxylated ceramide species, detected at m/z 1618.902. CID MS/MS top-down fragmentation analysis at low energy demonstrated that the A β protein binds to a GT1b isomer type structure (with a monosaccharide Neu5Ac to external galactose and a disialo element Neu5Ac-Neu5Ac to internal galactose). Thus, by chip-MS and tandem MS experiments it was possible to deduce the structure of this non-covalent complex as: A β -GT1b (d18:1/18:0). Similar results (GT1b isomer) were obtained also for the complex formed with the GG having a trihydroxylated ceramide, hence resulting a complex with A β -GT1b (t18:1/18:0) composition.

Acknowledgements

This project was supported by the Romanian National Authority for Scientific Research, UEFISCDI through projects PN-III-P4-ID-PCE-2016-0073, PN-III-P1-1.2-PCCDI-2017-0046 granted to ADZ and PN-III-P1-1.1-PD-2016-0256 granted to MS.

ANTIMICROBIAL EFFECT OF SOME NEW SALICYLAMIDE DERIVATIVES

Ienașcu, I.M.C.^{1,2}, Căta, A.¹, Ștefănuț, M.N.¹, Obistioiu, D.³, Popescu, I.M.⁴¹National Institute of Research and Development for Electrochemistry and Condensed Matter, 144 Dr. A. P. Podeanu, 300569, Timișoara, Romania²“Vasile Goldiș” Western University of Arad, Faculty of Pharmacy, Department of Pharmaceutical Sciences, 86 Liviu Rebreanu, 310045, Arad, Romania³Banat's Agricultural Science University, Faculty of Agriculture, Interdisciplinary Research Platform, 119 Calea Aradului, 300645, Timișoara, Romania⁴Banat's Agricultural Science University, Faculty of Agriculture, Department of Chemistry and Biochemistry, 119 Calea Aradului, 300645, Timișoara, Romania
imcienascu@yahoo.com**Abstract**

New 5-chloro-2-hydroxy-benzamide derivatives, esters, hydrazides, hydrazones, were obtained in good yields (60-93%), using conventional heating synthesis. The obtaining pathways of the synthesized compounds are presented in figure 1.

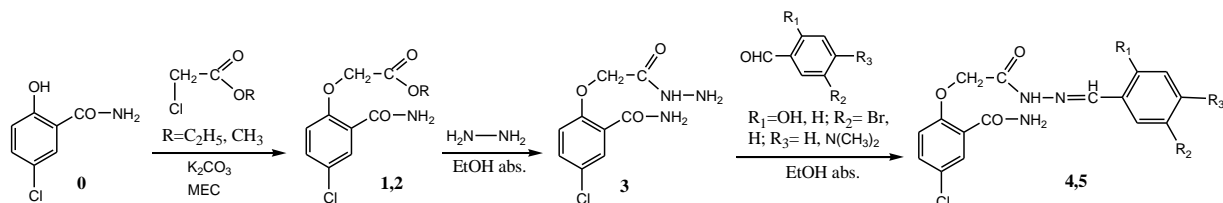


Figure 1. The obtaining pathways of the synthesized compounds

The synthesized compounds were characterized using modern physico-chemical methods (FTIR, ¹H- and ¹³C-NMR), the obtained results demonstrated the compounds identity.

The antimicrobial activity of the compounds was tested against some bacterial strains, *Staphylococcus aureus*, *Streptococcus pyogenes*, *Streptococcus mutans*, *Escherichia coli*, by measuring the optical density at 540 nm. The most effective compound was 5-chloro-2-hydrazinocarbonylmethoxy-benzamide and the most sensitive strain to the action of the tested compounds was *Staphylococcus aureus*. The tested compounds presented no inhibitory effect on *Escherichia coli*.

Acknowledgements

This work is part of the project PN 19 22 03 01 / 2019 “Supramolecular inclusion complexes of some natural and synthetic compounds with health applications”, carried out under NUCLEU Program funded by National Authority for Scientific Research (Romania).

References

- [1] J. Matyk, K. Waisser, K. Drazkova, J. Kunes, V. Klimensova, K. Palat, J. Kaustova, *Farmaco*. 60(5) (2005) 399.
- [2] K. Waisser, J. Matyk, H. Divisova, P. Husakova, J. Kunes, V. Klimensova, J. Kaustova, U. Mollmann, H.M. Dahse, M. Miko, *Arch Pharm*. 339(11) (2006) 616.

ELECTROCHEMICAL DENITRIFICATION OF WATER FOR DRINKING PURPOSE

Sorina Negrea^{1,2}, Monica Ihos¹, Mihaela Dragalina¹, Dorian Neidoni¹, Florica Manea³

¹National Research and Development Institute for Industrial Ecology ECOIND, Timisoara
Subsidiary, Street Bujorilor no. 115, code 300431, Timisoara, Romania

²"Gheorghe Asachi" Technical University of Iasi, Department of Environmental Engineering and
Management, Prof. Dimitrie Mangeron 73, 700050, Iasi, Romania

³Politehnica University of Timisoara, Department of Applied Chemistry and Engineering of
Inorganic Compounds and Environment, Faculty of Industrial Chemistry and Environmental
Engineering, V. Parvan 6, 300223 Timisoara, Romania

e-mail: monica_ihos@yahoo.com

Abstract

Electrocoagulation was used as method of groundwater denitrification for the purpose of obtaining drinking water. The experiments were carried out by using both synthetic solutions and groundwater from the West of Romania. The sacrificial anode was made of aluminium and the cell was equipped either with stainless steel or aluminium cathodes. Also, Linear Scan Voltammetry (LSV) experiments were carried out in order to know the behaviour of aluminium sacrificial anode during the anodic process.

Introduction

Groundwater is an important supply for drinking water and it is necessary to be aware of various components present in it for practical treatment approaches. The contamination of groundwater with nitrates has become a growing global challenge as a result of excessive fertilization, industrial activity and uncontrolled discharge of wastewaters [1]. The presence of nitrates in groundwater above the limits allowed by regulations in use can lead to health problems. In the human body, nitrates can easily be transformed into nitrites which react with red blood cells and methemoglobin is yielding. If the concentration of methemoglobin is above a certain limit the capacity of blood to transport oxygen to cells and tissues is impacted causing hypoxia and cyanosis [2,3]. Also, nitrites can react with secondary or tertiary amines to produce carcinogenic nitrosamines [4].

The chemical properties of nitrate make it difficult to remove from water using conventional processes such as filtration or activated carbon adsorption. As a result, more complex treatment processes must be considered. Thus, adsorption experiments have been carried out using functionalized chitosan-clinoptilolite nanocomposites [5] or applying electrostatic regeneration of functionalized adsorbent [6]. Denitrification of nitrate-contaminated groundwater using bioelectrochemical systems have been intensively studied [7-12]. Also, electrodialysis [13], hybrid nanofiltration-reverse osmosis filtration [14] and photocatalysis [15] alongside electrochemical processes [16] are suitable and effective alternatives for denitrification of groundwater.

Electrochemical processes because of their advantages, e.g., versatility, energy efficiency, easy operation, automation and environmental compatibility, are promising tools for water treatment. The aim of this study was the denitrification of nitrate-contaminated groundwater by electrocoagulation in order to develop an effective alternative to conventional methods.

Experimental

LSV experiments were performed by using a Princeton Applied Research VersaSTAT³-400, software VersaStudio 2.54.2, potentiostat-galvanostat and a Metrohm three electrode cell. A

silver/silver chloride electrode (Ag/AgCl) was used as reference electrode and a platinum plate of 1 cm² as a counter electrode. The working electrode was an aluminium plate with active surface area of 0.49 cm². Prior to the electrochemical measurements, the working electrode was carefully cleaned, degreased and treated by polishing with alumina powder (0.1 mm), and finally washed with distilled water. The interface of the working electrode with the aqueous medium was stabilized by repeated scans in the supporting electrolyte. The LSV experiments were carried out in either 0.1 M Na₂SO₄ or 0.1 M Na₂SO₄ + 0.01 M NaCl supporting electrolyte, in a potential range either between -2 → +2 V vs. Ag/AgCl or 0 → +2 V vs. Ag/AgCl, potential scan rate either 0.02 or 0.05 V/s and pH of 7.

The electrocoagulation experiments were carried out in a Plexiglas cell. It was equipped with three vertical anodes made of aluminium, each of 4.5x10.2 cm, and four cathodes made of stainless steel or aluminium having the same size as the anodes. The distance between the electrodes was 1 cm.

Volumes of 300 ml working solutions were introduced in the cell, and the applied current densities were 50, 75 and 100 A/m² when stainless steel cathodes were used and 10, 25 and 50 A/m² for the aluminium ones. Electrolysis duration was 60 minutes and samples were taken at every 15 minutes. All samples were filtered through a low porosity (0.2 µm) filter prior the analysis. The experiments were carried out with synthetic solutions and groundwater from the West of Romania. The synthetic solutions were of 100 mg/L nitrate in 0.1 M Na₂SO₄ + 0.01 M NaCl as supporting electrolyte. The groundwater was of 175 mg/L (F1) and 152 mg/L nitrate (F2), respectively.

All reagents were of analytical grade and the synthetic solutions were prepared with distilled water. The pH was adjusted to 7. No adjustment of the pH of groundwater was made, and it was 7.9 (F1) and 7 (F2), respectively.

The nitrate concentration was determined by using a Thermo Scientific Orion nitrate ion selective electrode.

Results and discussion

When aluminium is used as sacrificial anode it is important to know its behaviour during the anodic process as well as in the sequence of processes that occur in the electrocoagulation cell. Sulfate is widespread in groundwater. The aluminium behaviour in the anodic process and in presence of 0.1 M Na₂SO₄ is shown in Figure 1. The variation of current intensity as the potential was ranged from -2 to +2 V/Ag/AgCl showed that the aluminium dissolution was practically blocked in presence of Na₂SO₄.

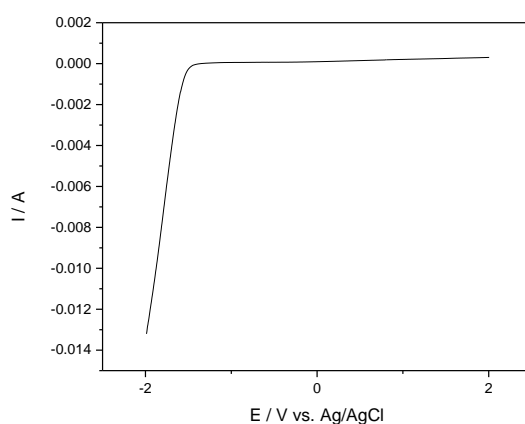


Fig. 1. Linear scan voltammogram of aluminium electrode in 0.1 M Na₂SO₄ potential scan rate: 0.02 V/s; potential range: -2 → +2 V/Ag/AgCl; pH 7

The experiments carried out did not lead to the expected results when the potential scan rate was increased in order to notice some activation and passivation of the electrode. At low polarization speed, namely 0.02 V/s, in 0.1 M Na₂SO₄, the electrode remained practically passive in a large potential range. The increase of the current (Figure 2), with the increase of the polarization speed to 0.05 V/s, can be interpreted by a compromise between the formation of an insulating superficial layer and the limitation of the processes by mass transport.

At a polarization rate of 0.05 V/s, the addition of 0.01 M NaCl did not change the shape of the polarization curves (Figure 3), but the current increased, that signifies the aluminium active dissolution by adding NaCl in the solutions subjected to electrocoagulation.

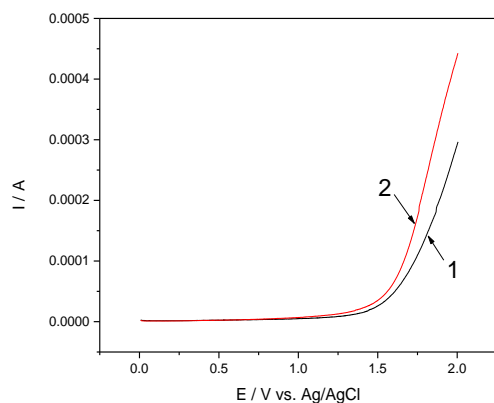


Fig. 2. Linear scan voltammograms of aluminium electrode in 0.1 M Na₂SO₄ potential scan rate: 0.02 V/s (1) and 0.05 V/s (2); potential range: 0 → +2 V/Ag/AgCl; pH 7

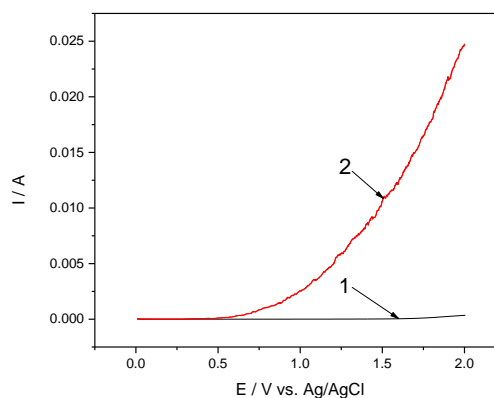


Fig. 3. Linear scan voltammograms of aluminium electrode in 0.1 M Na₂SO₄ (1) and 0.1 M Na₂SO₄ + 0.01 M NaCl (2) potential scan rate: 0.05 V/s; potential range: 0 → +2 V/Ag/AgCl; pH 7

When nitrate was added in 0.1 M Na₂SO₄ + 0.01 M NaCl supporting electrolyte in concentration of 30, 60 and 90 ppm N, respectively, it was found that the current decreased compared to the experiments in which the pollutant was not present (Figure 4). This behavior could be explained by a possible adsorption of the pollutant on the electrode surface.

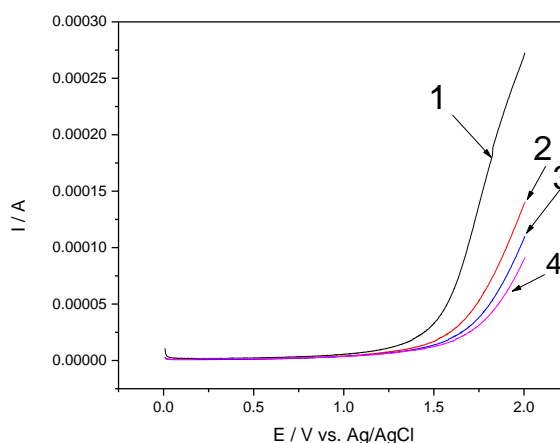


Fig. 4. Linear scan voltammograms of aluminium electrode in 0.1 M Na₂SO₄ + 0.01 M NaCl (1) and in presence of nitrate: 30 ppm N (2), 60 ppm N (3), 90 ppm N (4); potential scan rate 0.05 V/s; potential range: 0 → +2 V/Ag/AgCl; pH 7

Figures 5-8 show the working conditions and the nitrate removal efficiency obtained in this study. When the electrocoagulation carried out in 0.1 M Na_2SO_4 + 0.01 M NaCl supporting electrolyte, both stainless steel and aluminium cathodes, for any current density, the nitrate removal efficiency increased with the increase of electrolysis time. The concentration of nitrate was of 33.3 mg/L after 60 minutes of electrolysis by using stainless steel cathodes (Figure 5). This value was under the threshold limit of 50 mg/L nitrate stipulated in Romanian Law 458/2002 concerning the drinking water quality. Concentrations under the threshold limit stipulated in Romanian Law 458/2002 were achieved at lower current densities and shorter electrolysis time when the cell was equipped with aluminium cathodes (Figure 6). Thus, at 10 $\text{A}\cdot\text{m}^{-2}$ and 45 minutes of electrolysis, the nitrate concentration was 40 mg/L.

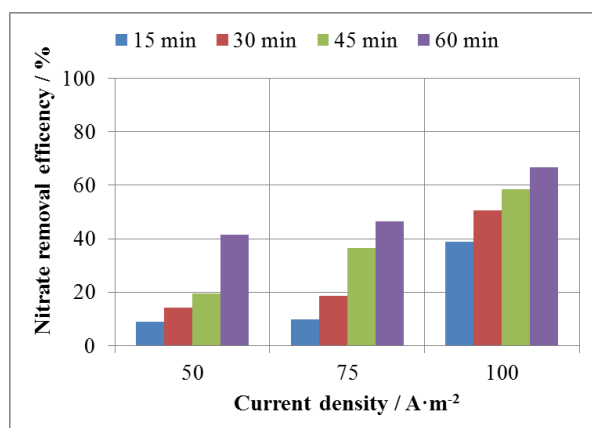


Fig. 5. Nitrate removal efficiency by electrocoagulation with stainless steel cathodes 0.1 M Na_2SO_4 +0.01 M NaCl supporting electrolyte; nitrate concentration: 100 mg/L; pH: 7

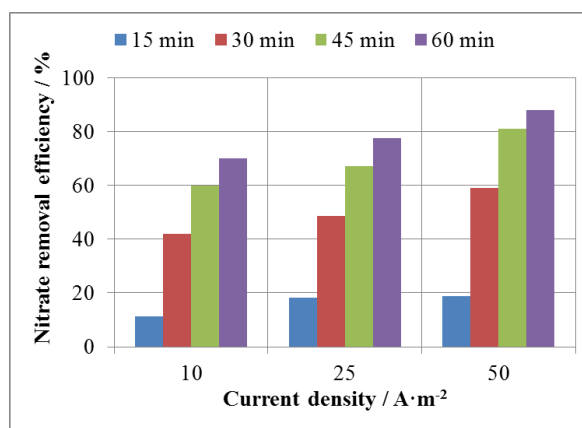


Fig. 6. Nitrate removal efficiency by electrocoagulation with aluminium cathodes 0.1 M Na_2SO_4 +0.01 M NaCl supporting electrolyte; nitrate concentration: 100 mg/L; pH: 7

The results obtained by using synthetic solutions provided useful information regarding the best working conditions for electrochemical denitrification of nitrate-contaminated groundwater from West part of Romania. Nitrate concentration under the threshold limit stipulated in Romanian Law 458/2002 were recorded for both groundwater samples (F1 and F2) at 50 $\text{A}\cdot\text{m}^{-2}$ and electrolysis time of 60 and 45 minutes, respectively (Figures 7 and 8).

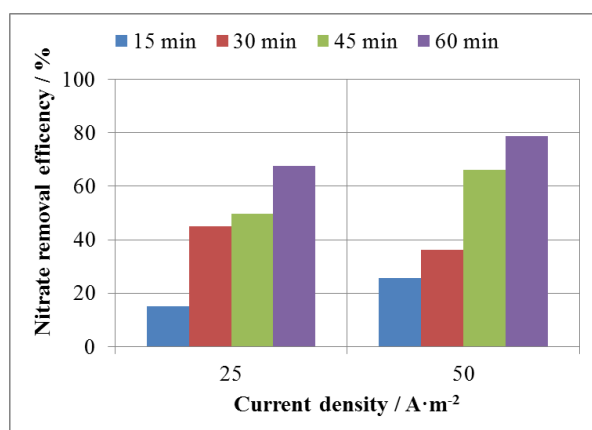


Fig. 7. Nitrate removal efficiency by electrocoagulation from groundwater (F1) nitrate concentration: 175 mg/l; pH: 7.9; cathodes: aluminium

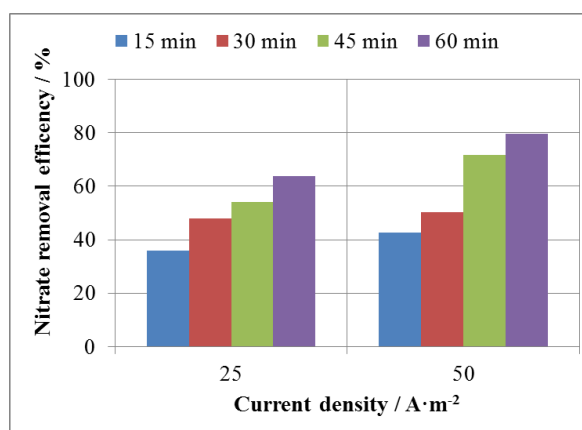


Fig. 8. Nitrate removal efficiency by electrocoagulation from groundwater (F2) nitrate concentration: 152 mg/L; pH: 7; cathodes: aluminium

The specific energy consumption was calculated according to equation (1) by using as working conditions: applied current density of 50 A/m² (1.15 A), electrolysis time of 60 minutes, cell voltage of 4 V, groundwater sample of 300 ml and it was of 15.3 kWh/m³. The pH of groundwater was in the range 7-8. In these conditions, the concentration of nitrate in the treated groundwater was under the threshold limit of 50 mg/L.

$$Q = U \cdot I \cdot t \cdot 10^{-3} / V \cdot 3600 \quad (1)$$

where:

Q = specific energy consumption, kWh/m³; U = cell voltage, V; I = current intensity, A; t = electrolysis time, s; V = electrolyzed solution volume, m³

Conclusion

Electrocoagulation with aluminium sacrificial anode was applied to denitrification of groundwater for drinking water purpose. The best results were achieved when aluminium cathodes were used. The best nitrate removal efficiency from groundwater from two sites in West of Romania was of about 80% and the concentration of nitrate was under the limit allowed by the regulations in use. The LSV experiments showed the aluminium sacrificial anode behaviour in the presence of sulfate and chloride that are often accompanying anions of nitrate in groundwater.

Acknowledgements

This work was carried out within the framework of a Core Program, managed by The Romanian Ministry of Research and Innovation, project code PN PN 18 05 03 02.

References

- [1] Z. Zhang, A. Chen, Sep. Purif. Technol. 164 (2016) 107.
- [2] S. Fossen Johnson, Curr. Probl. Pediatr. Adolesc. Health Care 49 (2019) 57.
- [3] N. Neander, C. A. Loner, J. M. Rotoli, J. Emerg. Med. 54 (2018), 685.
- [4] S. Zhai, Y. Zhao, M. Ji, W. Qi, Bioresource Technol. 232 (2017) 278.
- [5] F. Yazdi, M. Anbia, S. Salehi, Int. J. Biol. Macromol. 130 (2019) 545.
- [6] J. W. Palko, D. I. Oyarzun, B. Ha, M. Stadermann, J. G. Santiago, Chem. Eng. J. 334 (2018) 1289.
- [7] T. Peng, C. Feng, W. Hu, N. Chen, Q. He, S. Dong, Y. Xu, Y. Gao, M. Li, Biochem. Eng. J. 134 (2018) 12.
- [8] R. Liu, X. Zheng, M. Li, L. Han, X. Liu, F. Zhang, X. Hou, Water Res. 158 (2019) 401.
- [9] D. Cecconet, M. Devecseri, A. Callegari, A.G. Capodaglio, Sci. Total Environ. 613-614 (2018) 663.
- [10] D. Cecconet, S. Bolognesi, A. Callegari, A.G. Capodaglio, Sci. Total Environ. 651 (2019) 3107.
- [11] Y. Tong, Z. He, J. Hazard. Mater. 262 (2013) 614.
- [12] A. Bayrakdar, E. Tilahun, B. Çalli, Bioelectrochemistry 129 (2019) 228.
- [13] C. Onorato, L. J. Banasiak, A. I. Schäfer, Sep. Purif. Technol. 187 (2017) 426.
- [14] R. Epsztein, O. Nir, O. Lahav, M. Green, Chem. Eng. J. 279 (2015) 372.
- [15] D. S. Dharmagunawardhane, N. L. De Silva, U. B. Gunatilake, C.-F. Yan, J. Bandara, Mol. Catal. 470 (2019) 89.
- [16] Z. Zhang, A. Chen, Sep. Purif. Technol. 164 (2016) 107.

CHARACTERIZATION OF ROAD TRAFFIC POLLUTION IN AN URBAN STREET CANYON

Milana Ilić Mićunović¹, Boris Agarski¹, Zorica Miroslavljević²

¹*Department of Production Engineering, University of Novi Sad, 21000 Novi Sad, Trg Dositeja Obradovića 6, Serbia*

²*Department of Environmental Engineering, University of Novi Sad, 21000 Novi Sad, Trg Dositeja Obradovića 6, Serbia
e-mail: milanai@uns.ac.rs*

Abstract

Investigation of traffic-related air pollution is of great importance, due its impact of human health and the environment [1,2]. Traffic pollution in all larger cities is additionally burdened by tall buildings along a frequency roads, also known as “street canyon” [3]. Air dispersion and intensity of horizontal and vertical turbulence in a street canyon are very different from the ones that appear in a flat open region, with longer particle retention [4]. In this paper we investigated concentration of volatile organic compounds and road dust particles along the most frequent road in the second largest city in Serbia. The measurements were performed with personal sampler that was attached on operator, who was walking along the road. Absorber with collected volatile organic compounds that was examined with gas chromatography system, showed the highest concentration of benzene. The composition of dust particles, collected on the filter, was examined with scanning electron microscopy - energy dispersive spectrometry analysis. The results shown high levels of carbon, silicon, iron and aluminum, and presence of heavy metals. Size and shape of road dust particles was determined by the image analysis method, with ImageJ software. Based on the composition, size and morphological characteristics of the particles, we have identified the origin of the particles. The most particles originated from soil, motor vehicles (tire/brake abrasions) and particles generated during the road reconstruction/construction. This research enabled the assessment of the impacts on human health, and on the environment as well.

References

- [1] F. Rajé, M. Tight, F.D. Pope, Traffic pollution: A search for solutions for a city like Nairobi, *Cities* 82 (2018).
- [2] V. Tischer, G. Fountas, M. Polette, T. Rye, Environmental and economic assessment of traffic-related air pollution using aggregate spatial information: A case study of Balneário Camboriú, Brazil, *J. of Trans. & Heal.* 14 (2019) 100592.
- [3] N. Bukowiecki, P. Lienemann, M. Hill, M. Furger, A. Richard, F. Amato, A.S.H. Prévôt, U. Baltensperger, B. Buchmann, R. Gehrig, PM10 emission factors for non-exhaust particles generated by road traffic in an urban street canyon and along a freeway in Switzerland, *Atmos. Environ.* 44 (2010) 19.
- [4] O.V. Taseiko, S.V. Mikhailuta, A. Pitt, A.A. Lezhenin, Y.V. Zakharov, Air pollution dispersion within urban street canyons, *Atmos. Environ.* 43 (2009) 2.

MICROSTRUCTURE AND THERMAL CHARACTERIZATION OF Mo-DOPED Li_{6.87}Nb_{2.34}Ti_{5.78}O₂₁ SOLID-SOLUTION CERAMICS

Tamara Ivetić¹, Jelena Petrović², Imre Gúth¹, Kristina Čajko¹, Svetlana Lukić-Petrović¹

¹*University of Novi Sad Faculty of Sciences, Department of Physics, Trg Dositeja Obradovića 4, 21000 Novi Sad, Serbia*

²*Institute for Electronic Appliances and Circuits, Faculty Computer Science and Electrical Engineering, University of Rostock, Albert-Einstein 2, 18059, Rostock, Germany
e-mail: tamara.ivetic@df.uns.ac.rs*

Abstract

In this work, the microstructure and thermal properties of lithium-niobium-titanium-oxide (Li-Nb-Ti-O) solid-solution ceramics were investigated using the X-ray diffraction (XRD), Raman spectroscopy, scanning electron microscopy (SEM), and differential scanning calorimetry (DSC) techniques. XRD and SEM analysis confirmed that Li-Nb-Ti-O ceramic sample synthesized by solid-state method reaches the desired composition of so-called M-phase of the Li₂O-Nb₂O₅-TiO₂ ternary system (Li_{6.87}Nb_{2.34}Ti_{5.78}O₂₁) that should have excellent microwave dielectric properties. The M-phase was obtained with lower than 1000°C sintering temperature by doping with MoO₃ as flux material, which makes this kind of ceramic material suitable for the low temperature co-fired ceramic (LTCC) technology applications. The heat flow data obtained from DSC measurement were used to calculate the specific heat capacity (C_p) of synthesized Li_{6.87}Nb_{2.34}Ti_{5.78}O₂₁ solid-solution ceramics, which is the property of a material that tells about its stability and functionality.

Introduction

The modern wireless communications, such as mobile systems and its technology, is always searching for ways to miniaturize the mobile device's size. The LTCC technology offers the possibility of fabricating the highly integrated substrates and radio-frequency microwave circuits using a special combination of the ceramic materials and multi-layer/firing techniques. Co-fired ceramic devices are made by processing several layers independently which are assembled into a device as a final step. This allows co-firing the highly conductive materials (like silver) with passive ceramic elements (resistors, capacitors, and inductors). Silver is often used as a metallic electrode in such electrical systems because of its high conductivity and low cost. However, as Ag melting point is low (about 961 °C) the dielectric ceramics used in the co-fired technology with silver has to have besides the required dielectric properties for the desired application also a low sintering temperature [1]. The ternary Li₂O-Nb₂O₅-TiO₂ material system has been an attractive potential candidate for the LTCC applications for many years now. Especially, its so-called M-phase, which is described by the general formula Li_{1+x-y}Nb_{1-x-3y}Ti_{x+4y}O₃ (0.05<x<0.3, 0<y<0.182). As M-phase ceramics usually needs higher than 1100 °C synthesis temperature, the small additions of low-melting-temperature-oxides such as MoO₃ (795 °C) are added as a flux material to lower the synthesis temperature by mechanisms of liquid-phase sintering [2]. The M-phase compounds refer to the series of solid-solutions in the middle of the Li₂O-Nb₂O₅-TiO₂ ternary phase diagram. The M-phase grows into the large oriented anisotropic plate-like particles. Some describe the M-phase structure as the homologous series of solid-solutions phases (in trigonal crystal symmetry) with commensurate intergrowth LiNbO₃ layers separated by a single [Ti₂O₃]²⁺ corundum-type layer. Such M-phase type Li-Nb-Ti-O materials are featured with excellent and tuneable microwave dielectric properties (permittivity from 20 to 80) depending on the applied synthesis method, and the type and concentration of the functional additives used [3].

Various dielectric permittivity values of the dielectric ceramics used in LTCC are equally desirable. For example, the low permittivity dielectric ceramics with the fast signal transmission are used as microwave packaging substrates, while the medium dielectric permittivity (20-50) ceramics are used in the dielectric resonators/filters. Besides, studying the thermal properties of this kind of materials is of great interest as well, because the electronic systems, where these materials find applications, are often exposed to different and frequently extreme environmental conditions. The specific heat capacity and enthalpy change during the melting process were calculated using the obtained heat flow curve from DSC recordings [4].

Experimental

The Li-Nb-Ti-O ceramic sample was synthesized using a solid-state method. Starting precursors, the commercial powders of anatase TiO_2 , Nb_2O_5 , and LiCO_3 (all purchased from Sigma-Aldrich), were mixed in a molar ratio to reach the desired composition with the addition of not more than 0.5 wt. % of MoO_3 (sample is further marked in the text as Li-Nb-Ti-O-Mo). The mixed powders were milled in the planetary ball mill (Retsch GmbH PM100) in zirconia vial and by zirconia balls of 5 mm diameter. The ball milling was performed in ethanol for 4 h with the use of standard balls to powder mass ratio of 10:1 and 100 rpm speed rate. The obtained powder mixture was dried on air for 24 h and calcinated at 650 °C for 4h. The mechanically activated powder mixture was pressed by 10 mm diameter mold to form stable pellet that was finally sintered at 900 °C for 4h. XRD analysis was used for structural characterization and was performed on a MiniFlex600 (Rigaku, Japan) X-ray diffractometer with Cu-K_α radiation ($\lambda = 1.5406 \text{ \AA}$) at a tube voltage of 40 kV and a tube current of 15 mA, with steps of 0.02° and a counting time of $1^\circ/\text{min}$, in the 2θ angular range from 10° to 80° . With scanning electron microscope (JEOL JSM-6460LV), the morphology of the sample was investigated. The Raman spectrum was measured using the Centice MMS Raman spectrometer equipped with a CCD detector and a diode laser, operating at 785 nm (1.58 eV) with the power of 70 mW, as the excitation source. Non-isothermal differential scanning calorimetry (DSC) measurements were performed using NETZSCH STA 449 F3 Jupiter, equipped with DSC sample holders and using Al_2O_3 crucibles and samples in a powder form with a mass around 20 mg in an inert atmosphere of N_2 with a control flow rate of 20 ml/min. Temperature and heat flow calibration was performed for all the heating/cooling rates used in this research. Specific heat capacity measurements procedure used a sapphire crystal as reference material. The heating started at room temperature up to 40 °C with a hold for 30 min, then the heating continued up to 1200 °C with a heating rate of 10 K/min and hold for 30 min before the final cooling to room temperature.

Results and discussion

The obtained Li-Nb-Ti-O-Mo sample microstructure (Fig. 1) is characterized by the plate-like particles that strongly resemble the microstructure already described for the M-phase materials [1]. The obtained XRD result (Fig. 2) supports results from SEM findings (Fig. 1) that M-phase of $\text{LiO}_2\text{-Nb}_2\text{O}_3\text{-TiO}_2$ system was formed. Majority of XRD peaks were indexed according to COD reference card no. 1533457 that describes $\text{Li}_{6.87}\text{Nb}_{2.34}\text{Ti}_{5.78}\text{O}_{21}$ solid-solution crystal system with $P\bar{3}c1$ (no. 158) space group symmetry. Few impurity related diffraction peaks belong to LiNbO_3 and TiO_2 anatase (marked in Fig. 1) and no XRD peaks were found to relate to added MoO_3 compound.

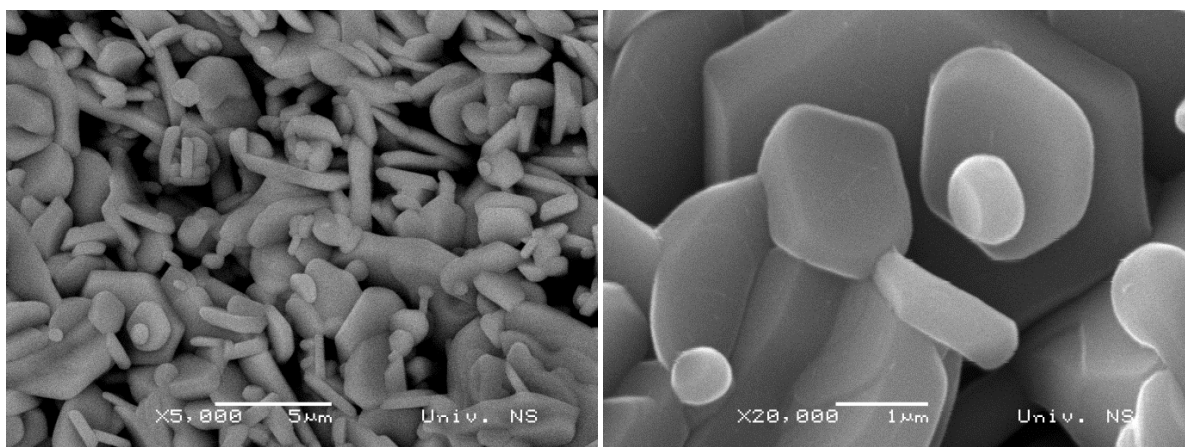


Figure 1. SEM images of synthesized Li-Nb-Ti-O-Mo ceramic sample

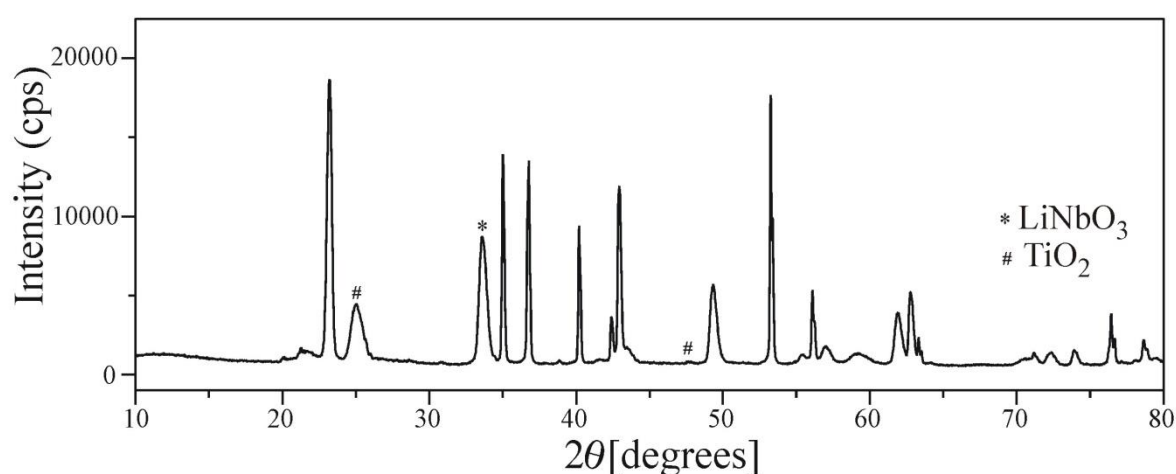


Figure 2. XRD pattern of synthesized Li-Nb-Ti-O-Mo ceramic sample

The Raman spectrum obtained by 785 nm excitation wavelength is shown in Fig. 3. The exact Raman peak positions (shift in cm^{-1}), intensity (counts) and full width at half maximum (FWHM) were determined by the amplitude version of Gaussian line-shape multi-peak fitting procedure (inset in Fig. 3). There are no past reports, as far as we know, on Raman spectrum for $\text{Li}_{6.87}\text{Nb}_{2.34}\text{Ti}_{5.78}\text{O}_{21}$ M-phase in the $P\bar{3}c1$ space group symmetry obtained by 785 nm excitation wavelength.

The DSC curve recorded for Li-Nb-Ti-O-Mo sample is shown in Fig. 4. The DSC spectrum features the endothermic peak at 1177 °C that characterizes the melting of $\text{Li}_{6.87}\text{Nb}_{2.34}\text{Ti}_{5.78}\text{O}_{21}$ compound. There was no change in mass. The DSC recording was used to calculate the specific heat capacity (C_p) of $\text{Li}_{6.87}\text{Nb}_{2.34}\text{Ti}_{5.78}\text{O}_{21}$. The melting enthalpy (ΔH_m) is calculated as the area below the heat capacity vs. temperature curve in the area where the change of this parameter is significant (the shaded area in the inset in Fig. 4) as $\Delta H_m = \int_{T_1}^{T_2} C_p(T) dt$.

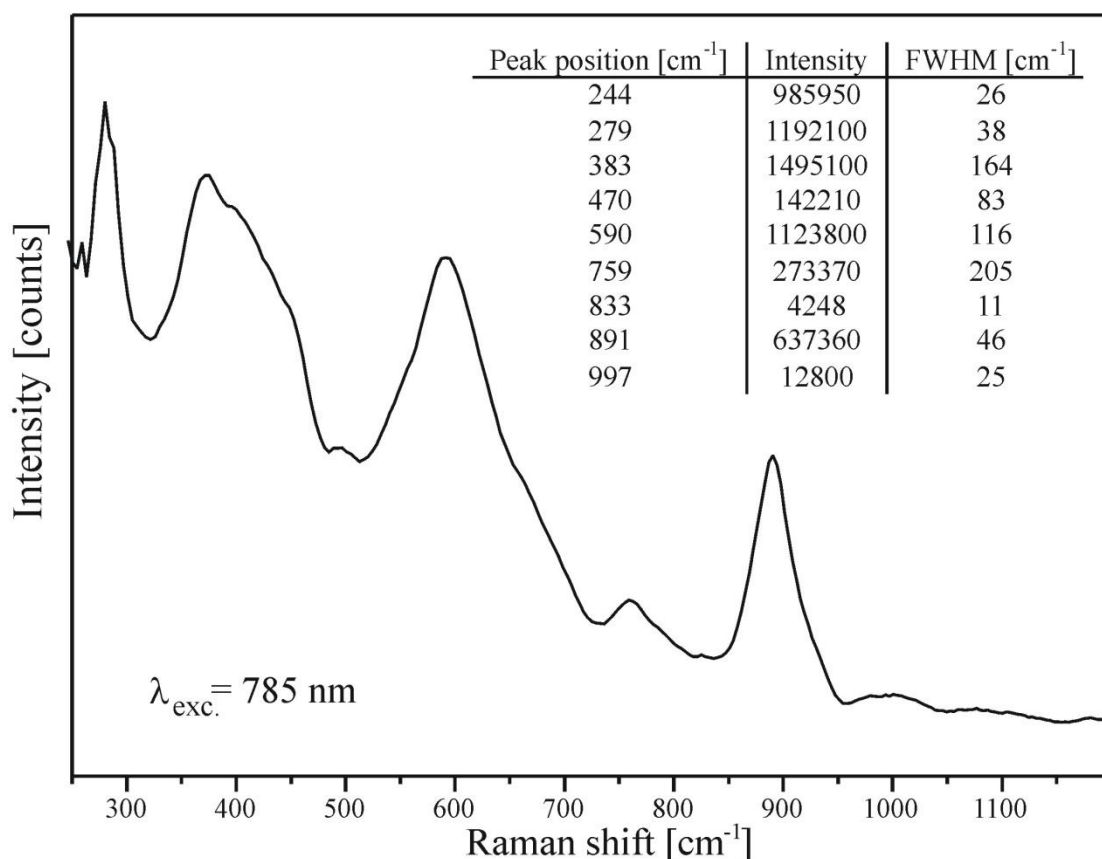


Figure 3. Raman spectrum of synthesized Li-Nb-Ti-O-Mo ceramic sample at room temperature obtained by 785 nm excitation wavelength

In the case of DSC measurement, the specific heat capacity of the sample at a given temperature and constant pressure, C_p , was calculated by a simple comparison of the heat flow rates into the sample and reference material (etalon-sapphire) [5] $C_p = \frac{\Phi_s - \Phi_0}{\Phi_{ref} - \Phi_0} \cdot \frac{m_{ref}}{m_s} C_p^{ref}$, where Φ_s , Φ_{ref} and Φ_0 represent heat flow rates through crucible loaded with sample material, crucible loaded with reference material and empty crucible, respectively. m_s and m_{ref} represent the mass of the sample and reference material respectively, while C_p^{ref} is the specific heat capacity of the reference material. Values for the heat capacity of sapphire between 200 °C to 2200 °C, required for specific heat calculation, are available in the NETZSCH Proteus software suite. The variation of the heat capacity with the temperature in $\text{Li}_{6.87}\text{Nb}_{2.34}\text{Ti}_{5.78}\text{O}_{21}$ crystalline solid is characterized by the melting temperature of 1177 °C and its belonging heat capacity maximum of $C_p = 18.7 \text{ J/gK}$ (shown as an inset in Fig. 4). By integrating the C_p melting peak area, the enthalpy change per unit weight of approximately $\Delta H_m = 364.7 \text{ J/g}$ was calculated for this thermal event (inset in Fig. 4).

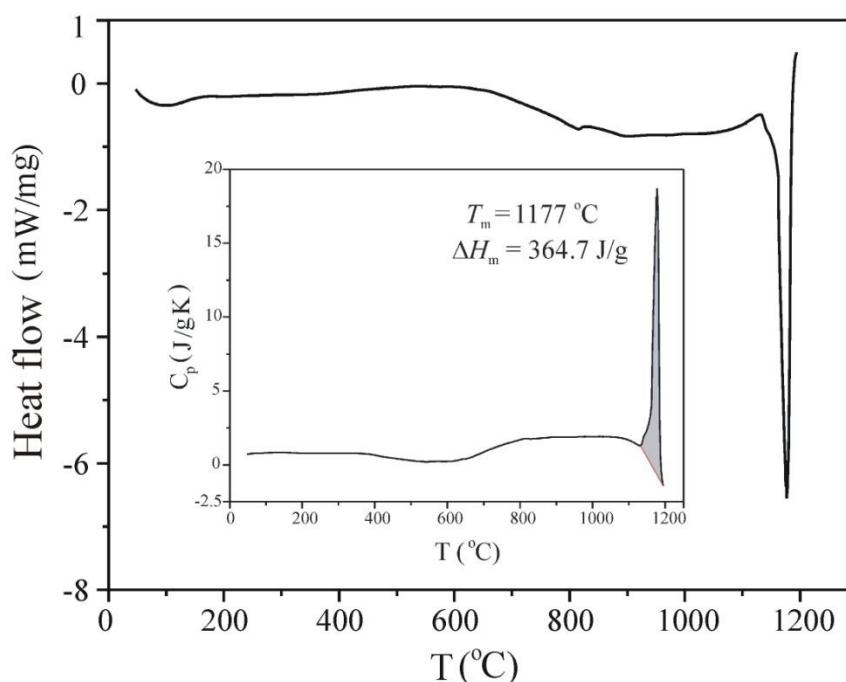


Figure 4. DSC curve of $\text{Li}_{6.87}\text{Nb}_{2.34}\text{Ti}_{5.78}\text{O}_{21}$ ceramic sample (inset shows the calculated variation of the specific heat capacity (C_p) with the temperature)

Conclusion

In this work, the Li-Nb-Ti-O ceramic was synthesized by the solid-state method and its microstructure and thermal properties were investigated. Synthesized Li-Nb-Ti-O is specially featured by 900 °C synthesis temperature (achieved by adding MoO_3 as flux material) and M-phase like superstructure, which makes it applicable for the LTCC technology. The microstructure analysis confirmed the formation of a member of the M-phase wherein the general formula $\text{Li}_{1+x-y}\text{Nb}_{1-x-3y}\text{Ti}_{x+4y}\text{O}_3$, the $x = 0.12$ and $y = 0.18$ give the final composition of $\sim\text{LiNb}_{0.34}\text{Ti}_{0.84}\text{O}_3$ which is equal to $\text{Li}_{6.84}\text{Nb}_{2.34}\text{Ti}_{5.78}\text{O}_{21}$ found by XRD. The results presented here give a good starting insight into the possible use of this kind of material. Exploring the obtained Li-Nb-Ti-O ceramics needs further electrical characterization, which will give a complete picture of the applicability of this material in the modern electrical devices.

Acknowledgments

This work was financially supported by the APV Provincial Secretariat for Higher Education and Scientific Research (project name: “Properties and electrical characteristics of doped amorphous chalcogenide materials and nanostructured ceramics”, project number: 142-451-2080/2019-04), and the Ministry of Education, Science and Technological Development of the Republic of Serbia (project number ON 171022).

References

- [1] Z. Liu, Y. Wang, W. Wu, Y. Li, J. Asian Ceram. Soc. 1 (2013) 2.
- [2] D. Zhou, C.A. Randall, H. Wang, L-X. Pang, X. Yao, J. Am. Ceram. Soc. 93 (2010) 1096.
- [3] H-F. Zhou, H. Wang, D. Zhou, L-X. Pang, X. Yao, Mater. Chem. Phys. 109 (2008) 510.
- [4] E. Morintale, A. Harabor, C. Constantinescu, P. Rotaru, Physics AUC 23 (2013) 89.
- [5] G.W.H. Höhne, W. Hemminger, H.-J. Flammersheim, Differential Scanning Calorimetry: An Introduction for Practitioners, Springer, Berlin, 1996.

DIRECT PHOTOLYSIS OF FUMONISIN B₁ IN AQUEOUS MEDIUM

Ivana Jevtić¹, Sandra Jakšić², Maria Uzelac³, Biljana Abramović³✉

¹*Higher Medical and Business-Technological School of Applied Studies, Šabac, Hajduk Veljkova 10, Šabac, Serbia*

²*Scientific Veterinary Institute „Novi Sad“, Rumenački put 20, Novi Sad, Serbia*

³*University of Novi Sad Faculty of Sciences, Department of Chemistry, Biochemistry and Environmental Protection, Trg Dositeja Obradovića 3, 21000 Novi Sad, Serbia*

✉ *biljana.abramovic@dh.uns.ac.rs*

Abstract

Fumonisin (FBs), secondary metabolites produced by fungi of the genus *Fusarium* [1], represent a major threat as potential organic pollutants. The FBs have been detected in different types of water [2], as well as produced them by fungi in untreated surface water [3]. Advanced Oxidation Processes (AOPs), have a high potential for water purification, including the removal of hazardous substances and pathogens from different types of water. AOPs are based on physicochemical processes that produce mainly hydroxyl radicals ($\bullet\text{OH}$), representing primary oxidants, which can lead to complete mineralization of pollutants. These processes can be initiated by UV or solar radiation. The photocatalytic degradation has become a powerful method for degradation and transformation of aflatoxin B₁ [4], zearalenone [5], and deoxynivalenol [6] into harmless substances. In this paper, we have investigated optimization of high performance liquid chromatography with fluorescence detector method for monitoring the stability of fumonisins B₁ (FB₁), B₂ (FB₂), and B₃ (FB₃) solutions as well as the efficiency of FB₁ degradation using direct photolysis under UV and solar radiation in ultrapure water. It was found that the sensitivity and separation of the FB₁ peak from *o*-phthalialdehyde–2-mercaptoethanol (used for derivatization) was optimally at isocratic elution using the MeOH–NaH₂PO₄ mobile phase, at a ratio of 75 : 25 (v/v). When studying the efficiency of direct photolysis of 1.47×10^{-6} mol/dm³ solution of FB₁ it was found that after 180 min of irradiation degradation efficiency was 88% using UV and 76% using solar radiation at pH 8.2. Also, the effect of pH in the range from 4.0 to 10.0 on the efficiency of direct photolysis of FB₁ was examined.

Acknowledgments

The authors acknowledge financial support of the Ministry of Education, Science and Technological Development of the Republic of Serbia (Project No. 172042).

References

- [1] K.A. Voss, G.W. Smith, W.M. Haschek, Anim. Feed Sci. Tech. 137 (2007) 299.
- [2] A. Waśkiewicz, J. Bocianowski, A. Perczak, P. Goliński, Sci. Total Environ. 15 (2015) 524.
- [3] B.R. Oliveira, A.T. Mata, J.P. Ferreira, M.T. Barreto Crespo, V.J. Pereira, M.R. Bronze, Environ. Sci. Pollut. Res. 25 (2018) 17519.
- [4] R. Liu, M. Chang, Q. Jin, J. Huang, Y. Liu, X. Wang, Eur. Food Res. Technol. 233 (2011) 1007.
- [5] E.S. Emídio, V. Calisto, M-R.R.R. de Marchi, V.I. Esteves, Chemosphere 193 (2017) 146.
- [6] X. Bai, C. Sun, D. Liu, X. Luo, D. Li, J. Wang, N. Wang, X. Chang, R. Zong, Y. Zhu, Appl. Catal. B-Environ. 204 (2017) 11.

ENVIRONMENTALLY FRIENDLY APPROACHES FOR CHEMICAL MODIFICATION OF CARBON-BASED NANOMATERIALS

Svetlana Jovanovic¹, Duska Kleut¹, Milica Budimir¹, Zois Syrgiannis^{2,3} and Biljana Todorović Marković¹

¹*Department of Radiation Chemistry and Physics, Vinca Institute of Nuclear Sciences, University of Belgrade, P. Box 522, 11000 Belgrade, Serbia*

²*Center of Excellence for Nanostructured Materials (CENMAT) and INSTM, unit of Trieste, Department of Chemical and Pharmaceutical Sciences, University of Trieste, Trieste, Italy*

³*Simpson Querrey Institute (SQI), Northwestern University, 2145 Sheridan Road, Evanston, IL, 60208, USA*

e-mail: svatlanajovanovicvucetic@gmail.com

Abstract

Carbon-based nanomaterials are under investigation for different applications, which often demands their chemical modification such as introducing the amino-functional groups or removing carboxyl and hydroxyl groups. In this paper, we are presenting approaches for changing the structure of selected carbon-based nanomaterials in which the use of reactive toxic chemicals is avoided. The methods such as gamma irradiation, thermal treatment with a source of N atoms and nascent hydrogen reduction are studied as possible methods for modification of carbon-based nanomaterials. In the phase of the cleaning, again environmentally friendly approaches are used: filtration, centrifugation, and dialysis. Due to selected methods for both modification and cleaning, the presented approaches are environmentally friendly, they avoiding the use of both aggressive toxic chemical in the synthetic phases as well as organic solvents in the phase of cleaning. Thanks to the avoiding of dangers chemical, these methods can lead to the lowering of the waste chemicals producing in the long-term future.

Introduction

Carbon-based nanomaterials are attracting great scientific attention since they were discovered.[1] Fullerenes are first discovered carbon-based nanomaterial, than carbon nanotubes, followed by graphene, graphene, and carbon quantum dots. All these materials possess unusual chemical, electrical and biological properties which made them interesting for application in therapy of carcinoma, bioimaging, solar cells, etc.[2-5]

Due to the need for carbon nanomaterials with different polarity and solubility, chemical structures as well as electrical conductivity, a large number of chemical reactions were applied to these materials in order to achieve these demands.[6-8] These reactions often involve the use of highly reactive, explosive and aggressive chemical, while the phase of cleaning is based to use of large volumes of different organic solvents such as 1,2-dichlorobenzene, methanol, and others. After reactions are done, the large amounts of residual, waste chemicals are left to be properly handled. Considering their high toxicity to humans and the environment, appropriate managing of this waste is necessary. Considering the increasing number of carbon nanomaterials application, the need for green approaches with reduced use of toxic chemicals for their modification also increasing.

Thus, we proposed a few approaches for modification of carbon nanomaterials using eco-friendly approaches. As a model system, we used graphene quantum dots and graphene oxide. We applied gamma irradiation on this material, using only water and a small amount of isopropanol as a medium in order to achieved chemical reduction. This chemical modification is often achieving using hydrazine, cancerogenic chemical. Also, thermal treatment with urea in order to incorporate N atoms in GQDs is based only on the application of GQDs and urea,

as well as the heat. As an alternative to hydrazine reaction, we investigated the possibility of use of nascent hydrogen reduction. We investigated the effects of proposed reaction on the morphology and chemical composition of GQDs and GO.

Experimental

Synthesis of carbon-based nanomaterials was achieved using electrochemical approach and modified Hummer's method for GQDs and GO production, respectively. Electrochemical synthesis of GQDs involves the use of graphite rods as both cathode and anode and 3% dispersion of NaOH in ethanol (96%) as an electrolyte. The current was set to 20 mA. Next day (in 24 h), the electrolyte was change color from yellowish to dark brown. It was collected and neutralized with HCl. Formed flocculated NaCl was removed by filtration and dialyze against MiliQ water (molecular weight cutoff 3500 Da) for 3 days to remove the residual NaCl. Graphene oxide was produced using a modified Hummer's method. Graphite powder (1 g) was dispersed in concentrated H_2SO_4 (23.3 ml). Then KMnO_4 (3 g) was slowly added to the reaction mixture placed in the ice bath. Next, after 1h the temperature was increased to 40 °C for 30 min and to 95 °C for 15 min. After that, the reaction mixture was poured into water (200 mL) and filtrated until the pH was 7.

Chemical modification of GQDs and GO were achieved using different approaches. Reduction of GO was conducted using *in situ* generated hydrogen. GO or GQDs were dispersed in water in a concentration of 1 mg/ml and the HCl acid (35%) was added in the final concentration of 1 mol/l. The pieces of Al foil were added in a concentration of 4 mg/ml. The final products were isolated using dialysis named GO-H and GQDs-H. In order to modify their structure, we used gamma irradiation, in a dose of 50 kGy and the medium for irradiation mixture of MiliQ water with isopropyl alcohol. This sample is named GQDs-50. To incorporate N atoms in GQDs, 50 mg GQDs and 1 g of urea was mixed and placed in a flask and heated for 5 minutes, with a heat gun. Then the mixture was diluted in water and filtered, followed by washing with water and methanol to remove free urea. This sample is named GQDs-U.

Atomic Force Microscopy (AFM) measurements were performed using Quesant microscope (Agoura Hills, CA). The microscope was working in the tapping mode, at room temperature, and in the air. Mica was used as a substrate. Samples were deposited using spin-coating. Absorption measurements were performed at UV-Visible UV-2600 Spectrophotometer (Shimadzu Corporation, Tokyo, Japan) in the ranges of wavelengths from 200 to 800 nm with 1 nm step. Spectra are recorded at 20 °C, in the air environment. Samples were prepared in the form of water dispersion, at a concentration of 0.25 mg/ml. The elemental composition of the samples was investigated by scanning electron microscopy (SEM, JEOL JSM-6390LV) with energy dispersive spectrometry (EDS, Oxford Aztec X-max), operating in vacuum at room temperature and an acceleration voltage of 3 keV.

Results and discussion

The results of AFM measurements are presented in Figure 1. AFM images of GQDs are presented on the left side while accompanied height profiles are presented in the upper left corner in the each AFM images. The right side, next to each AFM image, both height and diameter distributions are presented. These results showed that p-GQDs are mostly 15 to 20 nm in the height while an average diameter is in the range between 5 and 10 nm. For GQDs-H, the lower hight was observed, between 10 and 15 nm, and the diameter is around 6 nm. For GQDs-U, the largest fraction of dots is 3 nm in the height and an average diameter in the range between 5 and 10 nm. In the case of GQDs-50, the largest fraction is a 7 nm in height and 5 to 10 nm in diameter.

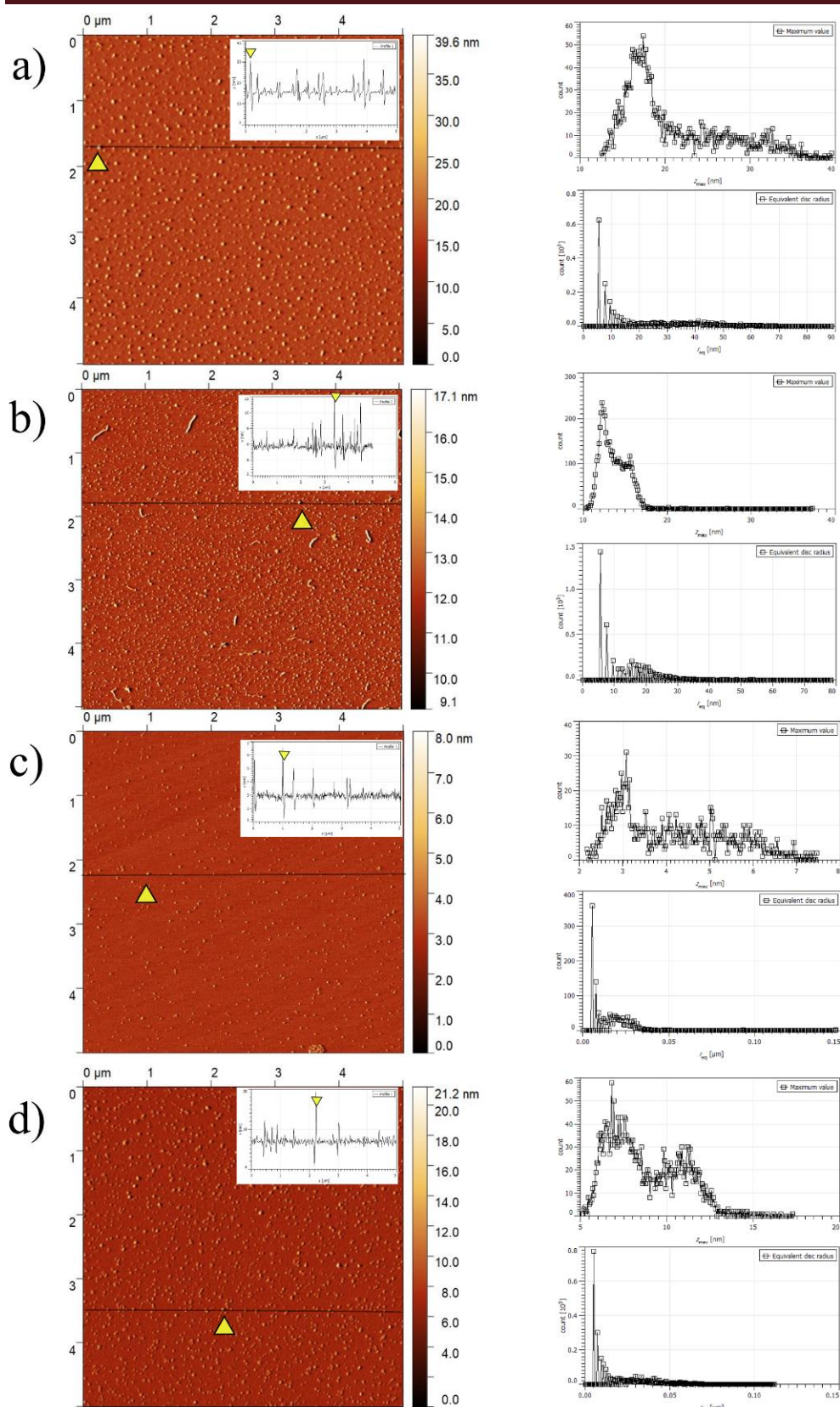


Figure 1. AFM images, profiles, height and diameter distributions for p-GQDs (a) and modified GQDs: GQDs-H (b), GQDs-U (c) and GQDs-50 (d).

The lowering in the height of GQDs after functionalization indicate reducing the number of functional groups.

The morphology of samples was also investigated using SEM microscope and while the EDS was employed to study the chemical composition of samples. In figure 2a), the SEM image of GQDs-50 has presented as well as the maps of O, Si, C atoms. It can be observed that sample contains 8% of O atoms, which is higher compared to GQDs-H (2%) [9] but significantly lower in comparison with p-GQDs, which has 37 % of O atoms.[10] These results indicate the lowering in the content of O containing functional groups.

UV-Vis spectra of all samples are present in figure 2b). The main absorption band for GQDs is located at 213 nm and it stems from π - π^* transitions due to the presence of graphene core. The additional band can be observed at around 320 nm and it stems from carboxy functional groups. Due to modification, the main absorption band has been shifted to the higher wavelengths. This change can be assigned to increasing of π -domains in GQD and GO structure.

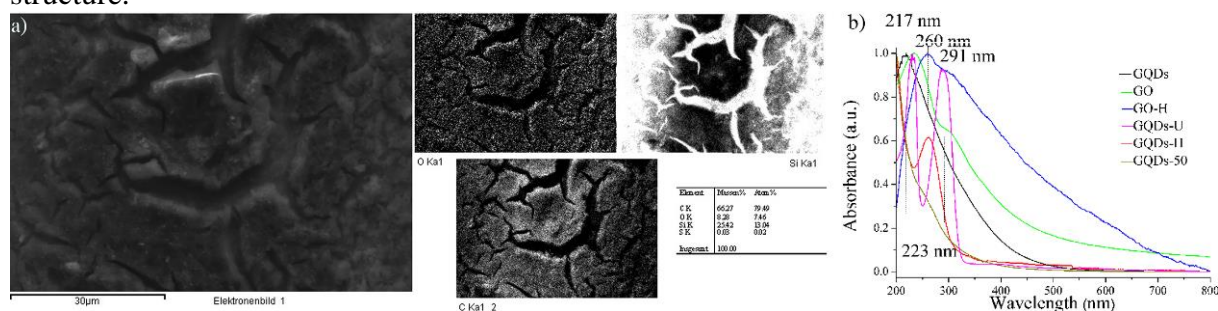


Figure 2. a) SEM image of GQDs-50 sample and elemental mapping, b) UV-Vis spectra of p-GQDs, GO, GO-H, GQDs-U, GQDs-H and GQDs-50 as indicated in spectra.

Conclusion

Proposed methods for structural modification of GQDs and GO appear to be efficient, eco-friendly methods for structural modification of carbon-based nanomaterials. By employing proposed reactions, the production of waste, residual, toxic reagents and solvents are avoided, while at the same time we achieved the chemical reduction of GO and GQDs. This structural modification is important from the aspect of the electronic application of these nanomaterials.

Acknowledgments

This research is supported by the Ministry of Education, Science and Technological Development of the Republic of Serbia through national project number 172003. Also, SEM measurements were conducted through support by the project of bilateral collaboration between the Republic of Serbia and Germany (project number 451-03-01732/2017-09/7).

References

- [1] N. Choudhary, S. Hwang, W. Choi, Carbon Nanomaterials: A Review, in: B. Bhushan, D. Luo, S.R. Schrick, W. Sigmund, S. Zauscher (Eds.) Handbook of Nanomaterials Properties, Springer Berlin Heidelberg, Berlin, Heidelberg, 2014, pp. 709-769.
- [2] S. Jovanović, Photoluminescence of carbon-based nanomaterials: Fullerenes, carbon nanotubes, graphene, graphene oxide, graphene and carbon quantum dots, in: E. Marsden (Ed.) Photoluminescence: Advances in Research and Applications, Nova Science Publishers, Inc., New York, USA, 2018, pp. 167-196.
- [3] N.T. Ho, T.V. Tam, H.N. Tien, S.J. Jang, T.K. Nguyen, W.M. Choi, S. Cho, Y.S. Kim, Solution-Processed Transparent Intermediate Layer for Organic Tandem Solar Cell Using Nitrogen-Doped Graphene Quantum Dots, Journal of Nanoscience and Nanotechnology, 17 (2017) 5686-5692.

- [4] Y. Fu, G. Gao, J. Zhi, Electrochemical synthesis of multicolor fluorescent N-doped graphene quantum dots as a ferric ion sensor and their application in bioimaging, *Journal of Materials Chemistry B*, 7 (2019) 1494-1502.
- [5] S.P. Jovanovic, Z. Syrgiannis, Z.M. Markovic, A. Bonasera, D.P. Kepic, M.D. Budimir, D.D. Milivojevic, V.D. Spasojevic, M.D. Dramicanin, V.B. Pavlovic, B.M. Todorovic Markovic, Modification of Structural and Luminescence Properties of Graphene Quantum Dots by Gamma Irradiation and Their Application in a Photodynamic Therapy, *ACS Appl Mater Interfaces*, 7 (2015) 25865-25874.
- [6] S. Jovanovic, Z.M. Markovic, B. Todorović Marković, Carbon based nanomaterials as agents for photodynamic therapy, in: F. Fitzgerald (Ed.) *Photodynamic Therapy (PDT): Principles, Mechanisms and Applications*, Nova Science Publishers, Inc., New York, 2017, pp. 35-108.
- [7] L.B. Li, L. Li, C. Wang, K.Y. Liu, R.H. Zhu, H. Qiang, Y.Q. Lin, Synthesis of nitrogen-doped and amino acid-functionalized graphene quantum dots from glycine, and their application to the fluorometric determination of ferric ion, *Microchim Acta*, 182 (2015) 763-770.
- [8] S.A. Miners, G.A. Rance, A.N. Khlobystov, Chemical reactions confined within carbon nanotubes, *Chemical Society Reviews*, 45 (2016) 4727-4746.
- [9] S. JOVANOVIĆ, O. HANSSLER, M. Budimir, D. Kleut, J. PREKODRAVAC, B. TODOROVIC MARKOVIC, Reduction of graphene oxide and graphene quantum dots using nascent hydrogen: investigation of morphological and structural changes in: 14TH MULTINATIONAL CONGRESS ON MICROSCOPY, September 15-20, 2019 in Belgrade, Serbia., 2019.
- [10] S.P. Jovanović, Z. Syrgiannis, Z.M. Marković, A. Bonasera, D.P. Kepić, M.D. Budimir, D.D. Milivojević, V.D. Spasojević, M.D. Dramićanin, V.B. Pavlović, B.M. Todorović Marković, Modification of Structural and Luminescence Properties of Graphene Quantum Dots by Gamma Irradiation and Their Application in a Photodynamic Therapy, *ACS Applied Materials and Interfaces*, 7 (2015) 25865-25874.

PRODUCT DEVELOPMENT OF SEA BUCKTHORN RESIDUAL POMACE TEA MIXTURE

Vanessza Klink¹, Dóra Székely¹, Mónika Stégerné-Máté¹, Éva Stefanovits-Bányai²,
Diána Furulyás^{1*}

¹*Department of Food Preservation, Szent István University, H-1118 Budapest, Villányi Street 29-43., Hungary*

²*Department of Applied Food Chemistry, Szent István University, H-1118 Budapest, Villányi Street 29-43., Hungary*

e-mail: Furulyas.Diana@etk.szie.hu

Abstract

Nowadays waste management is becoming increasingly important, as both consumers and companies are producing too much garbage that could be prevented. The food industry generates a large amount of by-products, which are in fact suitable for further processing. This study highlights an untapped area that is the further processing of the sea buckthorn by-product as a tea ingredient. Sea buckthorn berries are a source of polyphenols and carotenoids along with many vitamins, minerals, and trace elements. These biologically active compounds are also found in the residual pomace after food production. In this study dried sea buckthorn pomace (SBP) boiled with water at different temperatures (70 and 100%), with green tea and other flavoring agents (dried elderflower and orange flower) were analyzed. The antioxidant capacity (FRAP) and total polyphenol content (TPC) of the samples were measured. Preliminary experiments have shown that higher temperature water boiled SBP extract contains higher amounts of valuable components. As result of product development, most antioxidants and polyphenols were detected in a mixture of tea, which contained green tea, SBP and elderflower compared to the tested tea samples from the commercial. Nevertheless, each blend contained less valuable ingredients than natural green tea. This is due to the water-insoluble compounds in SBP so that they did not dissolve properly during soaking. Further studies are reasonable in which another sea buckthorn variety will be tested that contains water-soluble antioxidants and polyphenols.

Introduction

Sea buckthorn is from the family of the Elaeagnaceae. It can be a deciduous shrub with a height of 1.5-3 meters or a tree with a height of 8-10 meters [1]. Its 2-4 cm long lance-like leaves are placed rarely and have intact edges [6]. It has a single-seeded, dormant fruit, which is round or ovoid, 6-8 mm in diameter [4]. Sea buckthorn juice contains 8-10% dry matter, 2-4 % sugar, 1-2% fatty oil and valuable acids (mainly malic acid). Two coloring agents, fat soluble carotenoids and water-soluble yellow flavonoids give its colour. It also contains many biologically active substances such as vitamins A, C, B1, B2, E, F, K, P, proanthocyanidins (a type of polyphenol) and sitosterols. Several minerals and trace elements make it more valuable such as calcium, magnesium, potassium, iron, copper, manganese, zinc, folic acid, and titanium [6].

Tea is an indeciduous plant from the camellia family which has three isolable species, native to China, Assam, and Cambodia. This species is a shrub that grows to 2.7-4.5 meters high, is resistant to cold weather, and produces 5 cm long leaves for up to 100 years. It contains many compounds such as polyphenols, caffeine, amino acids, carbohydrates, and minerals. The complexity of the aroma of black tea is demonstrated by the fact that more than 550 compounds have been identified. It is interesting that the six different types of tea are made from the same plant, the difference is only in the way of processing. The six basic types of tea

are white, oolong, green, black, flavored and pressed teas, but there are more than 3000 subtypes.

Our goal, when conducting this experiment, was to find the right mixture of tea components which is the richest in antioxidants and polyphenols by adding sea buckthorn pomace [5].

Material and methods

‘Ascola’ sea buckthorn berries were used in the experiments which came from the 2018 harvest. In the first step of its processing berries were heated to 80 °C to assist compression and inactivates oxidative enzymes. The juice was extracted manually. Based on previous study the residual pomace was dried at 80 °C in an atmospheric dryer [3]. The extract of pomace was made two ways, with water at 75 °C and 100 °C. The purpose of the experiment was to ascertain if there was a significant difference between the two extracts, and a connection between the temperature of the boiling water and the extraction of the reducing compounds. Two types of green tea (Lipton and Nepal) were compared according to their nutrition value, taste and colour. to find the base of the tea mixture. Other flavorings were used in the tea mixture, these were elderflower and orange flower extracts. The sea buckthorn pomace tea mixture was prepared based on the results of the preliminary experiments. The formulas made during product development were compared with commercially available sea buckthorn tea blends. The mixtures and control samples were analyzed using two methods:

- Antioxidant capacity was determined based on Ferric Reducing Ability of Plasma (FRAP) method, by Benzie and Strain . Antioxidant capacity was defined in ascorbic acid equivalent (mg ascorbic acid equivalent/ 100 L).
- Total Polyphenol Content (TPC) was evaluated using a method by Singleton and Rossi. Results were specified in mg gallic acid equivalent/ 100 L.

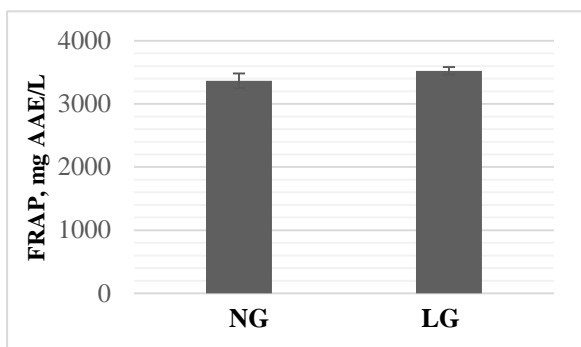
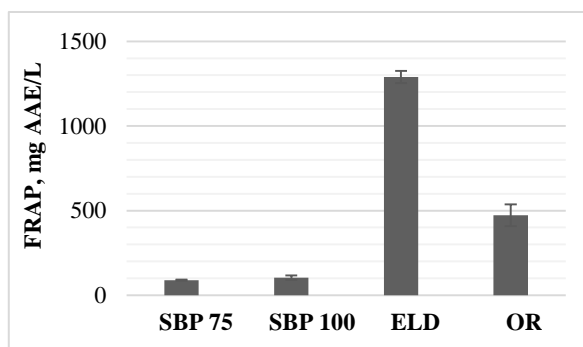
Results were calculated and after comparing they were represented by Microsoft Excel.

Results and discussion

Samples were measured to define antioxidant capacity and total polyphenol content in order to find the mixture(s) with the richest biologically active compounds.

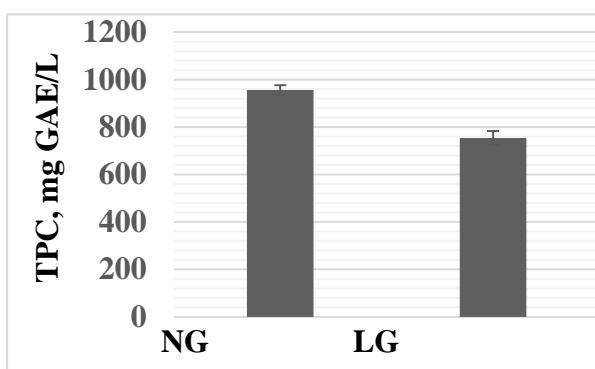
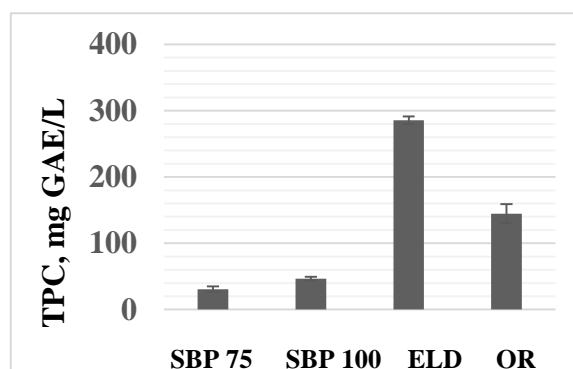
Sample shortened name	Components of the sample
NG	Nepal green tea
LG	Lipton green tea
SBP 100 °C	Sea buckthorn pomace tea made 100 °C
SBP 75 °C	Sea buckthorn pomace tea made 75 °C
OR	Orange-flower flavouring
ELD	Elder-flower flavouring
NSB	Naturland sea buckthorn tea (commercial)
OSB	Oxalis sea buckthorn tea (commercial)
NG+SBP	Nepal green tea+ sea buckthorn pomace tea
NG+SBP+OR	Nepal green tea+ sea buckthorn pomace tea, orange-flower flavouring
NG+SBP+ELD	Nepal green tea+ sea buckthorn pomace tea, elder-flower flavouring

Figure 1. Components and name of the tested tea types

**Figure 2.** Antioxidant capacity of green teas**Figure 3.** Antioxidant capacity of flavourings

In Figure 2., total antioxidant content concentrations in mg/ L are shown. There is no significant difference between the two green teas. Additional measurements are necessary which analyze the connection between the quantity of dissolving antioxidants and soaking time.

In Figure 3., total antioxidant content concentrations in mg/ L are shown. As Figure 3 is shown more antioxidant could dissolve from sea buckthorn pomace tea at the higher temperature (104.33 mg AAE/ L). At lower temperature this value is 89.24 mg AAE/L. Therefore 100°C water has no destructive effect, moreover, it slightly raises the amount of dissolving antioxidants. Despite, sea buckthorn pomace extracts have lower values than the orange-flower (472.5 mg AAE/L) and the elder-flower (1289.5 mg AAE/L) extracts, thus presumably there are water-insoluble antioxidants in sea buckthorn pomace.

**Figure 4.** Total polyphenol content of green teas**Figure 5.** Total polyphenol content of flavourings

As Figure 4 is represented the analysis of total polyphenol content shows significant difference. More polyphenol dissolved from Nepal green tea during the same soaking time (955.7 mg GAE/L). The difference between the two samples is 26.76 %. After the analysis of the antioxidant capacity and total polyphenol content unquestionably the Nepal green tea is able to the product development.

Figure 5 is shown a slightly greater value of sea buckthorn pomace tea made with 100 °C water (46.53 mg GAE/L) rather than made with 75 °C (30.86 mg GAE/L). Orange-flower (144.65mg GAE/L) and elderflower (285.61 mg GSE/L) had higher polyphenol content. The percentage difference between pomace extracts is 33,68%, between orange-flower and elderflower it is 49,35 %.

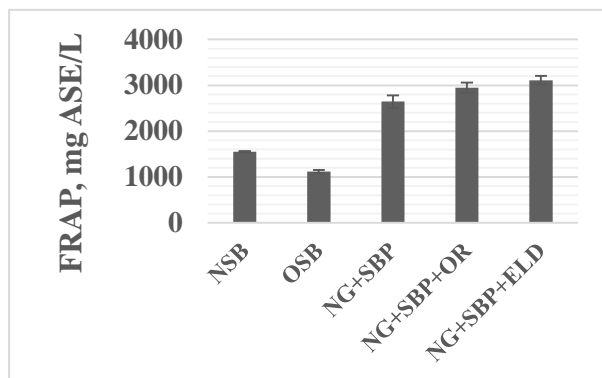
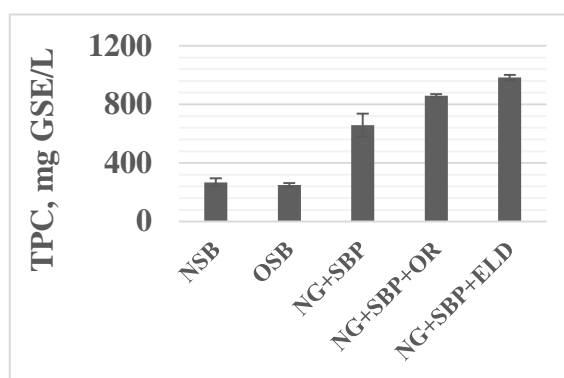
**Figure 6.** Antioxidant capacity of tea mixtures**Figure 7.** Total polyphenol content of tea mixtures

Figure 6. is represented that due to the different components, the percentage difference between control samples is 27.97 %. The basic mixture which contains green tea and sea buckthorn pomace took twice as big value than control samples (2647.37 mg ASE/L). Much more antioxidant could dissolve from orange-flower (472.5 mg ASE/L) and elderflower (1289.5 mg ASE/L) than sea buckthorn pomace (104.33 mg ASE/L). Thus tea mixture in which they are presented also contain a larger amount of antioxidant rather than the basic mixture. The orange-flower tea mixture's antioxidant capacity is 2948.32 mg ASE/L and the elderflower tea mixture's is 3110.59 mg ASE/L. Even so, all of the mixtures showed a lower value than Nepal green tea. The difference between mixtures and green tea is 7.53-21.3%. The reason is the additional sea buckthorn pomace extract, as it has low value because its antioxidants and polyphenols are just partly water-soluble. Accordingly further test needed with an another type of sea buckthorn which contains more water-soluble compounds.

Figure 7 is shown there is no significant difference between the control samples. The basic mixture which contains green tea and sea buckthorn pomace took more than twice as big value than control samples (657,36 mg GSE/L). Orange-flower (859,13 mg GSE/L) and elderflower mixture (983,51 mg GSE/L) have more valuable polyphenols. Only elder mixture's polyphenol content was higher than pure green tea, because of the additional sea buckthorn pomace (above).

Conclusion

The management of industrial waste is, without doubt, economic and environmental-friendly. The aim of this study was to extract bioactive compounds from sea buckthorn pomace to reduce industrial waste and create a valuable product. According to our results, elderberry tea mixture contained the most antioxidants and polyphenols. This mixture's values are much better than the control samples (almost four times). Still, except for elderberry mixture's polyphenol content, none of the mixtures reach the pure green tea's value. It is because sea buckthorn contains partly water-insoluble antioxidants and polyphenols. Therefore, further analysis is needed with another type of sea buckthorn.

Acknowledgements

This work was supported by the Hungarian Government through project No. EFOP-3.6.3-VEKOP-16-2017-00005.

References

- [1] J. Bernáth, Gyógy- és aromanövények, Mezőgazda Kiadó, Budapest, 2000, pp 350-354.
- [2] F. Benzie, J. Strain, Analytical Biochemistry 239, 1996, pp 70–76.
- [3] D. Furulyás, C. Rentsendavaa; F. Kis; K. Biró, M. Stéger-Máté, É. Stefanovits-Bányai, Preliminary study of optimal extraction of biologically active compounds from sea buckthorn (*Hippophae Rhamnoides* L.) pomace. Proceedings of the International Symposium on Analytical and Environmental Problems, (23), 2017, pp. 392-396.
- [4] L. Hornok, Gyógynövények termesztése és feldolgozása. Mezőgazda Kiadó, Budapest, 1990, pp 161-163.
- [5] J. Pettigrew, J. (2007): The Connoisseur's Guide to Tea, Apple Press, London, 2007, pp 10-36.
- [6] J. Rápóti, V. Romváry, Gyógyító növények, Medicina Könyvkiadó Zrt, Budapest, 1999, pp 173.
- [7] V.L. Singleton, J.A. Rossi, American Journal of Enology and Viticulture 16, 1965, pp 144–158.

POLYCYCLIC AROMATIC HYDROCARBONS IN URBAN AND RURAL SOILS OF VOJVODINA

Snežana Kravić, Zorica Stojanović, Ana Đurović, Zvonimir Suturović, Tanja Brezo-Borjan

University of Novi Sad, Faculty of Technology Novi Sad, Bulevar cara Lazara 1, 21000 Novi Sad, Serbia

e-mail: sne@uns.ac.rs

Abstract

Contents of 16 polycyclic aromatic hydrocarbons (PAHs) were determined in soil samples from urban and rural areas in Vojvodina Province, Serbia. Surface soil samples were collected from 15 different locations. The samples were Soxhlet extracted, cleaned-up and analyzed using gas chromatography-mass spectrometry in the selected ion monitoring mode. The total PAHs concentrations were in the range of 0.398-1.115 mg/kg for soils from urban areas, and 0.434-0.729 mg/kg for rural soils. Comparison with the relevant maximum allowed contents proposed by the Serbian legislative indicated that the concentration of PAHs in investigated soil samples is below the levels that would require the implementation of relevant soil remediation measures.

Introduction

Polycyclic aromatic hydrocarbons (PAHs) are a group of stable organic compounds consisting of two or more fused aromatic rings. PAHs originate from natural processes such as forest fires, volcanic eruptions, and diagenesis, and also from anthropogenic sources such as vehicle emissions, coal and fossil fuel power generation, petroleum refining, industrial processing, chemical manufacturing, oil spills, and coal tars [1]. Although hundreds of PAHs exist in the environment, only 16 have been selected by the US Environmental Protection Agency (US EPA) as priority pollutants due to their potential mutagenic, carcinogenic, and teratogenic effects on human health [2,3].

Due to widespread sources, PAHs are present in all environmental matrices, including soil, water and air. Soil is the most important sink for PAHs in the environment [4,5]. Due to their persistence and hydrophobicity, PAHs accumulate in the soil. It has been estimated that approximately 90% of total residues remain in the soil [6]. These harmful pollutants accumulated in soil can be carried into surface and ground water through precipitation, emitted into atmosphere by vaporization, and transported into crops from polluted soil and air via root and leaf adsorption [7], consequently resulting in direct or indirect exposure to humans. Considering the harmful effects of PAHs, it is important to monitor their concentration in the environment, especially in soil which is the most potent reservoir of PAHs.

The principal objective of the present study was to determine the concentration levels of PAHs in soil from urban and rural areas in Vojvodina Province.

Experimental

Soil sampling, extraction and purification

Surface soil samples were collected from 15 different sites in Vojvodina Province (Serbia) located in urban (8 sites) and rural (7 sites) areas. Samples were air-dried at room temperature, sieved to 100-mesh size particles and stored in amber glass containers at -4°C until analysis. A 10 g soil sample was Soxhlet extracted for 24 h with 200 ml methylene chloride. The extracts were concentrated to 0.5 ml by rotary vacuum evaporation and then 2

ml cyclohexane was added. The extracts were cleaned up using silica gel column chromatography (250 mm × 10 mm ID). The glass chromatography column was packed with glass wool, 10 g silica gel (100/200 mesh) and 2 cm anhydrous sodium sulfate. The column was rinsed with pentane (40 mL) before use. After adding the sample extract, the column was sequentially eluted with 25 ml of pentane and 25 ml of methylene chloride/pentane (2/3, v/v). The second eluate was vacuum-evaporated to near dryness and re-dissolved with acetonitrile (1 ml).

Gas chromatography-mass spectrometry

PAHs were analyzed using a gas chromatograph with mass selective detector (GC-MS, Hewlett-Packard 5890A-5971A) equipped with an ULTRA 1 column (25 m × 0.20 mm i.d., 0.33 µm film thickness), using helium as the carrier gas. The following temperature program was used: the initial temperature of 80°C was held for 5 min, increased at rate of 5°C/min to 250°C and held for 10 min, and then increased at the rate of 20°C/min to 280°C and held at this temperature for 15 min. The injection port was set at 290 °C. A 1 µl aliquot of sample extract was injected in split mode (split ratio 1: 20). The mass spectrometer was operated in the electron impact ionization mode and data were acquired using the selective ion monitoring (SIM) mode. Identification of PAHs was based on the selected ions and the relative retention time between samples and the standard solution containing individual PAHs. Quantification was done using the internal standard method. Five deuterium-labeled PAHs were used as internal standards: naphthalene-*d*8, acenaphthene-*d*10, phenanthrene-*d*10, chrysene-*d*12, and perylene-*d*12. The SIM program used to determine PAHs in soil is indicated in Table 1. All reported concentration values of PAHs are expressed on a dry weight basis of soil determined by drying the soil for 24 h at 100°C.

Table 1. SIM program used to determine PAHs

Group	PAHs	Time (min)	m/z	Dwell time (ms)
1	naphthalene, naphthalene - <i>d</i> 8	12.00	136, 128	50
2	acenaphthylene	19.00	152	50
3	acenaphthene - <i>d</i> 10, acenaphthene	21.50	164,154	50
4	fluorene	23.50	166	50
5	phenanthrene - <i>d</i> 10, phenanthrene, anthracene	28.00	188,178	50
6	fluoranthene, pyrene	34.00	202	50
7	chrysene - <i>d</i> 12, benzo[a]anthracene, chrysene	41.00	240, 228	50
8	benzo[b]fluoranthrene, benzo[k]fluoranthrene, benzo[a]pyrene, perylene- <i>d</i> 12	50.00	252, 264	50
9	indeno[1,2,3-cd]pyrene, dibenzo[ah]anthracene, benzo[ghi]perylene	59.00	276, 278	50

Results and discussion

The levels of the individual and the sum of 16 US EPA priority PAHs (Σ16PAHs) and seven carcinogenic PAHs (Σ7cPAHs=BaA+Chr+BbF+BkF+BaP+IcdP+DahA) determined in the soil samples, expressed as mg/kg dry weight, are given in Table 2.

Table 2. Concentrations of PAHs in soils from urban and rural areas in Vojvodina (mg/kg dry weight)

Compound/Abbreviation	Urban areas				Rural areas			
	Min	Max	Mean	SD	Min	Max	Mean	SD
Naphthalene/Nap	nd	0.101	0.045	0.029	0.005	0.054	0.022	0.017
Acenaphthylene/Acl	nd	0.017	0.017	0.002	nd	0.012	0.012	0.001
Acenaphthene/Acn	nd				nd			
Fluorene/Flu	nd	0.086	0.039	0.031	nd	0.031	0.021	0.009
Phenanthrene/Phe	0.046	0.183	0.090	0.048	0.004	0.132	0.069	0.042
Anthracene/Ant	nd	0.057	0.026	0.017	nd	0.102	0.054	0.046
Fluoranthene/Flt	0.060	0.184	0.136	0.047	0.056	0.142	0.097	0.038
Pyrene/Pyr	0.055	0.168	0.118	0.039	0.048	0.122	0.079	0.029
Benz[a]anthracene/BaA	0.046	0.174	0.105	0.057	0.015	0.098	0.058	0.032
Chrysene/Chr	nd	0.090	0.061	0.034	nd	0.052	0.031	0.020
Benzo[b]fluoranthene/BbF	0.026	0.191	0.112	0.058	0.045	0.165	0.096	0.050
Benzo[k]fluoranthene/BkF	nd	0.082	0.032	0.027	nd	0.032	0.025	0.010
Benzo[a]pyrene/BaP	0.046	0.142	0.073	0.029	0.049	0.091	0.070	0.014
Indeno[1,2,3-cd]pyrene/IcdP	nd	0.028	0.020	0.012	nd	0.041	0.036	0.007
Dibenz[a,h]anthracene/DahA	nd	0.042	0.028	0.012	0.012	0.044	0.022	0.012
Benzo[g,h,i]perylene/BghiP	nd	0.084	0.048	0.030	0.025	0.073	0.054	0.016
Σ_{16} PAHs	0.398	1.115	0.822	0.276	0.434	0.729	0.642	0.116
Σ_{7c} PAHs	0.140	0.549	0.361	0.146	0.157	0.372	0.280	0.077

SD - standard deviation; nd - not detected (below the limit of detection)

PAHs were detected in all analyzed soil samples. The content of Σ_{16} PAHs was in the range of 0.398-1.115 mg/kg for urban soils, and 0.434-0.729 mg/kg for rural soils. The most abundant PAHs found in urban soils were fluoranthene, pyrene, benzo[b]fluoranthrene and benzo[a]anthracene with mean concentrations of 0.136, 0.118, 0.112 and 0.105 mg/kg, respectively. In rural soils, the most frequently detected PAHs were fluoranthene, benzo[b]fluoranthrene, pyrene and benzo[a]pyrene with mean concentrations of 0.097, 0.096, 0.079 and 0.070 mg/kg, respectively.

Seven of the 16 PAH compounds prioritized by the EPA were determined as possible carcinogenic compounds for humans by the International Agency for Research on Cancer (IARC) [8]. The total levels of these compounds (Σ_{7c} PAHs) varied between 0.140 and 0.549 mg/kg for urban soils and 0.157-0.372 mg/kg for rural soils. The contribution of the seven carcinogenic PAHs to the total PAHs was similar for urban and rural soils, and it was about 43%.

The ring distributions of the PAHs that were determined in soil samples are given in Figure 1. In urban soils, the rate of 4-ring PAHs ranged between 38 and 53%, with average rate of 46%, followed by 6-ring, 3-ring and 5-ring compounds with average rate of 18, 17 and 15%, respectively. Similar ring distributions of PAHs were obtained for rural soils. The contribution of 4-ring PAHs varied between 28 and 50% (mean value was 38%), followed by 6-ring, 3-ring and 5-ring compounds with average rate of 25, 17 and 16%, respectively. It is evident that high molecular weight (HMW) PAHs with 4 to 6 rings were dominated. The mean percentage concentration of HMW PAHs was 79%, which correlated to those found in the literature [1, 4].

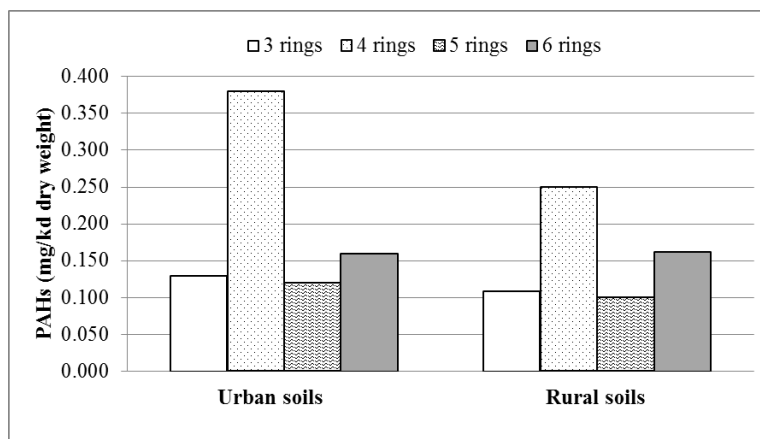


Figure 1. Ring distribution of PAHs in urban and rural soil from Vojvodina

Serbian law has no limitation for the maximum level of individual PAH compound, but the maximum allowed concentration (MAC) and remediation concentration (RM) for sum of 10 PAHs ($\Sigma_{10}\text{PAHs} = \text{Ant} + \text{BaA} + \text{BkF} + \text{BaP} + \text{Chr} + \text{Phe} + \text{Flt} + \text{IcdP} + \text{Nap} + \text{BgHiP}$) are defined. MACs are defined as the maximum values at which functional properties of the soil are still fully achieved and indicate level at which a sustainable soil quality is reached, while RM represent values at which basic functions of land are threatened or seriously disrupted, requiring remediation and other measures [4, 9]. According to the Serbian national limits for PAHs in soil [9] defined MAC and RM values for soil samples with organic matter less than 30% are 1 and 40 mg/kg, respectively. The concentration of $\Sigma_{10}\text{PAHs}$ for all samples was below the Serbian MAC, indicating no significant contamination. According to the obtained results soil from urban and rural areas of Vojvodina could be classified as suitable as residential soils.

Conclusion

Soil samples collected from urban and rural areas of Vojvodina were analyzed for pollution level of sixteen PAHs from the US EPA priority list. PAHs were detected in all samples with average concentrations of 0.822 mg/kg for urban soils, and 0.642 mg/kg for rural soils. The high molecular weight PAHs were predominant compounds in all samples. The concentration of $\Sigma_{10}\text{PAHs}$ was lower than maximum allowable limit set by the Serbian legislation, indicating no significant contamination of soil.

Acknowledgements

The present work was supported by the Ministry of Education, Science and Technological Development of the Republic of Serbia, under the Projects No. III 46009.

References

- [1] C. Wang, S. Wu, S. Zhou, H. Wang, B. Li, H. Chen, Y. Yu, Y. Shi, *Sci. Total Environ.* 527–528 (2015) 375.
- [2] J.S. Cvetkovic, V.D. Mitic, V.P. Stankov Jovanovic, M.V. Dimitrijevic, G.M. Petrovic, S.D. Nikolic-Mandic, G.S. Stojanovic, *Anal. Methods* 8 (2016) 1711.
- [3] G. Karaca, *Arch. Environ. Contam. Toxicol.* 70 (2016) 406.
- [4] B. Škrbić, N. Đurišić-Mladenović, Đ. Tadić, J. Cvejanov, *Environ. Sci. Pollut. Res.* 24 (2017) 16148.
- [5] C.Q. Yin, X. Jiang, X.L. Yang, Y.R. Bian, F. Wang, *Chemosphere* 73 (2008) 389.
- [6] Y. Hu, J. Wen, D. Wang, X. Du, Y. Li, *Chem. Ecol.* 29 (2013) 476.

- [7] L. Wang, S. Zhang, L. Wang, W. Zhang, X. Shi, X. Lu, X. Li, X. Li, *Int. J. Environ. Res. Public Health* 15 (2018) 607.
- [8] International Agency for Research on Cancer, *IARC Monographs on the evaluation of carcinogenic risks to humans*, 92 (2010) Lyon, France.
- [9] *Official Gazette of the Republic of Serbia* 88/2010.

VALIDATION METHOD FOR DETERMINATION OF PCB CONGENERS IN SOIL USING GC-MS

Aleksandar Krstić¹, Marija Ječmenica Dučić¹, Mina Seović¹, Djurica Katnić¹, Milena Pijović¹, Adrijana Šutulović¹, Gvozden Tasić¹

¹*Vinca Institute of Nuclear Sciences, University of Belgrade, Mike Petrovića-Alasa 12-14, 11000 Belgrade, Serbia*

e-mail: aleksandar.krstic@vinca.rs

Abstract

Polychlorinated biphenyls (PCBs) are the most highly toxic species of POPs. More than 200 PCB congeners exist in nature. [1] PCBs are highly toxic for humans. They enter the human body *via* inhalation, ingestion or sorption through the skin and the bloodstream transports them to the organs, muscles and adipose tissues, where they are accumulated. This study presents the validation of analytical method for determination of 7 PCBs congeners in soil: PCB 28, PCB 52, PCB 101, PCB 118, PCB 153, and PCB 180. The method is based on solid-liquid extraction with cyclohexane and the analysis by gas chromatography with mass spectrometric detection (GC-MS). [2] Samples were analyzed in SIM mode, and the analytes qualitative confirmation was performed comparing the mass spectra of analytical standards of PCB congeners with the NIST data base. The method developed can be applied in range from 0,005 to 10 mg/kg with the appropriate parameters of precision, accuracy, repeatability and linearity and can be used for simultaneous determination of low PCBs concentrations in different types of soil (agricultural, contaminated soil, etc.).

Introduction

For the first time, PCBs were synthesized in 1881. Their production in 20th century raised from 1000 tons/year in early 30s up to 200,000 tons/year in 1975 (Abraham et al, 2002). In the beginning of the 80s, the production and the use of PCBs were stopped due to their toxicity. They were classified as POPs – Persistent Organic Pollutants and covered by the Stockholm Convention on Persistent Organic Pollutants. PCBs consist of a skeleton with two benzene rings linked through a carbon atom. The aromatic structure can be substituted with one to ten chlorine atoms. PCBs are chemically inert compounds, remarkably resistant to elimination, addition, electrophilic substitution, oxidation and reduction. They are soluble in most organic solvents, oils and fats. PCBs penetrate through the soil surrounding places they were produced and used. [3] The concentration of PCBs on these sites is between 10 and 104 mg/kg, which is extremely higher than limits established by numerous national regulatory agencies (range of 0.01 to 50 mg/kg). The aim of presented study is validation of GC-MS method for determination of 7 PCB congeners in soil. Samples were prepared by liquid-solid extraction with cyclohexane and were analyzed in SIM mode. The validation parameters are: selectivity, linearity, repeatability, accuracy, precision, limit of detection (LOD), and limit of quantification (LOQ).

Experimental

The following chemicals were used: cyclohexane, HPLC grade (Fisher chemical), PCB standards mix 3, Dr Ehrenstorfer, sodium sulphate anhydrous (Centrohem), acetone p.a. (Fisher Chemical). Chromatographic analyses were carried out on the gas chromatograph coupled with mass detector Agilent Technologies 7890B GC System, Agilent Technologies 5977MSD. The gas chromatograph was equipped with a capilar column HP-5 MS Inert ((5% phenyl)-methylpolysiloxane, 30m x 0,25 mm, film thickness 0,25 µm. Agilent technologies).

The oven temperature was raised from 125°C to 200°C at a heating rate 25°C per minute. Then 200°C to 260°C at a heating rate 4°C per minute and isothermally held 10 min. As a carrier gas, helium at a flowrate 0,7 ml min⁻¹ was used. Injection volume was 1 µl and injected in a splitless mode. Calibration range was from 0,005 to 0,5 mg/l. Working standard solution was prepared by diluted working standard with concentration 10 ppm. For determination of accuracy, soil samples were spiked in 3 concentration levels, with 0,01 mg/l, 1,0 mg/l and 10,0 mg/l. Samples were prepared by measuring 10 g of dry soil samples in conical flasks and adding 50 ml cyclohexane, 50 ml acetone and specific volume of standard solution for spike. Then samples were shaken 30 min in orbital shaker. After time elapsed, cyclohexane aliquots were filtered through filter 0,22 µm into separation funnels and extraction was repeated with new aliquots of cyclohexane 50 ml and 30 min shaking. After that, aliquots were filtered into a separation funnels and shaken two times with 400 µl water. The extracts were filtered through a layer of anhydrous sodium sulphate and evaporated in vacuum evaporator to a volume of about 2 ml and then in stream of nitrogen to a final volume of 1 ml. Then samples were injected in GC-MS.

Results and discussion

Results of validation showed that the method for determination of low PCBs concentrations in soil was developed. Performed linearity test showed excellent linearity with correlation coefficient $R > 0,999$. Obtained low limits of detection (LOD of 0,002 mg/kg) and quantification (LOQ of 0,005 mg/kg) confirmed the method can be applied for determination of PCB congeners in traces. The precision criterion (<5%) was fulfilled for all analyzed congeners. Analysis results of samples spiked in 3 concentration levels showed the recovery was in range 92 – 110%, which fulfilled the accuracy criterion (Table 1) [4,5].

Table 1: Required criterion for accuracy

	Accuracy (recovery %)
I spike level	60-115
II spike level	80-110
III spike level	80-110

Table 2: Summary of results

Analytes	Regression equation	R	LOD (mg/kg)	LOQ (mg/kg)	Precision (%)
PCB 28	$y=565089x-2935$	0,999	0,002	0,005	4,01
PCB 52	$y=405060x-2118$	0,998	0,002	0,005	3,42
PCB 101	$y=354554x-2829$	0,999	0,002	0,005	4,90
PCB 118	$y=425740x-4459$	0,999	0,002	0,005	3,42
PCB 138	$y=296806x-3203$	0,999	0,002	0,005	4,61
PCB 153	$y=255957x-2929$	0,999	0,002	0,005	3,68
PCB 180	$y=185581x-2695$	0,998	0,002	0,005	4,12

Table 3: Recovery and repetability results

Analytes	Spike 0,1 mg/kg Recovery (%)	Spike 1,0 mg/kg Recovery (%)	Spike 10,0 mg/kg Recovery (%)	Repetability (%)
PCB 28	110	98	105	4,25
PCB 52	92	97	102	3,28
PCB 101	98	108	108	2,98
PCB 118	110	110	110	3,53
PCB 138	105	109	110	4,88
PCB 153	107	109	110	4,70
PCB 180	103	106	110	3,91

Conclusion

The method for the identification and quantification of the PCB congeners in soil by using gas chromatographic method with mass spectrometric detection analytical technique was developed and validated in presented study. Based on precision, accuracy, repeatability and linearity, it can be concluded that the measuring range of developed method is from 0.005 to 10,0 mg/kg. The method will be used for testing PCBs congeners in contaminated sites and another soil samples.

Acknowledgements

The work was supported by the Ministry of Education and Science of the Republic of Serbia, under the number OI 172045.

References

- [1] <https://www.epa.gov/sites/production/files/2015-09/documents/congenertable.pdf>
- [2] Reference standard: SRPS EN 15308:2010
- [3] <https://www.epa.gov/sites/production/files/2015-05/documents/biomonitoring-pcbs.pdf>
- [4] Validation and Qualification in Analytical laboratories, www.labcompliance.com 8. Quantifying Uncertainty in Analytical Measurement, EURACHEM/CITAC Guide CG4, 2000
- [5] EURACHEM/CITAC, Guide 25, 2000. 5. Text on Validation of Analytical Procedure, ICH 6. Method Verification and Validation

CONFORMATIONAL ANALYSIS OF ORGANO-SILICON DERIVATES ATTACHED ON SUPERPARAMAGNETIC IRON OXIDE (Fe_3O_4)

Horatiu Moldovan¹, Marius Chirita², Liviu Mocanu^{2*}

¹Politehnica University, P-ta Victoriei No. 2, RO-300006, Timisoara, Romania

²National Institute for Research and Development in Electrochemistry and Condensed Matter, Timisoara, PlautiusAndronescu Str. No. 1, RO-300224, Timisoara, Romania

*Corresponding author: mocanuliv@gmail.com

Continuing our previous works [1,2] the present study is a conformational analysis of the structure of the 3-(trimethoxysilyl propan)-1-amine, attached on the Fe_3O_4 superparamagnetic microparticles. The reason of this conformational study it is due to the fact that some physico-chemical properties of any compound depend in a determinant manner of its conformers. For instance (and especially) the steric properties or the electronic ones can be of major importance in the elementary processes of chemical mechanisms and are crucial in the ligand-substrate interactions. The latter ones constitute the main reason of our concerning related to the superparamagnetic properties of the Fe_3O_4 microparticles.

Keywords: superparamagnetic, magnetite, conformers

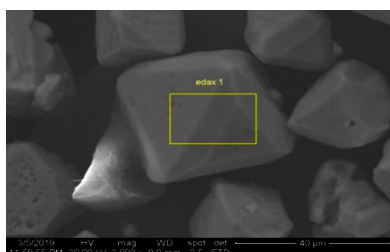


Fig.1 : SEM image of the MPTM's functionalized microcrystals

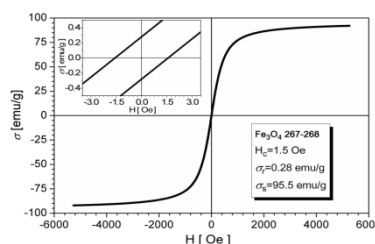


Fig.2 : Hysteresis loop of the sample

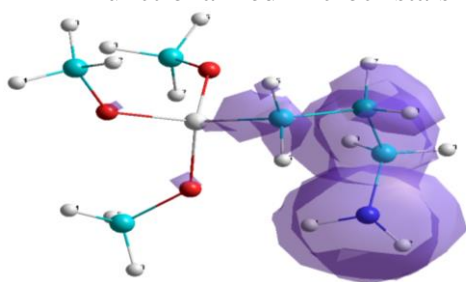


Fig 3 : One of the conformers and electronic distribution on the HOMO

References:

- [1] Horatiu Moldovan, Liviu Mocanu, Francisc Peter, Marius Chirita, *Surface Modification of Singlecrystalline Superparamagnetic Iron Oxide (Fe_3O_4) Microparticles with Various Functional Organo-Silicon Derivatives*. Titlu conferinta: "Physics Conference TIM 19", Timisoara, 29-31'st May 2019.
- [2] M. Chirita, M.L.Kiss, A. Ieta, I. Grozescu, NSTI-Nanotech 2013, Washington DC, USA, www.nsti.org, ISBN 978-1-4822-0581-7 Vol. 1, 20.

NUMERICAL STUDY OF ANISOTROPIC IRREVERSIBLE DEPOSITION OF EXTENDED OBJECTS ON A TRIANGULAR LATTICE

Ivana Lončarević¹, Ljuba Budinski-Petković¹, Slobodan Vrhovac², Zorica Jakšić²

¹*Faculty of Technical Sciences, University of Novi Sad, 21000 Novi Sad, Trg D. Obradovića 6, Serbia*

²*Institute of Physics, University of Belgrade, 11080 Zemun, Pregrevica 118, Serbia
e-mail: ivanalon@uns.ac.rs*

Abstract

The properties of the anisotropic random sequential adsorption (RSA) of objects of various shapes on a two-dimensional triangular lattice are studied numerically by means of Monte Carlo simulations. The depositing objects are formed by self-avoiding lattice steps. Anisotropy is introduced by positing unequal probabilities for orientation of depositing objects along different directions of the lattice. This probability is equal p or $(1 - p)/2$, depending on whether the randomly chosen orientation is horizontal or not, respectively. Approach of the coverage $\theta(t)$ to the jamming limit θ_{jam} is found to be exponential $\theta_{jam} - \theta(t) \propto \exp(-t/\sigma)$, for all probabilities. It was shown that the relaxation time σ increases with the degree of anisotropy in the case of elongated and asymmetrical shapes. However, for rounded and symmetrical shapes, values of σ and θ_{jam} are not affected by the presence of anisotropy.

Introduction

Deposition, or adsorption, of extended objects at different surfaces is of considerable interest for a wide range of applications in biology, nanotechnology, device physics, physical chemistry, and materials science [1,2]. Theoretically, several models have been developed to capture the basic physics of this situation, and by far the most studied is that of random sequential adsorption (RSA) [3]. In this model particles (objects) are sequentially deposited on the randomly chosen site of the substrate. When deposited, such objects are irreversibly attached to the site. If the chosen site is already occupied, the deposition is rejected, the particle is discarded, and the deposition is next attempted at a different randomly chosen site. For lattice models the approach of the coverage fraction to its jamming limit is given by the time dependence:

$$\theta(t) \sim \theta_{jam} - \Delta\theta \exp(-t/\sigma), \quad (1)$$

where parameters θ_{jam} , $\Delta\theta$, and σ depend on the shape and orientational freedom of depositing objects [4,5].

In order to account for inhomogeneous surfaces in our RSA model, we have introduced anisotropy in the deposition procedure. Namely, even when the deposition at a randomly chosen site is allowed, the probability for deposition is different along different directions of the underlying lattice. This simple modification introduces preferential direction in the deposition process and, depending on the shape of deposited objects, imposes this specific “patterning” on the deposited layer.

The main goal of the present study is to investigate the interplay between the anisotropy of deposition and the symmetry properties of deposited shapes. This work discusses the rapidity of the approach to the jamming state and the values of the jamming coverages for various degrees of anisotropy of the deposition process. Here we focus our interest on the influence of the order of symmetry axis of the shape on the kinetics of the deposition processes under anisotropic conditions.

Simulation method

The depositing shapes are modeled by directed self-avoiding walks on a triangular lattice. Examples of such walks for $l = 1, 2$, and 6 are shown in Table I. At each Monte Carlo step we randomly select a lattice site and try to deposit the shape of length l . If the selected site is occupied by a deposited object, the adsorption attempt is rejected. If the selected site is unoccupied, we fix the beginning of the walk that makes the chosen shape at this site.


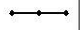



(x)	shape	n_s	ℓ
(A)		2	1
(B)		2	
(C)		1	2
(D)		3	
(E)		6	6

Table I. Various shapes (x) of length l on a triangular lattice. n_s denotes the order of symmetry axis of the shape.

Anisotropy is introduced by positing unequal rates for deposition of objects in the three possible directions. The choice of the horizontal direction occurs with probability p and for each of the other two directions with probability $(1 - p)/2$. Hence, the value of $p = 1/3$ corresponds to the isotropic case. We randomly pick one of the six possible orientations with a corresponding probability, start the l -step walk in that direction, and search whether all successive l sites are unoccupied. If so, we occupy these $l + 1$ sites and deposit the object; otherwise, the deposition attempt is rejected.

The Monte Carlo simulations are performed on a 2D triangular lattice of size $L = 128$. The time is counted by the number of attempts to select a lattice site and scaled by the total number of lattice sites. Periodic boundary conditions are used in all directions. The data are averaged over 1000 independent runs for each depositing object. The finite-size effects, which are generally weak, can be neglected for object sizes $< L/8$.

Results and discussion

We study the anisotropic irreversible deposition of objects of various shapes (Table I). In the case of isotropic deposition ($p = 1/3$), according to parameter σ (Eq.(1)), all extended shapes can be divided into four groups:

- (a) Shapes with asymmetry axis of first order, $n_s = 1$, with $\sigma \simeq 5.9$
- (b) Shapes with a symmetry axis of second order, $n_s = 2$, with $\sigma \simeq 3.0$
- (c) Shapes with a symmetry axis of third order, $n_s = 3$, with $\sigma \simeq 2.0$
- (d) Shapes with a symmetry axis of sixth order, $n_s = 6$, with $\sigma \simeq 0.99$.

This means that at late enough times, the rotational symmetries associated with specific shapes have a substantial influence on the adsorption rate of the objects. More symmetric shapes reach their jamming coverage faster; i.e., the relaxation time σ is smaller for more symmetric objects. At large times, adsorption events take place on the islands of unoccupied sites. The individual islands act as selective targets for specific deposition events. In other words, there is only a restricted number of possible orientations in which an object can reach

a vacant location, provided the location is small enough. For a shape of a higher order of symmetry n_s , there is a greater number of possible orientations for deposition into a selective target on the lattice. Hence, the increase of the order of symmetry of the shape enhances the rate of single-particle adsorption. This is reflected in the fact that the adsorption of asymmetric shapes is slower than the adsorption of more regular and symmetric shapes.

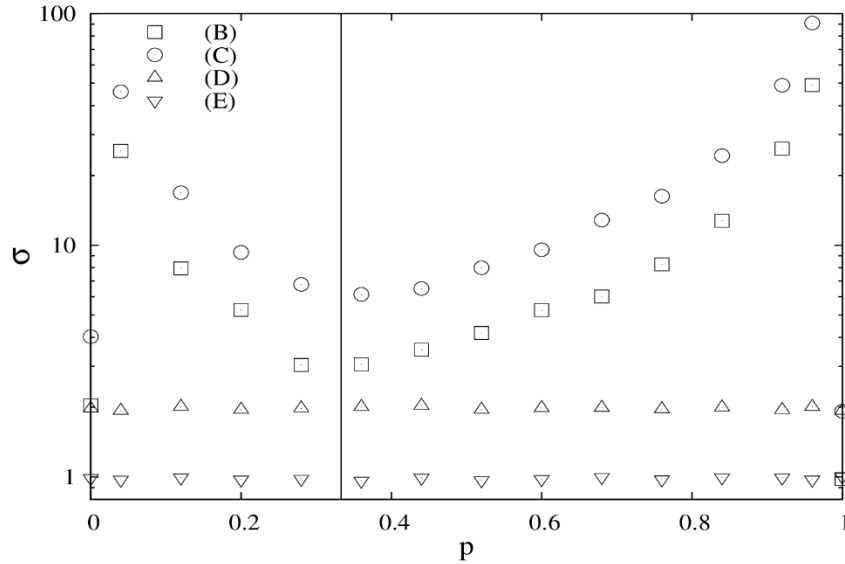


Figure 1. Dependence of the parameter σ [Eq. (1)] on probability p for shapes B, C, D, and E from Table I. The vertical line indicates the value of $p = 1/3$.

In the case of anisotropic deposition ($p \neq 1/3$), for all investigated shapes and all probabilities of adsorption in a horizontal direction, plots of $\ln[\theta_{jam} - \theta(t)]$ versus t are straight lines in the late times of the process. Analyzing the results for a large number of various shapes, we can see that the kinetics of anisotropic deposition is determined mainly by the symmetry properties of the object. For objects B, C, D and E (Table I), dependence of the parameter σ on the probability p is given in Fig. 1. For the k-mer B covering three lattice sites and for the angled object C, rapidity of the approach to the jamming limit is affected by the presence of anisotropy. The dependence of the parameter σ on the probability p is more prominent for the less symmetric object C. For the values of p close to zero, the deposition process is very slow. The relaxation time σ decreases with p , reaches a minimum for the isotropic case, and increases for higher values of p . For the less symmetric object C, $\sigma \simeq 4.0$ for $p = 0$, and $\sigma \simeq 2.0$ for $p = 1$. For $p = 1/3$, the expected result that $\sigma \simeq 6.0$ is obtained. Values of σ for the objects with symmetry axis of first order are twice higher than the corresponding values for the objects with symmetry axis of second order for each value of the probability p . Deposition of the objects with symmetry axis of third and sixth order is not affected by the presence of anisotropy. No matter what the value of the probability p is, $\sigma \simeq 2.0$ for the objects with symmetry axis of third order, and $\sigma \simeq 1.0$ for the objects with symmetry axis of sixth order.

As one can see from Fig. 2, the jamming coverage depends on the probability p for the shapes with symmetry axis of first and second order. On the contrary, for the objects with symmetry axis of third and sixth order, the values of θ_{jam} do not depend on p , and the isotropic values of

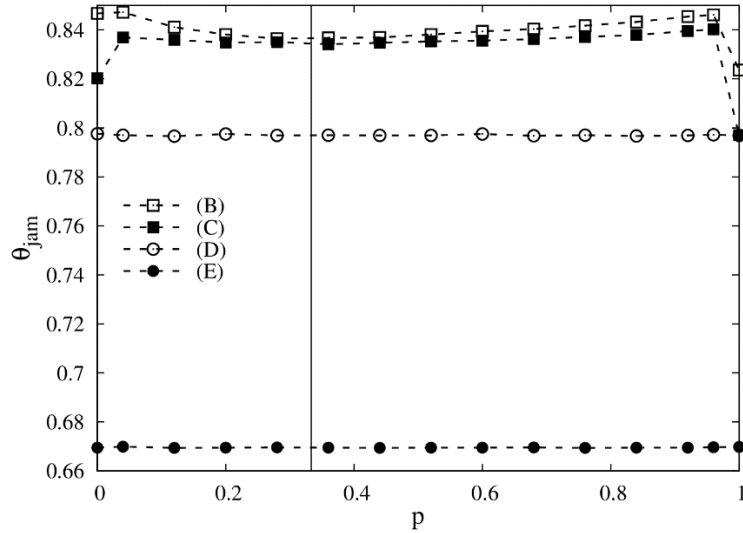


Figure 2. Dependence of the jamming coverage θ_{jam} on probability p for shapes B, C, D, and E from Table I. The vertical line indicates the value of $p = 1/3$.

jamming coverages are obtained [6]. At very early times of the process the depositing objects do not “feel” the presence of the already deposited ones and are placed randomly on to the lattice. However, in the late stages of deposition the objects must fit into small empty regions that favors the formation of clusters. Line segments and angled shapes deposited in the late stages of deposition must deposit parallel to the already deposited ones in order to avoid an intersection. This is reflected in the relatively high local packing of nearly parallel adsorbed objects in the vicinity of given object in the case of line segments and angled objects as compared to the triangles and hexagons. Such a different object view is the cause of the enhanced growth of very compact domains in the case of elongated shapes as compared to those in the case of more round (symmetric) shapes, resulting in a higher value of the jamming coverage fraction in the former case.

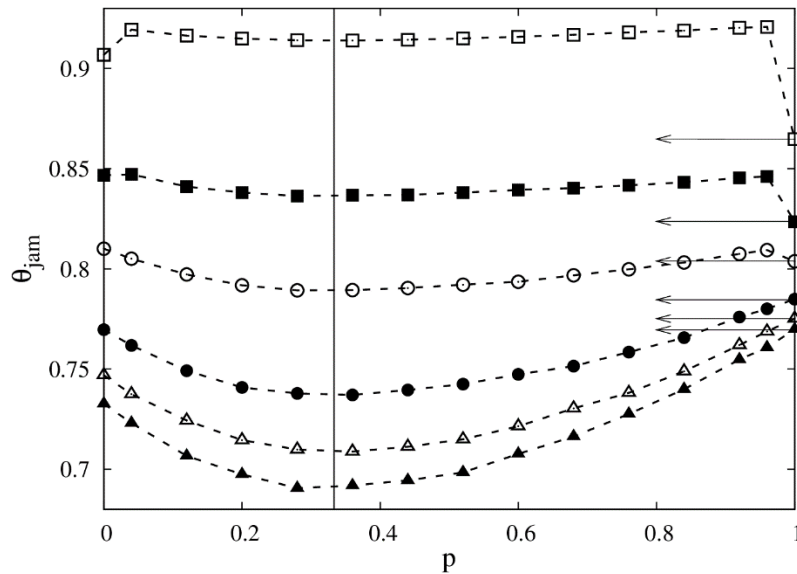


Figure 3. Dependence of the jamming coverage θ_{jam} on probability p for various k -mers.

The curves from top to bottom correspond to increasing values of $k = 2, 3, 4, 6, 8, 10$. The vertical line indicates the value of $p = 1/3$.

We also study the anisotropic RSA of k -mers. The simulations have been performed for line segments of lengths $l = 1, 2, \dots, 10$. For all investigated k -mers and for all probabilities p of

deposition in horizontal direction, plots of $\ln[\theta_{jam} - \theta(t)]$ versus t are straight lines for the late stages of deposition. Jamming coverage θ_{jam} also depends on the degree of anisotropy. From Fig.3 we can see that this dependence differs for k -mers of various lengths. For all objects, the jamming coverage θ_{jam} exhibits a local minimum near $p = 1/3$, i.e., for isotropic condition. For $k \geq 4$ this minimum is lower than the value of jamming coverage for deposition of k -mers in one dimension. However, the most striking feature is that a very small change in the probability p away from 0 or 1 brings an abrupt jump in the value of the jamming coverage θ_{jam} for the k -mers of small length ($k \leq 3$); e.g., when p changes from 0.96 to 1, the value of θ_{jam} for dimers drops from 0.92 to 0.86. The jump near $p = 0$ is smaller in magnitude.

Conclusion

We have investigated numerically the effect of anisotropy on the RSA of extended objects on a planar triangular lattice. A systematic approach is made by using the objects of different number of segments and rotational symmetries.

It was shown that the growth of the coverage $\theta(t)$ to the jamming limit θ_{jam} occurs via the exponential law (1), for all the shapes considered and for all values of probability p of deposition in a preferential direction. The simulations have shown that the kinetics of anisotropic deposition is determined mainly by the symmetry properties of the object. In the case of elongated and asymmetrical shapes, the relaxation time σ is found to increase with the degree of anisotropy. However, for rounded and symmetrical shapes, rapidity of the approach to the jamming state is not affected by the presence of anisotropy. A similar qualitative behavior of the jamming limit θ_{jam} in anisotropic condition is obtained; for highly symmetric objects, no dependence of the jamming coverage θ_{jam} on the probability p is observed within the statistical uncertainties. Nevertheless, the jamming coverage depends on the probability p for the shapes with lower-order symmetry axis.

Acknowledgements

This work was supported by the Ministry of Science of the Republic of Serbia, under Grant No. ON171017.

References

- [1] V. Privman, ed., Nonequilibrium Statistical Mechanics in One Dimension (Cambridge University Press, Cambridge, UK, 1997) (a collection of review articles).
- [2] V. Privman, ed., Colloids Surf. A 165, 1 (2000) (a collection of review articles).
- [3] J. W. Evans, Rev. Mod. Phys. 65, 1281 (1993).
- [4] Lj. Budinski-Petković and U. Kozmidis-Luburić, Phys. Rev. E 56, 6904 (1997).
- [5] Lj. Budinski-Petković, S. B. Vrhovac, and I. Lončarević, Phys. Rev. E 78, 061603 (2008).
- [6] I. Lončarević, Lj. Budinski-Petković, and S. B. Vrhovac, Eur. Phys. J. E24, 19 (2007).

THE ENERGETIC POTENTIAL OF THE URBAN AREAS FOR THE THERMO PHOTOVOLTAIC REGENERATIVE HYBRID SOLAR SYSTEMS

Corina Macarie, Ionel Balcu, Bogdan Taranu

*National Institute for Research and Development in Electrochemistry and Condensed Matter,
144 Dr. A. Paunescu Podeanu, 300569, Timisoara, Romania, Tel.: +40 256 222119
e-mail address: mac_cora@yahoo.com*

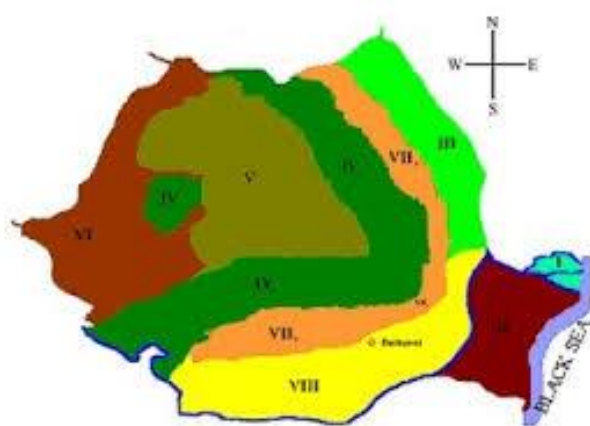
Abstract

Energetic potential of urban zones

The implementation of an energy strategy for exploiting *the* potential of renewable energy sources (SRE) is part of the coordinates of Romania's energy development in the medium and long term and offers the appropriate framework for making decisions regarding the energy alternatives[1].

Renewable sources have significant energy potential and offer unlimited availability for use locally and nationally. These ensure increased security in energy supply and limit the import of energy resources, under the conditions of sustainable economic development. The requirements are realized in the national context, through the implementation of policies of conservation of energy, the increase of the energy efficiency and by the superior valorisation of the renewable sources[2].

The following figure shows the distribution of renewable energy sources in eight geographical territories of Romania: the Danube Delta, Dobrogea, Moldova, the Carpathians, the Transylvanian Plateau, the Western Plains, the Subcarpathians and the Roman Plains:



- I- Danube Delta (solar energy);
- II- Dobrogea (solar energy, wind energy);
- III- Moldova (plateau plains: micro-hydro, wind energy, biomass);
- IV- Carpathians (IV1- Eastern Carpathians; IV2- South Carpathians; IV3- Western Carpathians, high potential in biomass, wind micro-hydrosis);
- V- Transylvania Plateau (high potential for micro-hydro and biomass);
- VI- Western Plain (high potential for geothermal and wind energy);
- VII- Subcarpathians (VII1- Geticisubcarpathians; VII2- Curvature subcarpathians; VII3- Moldovan subcarpathians: potential for biomass, micro-hydro);
- VIII- Southern Plain (biomass, geothermal energy, solar energy).

Territorial distribution of renewable resources

Recoverable hybrid solar systems

Hybrid solar systems allow the storage of excess solar energy during the day, and at night, on cloudy days or when there is a power outage in the grid, or the automatic use of energy stored in batteries.

Photovoltaic systems have a number of advantages over conventional systems for electricity production. Among the most important features of a photovoltaic system are energy independence, modularity, operating safety, reliability and lastly the free fuel (the sun)[3,4].

Thermophotovoltaic technology is based on the conversion of thermal radiation from a heat source into electricity using photovoltaic cells.

The major differences from the classical photovoltaic system are due to the small distances from the emitter source and the photovoltaic cells. Thus, the temperature of the emitting body can be much lower, and the transmitted power density is much higher. Thermal radiation contributes to the heating of photovoltaic cells by conduction. In addition, due to heat losses not transformed into electricity, the cells are additionally heated[4].

Acknowledgements

This work was supported by a grant of the Romanian Ministry of Research and Innovation CCCDI-UEFISCDI, project number PN-III-P1-1.2-PCCDI-2017-0404 / 31PCCDI/2018, within PNCDI III

References

- [1] http://www.minind.ro/domenii_sectoare/energie/studii/potential_energetic.pdf
- [2] http://mmediu.ro/new/wp-content/uploads/2014/01/2011-11-07_evaluate_impact_planuri_strategiaenergeticaactualizata2011.pdf
- [3] Mohammed Alghassab, Mohamed A. Zohdy, Modelling of a Residential Solar Energy Recuperation System Setup Open Journal of Energy Efficiency, 2016, 5, 135-147 <http://www.scirp.org/journal/ojee> ISSN Online: 2169-2645 ISSN Print: 2169-2637
- [4] <http://www.rasfoiesc.com/inginerie/electronica/MODELAREA-UNEI-CELULE-TERMOFOT74.php>

ENVIRONMENTAL SUSTAINABILITY OF MARGINAL SOILS BY MISCANTHUS CULTIVATION: A REVIEW

Jelena Maksimović¹, Zoran Dinić¹, Radmila Pivić¹, Aleksandra Stanojković-Sebić¹,
Željko Dželetović², Milena Mladenović Glamočlija³, Đorđe Glamočlija⁴

¹*Institute of Soil Science, Belgrade, Serbia*

²*Institute for Application of Nuclear Energy (INEP), Belgrade, Serbia*

³*Institute for Science Application in Agriculture (IPN), Belgrade, Serbia*

⁴*University of Belgrade, Faculty of Agriculture, Belgrade, Serbia*

Corresponding author e-mail: jelena.maks@yahoo.com; jelena.maksimovic@soilinst.rs

ABSTRACT

The paper discusses the possibilities of cultivating and using bioenergy crop in order to reduce climate change and protect the environment. Miscanthus is a perennial plant which annually produces great biomass of good quality and calorific value for energy. In addition to obtaining the second generation of fuel from its biomass, a new chemical conversion technique produces a product whose application can improve the quality of marginal soils. Based on the reviewed results, it was concluded that on marginal soils it is possible to plant the miscanthus seedlings and achieve expected yields. The Republic of Serbia has a large area of soil that could be used for this purpose, so it is recommended that additional research can be conducted to investigate the potential use of biochar in repairing this type of soil.

INTRODUCTION

Cultivation conditions

It originates from an area of temperate continental climate and the successful growth and development of plants require heat and large amounts of water. It uses absorbed water more efficiently than most arable crops, but under unfavorable water conditions, plant growth is limited, especially in the year of establishment. In the initial years, apart from optimal water supply, nitrogen nutrition has a major impact on biomass yield [1]. Irrigation of crops also increases the effect of the nitrogen nutrients used. Well formed plantation in the years of commercial exploitation has a strong deep-rooted root system and can absorb water accumulated in deeper soil horizons/layers.

Frost tolerance is also a cultivar trait, so that the newly introduced interspecies *Miscanthus x giganteus* hybrids tolerate winter frosts and cold weather in the spring better than native varieties and populations originating in the Far East [3].

Miscanthus grows and yields satisfactory yields on soils of various properties, from sand to soils with a high organic content [4, 5]. This energy crop can be grown under different agro-ecological conditions, but the value of biomass yield is greatly influenced by weathering during the growing season [6].

Production technology

As a perennial plantation, miscanthus is grown outside the crop rotation, and once planted it is used for 15-20 years. All agrotechnics can be performed by standard agricultural machinery [1]. The surface on which the planting is to be done should be prepared as for other agricultural crops. Plants use the nutrients very rationally by moving assimilants from the

underground to the aboveground organs during the growing season and returning them to the rhizomes before winter. Planting can be done in mid-April, when the danger of spring frosts passes, or in October. Planting requires 10,000-20,000 rhizomes per hectare [7]. In early years, a greater number of plants per unit area has the advantage of facilitating weed control [8]. Depending on the way of use, the biomass harvest using forage harvester is in period when the plants have reached the maximum height - at the end of August and the first half of September (for biodiesel or bioethanol) or during the winter when the miscanthus trees have the least water (for solid fuel) [9].

From the second year, the yield increased significantly, reaching its highest value after the third year. In the years of maximum production, over 100 t ha⁻¹ of fresh biomass (trees and leaves) and 15-25 t ha⁻¹ of dry trees can be obtained, and in very favorable weather conditions, or with irrigation, over 30 t ha⁻¹ can be obtained, with about 30% of water.

The transition to renewable energy and rehabilitation of degraded soils have been a topic of great interest in recent decades, thus for these purposes can serve plant species that have high annual biomass production, resistant to biotic and abiotic stress and require minimal investment in agrotechnics [7].

The cultivation of miscanthus on fertile soil is an irrational use of the potential of such a resource. To avoid conflict over the choice of plant species to use the most fertile soil between the needs for food production or for bioenergy production, it is recommended that marginal soils should be used for bioenergy crops. The marginal soils are usually described as unproductive or unsuitable for crop production due to poor soil properties, poor groundwater quality, drought, undesired topology, unfavorable climatic conditions, usually having no or little potential for profitability for conventional food crops [10]. Also, marginal soils include brownfields, previously contaminated soils, fallow agricultural soils due to unfavorable crop production conditions, degraded soils, or landfills [10]. The total area of arable and arable soils on the territory of the Republic of Serbia that could be suitable for cultivation of bioenergy crops is 2,462,529 ha [11].

PREVIOUS RESULTS AND DISCUSSION

Soil quality, organic matter concentration, and organism diversity are enhanced by growing miscanthus in contaminated and marginal soils [12]. The same authors point out that miscanthus has potential to stabilize and possibly remove metal contaminants slowly over time while being grown for its energy value. The effect of different doses and types of fertilizers on the yield of miscanthus cultivated on soils with limited production capacity (marginal soils) has been examined [13]. The results of the survey did not show a statistically significant impact of the applied fertilizers and the average yield in the year after planting was in the range 2.1-2.7 t ha⁻¹. Adverse climatic factors during the planting period and soil type resulted in low yields. Miscanthus cultivation is possible on marginal soils such as gleysols, planosols and technosols, with minimum application of agricultural measures only during the year of establishment. Due to favourable water conditions, gleysols may be recommended for miscanthus production [14].

A satisfactory average biomass yield (5.78 t ha⁻¹) was achieved on deposols with a significant difference between years [7]. Other authors also stated the possibility of establishing miscanthus and phytostabilization of ash and slag landfills, as the technogenic substrate extremely unfavorable for plant growth, by using this species [15]. Improved ecosystem services and low production costs justify lower miscanthus biomass yields in marginal agricultural sites [16].

Miscanthus use

Miscanthus represents a key candidate energy crop for use in biomass-to-liquid fuel-conversion processes and biorefineries to produce a range of liquid fuels and chemicals [17]. Miscanthus biomass application is primarily related to the production of second generation biofuels. An analysis of the biomass of miscanthus cultivated in the territory of Republic of Serbia yielded calorific values from 14.9 MJ kg⁻¹ to 18.3 MJ kg⁻¹, indicating that it is promising to introduce biomass of miscanthus as a renewable energy source [18, 19].

Using various thermochemical processes it possible to obtain a range of products that can also be used in agriculture. One of these products is biochar. Pyrochar and hydrochar differ in their physicochemical characteristics depending on the production process and the feedstock [20, 21]. Miscanthus can be a good raw material for biochar production because of the high yield and energy it generates at generally low investment requirements. Miscanthus biomass at harvest time is low in moisture content, which also reduces the cost of char production [20].

Promising results are shown by a relatively new process called hydrothermal carbonization (HTC) of biomass, where biomass is treated with hot compressed water instead of drying [19, 20]. The HTC process offers several advantages over conventional dry-thermal pre-treatments like slow-pyrolysis in terms of improvements in the process performances and economic efficiency, especially its ability to process wet feedstock without pre-drying requirement [20]. Hydrothermal carbonization in the temperature range from 180 to 220°C for 60 minutes is effective for obtaining miscanthus hydrochar. In terms of chemical and fuel properties, the hydrochar obtained at 220°C was the best demonstrated [22].

The use of biochar in agricultural practice to improve soil properties has shown a number of positive effects on water and nutrient retention capacity, reduction of volatilization of nitrous oxides, leaching of nitrates from soil, efficiency of applied fertilizers and productivity of cultivated plants [23]. It also has carbon sequestration capability [20], which contributes to the reduction of greenhouse gas emissions. The use of biochar in combination with phytoremediation techniques is a challenge for future research, since their interaction has the potential to remediate the soil contaminated with heavy metals [24]. *Miscanthus x giganteus* hybrid has the potential for both techniques (biochar feedstock and plant for phytoremediation).

CONCLUSION

Miscanthus cultivated on marginal soils does not compete for food production. According to the aforementioned data, the Republic of Serbia has sufficient land area that could be used for the cultivation of energy crops for the production of second generation biofuels. In addition to the positive impact of miscanthus cultivation on the soil condition and quality, using relatively new biomass processing technologies for this energy species the products of an exceptional importance are obtained, and they can, on the other hand, enhance the quality of marginal soils. The lower productivity of miscanthus on marginal soils is offset by improvements in the entire ecosystem and low production costs. In Serbia, commercial cultivation of miscanthus is represented on small areas, and the results presented in the paper on the yield of miscanthus are a part of the research that examined the possibility of its production on marginal soils.

The results presented refer to the first years after rhizomes planting on soil with poor properties, which has longer planting time compared to planting on fertile soil. It is to be expected that they will be higher and justify the investment over many years of plantation life, but what is more important is the fact that even in extremely unfavorable soil conditions the establishment of this bioenergy crop is possible. It is necessary to continue with this type of

research before reaching concrete conclusions and proposals for commercial cultivation, since in addition to the type of soil, weather conditions, that are very unstable in recent years, have an extreme impact. It would be environmentally and economically justifiable to invest in research which would include the use of biochar for the purpose of rehabilitation and reclamation of an agricultural soil, since previous research has shown that such a technique has the potential.

ACKNOWLEDGEMENTS

This research work was carried out with the financial support of Ministry of Education, Science and Technological Development of the Republic of Serbia, project TR 31018 and TR 37006.

REFERENCES

- [1] Ž. Dželetović, Uticaj azota i gustine zasada na morfološke osobine i prinos biomase vrste *Miscanthus x giganteus* Greef et Deu. Doktorska disertacija. Poljoprivredni fakultet, Zemun, 2010, str.122.
- [2] H.W. Zub, M. Brancourt-Hulmel, Agronomic and physiological performances of different species of *Miscanthus* energy crop, in: E. Lichtfouse, M. Hamelin, M. Navarrete, P. Debaeke (Eds.), Sustainable Agriculture, Volume 2. Springer, Dordrecht, Heidelberg, London, New York, 2011, pp. 987. doi:10.1007/978-94-007-0394-0.
- [3] A. D. Farrell, A. C. Clifton-Brown, I. Lewandowski, M. B. Jones, Genotypic variation in cold tolerance influences the yield of *Miscanthus*. *Annals of Applied Biology*. 149(3) (2006) 337-345. doi.org/10.1111/j.1744-7348.2006.00099.x.
- [4] Đ. Glamočlija, O. Laganin, Ž. Dželetović, S. Oljača, Mogućnosti iskorišćenja zemljišta Republike Srpske za gajenje novih bioenergetskih usjeva. *Agroznanje*. 9(2) (2008) 23-33.
- [5] Ž. Dželetović, J. Maksimović, I. Živanović, Yield of *Miscanthus* × *giganteus* during crop establishment at two locations in Serbia. *Journal on Processing and Energy in Agriculture*. 18(2) (2014) 62-64.
- [6] Đ. Glamočlija, N. Đurić, M. Spasić, The influence of agro-ecological conditions on the production properties of miscanthus. *Proceedings 8th International Symposium On Natural Resources Managment, Megatrend University, Faculty of Managment, Zaječar, Serbia, (2018) 173-178. ISBN 978-867747-590-1.*
- [7] J. Ikanović, V. Popović, S. Janković, S. Rakić, G. Dražić, Lj. Živanović, Lj. Kolarić, Ž. Lakić, *Miscanthus* biomass production growth on degraded land. *Radovi sa XXIX savetovanja agronoma, veterinara, tehnologa i agroekonomista*. 21(1-2) (2015) 115-124.
- [8] J. Maksimović, R. Pivić, A. Stanojković-Sebić, M. Vučić-Kišgeci, B. Kresović, Z. Dinić, Đ. Glamočlija, Planting density impact on weed infestation and the yield of *Miscanthus* grown on two soil types. *Plant, Soil and Environment*. 62(8) (2016) 384-388.
- [9] Ž. Dželetović, N. Mihailović, Đ. Glamočlija, G. Dražić, S. Đorđević, M. Milovanović, Žetva i skladištenje *Miscanthus*×*giganteus* Greef et Deu. *Poljoprivredna tehnika*. 34(3) (2009), 9-16.
- [10] M. A. Mehmood, M. Ibrahim, U. Rashid, M. Nawaz, S. Ali, A. Hussain, M. Gull, Biomass production for bioenergy using marginal lands. *Sustainable Production and Consumption*. (9) (2017) 3–21. doi:10.1016/j.spc.2016.08.003.
- [11] Z. Knežević, Mogućnosti za uzgajanje brzorastućih energetskih zasada sa aspekta raspoloživosti poljoprivrednog zemljišta u Republici Srbiji. *UNDP Srbija, Beograd, 2017, pp. 208.*

- [12] V. Pidlisnyuk, T. Stefanovska, E. E. Lewis, L. E. Erickson, L. C. Davis, *Miscanthus* as a Productive Biofuel Crop for Phytoremediation. *Critical Reviews in Plant Sciences*. 33(1) (2014) 1–19. doi:10.1080/07352689.2014.847616.
- [13] J. Maksimović, Ž. Dželetović, Z. Dinić, A. Stanojković-Sebić, O. Cvetković, R. Pivić, Assessment of the Main Agro-ecological Parameters Effects on the Cultivation of *Miscanthus x giganteus* Grown on Marginal Soils in the Republic of Serbia. *Agriculturae Conspectus Scientificus*. 83(1) (2018) 113–117.
- [14] G. Dražić, J. Milovanović, J. Ikanović, I. Petrić, Influence of fertilization on *Miscanthus x giganteus* (Greef et Deu) yield and biomass traits in three experiments in Serbia. *Plant, Soil and Environment*. 63(4) (2017) 189–193.
- [15] Ž. Dželetović, I. Živanović, R. Pivić, A. Simić, G. Lazić, J. Maksimović, Reclamation possibilities of perennial rhizomatous grasses for degraded soil. In: *Melioracije 13 - proceedings*. (January 24th 2013., Novi Sad, Serbia). Novi Sad: Univerzitet u Novom Sadu - Poljoprivredni fakultet, (2013) 130–137.
- [16] M. Von Cossel, I. Lewandowski, B. Elbersen, I. Staritsky, M. Van Eupen, Y. Iqbal, S. Mantel, D. Scordia, G. Testa, S. L. Cosentino, O. Maliarenko, I. Eleftheriadis, F. Zanetti, A. Monti, D. Lazdina, S. Neimane, I. Lamy, L. Ciadamidaro, M. Sanz, J. E. Carrasco, P. Ciria, I. McCallum, L. M. Trindade, E. N. Van Loo, W. Elbersen, E. Alexopoulou, Marginal Agricultural Land Low-Input Systems for Biomass Production. *Energies*. 12(16) (2019) 3123. doi:10.3390/en12163123.
- [17] N. Brosse, A. Dufour, X. Meng, Q. Sun, A. Ragauskas, *Miscanthus*: a fast-growing crop for biofuels and chemicals production. *Biofuels, Bioproducts and Biorefining*. 6(5) (2012) 580–598. doi:10.1002/bbb.1353.
- [18] O. Cvetković, R. Pivić, Z. Dinić, J. Maksimović, S. Trifunović, Ž. Dželetović, Hemijska ispitivanja *Miscanthus* gajenog u Srbiji - potencijalni obnovljiv izvor energije. *Zaštita materijala*. 57(3) (2016) 412–417. doi: 10.5937/ZasMat1603412C.
- [19] M. Mihajlović, J. Petrović, M. Stojanović, J. Milojković, Z. Lopičić, M. Koprivica, Č. Lačnjevac, Hydrochars, perspective adsorbents of heavy metals: - A review of the current state of studies. *Zastita Materijala*. 57(3) (2016) 488 – 495.
- [20] H. S. Kambo, A. Dutta, A comparative review of biochar and hydrochar in terms of production, physico-chemical properties and applications. *Renewable and Sustainable Energy Reviews*. (45) (2015) 359–378. doi:10.1016/j.rser.2015.01.050
- [21] M. Gronwald, M. Helfrich, A. Don, R. Fuß, R. Well, H. Flessa, Application of hydrochar and pyrochar to manure is not effective for mitigation of ammonia emissions from cattle slurry and poultry manure. *Biology and Fertility of Soils*. 54(4) (2018) 451–465. doi:10.1007/s00374-018-1273-x.
- [22] M. Mihajlović, J. Petrović, S. Maletić, M. K. Isakovski, M. Stojanović, Z. Lopičić, S. Trifunović, Hydrothermal carbonization of *Miscanthus x giganteus*: Structural and fuel properties of hydrochars and organic profile with the ecotoxicological assessment of the liquid phase. *Energy Conversion and Management*. (159) (2018) 254–263. doi:10.1016/j.enconman.2018.01.003.
- [23] I. Bargmann, M. C. Rillig, A. Kruse, J.-M. Greff, M. Kücke, Effects of hydrochar application on the dynamics of soluble nitrogen in soils and on plant availability. *Journal of Plant Nutrition and Soil Science*. 177(1) (2013) 48–58. doi:10.1002/jpln.201300069.
- [24] J. Paz-Ferreiro, H. Lu, S. Fu, A. Méndez, G. Gascó, Use of phytoremediation and biochar to remediate heavy metal polluted soils: a review. *Solid Earth*. 5(1) (2014) 65–75. doi:10.5194/se-5-65-2014.

THE STUDY OF SOME ELECTRICAL PROPERTIES OF Cu_2O COMPOUND BY *AB-INITIO* METHODS

Marinela Miclau, Daniel Ursu, Vajda Melinda, Liviu Mocanu*

National Institute for Research and Development in Electrochemistry and Condensed Matter,
Timisoara, PlautiusAndronescu Str. No. 1, RO-300224, Timisoara, Romania

*Corresponding author: mocanuliv@gmail.com

The cuprous oxide (Cu_2O) it is evidenced by high stability, natural abundance, non-toxicity, low production costs and remarkable electrical properties. All this makes possible a wide range of applications like gas sensor, catalyst, negative electrode for lithium batteries and solar cells. Considering the design of Cu_2O -based materials with improved electrical properties, a useful tool in this endeavor consists of a theoretical study based on *ab-initio* methods, possibly due to the development of specialized packages on quanto-chemical calculations. A first stage consists in determining the calculation parameters for the original structures, a kind of calibration of them. So it is necessary to calculate the basic properties- such as the band structure, respectively the density of states of the original material.

Keywords: cuprous oxide, band structure, density of states.

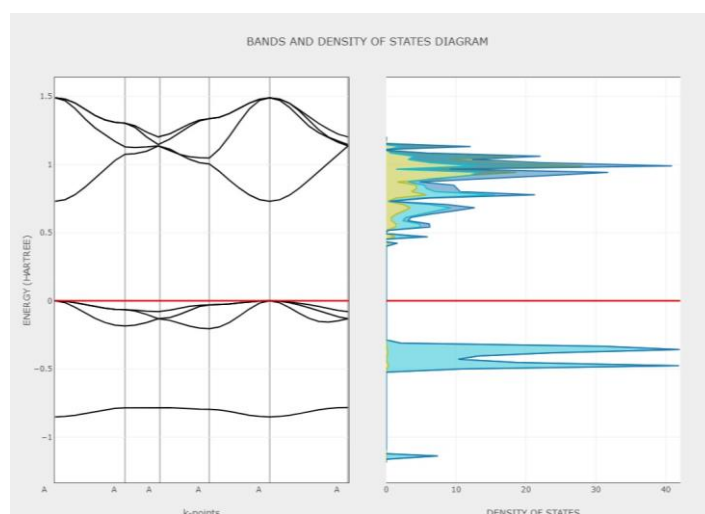


Fig.1 Band structure and density of states of Cu_2O

References

1. N-Type Conductivity of Cu_2O thin film prepared in basic aqueous solution under hydrothermal conditions. Daniel Ursu, Nicolae Miclau, Marinela Miclau Electronic Materials Letters (2018) 14, 405-412
2. Investigation of the p-type dye-sensitized solar cell based on full Cu_2O electrodes. Daniel Ursu, Melinda Vajda, Marinela Miclau. Journal of Alloys and Compounds 802 (2019) 86-92.
3. First principle investigation of hydrogen behavior in M doped Cu_2O (M= Na, Li and Ti)
A.Larabi. A. Mahmoudi, M.Mebarki, M.Dergal. Condensed Matter Physics , 2019, vol.22, No.2 23702:1-11.

HAZARDOUS WASTE MANAGMENT– PESTICIDE CONTAINER MANAGEMENT PROBLEM AND SOLUTIONS

Višnja Mihajlović¹, Una Marčeta¹, Bogdana Vujić¹, Jelena Mičić¹

¹ *University of Novi Sad, Technical Faculty Mihajlo Pupin, Department of Environmental Engineering, Djure Djakovica nn, Zrenjanin, Serbia e-mail: visnjamihajlovic@uns.ac.rs*

ABSTRACT

Use of pesticide increased every year, which in turn increase the quantity of pesticide containers. Pesticide containers, if are not managed properly, pose a risk for environment and health. In developed countries, system for pesticide container management are developed, and environmental impact of pesticide containers is reduced. However, developing and less developed countries are still struggling to develop system for pesticide container management. The aim of this paper is to analyze the current container system management in Serbia and identify the barriers and obstacles for development of sustainable pesticide container management.

INTRODUCTION

The problem of modern society is increasingly emphasized in providing sufficient quantities of food, the main source of which is the plant. Achieving high yields cannot be imagined without the use of mineral fertilizers and pesticides to control diseases, pests and weeds. Plant protection products play an important role in achieving higher yields and improving the quality of agricultural products. [1] Pests threaten cultivated plants and food stuffs by reducing plant fertility by 15 - 20% in developed countries and over 40% in underdeveloped countries [2]. Therefore, the use of agrochemicals is a necessity, but it occupies a special place in the environmental impact of agriculture due to numerous environmental problems in case of irrational use of these agents. [3]. Together with the plant protection products, the packaging also becomes available on the market, which becomes a waste after the use of the plant protection products. Packaging plays an important role in the safe delivery and use of plant protection products in the markets, minimizing the risk of loss in the supply chain as well as customer exposure. [1]

The main objective is that waste packaging contains minimal concentrations of the active substance and that it is harmless to human health and the environment, while on the other hand the economic impact is undeniable. [4] Solving the problem of packaging waste from plant protection products in Serbia has many obstacles, and the lack of experience in this field requires that we be informed as much as possible about the waste management system in EU Member States.

METHODOLOGY

In order to establish and operate a plant protection management system that ensures a high level of human health protection (for both users and consumers of agricultural products) and the environment (including flora and fauna), the following regulations apply in the European Union.

- Regulation (EC) No 1107/2009 - concerning the placing of plant protection products on the market and repealing Council Directives 79/117/EEC and 91/414/EEC [5],
- Regulation EU 540/2011 - list of approved active substances [6],

- Regulation EU 546/2011 - defines uniform principles for evaluation and authorization of plant protection products [7]
- Regulation EU 547/2011 - labelling requirements for plant protection products [8]
- Regulation EU 283/2013 - setting out the data requirements for active substances, [9]
- Regulation EU 284/2013 - setting out the data requirements for plant protection products [10]
- REGULATION (EC) No 396/2005 - define maximum residue levels of pesticides in or on food and feed of plant and animal origin [11]
- DIRECTIVE 2009/128/EC - framework for Community action to achieve the sustainable use of pesticides [12]
- DIRECTIVE 2009/127/EC - use of machinery for pesticide application [13]

These regulations include provisions on the placing on the market of plant protection products, the approval of active substances and the registration of plant protection products containing authorized substances, and contain restrictions on the maximum levels of residues of plant protection products in agricultural products, as well as proper storage and use.

The overall process involves two steps: first, the assessment and possible approval of the active substance at EU level, and then the assessment and approval by Member States of the plant protection products containing those substances. Implementation of mentioned regulations and Directives gives the framework for development of sustainable system for pesticide container management.

RESULTS AND DISCUSSION

Today, after a great experience in seeking to bring the hazardous waste system as closely as possible to high environmental requirements, additional options for hazardous waste management have been developed related to the advancement of technologies that generate less waste, substitution of hazardous substances with less hazardous waste, recycling and reuse existing hazardous waste and the like. This situation has resulted in the establishment of new technological standards, whose further improvements are measured by extremely short time intervals, and further progress in this area is inevitable. However, there is still different classification of pesticide containers after use across EU, Table 1.

Table 1: Classification of decontaminated (washed) packaging waste from plant protection products in Europe

Country	Classification of decontaminated (washed) packaging waste from plant protection products
Austria	Data are not available
Belgium	Non-hazardous waste
Bulgaria	Data are not available
Croatia	Hazardous waste
Cyprus	Data are not available
Czech Republic	Data are not available
Denmark	Non-hazardous waste
Estonia	Non-hazardous waste
Finland	Hazardous waste
France	If it is in accordance with the obligatory management program - non-hazardous, otherwise hazardous
Germany	Nonhazardous
Greece	Nonhazardous
Hungary	If it is in accordance with the obligatory management program - non-hazardous, otherwise hazardous
Ireland	Different classification at regional level
Italy	Non-hazardous
Latvia	Data are not available
Lithuania	Nonhazardous
Luxemburg	Nonhazardous
Malta	Data are not available
Netherland	Nonhazardous
Polska	Hazardous waste
Portugalia	Hazardous waste
Romania	Hazardous waste
Slovakia	Hazardous waste
Slovenia	Nonhazardous waste
Spain	Hazardous waste
Sweden	Data are not available
Turkey	Hazardous waste
United Kingdom	Nonhazardous waste

Table 1 shows a different approach to the classification of flushed waste packaging within the EU, with at least a third of countries classifying this packaging as hazardous. In some

countries it was not possible to access the data because this issue had not yet been addressed by the competent institutions. This level of inconsistency across Europe has major current and future implications for the PPP packaging collection and reuse program. [14].

Across the EU, there are two models for managing this type of waste: voluntary and mandatory.

A voluntary system model is a voluntary agreement model, that is, a model whereby a system is formed by polluters without a legal obligation or pressure from the authorities to do so.

Operators authorized by law are those operating within the scope of national legislation.

A sustainable system for collecting pesticide packaging waste is only feasible if funding is provided. This is most easily achieved when the operator is legally authorized.

Generally, as it is mandatory to register and authorize a preparation, so it is also mandatory to participate in the packaging waste collection system, to be a member of the operator.

The threat of statutory operators being set up by the state is often enough to establish a system on a voluntary basis.

Statutory certified dispatchers can specify the level of service they offer to their clients. A system that makes it easy to return empty packaging will be significantly more efficient.

The system must be economically independent if it is to be sustainable. Authorized operators are required by the government to determine how the system wants to be funded:

- Compensation to suppliers;
- Pesticide sales tax;
- General fee.

CONCLUSION

Creating an adequate model of packaging waste management is the first step in the process of setting up a system for removing packaging plant protection products.

The second and perhaps most important step is the proper flushing of waste packaging, which would make it possible to classify such packaging as non-hazardous waste according to the classification.

Solving the problem of hazardous packaging waste from plant protection products in Serbia faces a number of obstacles such as: lack of adequate storage, lack of export license company, lack of cement plant with adequate equipment and permit for destruction and many others. SECPA is working on establishing an efficient packaging waste management system and proposes a sustainable and efficient model of packaging waste management modeled on the German PAMIRA packaging waste management and waste management system.

REFERENCES

1. SECPA (2014) Serbian Crop Protection Association, Pesticide container management, Available at <http://www.secpa.rs/index.php/teme-i-dogadaji/zbrinjavanje-ambalaznog-otpada>
2. Sedlar A, Bugarin R, Đukić N. (2014) Pesticide application, Novi Sad.
3. Lješević M, Aleksić J, Spasić S. (2011) Applied ecology. The European Union's Under Strengthening Serbia-EU Civil Society Dialogue Project programme. UNECO.
4. Huyghebaert B, Mostade O, Sawa J. (2004) Management of empty pesticides containers. TEKA. Commission of motorization and power industry in agriculture 3: 117-126.
5. REGULATION (EC) No 1107/2009 OF THE EUROPEAN PARLIAMENT AND OF THE COUNCIL of 21 October 2009 concerning the placing of plant protection products on the market and repealing Council Directives 79/117/EEC and 91/414/EEC

6. COMMISSION IMPLEMENTING REGULATION (EU) No 540/2011 of 25 May 2011 implementing Regulation (EC) No 1107/2009 of the European Parliament and of the Council as regards the list of approved active substances
7. COMMISSION REGULATION (EU) No 546/2011 of 10 June 2011 implementing Regulation (EC) No 1107/2009 of the European Parliament and of the Council as regards uniform principles for evaluation and authorisation of plant protection products
8. COMMISSION REGULATION (EU) No 547/2011 implementing Regulation (EC) No 1107/2009 of the European Parliament and of the Council as regards labelling requirements for plant protection products
9. COMMISSION REGULATION (EU) No 283/2013 of 1 March 2013 setting out the data requirements for active substances, in accordance with Regulation (EC) No 1107/2009 of the European Parliament and of the Council concerning the placing of plant protection products on the market
10. COMMISSION REGULATION (EU) No 284/2013 of 1 March 2013 setting out the data requirements for plant protection products, in accordance with Regulation (EC) No 1107/2009 of the European Parliament and of the Council concerning the placing of plant protection products on the market
11. REGULATION (EC) NO 396/2005 OF THE EUROPEAN PARLIAMENT AND OF THE COUNCIL of 23 February 2005 on maximum residue levels of pesticides in or on food and feed of plant and animal origin and amending Council Directive 91/414/EEC
12. DIRECTIVE 2009/128/EC OF THE EUROPEAN PARLIAMENT AND OF THE COUNCIL of 21 October 2009 establishing a framework for Community action to achieve the sustainable use of pesticides
13. DIRECTIVE 2009/127/EC OF THE EUROPEAN PARLIAMENT AND OF THE COUNCIL of 21 October 2009 amending Directive 2006/42/EC with regard to machinery for pesticide application
14. ECPA. 2007. Crop Protection Plastic Containers. The case for a nonhazardous waste classification. European Crop Protection Association.

FOOD PRODUCT DESIGN - CHOCOLATE FORMULAS WITH ADDITION OF BREWER'S YEAST POWDER

**Diana Moigradean, Despina-Maria Bordean, Liana-Maria Alda, Daniela Stoin,
Antoanela Lena Cozma, Dan Dorin Raican, Mariana-Atena Poiana***

Faculty of Food Engineering, Banat's University of Agricultural Sciences and Veterinary Medicine „King Michael I of Romania” from Timisoara, Calea Aradului 119, Timisoara, RO 300645, Romania

*corresponding author e-mail: atenapoiana@yahoo.com

Abstract

The purpose of this study was to use the beer yeast as a substitute for cocoa powder in the chocolate manufacturing recipe with high antioxidant properties. It is known that beer yeast is rich in high antioxidant compounds. To preserve these properties, the beer yeast has been conditioned at a moderate temperature (65°C) to ensure its stability. Then, chocolate formulas, simple and with addition of beer yeast powder in different percentages, was obtaining. The total antioxidant capacity was measured by FRAP assay and to assess the total polyphenol content was used the Folin–Ciocalteu method. By incorporating the beer yeast powder into the chocolate recipe, an increase in the total phenolic content and total antioxidant capacity has been recorded compared to the control sample. Therefore, the total polyphenol content vary from 2.71 mM GAE/100 g DM in the control sample to 6.05 mM GAE/100 g DM in the chocolate formula with 40% yeast. Based on the results obtained from this study, we can affirm that the beer yeast can be used as an ingredient with high added value for designing innovative food products; in this case the chocolate with a more intense taste and flavor.

Introduction

Chocolate is characterized as solid dispersion of cocoa mass, sugar, additives, cocoa butter, lecithin, and flavonoids and there may be variations between types [6].

Yeasts have a rich history and a bright future in biotechnology. Their involvement and importance in traditional food fermentations are unparalleled by other organisms of biotechnological relevance. Most yeast species are nonpathogenic to humans and animals and it is likely that yeasts will be increasingly used in traditional processes as their safety is more extensively established [5]. *Saccharomyces cerevisiae* is the principal yeast utilized in biotechnology worldwide, due largely to its unique physiology and associated key roles in many food fermentations and other industrial processes [10] including wine, beer, coffee and chocolate. During wine fermentation, each strain of yeast releases distinctive metabolites, which contribute to flavor and aroma. So it, the beer yeast utilization in chocolate manufacturing recipe changes the chocolate taste and smell [9].

Experimental

Beer yeast conditioning

Fresh beer yeast was taken from the Ursus Breweries brewery from Timisoara- Romania, being by-product of the primary fermentation of brewer's wort. The beer yeast was kept in refrigerated condition (4-5°C) for 12 hours after which, was dehydrated in the laboratory condition. The dehydration process was performed with Food Dehydrator by Heinner/Germany at the working temperature of 65°C for 12 hours and at the fin of this process the moisture of beer yeast was 5.83%. The initial moisture of beer yeast was 64.34% wet basis.

Obtaining chocolate formulas

It was obtained, in manufacturing condition, the simple chocolate (no added) – C (control sample) and the chocolate formulas with addition of beer yeast powder in different percentages: 10, 20, 30 and 40% of total cocoa weight – which were noted: C1, C2, C3 and C4. Recipes for chocolate manufacturing formulas are shown in Table 1. It is noted that the cocoa powder content decreased proportionally with the percentage of yeast powder added in the chocolate formulas.

Table 1. The ingredients used to make chocolate formulas

Ingredients	C	C1	C2	C3	C4
sugar [g]	420	420	420	420	420
butter with 80% fat [g]	200	200	200	200	200
milk power [g]	255	255	255	255	255
cocoa power [g]	150	135	120	105	90
beer yeast powder [g]	0	15	30	45	60
water [mL]	135	135	135	135	135

Chocolate manufacturing recipe

The sugar and the water are boiled for 10 minutes until the sugar is melted. After melting the sugar, added the butter. Mixed until the butter melts, remove from heat and add the mixture of milk powder and cocoa and stir continuously until smooth. The beer yeast is added in chocolate in different percentages: 10, 20, 30 and 40% of cocoa weight. Pour the melted chocolate on a silicone molds. After 2-3 hours checked if the chocolate is cool, remove from the molds, packaged and remained at 18°C.

Chemical analysis

1 g of chocolate samples were grinded and were dissolved in 20 mL ethanol-water solution 45:55 (v/v), at room temperature. After 30 minutes, the samples was filtered and centrifuged for 10 min at 5000 rpm with Mikro 200 Microliter Centrifuges by Hettich Lab Technology / Germany. The supernatant were analyzed to determine the total phenolic content and the total antioxidant activity.

The **total antioxidant capacity** was measured by FRAP assay (Benzie and Strain 1996) [1]. FRAP reagent was prepared freshly by 10 mM TPTZ (2,4,6-Tris(2-pyridyl)-s-triazine) solution (diluted in HCl 40 mM), 20 mM $\text{FeCl}_3 \cdot 6\text{H}_2\text{O}$ solution and 300 mM sodium acetate buffer at pH 3.6 in the ratio of 1:1:10. Was added 0.5 mL hydroalcoholic extract samples diluted in the ratio 1:100 (v/v) in distilled water and 2.5 mL FRAP reagent. Absorbance was read at 593 nm, after 30 minutes, using an aqueous solution of FeSO_4 as standard. Correlation coefficient for calibration curve was: $r^2 = 0.9972$. Total antioxidant capacity was expressed as mM Fe^{2+} /100 g DM (dry matter).

The **total polyphenol content** was determined by Folin-Ciocalteu method (Singleton and al., 1999) [7]. Briefly, 0.5 mL hydroalcoholic extract beer yeast and chocolate samples and diluted in the ratio 1:50 (v/v) in distilled water, 2.5 mL of Folin-Ciocalteu reagent (diluted 1:10 in distilled water) and 2.0 mL Na_2CO_3 sol.7.5% was stirred and was kept at room temperature. After 2 hours, the absorbance was read at UV-VIS Spectrophotometer SPECORD 205 by Analytik Jena at wavelength $\lambda = 750$ nm using gallic acid for calibration curve ($r^2 = 0.9962$). The results were expressed as mM GAE/100 g DM.

Statistical analysis

All data are expressed as mean \pm standard deviation (SD) of three replicates ($n=3$). The simple linear regression analysis was performed using the computer software program Origin 8.0.

Results and discussions

Brewer's yeast power an excellent source of a variety of bioactive substances. The researchers found that brewer's yeast (*Saccharomyces cerevisiae*) contains probiotic, antioxidant and antimicrobial properties [3].

The antioxidant characteristics of the brewer's yeast power used as a functional ingredient to improve the antioxidant properties of the chocolate formulas are presented in Table 2.

Table 2. The antioxidant characteristics of the brewer's yeast power

Antioxidant characteristics	Values
Total antioxidant capacity [mM Fe ²⁺ /100 g DM]	147.22
Total polyphenol content [mM GAE/100 g DM]	59.42

The sensory properties of chocolate formulas with beer yeast are presented in Table 3.

Table 3. The chocolate sensory properties

The sensory properties	Appearance-exterior	Polished surface, without stains, scratches or air gaps
	Appearance- interior	Chocolate with homogeneous consistency
	Color	Dark-brown
	Consistency	Hard and brittle
	Taste and smell	Pleasant, taste and odor intense flavor due to the yeast
	The finesse	The product is unctuous

Table 4 presents the total antioxidant capacity and the total polyphenol content for the different formulas of chocolate with different percentages of beer yeast powder.

Table 4. Total antioxidant capacity and total polyphenol content of chocolate formulas

The chocolate formulas	Total antioxidant capacity [mM Fe ²⁺ /100 g DM]	Total polyphenol content [mM GAE/100 g DM]
C	18.68 \pm 1.17	2.71 \pm 0.10
C1	21.97 \pm 1.24	3.54 \pm 1.14
C2	24.93 \pm 1.27	4.33 \pm 1.16
C3	28.01 \pm 1.37	5.42 \pm 0.21
C4	31.14 \pm 1.45	6.05 \pm 0.26

Values are expressed as mean – standard deviation ($n = 3$).

A significant difference can be noticed between control sample (18.68 mM Fe^{2+} /100 g DM) and C4 chocolate formula (31.14 mM Fe^{2+} /100 g DM) for the total antioxidant activity. Chocolate antioxidant properties are often claimed; however, they are frequently different from the parent natural sources due to the industry or manufacturing productions. Therefore, the antioxidant property of chocolate and cocoa are not adequately taken into consideration by consumers who use of this food as a desert for its flavor and taste properties [8]. Cocoa has long been identified as a polyphenols-rich food [4]. The content of polyphenols can vary tremendously depending on the source of cocoa beans, primary and secondary processing conditions and process of chocolates making [2]. The recently researches has been showed that chocolate, especially dark chocolate, is one of the most polyphenol-rich foods along with tea and wine [4]

According to the data presented in Table 4, we can observe that with the increasing the percentage of yeast powder in the chocolate manufacture recipe increases the total polyphenols content. Therefore, the total polyphenol content vary from 2.71 mM GAE/100 g DM in the control sample to 6.05 mM GAE/100 g DM in the chocolate formula with 40% yeast. So, the percentage of beer yeast that replaces cocoa powder in chocolate formulas, increases antioxidant properties of this products.

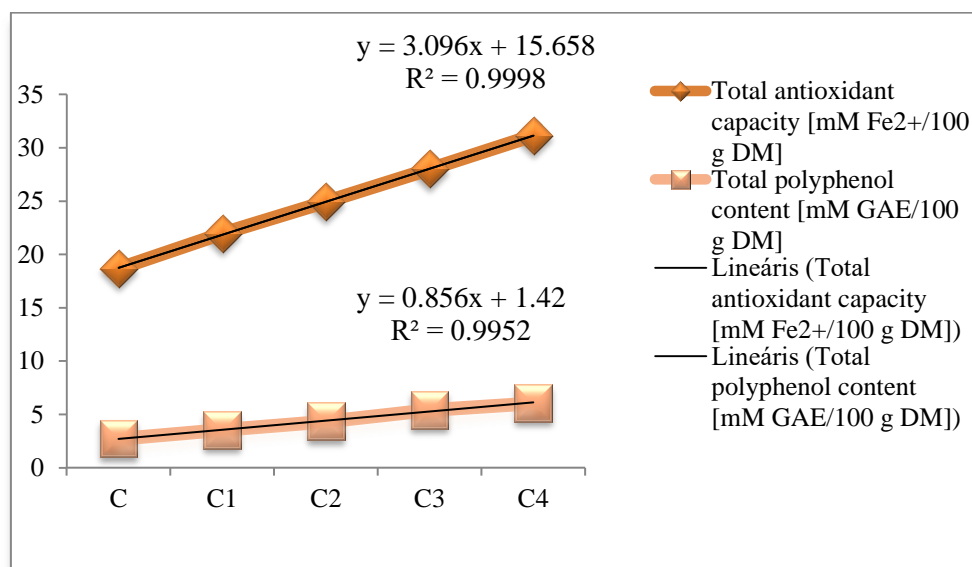


Figure 1. The relationships between the antioxidant properties chocolate formulas with beer yeast

All equations were revealed a positive relationship between the antioxidant properties of the chocolate formulas with beer yeast.

Figure 1 shows that there is a very good correlation between the antioxidant properties of the chocolate formulas. The coefficient of determination calculated is $R^2 = 0.9998$ for the total antioxidant capacity, respectively $R^2 = 0.9952$ for total polyphenol content.

Conclusion

The beer yeast is a sustainable raw material available in large quantities, rich in high antioxidant compounds.

The drying at a moderate temperature of 65°C represents a simple method of beer yeast conditioning in order to preserve its antioxidant properties.

The addition of the beer yeast does in different percentage not induce negative changes in the sensory attributes of chocolate formulas, especially taste, smell, texture and consistency.

By incorporating the yeast powder into the chocolate manufacturing recipe showed an increase in the total polyphenols content and total antioxidant capacity (FRAP value) compared to the control sample.

The order of total polyphenol content in the chocolate formulas showed a similar trend as the total antioxidant capacity.

Based on the results obtained from this study, we can affirm that the use of beer yeast as a ingredient with high added value for designing innovative food products - chocolate with a more intense flavor.

References

- [1] I.F.F Benzie, L. Strain, *Anal Biochem.* 239 (1996) 0-76.
- [2] K.A. Cooper, E. Campos-Gimenez, D.J. Alvarez, K. Nagy, J.L. Donovan, G. Williamson, *J. Agric. Food Chem.* 55 (2007) 2841-2847.
- [3] M. Fakruddin, N. Hossain, M.M. Ahmed, *BMC Complementary and Alternative Medicine* 17(64) 2017, DOI: 10.1186/s12906-017-1591-9.
- [4] A.M.M. Jalil, A. Ismail, *Molecules* 13 (2008) 2190-2219, DOI: 10.3390/molecules13092190.
- [5] E.A. Johnson, C. Echavarri-Erasun, *The Yeasts (Fifth Edition)*, Science Direct, 2011, pp 21-44.
- [6] M. Richter, S.C.D.S. Lannes, *Rev. Bras. Cienc. Farm.* 43(3) (2007) 357–369.
- [7] V.L. Singleton, R. Orthofer, R.M. Lamuela-Raventos, *Methods Enzimol.* 299 (1999) 152-178.
- [8] S. Vertuani, E. Scalambra, V. Trotta, A. Bino, G. Malisardi, A. Baldisserotto, S. Manfredini, *J Med Food* 17 (4) 2014, 512–516, DOI: 10.1089/jmf.2013.0110.
- [9] <https://www.sciencemag.org/news/2016/03/flavor-coffee-and-chocolate-thank-yeast-hitchhiked-human-migration>
- [10] <https://www.sciencedirect.com/topics/neuroscience/saccharomyces-cerevisiae>

EXTRACTION OF CHLOROPHYLL A, B AND CAROTENOIDS FROM *NANNOCHLOROPSIS OCULATA* AFTER HEAVY METAL ADSORPTION

Zamfira Dincă, Anamaria Iulia Török, Maria-Alexandra Hoaghia, Enikő Kovács,
Emilia Neag

INCDO-INOE 2000, Research Institute for Analytical Instrumentation, 67 Donath Street,
400293 Cluj-Napoca, Romania
e-mail: emilia.neag@icia.ro

Abstract

The main objective of the present study was to determine the most suitable solvent for photosynthetic pigments extraction from the *Nannochloropsis oculata* biomass after adsorption of Cu, Zn and Cd from mono and multicomponent solutions. The results revealed that the highest percentage removal of heavy metals from mono solutions was achieved for Zn 20 mg/L (96.2 %), followed by Cu 20 mg/L (92.6 %) and Zn 50 mg/L (92.1 %), respectively. Organic solvents, namely ethanol, methanol and acetone were tested for chlorophyll a, b and carotenoids extractions. It was observed that higher contents of *chlorophyll a* were obtained after extraction with methanol from algal biomass after Cd and Zn adsorption from single component solutions. After a comparative examination, the highest content of *chlorophyll b* was obtained after the extraction with acetone.

Introduction

Photosynthetic pigments, like *chlorophyll a*, *b* and carotenoids, are valuable bioactive compounds that can be extracted from microalgal biomass. These components play a vital role in sustaining life in both plants and animals and have beneficial effects on human health. Due to their usability in various fields, such as food, pharmaceutical or cosmetic industry, many studies have been carried out to enhance chlorophyll extraction and fractionation from microalgae [1]. In the extraction process the following parameters are important: type of solvent used, pressure, temperature and contact time. Each solvent has certain characteristics, more or less compatible, for an efficient extraction of photosynthetic pigments, taking into account the safety rules [2]. Acetone proved to be a poor extractant for chlorophyll from certain vascular plants and algae [3]. For algae and recalcitrant vascular plants, the most efficient extractant for chlorophylls was methanol [4], less volatile and flammable than acetone, but it is toxic if inhaled or absorbed through the skin [2]. For the chlorophyll analysis, ethanol was identified to be the most appropriate solvent due to its lower toxicity [2,5].

The aim of this study was to determine the contents of photosynthetic pigments (*chlorophyll a*, *b* and carotenoids) from *Nannochloropsis oculata* biomass after heavy metals adsorption using ethanol, methanol and acetone as solvents in the extraction process.

Experimental

Materials

The *Nannochloropsis oculata* biomass (powder) was purchased from Astaxa GmbH (Germany Milz Gerbergasse). The chemicals, such as nitric acid, hydrochloric acid, methanol, ethanol and acetone were of analytical grade and were purchased from Merck (Germany).

Batch adsorption experiments

The experiments were carried out in 250 mL Erlenmeyer flasks using 5 g of *Nannochloropsis oculata* biomass (powder) mixed with 100 mL synthetic heavy metals (Cu, Zn, Cd) solution at

various concentrations (20 - 300 mg/L) for 300 min and stirred at 75 rpm at room temperature. After adsorption, the biomass was separated from the liquid phase by filtration through Whatman filter paper with a diameter of 125 mm and dried in a universal oven (UFE 400, Memmert, Germany) for 6 hours at 60 °C. 20 mL of liquid phase were measured and carefully transferred to a clean and conditioned beaker. 7 mL of 65 % HNO₃ and 21 mL of 37 % HCl were added. Samples were left overnight at room temperature for pre-digestion. After digestion at controlled temperature, the samples were filtered and set for metals determinations.

The heavy metals content (Cu, Zn, Cd) was determined by inductively coupled plasma - optical emission spectrometer (OPTIMA 5300 DV, Perkin Elmer, Norwalk, USA), assembled with an CETAC U-6000 AT ultrasonic nebulizer.

The heavy metal amount in the adsorbent phase and the removal efficiency were calculated using the equations mentioned by Mudyawabikwa et al. [6].

Pigments extraction

0.5 g of *Nannochloropsis oculata* biomass after heavy metals adsorption experiments were mixed with 10 mL of different solvents for pigment extraction. The samples were sonicated for 15 min. After extraction, the samples were centrifuged at 4000 rpm for 8 minutes.

The absorbance was measured using a Lambda 25 Perkin-Elmer UV/VIS spectrophotometer. The obtained values were used to calculate the chlorophyll a (µg/mL), chlorophyll b (µg/mL) and carotenoid (µg/mL) content applying the equations mentioned by Lichtenthaler and Buschmann [7].

Results and discussion

Effect of heavy metals removal by *Nannochloropsis oculata* biomass

Cu, Zn and Cd removal by *Nannochloropsis oculata* biomass starting from different initial concentrations and mixtures are presented in Figure 1.

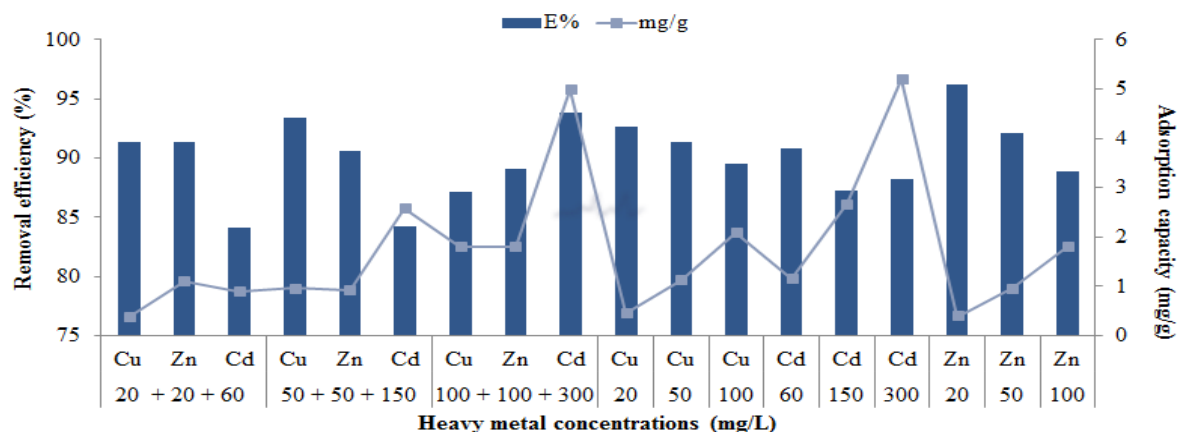


Figure 1. Influence of the initial heavy metal concentrations over the removal efficiency and amount in the adsorbent phase

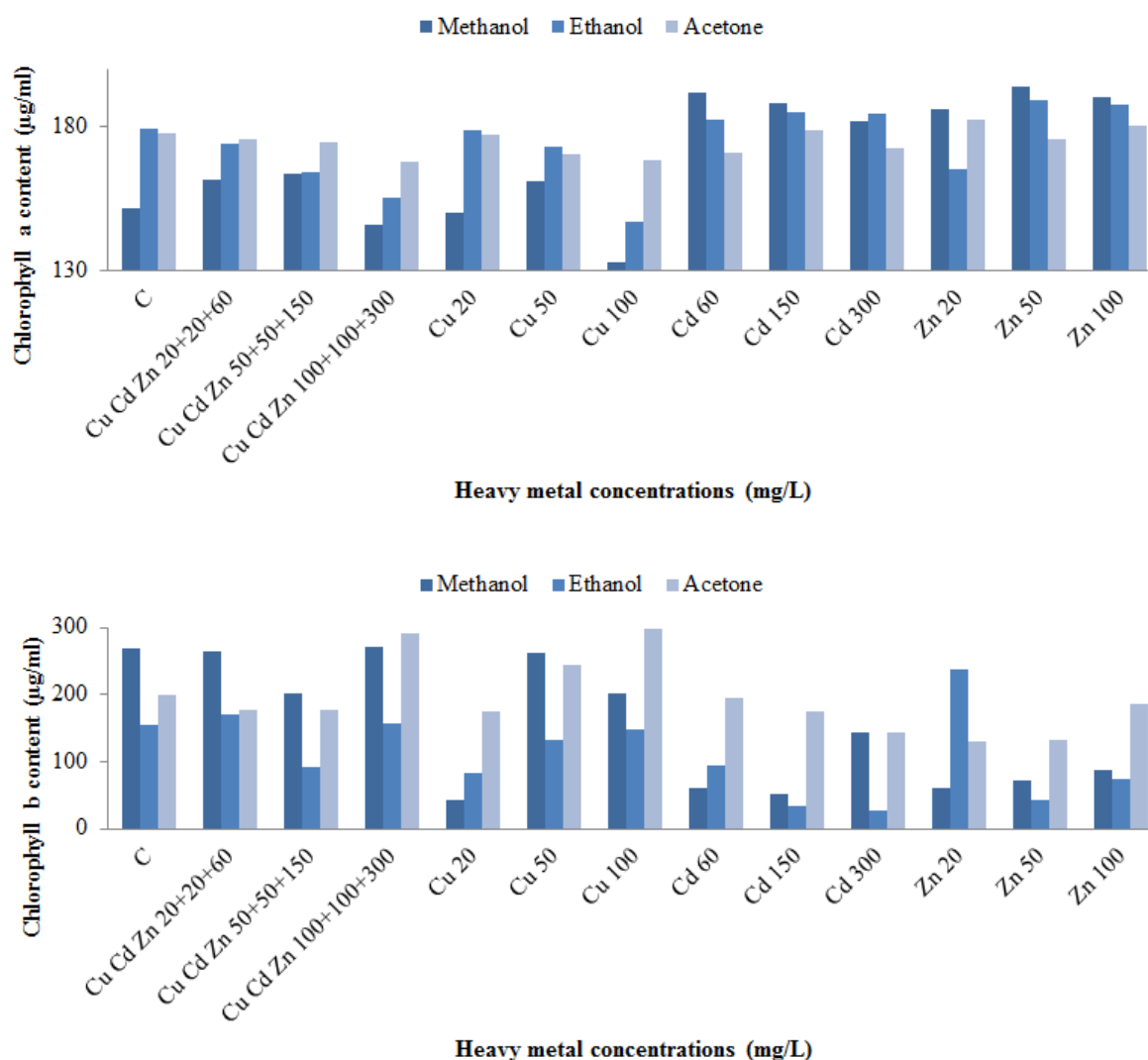
The biomass adsorption capacity improved with an increase of the initial concentrations of heavy metals. The results indicate that *Nannochloropsis oculata* biomass has a great capacity to remove high amounts of Cd from aqueous solutions, even in the presence of other metals, such as Cu and Zn. The removal efficiencies ranged from 84 % to 96 % for Cu, Zn and Cd, respectively. The highest removal efficiency and adsorption capacity was observed for Zn 20 mg/L (96 %) (mono component solutions) and Cd 300 mg/L (5.2 mg/g) (multicomponent

solutions). A gradually decrease in removal efficiencies was observed in the multicomponent solutions, compared with mono component solutions.

Effect of solvents for extraction of photosynthetic pigments

The effect of methanol, ethanol and acetone for photosynthetic pigments extraction from *Nannochloropsis oculata* biomass after heavy metals adsorption is presented in Figure 2.

Spectrophotometric analysis of photosynthetic pigments from *Nannochloropsis oculata* biomass after heavy metals adsorption showed changes in their content compared to the control sample.



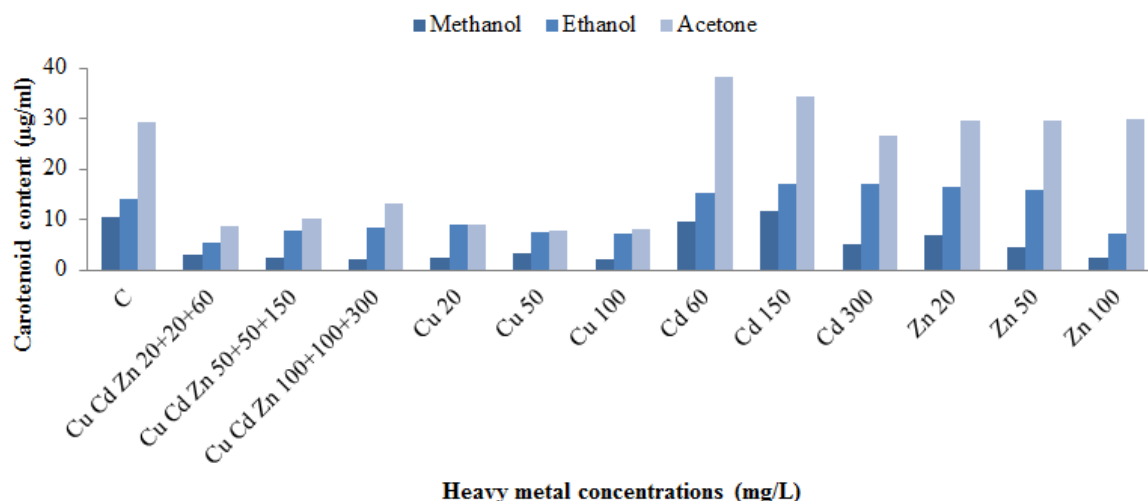


Figure 2. Chlorophyll a, b and carotenoid content after extraction with different organic solvents

The highest contents of *chlorophyll a* were achieved using methanol (193.7 µg/mL, 50 mg/L Zn) as an extraction solvent, followed by extraction with ethanol (189.0 µg/mL, 50 mg/L Zn) and acetone (182.2 µg/mL, 20 mg/L Zn) (Figure 2). The *chlorophyll a* content slowly increased with respect to the control sample after the extraction from the algal biomass used for Cd and Zn removal. Furthermore, lower *chlorophyll a* contents were extracted from *Nannochloropsis oculata* biomass after heavy metals removal from multicomponent solutions and Cu removal from monocomponent solutions.

The highest contents of *chlorophyll b* extraction (298.5 µg/mL, 100 mg/L Cu), were extracted with acetone, followed by methanol (271.0 µg/mL, Cu Cd Zn 100+100+300 mg/L) and ethanol (236.7 µg/mL, Zn 20 mg/L).

The highest *carotenoid* contents were achieved after extraction with acetone in all the samples used for heavy metal removal (Figure 2).

Conclusion

In the present study the influence of heavy metals on extraction of photosynthetic pigments in *Nannochloropsis oculata* biomass was investigated. The *Nannochloropsis oculata* biomass show a remarkable ability to remove higher concentrations of heavy metals from single (Zn 20 mg/L, 96.2 %) and multicomponent solutions (Cu Cd Zn 50+50+150 mg/L, 93.4% 90.6 % 84.2%). The obtained results showed that *Nannochloropsis oculata* biomass had a higher Cd removal capacity, than of Cu and Zn. The content of photosynthetic pigments varied by changing the concentrations of heavy metals. The highest measured *chlorophyll a* content was obtained using methanol. Acetone gave higher concentrations for carotenoids than methanol and ethanol in all the studied samples. Further studies will be conducted in order to determine the effect of metals on photosynthetic pigments from microalgae grown in a culture medium with an increased content of heavy metals.

Acknowledgements

This work was funded by Core Program, under the support of ANCS, project no. PN 19-18.01.01.

References

- [1] A. Hosikian, S. Lim, R. Holim, M. K. Danquah, Chlorophyll extraction from microalgae: A review on the process engineering aspects, *International Journal of Chemical Engineering*, 2010, Article ID 391632, 2010, pp.1-3.
- [2] N. Sumanta, C. I. Haque, J.Nishika, R. Suprakash, *Research Journal of Chemical Sciences*, 4(9), 2014, pp. 63.
- [3] S.W. Jeffrey, R.F.C. Mantoura, S.W Wright, *Phytoplankton pigments in oceanography: guidelines to modern methods*. UNESCO Monographs on Oceanographic Methodology, UNESCO Publishing, Paris, 1997, pp. 10.
- [4] R. J. Porra, The chequered history of the development and use of simultaneous equations for the accurate determination of chlorophylls a and b, *Photosynth. Res.*, 73, 2002, pp.149–156.
- [5] S. W. Wright, S. W. Jeffrey, F. R. C. Mantoura, Evaluation of methods and solvents for pigment analysis. In: *Phytoplankton pigments in oceanography: guidelines to modern methods*, UNESCO Publ., Paris, 1997, pp. 261–282.
- [6] B. Mudyawabikwa, H. H. Mungondori, L. Tichagwa, D. M. Katwire, *Water. Sci. Technol.* 75(10) (**2017**) 2390.
- [7] H.K. Lichtenthaler, C. Buschmann, *Current Protocols in Food Analytical Chemistry*, F4.3.1-F4.3.8 by John Wiley & Sons, Inc. (2001)

LEMNA MINOR L. AND PISTIA STRATIOTES L. IN THE ACCUMULATION OF TOTAL PHOSPHORUS FROM THE WATER

Dorian-Gabriel Neidoni¹, Mihaela Dragalina¹, Valeria Nicorescu¹, Amanda Izabela Siminic¹, Dan Alin Pop¹, Alexandru Pahomi²

¹National Research and Development Institute for Industrial Ecology- ECOIND, Timisoara
Subsidiary, 115 Bujorilor Str., 300431, Romania

²Faculty of Chemistry, Biology, Geography, Department of Biology-Chemistry, West
University of Timisoara, 16 Pestalozzi Str., 300115, Timisoara, Romania
e-mail: neidoni_dorian94@yahoo.com

Abstract

In this study we wanted to evaluate the absorption capacity of total phosphorus (TP) from water by two aquatic plants (*Lemna minor* L. and *Pistia stratiotes* L.) belonging to the same family (Araceae) which have a huge potential for remediation the water loaded with organic and inorganic substances (total phosphorus, total nitrogen, heavy metals, etc.). Four experimental variants with initial concentrations of total phosphorus in water of 4, 6, 8 and 10 mg/L (TP 4, TP 6, TP 8 and TP 10) at an ambient temperature of 25° C were used to achieve these things. The total amount of phosphorus was quantified at the initial moment and after 72 hours both in water (expressed in mg/L), and in plants (expressed in g/kg of dry matter), respectively. The best results were given by the *Lemna minor* L. plant at an initial phosphorus concentration in water of 6 mg/L.

Introduction

Phosphorus is an essential macronutrient for the harmonious growth and development of terrestrial and aquatic plants [1], but in large quantities, it harms the environment, especially water, because it is largely responsible for the occurrence of eutrophication, as reported by the OECD (World Economic Cooperation and Development Organization), which attributes over 80% of total phosphorus as the main cause of the appearance of eutrophication in water bodies [2]. Eutrophication has emerged as a global problem that produces a multitude of negative effects, such as the overgrowth of algae that leads to hypoxia, which in turn results in the killing of fish [3] and other aquatic organisms dependent on oxygen dissolved in water, which causes a major imbalance in aquatic ecosystems. Because of these negative effects caused by the excess of total phosphorus in the water, it is imperative to find a solution that is as efficient and sustainable as possible in eliminating it, and a solution could be the use of aquatic plants. The use of plants in naturally eliminating contaminants from a water source is called phytoremediation. This process uses the plant's metabolic system to remove nutrients and contaminants from the surrounding area and store them in their biomass [4].

Lemna minor L. and *Pistia stratiotes* L. are floating aquatic plants belonging to the Araceae family and which many authors report as being able to accumulate significant quantities of organic and inorganic substances from the aquatic environment, such as heavy metals (Cd, Pb, With etc.) [5], total nitrogen or phosphorus [6, 7]. These species are found almost all over the globe [4], but mainly in tropical [8], subtropical [4] and temperate [8] regions and develops in almost all types of freshwater (clean, polluted, muddy, stagnant) [9], having very high growth rates. *Pistia stratiotes* L. doubling its population within a few weeks [4], and *Lemna minor* L. being able to double its mass within a week [9], which is a major advantage because the need to add new plants to a remediation pond decreases [4]. These considerations mentioned above, make the two species of plants as ideal candidates in studies of phytoremediation of waters loaded with organic substances.

Experimental

Plant material

The *Lemna minor* L. and *Pistia stratiotes* L. plants were harvested from a natural pond and transferred to the laboratory, where they were thoroughly washed with distilled water to remove mud and impurities. Plants were acclimatized for 7 days to laboratory conditions, at a temperature range from 19° to 25° C, in tap water.

Experimental conditions

Approximately 10 grams of plant material were placed in 10 cm diameter transparent plastic containers, containing 250 ml of tap water enriched with total phosphorus (TP) up to concentrations of 4, 6, 8 and 10 mg/L (TP 4, TP 6, TP 8 and TP 10 variants). The experimental duration was 72 hours at 25° C ($\pm 0.5^\circ$ C), with a day/night cycle of 16/8, and the total amount of phosphorus in water, expressed in a mg/L, and in plants, expressed in a g/kg of dry matter (d.m.), was quantified at the initial moment and after 72 hours, during which the plants were in the water at preset temperature.

Methods of analysis

Plants. About 5 g of wet vegetal material was mixed for 5-10 minutes with 0.5-1 g of animal charcoal. The sample was transferred into an Erlenmeyer flask and 50 mL of 2% CH₃COOH was added, incubated for 10-15 minutes then it was filtered. 1 mL of the acetic acid extract was transferred in a 25 mL solution containing 3 mL of molybdenum reagent and 1 mL of ascorbic acid then the sample was incubated in the dark for 15-20 minutes. The detection of total phosphorus was spectrophotometrically analyzed at 600 nm.

Water. The determination of total phosphorus in water was performed using the Specord PC 205 spectrophotometer, Analytic Jena, according to SR EN ISO 6878: 2005.

Results and discussion

Water purification

The plants were grown in presence of four phosphorus concentrations, chosen based on the most commonly TP concentration values detected in untreated wastewater.

Figure 1 shows the decrease of the total amount of phosphorus in water after 72 hours at an ambient temperature of 25° C, for *Lemna minor* L. and *Pistia stratiotes* L. This temperature was chosen because most terrestrial and aquatic plants prefer a medium with relatively high temperature for cellular processes, especially for photosynthesis [10].

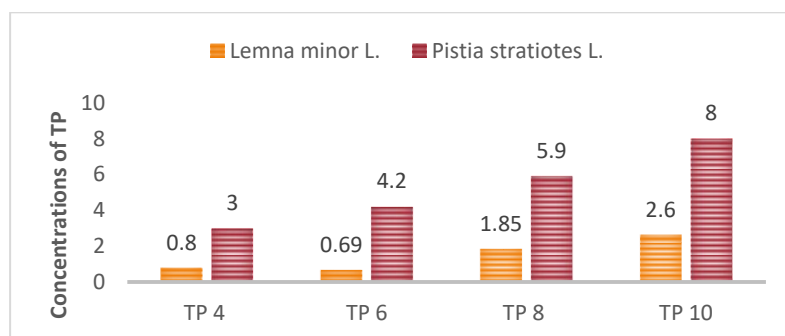


Figure 1. The decrease of the initial total phosphorus concentration in the water after 72 hours. The data represents the arithmetic average value of three replicates.

From figure 1 we can see the quite large difference between the two aquatic plants in terms of purification of total phosphorus-loaded water. For both species of plants the best results were in the case of the experimental variant with 6 mg/L initial TP in water, namely: for the *Lemna minor* L. plant a percentage decrease of 88.5% from 6 mg/L to 0.69 mg/L TP is observed, and

for the *Pistia stratiotes* L. species the percentage decrease is 30% from 6 mg/L to 4.2 mg/L TP. Comparing the treatment capacity of total phosphorus-loaded water, of the two aquatic plants, we can observe a markedly higher difference in favor of the species *Lemna minor* L. in all experimental variants.

Absorption of total phosphorus by *Lemna minor* L. and *Pistia stratiotes* L.

Table 1 shows the TP bioaccumulation by the two plant species. Comparing the initial quantities of phosphorus detected in plants, a higher affinity for phosphorus of the species *Lemna minor* L. is observed to the detriment of the species *Pistia stratiotes* L., these having in their body from the beginning 3.6 respectively 2.3 g/kg d.m.

In the case of *Lemna minor* L. the amount of phosphorus accumulated in its body is directly proportional to the amount of TP in the water, but the differences between the experimental variants TP 6, TP 8 and TP 10 are very small, which leads to the conclusion that, the value of 15.5 g/kg d.m. is the maximum amount of TP that can be accumulated by the body of the plant, regardless of whether the initial phosphorus dose is increased.

In the case of the first three experimental variants (TP 4, TP 6 and TP 8) for the species *Pistia stratiotes* L. the amount accumulated in the body of the plant is the same as in the case of the first species directly proportional to the initial amount of phosphorus in the water reaching a maximum of 9.0 g/kg d.m. For the experimental version TP 10, we observe a sudden decrease in the amount of phosphorus in the plant, compared to the previous version (TP 8= 9.0 g/kg d.m. and TP 10= 4.9 g/kg d.m.), which means that the plant reaches maximum saturation, and the bioaccumulation processes are stopped, the plant begins to gradually remove the TP from its body back into the water.

For the most efficient purification of the water loaded with TP, it is recommended to use the species *Lemna minor* L., to the detriment of the species *Pistia stratiotes* L., at initial quantities of TP in water of maximum 6 mg/L, for approximately 72 hours after which the plants can be renewed.

Because the plants present considerable amounts of TP in their bodies, after harvesting they can be used as a nutritional supplement for animal feed [11] or as a fertilizer for phosphorus-deficient soil.

Table 1. Total phosphorus accumulation in plants after 72 hours, expressed in g/kg d.m. The data represents the arithmetic average value of three replicates.

Experimental variants	<i>Lemna minor</i> L.		<i>Pistia stratiotes</i> L.	
	Initial	72 h	Initial	72 h
TP 4	3.6	10.7	2.3	5.7
TP 6	3.6	14.6	2.3	7.2
TP 8	3.6	15.0	2.3	9.0
TP 10	3.6	15.5	2.3	4.9

The data presented above are also supported by the data from the literature where Sudiastro et al. in 2019 [7], studied four different species of aquatic plants, among which *Lemna* sp. and *Pistia stratiotes* L. and concluded that regarding the removal of TP from wastewater from the agri-food industry, *Lemna* sp. it is the most efficient with a percentage of phosphorus removal of 36.15% by it. Other authors reported purification yields similar to those obtained in our experimental sets (45.5%-73.3%) after 96 hours of treatment with *Lemna gibba* L. in the presence of 8 mg/L TP, at a temperature range between 10 and 32° C [12].

Conclusion

This study demonstrated the ability of *Lemna minor* L. and *Pistia stratiotes* L. plants to accumulate TP from synthetic water. The degree of bioaccumulation of phosphorus by plants was influenced on the one hand by the studied species and on the other hand by the initial amount of phosphorus present in the water. Therefore, both species showed the best results in the experimental version TP 6, but the differences between the two species were significant, namely: the percentage decrease of TP in the species *Lemna minor* L. was 88.5%, and in the case of *Pistia stratiotes* L. was only 30%.

Regarding the bioaccumulation of organic substances by the plants in their body, there are notable differences between the two species. The degree of saturation for the *Lemna minor* L. species is around 15 g/kg d.m., while the *Pistia stratiotes* L. species reaches saturation around 9 g/kg d.m.

From the ones presented above, a general conclusion can be drawn, namely, that of the two species of floating aquatic plants, the species *Lemna minor* L. is far superior to the other, and is much better suited to the treatment of water loaded with TP.

Acknowledgements

The present research was financially supported by the Romanian National “Nucleu” Program (code PN 19 04 02 01).

References

- [1] D.G. Neidoni, V. Nicorescu, L. Andres, M. Ihos, M. Dragalina, I. Iordache, I. Siminic, S.C. Negrea, L.A. Diaconu, The 24th International Symposium on Analytical and Environmental Problems. (2018) 174.
- [2] C. Du, Q. Wang, Y. Li, H. Lyu, L. Zhu, Z. Zheng, S. Wen, G. Liu, Y. Guo, Int. J. Appl. Earth Obs. Geoinformation. 71 (2018) 29.
- [3] J. Mbabazi, T. Inoue, K. Yokota, M. Saga, J. Environ. Chem. Eng. 7 (2019) 102960.
- [4] N.A. Hanks, J.A. Caruso, P. Zhang, J. Environ. Manage. 164 (2015) 41.
- [5] S. Das, S. Goswami, A.D. Talukdar, Bull. Environ. Contam. Toxicol. 92 (2014) 169.
- [6] R.S. Putra, F. Cahyanaa, D. Novarita, Procedia Chem. 14 (2015) 381.
- [7] S.I.A. Sudiarto, A. Renggaman, H.L. Choi, J. Environ. Manage. 231 (2019) 763.
- [8] R. Gusain, S. Suthar, Process Saf. Environ. 109 (2017) 233.
- [9] L.C. Vieira, L.G. de Araujo, R.V. de P. Ferreira, E.A. da Silva, R.L.S. Canevesi, J.T. Marumo, J. Environ. Radioactiv. 203 (2019) 179.
- [10] M.D. Asfaw, S.M. Kassa, E.M. Lungu, W. Bewket, Ecol. Modell. 406 (2019) 50.
- [11] N. Muradov, M. Taha, A.F. Miranda, K. Kadali, A. Gujar, S. Rochfort, T. Stevenson, A.S. Ball, A. Mouradov, Biotechnol. Biofuels. 7 (2014) 30.
- [12] N. Boniardi, G. Vatta, R. Rota, G. Nano, S. Carra, The Chem. Eng. J. 54 (1994) 41.

**PRELIMINARY RESEARCH ON LAMINATE ULTRASONIC WELDING FOR
FABRICATION OF SANDWICH COMPOSITE FROM AMORPHOUS RIBBONS
AND CRYSTALLINE COOPER FOILS**

**Nicolaescu Mircea^{1,2}, Mina Popescu^{1,2}, Corina Orha¹, Emilia Florina Binchiciu³, Cosmin
Codrean²**

¹ *Department of Condensed Matter, National Institute of Research-Development for
Electrochemistry and Condensed Matter Timisoara, Plautius Andronescu 1, 300224
Timisoara, Romania*

² *Politehnica University of Timisoara, Faculty of Mechanics, blv. Mihai Viteazu no.30,
300222, Timisoara, Romania*

³ *National Institute in Welding and Material Testing - ISIM Timisoara, blv. Mihai Viteazu
no.30, 300222, Timisoara, Romania
e-mail: mircea.nicolaescu@student.upt.ro*

Abstract

With the evolution of society new materials or classes of materials must be developed. The lack of crystalline structure from the amorphous ribbons favors mechanical and electrical properties. The homogeneous structure of amorphous metal alloys offers unique mechanical, anti-corrosive, wear-resistant and magnetic properties, which makes them superior in many applications compared to the crystalline metals that have the same composition.

Yet, the major problem of amorphous metal alloys is their metastable character, these alloys being used only at low temperatures, but by introducing crystalline copper in the fabrication of sandwich composites, the usage temperature would increase.

In this study we present the results on the use of ultrasonic laminate welding for the fabrication of amorphous - crystalline composite materials.

Hybrid multilayer ultrasonic joints of the amorphous metal alloy with a thickness of 25 μm , having the chemical composition 87.2% Ni, 4.2% Fe, 1.3% Cr, 4.5% Si, 2.8% B and crystalline copper with 99.99% purity, with a thickness of 15 μm , were achieved. The amorphous ribbons were produced by the "Planar flow casting" process and the joint was made with an ultrasonic assembly at a frequency of 20 KHz.

The combined samples were characterized by X-ray diffraction (XRD), scanning electron microscopy (SEM), and Vickers micro-hardness.

Keywords: ultrasonic welding, amorphous ribbons, composite.

COMPARISON OF ANTIOXIDANT ACTIVITY BETWEEN TWO SWEET PEPPER GENOTYPES INFECTED WITH *ALTERNARIA ALTERNATA*

Marijana Peić Tukuljac¹, Dejan Prvulović¹, Slađana Medić-Pap², Dario Danojević²

¹University of Novi Sad, Faculty of Agriculture, Trg D. Obradovića 8, 21000 Novi Sad, Serbia

²Institute of Field and Vegetable Crops Novi Sad, M. Gorkog 30, 21000 Novi Sad, Serbia
e-mail: peictukuljacmarijana@yahoo.com

Abstract

The resistance of two sweet pepper varieties (cultivar Anita and breeding line 82/16) to fruit rot caused by fungus *Alternaria alternata* was evaluated. In order to determined antioxidant capacity of methanol extracts of tested fruits as well as its relation with phenolic compounds three different antioxidant tests were used and content of total polyphenols and total flavonoids was measured. The results suggested that not only phenolic compounds might be involved in antioxidant activity of pepper fruits, but also carotenoids and vitamins C and E

Introduction

Sweet peppers (*Capsicum annuum* L.) are one of most worldwide cultivated vegetable, especially in China, Mexico and Turkey [1]. Apart from its economic importance, peppers have significant place in human diets because of its high amount of vitamin C, vitamin E, capsaicinoids, carotenoids and phenolic compounds [2]. This valuable crop is mostly consumed as fresh fruits or in dried form used as a spice [1].

Many commercial varieties of pepper are susceptible to damage caused by different biotic factors (fungi, bacteria and insects) as well as abiotic factors (drought, metals in soils, ultraviolet radiation or in appropriate temperature). This could lead to significant losses of pepper crops so that is one of main reason why many researchers are focused on understanding the mechanisms of antioxidant protection [3].

Fungus *Alternaria alternata* can infects living plants and fresh fruits, especially after mechanical damage or insects injuries. This destructive fungus causes damage such as fruit rot, black spots on the fruit surface and internal mould of fruits. Fruit rot appears before or after harvest on mature pepper fruits more often than immature. One way to avoid fungal contamination is careful handling during harvesting, storing and other processes involved in pepper producing [1, 4, 5].

Because of pepper nutritional importance and widespread use, the aim of this study was to compare the resistance of two pepper cultivars on *Alternaria* infection. In this purpose were determined content of total polyphenols, total flavonoids and antioxidant activity measured by three different antioxidant tests.

Experimental

Genotype Anita and breeding line 82/16, used in this study, are sweet pepper cultivars with bell shaped fruits. Both varieties have light yellow color of fruits at technological maturity. These genotypes of pepper were grown in the experimental field of the Institute of Field and Vegetable Crops, Novi Sad, Serbia. Pepper seeds for seedlings production were sown on 30th of March. Seedlings were transplanted into the open field was done on 3rd of June. The distance between plants in the row was 25 cm, while the space between rows was 70 cm. All fruits were collected at the technological maturity stage.

The inoculation of fruits was done with monohyfal isolate *Alternaria alternata* (K-93) as described by Fallik et al. [6]. Fruits of pepper were inoculated with 40 µl spore suspension per puncture (3 puncture in each of the fruits). Fruits were put into PVC bags and incubated for

10 days at 20 °C in thermostat. Evaluation of infection was performed according to a method by Frans et al. [7].

Methanol extracts of sweet pepper fruits were prepared by homogenization of 4 g fresh plant material with 10 ml of 70% methanol. After an overnight extraction, the methanol extracts were centrifuged 15 min at 5000 rpm and the obtained supernatants used in further biochemical analyses were kept at 4 °C. The total polyphenol content was measured by spectrophotometry using Folin-Ciocalteu method [8]. Determination of total flavonoid content was performed by aluminium chloride colorimetric method based on building metal-complexes between flavonoid compounds and aluminium chloride. [9]. The concentration of total polyphenols and flavonoids were read (mg/ml) on the standard calibration curve were expressed as quercetin equivalents in mg per 100 gram of fresh weight (mg QE/100 g FW). The antioxidant capacity of fruits was measured by three the most widely used methods. 2,2-Diphenyl-1-picrylhydrazyl (DPPH) radical scavenging activity was determined using the method described by Yazdizadeh Shotorbani et al. [10] with some modification. This spectrophotometric method is based on reduction DPPH radical by antioxidant compounds. The ABTS assay is spectrophotometric method based on reduction the 2,2'-azino-bis(3-ethylbenzothiazoline-6-sulfonate) radical cation (ABTS^{•+}), which has a dark blue color, by an antioxidant into colorless ABTS. ABTS antioxidant activity of the tested extracts was measured according to Zheleva-Dimitrova et al. [11] with slight modification. Ferric reducing antioxidant power (FRAP) is based on measuring the reduction of ferric ion (Fe³⁺) to ferrous iron (Fe²⁺) by antioxidants in extracts. The FRAP assay was carried out as described by Thaipong et al. [12]. Determination of antioxidant activity by DPPH, ABTS and FRAP method was calculated from the standard curve constructed with Trolox. The results of DPPH, ABTS and FRAP were expressed as Trolox equivalents in mg per 100 g of fresh weight (mg Trolox/100 g FW).

All the assays were carried out in triplicate and the data were reported as mean ± standard deviation (Table 1). Statistic evaluation of data was analysed using software STATISTICA ver. 13.2 (StatSoft, Inc., USA). Analysis of variance (Factorial ANOVA) with the Bonferroni test was used to compare significant difference between the groups at the 5 % significance level ($p < 0.05$). The correlation coefficients were done by Spearman.

Results and discussion

The content of total polyphenols, total flavonoids and antioxidant capacity of sweet pepper extracts measured by DPPH, ABTS and FRAP tests is presented in Table 1. Polyphenols are a large group of secondary metabolites involved in non-enzymatic defence on damage caused by different biotic and abiotic agents [13]. In general, non-infected fruits of genotype Anita contained more phenolic compounds (150.20 mg QE/100 g FW) than non-infected fruits 82/16 cultivar (98.51 mg QE/100 g FW). Furthermore, infected fruits of both tested cultivars showed lower amount of polyphenols than non-infected fruits. Previous study of Kevers et al. [14] reported high concentration of polyphenols in fruits of peppers (from 215 to 296 mg CAE/100 g FW). However, these results cannot be compared with ours since these authors used different standard for expressing results.

The highest content of total flavonoids was obtained for non-infected fruits of Anita cultivar. The flavonoid content in our study was lower for both tested cultivars (from 8.61 to 13.96 mg QE/100 g FW for non-infected fruits) than previously reported by Medina-Juárez et al. (from 25.38 to 60.36 mg QE/100 g FW) [15], while the values obtained by Kevers et al. were even lower (from 2.1 to 4.8 mg QE/100 g FW) [14]. According to some researchers, this inconsistency in published results could be explained by the fact that concentration of polyphenols and flavonoids depends on varieties, the technological treatments and time of harvesting [15, 16].

Table 2. Phenolic compounds and antioxidant activity of methanolic extracts

Genotype	Anita		82/16	
Infection	Non-infected	Infected	Non-infected	Infected
Total polyphenols ¹	150.20 ± 4.28 ^a	86.93 ± 2.84 ^b	98.51 ± 6.55 ^c	88.81 ± 8.12 ^{bd}
Total flavonoids ¹	13.96 ± 1.74 ^a	5.25 ± 0.67 ^b	8.61 ± 0.18 ^c	5.03 ± 0.39 ^{bd}
DPPH ²	57.16 ± 3.49 ^a	46.21 ± 5.83 ^b	35.94 ± 1.69 ^c	57.18 ± 2.23 ^a
ABTS ²	43.30 ± 5.07 ^{ac}	34.24 ± 3.25 ^b	37.45 ± 1.5 ^{ab}	45.26 ± 4.01 ^c
FRAP ²	127.32 ± 7.97 ^a	116.05 ± 12.24 ^a	95.35 ± 7.10 ^b	133.41 ± 13.71 ^a

Value is a mean of three replicates ± standard deviation (SD)

¹Expressed as mg Quercetin/100 g FW ²Expressed as mg Trolox/100 g FW

Value without the same superscript within each column differ significantly at $p < 0.05$ (Bonferroni *post hoc* test)

Taking into account the ANOVA, interaction between genotype and infection show statistically significant ($p < 0.05$) influence on the all measured biochemical assays but genotype as a single factor do not have statistically significant influence on the values of ABTS and FRAP tests.

Infected Anita fruits expressed lower antioxidant activity than non-infected fruits. This could be in a close connection with the reduction of amount polyphenol compounds. Breeding line 82/12 was shown completely opposite results—in the infected fruits antioxidant activity was higher than non-infected peppers. This indicates the possibility that some other non-phenolic compounds have the main role in the mechanisms of antioxidant protection of pepper fruits. According to some authors, carotenoids, capsaicinoids, vitamins C and E have the most important role in the antioxidant activity [17, 18].

Table 3 Correlation coefficient between biochemical assays

	Total polyphenols ¹	Total flavonoids ¹	DPPH ²	ABTS ²	FRAP ²
Total polyphenols ¹			0,099918	0,123991	0,012174
Total flavonoids ¹	0,756846*	1,000000	-0,065872	0,021361	0,001740

*Statistically significant at $p < 0,05$ (Spearman correlation)

¹Expressed as mg Quercetin/100 g FW ²Expressed as mg Trolox/100 g FW

Considering the correlation coefficients, polyphenols and flavonoids are in a very weak correlation with all measured antioxidant tests in our study (Table 2). These results are in agreement with the report of Škrovánková et al [19].

Conclusion

The amount of measured polyphenols and flavonoids decreased in infected fruits of both tested genotypes. Taking into account the values of antioxidant tests, non-infected fruits of Anita cultivar show higher antioxidant activity than infected fruits. Even though antioxidant activity is higher in infected fruits than in non-infected fruits of breeding line 82/16, there is no correlation with phenols and flavonoids. The values of correlation coefficient between antioxidant tests and concentration of total polyphenols and flavonoids for both genotypes

might indicate that some other compounds have the principal role in antioxidant activity of tested pepper fruits.

Acknowledgements

This study was supported by the Ministry of Education, Science and Technological Development of Republic of Serbia under the project "Developing vegetable varieties and hybrids for outdoor and indoor production" (TR 31030).

References

- [1] J. Costa, R. Rodríguez, E. Garcia-Cela, A. Medina, N. Magan, N. Lima, C. Santos, Overview of Fungi and Mycotoxin Contamination in Capsicum Pepper and in Its Derivatives, *Toxins*, 2019, 11(1):27
- [2] I. Perucka, M. Materska, Antioxidant activity and content of capsaicinoids isolated from paprika fruits, *Polish Journal of Food and Nutrition Sciences*, 2003, 12/53(2):15-18
- [3] H. K. M. Padilha, E. dos S. Pereira, P. C. Munhoz, M. Vizzotto., R. A. Valgas., R. L. Barbieri, Genetic variability for synthesis of bioactive compounds in peppers (*Capsicum annuum*) from Brazil, *Food Science and Technology*, 2015, 35(3), 516–523
- [4] M. M. Wall and C. L. Biles, *Alternaria* Fruit Rot of Ripening Chile Peppers, *Postharvest Pathology and Mycotoxins*, 1993, 83:324-328
- [5] A. Halfon-Meiri and I. Rylski, Internal Mold Caused in Sweet Pepper by *Alternaria alternata*: Fungal Ingress, Etiology, 1983, 73(1):67-70
- [6] E. Fallik, S. Grinberg, S. Alkalai, S. Lurie, The effectiveness of postharvest hot water dipping on the control of grey and black moulds in sweet red pepper (*Capsicum annuum*), *Plant Pathology*, 1996, 45 (4): 644-649
- [7] M. Frans, R. Aerts, S. Laethem, B. Van Calenberge, L. Van Herck., K. Heungens, K. Van Poucke, S. Van Gool, J. Ceusters, Development of a quick screenig bioassay for internal fruit rot in bell pepper (*Capsicum annuum* L.). XVI Eucarpia Caspsicum and Eggplant Meeting, Kecskemet, Hungary, 12-14. September, 2016, 420-424.
- [8] P. C. Wootton-Beard, A. Moran, L. Ryan, Stability of the total antioxidant capacity and total polyphenol content of 23 commercially available vegetable juices before and after in vitro digestion measured by FRAP, DPPH, ABTS and Folin–Ciocalteu methods, *Food Research International*, 2011, 44 (1) : 217-224
- [9] A. Saha., R. Rahman., M. Shahriar., S. Saha., N. Al Azad., S. Das, Screening of six Ayurvedic medicinal plant extracts for antioxidant and cytotoxic activity, *Journal of Pharmacognosy and Phytochemistry*, 2013, 2 (2): 181-188
- [10] N. Yazdizadeh Shotorbani, R. Jamei, R. Heidari, Antioxidant activities of two sweet pepper *Capsicum annuum* L. varieties phenolic extracts and the effects of thermal treatment, *Avicenna Jurnal of Phytomedicine*, 2013;3(1):25–34.
- [11] D. Zheleva-Dimitrova, P. Nedialkov, G. Kitanov, Radical scavenging and antioxidant activities of methanolic extracts from *Hypericum* species growing in Bulgaria, *Pharmacognozy Magazine*, 2010, 6(22):74–78
- [12] K Thaipong, U. Boonprakob, K. Crosby, L. Cisneros-Zevallos, D. Hawkins Byrne, Comparison of ABTS, DPPH, FRAP, and ORAC assays for estimating antioxidant activity from guava fruit extracts, *Journal of Food Composition and Analysis*, 2006, 19(6-7), 669–675
- [13] D. M Pott, S. Osorio, J. G Vallarino, From Central to Specialized Metabolism: An Overview of Some Secondary Compounds Derived From the Primary Metabolism for Their Role in Conferring Nutritional and Organoleptic Characteristics to Fruit, *Front Plant Science*, 2019;10:835

- [14] C. Kevers, M. Falkowski, J. Tabart, J.-O Defraigne, J. Dommes, J. Pincemail, Evolution of Antioxidant Capacity during Storage of Selected Fruits and Vegetables, *Journal of Agricultural and Food Chemistry*, 2007, 55(21), 8596–8603
- [15] L. Á. Medina-Juárez, D. M. A. Molina-Quijada, C. L. Del Toro Sánchez, G. A. González-Aguilar, N. Gámez-Meza, Antioxidant activity of peppers (*Capsicum annuum* L.) extracts and characterization of their phenolic constituents, *Interciencia*, 2012, 37 (8): 588-593
- [16] N. Zaki, A. Hakmaoui, A. Ouattmane, A. Hasib, A. Fernandez-Trujillo, Bioactive components and antioxidant activity of Moroccan paprika (*Capsicum annuum* L.) at different period of harvesting and processing, *Biology Agriculture and Healthcare*, 2013, 3(8):1-8
- [17] J.-S. Kim, J. Ahn, S.-J. Lee, B. Moon, T.-Y Ha, S. Kim, Phytochemicals and Antioxidant Activity of Fruits and Leaves of Paprika (*Capsicum Annuum* L., var. Special) Cultivated in Korea, *Journal of Food Science*, 2011, 76(2), 193–198.
- [18] M. H. Gnayfeed, H. G Daood, P. A. Biacs, C. F. Alcaraz, Content of bioactive compounds in pungent spice red pepper (paprika) as affected by ripening and genotype, *Journal of the Science and Food Agriculture*, 2001, 81(15):1580-1585
- [19] S. Škrovánková, J. Mlček, J. Orsavová, T. Juríková, P. Dřimalová, Polyphenols content and antioxidant activity of paprika and pepper spices, *Potravinárstvo Slovak Journal of Food Sciences*, 2017, 11(1), 52-57

CHEMOMETRICS STUDY OF GERMS PLANT FOR DETERMINING THE ANTICANCER ACTIVITY

Alina-Maria Petrescu¹, Lauriana-Eunice Zbîrcea^{1,6}, Maria-Roxana Buzan^{1,6}, Marieta – Elena Furdui^{1,2}, Gianina-Loredana Jucos¹, Feng Chen Ifrim^{1,3}, Gheorghe Ilia^{1,4}, Virgil Paunescu^{1,5}

¹OncoGen Centre, County Hospital "Pius Branzeu", Blvd. Liviu Rebreanu 156, RO-300736, Timisoara, Romania, alinapetrescu79@gmail.com

²West University of Timisoara, Physics Faculty, Blvd. Vasile Parvan, number 4, 300223, e-mail: marieta.furdui93@e-uvt.ro

³Department of Marketing medical technology, Carol Davila University of Medicine and Pharmacy, 020021, Romania; adsm.adsm@yahoo.com

⁴Institute of Chemistry of the Romanian Academy, 24 Mihai Viteazu Bvd. 300223, Timisoara, Romania, ilia@acad-icht.tm.edu.ro; gheilia@yahoo.com

⁵Department of Immunology, University of Medicine and Pharmacy "Victor Babes", Eftimie Murgu Sq. 2, Timisoara, 300041, Romania; virgilpaunescu@oncogen.com

⁶University of Medicine and Pharmacy "Victor Babes", Eftimie Murgu Sq. 2, Timisoara, 300041, Romania, zbircea.lauriana@umft.ro; buzan.roxana@umft.ro

Abstract

This project started from the premise that in nature, there are substances capable of preventing the occurrence of cancer, or, at least keeping it in its early stages, by using plant germs.

Germs were obtained from Biovita germs machine, like: watercress, unshelled and genetically modified soybeans, hyssop, sage, fennel, amaranth, broccoli, radish, alfalfa, cumin, caraway, rye, wheat, buckwheat, and the next step was to extract the substances from these germs, and analyzed by LS/MS, for the identification of polyphenolic compounds, which are antioxidants, which play a very important role in the prevention of cancer, mainly alpha-linolenic acid, the main source of omega 3 fatty acids, essential for the human body.

The process was carried out in several stages, namely: the germination period was 4-5 days, followed by maceration in hydroalcoholic solution with 99% ethyl alcohol, then the decoction and percolation in the system provided with separating funnel, filter and Erlenmayer glass.

The antioxidant activity was determined using spectrophotometry (Tecan Sunrise™ – A Reliable Absorbance Reader), using as a calibration sample, ascorbic acid, the absorbance of which was already known from the literature data, namely 600 nm. The presence of riboflavin, at an absorbance of 440 nm, allantoin, 517 nm, quercetin, at an absorbance of 385 nm, choline, at 570 nm, and thiamine at an absorbance of 520 nm, was identified. The calibration curve was obtained based on the values of the concentrations used and the absorbance obtained. The scavenging was determined, on the basis of which the antioxidant activity was identified.

DEVELOPMENT OF MODERN HIGH RESOLUTION MASS SPECTROMETRY PLATFORM FOR GLYCOLIPID MAPPING IN DEFINED HUMAN BRAIN REGIONS

Alina Petrut¹, Anca Simulescu², Raluca Ica¹, Mirela Sarbu¹, Cristian V.A. Popescu³,
Alina D. Zamfir^{1,4}, Andrei J. Petrescu³

¹National Institute for Research and Development in Electrochemistry and Condensed Matter, Timisoara, Romania; ²“Victor Babes” University of Medicine and Pharmacy, Timisoara, Romania; ³Institute of Biochemistry of the Romanian Academy, Bucharest, Romania; ⁴“Aurel Vlaicu” University of Arad, Arad, Romania
e-mail: alina_mld@yahoo.com

Abstract

Gangliosides (GGs) are present and concentrated on cell surfaces, with the two lipid chains of the ceramide moiety embedded in the plasma membrane and the oligosaccharide chain located on the extracellular surface, where they constitute points of recognition for extracellular molecules or surfaces of neighbouring cells. Gangliosides are found predominantly in the nervous system, were involved in a series of biological and pathological processes.

The introduction of electrospray (ESI) ion sources into biological mass spectrometry (MS) addressed the fundamental issue of how to analyze minute amounts of complex biological samples. A strategy to characterize and monitor the changes with age of the GG profile in different developmental stages of human cerebellum, by ESI Orbitrap MS and tandem MS (MS²) is presented here. Two native ganglioside mixtures originating from normal human fetal cerebellum in the 15th (Cc15) and 40th (Cc40) gestational week were subjected to Orbitrap MS and multistage MS (MSⁿ) by collision induced dissociation (CID) analysis under thoroughly optimized experimental conditions. Both native GGs were dissolved in pure methanol up to final concentration of 10 pmol/μL. After only 2 min of signal acquisition in the negative ion mode, over 100 species have been detected and identified, among them several potential biomarkers. Although a similar number of species were identified in both mixtures, the GG profile was found to be essentially different. Obtained results also indicated differences in the expression of polysialylated species in the two ganglioside mixtures, which support an earlier hypothesis regarding the direct correlation between sialylation degree and brain developmental stage.

The method provided elevated ionization efficiency, high speed of analysis, almost 100% in-run and run-to-run reproducibility at a sample consumption per experiment situated in the femtomole range.

Acknowledgements

This project was supported by the Romanian National Authority for Scientific Research, UEFISCDI through projects PN-III-P4-ID-PCE-2016-0073, PN-III-P1-1.2-PCCDI-2017-0046 granted to ADZ and PN-III-P1-1.1-PD-2016-0256 granted to MS.

INFLUENCE OF HIGHWAY DISTANCE ON HEAVY METALS DYNAMICS IN THE SOIL-FRUIT SYSTEM

Radmila Pivić¹, Zoran Dinić¹, Jelena Maksimović¹ Aleksandra Stanojković-Sebić¹

¹*Institute of Soil Science, Belgrade, Teodora Drajzera 7, Serbia
e-mail: drradmila@pivic.com*

Abstract

At five locations of apple orchards grown on eutric cambisol at a different distance from the E 75 highway, the presence of heavy metals in soil and plant material was examined. In the soil samples it were determined pH in 1M KCl, CaCO₃, total C, SOM, content of clay and content of total and available forms of Cu, Ni, Pb and Zn. Content of Cu, Ni, Pb and Zn was analyzed in the plant material. In the tested soil samples, the content of the total forms of the tested elements is within the limits of maximum allowable concentrations, while in the tested plant material, only the content of lead in one of the five tested apple samples is within the permitted limits. In apple samples from locations 30 m away from the highway, the lead content is well above the limit values, which requires further research to determine whether the increased concentration of this element is due to aerosol pollution or protective equipment applied.

Key words: Highway, soil, apple, heavy metals

Introduction

Metals are the main inorganic pollutants related to traffic. Common source of soil and plant contamination with heavy metals is traffic [8]. Metals are also found in road dust, emitted by vehicles, particles from the deterioration of the track pavement, industrial activities, and naturally from the soil minerals [7, 20]. Fast development of industry, continuously increasing population, and intensification of road traffic are regarded as the foremost causes of ecosystem pollution in urban areas [9]. Cr and Ni are more associated with the corrosion of vehicles and their chrome parts [3]. Numerous studies on roadside soil pollution have focused on total emission loads of heavy metals into open grassland and agricultural areas [18]. Generally, total heavy metal contents in roadside soils were found strongly dependent on traffic density and showed an exponential decrease with distance from the road, reaching background levels 10-100 meters. The most frequently reported heavy metals of concern have been Pb, Zn and Cu. Among the contaminants that are transferred to plant tissue are Cd, Cr, Cu, Ni, Pb, Zn and their uptake depends on their concentration in the soil solution, which in turn is affected by the level and form of metal present and soil pH. In general, the solubility and uptake of metals are less at higher soil pH [12]. The mobility of the trace elements and their translocation in the plant are influenced by the content of the clay fraction, organic matter and pH value of soil [4]. Plants are the intermediaries through which elements from the soil and partly from the air and water are transferred to the human body by consumption. Some of the elements are necessary for growth and development of crops and without them they cannot survive, some of them have stimulating effect on plant growth, while a group of elements at high concentrations affects very toxically on the plants [18]. Concentrations of metals in plants vary with plant species [1]. Plant uptake of heavy metals from soil occurs either passively with the mass flow of water into the roots, or through active transport crosses the plasma membrane of root epidermal cells [13]. Heavy metals are naturally present in the environment, however, the dynamic development of industry and motorization, as well as the

continuing over-intensive use of various chemical compounds in agriculture, causes constantly increase of toxic heavy metals in the environment [2].

Material and Methods

Sampling of soil samples to a depth of 30 cm and apples from the orchard was performed in orchard established on soil type Eutric Cambisol [19], at a distance of 30, 50 and 400 meters from the highway lane E 75 during August and September 2010, as part of research within the project "Investigation of the presence of dangerous and harmful substances in agricultural soil on the most important crop and vegetable crops in the E 75 highway zone", which covered the entire section of the above mentioned highway. Table 1 presents the coordinates of the sampling locations and the distance from the highway lanes.

Table 1.-List of locations of samples and type of soil

Study site	(m from route lanes)	Coordinate	
		X	Y
1	D(30)	7475052	4935866
2	D(50)	7475069	4935835
3	D(30)	7490188	4937435
4	D(50)	7490165	4937420
5	D(400)	7490042	4937222

Soil analysis

In the laboratory, composite soil samples were dried and passed through a 2-mm sieve. Soil pH in water and in 1M KCl was analyzed potentiometrically, using glass electrode (SRPS ISO 10390:2007); calcium carbonate by volumetric method SRPS ISO 10693: 2005- Determination of carbonate content; total contents C was analyzed on elemental CNS analyzer Vario EL III [16]. SOM (soil organic matter) was calculated using the formula: SOM content (%) = organic C content (%) x factor 1.724 in carbonless soil samples, ie SOM content (%) = (organic C content (%) - 0.12 x% CaCO₃) x factor 1.724 for carbonate soil samples [5]; granulometric composition was analyzed by standardized method by sieving and sedimentation (ISO 11277: 2009(E), 2009). Determination of trace elements in ICP-AES soil extracts was analyzed by standardized method ISO 22036: 2008; Available forms of Ni, Pb, Cu, Zn - DTPA buffer solution extraction and determination by ICP using method: SRPS ISO 14870: 2005. Reference soil NCS ZC 73005 (Soil Certificate of Certified Reference Materials approved by China National Analysis Center Beijing China) and reagent blanks were used as the quality assurance and quality control (QA/QC) samples during the analysis.

Plant analysis

Analyzed aerial parts of the study plant species were dried for 2 hours at 105°C, using gravimetric method for determination of dry matter content of plant tissue. The dry matter determination is used to correct the sample element concentration to an absolute dry matter basis [15]. The content of heavy metals in selected plants was determined with an inductively coupled plasma optical emission spectrometer ICAP 630 (ICP-OES), after the samples were digested with concentrated HNO₃/H₂O₂ for total form extraction.

Results and discussion

Soil suitable for the production of health safe food should not contain dangerous and harmful substances, so it is very important to know their content and distribution. High concentrations of heavy metals in soil pose a significant risk to the agro-ecosystem because of their persistancy and, when incorporated in to the soil, remain present for many years, building

strong links with soil components. The origin and content of heavy metals is primarily of geochemical origin, but also due to atmospheric deposition as is the case on soil adjacent to roads. Likewise, one of the causes of the increased content of heavy metals may be of anthropogenic character by the application of fertilizers and pesticides containing increased concentrations of heavy metals that accumulate in it. The land on which the apple plantations are based belongs to the type Eutric Cambisol [19]. The obtained values of the content of the studied Physical and chemical properties of tested soil samples and microelements and heavy metals are shown in Table 2 and 3.

Table 2. Physical and chemical properties of tested soil samples

Study site	Clay fraction (<0.002 mm) %	pH 1M KCl	C (%)	CaCO ₃ (%)	SOM (%)
1	12.1	6.10	3.11	0.41	5.27
2	11.3	4.40	1.90	BLMD	3.27
3	7.8	6.30	2.03	BLMD	3.50
4	8.2	6.20	1.99	BLMD	3.43
5	7.5	3.60	2.35	BLMD	4.05

SOM-soil organic matter; BLMD-below the limit of the method detection

Table 3. The content of total and available forms trace elements in soil samples

Study site	Soil total forms				Soil available forms			
	Cu	Ni	Pb	Zn	Cu	Ni	Pb	Zn
	(mg kg ⁻¹)							
1	19.62	34.19	34.84	80.31	2.50	1.10	2.12	4.65
2	28.82	34.68	32.60	71.91	7.80	2.39	3.09	7.12
3	23.85	48.20	50.60	73.76	4.20	2.32	1.86	4.38
4	23.68	49.74	29.83	66.66	4.10	2.64	1.55	4.64
5	38.05	41.12	32.58	80.21	11.40	3.00	3.50	6.12

The interpretation of data on the trace elements content in soil samples was done according to the Rule book of maximum permissible levels (MPL) of dangerous and hazardous materials in soil and water for irrigation and methods for analysis [17], where MPL for Cu is 100 mg kg⁻¹, MLP for Zn is 300 mg kg⁻¹, MPL for Ni is 50 mg kg⁻¹ and MLP for Pb is 100 mg kg⁻¹.

The interpretation of the results of the heavy metal content in the tested apple fruit was based on additional literature sources were used for data analysis: recommendations of the World Health Organisation on maximum allowable concentrations of heavy metals in fruits and vegetables [6] and scientific literature [14,10,11], Table 4.

Table 4. Average and toxic concentration of heavy metals in plants

Element	Limit values WHO	Normal content in plants Kloeke et al. *	Critical contents for plant food Kloeke et al. *	Critical concentration Kastori et al.**	Toxical concentration Kastori et al.**
		(mg kg ⁻¹)			
Cu		3-15	15-20	15	20
Ni		0.1-5	20-30	20	30
Pb	0.3		0.1-0.2	0.1	0.2
Zn		15-150	150-200	150	200

Table 5. shows the percentages of examined Cu, Ni, Pb and Zn in the fresh matter of the apple fruit by test locations.

Table 5. The content of the tested elements in the apple fruit calculated on fresh matter

Location	1	2	3	4	5
Element	(mg kg ⁻¹) fresh matter				
Cu	1,38	0,99	1,31	0,98	1,04
Ni	0,7	0,77	0,29	0,26	1,78
Pb	1,64	0,28	1,49	0,19	0,26
Zn	8,98	14,55	12,63	8,38	9,01

The obtained results indicate that the content of the tested elements above the MPC was not detected in the tested soil samples. In the samples of apple fruits only in sample 4, the content of Pb is within the allowed limits, therefore, further investigations would require a more detailed examination of the possible impact of aerial contamination and contamination of the fruits due to the use of plant protection products. In samples 1 and 3, the lead content is well above the limit value, and since it was sampled at a distance of 30 m from the highway, it is assumed that the the main cause of contamination is motor vehicle exhausts since the use of lead-containing petroleum products ceased in 2011.

Acknowledgment: This research was financially supported by the Ministry of Education, Science and Technological Development, Republic of Serbia [Project TP 37006].

References

- [1] B.J., Alloway, 1994. Toxic metals in soil–plant systems. Chichester, UK: John Wiley and Sons.
- [2] N., Blagojević, B., Damjanović-Vratnica, V., Vukašinović-Pešić, D. Đurović. Heavy Metals Content in Leaves and Extracts of Wild-Growing *Salvia Officinalis* from Montenegro, Polish Journal of Environmental Studies, (2009) 18, (2):167-173.
- [3] J.A., Carrero, I., Arrizabalaga, J., Bustamante, N., Goienaga, G., Arana, J.M., Madariaga, Diagnosing the traffic impact on roadside soils through a multianalytical data analysis of the concentration profiles of traffic-related elements. Sci Total Environ (2013) 458-460:427–434. <https://doi.org/10.1016/j.scitotenv.2013.04.047>
- [4] Z., Dinić, J., Maksimović, A., Stanojković-Sebić, R., Pivić. The content of trace elements in forage crops grown on diverse soils of the Mali Zvornik municipality in Serbia, 11th International Scientific/Professional conference Agriculture in nature and environment protection, Vukovar, Hrvatska, (2018) P58.
- [5] R., Džamić, D., Stevanović, M., Jakovljević (1996): Agrochemistry Manual. Faculty of Agriculture, University of Belgrade, Serbia, (in Serbian).
- [6] FAO/WHO Expert Committee on Food Additives (1999). Summary and conclusions. Pro. of the 53rd Meeting Joint FAO/WHO Expert Committee on Food Additives, Rome, Italy.
- [7] W., Gope, R.E., Masto, J., George, R.R., Hoque, S., Balachandran. Bioavailability and health risk of some potentially toxic elements (Cd, Cu, Pb and Zn) in street dust of Asansol, India. Ecotoxicol Environ Saf (2017) 138:231–241.
- [8] B.A., Gworek, M., Deckowska M., Pierscieniak. Traffic Pollutant Indicator: Common Dandelion (*Teraxacum Officinale*), Scots Pine (*Pinus Silvestris*), Small-Leaved Lime (*Tilia Cordata*), Polish Journal of Environmental Studies, (2011) 20,(1):87-92.
- [9] B., Jankiewicz, D., Adamczyk. Assessing Heavy Metal Content in Soils Surrounding a Power Plant, Short commu., Polish Journal of Environm. Studies (2010) 19,(4), pp.849-853.
- [10] R., Kastori, N., Petrović, I., Arsenijević-Maksimović. Teški metali u životnoj sredini (R. Kastori, ed.). Naučni institut za rat. i povrtarstvo, Novi Sad, (in Serbian) (1997) pp.196-257.

- [11] R., Kastori, P., Sekulić, N., Petrović, I., Arsenijević-Maksimović. Osvrt na granične vrednosti sadržaja teških metala u zemljištu u nas i u svetu. Zbornik radova Instituta za ratarstvo i povrtarstvo (2003) 38: 49-58.
- [12] M.G., Kibblewhite. Contamination of agricultural soil by urban and peri-urban highways: An overlooked priority? *Environmental Pollution* 242 (2018) 1331e1336.
- [13] I.S., Kim, H.K., Kang, P., Johnson-Green, E.J., Lee. Investigation of heavy metal accumulation in *Polygonum thunbergii* for phytoextraction. *Environ Pollut* (2003) 126:235-43.
- [14] A., Kloeke, D.R., Sauerbeck, H., Vetter. The contamination of plants and soils with heavy metals and the transport of metals in terrestrial food chains. In: J. O. Nriagu, Editor, *Changing Metal Cycles and Human Health: Report of the Dahlem Workshop on Changing Metal Cycles and Human Health*, Germany, Springer, Berlin, (1984) pp.113-141.
- [15] R.O., Miller. Determination of dry matter content of plant tissue: gravimetric moisture, In: Kalra Y.(ed.) *Handbook of reference methods for plant analysis*, CRC Press, Taylor&Francis Group, Boca Raton, Florida, USA, (1998) pp.51-52.
- [16] D.W., Nelson, L.E., Sommers. Total Carbon, Organic Carbon, and Organic Matter. In: *Methods of Soil Analysis. Part 3*. Ed Sparks D.L. SSSA, Madison, Wisconsin, USA, (1996) 961-1010.
- [17] Official Gazette of Republic of Serbia, 1994:23. Rule book of allowed concentrations of dangerous and hazardous materials in soil and in water for irrigation and methods for analysis.
- [18] R., Pivić, A., Stanojković-Sebić, D., Jošić. Assessment of soil and plant contamination by select heavy metals along a major european highway. *Pol. J. Environ. Stud.* (2013) 22 (3), 1465–1472.
- [19] WRB (2015): World Reference Base for Soil Resources 2014 International soil classification system for naming soils and creating legends for soil maps Update 2015. Food and Agr. Organization of the United Nations, Rome, [://www.fao.org/3/i3794en/I3794en.pdf](http://www.fao.org/3/i3794en/I3794en.pdf)
- [20] S. Zanello, V.F., Melo, N., Nagata. Study of different environmental matrices to assess the extension of metal contamination along highways. *Environmental Science and Pollution Research* (2018) 25:5969–5979 <https://doi.org/10.1007/s11356-017-0908-z>

A COMPARATIVE STUDY BETWEEN CORROSION PROTECTION OF DIFFERENT SUBSTITUTED Pt-METALLOPORPHYRINS

Nicoleta Plesu¹, Milica Tara-Lunga Mihali¹, Eugenia Fagadar-Cosma¹

¹*Institute of Chemistry "Coriolan Dragulescu", M. Viteazul Ave. 24, 300223-Timisoara, Romania, Tel: +40256/491818; Fax: +40256/491824*

** email: plesu_nicole@yahoo.com*

Organic compounds containing N, S and O heteroatoms, and / or aromatic or other π -electronic systems, exhibit excellent potential for corrosive protection. The porphyrin molecule, by its extended aromatic structure promises to be a potential corrosion inhibitor due to its strong binding ability to metal surfaces. The metal present in the metalloporphyrins inner core presents as good adsorption properties as porphyrin-base molecules. [1]. The current investigation presents the comparative results of two different substituted Pt-porphyrin compounds (**Figure 1**), namely: Pt(II)-5,10,15,20-tetra(4-methoxy-phenyl)-porphyrin (Pt-TMeOPP) bearing inductive donor methoxy groups and Pt(II) -5,10,15,20-tetra-allyloxyphenylporphyrin (Pt-TAPP), that is grafted with electron withdrawing allyloxy groups regarding corrosion inhibitor properties for carbon steel in 3% NaCl solutions.

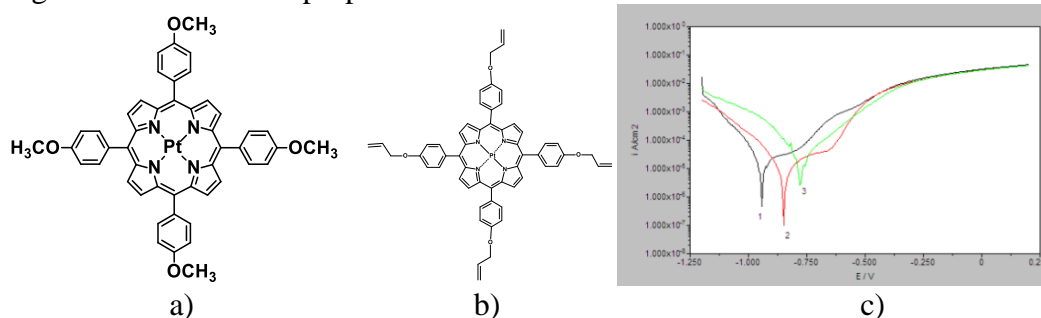


Figure 1. a) Porphyrin (Pt-TMeOPP), b) (Pt-TAPP) structures and c) potentiodynamic polarization curves for carbon steel after 60 min. immersion in 3 % NaCl solutions without (1) and with porphyrins: Pt-TMeOPP (2) and Pt-TAPP (3), scan rate = 1 mV/s.

The Pt-TMeOPP molecule satisfies the criteria of an effective inhibitor and can form a protective layer on metal surface (cover properly the active centers of the metal surface) avoiding the aggressive species to reach to the metal surface. The Pt-TMeOPP shows good anticorrosive protection to iron in saline solution. The polarization resistance increase from 53.9 Ohm (iron in saline media) to 1271 Ohm in the presence of this metal porphyrin. The corrosion rate is 0.10 mm/year less than 0.26 mm/year for iron in saline solution and 0.48 mm/year for Pt-TAPP. Thus, Pt-TAPP has not provided a suitable anticorrosive protection due to peripheral functional group, steric hindrance and electron density at donor reaction sites that affect the binding stability to metal surface. This Pt-porphyrin appears to form a thin, porous and incomplete layer on iron surface resulting in inefficient protection.

Acknowledgements

The authors are acknowledging UEFISCDI PN-III-P1-1.2-PCCDI-2017-1-Project ECOTECH-GMP 76PCCDI/2018 and the Romanian Academy for financial support in the frame of Programme 3/2019 from ICT.

References

[1] K.S. Lokesh, M. de Keersmaecker, A. Adriaens. *Molecules* 17 (2012) 7824.

EFFECT OF INTERMOLECULAR INTERACTIONS ON PHASE COMPATIBILITY AND MATERIAL PROPERTIES IN ORGANIC-INORGANIC COMPOSITE BLENDS

Adina Maria Dobos¹, Anca Filimon¹, Adriana Popa^{2*}

¹Department of Physical Chemistry of Polymers, "Petru Poni" Institute of Macromolecular Chemistry, Aleea Grigore Ghica Voda 41 A, 700487 Iasi, Romania

²"Coriolan Drăgulescu" Institute of Chemistry, 24 Mihai Viteazul Blv., 300223, Timisoara, Romania

*e-mail: apopa_ro@yahoo.com

Abstract

The concentrated solutions of cellulose acetate (CA) in tetrahydrofuran (THF) with different content of tetraethyl ortosilicate (TEOS) (1.0-2.0 (wt.%/wt.)) were analyzed in terms of the intermolecular interactions by dynamic viscometric measurements and Fourier-transform infrared spectroscopy (FTIR) analysis. For all studied systems the flow behavior is governed by hydrogen and covalent bonds that have an impact on the dynamic viscosities and flow activation energy (E_a), implicitly. Thus, was observed that the flow activation energies increase with the increasing of TEOS content in CA solutions. This means that, besides to polymer/solvent interactions, which established between the cellulose acetate and tetrahydrofuran, new hydrogen and covalent bondings generated by silanol groups of TEOS and -OH groups of CA occurs, leading to an increase in E_a (Fig. 1).

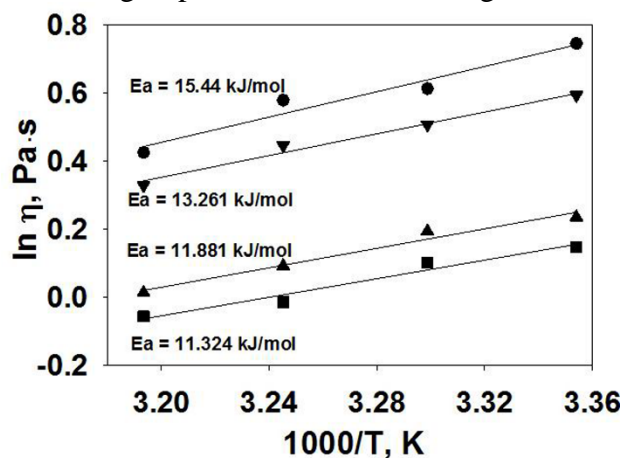


Fig. 1. Plot of $\ln \eta_s$ versus $1000/T$ for CA/TEOS blends at different mixing ratios: (■) CA, (▲) CA/1wt.% TEOS, (▼) CA/1.5wt.% TEOS, (●) CA/2wt.% TEOS.

A higher value of E_a corresponds to a low polymer flexibility which slows the flow process and determines the appearance of gel behavior. In addition, SiO_2 resulting from the hydrolysis and condensation of TEOS, which take place during the process of the solutions obtaining, may generates crosslinking points in the polymeric systems, increasing its rigidity and leading to high values of E_a . These results are also reflected in FTIR spectra of the films corresponding to the solutions rheological analyzed, where the shape and intensity of the peaks confirm the occurrence of some additional interactions with increasing of TEOS content in CA casting solution. It was demonstrated thus, that, for a TEOS content less than 1.00 wt.%/wt.% and greater than 1.5 wt.%/wt.%, the intermolecular interactions prevent the formation of films/membranes.

Consequently, the results of this study are essential in different fields of applicability, considering the intermolecular interactions impact in the process of the supramolecular structures obtaining.

EFFECT OF DIFFERENT SWELLING AGENTS ON TEXTURAL AND STRUCTURAL PROPERTIES OF MODIFIED MESOPOROUS SILICA

Alexandru Popa¹, Silvana Borcanescu¹, Paul Barvinschi², D. Bajuk-Bogdanović³,
S. Uskoković-Marković⁴, I. Holclajtner-Antunović³

¹*Institute of Chemistry Timișoara, Bl. Mihai Viteazul 24, 300223 Timisoara, Romania*

²*Faculty of Physics, West University of Timisoara, B-dul V. Parvan, Nr. 4, 300223 Timisoara, Romania*

³*Faculty of Physical Chemistry, University of Belgrade, P.O. Box 47, 11158 Belgrade, Serbia*

⁴*Faculty of Pharmacy, University of Belgrade, P.O. Box 146, 11001 Belgrade, Serbia*

e-mail: alpopa_tim2003@yahoo.com

Abstract

In this study was carried out the preparation of some large-pore ordered mesoporous silicas using a proper surfactant with different swelling agents. In order to use a micelle swelling agent with a moderate swelling ability we selected three swelling agents: 1-phenyl-decane, butyl benzene and mesitylene. The aim of these synthesis was to achieve a pore diameter enlargement but in the same time to avoid the formation of heterogeneous and/or poorly defined nanostructure of silica.

These composites were characterized by FT-IR spectroscopy, X-ray diffraction at low angles, nitrogen physisorption at 77 K, SEM-EDS. In the view of a possible use of these amino-functionalized mesoporous silicas as adsorbents for CO₂ removal, their adsorption-desorption properties towards CO₂ were investigated by the TPD method.

CO₂ adsorption isotherms of amino-functionalized mesoporous silicas measured at 50, 60 and 70 °C showed that the adsorption capacity (mg CO₂/g adsorbent) depend on the temperature of adsorption and on the type of swelling agents and amination reagents used.

Introduction

Solid sorbents adsorption is considered as a potential option for the CO₂ capture process. In the literature adsorption of CO₂ was investigated over a wide range of conditions on a series of mesoporous silica adsorbents comprised of conventional silica, MCM-41 and SBA-15 molecular sieves [1-3].

L. Bakhtiari et al. was shown that the use of swelling agent was an effective technique to control the pore characteristics in the mesoporous particles. The results showed that the use of an optimum amount of 1-dodecanethiol (swelling agent) can increase the pore diameter size and the distance between the pore centers [4].

So, the synthesis of mesoporous materials with amine functionalized groups with high adsorption capacity and selectivity for CO₂ capture process is an important task for the future.

Three different modified mesoporous silica compounds were synthesized by the hydrolysis of tetraethyl orthosilicate using as surfactant a P123 block copolymer and 3 different compounds as swelling agents: 1-phenyl-decane, butyl benzene and mesitylene. The prepared compounds were denoted as: SSBA-15-Dec, SSBA-15-BB and SSBA-15-Mes.

These composites were characterized by FT-IR spectroscopy, X-ray diffraction at low angles, nitrogen physisorption at 77 K, SEM-EDS and evaluated by the adsorption of CO₂ and its temperature programmed desorption – TPD.

Experimental

Three different modified mesoporous silica compounds were synthesized by the hydrolysis of tetraethyl orthosilicate using as surfactant a P123 block copolymer and 3 different compounds as swelling agents: 1-phenyl-decane, butyl benzene and mesitylene. The prepared compounds were denoted as: SSBA-15-Dec, SSBA-15-BB and SSBA-15-Mes.

For the synthesis of SSBA-15-Dec: 4.6 g of Pluronic P123 was dissolved in 145 ml of HCl solution and stirred at 40 °C until the solution became clear. Then, 9.0 g of 1-phenyl-decane was added to the solution with stirring at 40 °C for 1 h. Finally, 0.05 g of NH₄F was added under stirring, followed by 9.0 g of TEOS. The above mixture was stirred at 40 °C for 24 h and then transferred to an autoclave for further reaction at 100 °C for 48 h. The preparation method was almost the same for SSBA-15-BB and SSBA-15-Mes with the difference of swelling agent which was butyl benzene and mesitylene, respectively. After filtration and drying, the adsorbents were obtained as white solids.

Textural characteristics of the outgassed samples were obtained from nitrogen physisorption at 77K using a Quantachrome instrument, Nova 2000 series instrument. The specific surface area S_{BET} , mean cylindrical pore diameters d_p and adsorption pore volume V_{pN_2} were determined. Powder X-ray diffraction data were obtained with a XD 8 Advanced Bruker diffractometer using the Cu K α radiation in the range $2\theta = 0.5^\circ$ to 5° and $2\theta = 5^\circ$ to 60° . The FTIR absorption spectra were obtained with: Jasco 430 spectrometer in the 4000 - 400 cm⁻¹ range, using KBr pellets. Microstructural characterization by SEM-EDS of the composites particles was carried out with a Jeol JSM 6460 LV instrument equipped with an EDS analyzer.

Adsorption measurements of CO₂ were carried out using a thermogravimetric analyzer TGA/SDTA 851-LF 1100 Mettler apparatus. High-purity CO₂ and 50% CO₂ in N₂ at 1 atm was used for the adsorption runs. Each sample was pretreated in flowing N₂ at 150 °C for 30 min, then cooled to the desired adsorption temperature and exposed to CO₂ for 120 min. Temperature programmed desorption (TPD) was performed by heating the sample from adsorption temperature to 180 °C with 10 °C/min and held at 180 °C for 30 min in N₂ flow 50 ml/min to regenerate the sorbent. The CO₂ adsorption capacity of the adsorbent in millimole of CO₂ per gram of adsorbent was calculated from the mass gain of the sample in the adsorption process.

Results and discussion

From N₂ adsorption-desorption isotherms (not shown) of parent samples (SSBA-15-Dec, SSBA-15-BB and SSBA-15-Mes) and grafted ones it could be concluded that all samples have a typical IV type of adsorption isotherms and a H1 type hysteresis loop, meaning that all materials have an orderly mesoporous pore structure.

Table 1 Textural properties of molecular sieves SBA-15 and modified mesoporous silica SSBA-15

No.	Sample	Specific surface area (m ² /g)	Pore volume BJH _{Des} (cc/g)	Average pore diameter BJH _{Des} (nm)
1	SBA-15	725	1.19	6.2
2	SSBA-15-Dec	766.5	1.29	6.62
3	SSBA-15-BB	579.8	1.30	9.81
4	SSBA-15-Mes	655.1	1.44	9.73

The effect of swelling agent could be observed for all textural properties (Table 1). For all 3 composites the specific surface area has close values and comparative with parent SBA-15 values, but the pore volume of prepared composites is larger than for parent SBA-15. The

average pore diameter for SSBA-15-BB and SSBA-15-Mes was around 10 nm, which was larger than the pore size of conventional rope-like SBA-15 (6.2 nm).

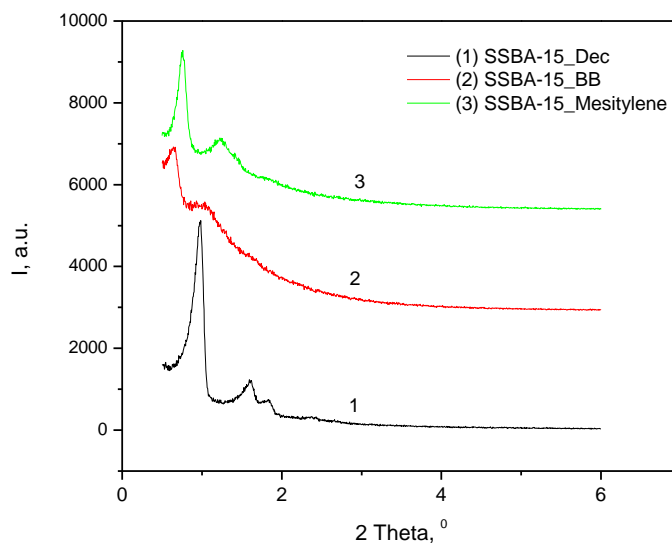


Fig. 1 XRD spectra of SSBA-15 with 3 different swelling agents: 1-phenyl-decane (a), butyl benzene (b) and mesitylene (c).

Figure 1 shows XRD patterns at low angles of the SSBA-15 samples prepared with 3 different swelling agents. As seen in this figure, SSBA-15-Dec sample show three well-resolved typical diffraction peaks, which are associated with a bi-dimensional $p6mm$ hexagonal symmetry of the pores of classical SBA-15: one intense reflection centered at 0.87° and two lower intensity peaks at about 1.45° and 1.68° , which can be indexed as the (100), (110) and (200) hkl reflections, respectively.

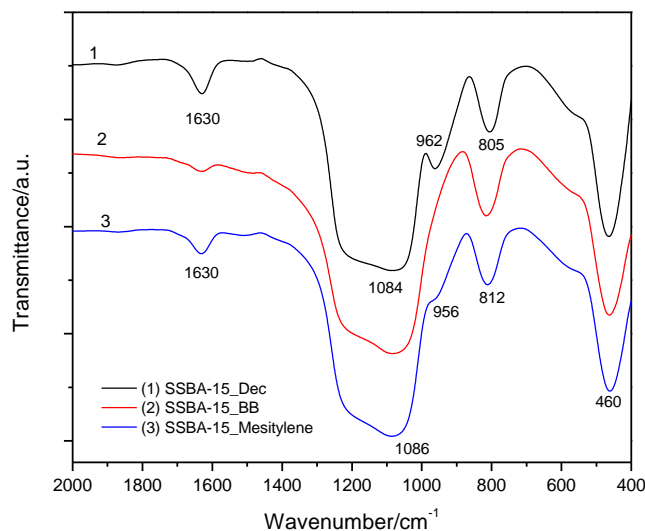


Fig. 2 Infrared spectra of SSBA-15 with 3 different swelling agents: 1-phenyl-decane (a), butyl benzene (b) and mesitylene (c).

SSBA-15-BB (0.64, 0.82) and SSBA-15-Mes (0.76, 1.24) have only 2 well resolved peaks which are shifted to lower angles by comparing with SSBA-15-Dec sample. The main

diffraction peak corresponding to (100) reflection is shifted to 0.64° for SSBA-15-BB, while for SSBA-15-Mes this peak is shifted to 0.76° .

All modified mesoporous silica prepared with 3 different swelling agents SSBA-15-Dec, SSBA-15-BB and SSBA-15-Mes showed that the characteristic IR bands of silica are evidenced by the three strong absorption bands at 1086, 810 and 460 cm^{-1} (Fig. 2). The IR bands at 1086 cm^{-1} belong to the anti-symmetric vibrations ν_{as} (Si–O–Si) and at 810 cm^{-1} to the symmetrical ν_{s} (Si–O–Si) bond. The IR bands 460 and 962 cm^{-1} have been assigned to the bending vibration of the bond δ (Si–O–Si) and the vibration of the silanol's group (Si–OH), respectively.

SEM images (Fig. 3 a-c) showed the changes of surface morphology on these obtained SSBA-15 particles in function of different swelling agents. Structural morphology of SSBA-15 modified with 1-phenyl-decane as swelling agent showed particles with long range well-ordered which have close aspect with conventional rope-like SBA-15. In fact, from textural analysis was evidenced that textural parameters of SSBA-15-Dec have values close to conventional SBA-15.

In contrast, the surface morphology of SSBA-15-BB and SSBA-15-Mes is different from SSBA-15-Dec and were consisted of cuboid-like particles. Also, from the values of textural parameters of modified SSBA-15 could be seen that SSBA-15-BB and SSBA-15-Mes have lower values of surface area but larger pore size than conventional SBA-15 and SSBA-15-Dec.

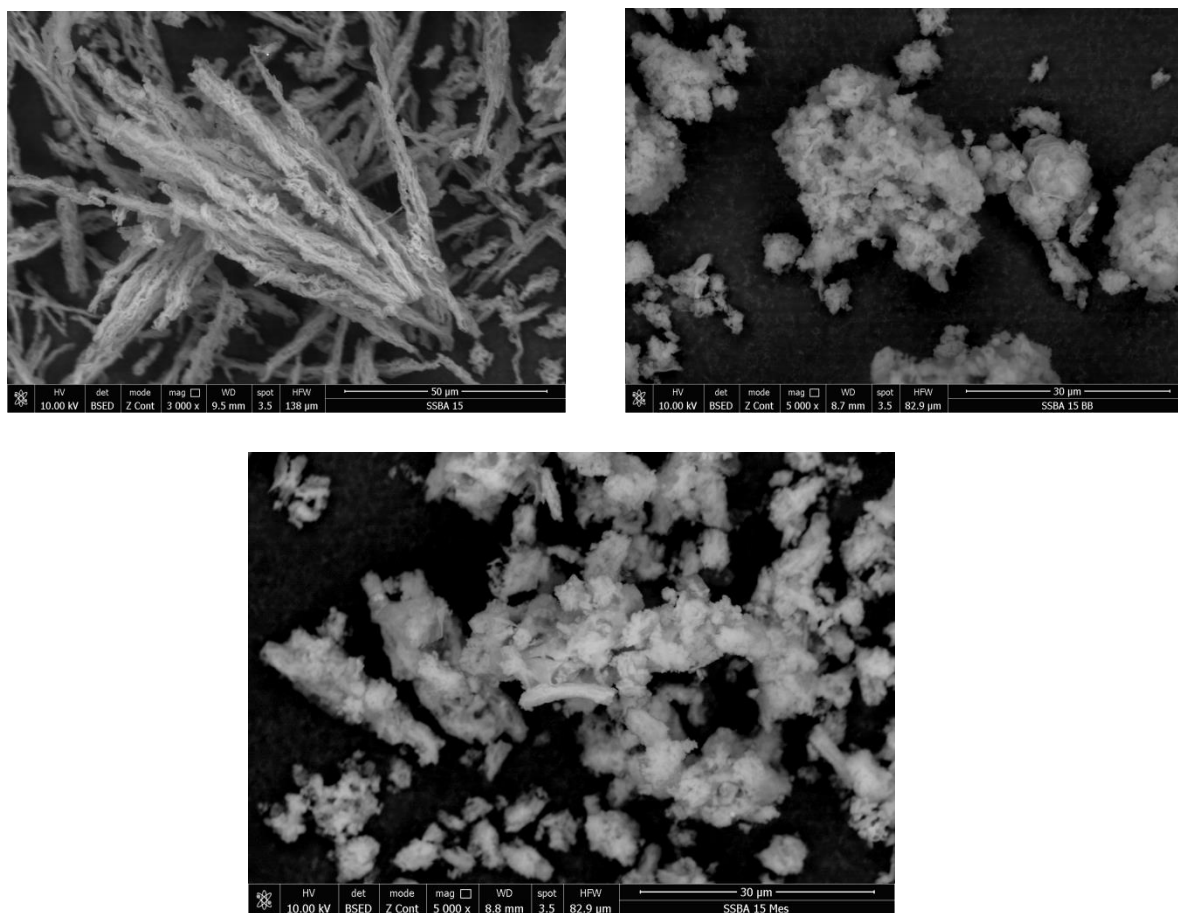


Fig. 3 SSBA-15 prepared with 3 different swelling agents: 1-phenyl-decane (a), butyl benzene (b) and mesitylene (c).

The adsorption of CO₂ and its TPD using thermogravimetry were studied for amino-functionalized molecular sieves. As we mention in experimental part each sample was pre-treated in flowing N₂ at 150 °C, then cooled to the desired adsorption temperature (50, 60 and 70 °C), and exposed to 50% CO₂/N₂ (70 ml/min) for 120 min. The desorption step was run in the range started from adsorption temperature until 180 °C with an increasing temperature rate of 10°C/min and with a isotherm at 180 °C for 30 minutes.

Table 3. The amounts of the captured CO₂ on molecular sieves at different temperatures.

No.	Sample	$n_{CO_2}/g\ SiO_2$ [mmol/g]		
		50°C	60°C	70°C
1.	SSBA-15-Dec-sil	2.24	1.94	1.54
2.	SSBA-15-BB-sil	2.82	2.89	2.28
3.	SSBA-15-Mes-sil	3.58	3.12	2.45

The CO₂ adsorption capacity of the adsorbent in mmole of CO₂ per gram of adsorbent could be seen from the mass gain of the sample in the adsorption process and was calculated more accurate from the mass loss during the desorption step. In Table 3 is shown the amounts of the captured CO₂ on all SSBA15 adsorbents. The best results were obtained with SSBA-15 - Mes-sil sample for the adsorption capacity of CO₂ at 50°C (3.6 mmole CO₂/g SiO₂) and at 60°C (3.1 mmole CO₂/ g SiO₂).

Conclusion

Three different modified mesoporous silica compounds were synthesized by the hydrolysis of tetraethyl orthosilicate using as surfactant a P123 block copolymer and 3 different compounds as swelling agents (1-phenyl-decane, butyl benzene and mesitylene) in order to achieve a pore diameter enlargement of silica.

From the values of textural parameters of modified SSBA-15 could be seen that SSBA-15-BB and SSBA-15-Mes have lower values of surface area but larger pore size than conventional SBA-15 and SSBA-15-Dec.

From the amounts of the captured CO₂ on all SSBA15 adsorbents by TPD, the best results were obtained with SSBA-15 - Mes-sil sample at 50° and at 60°C .

Acknowledgements

These investigations were partially financed by Romanian Academy Project No. 4.3.

References

- [1] Cao L, Man T, Kruk M, Synthesis of Ultra-Large-Pore SBA-15 Silica with Two-Dimensional Hexagonal Structure Using Triisopropylbenzene As Micelle Expander. *Chem Mater.* 21 (2009) 1144.
- [2] Kruk M, Cao L, Pore Size Tailoring in Large-Pore SBA-15 Silica Synthesized in the Presence of Hexane. *Langmuir.* 23 (2007) 7247.
- [3] Popa A, Sasca V, Verdes O, Ianasi C, Suba M, Barvinschi P, Effect of the amine type on thermal stability of modified mesoporous silica used for CO₂ adsorption, *J Therm Anal Calorim.* 134 (2018) 269.
- [4] Bakhtiari L, Javadpour J, Rezaie H R, Erfan M, Shokrgozar M A, The effect of swelling agent on the pore characteristics of mesoporous hydroxyapatite nanoparticles, *Prog Nat Sci-Mater.* 25 (2015) 185.

THE APPLICATION OF CARBONIZED ASH FOR THE SOLIDIFICATION AND STABILIZATION OF SEDIMENT WITH HIGH CONTENT OF Zn AND As

Nenad Popov¹✉, Srđan Rončević², Snežana Maletić², Nataša Varga², Sandra Jakšić¹, Željko Mihaljev¹, Milica Živkov Baloš¹

¹Scientific Veterinary Institute „Novi Sad“, Rumenački put 20, Novi Sad, Serbia

²University of Novi Sad Faculty of Sciences, Department of Chemistry, Biochemistry and Environmental Protection, Trg Dositeja Obradovića 3, 21000 Novi Sad, Serbia

✉ nenad.p@niv.ns.ac.rs

Abstract

Large quantities of ash generated by combustion of biomass require a sustainable management strategy [1]. The chemical composition of ash includes heavy metals that classified this kind of material as toxic waste. Accumulation of heavy metals as persistent and toxic substances in sediment can cause potential ecological risks [2]. The characteristics of sediment and examination of level of metal content can determine whether its remediation is necessary. The highest applicable technique of sediment remediation is solidification/stabilization (S/S). The application of this technique results in immobilization of pollutants into less soluble forms less available to the living world [3]. The ash produced by combustion of sunflower stem, after carbonization, was applied as a potential immobilization agent for the solidification/stabilization treatment of the sediment of the Greater Backa Canal. Carbonization causes decrease in leaching of metals by forming new adsorption zones and lowers porosity of a solidifier [4]. The results of the analyses showed that CO₂ combined with (OH)₂ forms CaCO₃, while in the combination with heavy metal oxides it forms their carbonates [5]. This paper presents the preliminary results of single step leaching test DIN 3841-4 S⁴ [6], and TCLP [7], which were used for testing newly formed mixture of sediment and non-carbonized/carbonized ash. The value of Zn and As concentrations in the eluates of the tested samples was monitored for successful evaluation of the treatment efficiency and risk assessment of newly emerging waste for human health and the environment.

Acknowledgments

The authors acknowledge financial support of the Ministry of Education, Science and Technological Development of the Republic of Serbia (Project No. 31011).

References

- [1] Izquierdo M., Moreno N., Font O., Querol X., Alvarez E. D., Nugteren H., Luna Y., Fernández-Pereira C. Fuel 87, 1958–1966, (2008).
- [2] Dalmacija M. PhD thesis, Faculty of Science, University of Novi Sad, 18, (2010).
- [3] Hunce S. Y., Akgul D., Demir G., and Mertoglu B. Waste Management 32(7), 1394–1400, (2012).
- [4] Halim C. E., Amal R., Beydoun D., Scott A. J., Low G. Cement and Concrete Research 34(7), 1093-1102, (2004).
- [5] Jianguo J., Maozhe C., Yan Z., Xin X. Journal of Environmental Management 128, 807-821, (2013).
- [6] DIN 38414 S⁴ Beuth Verlag. Berlin, (1984).
- [7] US EPA SW-846 Test Method 1311. Environmental Protection Agency 35, (1992).

RELATIVE DEPENDENCE BETWEEN OPERATING PARAMETERS AND QUALITY OF BITUMEN OBTAINED IN AN ASPHALT AIR BLOWING PROCESS

Rosu Dan

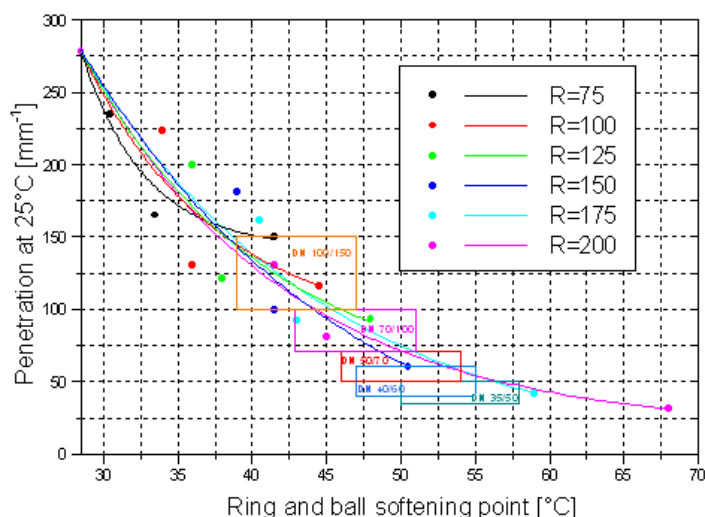
National Institute for Research and Development in Electrochemistry and Condensed Matter, Timisoara, A.P. Podeanu no.1, 300569, Romania
e-mail: antiquitera@yahoo.ca

Abstract

The bitumen blowing process is used mainly for the production of industrial bitumen grades with a high softening point and low penetration [1]. A number of factors affect the properties of the final product produced by air blowing: source and type of blowing flux, air feed rate, blowing time, and the blowing temperature [2].

Air blowing of feed stock was carried out in a static mixing gas-liquid reactor at 280 °C. Softening point of feed material was 28.5 °C, and penetration at 25°C was 278 mm⁻¹.

The relationship between softening point and penetration is the most important consideration in an asphalt air blowing process. Graphical representation of these relationship is called “blowing curve”



Blowing curves as function of volumetric air-feed stock ratio (R) in the air blowing process

The softening point dependence of the penetration is given by the equation:

$$Pen = (278 - a) \cdot e^{-b \cdot (SP - 28.5)} + a$$

It was obtained four main sorts of paving asphalt (romanian standard): DN 40/60, DN 50/70, DN 70/100 and DN 100/150

References

- [1] S. Parkash, Petroleum Fuels Manufacturing Handbook, McGraw-Hill, 2010.
- [2] V.P. Puzinauskas, E.T. Harrigan, R.B. Leahy, Current Refining Practices for Paving Asphalt Production, Strategic Highway Research Program Report SHRP-A/FR-91-102, 1990.

CHEMICAL SYNTHESIS AND CHARACTERIZATION OF LEAD DIOXIDE NANOPOWDER

Branislava Savić¹, Sanja Živković¹, Dalibor Stanković¹, Miloš Ognjanović¹, Tanja Brdarić¹, Gvozden Tasić¹, Ivana Mihajlović²

¹*Vinča Institute of Nuclear Sciences, University of Belgrade, Mike Petrovića Alasa 12–14,
11000 Belgrade, Serbia*

²*University of Novi Sad, Faculty of Technical Sciences, Department of Environmental
Engineering, Trg Dositeja Obradovića 6, 21000 Novi Sad, Serbia
e-mail: savicbrislava87@gmail.com*

Abstract

Lead dioxide (PbO₂) is one of the very interesting materials that have a lot of applications. In this work, nano-sized PbO₂ was synthesized by the chemical method. The composition, morphology and crystal structure of the nanopowder were characterized using Fourier Transform Infrared Spectrometry (FT-IR) and field emission scanning electron microscopy with energy dispersive X-ray spectrometer (FESEM-EDX). The obtained data indicate that a nanopowder PbO₂ with an average crystalline size of about 20 to 40 nm was formed. The synthesized nanomaterial PbO₂ could have a wide range of applications in wastewater treatment, e.g. to remove organic pollutants such as phenols.

Introduction

Nano-sized materials are of great scientific and technological importance in various fields of chemistry and environment protection [1]. A number of scientists investigations including physical, chemical and biological methods have been developed for nanoparticle preparation. It is well known that properties of nanoparticles depend on morphology, the size of the particles, the composition of the phases i.e. of the synthesis process.

The lead dioxide (PbO₂) is often cited as a promising material for chemistry and environmental protection applications, including its use for the oxidation of organic compounds in wastewater [2, 3], as a stationary phase for solid-phase microextraction [4]. Recently, it was reported that different morphologies of the PbO₂ nanoparticles (nano-rods, hollow spheres, trigonal nano-plates, nano-wires, macroporous, and hexagonal flower array) were synthesized by ultrasonic irradiation [5], hydrothermal method and electrochemical methods [6, 7].

The aim of the presented study is the synthesis and characterization of lead dioxide nano-powders. In the presented work, lead dioxide nano-powders were prepared using chemical method of preparation. Herein, the morphology and structure of PbO₂ were investigated using FT-IR and FESEM-EDX. The novel synthesized nanomaterial could be used in different applications for environmental protection.

Experimental

All chemical reagents were of analytical grade or better. Potassium persulfate (K₂S₂O₈), lead (II) acetate (Pb(CH₃COO)₂) and NaOH were all obtained from Sigma-Aldrich and used as received.

Functional groups were analyzed by Thermo scientific (Nicolet iS5, iD7) FT-IR spectrometer. The FT-IR spectra were recorded in the range from 400 cm⁻¹ to 4000 cm⁻¹.

The morphology of the PbO₂ was determined by FE-SEM (FEI Scios 2). The micrographs were recorded with 25000 x magnification.

The synthesis of nanosized PbO₂ using PbO nanomaterial synthesis of nanosized lead oxides was conducted according to the procedure proposed by *M. Alagar et al.* [7], and *W. Li et al.* [9]. PbO nanomaterial, used as precursor for the synthesis of nanosized PbO₂, was prepared by mixing lead (II) acetate solution with NaOH solution and resulting mixture was heated up to 90 °C. The obtained precipitate was filtered and dried at 90 °C. Then, this material was mixed with deionized water and treated with potassium persulfate in hydrothermal reactor at 120 °C for 2 h. The obtained material was washed several times with deionized water and dried at 70 °C.

Obtained PbO₂ material was characterized by FT-IR and FESEM-EDX methods.

Results and discussion

FT-IR studies:

The FT-IR spectra of PbO₂ nanoparticles (Figure 1.) showed a broad band at 445.58 cm⁻¹ due to PbO₂ vibration mode. A peak at 511.34 cm⁻¹ indicates the presence of oxides. This shows that the synthesised nanopowder consists of lead and oxide.

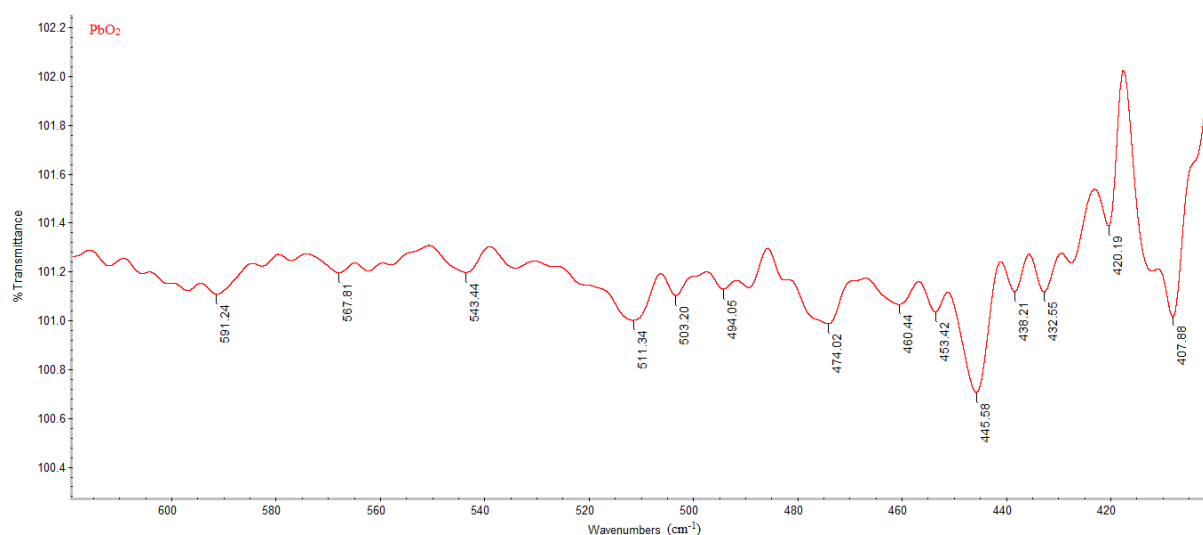


Figure 1. FT-IR spectrum of PbO₂ nanoparticles

SEM studies:

SEM morphological and nanostructural studies of the PbO₂ nanoparticles are shown in Figure 2. The size of nanoparticles is from 20 nm to 40 nm.

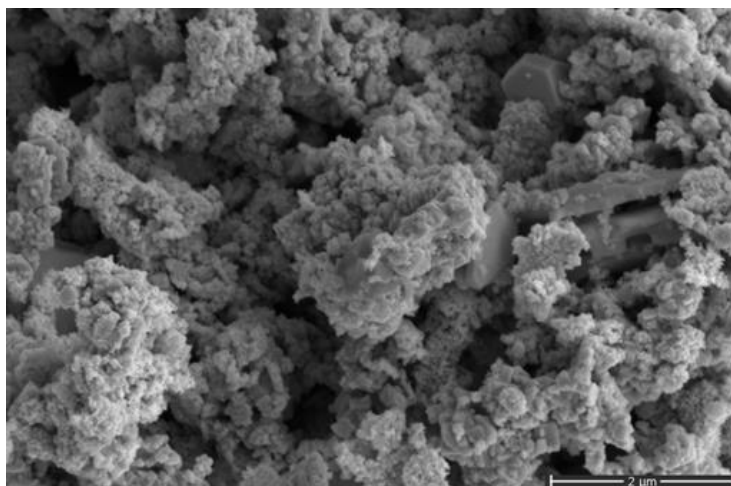


Figure 2. SEM picture showing PbO₂ nanoparticles

Conclusion

In summary, PbO₂ nanoparticles were synthesized by chemical method. The nanopowder contains a crystallites from 20 to 40 nm. The synthesized nanopowder could be appropriate for electrochemical degradation of organic pollutants and can be used as electrode material. The future investigation should be focused on the detailed physical characterization of synthesized material, as well as the application of nano-sized PbO₂ in wastewater treatment of organic pollutants.

Acknowledgements

This study was financially supported by the "Serbian Ministry of Education, Science and Technological Development" (project no. TR 37021).

References

- [1] R.F. do Nascimento, O.P. Ferreira, A. J. De Paula, V. de Oliveira Sousa Neto (Eds.), *Nanomaterials Applications for Environmental Matrices, Water, Soil and Air*, Elsevier, Netherlands, 2019, pp. 528.
- [2] S.P. Tong, C.A. Ma, H. Feng, A novel PbO₂ electrode preparation and its application in organic degradation, *Electrochem. Acta* 53 (2008) 3002–3006.
- [3] X. Duan, F. Ma, Z. Yuan, L. Chang, X. Jin, Electrochemical degradation of phenol in aqueous solution using PbO₂ anode, *J. Taiwan Inst. Chem. Eng.* 44 (2013) 95–102
- [4] A. Mehdiinia, M.F. Mousavi, M.J. Shamsipur, *Chromatogr A*. 2006 Nov 17;1134(1-2):24-31. Epub 2006 Sep 25.
- [5] S. Ghasemi, M.F. Mousavi, M. Shamsipur, H. Karami, Sonochemical-assisted synthesis of nano-structured lead dioxide. *Ultrason. Sonochem.* 15 (2008) 448-455.
- [6] Fu, Z. A. Hu, L. J. Xie, X. Q. Jin, Y. L. Xie, Y. X. Wang, Z. Y. Zhang, Y. Y. Yang, H. Y. Wu, *Int. J. Electrochem. Sci.*, 4 (2009) 1052.
- [7] H. Xu, D. Shao, Q. Zhang, H. Yang, Y. Wei, Preparation and characterization of PbO₂ electrodes from electro-deposition solutions with different copper concentration, *RSC Adv.* 4 (2014) 25011–25017.
- [8] M. Alagar, T. Theivasanthi, A. Kubera Raja, Chemical Synthesis of nano-sized particles of lead oxide and their characterization studies, *J. of Applied Sci.*, 12 (4) (2012) 398-401.
- [9] W. Li, Huayun Y., Q. Liu, Hydrothermal synthesis of PbO₂/RGO nanocomposite for electrocatalytic degradation of cationic red X-GRL, *J. of Nanomaterials*, (2017), Article ID 1798706.

NOVEL REACTOR WITH MULTIPLE ZINC ELECTRODES FOR SCALE PREVENTION

Marjana Simonič¹

¹*Faculty of Chemistry and Chemical Engineering, University of Maribor, Smetanova 17,
Maribor, Slovenija
e-mail: marjana.simonic@um.si*

Abstract

The use of zinc reactor system with multiple electrodes was studied. Physico-chemical analyses of water and X-ray powder diffraction (XRD) of scale were performed without treatment and after the water passed through the reactor. The results showed that chemical parameters were remained the same after the treatment. Very small concentration of Zn^{2+} was detected in water after the treatment. The XRD analyses showed that in drinking water the share of calcite was higher, while only aragonite was formed after the treatment.

Introduction

Carbonate CaCO_3 precipitation in drinking water is a crystal mixture of calcite and aragonite at certain ratio between them. The share of calcite is affected by temperature, pH, ion concentration and suspended solids

In our previous study it was proved that Zn substantially inhibited the nucleation rate of CaCO_3 [1]. Crystallization of aragonite CaCO_3 was studied [2]. It was discovered that the morphology of carbonate precipitate differs a lot upon the crystal structure. Recently, a lot of efforts have been done to generate green inhibitors, either from plant extraction or by using natural organic molecules. [3] However, it is complicated if chemicals are added directly into the water and could affect the chemical water quality.

The main objective of the present research, was to study the effect of reactor with multiple Zn electrode on scaling and CaCO_3 crystal morphology was studied. The calcite/aragonite ratio was studied by means of a chemical analysis and X-ray powder diffraction. A mechanism has been proposed that the surface reaction of Zn-ions with CaCO_3 might be rate determining step in the crystallization process.

Experimental

Untreated water samples were taken from waterworks (Maribor, Slovenia). Water flowed through the Zn-reactor (Figure 1) directly from the water pipe. The sample was taken at the outflow from the reactor. Samples of untreated and treated waters were saved for chemical and XRD analyses.

The device in Figure 1 operates due to certain potential difference which is governing the process of scale prevention. Inside the reactor there are multiple zinc electrodes as seen from Figure 1. Due to potential difference the device inhibits the scale formation. For the proper working the ratio between zinc versus copper electrode area ($S_{\text{zn}}/S_{\text{cu}}$) is very important.

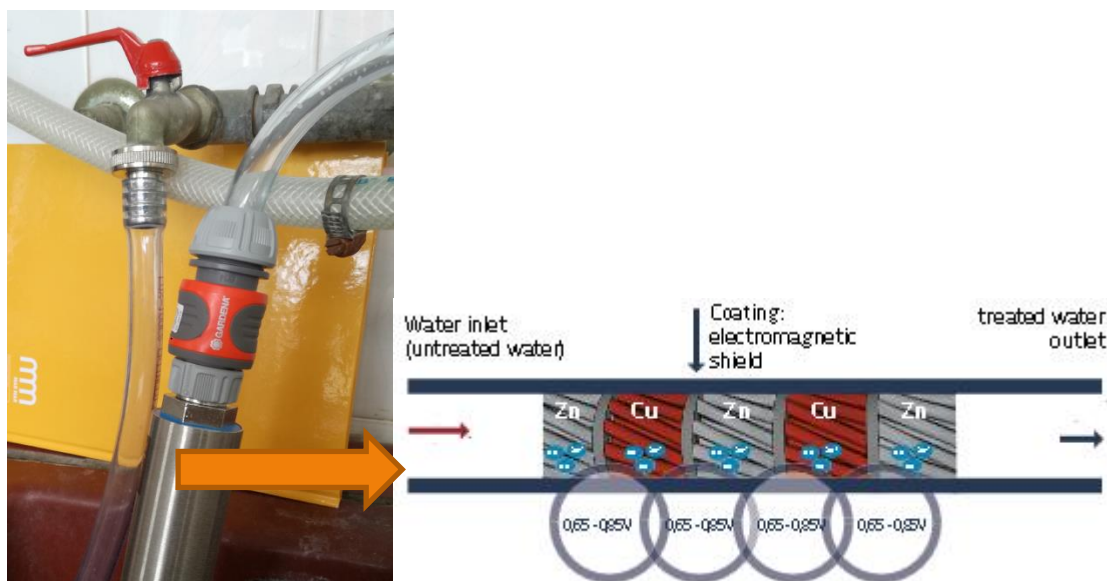


Figure 1. Zinc reactor

The chemical analysis of water was made in three replicates. The standard methods are gathered in Table 1.

Table 1. The methods used for water analyses

Parameter	Standard method	Apparatus
T (°C)	ISO 10523	Thermometer
pH	ISO 10523	pH-meter, MA 5740
TH (°d)	38409-H6 (1986)	Titration
Ca^{2+} , Mg^{2+} (mg/L)	38406-E3 (1982)	Titration
Zn^{2+} , Cu^{2+} (µg/L)	ISO DIN 11885 (1993)	ICP-MS/Perkin Elmer Elan 6000

X-ray powder diffraction data were collected with an AXS-Bruker/Siemens/D5005 diffractometer, using Cu-K α radiation at 293 K. The samples were scanned with positin sensitive detector and measured in range $10^\circ < 2\Theta < 80^\circ$, with the step of 0,01 and scanning speed of 2 s per step. Determination of phases in the sampe was done with Search/Match program.

Results and discussion

Water was taken after passing through the Zinc reactor. Results of chemical analyses are shown in Table 2.

All experiments were performed at room temperature.

Table 2. The methods used for water analyses

Analysis	Drinking water	Treated water
T(°C)	20	20
Ca ²⁺ (mg/L)	65,7	65,7
Mg ²⁺ (mg/L)	21,3	21,3
Zn ²⁺ (mg/L)	< 0,01	< 0,01
Cu ²⁺ (mg/L)	<0,01	<0,01
TH (°d)	14,1	14,1

It is clearly seen that chemical water quality remained the same after the treatment. Also none of the Zn concentration difference was noted. Copper concentration was also measured due to the content of the reactor. The concentration in drinking water was below 10 µg/L.

XRD analysis of scale formed in untreated water and in treated water was performed. The diffractogram of the precipitate from untreated water showed some calcite crystals peaks (denoted C in Figure 1a). Zinc reactor device induced changes to the crystal morphology and promoted crystallization in the aragonite rather than calcite. Only aragonite in powdered form was formed after the treatment (Figure 1b).

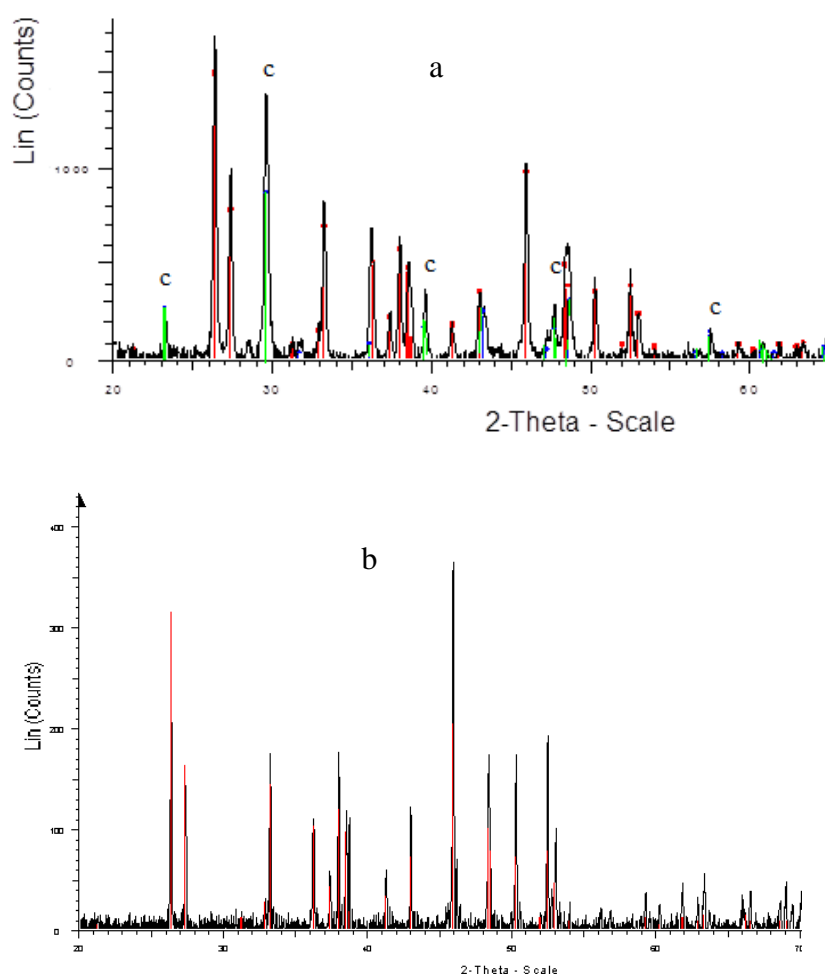


Figure 2. XRD analysis of CaCO_3 (a pattern denotes the untreated water, b treated water)

Since the product is novel, the operating time of reactor could be estimated at 10 years according to the results. Due to calcite formation inhibition the pipes are preserved and there is prolonged the lifetime of pipes. Further, no chemical cleaning is needed for scale removal inside the entire water pipeline system. Therefore, device minimizes operational costs.

Conclusion

The trace amounts of Zn substantially inhibit the nucleation rate of calcium calcite. The Zinc concentrations below 10 µg/L enable the formation of aragonite and disable the formation of calcite. Already after analyses of the scale it was found the powdered form of aragonite was formed.

Acknowledgements

The research work was produced within the framework of the program P2-0032 Process System engineering and sustainable development, financially supported by Slovenian Research Agency. Also thanks Energywater for cooperation.

References

- [1] M. Simonič, I. Ban. Open Chem. 11 (2013) 698.
- [2] H. Guo, Z. Qin, P. Qian, P. Yu, S. Cui, W. Wang. 22 (2011) 777.
- [3] M. Chaussemier, E. Pourmohtasham, D. Gelus, N. Pécoul, H. Perrot, J. Lédion, H. Cheap-Charpentier, O. Horner. Desalination 356 (2015) 47-55.
- [4] Z. Amjad. The science and technology of industrial water treatment, 1st ed., CRC Press, 2010.

REMOVAL OF HERBICIDE TEMBOTRIONE FROM WATER USING VARIOUS NEWLY SYNTHESIZED PHOTOCATALYSTS

Daniela Šojić Merkulov¹, Marina Lazarević¹, Paula Sfirloagă², Biljana Abramović¹

¹*University of Novi Sad Faculty of Sciences, Department of Chemistry, Biochemistry and Environmental Protection, Trg Dositeja Obradovića 3, 21000 Novi Sad, Serbia
e-mail: daniela.sojic@dh.uns.ac.rs*

²*National Institute of Research and Development for Electrochemistry and Condensed Matter, Dr. Aurel Păunescu Podeanu 144, 300569, Timișoara, Romania*

Abstract

Tembotrione [2-(2-chloro-4-methylsulfonyl-3-(2,2,2-trifluoroethoxy)methyl)benzoyl cyclohexane-1,3-dione] is the most recently commercialized triketone herbicide worldwide in 2007 with a purpose to control weeds in corn farming [1]. Because of their stability, many herbicides that are used in agriculture may be leached and thus contaminate surface and ground water [2]. Besides, their uptake by the plant root may cause herbicide accumulation in plants and through the food chain becomes a threat to the living beings. Research into the chemical treatment of wastewater and drinking water has focused on improving the efficiency of removal of harmful organic compounds, among which pesticides have an important role, using catalytic and photochemical methods [3]. Heterogeneous photocatalysis represents low-cost, versatile, environmentally friendly, and one of the most promising green chemistry method for removal of different contaminants [4]. The activity of various photocatalysts (TiO₂, ZnO, and MgO) in the case of tembotrione removal from ultrapure water was investigated in this paper using combined adsorption and photocatalytic degradation processes under simulated sunlight and UV irradiation. Effect of different concentration of ammonium persulfate has also been investigated in the presence of all mentioned photocatalysts. Kinetics of tembotrione removal were monitored using HPLC with UV/vis DAD detector.

Acknowledgments

The authors acknowledge financial support of the Ministry of Education, Science and Technological Development of the Republic of Serbia (Project No. 172042).

References

- [1] E. Dumas, M. Giraudo, E. Goujon, M. Halma, E. Khili, M. Stauffert, I. Batisson, P. Besse-Hoggan, J. Bohatier, P. Bouchard, H. Celle-Jeanton, M. Costa Gomes, F. Delbac, C. Forano, P. Goupil, N. Guix, P. Husson, G. Ledoigt, C. Mallet, C. Mousty, V. Prévot, C. Richard, S. Sarraute, J. Hazard. Mater. 325 (2017) 136.
- [2] D.B. Donald, A.J. Cessna, E. Sverko, N.E. Glozier, Health Perspect. 115 (2007) 1183.
- [3] C.B. Ong, L.Y. Ng, A.W. Mohammad, Renew. Sustain. Energy Rev. 81 (2018) 536.
- [4] M.E. Borges, M. Sierra, E. Cuevas, R.D. García, P. Esparza, Sol. Energy 135 (2016) 527.

SYNTHESIS AND CHARACTERIZATION OF THIENO [3, 2-B] THIOPHENE DERIVATIVE INTERMEDIATE IN SYNTHESIS OF LIQUID CRYSTAL COMPOUNDS

Spirache Maria Angela¹, Haidu Daniela¹, Badea Valentin² and Cseh Liliana^{1*}.

¹*Institute of Chemistry Timisoara of Romanian Academy, 24 Mihai Viteazu Bvd., 300223 – Timisoara, Romania*

²*Politehnica University of Timișoara, Faculty of Industrial Chemistry and Environmental Engineering, 6 Vasile Parvan Bvd, 300223 - Timișoara, Roumania
angelaspirache@gmail.com*

Liquid crystals (LCs) represent truly fascinating materials in terms of their properties, their importance for the fundamental understanding of molecular self-assembly, and their tremendous success in commercial applications. [1] Liquid crystals, the fourth state of matter, are a class of compounds which exhibit liquid crystalline behavior, which appears under temperature or solvent. The molecular order of LCs is intermediate between that of an ordered solid crystal and a disordered liquid. LCs combines the physical properties of the crystalline and liquid states. [2]

The compounds based on thieno groups and thiophene derivative with various classes of π -conjugated polycyclic molecules have been presented, better electronic characteristics and also more resistant to degradation. These compounds are versatility because of a variety of combinations of aromatic and heteroaromatic units that provide desired tuning for target structures. Many heteroacene derivatives based on thiophene units have recently been suggested as promising materials for electronic and optoelectronic devices. [3]

Here we report the synthesis of some intermediates base on thieno [3, 2-b] thiophene core used in the synthesis of new liquid crystals. The characterization and purity of compounds were confirmed through elemental analysis, 1D⁺ NMR, UV-Vis.

Acknowledgements: This work was supported by a grant of Ministry of Research and Innovation, CCCDI - UEFISCDI, project number PN-III-P3-3.1-PM-RO-CN-2018-0139/19/2018, within PNCDI III

[1] Tschierske C., *Top. Curr. Chem.*, **2012**, 318, 1-108.

[2] Binnemans K., *Chem. Rev.*, **2005**, 105, 4148–420.

[3] Irgashev R. A., Karmatsky A. A., Rusinov G. L., Charushin V. N., *J. Amer. Chem. Soc.*, **2016**, 138, 804–807.

INFLUENCE OF DIFFERENT COMBINATIONS OF WALL MATERIALS ON THE ENCAPSULATION OF BUTTERNUT SQUASH WASTE EXTRACT

**Sladana Stajčić, Jasna Čanadanović-Brunet, Gordana Četković,
Vesna Tumbas Šaponjac, Jelena Vulić, Vanja Šeregelj**

*University of Novi Sad, Faculty of Technology Novi Sad,
Bulevar Cara Lazara 1, 21000 Novi Sad
e-mail: sladj@uns.ac.rs*

Abstract

The aim of this study was to evaluate the effect of different amounts of carrier agents (maltodextrin, inulin and pea protein) on the content of phenolics and carotenoids from butternut squash waste extract in encapsulates obtained by freeze-drying technique. Using Simplex-Centroid experimental design and response surface methodology (RSM), the highest content of both phenolics and carotenoids in the encapsulate was determined for a wall blend ratio 53.9 % pea protein, 46.1 % maltodextrin and 0% inulin.

Introduction

The fruits and vegetables processing industry produce very large amounts of waste materials, which are promising sources of bioactive compounds, such as phenolics and carotenoids. The applications of bioactive compounds from waste have recently attracted great interest in the food and pharmaceutical industries. However, the effectiveness of bioactive compounds depends on preserving their stability, bioactivity and bioavailability. Encapsulation, technique by which sensitive ingredients are packed within a coating or wall material, can effectively alleviate these deficiencies. Different encapsulation techniques and/or wall materials have been applied in order to achieve desired properties of encapsulates.

Experimental

Freeze-dried butternut squash waste was extracted with acetone:ethanol mixture (36:64 v/v) in solid to solvent ratio 1:10 w/v according to the procedure of Šeregelj et al. (1). The content of carotenoids in the butternut squash waste extract was analyzed by the method of Nagata and Yamashita (2). The amount of total phenolics in extract was determined according to the Folin-Ciocalteu method (3). Three carrier agents, including maltodextrin (M), inulin (I) and pea protein (P) were used as wall materials for freeze-drying encapsulation of phenolics and carotenoids from butternut squash waste extract. The composition of the wall materials mixture was optimized using response surface methodology (RSM) in order to obtain the optimum encapsulate (OE) with the highest content of both phenolics and carotenoids. The encapsulates were prepared according to the modified method developed by Indrawati et al. (4). Contents of total phenolics and carotenoids in the encapsulates were determined spectrophotometrically by following a modified Saénz et al. and Barbosa et al. methods, respectively (5, 6). The characterisation in terms of water activity, hygroscopicity, water solubility, bulk density, tapped density and color properties of the optimum encapsulate was also conducted (7).

Results and discussion

Total phenolic and carotenoid content in extract were 294.69 mg/100 g and 14.26 mg/100 g dried squash waste, respectively. The content of total phenolics from squash waste in the encapsulates ranged from 24.57 to 65.16 mg/100 g. The content of total carotenoids in the encapsulates were in range from 2.39 to 3.08 mg/100 g. Using RSM, the highest content of

both phenolics and carotenoids in the encapsulate was determined for a wall blend ratio 53.9 % P, 46.1 % M and 0 % I. The total phenolic and carotenoid content in the OE (63.41 mg/100 g and 3.08 mg/100 g, respectively), prepared using the calculated optimum wall materials mixture, did not differ significantly from the predicted values. OE was characterised in terms of water activity (0.014), hygroscopicity (12.30 g of moisture per 100 g dry solids), water solubility (60.00 %), bulk density (0.21 g/ml), tapped density (0.33 g/ml) and color properties ($L^* = 62.65$, $a^* = 0.88$ and $b^* = 34.47$).

Conclusion

The experimental mixture design and response surface methodology was adequate, allowing for the selection of the best mixture of wall materials. The maltodextrin/pea protein interactions can give the improvement in preservation of both phenolics and carotenoids from butternut squash waste extract in encapsulate during freeze-drying encapsulation.

Acknowledgements

This research is part of the Project TR 31044 which is financially supported by the Ministry of Education, Science and Technological Development of the Republic of Serbia.

References

- [1] V.N. Šeregelj, G.S. Četković, J.M. Čanadanović-Brunet, V.T. Tumbas Šaponjac, J.J. Vulić, S.S. Stajčić, *Acta Periodica Technologica*. 48 (2017) 261.
- [2] M. Nagata, I. Yamashita, J. Jap. Soci. Food Sci. Tehnol. 39 (1992) 925.
- [3] V.L. Singleton, J.A. Rossi, *American Journal of Enology and Viticulture*. 16 (1965) 144.
- [4] R. Indrawati, H. Sukowijoyo, R.D.E. Wjayantu, L. Limantara, *Procedia Chemistry*. 14 (2015) 353.
- [5] C. Saénz, S. Tapia, J. Chávez, P. Robert, *Food Chem*. 114 (2009) 616.
- [6] M.I.M.J. Barbosa, C.D. Borsarelli, A.Z. Mercadante, *Food Res. Int*. 38 (2005) 989.
- [7] V. Šeregelj, V. Tumbas Šaponjac, S. Lević, A. Kalušević, G. Četković, J. Čanadanović-Brunet, V. Nedović, S. Stajčić, J. Vulić, A. Vidaković, J. *Microencapsul.* (<https://doi.org/10.1080/02652048.2019.1668488>).

PARTIAL CHARACTERIZATION OF EXTRACTS FROM SOME *BRASSICACEAE* VEGETABLES

Mariana Nela Ștefănuț^{1*}, Adina Căta¹, Ioana Maria Carmen Ienașcu^{1,2}

¹National Institute of Research and Development for Electrochemistry and Condensed Matter, Dr. A. P. Podeanu 144, 300569 Timișoara, Romania, mariana.stefanut@gmail.com

²“Vasile Goldiș” Western University of Arad, Faculty of Pharmacy, 86 Liviu Rebreanu, 310045, Arad, Romania

Extraction of biological active compounds from Romanian cabbage, broccoli and rapeseeds was performed by classical methods: maceration, extraction under pressure, and two *eco-friendly* modern methods, extraction in ultrasonic field (59 kHz, 15-30min.) and extraction in microwaves field (2450 MHz, 15 min.). The extracts were characterized by DPPH (0.85-1.1 mmol/L Trolox) and FRAP (8.2-19.6 mmol/L Trolox) methods, total phenolics determination (660-3900 GAE/L). Toxicity was evaluated by determination of concentrations for some heavy metals (by AAS method) and determination of some pesticides (HPLC). In order to be compared, extracts were evaporated under vacuum (Laborota 4000, Heidolf) and finally, were putted in 10 mL marked flasks.

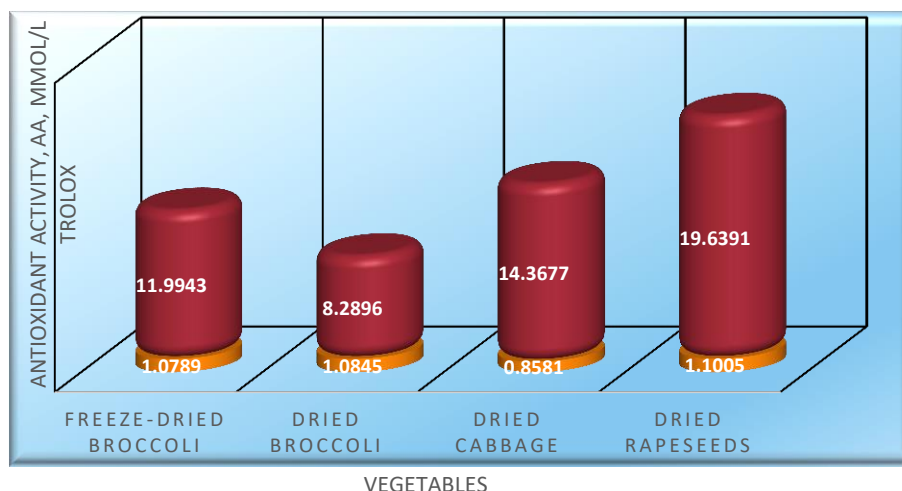


Figure 1. Antioxidant activity of extracts from some Brassicaceae (blue- DPPH; red-FRAP)

The best method for extraction of biological active compounds from cabbage, broccoli and rapeseeds, was microwave technique. Ethanol or ethanol 70% was the solvent choose because the extracts are destined to alternative medicine, pharmacy and food industry.

Acknowledgements

This work is part of the project PN 19 22 03 01 / 2019 “Supramolecular inclusion complexes of some natural and synthetic compounds with health applications”, carried out under NUCLEU Program funded by National Authority for Scientific Research (Romania).

References

- [1] Fernández-León A.M., Lozano M., González D., Ayuso M.C., Fernández-León M.F., Czech J. Food Sci. 32(6), 2014, 549-554.
- [2] Brand-Williams W., Cuvelier M.E., Lebensm.Wiss.Technol., 28, 1995, 25-30.

NUTRITIONAL PROFILE EVALUATION OF THE GLUTEN-FREE BREAD OBTAINED FROM FLOUR MIXTURES WITH HIGH NUTRITIONAL VALUE

Stoin Daniela^{1*}, Lavrik Ilya Petrovich², Jianu Călin¹, Velciov Ariana – Bianca¹,
Moigrădean Diana¹, Popescu Sofia¹

¹University of Agricultural Sciences and Veterinary Medicine of Banat "King Mihai I of Romania" Timisoara, Faculty of Food Engineering, Food Science Department, 300645, Timisoara, Calea Aradului, nr. 119, Roumania

²Russian State Agrarian University - Moscow Timiryazev Agricultural Academy, Timiryazevskaya st., 49, 127550, Russian Federation, Moscow

* author's email address: danielastoin@yahoo.com

Abstract

The aim of this study was to obtain and to characterize some gluten-free flour mixtures with high nutritional value by partially replacing rye flour (RF) with flax flour (FF) and millet flour (MF) and to evaluate the nutritional profile of gluten-free bread obtained from these mixtures. RF was replaced by 10%, 20%, 30% and 40% FF and MF, respectively. The determinations made for studied flour, flour mixtures and gluten-free bread samples were the following: moisture content, protein content, ash content, fat content, fiber content and total carbohydrate content. The gluten-free bread samples studied were obtained by the direct method. According to the results regarding the physico-chemical composition of the flours and M1 ÷ M4 flours mixtures, it can be appreciated that all these mixtures are suitable to be incorporated in gluten-free bread according to the established substitution amount, because the obtained results highlight their superior nutritional profile. The results obtained regarding the physico-chemical composition of the studied bread samples show the superior nutritional profile of all four bread samples (BM1, BM2, BM3 and BM4) compared to CB.

Keywords: *flour mixtures, high nutritional value, gluten free bread, nutritional profile*

DETERMINATION OF POLYPHENOLIC CONTENT IN BY-PRODUCT FROM SUNFLOWER SEED INDUSTRY

Zorica Stojanović¹, Snežana Kravić¹, Ana Đurović¹, Nada Grahovac², Ranko Romanić¹

¹*University of Novi Sad, Faculty of Technology Novi Sad, Bulevar cara Lazara 1, 21000 Novi Sad, Serbia*

²*Institute for Field and Vegetable Crops, Maksima Gorkog 30, 21000 Novi Sad, Serbia
e-mail: zorica.stojanovic@uns.ac.rs*

Abstract

The production of sunflower oil yields a considerable amount of by-product such as sunflower seed cake which remains after isolation of oil from sunflower seeds. Sunflower seed cake is usually used to produce animal feed and fertilizer of low quality, as well biomass for energy generation and partially ends up as waste. Due to the huge amount of this by-product released every year from sunflower oil industry as a waste, if it is valorised properly, it can be very beneficial from both economic and environmental aspects. Polyphenols are secondary metabolites of plants with a high antioxidant power. Chemically they are compounds that have more than one hydroxyl groups attached to one or more benzene rings [1]. Polyphenols are not clarified as human nutrients, but they have many beneficial effects on human health and, therefore, are called nutraceuticals [2]. In recent years polyphenols rich products are suggested as preventing and treating agents in specific diseases.

In this study, sunflower seed cake samples from non-oil type of sunflower (n=20) were analysed in order to assess the content of polyphenols. Ultrasound extraction at 30 °C (t=10 min) was used as extraction technique while 80% ethanol was applied as extraction solvent. Thereafter, the ethanol was removed and dry residue was dissolved in methanol. In the obtained extracts, total phenols were estimated according to Folin-Ciocalteu (FC) assay [3] and results are expressed as mg chlorogenic acid/100 g on dry matter basis (d.m.). By FC method, total phenols content can be determined. However, since most of food phenolics have more than one hydroxyl group, food phenolics are also called polyphenols, thus, polyphenols content can be approximately assessed by FC method. From obtained results it is evident that sunflower seed cakes contained significant amount of biologically highly valuable polyphenols. The total polyphenolic content was found to be in the range from 536 to 732 mg of chlorogenic acid/100 g d.m. in sunflower seed cakes. The results proved that this by-product is an interesting source of antioxidant compounds that may be recovered and used for the development of functional ingredients in food products.

Acknowledgements

This work is financially supported by the Ministry of Education, Science and Technological Development of Republic of Serbia (Projects TR 31014 and III 46009).

References

- [1] W. Vermerris, R. Nicholson, Phenolic compound biochemistry, Springer, West Lafayette, IN, 2006, pp. 2.
- [2] A.P. Gollucke, R.C. Peres, A.Jr. Odair, D.A. Ribeiro, Recent Pat. Food Nutr. Agric. 5 (2013) 214.
- [3] M. Kosar, H.J.D. Dorman, R. Hiltunen, Food. Chem. 91 (2005) 525.

AMINE FUNCTIONALIZED KIT-6 FOR CO₂ ADSORPTION AT DIFFERENT TEMPERATURES

Mariana Suba, Orsina Verdeş, Alexandru Popa, Silvana Borcănescu

*"Coriolan Drăgulescu" Institute of Chemistry, Mihai Viteazul No.24, 300223 Timisoara
E-Mail: marianasuba@gmail.com*

Abstract

In this paper, pure KIT-6 was synthesized and functionalized with 3-aminopropyl triethoxysilane (APTES) by grafting in aqueous solvent at 80°C. The as-prepared composites were characterized by X-ray diffraction at low angles, FT-IR spectroscopy, TGA-DTA coupled with mass-spectrometry, SEM and N₂ physisorption techniques followed by testing for CO₂ adsorption at different temperatures. The CO₂ adsorption/desorption performance was investigated by TGA-DTA coupled with mass-spectrometry using TPD method. The results showed that the CO₂ adsorption capacity decreases with increasing temperature from 40 to 70 °C.

Introduction

A major problem in recent years is the high level of CO₂ emissions on the environment with serious negative effects. In the last half century large quantities of carbon dioxide have been released into the atmosphere, which contributes substantially to global warming - the greenhouse effect. Thus, the research directions were directed towards obtaining materials with CO₂ adsorption-desorption properties [1-3].

There is a direct correlation between increasing CO₂ concentration and the greenhouse effect that causes global warming. In recent decades, there has been growing interest in developing materials that can be used to capture and store CO₂. In the literature, CO₂ adsorption has been studied under various conditions on a series of mesoporous silica adsorbents composed of conventional silica molecular sieves MCM-41, SBA-15 and KIT-6 [4].

Mesoporous silica, KIT-6 is of particular interest to other materials such as MCM-41 and MCM-48, due to its three-dimensional structure with a large diameter mesopore and an easy method of synthesis. [5].

Experimental

KIT-6 mesoporous silica was synthesized following the method described by Kleitz *et al.* [6]. First, 3.69 g triblock copolymer pluronic P123 (EO₀₂PO₇₀EO₂₀) was dissolved in 132 g distilled water and 6.75 g 37% HCl under vigorous stirring at 35 °C for 8 h. After complete dissolution, 3.63 g n-butanol was added to this solution. The mixture remained under stirring at 35 °C for 1 h. To this, 7.92 g tetraethyl orthosilicate (TEOS, 99% Fluka) was added to the homogeneous solution and stirring for 24 h at 35 °C. Then, this mixture was transferred into a Teflon-lined stainless steel autoclave and heated at 100 °C for 24 h under static hydrothermal conditions. The solid product obtained after hydrothermal treatment was separated by vacuum filtration and washed with a 2% HCl-ethanol solution. Finally, the sample was calcined in air atmosphere at 550 °C for 6 h to remove the organic template. The resulting sample was denoted KIT-6.

Modified KIT-6 denoted as KIT-6 Sil was prepared as follows: 0.5 g of KIT-6 was dispersed in 50 ml toluene and 0.79 ml of 3-aminopropyl triethoxysilane was added later to the solution. The above mixture was refluxed at 110 °C for 12 h, and then the solid was

collected by filtration, washed by ethanol and air-dried at 80 °C. The grafting reaction was carried out at 110 °C for 5 h. After filtration and drying, the absorbents were obtained as white solids.

The thermal analyses were carried out using a thermoanalyzer system Mettler TGA/SDTA 851/LF/1100 coupled with mass-spectrometry (MS). The measurements were conducted in dynamic atmosphere of air (50 ml/min), using the alumina plates crucibles of 150 μ l.

The FTIR absorption spectra were recorded with a Jasco 430 spectrometer (spectral range 4000-400 cm^{-1} range, 256 scans, and resolution 2 cm^{-1}) using KBr pellets

Powder X-ray diffraction data were obtained with a XD 8 Advanced Bruker diffractometer using the Cu K α radiation in the range $2\theta = 0.5 \div 5^\circ$ and $2\theta = 5 \div 60^\circ$.

The specific surface areas of samples were calculated from the nitrogen adsorption-desorption isotherms using a Quantachrome instrument, Nova 2000 series.

Scanning electron micrographs (SEM) were recorded using Jeol JMS 6460 LV instrument equipped with an Oxford Instruments EDS (energy dispersive spectroscopy) analyser.

Adsorption tests were carried out using the same thermogravimetric analyzer connected to a gas delivery manifold. High-purity CO₂ and 30% CO₂ in N₂ at 1 atm was used for the adsorption runs, and N₂ was used as a regenerating purge gas for CO₂ desorption. Each sample was pretreated in flowing N₂ at 150 °C, then cooled to the desired adsorption temperature (60 °C), and exposed to 30% CO₂/N₂ (70 ml/min) for 90 min. The CO₂ adsorption capacity of the adsorbent in milligrams of CO₂ per gram of adsorbent was calculated from the weight gain of the sample in the adsorption process.

Results and discussion

The XRD model of KIT-6 and KIT-6 Sil are shown in Fig. 1. and confirm the cubic structure Ia3d specific to mesoporous sieves of KIT -6 type [7] by the presence of the two diffraction peaks at small angles of 0.96 and 1.83°, corresponding to the crystal planes Miller (211) and (220).

In the case of KIT-6 Sil, the peaks were also retained but the intensities decreased with introduction of 3-aminopropyl triethoxysilane. This also shows that APTES was successfully grafted onto KIT-6.

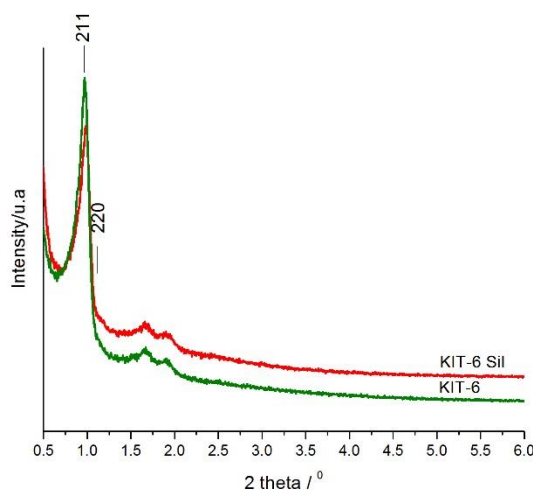


Fig. 1. XRD patterns of KIT-6 and KIT-6 Sil

The FT-IR spectra were recorder in the range 500-4000 cm^{-1} to confirm the APTES in the absorbent as can see in Fig. 2. In the APTES grafted, the peaks around 1387 cm^{-1} and 1548 cm^{-1} represent the $-\text{NH}_2$ and $-\text{NH}$ groups associated with the surface [5]. The peaks intensity of KIT-6 Sil was found higher compared with KIT-6.

The broad peaks at around 3734 and 3844 cm^{-1} represent the $-\text{NH}$ and $-\text{OH}$ stretching vibrations. The other peaks at 2042 cm^{-1} and 1632 cm^{-1} represent CO_2 and the physically adsorbed water [8, 9].

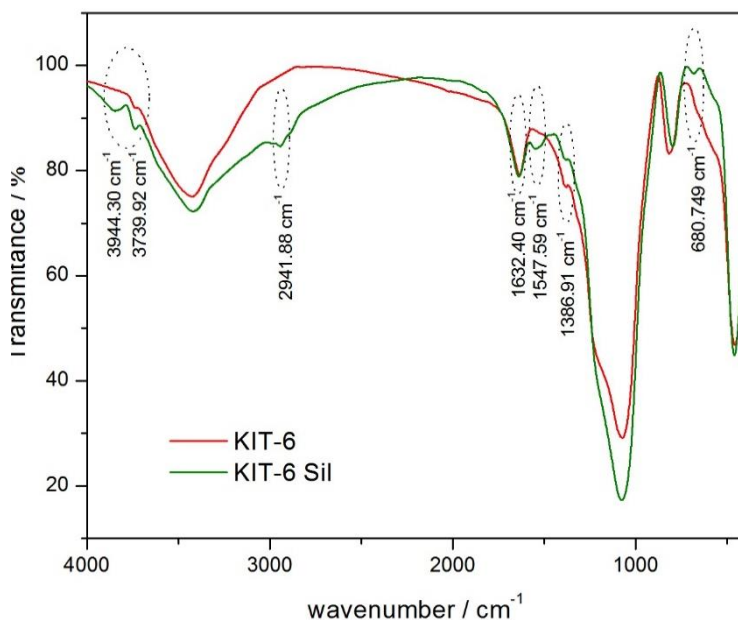


Fig. 2. FTIR spectra of parent KIT-6 and KIT-6 Sil

The textural parameters of synthesized KIT-6 and KIT-6 Sil are shown in Table 1. After grafting of APTES the surface area and pore volume decreased from 715 to 560 (m^2/g) and from 0.967 to 0.950 (cm^3/g) respectively. The data reveal a gradual reduction in surface area and pore volume after modification with silane coupling agent 3-aminopropyl triethoxysilane. These decrease can be attributed to the increase in agglomeration of silica particles or/and the filling of pore with APTES.

All composites display a type IV isotherm with H1 hysteresis loop according to the IUPAC classification, which is characteristic of mesoporous materials. It could be observed a sharp increase in volume adsorbed at $p/p_0 = 0.5-0.8$ characteristic of highly ordered of composite (not shown).

Table 1. Textural properties of KIT-6 and KIT-6 Sil composites

No.	Samples	Specific surface area (m^2/g)	Pore volume BJH _{Des} (cm^3/g)	Average pore diameter BJH _{Des} (nm)
1	KIT-6	715	0.967	6.570
2	KIT-6 Sil	560	0.950	5.462

Scanning electron micrographs images were used to observe the morphology of the KIT-6 and KIT-6 Sil particles. The image of KIT-6 shows that the particles are appeared to be spherical (Fig.3a) due to aggregation of fine threads of KIT-6. The spherical morphology is

slightly modified after amine functionalization as seen in (Fig. 3b). After introduction of APTES, the threads are easily dispersed and thus destroyed the spherical morphology [10]

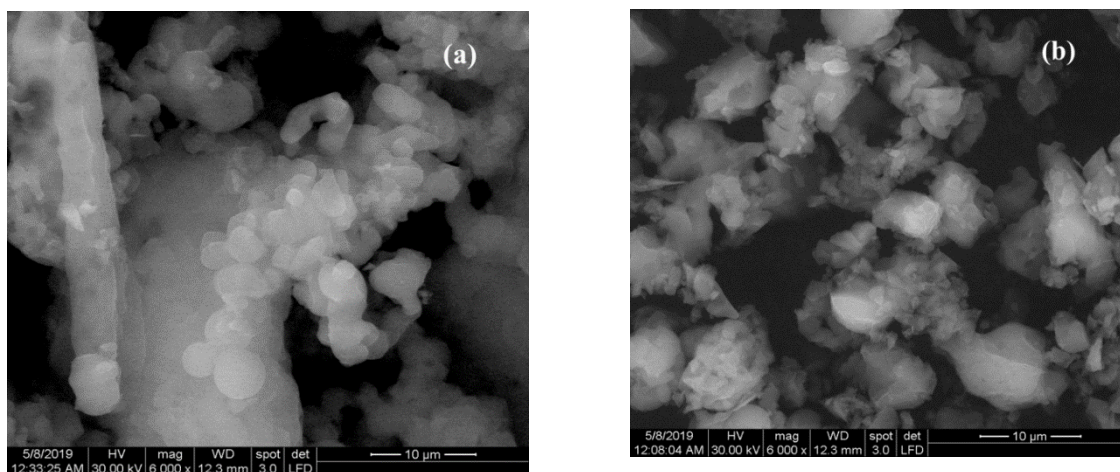


Fig. 3. SEM images of KIT-6 (a) and KIT-6 Sil (b)

The CO₂ adsorption capacity of the adsorbent in mmol of CO₂ per gram of adsorbent was determined from the mass gain of the sample in the adsorption process and was calculated more precisely from the mass loss during the desorption step. In Table 2, the amounts of the captured CO₂ on KIT-6 Sil adsorbent in the temperatures between 40-70 °C are shown. By increasing the temperature, the adsorption capacity and efficiency of amino groups decrease from 2.23 to 0.95 mmol CO₂/g SiO₂, and from 0.51 to 0.22 mmol CO₂/mmol NH₂ respectively. The best result was obtained for KIT-6 Sil at 40 °C which means an adsorption capacity of 2.23 mmol CO₂/g SiO₂ and an efficiency of amino groups of 0.51 mmol CO₂/mmol NH₂.

The results are promising and showed that both the adsorption capacity (mmol CO₂/g adsorbent) and the efficiency of amino groups (mmol CO₂/mmol NH₂) depend of the temperature at which the experiment performed.

Table 2. The amounts of the capture CO₂ using KIT-6-Sil at different temperatures

No.	Sample	Temp (°C)	n _{CO₂} /gSiO ₂ (mmol/gSiO ₂)	n _{CO₂} /n _{NH₂} (mmol/mmol)
1	KIT-6-Sil	40	2.23	0.51
2	KIT-6-Sil	50	1.76	0.40
3	KIT-6-Sil	60	1.31	0.29
4	KIT-6-Sil	70	0.95	0.22

The results are promising and showed that both the adsorption capacity (mmol CO₂/g adsorbent) and the efficiency of amino groups (mmol CO₂/mmol NH₂) depend of the temperature at which the experiment performed.

Conclusion

In this paper, the preparation of KIT-6 and KIT-6 Sil by grafting of amino-functionalized using a silane coupling agent 3-aminopropyl triethoxysilane (APTES) were carried out.

The small angles of XRD showed that KIT-6 has a cubic structure which indicates that the synthesis was successful. In the case of KIT-6 Sil appears a decrease in peaks intensity by partial blocking of pores and result that APTES was successfully grafted onto KIT-6. The FT-IR indicated that the KIT-6 Sil present all the characteristic bands of amino-functional groups, providing the grafting of amines onto KIT-6.

The CO₂ adsorption/desorption of KIT-6 Sil showed that both the adsorption capacity (mmolCO₂/g adsorbent) and the efficiency of amino groups (molCO₂/mol NH₂) depend on the temperatures. The best results were obtained for KIT-6-Sil at 40 °C.

References

- [1] L. Yamin, Y. Xiaojing, *Applied Energy*, 211 (2018) 1080.
- [2] Y. Belmabkhout, R. Serna-Guerrero, A. Sayari, *Ind Eng Chem Res*, 49 (2010) 359.
- [3] B Ma, L Zhuang, S Chen, *J Porous Mater.*, 23 (2016) 529.
- [4] A. Popa, V. Sasca, O. Verdes, M. Suba, P. Barvinschi, *J Therm. Anal. Calorim.*, 134 (2018) 269.
- [5] R. Kishor, AK. Ghoshal, *Chemical Engineering Journal*, 262 (2015) 882-890.
- [6] F. Kleitz, S. H. Choi, R. Ryoo, *Chem. Commun.*, (2003) 2136
- [7] W. Junhui, L. Yang, Z. Zhongshen, H. Zhengping, *J. Mater. Chem. A*, (2015) 3.
- [8] S. Shylesh, A.P. Singh, *J. Catal.* 228 (2004) 333–346.
- [9] CS Srikanth, *SSC Chuang* , *J. Phys. Chem. C* 117,(2013) 9196.
- [10] P. Visuvamithiran, M. Palanichamy, K. Shanthi, V. Murugesan, *Applied Catalysis A: General* 462– 463 (2013) 31.

CHARACTERIZATION OF RECYCLED RESINS WITH AMINOPHOSPHONIC GROUPS FOR A FUTURE ANTIMICROBIAL TEST

Ileana Nichita^{1*}, Lavinia Lupa², Adriana Popa³, Valentin Radu Gros¹

¹“Banat” University of Agricultural Science and Veterinary Medicine, 119 Calea Aradului, 30465 Timisoara, Romania

²Faculty of Industrial Chemistry and Environmental Engineering, Politehnica University of Timisoara, 6 Vasile Parvan Blv, 300223 Timisoara, Romania

³Institute of Chemistry “Coriolan Dragulescu”, 24 Mihai Viteazul Blv, 300223 Timisoara, Romania

*e-mail: nichita_ileana@yahoo.com,

e-mail: apopa_ro@yahoo.com

Abstract

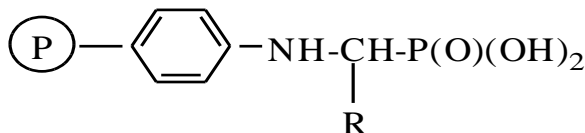
This article describes analysis of resins with functional group (by type aminophosphonic groups) recuperated from a biological environment for the use in a new study of antimicrobial test. Their stability was confirmed by Fourier transform infrared spectroscopy, energy-dispersive X-ray analysis and scanning electron microscopy.

Introduction

Bacteria show a significant role in our life. They are dispersed in soil, air and water. They may cause numerous health related problems. For prevent the infection of bacteria some materials were employed as antimicrobial agents. One of the remarkable substances is aminophosphonic acid. It has an important role in biological system [1]. The compounds of aminophosphonic acid can be use as enzyme inhibitors, potential antibiotics and pharmacological agents [1].

In the past decade, the field of macromolecular systems with antimicrobial properties has intensive development including the chemical modification of known polymers with bioactive groups by polymer-analogous reactions [2-5].

This study concerns the characterization of recycled resins with aminophosphonic groups (see figure 1) [6] for using in a new antimicrobial test. The efficacy of the aminophosphonic pendant groups grafted on styrene-6.7%divinylbenzene copolymers was investigated by Fourier transform infrared spectroscopy, energy-dispersive X-ray analysis and scanning electron.



Where: R= -C₆H₅ (1Ba-Bz), -C₂H₆ (2Ba-Pr); P- styrene-6.7%divinylbenzene copolymers

Figure 1. Aminophosphonic pendant groups grafted on styrene-6.7%divinylbenzene copolymers

Experimental Part

Instruments

Fourier transform infrared spectroscopy (FTIR) using a JASCO-FT/IR-4200 spectrophotometer. Energy-dispersive X-ray analysis (EDAX) and scanning electron microscopy (SEM) were carried out using a Quanta FEG Microscope equipped with EDAX ZAF quantifier.

Method of work

All six samples (1Ba-Bz (1), 2Ba-Pr (1), (1Ba-Bz (2), 2Ba-Pr (2) and (1Ba-Bz (3), 2Ba-Pr (3) were recovered from antibacterial solutions where they were tested against one specie of Gram-positive bacteria (*Staphylococcus aureus*) (code: 1-*S. aureus*) and one specie of Gram-negative bacteria (*Pseudomonas aeruginosa*) (code: 2-*P. aeruginosa*) and a specie of yeast (*Candida albicans*) (code: 3-*C. albicans*). Then, the samples were filtrated, autoclaved at 1 atm pressure and temperature of 120 °C for 30 minutes. These recuperated samples were characterized by FTIR, SEM and EDAX for confirming the presence of active aminophosphonic groups' pendant.

Results and discussion

All the aminophosphonic acid groups grafted on styrene-6.7%divinylbenzene copolymer were analyzed after recovery by FTIR analysis. The absorption bands of samples (see table 1) are presented in the region 3300-3500, 1200-1250 and 1000-1100 cm^{-1} for -NH, P=O and P-OH respectively [6].

Table 1. FTIR spectra for the aminophosphonic acid groups grafted on styrene-6.7%divinylbenzene copolymer.

	1- <i>S. aureus</i>		2- <i>P. aeruginosa</i>		3- <i>C. albicans</i>	
	1Ba-Bz (1)	2Ba-Pr (1)	1Ba-Bz (2)	2Ba-Pr (2)	1Ba-Bz (3)	2Ba-Pr (3)
-NH	3413.39	3358.43	3406.64	3411.46	3415.31	3423.03
P=O	1213.97	1212.04	1213.97	1212.04	1213.97	1209.14
P-OH	1076.08	1072.23	1073.19	1072.19	1075.12	1171.54

In figure 2 is presented EDAX image of 2Ba-Pr (2) after recover from the test with *P. aeruginosa*. It confirm the presence of chemical elements as P, N, Cl, O and C in the of aminophosphonic groups grafted on copolymer

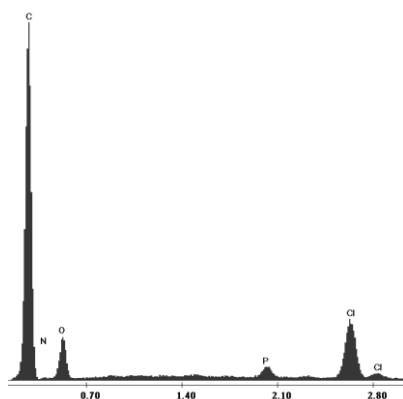


Figure 2. EDAX image of 2Ba-Pr (2) after recover from the test with *P. aeruginosa*
Elemental analysis of all six samples (1Ba-Bz (1), 2Ba-Pr (1), (1Ba-Bz (2), 2Ba-Pr (2) and (1Ba-Bz (3), 2Ba-Pr (3), are shown in Table 2. Composition of these chemical elements confirm the possibility of reuse of these polymers in a new antimicrobial test.

Table 2. Composition of aminophosphonic groups grafted on copolymer after recover them determined by elemental analysis

Elem. / Wt%	1- <i>S. aureus</i>		2- <i>P. aeruginosa</i>		3- <i>C. albicans</i>	
	1Ba-Bz (1)	2Ba-Pr (1)	1Ba-Bz (2)	2Ba-Pr (2)	1Ba-Bz (3)	2Ba-Pr (3)
C	80.02	75.80	80.39	75.57	75.03	69.07
N	4.26	7.03	5.10	2.01	7.17	9.37
O	15.13	16.86	13.82	21.15	17.60	21.38
P	0.22	0.09	0.25	0.29	0.10	0.05
Cl	0.36	0.22	0.43	0.97	0.10	0.14

Determination of the FTIR spectra and energy-dispersive X-ray analysis (EDAX) after the first cycle of antibacterial activity confirmed that the aminophosphonic acid groups can be used as the active groups in a new the antibacterial test.

The morphology of the resins grafted with aminophosphonic pendant groups can be directly visualized by SEM images (Figure 2 and 3)

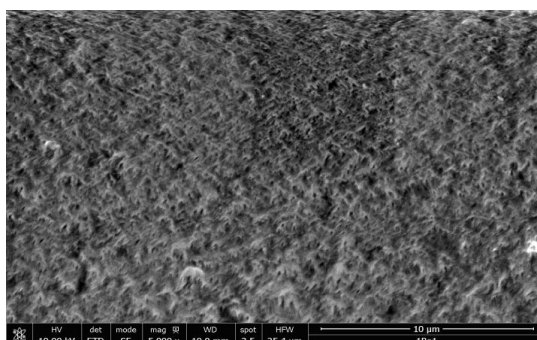


Figure 2. SEM image 1Ba-Bz (1) after recover from the test with *S. aureus*

The surface of the 1Ba-Bz (1) (see figure 2) is rough with interconnected micro-particles and many micro-pores.

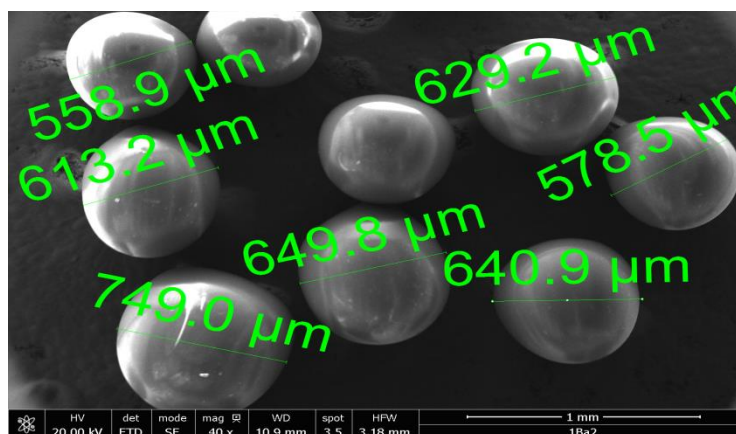


Figure 3. SEM image 1Ba-Bz (2) after recover from the test with *P. aeruginosa*

The beads (see figure 3) are approximately spherical with an average diameter that there is a range from 570 to ~ 750 μm.

The functional groups by type aminophosphonic acid on the bead surface are stable, and antibacterial properties are possible in a repeated application using the same beads.

Conclusion

The investigation of the functional aminophosphonic groups grafted on copolymer styrene-6.7% divinylbenzene recovered from a biological environment confirms the stability of their functional groups.

This is the reasons to recommend their application for a new antimicrobial test.

References

1. Ch. Mohan, B. Hari Babu, C. Naga Raju, R. Usha Nagalakshmi, E-Journal of Chemistry, 2008, 5(4), 679-687.
2. L. Timofeeva, N. Kleshcheva, Appl Microbiol Biotechnol, 2011, 89, 475–492.
3. I. Nichita, A. Popa, E.S. Dragan, S. Iliescu, G. Ilia, Journal of Biomaterials Science, Polymer Edition, 2015, 26(8), 483–496.
4. A. Popa, C.M. Davidescu, R. Trif, G. Ilia, S. Iliescu, G. Dehelean, Reactive and Functional Polymers, 2003, 55(2), 151-158.
5. I. Nichita , A. Popa , R.V. Gros, S. Iliescu, M. Stoia , M. Seres, A. Morar, Proceedings of 22nd International Symposium on Analytical and Environmental Problems, Szeged, Hungary, 10 October, 2016, 243-246, ISBN 978-963-306-507-5.
6. I. Nichita, L. Lupa, M. Stoia , E.S. Dragan, A. Popa, Polymer Bulletin, 2019, 76, 4539–4557, <https://doi.org/10.1007/s00289-018-2613-6>.

Acknowledgments:

The authors are grateful to Marcela Stoia (Faculty of Industrial Chemistry and Environmental Engineering, Timisoara, Romania) for image of EDAX and SEM.

TOXICITY ASSESSMENT OF CEFTRIAXONE, THIOTRIAZINONE AND THEIR MIXTURE FORMED DURING PHOTOCATALYTIC DEGRADATION USING TiO₂ AND ZnO

Maria Uzelac¹, Dragana Četojević-Simin², Biljana Abramović^{1,✉}

¹*University of Novi Sad Faculty of Sciences, Department of Chemistry, Biochemistry and Environmental Protection, Trg Dositeja Obradovića 3, 21000 Novi Sad, Serbia*

²*University of Novi Sad, Faculty of Medicine, Oncology Institute of Vojvodina, Dr Goldmana 4, 21204 Sremska Kamenica, Serbia*
✉*biljana.abramovic@dh.uns.ac.rs*

Abstract

Annual consumption of pharmaceutical compounds has increased worldwide and great attention has been focused on their presence in different aquatic environments in many countries [1]. After the administration, drug molecules are absorbed, distributed, metabolized, and finally excreted from the body [2]. As one of the most frequently used antibiotics, ceftriaxone sodium has been widely used in human treatment and animal husbandry due to its broad-spectrum antimicrobial capability, which results in the release of residues into wastewater, causing environmental, ecological, and health issues, threatening biota, and disrupting indigenous microbial populations [3]. Ceftriaxone is subjected to hydrolysis and it is supposed that the main stable product of hydrolysis of ceftriaxone is thiotriazinone [4]. Thiotriazinone is mainly used in the preparation of beta-lactam antibiotics with proven effects as antibacterial agents and human leukocyte elastase inhibitors [5]. In this paper, photocatalytic degradation of antibiotic ceftriaxone and its intermediate thiotriazinone using TiO₂ Degussa P25 and ZnO under solar radiation was investigated. Also, toxicity of ceftriaxone and thiotriazinone alone and in mixtures with its photocatalytic degradation intermediates obtained by using TiO₂ Degussa P25 and ZnO under solar radiation in the presence of O₂ was evaluated in vitro in a panel of three histologically different cell lines: rat hepatoma (H-4-II-E), human colon adenocarcinoma (HT-29) and human fetal lung (MRC-5).

Acknowledgments

The authors acknowledge financial support of the Ministry of Education, Science and Technological Development of the Republic of Serbia (Project No. 172042).

References

- [1] M. Petrovic, P. Verlicchi, *Contrib. Sci.* 10 (2014) 135.
- [2] K. Ikehata, N.J. Naghashkar, *Ozone-Sci. Eng.* 28 (2006) 353.
- [3] Y. Zhao, X. Liang, Y. Wang, H. Shi, E. Liu, J. Fan, X. Hu, *J. Colloid Interf. Sci.* 523 (2018) 7.
- [4] W. Arjharn, V. Vongsutilers, P. Thantiworasit, N. Suthumchai, J. Klaewsongkram, B. Tuesuwan, *Thai J. Pharm. Sci.* 40 (2016) 5.
- [5] R. Ghiorghiasa, A.R. Petrovici, I. Rosca, L. Miron, *Dig. J. Nanomater. Bios.* 11 (2016) 235.

LIPOPEPTIDE PROFILING OF A *BACILLUS* STRAIN BY HPLC-HRMS TECHNIQUE

Attila Bartal, Henriett Hunkár, Mónika Vörös, Csaba Vágvolgyi, András Szekeres¹

¹*Department of Microbiology, Faculty of Sciences,
University of Szeged, 6726 Közép fasor 52, Szeged, Hungary
e-mail: bartaloszi@gmail.com*

Abstract

Surfactins, iturins and fengycins are lipopeptide-type biosurfactants produced by the gram-positive *Bacillus* strains. They consist of an oligopeptide amino acid loop and a hydrophobic fatty acid chain. These lipopeptides are proved to exhibit various biological activities, such as anti-tumor, anti-viral and anti-inflammatory effects. According to these properties, different therapeutic and environmental applications of these compound groups are considered. Their chemical composition may vary in the length of the fatty acid chain and in the sequence of the amino acids of the peptide loop, generating a wide spectrum of different homologues and isomers. These isoforms can be discerned by fragmentation in mass spectrometry. Depending on the cultivation conditions the production of biosurfactants is affected, resulting in various rates of the different isoforms produced.

In this work a mixture of lipopeptides were extracted from the *Bacillus* strain SZMC 6178J and was examined by HPLC-HESI-MS techniques. To increase the separation of the fractions with higher masses a gradient elution was applied using a non-polar solvent system, which led to the elution and characterization of their structures. The quantitative examinations of the effects of the culture media modified by various carbon sources and metal ions on the composition and ratio of the different surfactin isoforms produced were carried out by a triple quadrupole mass spectrometric system in full scan mode. We observed that the application of metal ions commonly used for enhancing surfactin production resulted in the almost complete loss of lipopeptide biosynthesis of the bacteria. The qualitative measurements of the carbon source modified samples were achieved by an OrbiTrap high resolution mass spectrometer in parallel reaction monitoring mode. Both the length of the linked fatty acids and the peptide sequences were also investigated during the MS² spectra analyses of the hydrogenated precursor ions. The results led to the detection and identification of 16 different surfactin variants. Observation of the relative ratios of the different homologues and isoforms showed that the [Sur] and [Val7] variants and molecules with C14 and C15 chain lengths were the most common in the samples.

This work was supported by the Hungarian Scientific Research Fund by grants NKFI K-128659 and this work was connected to the project GINOP-2.3.2-15-2016-00012. The infrastructural background was established with the support of GINOP-2.3.3-15-2016-00006.

RECYCLING OF FILTER TEA INDUSTRY BY-PRODUCTS: PRODUCTION OF *A. MILLEFOLIUM* EXTRACTS USING SUBCRITICAL WATER EXTRACTION

Jelena Vlatić¹, Maja Molnar², Martina Jakovljević², Senka Vidović¹, Stela Jokić², Kristian Pastor¹, Natasa Nastic¹

¹*Department of Inorganic and Analytical Chemistry, University of Szeged, H-6720 Szeged, Dóm tér 7, Hungary*

²*Josip Juraj Strossmayer University of Osijek, Faculty of Food Technology, Franje Kuhača 18, 31000, Osijek, Croatia*
e-mail: vlaticjelena@gmail.com

Abstract

Medicinal plants are most commonly used in the form of herbal tea, individually or in a tea blend. In the process of production filter tea, "herbal dust" or very small particles are formed during grinding of the plant material. As the particles of herbal dust are smaller (<0.315 mm) with respect to the particle size of filter paper, this fraction cannot be used in form of filter tea and is considered as a by-product in the tea production process [1]. Considering the significant content of bioactive compounds in this type of material, it would be beneficial to develop an adequate way of additional exploitation of the by-product and its transformation into high-quality products.

A medicinal plant with pharmacological properties that are recognized worldwide is *Achillea millefolium* which is included in the national Pharmacopoeias of many countries. Many scientific researches confirmed the biological activity of *A. millefolium* preparations such as anti-inflammatory, antitumor, antioxidant, antimicrobial, liver protective activities, and gastroprotective activity [2].

Introduction

The aim of this study was to develop procedures for obtaining *A. millefolium* extracts with a high content of polyphenolics by applying innovative green technology - subcritical water extraction (SWE). During the extraction with subcritical water, Maillard and caramelization reactions take place and have formation of neoantioxidants as a consequence, which are the reason for the increased antioxidant activity. Hydroxymethylfurfural (HMF) is an indicator of the Maillard reaction [3]. Several studies show that HMF and related compounds induce the genotoxic and mutagenic effect in human cells and promote colon cancer in rats [3]. Therefore, the goal of this research was to establish the conditions of extraction that provide the highest quality of extracts in terms of content of antioxidant components with the lowest formation of HMF.

Experimental

SWE extraction was performed at different process parameters (temperature 120–200 °C, extraction time 10–30 min, and HCl concentration 0–1.5%). The content of polyphenols in obtained extracts was determined by applying spectrophotometric methods, and the content of individual components present in extracts was determined by HPLC analysis. Additionally, HMF content in extracts was determined.

Results and discussion

There was no HMF present in extracts at the highest temperature of extraction (200°C; 20 min and without HCl) which provided the highest content of phenols (128.20 mg/GAE/g SE). HPLC analysis was used to determine the content of chlorogenic acid and its highest content was recorded in the extract obtained at 120°C, 20 min and without addition of HCl. The same

extract also possessed the highest content of flavonoids (79.19 mg CAT/g SE). The presence of chlorogenic acid was not detected at the highest temperature due to potential degradation, while at lower temperatures the content of chlorogenic acid was in range of 16.8-30.4 µg/mL of extract. In addition, HMF was detected in almost all samples except in those obtained at higher temperatures and it ranged between 5.8 and 39.3 µg/mL.

Conclusion

In the present study, SWE was successfully applied for valorization of *A. millefolium* “herbal dust” through the extraction of bioactive components and production of high quality extracts.

References

- [1] M. Ramić, S. Vidović, Z. Zeković, J. Vladić, A. Cvejin, B. Pavlić, Ultrasonic. Sonochem. 23 (2015) 360-368.
- [2] A.M. Cavalcanti, C.H. Baggio, C.S. Freitas, L. Rieck, R.S. De Sousa, J.E. Da Silva-Santos, M.C.A. Marques, J. Ethnopharmacol. 107 (2006) 277-284.
- [3] M. Plaza, V. Abrahamsson, C. Turner, J. Agric. Food Chem. 61 (2013) 5500-5510.

WASTEWATER TREATMENT WITH MICROALGAE AND CHARACTERIZATION OF THE OBTAINED BIOMASS

Jelena Vladic¹, Luisa Gouveia², Alice Ferreira², Senka Vidovic¹

¹*Faculty of Technology, University of Novi Sad, Bulevar cara Lazara 1, 21000 Novi Sad, Serbia*

²*LNEG – Laboratório Nacional de Energia e Geologia, I.P./Bioenergy Unit, Estrada do Paço do Lumiar 22, 1649-038, Lisbon, Portugal
e-mail: vladicjelena@gmail.com*

Abstract

Wastewater treatment using microalgae possesses numerous benefits when compared to the conventional treatment. Apart from a significant reduction in expenses of purification of wastewater, it also decreases costs of microalgae production. In addition, there are additional benefits of using microalgae in wastewater treatment such as: reduction in toxic solid sludge formation; reduction of greenhouse gases; reduction of necessity for forced aeration because the oxygen required for aerobic bacteria is provided by the microalgae photosynthesis; production of microalgae biomass, which is a great source of energy due to the process of absorbing nutrients present in the wastewater [1-3].

Microalgae represent a source of significant components such as proteins, sugars, lipids, pigments (carotenoids and chlorophylls), and antioxidant components. Therefore, the obtained biomass, depending on its chemical composition and quality, can be used in different fields.

Introduction

The main goal of this work was to evaluate the potential of *Scenedesmus obliquus* microalga for treating wastewater from poultry industry. Moreover, the goal was to determine the composition of the obtained biomass in terms of content of proteins, lipids, carbohydrates, chlorophylls, and bioactive compounds. Based on the composition, the potential application(s) of the obtained biomass can be determined.

Experimental

The effluent was characterized in terms of pH, COD, and nitrogen (ammonia and Kjeldahl nitrogen) and phosphorus concentrations, before cultivation. In order to assess the efficiency of the wastewater treatment by microalgae, the same analyses were performed at the end of the cultivation, after biomass settling and filtration. The obtained biomass was characterized in terms of its crude protein, total sugars, and chlorophylls (a and b). In addition, biomass productivity was determined.

Results and discussion

The efficiency of removing of Kjeldahl nitrogen was approximately 45% in poultry wastewater, while regarding COD removal, high efficiency of 97.68% was achieved. The results of biochemical characterization of microalgae biomass after the effluent treatment indicate that the process resulted in production of valuable biomass. The content of proteins of the *S. obliquus* biomass after treatment of poultry wastewater was 35.8%. The content of sugars was approximately 6%. Additionally, the content of chlorophyll in biomass obtained after poultry wastewater treatment was 4.2 µg/mg.

Conclusion

The obtained results indicate that microalgae *S. obliquus* possess the potential in wastewater poultry treatment and the obtained biomass can be used as potential feedstock for biofuel and biofertilizer production or as a source of animal feed.

Acknowledgements

Part of this work was supported by the COST Action No ES1408 and Provincial Secretariat for Higher Education and Scientific Research No 142-451-2576/2019-01.

References

- [1] A.P. Batista, L. Ambrosano, S. Graça, C. Sousa, P. Marques, B. Ribeiro, E.P. Botrel, P.C. Neto, L. Gouveia, Bioresour. Technol. 184 (2015) 230-235.
- [2] W.J. Oswald, J. Appl. Phycol. 15, 2 (2003) 99-106.
- [3] L. Gouveia, S. Graça, C. Sousa, L. Ambrosano, B. Ribeiro, E.P. Botrel, P.C. Neto, A.F. Ferreira, C.M. Silva. Algal Res. 16 (2016) 167-176.

ENVIRONMENTAL FRIENDLY LEAD FREE PIEZOELECTRIC CERAMICS

Farkas Iuliana, Bucur Alexandra Ioana, Bucur Raul Alin

*National Institute for Research and Development in Electrochemistry and Condensed Matter,
Condensed Matter Department, No.1 Plautius Andronescu, 300224 Timisoara Romania.
e-mail: iulia_b24@yahoo.com*

Abstract

The interconnectivity between mechanical and electrical energy specific for the ferroelectric ceramics, enables their application in a wide range of devices. Lead oxide based ferroelectrics are the most widely used materials for actuators, sensors and microelectronic applications, due to their excellent piezoelectric properties. Because of the toxicity of lead oxide, researchers are now focusing on to substituting this compound [1]. Lead-free piezoelectric materials are nowadays receiving increasing attention, since recent reports showed that they are promising candidates for lead-free piezoelectric materials [2]. Of considerable interest is the (K,Na)NbO₃ (KNN)-based system, which possesses a relatively high Curie temperature and good piezoelectric properties. Also, the temperature independence of the morphologic phase boundary (MPB) for such materials enables a good temperature stability of the piezoelectric and ferroelectric properties [3, 4].

In this study, lead-free KNN piezoelectric ceramics doped with x mol % SmBO₃ (x= 0,25; 0,5; 0,75; 1; 2,5; 5 and B= Al, Co, Cr, Fe, Mn), were prepared by conventional ceramic processing. The crystalline structures of the obtained ceramics were analyzed by X-ray diffraction using a PanAnalytical X'Pert Pro MPD diffractometer. The microstructure was analyzed using SEM techniques. The dielectric measurements (room temperature, from 100Hz up to 5MHz) were performed with a 42 Hz–5 MHz Programmable Impedance/LRC meter TEGAM model 3550. The planar piezoelectric properties were measured using the resonance method with an impedance analyzer Agilent E5100A. The increase of the piezoelectric properties and decrease in grain size proves that such piezoelectric ceramics can be used for sensing applications.

References

- [1] Restriction of Hazardous Substances in Electrical and Electronic Equipment (RoHS 2), Directive 2011/65/EU.
- [2] J. Rodel, W. Jo, K.T.P. Seifert, E.M. Anton, T. Granzow, D. Damjanovic, J. Am. Ceram. Soc. 92, 1153 (2009).
- [3] X. Wang, J. Wu, D. Xiao, J. Zhu, X. Cheng, T. Zheng, B. Zhang, X. Lou, X. Wang, J. Am. Chem. Soc. 136, 2905 (2014).
- [4] L.J. Rigoberto, G.V. Virginia, M.P. Cruz, M.E. Villafuerte-Castrejon, J. Electron. Mater. 44, 2862 (2015).

HIGH ASPECT RATIO HYDROXYAPATITE FOR LOW DENSITY AEROGELS

Alexandra Ioana Bucur, Bogdan-Ovidiu Taranu, Iuliana Sebarchievici, Cristina Mosoarca, Mihai Cosmin Pascariu, Corina Orha, Radu Banica

*National Institute for Research and Development in Electrochemistry and Condensed Matter
no 144 dr P. A Podeanu, Timisoara 300569, Romania
alexandra.i.bucur@gmail.com*

Abstract

Aerogels are materials with huge potential for a number of applications such as thermal insulation, catalyst carriers, electrodes or flame retardant materials, etc [1]. HA is a well-known biocompatible material [2]. Making this material in the shape of aerated low-density structures brings advantages regarding, among others, the bone cells growth inside this ceramic matrix, with high potential to improve the biocompatibility aspects [3, 4]. The aspect ratio of the original crystals is one of the factors that plays an important role in obtaining tridimensional structures. The purpose of the present study was to obtain tridimensional low density structures based both on a high aspect ratio and pseudo-spherical HA particles.

Two HA samples were prepared, one by simple precipitation, and the other by precipitation followed by hydrothermal crystallization at 200°C. The synthesized materials were used in order to obtain low density tridimensional structures by applying the freeze-drying method.

Both samples were further used as aqueous suspension, frozen at -25°C for 18h, then freeze-dried for 18h and sintered at 750°C, heating rate 5 deg/min, and naturally cooled to room temperature. The powders were characterized by SEM, XRD and FT-IR, and the freeze-dried structures were studied by SEM.

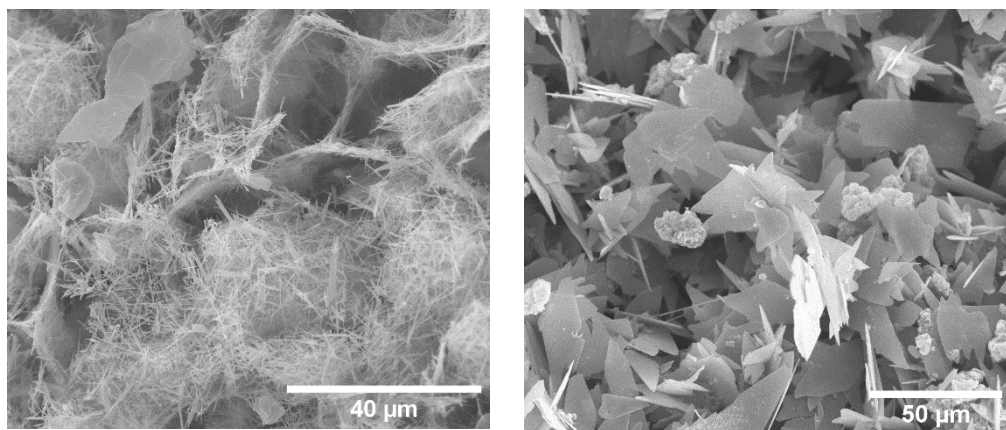


Fig. 1 SEM images of tridimensional freeze-dried structures: left – from hydrothermally synthesized HA; right – from precipitated HA

The results proved the formation of pure phase HA powders. The hydrothermal treatment leads to the improvement of the crystallinity and aspect ratio of the particles. As a result of the hydrothermal treatment, long crystals with lengths of 5-10 µm and widths of 0.1-1 µm are formed, superstructured in highly porous microspheres. Using particles with a large shape coefficient (nanowires) obtained hydrothermally, aerogels of the same porosity but with higher mechanical strength can be obtained than by using precipitated particles

Acknowledgements

This work was financed by the National Program NUCLEU, Project Code PN 19 22 01 01, Contract No 40N/2019

References

- [1] Guo W, Liu J, Zhang P, Song L, Wang X, Hu Y, Compos. Sci. Technol. 158 (2018) 128-136
- [2] Fidancevska E., Ruseska G., Bossert J., Lin Y.-M., Boccaccini A.R., Mater. Chem. Phys. 103 (2007) 95–100
- [3] Parandoush, P., Fan, H., Song, X., Lin, D., J. Micro. Nano.-Manuf., 6(1) (2017) 011007
- [4] Zhang Y.-G., Zhu Y.-J., Chen F., Sun T.-W., ACS Appl. Mater. Interfaces 9 (2017), 7918–7928

NEW ENVIRONMENTAL BUILDING MATERIAL WITH SELF-CLEANING PROPERTY

Madalina Ivanovici^{1,2}, Paulina Vlazan¹, Stefan Novaconi¹, Cristina Mosoarca¹, Florina Stefania Rus^{1,*}

¹National Institute for Research and Development in Electrochemistry and Condensed Matter, 300569 Timisoara, Aurel Paunescu Podeanu Street No. 144, Romania

²Politehnica University of Timisoara, 300006 Timisoara, Piata Victoriei No. 2, Romania

*Corresponding author e-mail: rusflorinastefania@gmail.com

Abstract

Developing self-cleaning building materials has gained a lot of interest among the researchers due to the beneficial effect on the environment regarding the indoor and outdoor air quality and due to the enhancement of the maintenance normally required for the construction materials. A known method for functionalizing the materials is represented by including active components – photocatalytic compounds in the composition of the construction materials. Under the solar irradiation, these materials have the ability to degrade various pollutants coming from the environment, especially from the atmosphere [1]. As materials used for photocatalytic activation, there may be mentioned mortar, cement, asphalt, plaster, glass or even paints [2, 3].

The aim of the present study was to obtain a new building material with self-cleaning property consisting of glass foam as a valuable building material and tungsten trioxide as the photoactive compound. The glass foam is an interesting material which possesses a combination of different properties of value in the construction field such as thermal and sound insulating properties, chemical and mechanical stability and high resistance to fire and moisture [4]. The tungsten trioxide was selected because it has been reported to be a photocatalyst that absorb a wide spectrum of the visible light and because it is cheap and stable in acidic or oxidative environment [5].

The foam glass functionalized with WO_3 was synthesized by hydrothermal method and the raw materials involved are glass waste from household activities, waste of calcium carbonate from marble industry and tungsten trioxide nanoparticles obtained in a previous study by combustion method. The identification of the main chemical elements and bonds of the material was performed by Raman and FT-IR analyses. 3D laser scanning microscopy was employed for characterizing the surface morphology of the material. In figure 1, 2D image and 3D images of the sample at 100 μm and 400 μm scale are presented.

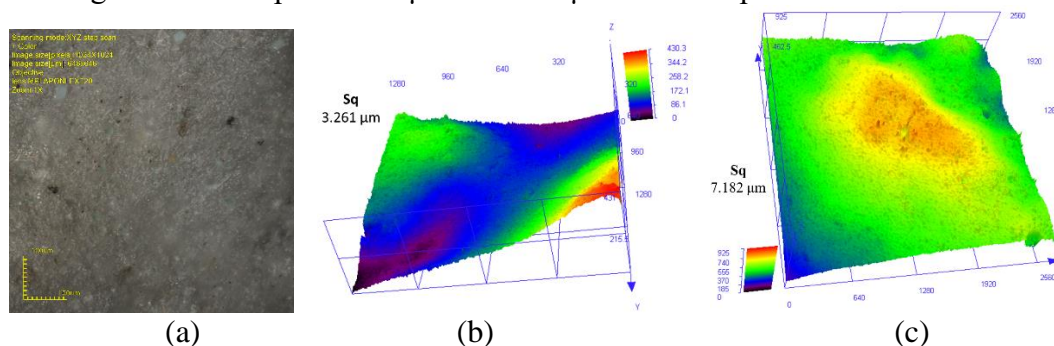


Figure 1. (a) 2D image and (b) 3D image of glass foam functionalized with WO_3 performed at 20X magnification and (c) 3D image performed at 5X magnification

As a measure of the surface texture, the values of the surface roughness at both scales were calculated for each analyzed surface. The values of the surface roughness are 3.261 μm

for image recorded with 20X magnification (figure 1(a) and (b)), respectively 7.182 μm for image recorded with 5X magnification (figure 1(c)).

In order to validate the self-cleaning properties of the glass foam functionalized with WO_3 , the material was subjected to a photocatalytic test. In this sense, the capacity of the material to degrade methylene blue (MB) - an organic dye, under artificial solar irradiation was evaluated by recording the absorbance of the MB aqueous solution with UV-VIS spectrophotometer for 2 hours, at every twenty minutes. Former to the exposure to simulated solar light, the material was maintained in the MB aqueous solution (20 ml with initial concentration of 5 mg L^{-1}), in dark conditions, for 20 minutes to reach the adsorption-desorption equilibrium. The decrease of the MB absorbance during the photocatalytic experiment is shown in figure 2. The removal of MB reached a value of 55.5%.

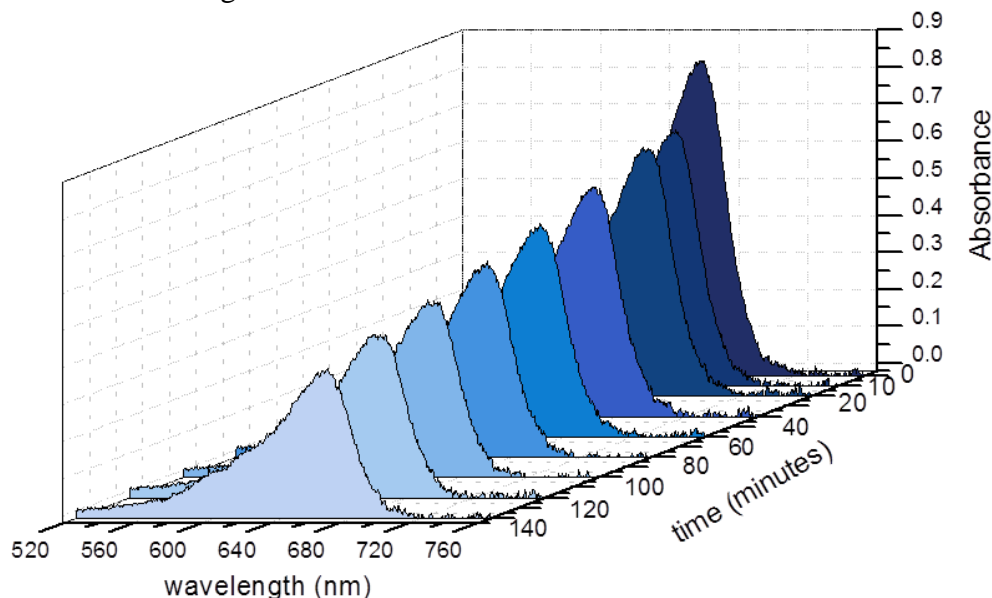


Figure 2. MB absorbance variation in time during the photocatalytic experiment

Acknowledgements

This experimental study was financed by the project PN-III-P1-1.2-PCCDI-2017-0391/CIA_CLIM-Smart buildings adaptable to the climate change effects, granted by Romanian Ministry of Research and Innovation, CCCDI-UEFISCDI.

References

- [1] R. Paolini, D. Borroni, M. Pedferri, M. V. Diamanti, Constr. Build. Mater. 192 (2018) 126.
- [2] A. Andaloro, E.S. Mazzucchelli, A. Lucchini, M.P. Pedferri, JFDE 4 (2016) 115.
- [3] S.H. Chermahini, S. Eslamian, K. Ostad-Ali-Askari, V. P. Singh, N. R. Dalezios, Adv. Civ. Eng. 1 (2018) 1.
- [4] A. M. Papadopoulos, Energ. Buildings 37 (2005) 77.
- [5] H. Zheng, J.Z. Ou, M. S. Strano, R.B. Kaner, A. Mitchell, K. Kalantar-zadeh, Adv. Func. Mater. 21 (2011) 2175.

UV AND SUNLIGHT-DRIVEN DEGRADATION OF CIPROFLOXACIN IN THE PRESENCE OF CATALYSTS TiO₂, ZnO AND MgO

Nina Finčur¹, Paula Sfirloagă², Daniela Šojić Merkulov¹, Biljana Abramović¹

¹University of Novi Sad Faculty of Sciences, Department of Chemistry, Biochemistry and Environmental Protection, Trg Dositeja Obradovića 3, 21000 Novi Sad, Serbia

²National Institute of Research and Development for Electrochemistry and Condensed Matter, Dr. Aurel Păunescu Podeanu 144, 300569, Timișoara, Romania
e-mail: nina.fincur@dh.uns.ac.rs

Abstract

Advanced Oxidation Processes (AOPs) are used to remove a wide range of organic pollutants [1]. These processes are recommended for the removal of pollutants that are very stable because they allow the complete mineralization of pollutants or their partial degradation to less harmful compounds or compounds that are biodegradable [2]. AOPs are based on the formation of highly reactive chemical species that can break down even the most stable molecules to biodegradable compounds. The most important oxidizing agent is the non-selective hydroxyl radical, which can oxidize and mineralize organic molecules, producing CO₂, H₂O, and inorganic ions [3]. Heterogeneous photocatalysis has been recognized as a promising method for the removal of organic pollutants from water [4]. The presence of pharmaceutically active compounds in natural waters is a problem for the aquatic living world, since these compounds from the wastewater treatment plants can reach the environment in almost unchanged form [5]. Antibiotics have been widely used in human clinical, animal husbandry, and aquaculture for almost one hundred years, playing an important role in the treatment of infectious diseases [6]. Antibiotics have been detected in the effluent of sewage treatment plants, surface waters, and ground waters. Thus, it is necessary to remove antibiotic pollutants from the source of wastewater [7]. Ciprofloxacin belongs to fluoroquinolones class, which represents one of the most important class of synthetic antibiotics. In this paper, photodegradation of ciprofloxacin was studied using heterogeneous photocatalysis under UV and simulated sunlight. Newly synthesized nanopowders ZnO, TiO₂ and MgO were used as photocatalysts. Besides, the effect of (NH₄)₂S₂O₈ concentration on the efficiency of the ciprofloxacin removal, using TiO₂ and both type of radiation, was observed.

Acknowledgments

The authors acknowledge financial support of the Ministry of Education, Science and Technological Development of the Republic of Serbia (Project No. 172042).

References

- [1] C. Byrne, G. Subramanian, S.C. Pillai, J. Environ. Chem. Eng. 6 (2018) 3531.
- [2] S. Teixeira, R. Gurke, H. Eckert, K. Kühn, J. Fauler, G. Cuniberti, J. Environ. Chem. Eng. 4 (2016) 287.
- [3] S. Malato, P. Fernández-Ibáñez, M.I. Maldonado, J. Blanco, W. Gernjak, Catal. Today 147 (2009) 1.
- [4] M.A. Behnajady, N. Modirshahla, R. Hamzavi, J. Hazard. Mat. B133 (2006) 226.
- [5] O.K. Dalrymple, D.H. Yeh, M.A. Trotz, J. Chem. Technol. Biotechnol. 82 (2007) 121.
- [6] Y. Zhao, S. Hou, D. Liu, C. Zhong, Ind. Eng. Chem. Res. 57 (2018) 15132.
- [7] A.K. Sarmah, M.T. Meyer, A.B. Boxall, Chemosphere 65 (2006) 725.

STUDIES REGARDING OBTAINMENT AND THE CHARACTERIZATION OF DIFFERENT TYPES OF HOMEMADE CHOCOLATE WITH FRUIT ADDITION

Georgeta-Sofia Popescu^{1*}, Ariana - Bianca Velciov^{1*}, Adrian Riviş¹, Antoanela Cozma¹, Daniela Stoin¹, Florina Radu¹, Iulia Bucurescu¹

¹ Faculty of Food Engineering, Food Science Department, Banat's University of Agricultural Sciences and Veterinary Medicine "King Michael I of Romania" Timisoara

*corresponding authors: A.B. Velciov (ariana.velciov@yahoo.com), GS Popescu (sofia.pintilie@gmail.com)

Abstract

It is known that homemade chocolate is the most important and popular sweet product used in the diet of children and adults, due to its attractive taste and caloric value.

The special nutritional qualities of chocolate are conferred by compounds with biological activity in its composition. The representative compounds from chocolate are antioxidants, macro- and micronutrients, sugar, and stimulants such as caffeine and theobromine.

In our study we show how fruits addition can influence the physico-chemical properties of homemade chocolate. The used fruits were been frozen fruit.

Experimental part is based on some physico-chemical determination (content of water, dry content, total mineral content et al.) in order to evaluate the nutritional characteristics of the product.

Key words: *chocolate, diet, sour cherry fruit, caloric value*

Introduction

The history of chocolate starts from the cocoa tree cultivated by the Mayan populations of the Yucatan in the 6th century AD, which would have left us a fruit, compared, since then, with gold. Chocolate came to Europe in the 16th century. From that moment, the modern chocolate industry has developed, and cocoa seeds are now processed in different ways [1].

Nowadays, chocolate is recognized for its beneficial health qualities. Thus, it is shown that, eaten in moderate amounts, chocolate is lauded for its remarkable antioxidant potential due to the high content of biologically active phenolic compounds from cocoa powder.

The purpose of this study was to evaluate the physical, chemical characteristics (content of water, dry content, total mineral content, total antioxidant capacity) and sensory aspects in case of simple homemade chocolate and homemade chocolate with fruit addition, in order to evaluate the nutritional characteristics of the chocolate products.

Material and Methods

Chemicals and materials: All chemicals and reagents were analytical grade or purest quality purchased from Sigma, Merck, Aldrich and Fluka, bidistilled water was used. Absorption determination for CUPRAC and total polyphenols content was made using SPECORD 205 spectrophotometer by Analytik Jena.

Humidity, dry mater and total mineral content

Samples weight was measured by using a digital balance with a sensitivity of 0.001 g. Gravimetric method was used to determine the moisture of samples, using a moisture analyzer Nabertherm model 6/11 with automated programming and electronic display. The level of moisture was tested for all samples by heating a known weight of sample in the hot air oven (100±5°C) until constant weight [2].

Moisture content can be determined from total solid content (TSC) as below [3]:

Moisture (%) = $100 - \text{TSC}(\%)$, where total solid content (TSC) represent dry matter.

In order to determine the total mineral content (ash), the samples were washed with deionised water, dried, chopped, dried and then calcined in the Nabertherm LE4 oven (Germany), at 505 °C. The temperature was gradually raised to 505 °C (when the ash became gray-white and the mass of crucible with the burned sample remained constant).

Evaluation of total antioxidant capacity (TAC) by CUPRAC method: CUPRAC method [4-9] depends upon the reduction of cupric neocuproine complex to the cuprous neocuproine complex by a reductant at low pH. The neocuproine complex can be monitored at 450 nm.

As reference substance, we have used Trolox (6-hydroxy-2,5,7,8-tetramethylchroman-2-carboxylic acid), an antioxidant with a structure similar to vitamin E. Reagents: 0.01M CuCl_2 , 7.5·10⁻³M neocuproine (2,9-Dimethyl-1,10-phenanthroline) and acetate buffer. 1mL 0.01M CuCl_2 solution were mixed with 1mL neocuproine (7.5·10⁻³M) and 1 mL acetate buffer. At this solution was added 1.1 mL sample (alcoholic extract). For blank it was used ethanol 20%. The absorption was read after 1/2 hours at 20°C, at 450 nm. All determinations were performed in triplicate. Total antioxidant capacity (TAC) by CUPRAC in all samples were expressed as mmol Trolox/g fresh weight (FW).

All analytical determinations were made in triplicate.

Samples preparation: The following ingredients were used to make homemade chocolate: 250 g powdered milk, 250 g sugar, 150 g margarine, 50 g cocoa, 50 g sour cherries and 90 mL water. The ingredients are homogenized by heating.

Results and discussion

The obtained data regarding water content and dry matter content in our homemade chocolate samples are represented in fig. 1.

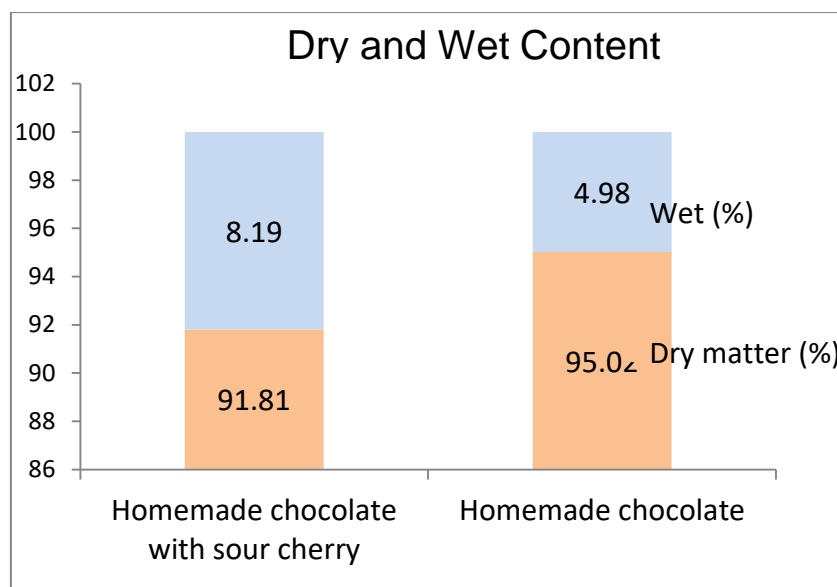


Figure 1. Content of humidity and dry mater in homemade chocolate samples

In the present study water content values are higher in homemade chocolate with fruit addition (8.19%) that in simple homemade chocolate (4,98%). This can be explained by the fact that the fruits come with a water content.

The different values in water content are depending on the recipe for the preparation of chocolate and also on the quantities and type of ingredient used.

In fig. 2 we are presenting total mineral content (ash) values.

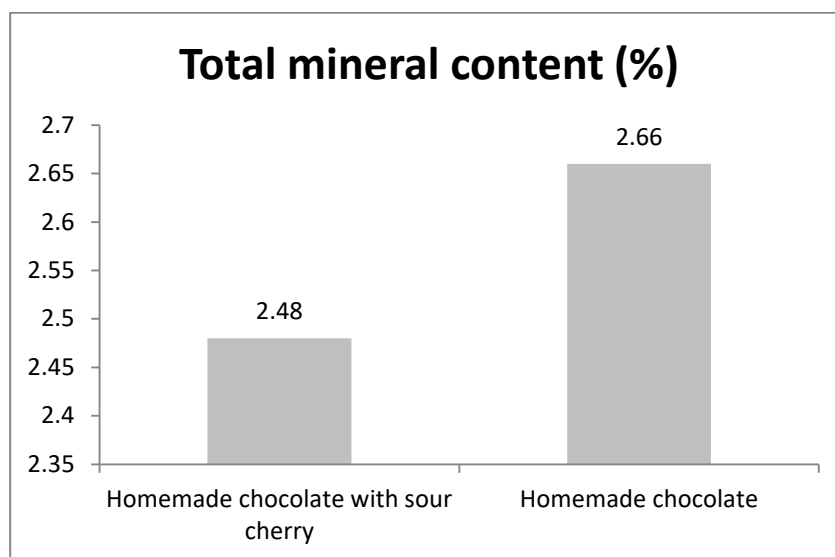


Figure 2. Total mineral content in homemade chocolate samples

The content of total mineral substances is higher in simple homemade chocolate.

The results for total antioxidant capacity (TAC) by CUPRAC method are presented in figure 3 and figure 4.

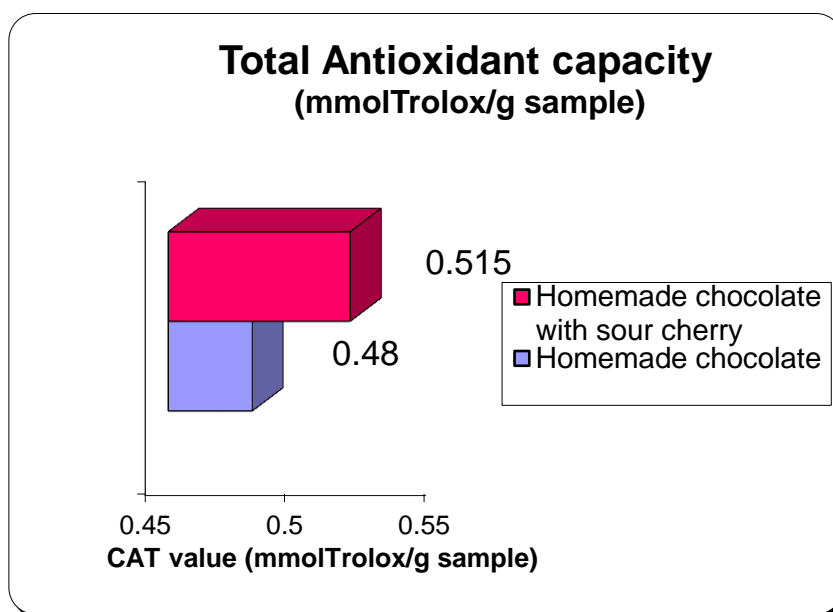


Figure 3. Total antioxidant capacity of homemade chocolate samples

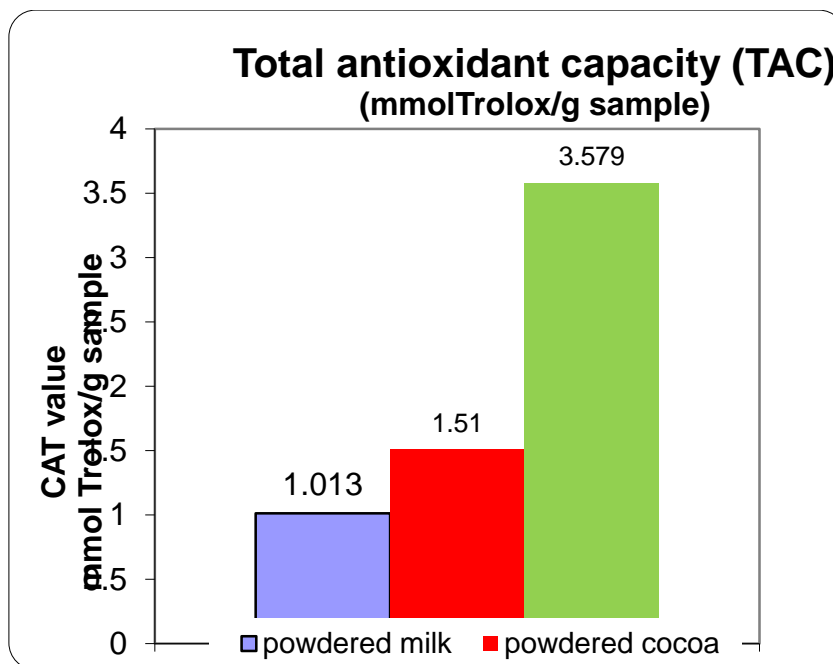


Figure 4. Total antioxidant capacity of ingredients used for obtained homemade chocolate

The TAC value is between 0.48 and 3.60 mmolTrolox/g sample. The ingredients have higher TAC values. The highest TAC value is in the case of cherry fruits. It was expected that more value would be for cocoa. It seems that the cocoa used was old or of poor quality. It is noted that the chocolate has a low TAC value, because she is obtained by heat treatment of the ingredients.

The results obtained from the processing of the data from the sensory analysis data sheet suggest that, overall, simple homemade chocolate was the most appreciated in terms of consistency (see fig.5).

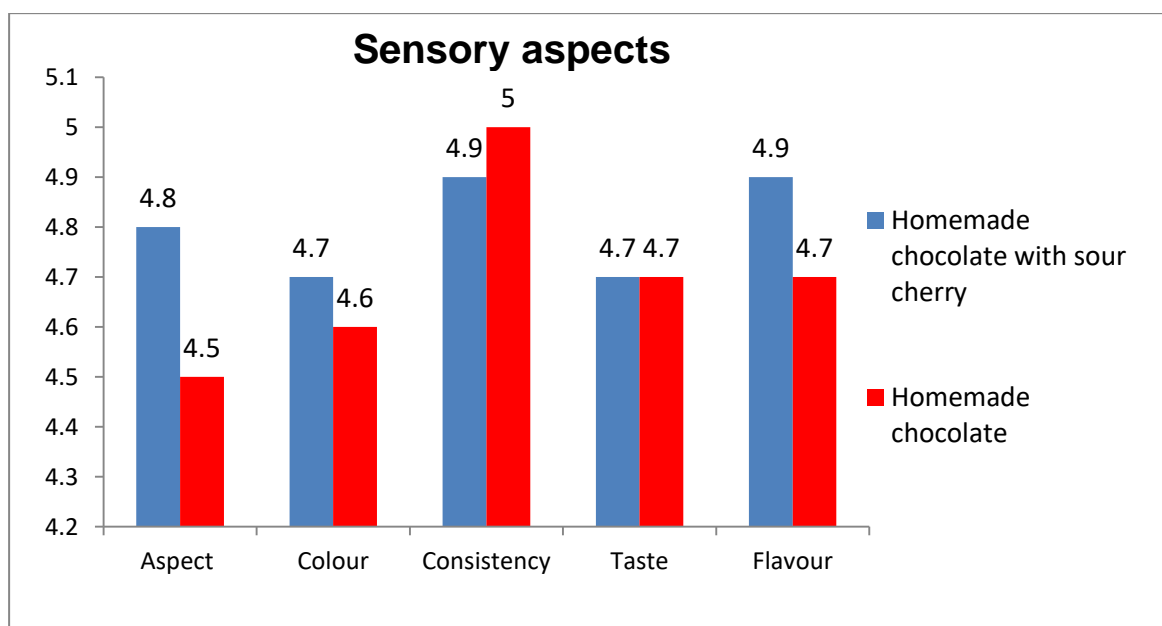


Figure 5. Sensory aspects for homemade chocolate

In contrast, homemade chocolate with fruit is more appreciated for its colour, appearance/aspect and flavour.

Conclusion

Homemade chocolate is a food with high nutritional value, attractive appearance, which is at the same time an important source of energy. Due to the antioxidants contained in cocoa powder, as well as the fruits added to our recipe, which are high in vitamin C, homemade chocolate is a food product successfully used to combat cell aging due to the free radical initiation process and prevention of oxidative stress with negative role on health.

Acknowledgements

The present paper was funded by the Research Project "Research on the use of biologically active substances in order to obtain high-nutrition foods", No 1545/28.02.2019.

References

1. Latif R. - Chocolate/cocoa and human health: a review, *Neth J Med*, 2013 vol. 71, no 2, pp. 63-68
2. AOAC, Official Methods of Analysis, AOAC, Washington, DC, USA, 16th ed., 1995;
3. Velciov A.B., Popescu G.S., Cozma A., Stoin D., Riviş A., Bujancă G., Pinte M., Green Fresh Smoothie – some physico-chemical and nutritional aspects, *Proceedings of the 23th Symposium on Analytical and Environmental Problems*, 2017, pp. ISBN 978-963-306-563-1;
4. Popescu S., Furdi F., Andronesu A., Bordean D., Velciov A., Velicevici G., Petolescu C., Botau D., Biochemical variability in several tomato varieties fruits, *Journal of Horticulture, Forestry and Biotechnology*, 17(2), 386-388, 2013.
5. Popescu (Pintilie) G.S., Velciov A.B., Costescu C.I., Gogoasă I., Grăvilă C., Petolescu C., Chemical characterization of white (*Morus alba*), and black (*Morus nigra*) mulberry fruits, *Journal of Horticulture, Forestry and Biotechnology*, 18(3), 133-135, 2014.
6. Popescu S., Manea D., Velciov A., Cristea T., Cârciu G., Cherry fruits source of biominerals and bioactive compounds, pp. 335-341 in 15th International Multidisciplinary Scientific Geoconference – Micro and nano technologies. *Advances in Biotechnology Section*, vol. I, Albena, Bulgaria, 2015
7. Dragan S, Iosif G, Socaciu C (Eds.) (2008). *Alimentatia functionala cu componente bioactive naturale in sindromul metabolic*, Eurostampa, Timișoara.
8. Ferretti G, Bacchetti T, Belleggia A, Neri D (2010). Cherry Antioxidants: From Farm to Table, *Molecules* 15:6993-7005.
9. Malichacova S, Timoracka M, Bystricka J, Vollmannova A, Cery J (2010). Relation of total antiradical activity and total polyphenol content of sweet cherries (*Prunus avium* L.) and tart cherries (*Prunus cerasus* L.). *Acta agriculturae Slovenica* 95(1):21-28.

ELECTRO-OXIDATION OF ASCORBIC ACID ON PEROVSKITE-MODIFIED ELECTRODES

Iuliana Sebarchievici*, Bogdan-Ovidiu Taranu, Stefania Florina Rus, Paulina Vlazan, Maria Poienar, Paula Sfirloaga

*National Institute of Research&Development for Electrochemistry and Condensed Matter,
144 Dr. Aurel Păunescu-Podeanu, RO-300569 Timișoara, Romania*

**e-mail: iuliana.sebarchievici@gmail.com*

Abstract

The main purpose of this research was to obtain LaMnO_3 perovskite-modified graphite electrodes, to characterise them and to observe their electrochemical behaviour in the presence of ascorbic acid. The morphology of the perovskite films were studied by scanning electron microscopy (SEM) and their double-layer capacitance was determined using cyclic voltammetry. The results are promising, but the electrocatalytic activity of the films for the oxidation of ascorbic acid needs to be improved.

Introduction

Perovskite-type oxides have received extensive attention due to their high electronic conductivity, mobility of the oxide ions within the crystal, variations on the oxygen content, photocatalytic and magnetic properties, electrically active structure, chemical stability and thermoelectric and dielectric properties. They are widely used in the research of fuel cells, electrochemical sensors and as catalysts in oxidation and reduction processes [1]. Ascorbic acid (AA) is an important nutrient and most of the methods for quantifying it were developed based on its reducing properties. Electrochemical methods have gained the most success among the different techniques for quantifying the concentration of AA in solutions. AA is easily oxidized to dehydroascorbic acid and this reaction can be induced and monitored by cyclic voltammetry [2]. In the past, we reported a simple procedure for the preparation of carbon modified electrodes by the *slow evaporation* of a N,N-dimethylformamide (DMF) solution containing the catalyst. These electrodes were also used for the electro-oxidation of AA [3].

In the present work, we used a LaMnO_3 perovskite-type material, to modify the surface of graphite electrodes and we studied their electrochemical behaviour.

Experimental

The electrochemical characterization of the LaMnO_3 powder was investigated in a conventional three-electrode cell equipped with a Pt wire counter electrode, an Ag/AgCl (sat. KCl) reference electrode and a modified graphite (G) disk electrode ($S = 0.28 \text{ cm}^2$) as working electrode. The G disk was used as a substrate on which a thin layer of the perovskite was placed. The perovskite suspension was prepared by adding 10 mg of LaMnO_3 powder in 500 μL of DMF. After 30 min in an ultrasonic bath, a volume of 15 μL of the suspension was applied on the surface of the G disk and allowed to slowly evaporate. The SEM technique was employed to study and confirm the uniformity of the deposited layer (data not shown).

Electrochemical experiments were carried out using a potentiostat type Voltalab PGZ 402. The double-layer capacitance of the modified electrode – electrolyte interface was determined by recording cyclic voltammograms in 0.1 M KCl, at various scan rates between -0.2 and 0.2 V. The capacitive current density was calculated as the average of anodic and cathodic currents taken at a potential where only double-layer adsorption and desorption features were observed (0 V vs Ag/AgCl). The capacitance was obtained from the slope of the

linear dependence of capacitive current density *versus* scan rate [4]. The oxidation reaction of AA was carried out in 0.1 M KCl at a scan rate of 100 mV/s.

Results and discussion

The characteristic voltammetric peak of AA in 0.1 M KCl solution appears at ~ 0.5 V and is assigned to the oxidation of AA to dehydroascorbic acid (Figure 1).

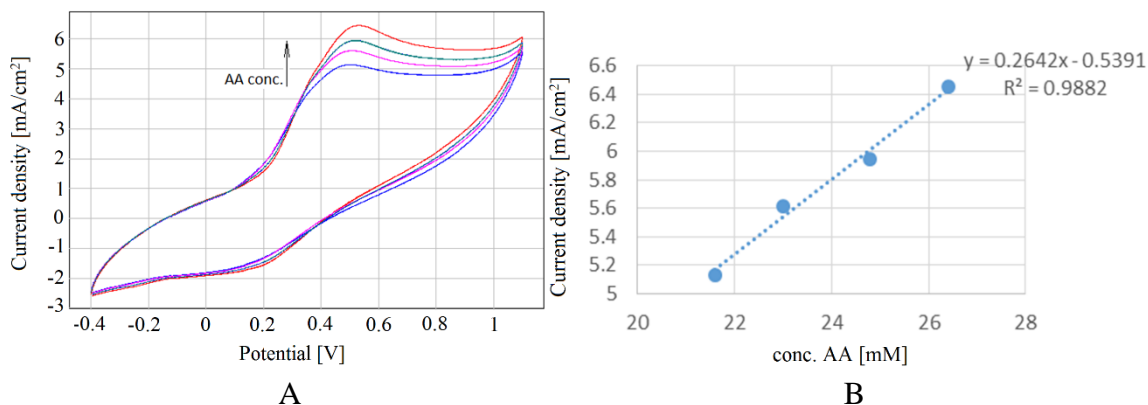


Figure 1. (A) Cyclic voltammograms obtained for the perovskite modified electrode at different ascorbic acid concentrations (21.6, 23, 24.8, 26.4 mM), in 0.1M KCl solution, at a scan rate of 100 mV/s. (B) The corresponding plot of anodic density current *vs* ascorbic acid concentration

In case of the modified electrode the oxidation peak current attributed to the presence of AA in the electrolyte solution increased by comparison with that observed for the unmodified G electrode, which indicates that the perovskite material serves to improve the electrode's catalytic properties (data not shown). Thus, the presence of LaMnO₃ perovskite as a modifier facilitates the rate of the charge transfer. The increase of the intensity of the anodic current can be noticed as the concentration of AA becomes higher. These results constitute the premises for further investigations of the possibility to use this electrode as an ascorbic-acid sensor. Also, the capacitance of the perovskite-modified G electrode was obtained from the slope of the linear dependence of the capacitive current density *versus* the scan rate and was found to be $3.96 \cdot 10^{-3} \text{ F cm}^{-2}$ (*versus* $1.25 \cdot 10^{-3} \text{ F cm}^{-2}$ for the unmodified electrode).

Conclusion

The LaMnO₃ perovskite material was deposited from suspension as a uniform film on the surface of graphite electrodes, which was confirmed by SEM imaging. The electrocatalytic behaviour of the modified electrodes in the presence of ascorbic acid indicates that LaMnO₃ is a promising material for the development of novel ascorbic acid sensors.

Acknowledgements

The authors are acknowledging INCEMC Timisoara for financial support as part of the PN 19 22 02 01, 40N/2019 NUCLEU project.

References

- [1] N.F. Atta, S.M. Ali, E.H. El-Ads, A. Galal, *Electrochim. Acta.* 128 (2014) 16-24.
- [2] S.M. Chen, Y.L. Chen, *J. Electroanal. Chem.* 573 (2004) 277–287.

- [3] I. Sebarchievici, E. Fagadar-Cosma, B. Taranu, M. Birdeanu, S.F. Rus, I. Taranu, A. Lascu, Electro-oxidation of ascorbic acid by Mn(III)porphyrin-silica hybrid film prepared by Pulsed Laser Deposition, TIM15-16 Physics Conference Timisoara, Romania (2016) AI-P04.
- [4] A. Kellenberger, D. Ambros, N. Plesu, Int. J. Electrochem. Sci. 9 (2014) 6821 – 6833.

EFFECT OF WASTEWATER SLUDGE ON MICROBIOLOGICAL AND BIOCHEMICAL CHARACTERIZATION IN SECALE CEREALE L. RHIZOSPHERE

Hosam Bayoumi Hamuda

*Environmental Engineering Institute, Óbuda University, H-1034 Budapest Doberdo Út 6,
Hungary*

e-mail: bayoumi.hosam@rkk.uni-obuda.hu

Abstract

Pot experiment was conducted to study the effects of wastewater sludge treatment on biological properties of rye rhizosphere after 9 weeks cultivation. Soil was kovárvány brown forest soil collected from Nyíregyháza and treated with different doses of the sludge. Different microbial properties and enzymatic activities were studied. Results indicated that the enzymatic activities in soil samples treated with the sludge were increased with higher sludge doses. There was an increase in the density of the microbial population in the rye rhizosphere as the sludge dose increased. Results demonstrated that Gram negative bacteria were dominant in the rye plant rhizosphere and the ratio between Gram-negative and Gram-positive bacteria was 2.367. Finally, soil amended with the sludge stimulates the biochemical and microbial properties of the rye rhizosphere. For maintaining the soil quality, the authors recommend to treat the acidic soil with a ratio of 40–60% of this sludge to improve the fertility of the soil.

Introduction

Application of sewage sludge compost as a fertilizer on landscaping provides a potential way for the effective disposal of sludge. Monitoring of microbiological and biochemical parameters is one of the most essential properties to qualify soil health when treated with wastewater sludge. Today, one of the most pressing environmental problems is the increasing volume of waste, including wastewater sludge treatment, utilization and disposal. The possible way to use wastewater sludge as organic fertilization is utmost importance because it improves soil structure and induces useful microbiological processes. Wastewater sludge is environmentally polluting and on the other hand, suitable for organic farming as organic fertilizer. As a result of wastewater sludge treatment, the amount of microorganisms in the soil usually increases. The nutrient flow for the soil is determined by the activity of enzymes, in addition to the physical, chemical parameters, plant cover and microbial activity. The organic matter of wastewater sludge is decomposed by heterotrophic nutrition prokaryotes and fungi. Biodegradation is basically the result of microbial and biochemical processes, therefore all factors that have an impact on the structure, function and enzymatic activity of microorganisms affect the rate of degradation. Microbial mineralization products of organic constituents differ in aerobic and anaerobic conditions. During the present work, we investigated the effects of wastewater sludge on the biological properties of the amended soils in the rhizosphere of rye plant.

Experimental

The origin of soil samples were: Kovárvány brown forest soil (KBET) was from the Center for Agricultural and Technical Sciences at the Nyíregyháza Research Institute of the University of Debrecen. Soil samples were collected from the upper layer of 0-25 cm. Some chemical properties of communal wastewater sludge from the municipal wastewater treatment plants (Nyíregyháza) and soil samples are presented in Table 1. The air dried soil was

thoroughly mixed with wastewater sludge so, the final mixture contained wastewater sludge in the soil sample was as following percentages: 0% (wastewater -free control soil), 20, 40, 60 and 100% (wastewater sludge only, without soil). Rye (*Secale cereale* L.) seeds were sterilized and planted in plastic containers of 3 kg of tested soil as prepared above. After 10 days of germination, young plants were reduced to be 10 plants/pot.

Table 1
Properties of the soils and sludge used in the model experiment

Parameters	Soil type: KBET	Wastewater sludge: NySzv
pH _(KCl)	5.78	6.71
a) Dry matter content, %	na	53
b) Organic matter, %	na	21.7
c) Humus content, %	2.54	na
d) Total-N, mg·kg ⁻¹	na	7470
NO ₃ -N, mg·kg ⁻¹	23	na
NH ₄ -N, mg·kg ⁻¹	5.6	na
Mg, mg·kg ⁻¹	214	2507
Na, mg·kg ⁻¹	64	994
P ₂ O ₅ , mg·kg ⁻¹	318	28720
K ₂ O, mg·kg ⁻¹	412	3171
Zn, mg·kg ⁻¹	1.7	537
Cu, mg·kg ⁻¹	1.4	110.4
Mn, mg·kg ⁻¹	55	421
Fe, mg·kg ⁻¹	945	11308
Cd, mg·kg ⁻¹	1.7	2.3
Pb, mg·kg ⁻¹	1.3	66.9

na: no data available

Heterotrophic and aerobic soil microorganisms

The total plate count of aerobic bacteria, aerobic endospore-forming bacteria, filamentous fungi, yeasts, cellulose decomposers and phosphate-solubilizers in the rye rhizosphere was determined by means of a soil suspension. The roots separated from the plants were washed in sterile tap water to remove sticky soil particles followed by washing with a sterile 0.85% NaCl solution again. Ten grams of the washed roots were cut and placed in 90 ml of sterile saline. The total numbers of colony forming units (CFU) of culturable microorganisms were determined by serial dilution and plating on selective media. Plate counts of culturally viable bacteria and endospore-forming bacteria were made on Tryptone Soya Agar (TSA; Oxoid, Basingstone, Hampshire, England) amended with 0.1 g/l cyclohexamide. For fungi the Martin's medium for fungi [1] was Rose Bengal Agar (RB; Oxoid) amended with 30 mg/l streptomycin sulphate. Yeasts were cultivated on Malt Extract Agar, actinobacteria were counted on Glycerol Casein Agar [2] amended with 0.05 g/l cyclohexamide. Examination of phosphate solubilisation was done in the medium described by Goldstein [3] for the selection of phosphate solvents. Dicalcium phosphate agar plates were inoculated, so that pure ring-producing strains around their cells are phosphate-free. Cellulose agar plates were seeded using two types of media (PDA: fungi and Nutrient agar: bacteria), which included the carboxymethylcellulose Congo red (CMC-Congo red) substrate as determined by Hendricks et al. [4]. All plates were inoculated with 0.1 ml of soil suspension and cultured at 25°C for 4 to 7 days for fungi, 30°C for 2 days for heterotrophic and endospore-forming bacteria and for 10 days for actinobacteria. Isolation and identification of microorganisms were done according to their morphological characteristics (colour, shape, appearance, cell size). Cultivable aerobic heterotrophic bacterial isolates belonging to different genes were studied by colony and cell morphology, Gram staining, spore staining, oxidase and catalase reactions, oxidation and fermentation of glucose, and motion and pigmentation.

Monitoring the enzymatic activity

Dehydrogenase activity ($\mu\text{g INTF/g}^{-1}$ dry soil) was measured according to García et al. [5]. Phosphatase activity ($\mu\text{mol p-nitrophenol (PNP)/g}^{-1}$ dry soil/ h^{-1}) regard to the method of Tabatabai and Bremner [6]; β -glucosidase activity ($\mu\text{mol p-nitrophenol/g}^{-1}$ dry soil/ h^{-1}) was determined by the method described by Masciandaro et al. [7]. Invertase activity was measured by Siegenthaler [8] using p-nitrophenyl α -D-glucopyranoside (Fluka, Buchs, Switzerland). After adding a solution containing p-nitrophenol, tris buffer (pH 9.5); it is converted to nitrophenolate anion which can be measured by a spectrophotometer due to the pH effect. The extinction value at 400 nm is multiplied by 21.64 in an invertase number. The aryl sulfatase activity ($\mu\text{mol nitrophenol g}^{-1}$ dry soil/ h^{-1}) was determined according to Tabatabai and Bremner [6] (absorption of p-phenol at 400 nm after incubation with PNP sulphate).

Results and discussion

Composition of microbial population: It was found that population of the different microbial groups increased by the addition of sludge to soil. This suggests that microbial populations are able to utilize large quantities of organic matter and use wastewater sludge as energy sources (Figure 1).

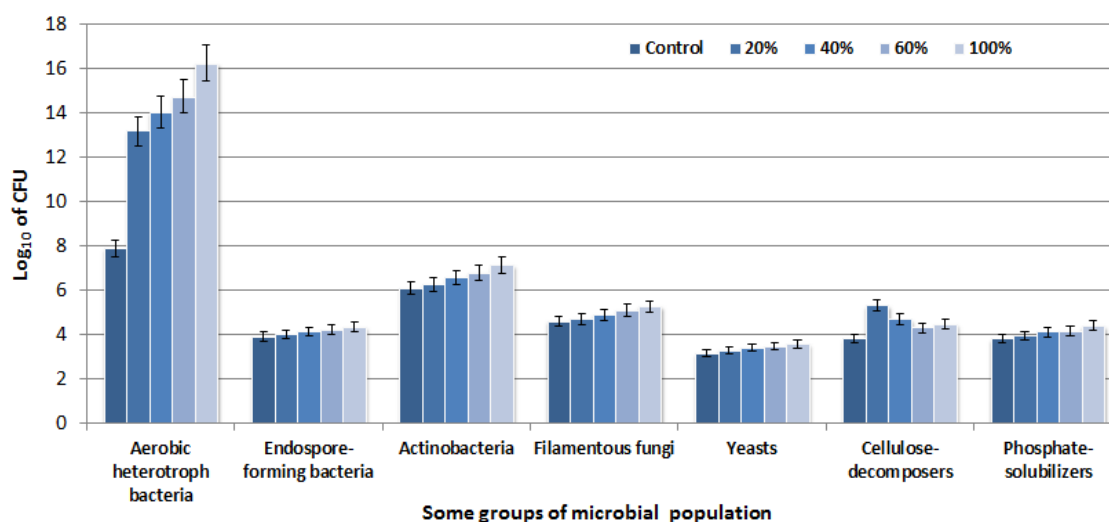


Figure 1. Effect of sludge application on microbial structure in soil of Nyíregyháza

The most common isolates were belong to genera of *Achromobacter*, *Acinetobacter*, *Aeromonas*, *Alcaligenes*, *Arthrobacter*, *Azotobacter*, *Bacillus*, *Brevundimonas*, *Burkholderia*, *Cellulomonas*, *Chromobacterium*, *Chryseobacterium*, *Corynebacterium*, *Enterobacter*, *Escherichia*, *Flavobacterium*, *Klebsiella*, *Microbacterium*, *Micrococcus*, *Pseudomonas*, *Rhodococcus*, *Serratia*, *Stenotrophomonas*, *Staphylococcus*, *Streptococcus*, *Streptomyces* and *Zooglea*. The number of filamentous fungi was greater than in the control and more than 350 representative fungal strains were isolated. These isolates belong to the following genera: *Alternaria*, *Aspergillus*, *Cephalosporium*, *Cladosporium*, *Fusarium*, *Geotrichum*, *Mucor*, *Penicillium*, *Rhizopus* and *Trichoderma*. In addition, there are many strains belonging to the *Saccharomyces* genus (Figure 1).

Bacterial communities: It was found that Gram negative bacteria were dominated in the rye rhizosphere treated with the sludge. The proportion of Gram-negative to Gram-positive bacteria was 3.24.

Enzymatic activities: The results of measuring dehydrogenase activity confirm the microbial population. Also, the enzymatic activity exceeded in higher values than the control

samples. Soil dehydrogenase activity refers to the total oxidative activity of the soil microbial activities and can therefore be a good indicator of the degree of microbial activity. Sludge addition increased dehydrogenase activities for each treatment (Figure 2).

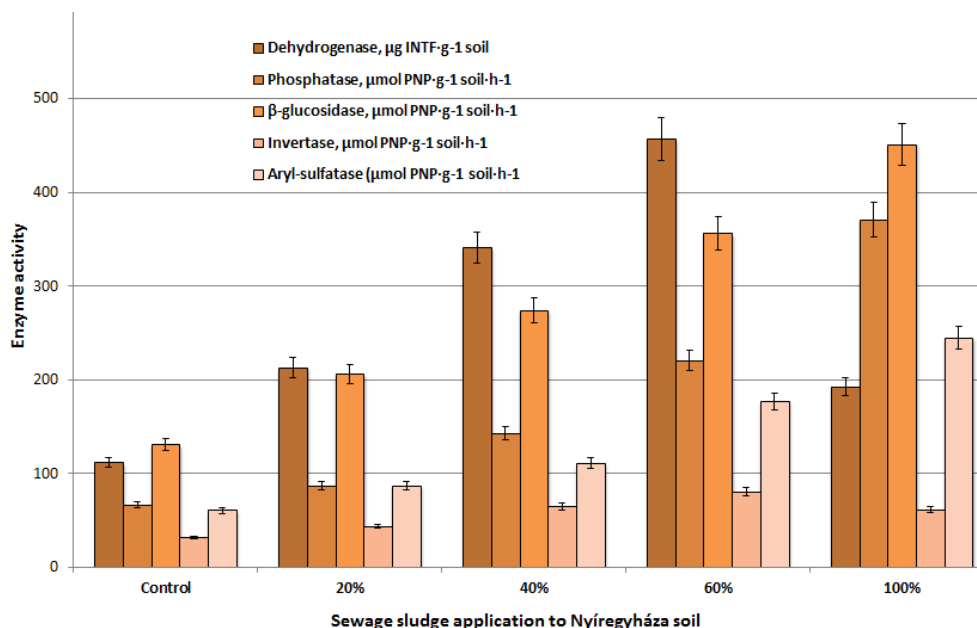


Figure 2. Effect of sludge application on the activities of some enzymes in soil

The highest enzymatic activities of urease, protease, phosphatase, β -glucosidase and aryl sulfatase (Figure 2) were observed. The higher enzyme activity can be explained by the increases of microbial activity that is caused by the high nutrient and organic content of sludge. Protease activity increased significantly after 9 weeks of growth time. During the experiment, the plant grown in sludge treated soil had a positive effect on the microbial growth and increases the β -glucosidase.

Evaluation of results: Investigation of the data showed that there is more and more evidence that such parameters are also sensitive indicators of the composition and function of the stressed soil caused by the use of sludge because microbiological activity directly affects the stability of agro-ecological systems and fertility. There is also a growing interest in the use of soil enzymes as indicators of soil fertility, because the activity of soil enzymes is sensitive to many factors.

Since the enzyme activity is substrate-specific, it is difficult to predict the nutrient supply of the soil from the activity of an enzyme, and the parallel measurement of several properties can better describe the microbiological activity of the soil. The number of heterotrophic microorganisms in the soil usually increases following the addition of sludge. In fact, microorganisms capable of utilizing the organic material of sludge are rapidly propagating.

According to Stadelmann and Furrer [9], the number of aerobic bacteria and beetles increased due to sludge addition. The sludge application causes an increase in the microbial populations. Environmental factors also affect microbial activity and mineralization of sludge. Wastewater sludge and its management affect the quality of the organic material, its degradation speed, the time required for it, and the amount of nutrient released. Our results confirm the statement by Garcia et al. [6] that microbial and dehydrogenase activity is directly related to each other and depends on the metabolic state of microbial populations in soil. Crecchio et al. [10] observed that with increasing use of communal waste compost the organic C, N,

dehydrogenase, β -glucosidase, urease, nitrate reductase and phosphatase activity of the soil increased with the composition of the bacterial communities living in soil did not change significantly. However, in our case, the activity of soil enzymes and the density of microbial populations increased with the addition of sludge. Sludges, as products obtained by wastewater treatment, contain organic matter, micro and macronutrients and are potentially useful for any agriculture use. They may contain undesirable harmful materials. For these reasons, the use of sludges in agriculture, at European Union (EU) level, is regulated by the EU Sludge Directive 86/278/EEC. One of the current Council Directive of 12 June 1986 aims on the protection of soil environment, when sludge is applied in agriculture is to avoid toxicity effects on soil, plants and man [11]. Considerable improvement in dehydrogenase activity and aggregate associated organic matter was observed particularly when higher amount of sludge was applied our results are confirmed with the observation of Mondala et al. [12]. The greater soil urease and invertase activities in spring soil amended with sludge provided evidence of increased soil microbial population [12]. Soil microorganisms excrete a variety of enzymes such as urease, invertase, dehydrogenases, cellulases, amylases and phosphatases that have long been recognized as a primary means of degrading xenobiotics in soil and water ecosystems [13]. Therefore, in municipal solid waste composts use over agricultural lands, heavy metal contents should always be taken into consideration and excessive uses should be avoided [14].

Conclusion

Findings showed that microbial activity in the soil depends on the C and N content; soil enzymatic activity increase with the addition of sludge. Therefore, the wastewater sludge utilized in the present study could be used as a valuable organic fertilizer in rye cultivation land and could also act as an eco-friendly method for the recycling of wastewater sludge.

References

- [1] P.J. Martin, *Soil Sci.*, 69 (1950) 215-232.
- [2] T.S. Williams, H.M.E. Wellington, American Society of Agronomy, Madison, WI, 1982.
- [3] H.A. Goldstein, *Am. J. Altern. Agric.*, 1 (1986) 51–57.
- [4] W.C. Hendricks, D.J. Doyle, B. Hugley, *Appl. Environ. Microbiol.*, 61 (1995) 2016-2019.
- [5] C. García, T.M. Hernandez, F. Costa, *Commun. Soil Sci. Plant Anal.*, 28 (1997) 123-134.
- [6] M. Tabatabai, M.J. Bremner, *Soil Biol. Biochem.*, 1 (1969) 301–307.
- [7] G. Masciandaro, B. Ceccanti, C. Garacia, *Agrochimica*, 38 (1994) 195-203.
- [8] U. Siegenthaler, *Mitt. Gebiete Lebensm. Hyg.*, 68 (1977) 251-258,.
- [9] X. Stadelmann, J.O. Furrer, D. Reidel Publ. Co. Dordrecht, 141-166, 1983.
- [10] Crecchio, M. Curci, M.R.D. Pizzigallo, P. Ricciuti, P. Ruggiero, *Soil Biol. Biochem.*, 36 (2004) 1595-1605.
- [11] Commission of the European Communities, COM(1999) 752 final, 1-92, 2000.
- [12] S. Mondala, R.D. Singhb, A.K. Patrab, B.S. Dwivedi, *Environ. Nanotechnol. Monit. Manag.*, 4 (2015) 37-41.
- [13] G.F. Antonious, *J. Environ. Sci. Health, Part A* vol. 44, (2009) 1019-1024.
- [14] O. Yuksel, *Environmental Monitoring and Assessment*, 187 (2015) 313.

ASSESSMENT OF THE USEFULNESS OF LIBS AND ICP-MS FOR THE CHARACTERIZATION OF NANOPARTICLES IN INDUSTRIAL AND ENVIRONMENTAL SAMPLES

Dávid Palásti^{1,2}, Albert Kéri^{1,2}, Lajos Villy^{2,3}, Tíria Biros¹, Ádám Bélteki¹, Bálint Leits^{2,3}, Patrick Janovszky^{1,2}, Attila Kohut^{2,3}, Zoltán Galbács^{1,2}, Éva Kovács-Széles⁴, Zsolt Geretovszky^{2,3}, Gábor Galbács^{1,2*}

¹*Department of Inorganic and Analytical Chemistry, University of Szeged, 6720 Szeged, Dóm square 7, Hungary*

²*Department of Materials Science, Interdisciplinary Excellence Centre, University of Szeged, 6720 Szeged, Dugonics sq. 13, Hungary*

³*Department of Optics and Quantum Electronics, Univ. of Szeged, 6720 Szeged, Dóm square 9, Hungary*

⁴*Nuclear Security Department, Hungarian Academy of Sciences Centre for Energy Research, 1121 Budapest, Konkoly-Thege M. way 29-33, Hungary
e-mail: galbx@chem.u-szeged.hu*

Abstract

The need for analytical techniques capable for the detection and characterization of nanoparticles (NPs) in industrial and environmental matrices also grows along with the quickly expanding use of NPs in various products. Two candidate analytical techniques are laser induced breakdown spectroscopy (LIBS) and inductively coupled plasma mass spectrometry (ICP-MS). Both of these sensitive and versatile techniques provide elemental compositional information. Based on the success of the application of LIBS in aerosol analysis this technique can be expected to be similarly useful in NP monitoring applications, such as the detection of NPs in liquid or gaseous matrices, or for the monitoring of the properties of NPs produced by physical generation methods (e.g. electrical discharges or laser ablation). ICP-MS on the other hand has already proven itself useful in the literature, both in the solution or single particle analysis (spICP-MS) modes, for the characterization of nanoparticles. In recent years we also reported about the successful development of several ICP-MS based analytical methods for the compositional and dimensional analysis of NPs (e.g. [1, 2]).

In our study we assessed the potential of LIBS and ICP-MS for nanoparticle detection and characterization both in on-line (only for LIBS) or off-line (following collection on a filter) mode. Dispersions of various types of nanoparticles (e.g. monometallic, bimetallic, oxide) in simulated or real liquid and gaseous industrial and environmental matrices were measured. Some NPs were obtained commercially, while others were generated by in-laboratory developed electrical (spark or arc) discharge generators. Additional and reference characterization of the nanoparticles were performed by electron microscopy (SEM, TEM) and scanning mobility particle sizer (SMPS). Size and mass detection limits were also calculated for on-line LIBS detection of nanoaerosols and for spICP-MS detection of NPs in aqueous nanodispersions.

Introduction

Nanoparticles (NPs) can be the product of natural phenomenons or various industrial processes. Due to their favorable properties, their application has expanded to a wide range of industries, such as textiles, pharmaceuticals, food, construction electronics and so on. As their application shows an increasing trend, it is becoming necessary to detect them in both environmental and industrial samples. In our present study, we investigated the potential of

LIBS and ICP-MS for nanoparticle detection and characterization both in on-line (only for LIBS) or off-line (following collection on a filter) mode. Dispersions of various types of nanoparticles (e.g. monometallic, bimetallic, oxide, polymer) in simulated or real liquid and gaseous industrial and environmental matrices were measured.

Experimental

A quadrupole Agilent 7700X inductively coupled plasma mass spectrometer (ICP-MS), equipped with standard Agilent accessories, was used in our experiments. Sample introduction was performed by an Agilent I-AS autosampler and a Micro Mist pneumatic nebulizer equipped with a Peltier-cooled Scott-type spray chamber. The sample uptake rate was 400 $\mu\text{L}/\text{min}$. The ICP plasma and interface parameters were set up according to standard conditions (RF forward power: 1550 W, plasma gas flow rate: 15.0 L/min, carrier gas flow rate: 1.05 L/min, sampling depth: 10.0 mm). An in-house developed spark discharge generator (SDG) and an arc discharge generator (ADG) were used to generate well characterized gold and copper NPs, respectively. In the SDG, the operating time was kept constant and the spark repetition rate was changed between 50 and 250 Hz (this directly influences the numerical concentration of the produced nanoparticles). The nanoparticles were collected on a glass membrane filter in continuous Ar gas flow. The NPs were characterized by scanning mobility analyzer (SMPS) TSI model 3082 and transmission electron microscopy (TEM) FEI Tecnai G2 20 X-TWIN. In our experiments LIBS spectra were recorded with a LIBSCAN 25+ instrument ($\lambda=1064$ nm, 50 mJ impulse energy). Commercially obtained NPs. Pt nanoparticles (46 nm, citrate stabilized, (NanoXact, NanoCompsix Inc.) and Ag nanoparticles (59 nm, Pelco NanoXact, Ted Pella Inc.)

Results

Nanoparticles may also be generated during the wear of the catalytic converters of cars, which is then released into the environment. In this simulation experiment, Pt nanoparticles were added to the collected environmental water matrix (Szeged, Vér tó). The sample was homogenized, filtered on a 0.22 μm pore-size PTFE membrane filter, diluted and measured by spICP-MS. The NPs can be detected in such a complex environmental matrix. Silver nanoparticles are widely used in textile industry because of their antimicrobial effects. In our experiment, we simulated the washing procedure of Ag NP coated textiles. The washing was simulated by vortexing the textile piece for 45 minutes in 0.4 g/L Na_2CO_3 . The released washing water was diluted and measured with spICP-MS for the detection of silver nanoparticles. The Ag NPs were well detectable and barely degraded in size during the washing procedure. On-line measurement of nanoaerosols may be useful in the monitoring of ambient air samples or the production of nanoparticle synthesis in gases. These measurements can be carried out with a portable, robust equipment, in natural or industrial environment. In our experiments, we tested this using SDG and ADG produced Au and Cu NPs. We found that the SDG-generated Au nanoparticles (diameter of ca. 36 nm) did not contain sufficient amount of material to be detected in the on-line mode, but the ADG-produced Cu particles (with the diameter of around 236 nm) were well detectable.

Conclusion

In this work we successfully demonstrated that both LIBS and ICP-MS can be used to detect or characterize nanoparticles. The LIBS method was found to be suitable for particle detection with both on-line and off-line approaches in the case of sufficiently large nanoparticles. ICP-MS can provide accurate compositional and size information about NPs.

Acknowledgements

The authors gratefully acknowledge the financial support from various sources including the Ministry of Human Capacities (through project No. 20391-3/2018/FEKUTSTRAT) and the National Research, Development and Innovation Office (through projects No. K_129063, and EFOP-3.6.2-16-2017-00005 (Ultrafast physical processes in atoms, molecules, nanostructures and biological systems) of Hungary.

References

- [1] A. Sápi, A. Kéri, I. Kálomista, D.G. Dobó, Á. Szamosvölgyi, K.L. Juhász, Á. Kukovecz, Z. Kónya, G. Galbács, *J. Anal. At. Spectrom.* 32 (2017) 996.
- [2] A. Kéri, I. Kálomista, D. Ungor, Á. Béltéki, E. Csapó, I. Dékány, T. Prohaska, G. Galbács, *Talanta* 179 (2018) 193.

THE IMPROVEMENT OF THE BIODEGRADABILITY OF DICLOFENAC AND SULFAMETHOXAZOLE BY COMBINED COMETABOLISM AND GAMMA IRRADIATION TREATMENT

Anikó Bezsényi^{1,2}, Gyuri Sági³, Magdolna Makó¹, György Palkó¹, Tünde Tóth³, László Wojnárovits³, Erzsébet Takács³

¹*Budapest Sewage Works Pte Ltd., H-1087 Asztalos Sándor str. 4, Budapest, Hungary*

²*Óbuda University, H-1034 Bécsi út 96b, Budapest, Hungary*

³*Institute for Energy Security and Environmental Safety, Centre for Energy Research, Hungarian Academy of Sciences, H-1121, Konkoly-Thege Miklós út 29-33, Budapest, Hungary*

e-mail: bezsenyia@fcsm.hu

Abstract

The two forms of most common biological purification used (activated sludge and biofilm) cannot effectively remove pharmaceuticals, such as diclofenac and sulfamethoxazole. However, a biological phenomenon called cometabolism can improve the removal efficiency. In the case of cometabolism, an easily degradable substrate (growth substrate) is added to the wastewater to be treated, which supplies the microorganisms with sufficient energy for biodegradation. Such easily degradable molecules (e.g. methanol, acetic acid, ethylene glycol) are also formed in the anaerobic steps of wastewater treatment systems and are utilized as growth substrates. The rate of oxidative degradation of pharmaceuticals (measured by using oxygen uptake rate) was shown to greatly increase in the presence of easily degradable growth substrates in the case of activated sludge. In the biofilm system which is another form of biological wastewater treatment, the rate of cometabolism remained low, most possibly because it has much narrower bacterial diversity than activated sludge. However, the efficiency of oxidative degradation can be significantly improved by using an advanced oxidation process, ionizing radiation treatment, before cometabolism. This combined treatment, irradiation and cometabolism is recommended for the degradation of recalcitrant organic compounds.

Introduction

The conventional wastewater treatment technologies are not suitable for removing hardly biodegradable micro-pollutants (xenobiotics), such as pharmaceuticals. These compounds often pass through the treatment systems in unchanged form and enter the surface waters [1, 2]. The pharmaceuticals, especially antibiotics remaining in the treated wastewater have several adverse effects on the environment: short-term and long-term toxicity, endocrine disruption or induction of resistant pathogens [3, 4].

The decomposition of xenobiotics can be enhanced by the stimulation of natural processes, so called cometabolism (co-oxidation), whereby a complex non-biodegradable molecule can be degraded in the presence of an easy-to-degrade substrate (growth substrate) [5]. Simple organic compounds (methanol, ethanol, formic acid, acetic acid, propionic acid, butyric acid, valeric acid, caproic acid or hexanoic acid, lactic acid, ethylene glycol, etc.) are formed by hydrolysis and microbiological fermentation from complex organic molecules in wastewater. Industrial by-products (acids and alcohols) can also be used for feeding the bacterial community. However, depending on the composition and diversity of the microbiota, other elements can be successfully utilized and it also affects the efficiency of cometabolism. The biomass of each wastewater treatment plant has a special composition, so its removal efficiency and biotransformation capability for micro-pollutants are also different [6, 7].

Several technological innovations are aimed at removing micro-pollutants, among these advanced oxidation processes (AOP) based on hydroxyl radicals ($\cdot\text{OH}$) are highly effective [8, 9, 10]. This process eventually results in the formation of simpler, biodegradable (available to microorganisms) organic compounds.

The aim of this work was to improve the removal efficiency of the biological treatment for hardly biodegradable pharmaceuticals, namely sulfamethoxazole (SMX, antibiotic) and diclofenac (DCF, analgesic, non-steroidal anti-inflammatory drug). For this purpose AOP and cometabolism, as well as their combination were tested. The phenomenon of cometabolism was studied by the addition of simple growth substrates (methanol, acetic acid, ethylene glycol), and γ radiation was used as an advanced oxidation process at three different doses. The change in the bioavailability of the compounds was followed by respiratory tests on wastewater activated sludge and biofilm cultures.

Experimental

As an advanced oxidation method, γ irradiation was used with 0.5, 1.0 and 2.0 kGy doses. Irradiations were performed by a ^{60}Co (1.85PBq) SSL-01 panoramic type gamma source, with 9.4 kGy h^{-1} dose rate. The samples containing pharmaceuticals in 0.1 mmol L^{-1} concentration were continuously aerated and kept at room temperature during the treatment. H_2O_2 generated during ionizing radiation treatment was eliminated with dosing 0.25 g L^{-1} manganese(IV) oxide at pH 10.0 (stirred at 20°C for 10 minutes). After filtration with $0.22 \mu\text{m}$ regenerated cellulose membrane filter the solutions were neutralized. This step is necessary to avoid toxicity and measurement interfering effects by elevated oxygen levels.

Organic matter content was expressed as chemical oxygen demand (COD) as the organic matter is oxidized by sulfuric acid and a known excess of potassium dichromate ($\text{K}_2\text{Cr}_2\text{O}_7$) at high temperature (2 h, 170°C). The remaining unreduced $\text{K}_2\text{Cr}_2\text{O}_7$ is titrated with ferrous ammonium sulfate (ISO 6060:1989).

The respiratory tests (on the basis of ISO 8192:1986 standard) were carried out with two types of wastewater bacterial cultures: activated sludge and biofilm biomass collected from the South-Pest Wastewater Treatment Plant. The cultures were used for testing freshly without storage and were washed several times with tap water. Oxygen consumption of the culture was measured in 300 mL Karlsruher bottles with an FDO® 925 oxygen sensor at 20°C . The mixtures were made with tap water. The respiration intensity is expressed in oxygen uptake rate (OUR, $\text{mg O}_2 \text{ L}^{-1} \text{ h}^{-1}$).

The cometabolic effect is achieved by the addition of simple organic substrates with the same load levels in each bottle: 25 mg dry matter of biomass, $150 \text{ mg O}_2 \text{ L}^{-1}$ COD-equivalent substrate and 150 mL of irradiated pharmaceutical solutions. The blank test mixtures contained only biomass and substrates, while the control mixtures treated/untreated pharmaceutical samples and substrates without biomass. All data used to evaluate the results are corrected for endogenous OUR values (absence of pharmaceutical and growth substrate) and control values (currently tested pharmaceutical and growth substrate without biomass). The dissolved oxygen uptake is increasing in the presence of biodegradable compounds, and it is reduced in the presence of toxic substances.

Results and discussion

In order to study the combined effect of gamma radiation and cometabolism, we had to perform a number of preliminary experiments. First we had to identify the growth substrates that the bacterial cultures could utilize for the cometabolic biodegradation of the tested pharmaceuticals (DCF, SMX). If a bioculture (activated sludge, biofilm) is capable of efficient cometabolic degradation alone, the effect of gamma radiation is less detectable. According to this guiding principle we selected a poorly, a medium and a highly active

growth substrate and the less effective bacterial culture for further testing that worked similarly for both pharmaceuticals: methanol, ethylene glycol and acetic acid.

During the preliminary tests we found that activated sludge is efficient in cometabolism alone, the effect of irradiation treatment is further tested on the biofilm, which was less effective in cometabolism. The OUR data for the selected three substances are summarized in Fig.1.

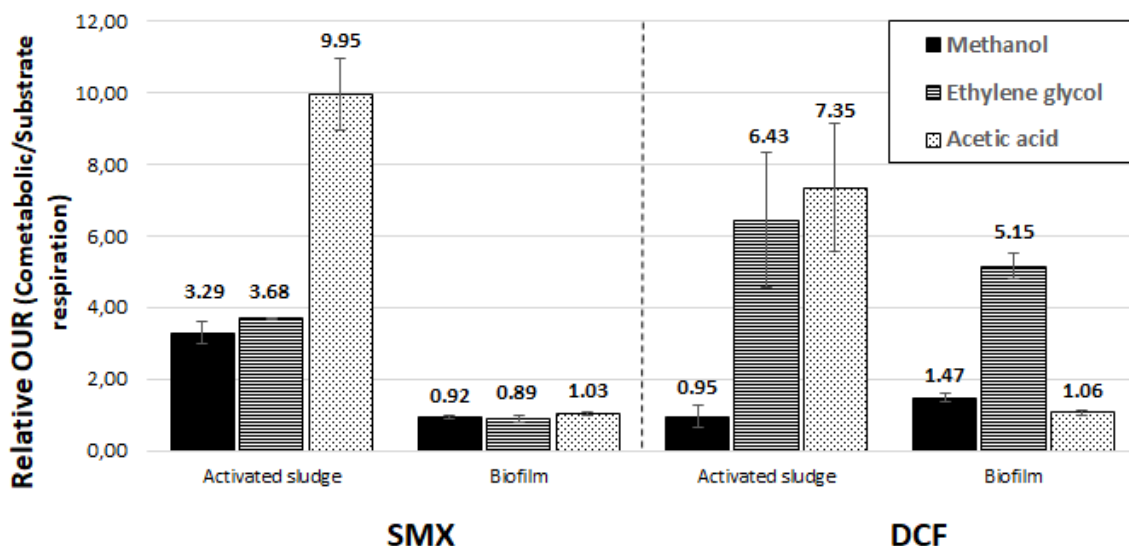


Figure 1. Relative OUR values for SMX (a) and DCF (b) with the three selected substrates using activated sludge or biofilm.

As Fig. 2 shows the untreated pharmaceuticals were not eliminated by the biofilm bacterial culture ($0 \text{ mg L}^{-1} \text{ h}^{-1}$, i.e. no metabolic activity). However, in the irradiated samples bioavailability of both pharmaceuticals was observed and the effect was enhanced with the dose. At 0.5, 1.0 and 2.0 kGy absorbed doses for SMX solutions 0.16 , 0.27 and $0.35 \text{ mg L}^{-1} \text{ h}^{-1}$, while for DCF 0.01 , 0.14 and $0.31 \text{ mg L}^{-1} \text{ h}^{-1}$ oxygen consumptions were measured, respectively. The chemical oxygen demand (COD) decreased due to the irradiation treatment from 54 mg L^{-1} (not irradiated), to 52 mg L^{-1} (0.5 kGy), 37 mg L^{-1} (1.0 kGy) and 30 mg L^{-1} (2.0 kGy), for SMX, and from 48 mg L^{-1} (not irradiated) to 40 mg L^{-1} (0.5 kGy), 39 mg L^{-1} (1.0 kGy) and 34 mg L^{-1} (2.0 kGy) in the case of DCF (Fig. 2 inset). This indicates radiation induced degradation of the pharmaceuticals.

The post-irradiation OUR value with growth substrate are shown in Fig. 3. The values measured for the growth substrate (without irradiation) were subtracted. The OUR increment values of the figure show the effect of cometabolism and irradiation together. The higher the OUR values, the more pronounced the effect of irradiation on cometabolism.

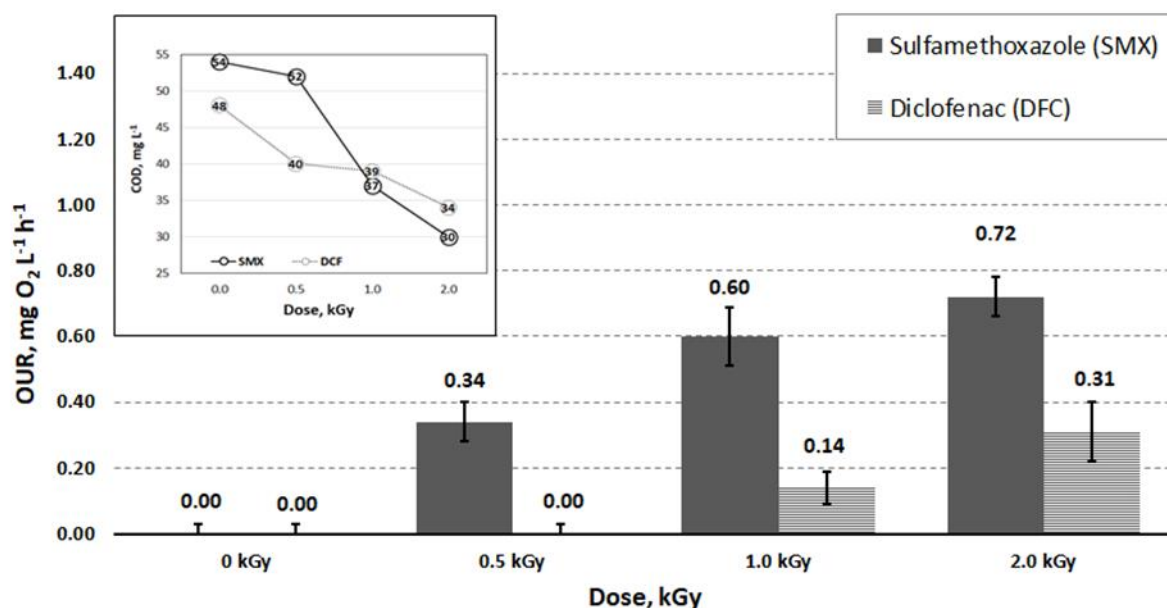


Figure 2. The effect of irradiation on oxygen uptake rate and chemical oxygen demand values (inset) of two pharmaceutical compounds (SMX and DCF).

The efficiency of the cometabolism can be increased by irradiating the samples with a relatively low dose. At 0.5 kGy absorbed dose, the increase in co-oxidative respiration for SMX was 0.47 mg L⁻¹ h⁻¹ with acetic acid, 1.60 mg L⁻¹ h⁻¹ with ethylene glycol and 2.24 mg L⁻¹ h⁻¹ with methanol. For DCF the increase was 0.53 mg L⁻¹ h⁻¹ with acetic acid, 2.05 mg L⁻¹ h⁻¹ with ethylene glycol and 4.19 mg L⁻¹ h⁻¹ with methanol. No improvement was observed at higher doses (Fig. 3). Above 0.5 kGy there is a very high oxidation percentage and there is considerable depletion in the organic material (Fig. 2, inset).

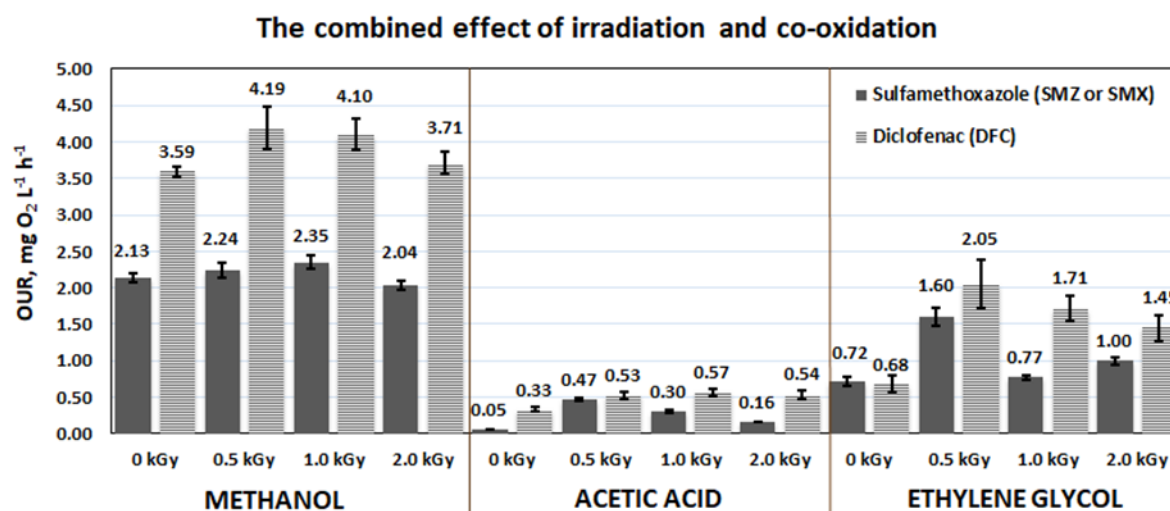


Figure 3. The effect of irradiation on oxygen uptake rate (OUR) increment in the presence of pharmaceuticals (SMX and DCF) and growth substrate (methanol, acetic acid and ethylene glycol) with the values measured for the growth substrate subtracted.

If acetic acid was added to the irradiated SMX solution, the OUR was almost ten times higher than without treatment (0.05 to 0.47 mg L⁻¹ h⁻¹). Ethylene glycol mixed with irradiated DCF solution resulted in a triple respiration intensity relative to the untreated cometabolic effect (0.68 to 2.05 mg L⁻¹ h⁻¹). The effect of treatment on the methanol as growth substrate is barely detectable (SMX: from 2.13 to 2.24 mg L⁻¹ h⁻¹, DCF: from 3.59 to 4.19 mg L⁻¹ h⁻¹). Based on

these results, significant improvement can be achieved in the case of the inherently weak substrate. In the case of a highly active substrate, methanol, irradiation does not improve significantly the efficiency.

Conclusion

The biodegradation of sulfamethoxazole and diclofenac was stimulated separately by the two tested methods: cometabolism and advanced oxidation treatment (by high-energy ionizing radiation). Two type of bioculture (activated sludge and biofilm) and 10 organic molecules were tested, and finally methanol, acetic acid and ethylene glycol were selected as growth substrates for cometabolism by biofilm biomass. Both pharmaceuticals showed cometabolic effect, but it was really significant for activated sludge. The biodegradability of sulfamethoxazole and diclofenac in 0.1 mmol L^{-1} aqueous solutions was enhanced by irradiation. A further increase was observed when the two methods, cometabolism and irradiation were combined. The the efficiency of the cometabolism can be enhanced by irradiation up to 0.5 kGy . No improvement was observed at higher doses most possibly due to the depletion of organic molecules by irradiation. Acetic acid added to the sulfamethoxazole almost ten times, the ethylene glycol mixed with diclofenac three times increased the respiration intensity as compared to the values obtained without irradiation.

The use of advanced oxidation techniques combined with cometabolic technology can be a successful and cost effective development path for the removal of pharmaceuticals. These two methods can be combined at the end of the wastewater treatment technology as a fourth stage.

References

- [1] A. Jelić, M. Gros, M. Petrović, A. Ginebreda, D. Barceló, H. Guasch, A. Ginebreda, A. Geiszinger (Eds.), *Emerging and Priority Pollutants in Rivers, The Handbook of Environmental Chemistry*, vol 19. Springer, Berlin, Heidelberg pp. 2012. pp. 1.
- [2] A. Joss, S. Zabczynski, A. Göbel, B. Hoffmann, D. Löffler, C.S. McArdell, T.A. Ternes, A. Thomsen, H. Siegrist *Water Res.* 40 (2006) 1686.
- [3] K. Fent, A. Weston, D. Caminada *Aquatic Toxicology* 76 (2006) 122.
- [4] A. Pruden, R. Pei, H. Storteboom, K.H. Carlson *Environ. Sci. Technol.* 40 (2006) 7445.
- [5] S. Evangelista, D.G. Cooper, V. Yargeau, *Chemosphere* 79 (2010) 1084.
- [6] D.E. Helbling, D.R. Johnson, M. Honti, K. Fenner *Environ. Sci. Technol.* 46 (2012) 10579.
- [7] S. Xia, R. Jia, F. Feng, K. Xie, H. Li, D. Jing, X. Xu *Bioresource Technol.* 106 (2012) 36.
- [8] F.C. Moreira, J. Soler, M.F. Alpendurada, R.A.R. Boaventura, E. Brillas, V.J.P. Vilar *Water Res.* 105 (2016) 251.
- [9] M. Tokumura, A. Sugawara, M. Raknuzzaman, M. Habibullah-Al-Mamun, S. Masunaga *Chemosphere* 159 (2016) 317.
- [10] S. Zhang, S. Gitungo, L. Axe, J.E. Dyksen, R.F. Raczko *Water Research* 105 (2016) 85.

EFFECT OF SUGAR BEET SHREDS PARTICLE SIZE ON BIOSORPTION OF Cu(II) IONS FROM AQUEOUS SOLUTIONS IN A FIXED-BED COLUMN

Nevena Blagojević, Dragana Kukić, Vesna Vasić, Marina Šćiban, Jelena Prodanović, Oskar Bera

*Faculty of Technology, University of Novi Sad, Bul. Cara Lazara 1, Novi Sad, Serbia
+381638687534, nevenan@uns.ac.rs*

Biosorption process is one of the most widely used methods for the removal of heavy metals from water with advantage of low operating costs, high treatment efficiency and no contaminative by-product released into treated water. This technological process is influenced by various process parameters, such as pH, temperature, initial metal ion concentration, sorbent dosage, etc [1]. Furthermore, the biosorbent properties, such as composition, surface structure and particle size, may also affect the biosorption performances [2]. This study investigates the influence of biosorbent particle size, namely sugar beet shreds, on the uptake of Cu(II) ions from aqueous solutions, in a fixed-bed column. Concentration (C_0) and the pH of the inlet solution were $100 \text{ mg}\cdot\text{L}^{-1}$ and 4.5, respectively, and 10 g of the adsorbent were used. Sugar beet shreds were milled and sieved through the set of sieves, and three fractions were used for the adsorption experiments: 224-400, 400-600 and 600-800 μm . Results obtained for the concentration of the copper ions in consecutive effluent aliquots (C) were fitted with the parallel sigmoidal (PS) model [3], since this model fits the experimental data more accurately than any other commonly used model. Namely, coefficient of determination, R^2 , for the samples with ascending particle sizes were 0.9991, 0.9998 and 0.9982, respectively, and sum of squared errors, SS_{er} , for the same samples were $2.27\cdot 10^{-3}$, $0.8\cdot 10^{-3}$ and $0.5\cdot 10^{-3}$, respectively. Two-stage nature of the biosorption process has been confirmed by the low values of the one phenomenon moiety in the overall adsorption process, p (0.31, 0.40 and 0.35, respectively). However, there is no significant differences between samples with different particle sizes, regarding this parameter. The efficiency of the adsorption process is calculated as the ratio of the amount of metal ion adsorbed and the amount of metal ion fed into the column, using PS mathematical model equation. The most efficient was the process applying the smallest biosorbent particles, 224-400 μm , achieving the efficiency of 60.67%. This could be attributed to the fact that smaller particles provided a larger and easily accessible surface area for the same amount of biomass, making more binding sites available for the metal uptake [4]. The sample with particle sizes 400-600 μm achieved 44.24% adsorption efficiency, while the sample with the largest particles achieved efficiency of 52.25%. The higher efficiency of the largest fraction could be attributed to the fact that the smaller total surface area of this sample has been compensated with contribution of some additional adsorption mechanisms, unlikely to occur in the sample with smaller particles.

Acknowledgements

This research was supported by the grants III43005 and III46009 (Ministry of Education, Science and Technological Development, Republic of Serbia).

References

- [1] Kanamarlapudi, S., Chintalpudi, V., and Muddada, S. (2018) Application of biosorption for removal of heavy metals from wastewater. in: J. Derco, B. Vrana (Eds.), Biosorption, IntechOpen, pp. 70–116.
- [2] El-Sayed, H.E.M. and El-Sayed, M.M.H. (2014) Assessment of food processing and pharmaceutical industrial wastes as potential biosorbents: a review. *BioMed Research*

- International*. 2014 146769.
- [3] Blagojev, N., Kukić, D., Vasić, V., Šćiban, M., Prodanović, J., and Bera, O. (2019) A new approach for modelling and optimization of Cu(II) biosorption from aqueous solutions using sugar beet shreds in a fixed-bed column. *Journal of Hazardous Materials*. 363 366–375.
- [4] Barka, N., Ouzaout, K., Abdennouri, M., and Makhfouk, M. El (2013) Dried prickly pear cactus (*Opuntia ficus indica*) cladodes as a low-cost and eco-friendly biosorbent for dyes removal from aqueous solutions. *Journal of the Taiwan Institute of Chemical Engineers*. 44 (1), 52–60.

CHEMICAL ANALYSIS OF SOIL POLLUTING LUBRICANT OILS PRIOR TO DESIGN A SOIL REHABILITATION PROCEDURE

Attila Bodor^{1,2,3}, György Erik Vincze¹, Péter Petrovski¹, Naila Bounedjoum¹, Krisztián Laczi¹, Balázs Szalontai³, Gábor Rákhely^{1,2,3}, Katalin Perei^{1,2}

¹*Department of Biotechnology, University of Szeged, H-6726 Szeged, Közép fasor 52, Hungary*

²*Institute of Environmental and Technological Sciences, University of Szeged, H-6726 Szeged, Közép fasor 52, Hungary*

³*Institute of Biophysics, Biological Research Centre, H-6726 Szeged, Temesvári krt. 62, Hungary*
e-mail: bodor.attila@gmail.com

Abstract

Excessive consumption of petroleum products carries the risk that these toxic chemicals enter and accumulate in the environment endangering natural habitats or human health. Areas being close to vehicle traffic or where handling and maintenance operations of vehicles take place are considered to be particularly vulnerable, thus, we aimed at investigating a railway marshalling yard polluted by used lubricant oils (ULO). Quantitative determination of total petrol hydrocarbons in the polluted soil revealed a high level of pollution. Apart from the presence of open-chain or branched paraffins and aromatics, Fourier transform infrared spectroscopy identified intermediates from the microbial degradative pathways of hydrocarbons. Occurrence of metabolically active microorganisms even in this highly ULO-contaminated soil indicates that biological rehabilitation techniques can be preferable over more invasive and expensive physico-chemical methods to meet the soil standard.

Introduction

Lubricating oils (LOs) are widely used as friction-reducing, cooling and anti-corrosion agents on mechanical moving parts of motorized vehicles, which undergo a great variety of physicochemical changes during normal operation [1]. Used lubricating oils are complex chemicals consisting of a hydrocarbon mixture with varied carbon counts and diverse structures, additives and a considerable level of such harmful compounds as polychlorinated and polyaromatic hydrocarbons (PCBs and PAHs) or heavy metals [2-4]. Since ULOs can strongly bind to soil particles, persist in soil and cause changes in its physical, chemical and biological properties [5], contamination usually results in narrowing the soil spectra for later uses.

Experimental

Areas being close to vehicle traffic or where handling and maintenance operations of vehicles take place are considered to be particularly vulnerable, since the probability of contamination inevitably increases in these places [6]. ULOs, leaking from locomotives and polluting the soil, have been a long-standing environmental problem at a railway marshalling yard near Szeged, Hungary. We aimed at determining the level of total petrol hydrocarbons (TPH) in the polluted soil and elucidating changes in chemical composition of ULO exposed to natural weathering processes. Fourier transform infrared spectroscopy (FTIR) was applied to compare chemical properties of spent ULO to fresh MK8 locomotive LO. Determination of pollution level and chemical properties of the pollutant are essential for designing appropriate environmental soil rehabilitation processes.

Results and discussion

Soil samples were collected from the upper layer of soil along a transect on the ULO-polluted train track. TPH levels in samples A-F (Fig. 1.) exceeded the pollution limit of 100 mg TPH/kg soil set out in Government Decree 6/2009 (IV. 14.) [7].

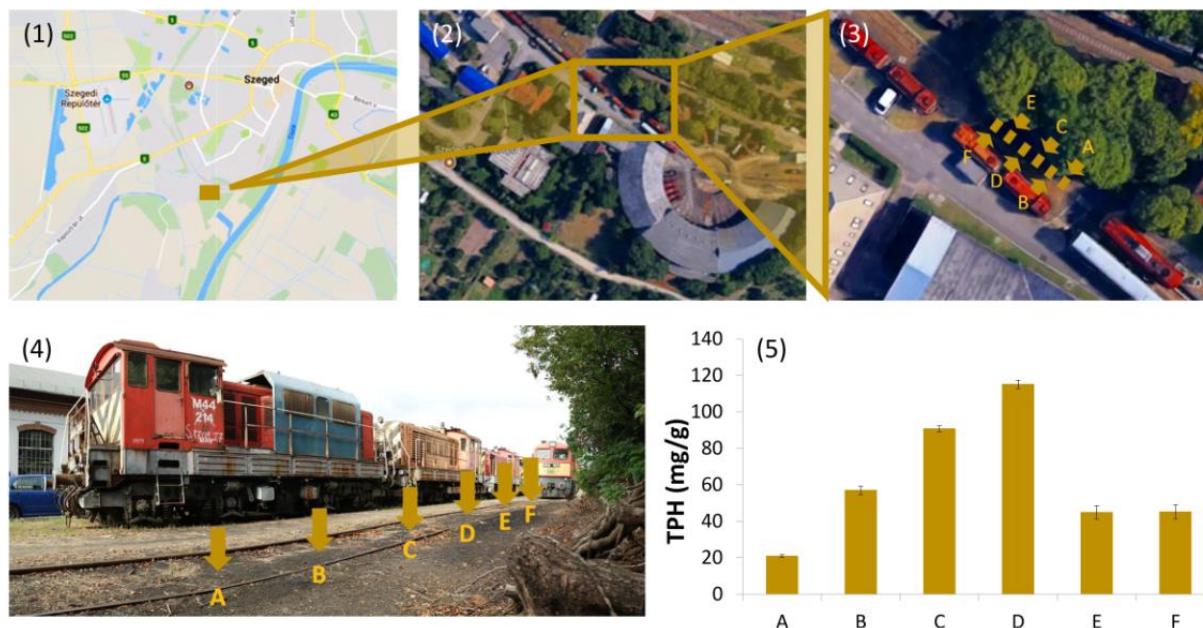


Figure 1. Sampling site: 1-2) ULO-polluted area of a railway marshalling yard near Szeged, 3-4) soil sampling points and 5) TPH levels in ULO-contaminated soil samples (A-F).

Comparison of FTIR spectra of spent ULO and fresh MK8 LO (Fig. 2.) revealed that LOs primarily composed of open-chain and branched paraffins [8-10]. Absorbance bands of C-H stretching vibrations in spent ULO are a bit shifted indicating disordered oil structure and shortened hydrocarbon chains possibly due to microbial ULO-degradation in soil. Alcohols and carboxylic acids are also intermediers in the degradative pathways of hydrocarbons [1, 8, 11]. Bands corresponding to the presence of esters, ethers and amines [9, 12] further proves that metabolically active microorganisms can be found in polluted soils despite the high level of ULO-contamination. Metal-containing additives of LOs (zinc dialkyl dithiophosphates - ZDDPs) detergents (sulfonates, phenolates and carboxylates) and antifoams were also present according to the absorption bands of their P-O-C, P=S and Si-H bonds [12-14]. Increased concentration of aromatics was also detected in spent ULO compared to the FTIR spectrum of fresh LO [12].

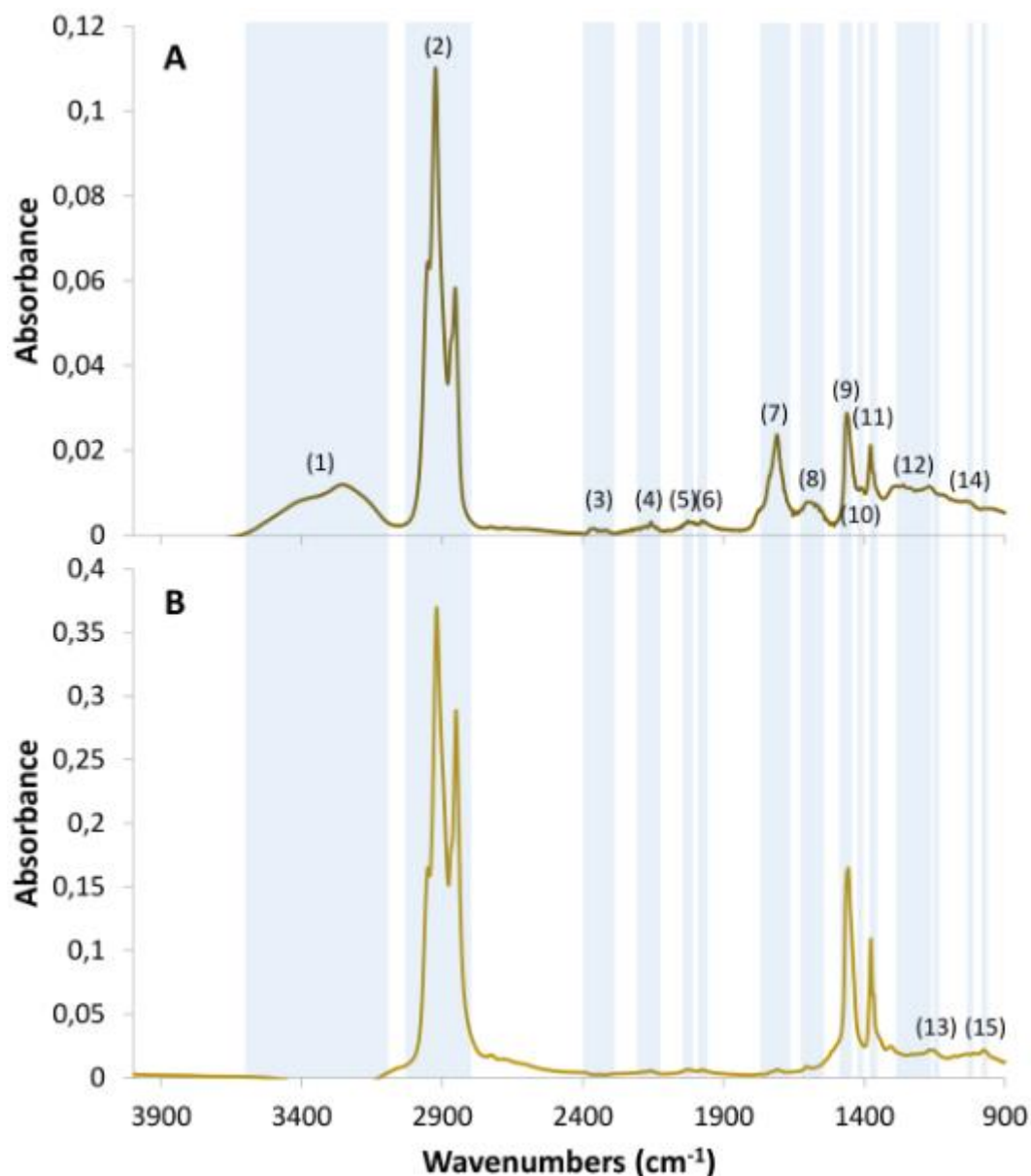


Figure 2. FTIR spectra of MK8 lubricating oil: A) spent ULO and B) fresh LO. Absorbance bands: (1) O-H stretching in alcohols; (2) C-H stretching in hydrocarbons; (3) NH_2^+ deformation and NH^+ stretching in amines; (4) Si-H stretching; (5) $\text{N}=\text{C}=\text{S}$ stretching in isothiocyanates; (6) C-H bending in aromatics; (7) $\text{C}=\text{O}$ stretching in esters, ketones and carboxylic acids; (8) C-C stretching in aromatic rings; (9) C-H bending in hydrocarbons; (10) $\text{S}=\text{O}$ stretching in sulfates and sulfonates; (11) C-H branching vibration in hydrocarbons; (12) C-O-C stretching in esters and ethers; (13) sulfonate salts, methacrylates; (14) C-N stretching in amines; (15) P-O-C and P=S bonds in zinc dialkyl dithiophosphates (ZDDPs).

Conclusion

Detection of biomolecules and intermediers from ULO-biodegradation indicate the presence of metabolically active microorganisms even in this highly ULO-contaminated soil, hence biological rehabilitation techniques can be preferable over more invasive and expensive physico-chemical methods to meet soil standards.

Acknowledgements

The authors also thank the Hungarian State Railways for making their work possible. The support and advices by Mr. Péter Tóth (MÁV Szolgáltató Központ Zrt.), Ms. Bernadett Kolozsi (MÁV Szolgáltató Központ Zrt.) and Mr. Gyula Gyarmati (MÁV-START Zrt.) are gratefully acknowledged. The authors would like to express their gratitude towards Ms. Sarolta Papp for the excellent technical assistance. The project was supported by the European Union and Hungarian State (grant agreement no. EFOP-3.6.2-16-2017-00010).

References

- [1] Pinheiro, C.T., Rendall, R., Quina, M.J., Reis, M.S. and Gando-Ferreira, L.M., 2016. Assessment and prediction of lubricant oil properties using infrared spectroscopy and advanced predictive analytics. *Energy & Fuels*, 31(1), pp.179-187.
- [2] Dorsey, A., Rabe, C. and Thampi, S., 1997. Toxicological profile for used mineral-based crankcase oil. *Public Health Service Press*, Atlanta, GA, USA.
- [3] Vazquez-Duhalt, R. and Greppin, H., 1986. Biodegradation of used motor oil by bacteria promotes the solubilization of heavy metals. *Science of the Total Environment*, 52(1-2), pp.109-121.
- [4] Vazquez-Duhalt, R., 1989. Environmental impact of used motor oil. *Science of the Total Environment*, 79(1), pp.1-23.
- [5] Paria, S., 2008. Surfactant-enhanced remediation of organic contaminated soil and water. *Advances in Colloid and Interface Science*, 138(1), pp.24-58.
- [6] Odjegba, V.J. and Sadiq, A.O., 2002. Effects of spent engine oil on the growth parameters, chlorophyll and protein levels of *Amaranthus hybridus* L. *Environmentalist*, 22(1), pp.23-28.
- [7] National Legislation Database 2010, Hungary, accessed 10 September 2019, <http://njt.hu/cgi_bin/njt_doc.cgi?docid=123507.291524>
- [8] Nespeca, M.G., Piassalonga, G.B. and de Oliveira, J.E., 2018. Infrared spectroscopy and multivariate methods as a tool for identification and quantification of fuels and lubricant oils in soil. *Environmental Monitoring and Assessment*, 190(2), p.72.
- [9] Simons, W.W., 1978. Sadtler handbook of infrared spectra. Sadtler Research Laboratories.
- [10] Koji, N. and Solomon, P.H., 1977. Infrared absorption spectroscopy. *QD95 N*, 383.
- [11] Merck IR Spectrum Table & Chart 2019, Germany, accessed 10 September 2019, <<https://www.sigmaaldrich.com/technical-documents/articles/biology/ir-spectrum-table.html>>.
- [12] Kupareva, A., Mäki-Arvela, P., Grénman, H., Eränen, K., Sjöholm, R., Reunanen, M. and Murzin, D.Y., 2012. Chemical characterization of lube oils. *Energy & Fuels*, 27(1), pp.27-34.
- [13] Zięba-Palus, J., Kościelniak, P. and Łacki, M., 2001. Differentiation of used motor oils on the basis of their IR spectra with application of cluster analysis. *Journal of Molecular Structure*, 596(1-3), pp.221-228.
- [14] Isa, F.M. and Haji-Sulaiman, M.Z., 1997. An investigation of the relationship between used engine oil properties and simulated intake valve deposits. Proceedings of the Institution of Mechanical Engineers, Part D: *Journal of Automobile Engineering*, 211(5), pp.379-389.

DUST LOAD OF AGRICULTURAL ORIGIN, WITH PARTICULAR REGARD TO ITS TOXIC ELEMENT CONTENT.

Katalin Csányi^{1*}, Barta Károly¹, Andrea Farsang¹

¹*Department of Physical Geography and Geoinformatics, University of Szeged, H-6720*

Szeged, Egyetem u. 2-6, Hungary

**e-mail: csanyi@geo.u-szeged.hu*

Abstract

There is a worldwide increasing interest in air pollution problem today. Wind transport and deposition of soil is recognized worldwide as an important environmental problem, as a large proportion of the environmental dust consists of fine particles from natural soil. Coarse and fine particles are released into the atmosphere through a variety of mechanisms, depending on the composition, size, concentration and duration of the particles in the atmosphere. Thus, mineral aerosols have a significant impact on air quality at local, regional and continental levels. Particles smaller than 10µm in diameter (PM₁₀ and PM_{2.5}) are easily transported by the wind. Eroded soil contains organic matter, heavy metals, pesticides, fertilizers, etc. Therefore, the study of the spatial and temporal changes in the content of soil toxic elements (pesticides, heavy metals) due to deflation is important from an environmental and human health point of view. The finer particles of soil transported by the wind, when introduced into the towns / villages, can contribute to the dust load of the settlements through dry and wet atmospheric deposition. So, it is important to examine the spatial and temporal variations in the harmful and pollutant content of the topsoils. These effects can be tested by wind tunnel experiments. [1, 2]

In this study, we investigated the behavior of pesticides in wind-eroded sediment portable wind tunnel and a Wet Active Sediment Trap (WAST) and. WAST is a horizontal active trap that is patterned at different heights, isokinetic, wet trap to collect the suspended soil fractions [3]. Trap inlets are 5-10 cm, 20-25 cm, 50-55 cm high. The rolling soil fractions were collected too, in a tray at the end of the wind tunnel. In summer 2019, we collected chernozem and sandy soils from arable land near Szeged and took ex-situ measurements. Before the experiment, a part of the soil samples were treated with chlorpyrifos (2l/ha) and pendimethalin (5l/ha). Control soil samples were also measured.

We examined the topsoil samples (pH (H₂O), CaCO₃, Arany yarn test, OM %, total salt content, humidity and pendimethalin and chlorpyrifos contents and the toxic element contents in the collected soil fractions. Pesticide measurements are made by LC-MS according to hungarian standards.

First results indicated that that chlorpyrifos and pendimethalin contents were higher in the rolling particles and in the particles collected at 5-10 cm.

Keywords

dust, wind-eroded soil, toxic elements, wind tunnel

Acknowledgements

Supported by the ÚNKP-19-3-I. New National Excellence Program of the Ministry for Innovation and Technology. The study was carried out with the support of OTKA 1K 116981.

References

- [1] Toy, T.J., Foster, G.R., Renard, K.G.: Soil erosion: Processes, Prediction, Measurement, and Control. New York: John Wiley and Sons, 338 p. (2002).
- [2] Gossens, D.: On-site and off-site effects of wind erosion. In: Wind erosion on agricultural land in Europe (ed.:Warren, A.). Office for Official Publications of the European Communities. EUR 20370, pp. 29-38. (2002)
- [3] Farsang, A.: A víz- és szélrózió szerepe a talaj humusz- és elemtartalmának horizontális átrendeződésében. MTA doktori értekezés. Szeged, 183 p. (2016).

DEVELOPING ENVIRONMENTAL AWARENESS IN THE PUBLIC ADMINISTRATION: A PILOT STUDY

Zsófia Csonka¹, László Berényi²

¹ Faculty of Science of Public Governance and Administration, National University of Public Service, H-1083 Budapest, Üllői út 82., Hungary

² Institute of E-Government, National University of Public Service, H-1083 Budapest, Üllői út 82., Hungary
e-mail: csonkazsofi98@gmail.com

Abstract

Government and public administration have a multifaceted role in defining and achieving sustainability by developing policies and supporting the implementations. Since this area is a notable employer, personal opinions of the present and future employees deserve attention. Several studies are dealing with the attitude of higher education students towards sustainability, but public administration manager students are usually out of scope. This paper shows the results of a pilot study among 34 public administration manager students. The results include that the respondents are active in certain activities, but these are limited to simple and attractive issues like selective waste collection. The most important governmental responsibilities are defining and supporting tasks related to environmental protection, indirect tasks (framing) are rated less important. The main experience of the survey is that a system-oriented and integrated approach is desired.

Introduction

Pro-environmental personal behavior is essential for achieving sustainability. Since both sustainability and human behavior are complex concepts, there are no simple answers to the emerging challenges. UN [1] defined 17 sustainable development goals (SDGs) including environmental, social and human ones. The most important components of environmentally conscious behavior are the knowledge, shared values, attitudes, intentions and the evaluation of actions [2] [3] [4] [5]. However, only the implemented actions bring sustainability closer to the present, such occurrence should be consciously increased. Li and Hu [6] or Bukovics [7] confirm the importance of relevant information available, others deal with exploring the patterns of personal attitudes ([8] [9] [10] [11]). Due to the conceptual diversity and a large number of influencing factors, the role of empirical studies is appreciated.

Attention paid to public administration can be justified by two reasons. Once, public services appear in a wide area of life, so it is an excellent medium for presenting the expected behavioral patterns. Secondly, there are 471 800 people (2016 data of the KSH) working in various positions for the public administration, so the government is the largest employer in Hungary. Developing environmental awareness among them may also lead to notable impacts on the national level. Bukovics et al. [7] pointed out the need for this special approach to sustainable public administration that focuses on the functioning of society.

The 'Good State and Governance Report' [12] [13], managed by the National University of Public Service, covers the strategy and the measurement initiation of the issues above. Sustainability is evaluated in five dimensions:

- Climate change
- Natural resources
- Energy and water management
- Environmental burdens (emissions)
- Social sustainability.

Just social sustainable is marked 'in need of development'.

Several studies are dealing with the attitudes of higher education students (see e.g. [8] [10] [14]) but these usually focus on business/MBA students. Exploring the characteristics of public service students contributes greatly to the knowledge base of the field.

Experimental

The paper presents the results of a pilot study among 34 public administration manager students (82.4% female, 17.6% male). The representativeness of the sample is not ensured, conclusions are limited to the sample. The main purpose of the research is to prepare a wider survey. The survey uses an online questionnaire about the opinions and attitudes to environmental issues, evaluation of environmental and social problems as well as the role and engagement of the government. Due to the pilot nature of the research and the small sample size, it is not worth to run statistical tests for relationship analysis. This paper selects some results:

- personal approach to environmental protection (measured on a 5-point scale),
- barriers of sustainability (respondents were asked to mark at most 3 items of a list),
- role of government (respondents were asked to put items in order).

Results and discussion

Environmental considerations are presented in some activities of the students. Figure 1 summarizes the distribution of the responses measured on a 5-point scale. The waste collection shows a 'greener picture' than other items of the survey. Voluntary actions are not typical as well as environmental considerations in e.g. selecting the travel mode of the holiday journey.

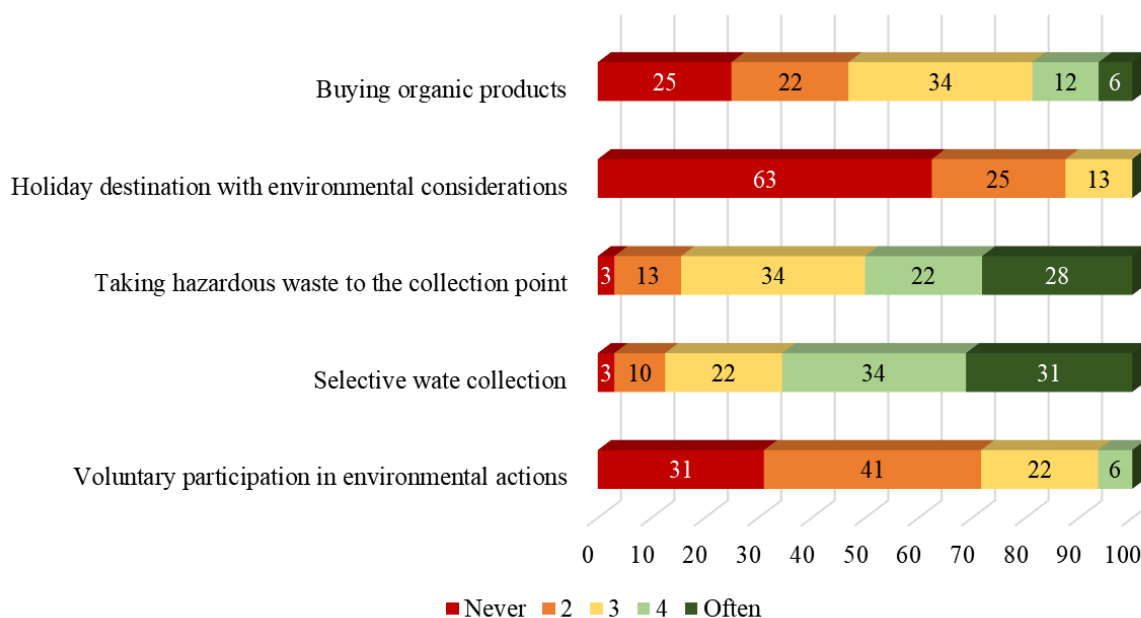


Figure 1: Considerations of environmental aspects in some activities (own edition)

The most relevant barrier of environmentally conscious living is the need for comfort based on the evaluation of the respondents (Figure 2). Financial reasons are marked by 46.9% of the respondents as one of the three most relevant items. It is surprising, that a high proportion of them do not consider environmental problems serious (41.2%). However, it is encouraging that only 11.8% thinks that the conditions of sustainable living are not available.

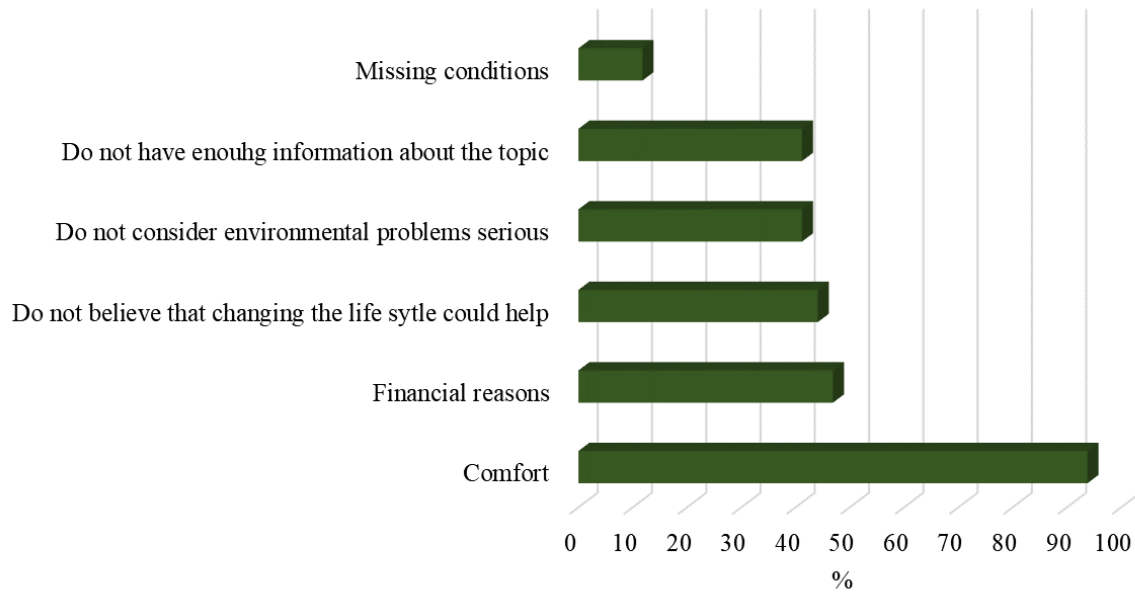


Figure 2: Barriers of sustainability (own edition)

The role of government is complex in managing sustainability from legislation to business activities including education and supporting social changes. The survey asked the respondents to rank 7 statements. Accordingly, the order is as follows, based on the mean value of the ranking numbers:

1. Establishing a legal, economic and technical regulatory framework for achieving environmental goals (3.4)
2. Defining the priority tasks of environmental protection (3.5)
3. Providing the economic and financial foundations of environmental protection (3.6)
4. Carrying out environmental state administration tasks (4.0)
5. Exploring the state of the environment and determining the status to be reached (4.1)
6. Defining and realizing R&D, education and information tasks (4.4)
7. Enforcement of environmental requirements in other state tasks (5.0)

The distribution of the rankings shows a more nuanced picture of the opinions. Figure 3 highlight the ratios of high priority (Rank 1 and 2), middle (Rank 3 to 5) subordinated (Rank 6 and 7) issues.

Beyond providing the economic and the financial background, the respondents considered defining the priorities as an important governmental task as well as R&D, education and information tasks. However, 44.1% of the respondents rated this item the least important. Medium values are assigned to establishing a regulatory framework and state administration tasks. An interesting experience of the survey is that an integrated approach is not expected, 58.6% considered enforcing environmental requirements in other governmental tasks the least important item.

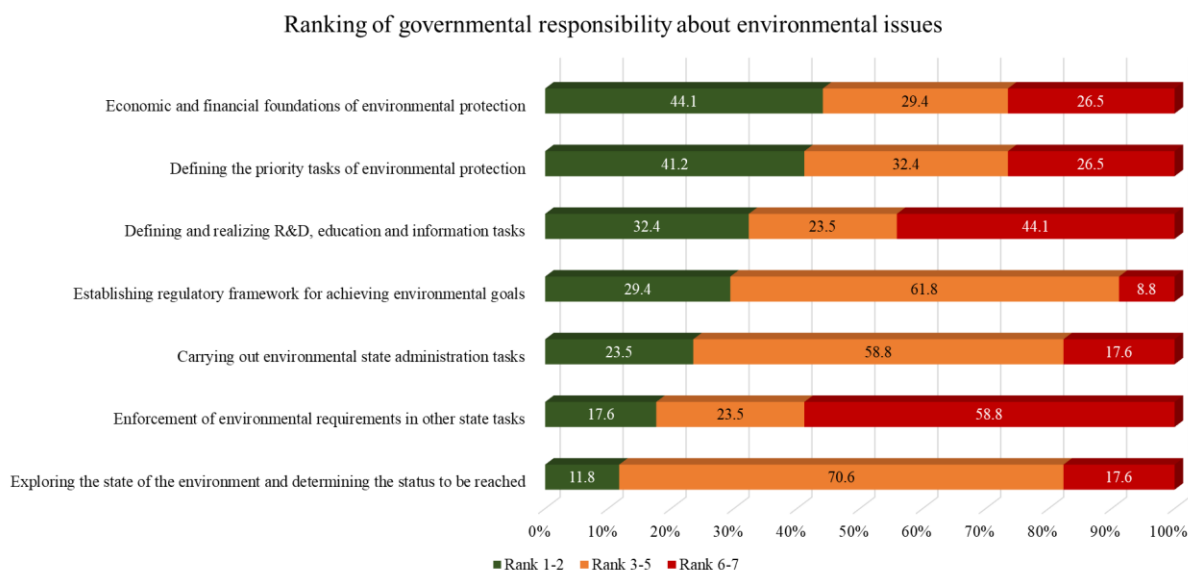


Figure 3. Ranking of governmental responsibility about environmental issues (own edition)

Conclusion

The government has a multifaceted role in defining and achieving sustainability. The attitudes of public administration manager students as future public servants may influence the success of the progress. However, there is very little attention to their characteristics in the literature. However, the results presented in this paper are not representative and the conclusion is limited to the sample, the experience helps to prepare extensive research. The main conclusions of the research are as follows:

- the respondents are active in certain activities, but these are limited to some simple and attractive issues like selective waste collection,
- comfort is considered the most important barrier of sustainability,
- Defining and supporting tasks related to environmental protection are the most important governmental responsibilities; indirect tasks (framing) are rated less important,
- integrated approach and system-oriented thinking must be developed.

Acknowledgments

The research was supported by the ÚNKP-18-1 New National Excellence Program of The Ministry of Human Capacities, Higher Education Undergraduate Student Research Scholarship (ÚNKP-18-1-I-NKE-88).

References

- [1] The Sustainable Development Goals. (2017). New York: United Nations Publications.
- [2] Á. Zsóka, Zs. Marjai-Szerényi, A. Széchy, T. Kocsis, Greening due to environmental education? Environmental knowledge, attitudes, consumer behavior and everyday pro-environmental activities of Hungarian high school and university students, *Journal of Cleaner Production*. 48 (2013) 126-138.
- [3] A. Zsóka, Consistency and “awareness gaps” in the environmental behaviour of Hungarian companies, *Journal of Cleaner Production*. 16(3) (2008) 322-329.
- [4] S. Bamberg, How does environmental concern influence specific environmentally related behaviors? A new answer to an old question, *Journal of Environmental Psychology*. 23(1) (2003) 21-32.

- [5] L. Varela-Candamio, I. Novo-Cortib, M.T. García-Álvarez, The importance of environmental education in the determinants of green behavior: A metaanalysis approach, *Journal of Cleaner Production*. 170 (2018) 1565-1578.
- [6] Z. Li, B. Hu, Perceived health risk, environmental knowledge, and contingent valuation for improving air quality: New evidence from the Jinchuan mining area in China, *Economics & Human Biology*. 31 (2018) 54-68.
- [7] I. Bukovics, L. Földi, M. Besenyei, Zöld-beszéd, Külső és belső kommunikáció a fenntarthatóságról. Budapest: Nemzeti Közzolgálati Egyetem, 2014.
- [8] A.M. Lämsä, M. Vehkaperä, T. Puttonen, H.L. Pesonen, Effect of business education on women and men students' attitudes on corporate responsibility in society, *Journal of Business Ethics*. 82(1) (2008) 45-58.
- [9] N. Deutsch, L. Berényi, Personal approach to sustainability of future decision makers: a Hungarian case, *Environment Development and Sustainability*. 20(1) (2018) 271-303.
- [10] J.L. Vázquez, A. Lanero, M.P. Garcia, Analyzing CSR conceptions of business students: Some Preliminary Evidences in Spain, *Bulletin UASVM Horticulture*. 68(2) (2011) 246-252.
- [11] M. Segon, C. Booth, Business ethics and CSR as part of MBA curricula: an analysis of student preference, *International Review of Business Research Papers*. 5(3) (2009) 72-81.
- [12] T. Kaiser (ed.), *Good State and Governance Report 2017*. Budapest: Nordex Nonprofit Kft. – Dialóg Campus Kiadó, 2018.
- [13] T. Kaiser (Ed.), *Jó állam jelentés 2018*. Budapest: Nordex Nonprofit Kft. – Dialóg Campus Kiadó, 2019.
- [14] A. Sobczak, G. Debucquet, C. Havard, The impact of higher education on students' and young managers' perception of companies and corporate social responsibility: an exploratory analysis. *Corporate Governance, The European Journal of Business in Society*. 6(4) (2006) 463-474.

ANALYSIS OF AWARENESS OF ELECTRICAL ENERGY CONSUMPTION IN COMPANIES AND HOUSEHOLDS

Ivana Dolga¹, Vladimir Dj. Djaković¹, Ladin Gostimirović², Nebojša M. Ralević¹

¹*University of Novi Sad, Faculty of Technical Sciences, Department of Fundamentals Sciences, Novi Sad, Serbia*

²*Visoka poslovno tehnička škola, Doboj, Bosnia and Herzegovina, Republic of Srpska*
e-mail: ivana.dolga@gmail.com, v_djakovic@uns.ac.rs, ladin74@gmail.com, nralevic@uns.ac.rs,

Abstract

In this paper are shown results of the research about the awareness of the employed persons in Doboj (BiH) about the energy consumption and costs in companies and also in households. Analysis is performed based on the respondent answers and correspondent tests of questionnaires collected among employed persons. Questionnaire is organized in three main topics about other sources of energy, including fossil fuels and renewable energy as a supplementation and/or replacement for the electric energy. In the conducted research 150 fulfilled questionnaires were collected, representing the respondents opinion about the importance of source of energy related to companies' energy costs. In this paper relation between of awareness about the energy consumption costs in the company and awareness of the consumption of electricity and the possibility to make household savings in electricity costs.

Keywords: Electric energy, renewable energy, fossil fuels, costs of energy.

Introduction

Survey "Renewable energy sources" was conducted in Doboj (BiH) Municipality and 150 completed surveys were collected, which represents data sample for this analysis. Survey contains of personal data questions and questions about an opinion on efficient consumption and renewable energy sources (1st competitiveness and consumption, 2nd sources of energy). Questions are constructed in line with the possible answers with the scale of 5 possible answers: A - insignificant, B - less significant, C - intermediate, D - very significant, E - extremely significant. Respondents are the employed persons from Doboj (BiH) and they have been expressed their views on the question that they were asked.

Analysis is based on the criterion question:

Electricity consumption has a significant share in the total cost of the company.

How responded reacted to this criterion question represents their opinion about the consumption of electricity within the work they deal with. Based on the criterion question the entire sample is divided into 5 groups depending on their answers to that question.

The 5 groups are represented in the following way:

A - insignificant (0 respondents), B - less significant (4 subjects), C - intermediate (36 subjects), D - very significant (69 respondents) and E - extremely significant (41 subjects). Given distribution of the answers to the criterion question, shows that the group A is completely insignificant and because there are no respondents it won't be used it in the future, while the results of the group B is taken with the reserve because of the small number of respondents, and it cannot be considered as a relevant result. Focus will be on the difference

in attitudes between groups: C - intermediate significant (36 subjects), D - very significant (69 respondents) and E - extremely significant (41 respondents).

Methodology

Goal of this research is to determine whether there are differences between the 4 mentioned groups and on which question or a questions differences exist. Differences are important for the respondents who consider that electricity consumption has a significant share in the total costs of the company and the test hypotheses are created in the following way:

H1 – Groups defined by criteria question (CQ) have different opinion (answer) on the question “Energy consumption in the economy is high” (ENERGY IN THE ECONOMY)

H2 - Groups defined by criteria question have different opinion (answer) on the question “Households can be more economical when consuming electricity” (ELECTRICITY IN HOUSEHOLDS) ”.

Analyses used in this research are MANOVA and ANOVA analysis and data processing and calculations are done with R-project. For testing whether there was a difference on all groups the MANOVA analysis was done and if the difference is obtained as a result of MANOVA, tests between which groups differences exists is later done with ANOVA analysis.

Results

In relation to the criterion question first test was done on the first question:

1. “Energy consumption in the economy is high” (ENERGY IN THE ECONOMY).
2. “Electricity consumption has a significant share in the total cost of the company” (criterion question, CQ)

MANOVA results are shown in the table below

	Df	Sum Sq	Mean Sq	F value	Pr (>F)
CQ	3	23.83	7.943	14.14	0.000
Residuals	146	82.04	0.562		

There is a significant difference ($p < 0.05$), so hypothesis H1 is proven.

Next analysis, **ANOVA was done on questions:**

1. “Energy consumption in the economy is high” (ENERGY IN THE ECONOMY)
2. “Electricity consumption has a significant share in the total cost of the company” (criterion question, CQ).

Groups defined by criteria question	Diff	lower	upper	p adjusted
(B - less significant) - (E - extremely significant)	-2.08537	-3.10587	-1.06487	2.4E-06
(C - intermediate) - (E - extremely significant)	-0.80759	-1.25256	-0.36262	3.27E-05
(D - very significant) - (E - extremely significant)	-0.54189	-0.92604	-0.15773	0.001935
(C - intermediate) - (B - less significant)	1.277778	0.250999	2.304557	0.008133
(D - very significant) - (B - less significant)	1.543478	0.541553	2.545403	0.000568
(D - very significant) - (C - intermediate)	0.265701	-0.13484	0.666242	0.315015

In the cases where p value is less than 0.05 (all rows except the last one) the conclusion is that there is significant difference.

Significant differences are between following groups: (B - less significant) - (E - extremely significant) where $p=2.4E-06$, (C - intermediate) - (E - extremely significant) where $p=3.27E-05$, (D - very significant) - (E - extremely significant) where $p=0.001935$, (C - intermediate) - (B - less significant) where $p=0.008133$, (D - very significant) - (B - less significant) where $p=0.000568$.

We can conclude that the groups for which difference is shown, have different opinion about the given question “Energy consumption in the economy is high” (ENERGY IN THE ECONOMY).

Answer frequencies for the Groups are shown in the table below:

Criteria group	A - insignificant		B – less significant		C - intermediate		D – very significant		E – extremely significant	
	n	%	n	%	n	%	n	%	n	%
B - less significant	0	0.00	3	75.00	0	0.00	1	25.00	0	0.00
C - intermediate significant	0	0.00	0	0.00	10	27.78	24	66.67	2	5.56
D - very significant	0	0.00	2	2.90	15	21.74	30	43.48	22	31.88
E - extremely significant	0	0.00	2	4.88	1	2.44	9	21.95	29	70.73

On the left side in the above table are given groups obtained by dividing the respondents on the criterion question “Electricity consumption has a significant share in the total cost of the company” (criterion question, CQ). In the head row are given answers of respondents for the question “Energy consumption in the economy is high” (ENERGY IN THE ECONOMY).

The most frequents answers per groups are:

- for the group C - intermediate significant the most frequent answer is D – very significant (24 answers)
- for the group D - very significant the most frequent answer is D - very significant (30 answers)
- for the group E - extremely significant the most frequent answer is E – extremely significant (29 answers)

Second test was done on the third question in relation to the criterion question:

3. “Households can be more economical when consuming electricity” (ELECTRICITY IN HOUSEHOLDS)
2. “Electricity consumption has a significant share in the total cost of the company” (criterion question, CQ)

MANOVA results are shown in the table bellow

	Df	Sum Sq	Mean Sq	F value	Pr (>F)
CQ	3	10.37	3.456	3.612	0.0148
Residuals	146	139.69	0.957		

In this case there is the statistically significant difference because $p = 0.0148$ which is less than 0.05. Hypothesis H2 is proven.

Next analysis, ANOVA was done on questions:

3. “Households can be more economical when consuming electricity” (ELECTRICITY IN HOUSEHOLDS)
2. “Electricity consumption has a significant share in the total cost of the company” (criterion question, CQ)

Groups defined by criteria question	Diff	lower	upper	p adjusted
(B - less significant) - (E - extremely significant)	-0.5	-1.83161	0.831612	0.763416
(C - intermediate) - (E - extremely significant)	-0.58333	-1.16396	-0.00271	0.048469
(D - very significant) - (E - extremely significant)	0.028986	-0.47229	0.530257	0.998785
(C - intermediate) - (B - less significant)	-0.08333	-1.42314	1.256473	0.99849
(D - very significant) - (B - less significant)	0.528986	-0.77839	1.836361	0.719384
(D - very significant) - (C - intermediate)	0.612319	0.089667	1.13497	0.014527

In the cases where p value is less than 0.05 (second and the last row in the table above) the conclusion is that there is significant difference.

Significant differences are between following groups: (C - intermediate) - (E - extremely significant) where $p=0.048469$, (D - very significant) - (C - intermediate) where $p=0.014527$. We can conclude that the groups for which difference is shown, have different opinion about the given question “Energy consumption in the economy is high” (ENERGY IN THE ECONOMY).

Answer frequencies for the Groups are shown in the table below:

	A - insignificant		B – less significant		C - intermediate		D – very significant		E – extremely significant	
Criteria group	n	%	n	%	n	%	n	%	n	%
B - less significant	0	0.00	0	0.00	3	75.00	0	0.00	1	25.00
C – intermediate significant	1	2.78	3	8.33	16	44.44	12	33.33	4	11.11
D - very significant	0	0.00	5	7.25	12	17.39	28	40.58	24	34.78
E - extremely significant	3	7.32	0	0.00	8	19.51	13	31.71	17	41.46

On the left side in the above table are given groups obtained by dividing the respondents on the criterion question “Electricity consumption has a significant share in the total cost of the company” (criterion question, CQ). In the head row are given answers of respondents for the question “Households can be more economical when consuming electricity” (ELECTRICITY IN HOUSEHOLDS).

The most frequents answers per groups are:

- for the group C - intermediate significant the most frequent answer is C – intermediate significant (16 answers),
- for the group D - very significant the most frequent answer is D - very significant (28 answers), and frequent answer is E - extremely significant (24 answers),
- for the group E - extremely significant the most frequent answer is E – extremely significant (17 answers) and D – very significant (13 answers).

Discussion

It has been shown that the respondents, who have the opinion that the price of electricity has a significant share in the costs of companies, also consider that the electricity consumption in the economy is high, and that the consumption in households can be more economical. Higher awareness of the respondents to the criterion question asked indicates greater awareness for the questions “Energy consumption in the economy is high” (ENERGY IN THE ECONOMY) and “Households can be more economical when consuming electricity” (ELECTRICITY IN HOUSEHOLDS).

Conclusion

For hypothesis H3 results indicated that there are no significant differences between criteria groups.

For hypothesis H1 and H2 results indicate statistically significant difference between criteria groups.

Respondents who have demonstrated high level of awareness about the energy consumption costs in the company (“Electricity consumption has a significant share in the total cost of the company” - criterion question), also have demonstrated high level of awareness of the consumption of electricity and the possibility to make household savings in electricity costs.

It is general conclusion that more respondents indicated very high level of awareness about electric energy consumption and also about costs that are created from the electric energy consumption at home and at their place of work.

Acknowledgements

The authors acknowledge the financial support of the Ministry of Education, Science and Technological Development of the Republic of Serbia, within the Project No. TR34014.

References

- [1] Martin Kaltschmitt, Wolfgang Streicher, Andreas Wiese (ed): Renewable energy. Technology, economics and environment, Springer, Berlin/Heidelberg. 2007.

EFFECT OF FLOW BREAKERS ON THE VUV PHOTOLYSIS OF AQUEOUS SOLUTION OF COUMARIN

Luca Farkas, Máté Náfrádi, Tünde Alapi

*Department of Inorganic and Analytical Chemistry, University of Szeged, H-6720 Szeged,
Dóm tér 7, Hungary
fluca@chem.u-szeged.hu*

Abstract

Vacuum ultraviolet (VUV) photolysis is one of the Advanced Oxidation Processes (AOPs) for the elimination of trace pollutants from water and air. During VUV photolysis reactive species (mainly $\bullet\text{H}$ and $\bullet\text{OH}$) can be generated directly from water without the addition of any chemicals. The penetration depth of VUV radiation in water is very small, only 0.04 mm, so reactive species form and react with organic compounds and dissolved O_2 in this extremely thin layer. Carbon centered radicals can react at a longer distance from the light source, and their fast reaction with dissolved O_2 results in an O_2 poor layer, wider than the photo reaction zone. Consequently VUV irradiated solution is an extremely inhomogeneous system.

To reduce the inhomogeneity of the VUV irradiated aqueous solution flow breakers (PTFE rings) were used to enhance the mass transfer into the zone determined by the reactions of primary, carbon centered and peroxy radicals. Coumarin and its hydroxylated byproduct, the umbelliferone (7-hydroxy-coumarin) were used as model compounds. The effects of the PTFE rings on the transformation rate of coumarin and formation rate of umbelliferone were investigated in O_2 -saturated and O_2 -free solutions. The detailed investigation of the concentration effect of both dissolved O_2 and coumarin is also reported in this work.

Introduction

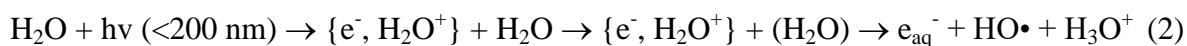
Advanced Oxidation Processes (AOPs) include chemical, photochemical, and electrochemical processes, based on the producing reactive species (especially $\text{HO}\bullet$). These species can react with organic pollutants and possibly mineralize those in the presence of dissolved O_2 . VUV photolysis, one of the AOPs, is based on high energy UV-radiation (wavelength <200 nm). VUV light has enough energy to break the bound in water molecule and consequently produce $\text{HO}\bullet$ and $\text{H}\bullet$ reactive species.

Two typical VUV light sources exist. One of them is the low-pressure mercury vapour lamp, which emits both 254 nm UV and 185 nm VUV light. The other light source is the Xe excimer lamp, which emits quasi-monochromatic light with a wavelength maximum at 172 nm. There are several benefits of the excimer lamps, such as high average specific power radiation, high energy of emitting photons, quasi-monochromatic radiation, high spectral power density, absence of visible and IR radiation, low heating of radiating surface (cold lamps), no fixed geometry and no warm up time. [1]

In the case of 172 nm VUV radiation, the VUV irradiated zone is only 0.04 mm wide, because of the high molar absorbance of water at this wavelength. The primary reactive species ($\text{HO}\bullet$, $\text{H}\bullet$ and e_{aq}^-), having a short lifetime, form and react within this zone.



$$\Phi(\text{HO}\bullet) = 0.42 [2,3]$$



$$\Phi(\text{e}_{\text{aq}}^-) = 0.045 - 0.05 [2,3]$$

The carbon centered radicals, which formed due to the reaction of organic pollutants with primary radicals, react fast with dissolved O_2 . Because of the extremely high concentration of $HO\bullet$, $H\bullet$, and carbon centered radicals, an O_2 poor layer forms close to the wall of the light source. Thus the VUV irradiated solution can be characterized as an extremely inhomogeneous system, since both radical's concentration (primary and carbon centered radical) and dissolved O_2 concentration decreases fast with the distance from the outside of the light source. [4].

The aim of this work was the investigation of the effect of flow parameters on the inhomogeneity of the zone characterized by O_2 depletion and radical reactions. Coumarin was used as a model compound. According to the publications reported previously [5], the formation rate of umbelliferone, which is the hydroxylated product of coumarin, is proportional to the formation rate of $HO\bullet$.

Experimental

The Xe_2^* excimer lamp (Radium XeradexTM, 130 mm long, 46 mm diameter, 20 W) was centred in a high purity silica quartz envelope (53 mm diameter), which transmits the 172 nm light. The thickness of irradiated water layer was 5 mm. The aqueous solution was circulated continuously (375 mL min^{-1}) between the reactor and the liquid containing reservoir. Double walled, water cooled reactor was used and the temperature was set to $25 \pm 0.5^\circ \text{C}$. Samples were taken from the reservoir. The total volume of the circulated solution was 500 mL. The photon flux emitted by the excimer lamp (20 W) at $172 \pm 14 \text{ nm}$ determined by methanol actinometry was found to be $3.0 \times 10^{-6} \text{ mol}_{\text{photon}} \text{ s}^{-1}$ [6]. For investigation of the flow parameters 7 PTFE rings was placed into the reactor to break the laminar flow and increase the turbulence. These rings were 5 mm tall and 3 mm wide.

The transformation of coumarin was followed using spectrophotometry (Agilent 8453) at 277 nm. Fluorescence spectroscopy (Hitachi F4500) was applied to determine the concentration of umbelliferone. The wavelength of excitation was 387 nm, the determination of concentration was based on the intensity of the emitted fluorescence light at 455 nm.

Results and discussion

Dissolved O_2 generally enhances the transformation rate of organic substances due to the formation of peroxy radical. The formation of peroxy radical opens up a new pathway for the further transformation of carbon centered radicals and hinders the backward reactions. In the case of VUV photolysis of aqueous solution, the formation rate of $H\bullet$ is equal with the formation rate of $HO\bullet$. Moreover, rate constants of the reaction of coumarin with $H\bullet$ ($2.50 \times 10^9 \text{ M s}^{-1}$) and $HO\bullet$ ($6.88 \times 10^9 \text{ M s}^{-1}$) has similar values, thus both radicals can initiate the transformation with high rate. Dissolved O_2 reacts with $H\bullet$ and transform that into $HO_2\bullet$ having very low reactivity [7]. In the case of 172 nm VUV irradiated $5.0 \times 10^{-4} \text{ M}$ coumarin solution, there was no significant effect of O_2 on the transformation rate, most probably because the positive effect (formation of peroxy radical) and negative effect (scavenging of reactive $H\bullet$) of O_2 compensate each other (Table 1 and Fig. 2.).

The reaction between coumarin and $HO\bullet$ produce umbelliferone (7-hydroxy-coumarin). However the dissolved O_2 has no significant effect on the transformation rate of coumarin, the formation rate of umbelliferone was about two times higher in the presence of O_2 than in O_2 -free solution. The formation of umbelliferone from coumarin is reported to be highly O_2 -dependant: in the presence of dissolved O_2 , umbelliferone forms via peroxy radicals, while in O_2 -free solutions the hydroxylated products can be resulted only by the disproportionation and has lower yield [8] (Fig. 2). Consequently, the formation of umbelliferone requires $HO\bullet$ initiated transformation of coumarin, while dissolved O_2 highly enhances that via peroxy

radical formation. Transformation of coumarin and decomposition of umbelliferone take place parallel in the VUV irradiated solutions as Figure 1 shows that.

Figure 1. The concentration of coumarin and umbelliferone versus the time of irradiation in

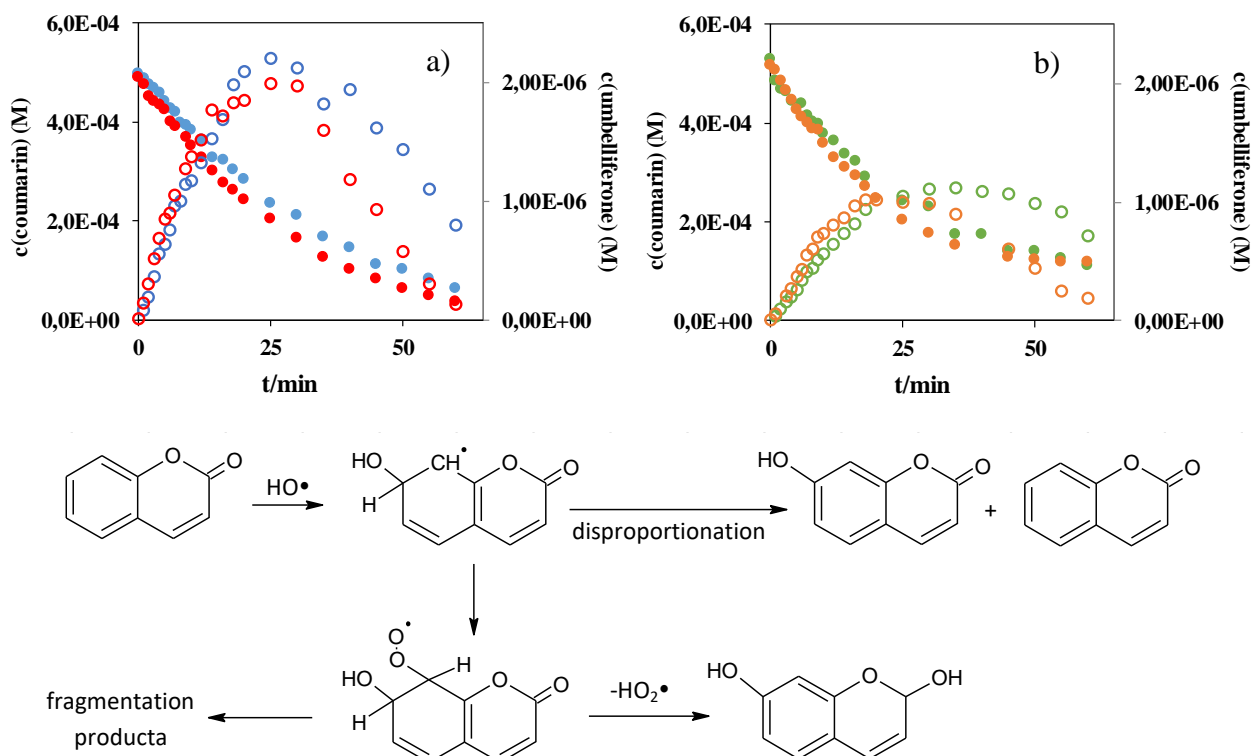


Figure 2. Formation of 7-HO-COU in the presence (a) and absence (b) of dissolved O_2

For further investigation of the dissolved O_2 effect, its concentration was changed between 0 and 100% in the gas flow bubbled through the solution. Thus the dissolved O_2 concentration was changed between 0 and 40 mg dm⁻³ in the aqueous solution. As Fig. 3 shows, the increase of O_2 concentration in gas phase from 0 to 12% caused a slight decrease of the coumarin transformation rate. The further increase of O_2 concentration slightly increased that. The effect of this factor is much more pronounced in the case of the formation of the hydroxylated product, umbelliferone. The formation rate of umbelliferone significantly increased when O_2 concentration was changed from 0 to 50%. The further increase of O_2 concentration has no effect.

Table I. Initial transformation rates determined at 5.0×10^{-4} M initial concentration of coumarin

	Initial transformation or formation rate	O_2 -saturated solution	O_2 -free solution
without PTFE rings	r_0 (coumarin) ($\times 10^{-7}$ M s ⁻¹)	1.97	2.13
	r_0 (umbelliferone) ($\times 10^{-9}$ M s ⁻¹)	2.27	0.93
with PTFE rings	r_0 (coumarin) ($\times 10^{-7}$ M s ⁻¹)	2.87	3.12
	r_0 (umbelliferone) ($\times 10^{-9}$ M s ⁻¹)	2.55	1.22

As that was mentioned previously, the VUV irradiated aqueous solution is a very inhomogeneous system: both $\text{HO}\cdot$ and $\text{H}\cdot$ concentration and dissolved O_2 concentration strongly decreases with the distance from the wall of the light source. Installation of flow breakers (PTFE rings) in the reactor is aimed the breaking of this inhomogeneity via turbulence in the flow. As Fig. 3 shows, in the presence of PTFE rings higher transformation rate of coumarin was reached, mainly in O_2 -free solution, when the increase was about 40%. Surprisingly the presence of O_2 decreased the positive effect of the flow breakers.

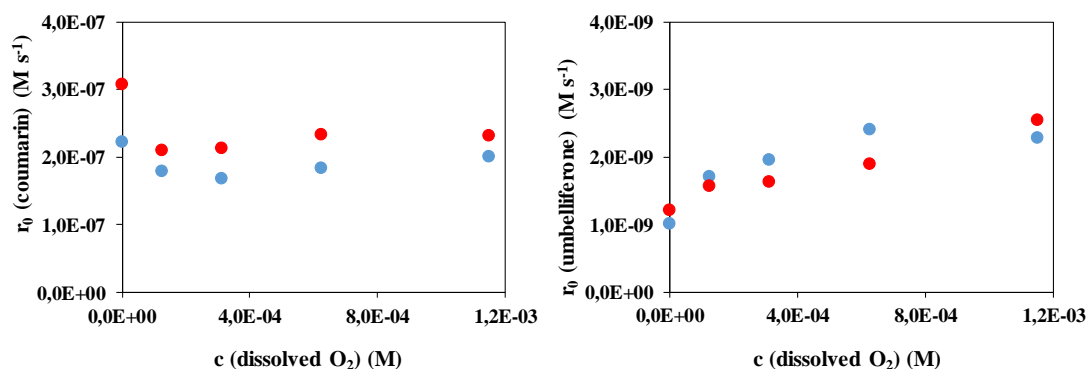


Figure 3. The effect of dissolved O_2 and PTFE rings on the transformation of coumarin (5.0×10^{-4} M) and formation of umbelliferone

●: without PTFE rings; ●: with PTFE rings

The effect of flow breakers and dissolved O_2 on the transformation rate of coumarin and formation rate of umbelliferone was investigated at various initial concentrations too. Since the transformation can be initiated by $\text{H}\cdot$ and $\text{HO}\cdot$, the transformation rate of coumarin can be described by the following equation: $r_{\text{cou}} = k_{\text{H}\cdot} \times [\text{H}\cdot] \times [\text{c}_{\text{cou}}] + k_{\text{HO}\cdot} \times [\text{HO}\cdot] \times [\text{c}_{\text{cou}}]$. The value of $[\text{H}\cdot]$ and $[\text{HO}\cdot]$ is determined by the photon flux and quantum yield of their formation from water via absorption of 172 nm VUV light. The quantum yield is 0.42 for $\text{H}\cdot$ and $\text{HO}\cdot$ formation too. Moreover, as that was described previously, $[\text{H}\cdot]$ is decreased by the dissolved O_2 , which has to be taken into account. Thus the increase of the transformation rate with increase of the initial concentration of coumarin is expected. Above a given initial concentration, the transformation rate must be determined by the formation rate of primary radicals ($\text{H}\cdot$ and $\text{HO}\cdot$) and has to be independent on the coumarin concentration. As that was expected, at first the coumarin transformation rate increased with its initial concentration. Above 5.0×10^{-4} M, that was found to be independent on the coumarin concentration and determined by the formation rate of $\text{H}\cdot$ and $\text{HO}\cdot$ radicals. The positive effect of the flow breakers could be observed only in O_2 -free solution and this effect was pronounced better with the increase of the coumarin concentration. Probably the PTFE rings are able to enhance the mass transfer into the zone determined by the reactions of various radicals, but not able to affect the primary radical and dissolved O_2 concentrations in the VUV irradiated, very thin photoreaction zone. The latter supposition was confirmed by the fact that, the formation rate of hydroxylated product cannot be affected by the flow breakers.

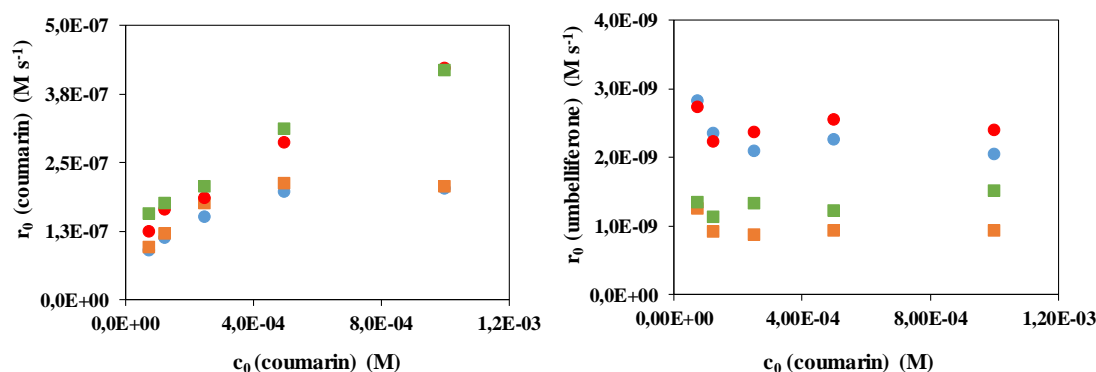


Figure 4. The effect of initial concentration and PTFE rings on the transformation rate of coumarin and the formation rate of umbelliferone

●: without PTFE rings, O_2 ; ●: with PTFE rings, O_2 ; ■: with PTFE rings, N_2 ; ■: without PTFE rings, N_2

Conclusion

- The presence of dissolved O_2 increases the formation rate of umbelliferone, but there is no significant effect on the transformation rate of coumarin
- Flow breakers are able to increase the transformation rate of coumarin in O_2 -free solution, but there is no effect on the formation rate of umbelliferone.

Acknowledgement

This publication was supported by the János Bolyai Research Scholarship of the Hungarian Academy of Sciences, UNKP-19-3-SZTE-207 and UNKP-19-4-SZTE-115, new national excellence programs of the Ministry for Innovation and Technology.

References

- [1] T. Alapi, K. Schrantz, E. Arany, Zs. Kozmér; Ed.: Mihaela I. Stefan, Advanced oxidation processes for water treatment : fundamentals and applications. IWA, 2018
- [2] G. Heit, A. Neuner, P.-Y. Saugy, A. M. Braun; J. Phys. Chem. A 1998, 102, 5551-5561
- [3] E. J. Hart, M. Anbar; Journal of Molecular Structure, 1970, 9, p. 486-486
- [4] S. Al-Gharabli, P. Engeßer, D. Gera, S. Klein, T. Oppenlander, Chemosphere, 2016, 144, 811-5
- [5] Y. Manevich, K. D. Heldt, John E. Biaglow. Radiation Research., 1997, 148, 580-591.
- [6] E. Arany, R. Szabó, L. Apáti, T. Alapi, I. Ilisz, P. Mazellier, A. Dombi, K. Schrantz, J Hazard Mater, 2013, 262, 151-7.
- [7] M. R. Gopakumar, K. Kini, U. R. Ashawa, S. C. Bhandari, N. S. Krishnan, G. U., Krishnan, D., Radiation Effects, 1977, 32, 199-203
- [8] G. Louita, S. Foley, J. Cabillic, H. Coffigny, F. Taran, A. Valleix, J. P. Renault, S. Pin, Radiation Physics and Chemistry, 2005, 72 (2-3), 119-124.

**ENZYMATIC *N*-ALKOXYCARBONYLATION OF 1-SUBSTITUTED
6,7-DIMETHOXY-1,2,3,4-TETRAHYDROISOQUINOLINES.
SUBSTRATE SPECIFICITY**

Dániel Gombkötő, Enikő Forró, Ferenc Fülöp

*Institute of Pharmaceutical Chemistry, University of Szeged, H-6720 Szeged, Eötvös u. 6., Hungary
e-mail: gombkoto.daniel@pharm.u-szeged.hu*

Abstract

In view of substrate specificity, CAL-B-catalysed asymmetric *N*-alkoxycarbonylations of 1-substituted 6,7-dimethoxy-1,2,3,4-tetrahydroisoquinolines (Et, Pr, *i*Pr, *t*-Bu, Ph) have been studied. High enantioselectivities (>200) were observed, when the reactions were performed from the substrates' HCl salts in triethylamine in the presence of allyl phenyl carbonate at 60°C using incubator shaker. The reaction time increased with increasing substituent size in position 1; however, the isopropyl- and *t*-buthyl-substituted compounds proved to be too bulky for the optimum activity of CAL-B.

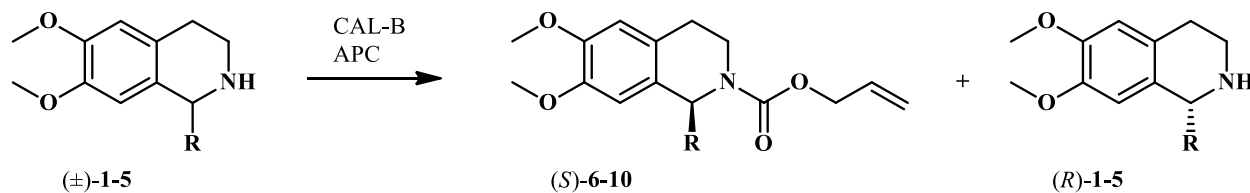
Introduction

Isoquinoline alkaloids constitute one of the largest groups of natural substances. They possess a skeleton with various biological properties including analgesic effect (morphine), antibacterial activities (berberine), and antispasmodial activities (papaverine)¹. Additionally, a novel effect of tetrahydroisoquinolines as phosphodiesterase type 4 (PDE4) inhibitor has recently been discovered, which led to the discovery of an effective antipsoriasis agent (skin disease)². The class of isoquinolines are associated with pivotal pharmacological effects, which attracts increasing attention in medicinal and pharmaceutical research. In this work, we aimed to investigate lipase catalyzed kinetic resolution of a homolog series of 1-substituted tetrahydroisoquinolines (±)-**1-5**.

Experimental

Larger part of lipases (CAL-A, CAL-B, AY, AK, PPL) were from Sigma-Aldrich, the PS-IM was from Amano Pharmaceuticals. The substrates were synthesised according to the literature³. The aldehydes and the solvents were from Sigma-Aldrich and VWR. The selected acyldonor [allyl phenyl carbonate (APC)] was also from Sigma-Aldrich. For the substrates synthesis Discover CEM microwave reactor was applied. The enantiomeric excess (*ee*) values for the unreacted isoquinolines and the *N*-alkoxycarbonylated enantiomers were determined by Jasco HPLC with Chiralpack IA column after derivatization with acetic anhydride. (*n*-hexane/isopropyl alcohol 93/7 ratio, 1 ml/min flow rate). Optical rotations were measured with Perkin-Elmer 341 Polarimeter. NMR spectrograms were made by Bruker Avance DRX 400.

Results and discussion



R: ethyl, propyl, isopropyl, *tert*-buthyl, phenyl

Figure 1. Scheme of the reactions

Racemic 1-substituted 6,7-dimethoxy-1,2,3,4-tetrahydroisoquinolines were synthesized with 45-65% yield, in microwave induced Pictet-Spengler reactions, as described in the literature³. Next, an adequate analytical method has been optimised to follow the enzymatic reactions. With the method all of the starting racemates such as the chemically prepared *N*-acylated products have been baseline separated. Preliminary experiments were designed in order to establish the optimum conditions for the enzymatic resolution of model compound (R: ethyl)-1, the effects of enzyme, solvent, quantity of acyl donor and temperature on *E* and the reaction rate being examined. Finally, preparative-scale enzymatic reactions were carried out. When the alkoxy-carboxylations of (±)-2-5 compounds with 4 eq allyl phenyl carbonate performed under the optimized conditions: CAL-B, in triethylamine, 60°C in batch reactor, conversion of 50% was reached in 1-3 days for (±)-1,2,5 which excellent *E* (>200). Unfortunately in case of resolution of (±)-3,4 no products formed even after 7 days. On the bases of preliminary reactions, preparative scale resolutions were performed with (±)-1,2,5 under the optimal conditions (CAL-B, APC, Et₃N, 60°C).

Conclusion

Kinetic resolution of 1-substituted-6,7-dimethoxy-1,2,3,4-tetrahydroisoquinolines have been prepared through CAL-B catalyzed *N*-alkoxycarbonylation. Excellent enantioselectivity (*E*>200) when solvent was triethylamine, in presence of 4 eq APC, and the temperature was 60°C. The unreacted (*R*)-1,2,5 and alkoxy-carboxylated (*S*)-6,7,10 products were isolated with *ee* 95-97, yield 32-42%. To follow the enzymatic reactions and determine conversion, enantioselectivities and enantiomeric excess an adequate analytical method was optimized with HPLC.

Acknowledgements

The authors thank to the Hungarian Scientific Research Council (OTKA K129049) and the Ministry of National Economy, National Research, Development and Innovation Office (GINOP-2.3.2-15-2016-00014) for financial support.

References

- (1) Nishihachijo, M.; Hirai, Y.; Kawano, S.; Nishiyama, A.; Minami, H.; Katayama, T.; Yasohara, Y.; Sato, F.; Kumagai, H. Asymmetric Synthesis of Tetrahydroisoquinolines by Enzymatic Pictet-Spengler Reaction. *Bioscience, Biotechnology, and Biochemistry* **2014**, 78 (4), 701–707. <https://doi.org/10.1080/09168451.2014.890039>.
- (2) Zhang, X.; Dong, G.; Li, H.; Chen, W.; Li, J.; Feng, C.; Gu, Z.; Zhu, F.; Zhang, R.; Li, M.; et al. Structure-Aided Identification and Optimization of Tetrahydro-Isoquinolines as Novel PDE4 Inhibitors Leading to Discovery of an Effective Antipsoriasis Agent. *Journal of*

Medicinal Chemistry **2019**, 62 (11), 5579–5593.
<https://doi.org/10.1021/acs.jmedchem.9b00518>.

(3) Eagon, S.; Anderson, M. O. Microwave-Assisted Synthesis of Tetrahydro- β -Carbolines and β -Carbolines: Microwave-Assisted Synthesis of β -Carbolines and Congeners. *European Journal of Organic Chemistry* **2014**, 2014 (8), 1653–1665.
<https://doi.org/10.1002/ejoc.201301580>.

MAPPING OF ELECTROSMOG EFFECTS IN URBANISED ENVIRONMENT

Anna Gutási, Marianna Radács, Ildikó Trója, István Varga, Péter Hausinger, Márta Gálfi, Zsolt Molnár

*Institute of Applied Natural Science, Faculty of Education, University of Szeged Hungary
Department of Environmental Biology and Education, Juhász Gyula Faculty of Education,
University of Szeged*

e-mail: gutasi.anna@gmail.com

Abstract

Physical, biological, and chemical conditions determine the evolution in Earth. As societies have evolved, the equilibrium previously realized has shifted, so today evolution is taking place under new conditions. The study of changes in the terrestrial environment has a significant impact on the electric and / or magnetic fields induced by societies, which are commonly known as electrosmog. In this present work, a model system for mapping electrosmog effects was developed, and a database for this was started to build.

Introduction

The conditions of evolution (physical, chemical, biological factors) determined the formation, operation and survival of terrestrial systems. With the presence of societies, natural conditions, that is, the terrestrial environment, have been transformed, altering its network of relationships [1, 2]. Accordingly, evolution is nowadays defined by new environmental conditions, and societal devices generating electromagnetic fields are also significantly involved in this relationship [3]. The biological matter pattern, so the life is evolved with the constant presence of natural background radiation. Natural (non-human) electromagnetic radiation is thus an integral part of our lives. Natural background radiation of Earth (under which Earth's life has evolved) has been modified by anthropogenic activities, and the resulting increase in electromagnetic energy is treated as electrosmog [4]. The electromagnetic fields and energy emitted by electrical equipment, due to the properties of living systems, have a behavioural effect on living organisms. In 1996, the World Health Organization (WHO) set up the International Electromagnetic Field Project to examine the potential health risks associated with electromagnetic field emission technologies [5]. The WHO team of experts has recently described the health implications of electromagnetic field (EMF) spaces in a summary article. Most power grids operate at 50 or 60 cycles per second, or hertz (Hz). The magnetic field value of some devices may be as high as a few thousand microteslas [6].

Aims

In this work we wanted to study the significance of electromagnetic fields (EMFs) in relation to ground conditions, which act as physical environmental loads. For dose-response studies, we also considered the processing of statistical research and on-site EMF measurement data documented by our team.

Methods

In this work, a structured nameplate of model household electrical appliances was constructed using Central Statistics Office (KSH) data. We have identified equipment that generates electromagnetic fields. Load levels are assigned in this data structure. In this way, the volume of indoor electric field transmitted by the on-mode presence of the respective household

appliances, appliances and fittings can be properly tracked. In these measurements, the electric field strength and magnetic induction emitted at different distances (0 m, 0.25 m, 0.5 m, 1 m, 2 m) were measured by the electrical equipment involved in the design of the model households, which is present in all households. In this way we can follow the decrease of the field strength with distance. For indoor measurements, the measurement points are designed so that they are located along busy areas of the population. The main reason for this is that our study was also targeted at society and the exposure effect it had on it. In addition, characteristic points that are outstanding in terms of exposure (eg. transformer station, high voltage column) were selected. In our field measurements, we used the ME 3951A handheld meter to measure low frequency (50 Hz-400kHz) field strengths in the range 0-1999 V / m.

Results and discussion

Model households were developed according to the load levels and are shown in Table 1.

1 st level	2 nd level	3 rd level	4 th level
washing machine	washing machine	washing machine	washing machine
television	television	television	television
refrigerator	refrigerator	refrigerator	refrigerator
landline phone	landline phone	landline phone	landline phone
traditional reading lamp	traditional reading lamp	traditional reading lamp	reading lamp with halogen bulb
	microwave oven	microwave oven	microwave oven
	kettle	kettle	kettle
	extension cord	extension cord	extension cord
		cell phone	cell phone
		computer (internet, router)	computer (internet, router)
			air conditioner

Table 1. Load levels of model households by working household appliances

The following table presents the timeframe EMF data for our model households from the Southern Great Plain region. The design criterion for model households was to adequately represent the evolution of EMF exposures in relation to household development. Below is a summary of the electric field strength emitted by each household appliance, followed by the summed exposure of model households.

	Field strength (V/m)	Frequency-weighted field strength (V/m)		
		2004	2011	2012
Numbers of households		175974	181889	192556
Numbers of cell phones	12.9	17.62	22.11	22.03
Computer (internet+ modem/router)	965.64	241.41	612.87	655.87
Washing mashine	2.92	3.17	3.02	3.03
Microwave oven	17.04	10.91	14.00	14.38
Television	158.1	224.66	261.80	268.17
Refrigerator	1.99	2.05	2.07	2.05

Air conditioner	64	3.20	2.51	2.35
Landline phone	9.9	5.67	4.58	3.10
Traditional reading lamp	136	435.2	380.8	272.0
Kettle	50	10.0	40.0	65.0
Extension cord	150	375.0	420.0	525.0
Reading lamp with halogen bulb	390	468.0	780.0	1326.0
1st level		670.75	652.27	548.35
2nd level		1060.6	1319.14	1152.73
3rd level		1325.69	1761.25	183.63
4th level		1361.69	2162.96	3093.98

Table 2 Measured electric field strength of household appliances ($E = V / m$), weighted by frequency, in Csongrad County

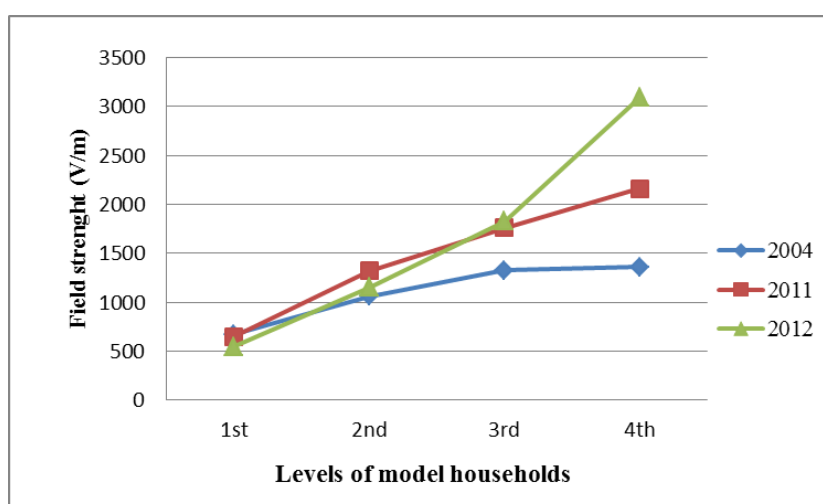


Figure 1. Tracking the increase in electromagnetic exposure through model households in Csongrad County

The figure above shows the value of the total field strength measured by the levels of the model household we have created, according to the years we examined in Csongrad County. The X-axis shows the load levels created, which are shown in ascending order. The Y-axis shows the electric field strength values that we have calculated or calculated from statistical data.

<i>Serial number</i>	<i>County</i>	<i>Denomination</i>	<i>Eastern longitude</i>	<i>North latitude</i>	<i>E (V/m)</i>
69	Csongrád	Road of number 4421 between Hódmezővásárhely and Békéssamson	20.3925	46.410278	>1999
109	Csongrád	Szeged, József Attila boulevard	20.156667	46.268889	1392,0

Table 3. Outstanding points of outdoor measurements in Csongrád County based on GPS coordinates

The measuring limit (1999 V / m) was reached by the test instrument at the high-voltage column shown in road of number 4421, which is adjacent to arable land. Another outstanding value was Szeged, József Attila boulevard point near the transformer station. Outstanding values are shown in the table.

Conclusion

In our conclusions, we find it very important that members of society are aware of the sources of exposure that they may encounter in their daily lives. The society should be aware of the positive and negative effects of the exposures involved, such as the nature of the environmental electromog, its source and its causal potential. In order to verify the real presence of EMF effects, we have developed indoor and outdoor measurement procedures and started building a real database.

Acknowledgement

EFOP-3.4.3-16-2016-00014, EFOP-3.6.1-16-2016-00008, TÁMOP-4.2.4.A/2-11/1-2012-0001

References

- [1] L. Zombory. Élet a sugárözönben, Magyar Tudomány, 2002, 8, pp: 989.
- [2] E. Mészáros. Az élet keletkezése az őslégkör összetétele és az éghajlat tükrében, Magyar Tudomány, 2008, 6; pp: 656
- [3] W. Daehn. Electromog & electromagnetic CAD; Proceedings of the International Conference and Exhibition on High-Performance. Computing and Networking, 1994, 1, 94-98.
- [4] M. Blank. Biological effects of electromagnetic fields. Bioelectrochemistry and Bioenergetics, 1993, 32, 203-210.
- [5] WHO – Extremely low electromagnetic fields; Environmental health criteria, 2007 pp: 238.
- [6] L. Hardell, C. Sage. Biological effects from electromagnetic field exposure and public exposure standards. Biomedicine & Pharmacotherapy, 2008, 62, 104-109.

PHYTOCHEMICAL INVESTIGATION OF *EUPHORBIA TRIGONA*

Reham Hammadi¹, Norbert Kúsz¹, László Papp², Judit Hohmann^{1,3}, Andrea Vasas¹

¹ Department of Pharmacognosy, University of Szeged, Eötvös u. 6, H-6720 Szeged, Hungary

² Botanical Garden, Eötvös Loránd University, Illés u. 25, H-1083 Budapest, Hungary

³ Interdisciplinary Centre of Natural Products, University of Szeged, Eötvös u. 6, H-6720 Szeged, Hungary

e-mail: reham.hammadi@pharmacognosy.hu

Introduction

Euphorbia is the largest genus in the family Euphorbiaceae, comprising more than 2 000 species worldwide. Detailed study of the profile of all secondary metabolites could contribute to taxonomic subdivision of this complex genus. The most important compounds of *Euphorbia* plants are diterpenes. Hitherto many secondary metabolites with specific types of diterpene skeletons in the genus have been found to possess a number of interesting biological activities, including antiproliferative, antiviral, ion-channel modulating, and multidrug resistance (MDR) reversing activities [1].

The present work deals with the phytochemical investigation of *Euphorbia trigona* Miller. *E. trigona* is a thorny succulent plant, which grows up to 6 m in height. It is indigenous to southwest tropical Africa where its latex is applied in severe cases of constipation or in case of an epileptic attack. The irritancy of the latex was proven in human experiment, and ingenol esters were reported [2].

Results and discussion

The fresh aerial parts of *E. trigona* has been chopped and percolated with methanol at room temperature. The crude methanol extract was concentrated, and then dissolved in 50% methanol. Thereafter, solvent-solvent partition was performed by using *n*-hexane, chloroform, ethyl acetate and butanol. Diterpenes were accumulated in the chloroformic phase. After multiple separation process, including TLC, vacuum liquid chromatography, preparative TLC, and HPLC, nine compounds were isolated from the chloroformic fraction. The structures of the components were determined by 1D and 2D NMR (¹H-¹H COSY, HSQC, and HMBC) and MS measurements, and comparing them with literature data. The isolated compounds proved to be diterpenes; five of them are ingol-, and four components are ingenol esters. They are tri- or tetra esters, substituted with acetyl, benzoyl, angeloyl and tigloyl groups. The compounds were isolated previously from other *Euphorbia* species, e.g. *E. nivulia* and *E. kamerunica* [3, 4].

Conclusion

With a combination of different chromatographic techniques, nine polyacylated diterpenes were isolated from the chloroformic phase of *E. trigona* methanol extract.

Acknowledgements

Support from the GINOP-2.3.2-15-2016-00012 is gratefully acknowledged.

References

- [1] A. Vasas, J. Hohmann, Chem. Rev. 114 (2014) 8579.
- [2] S.M. Worobec, T.A. Hickey, A.D. Kinghorn, D.D. Soejarto, D. West, Contact Dermatitis 7 (1981) 19.

- [3] V. Ravikanth, V.L. Niranjana Reddy, T. Prabhakar Rao, P.V. Diwan, S. Ramakrishna, Y. Venkateswarlu, *Phytochemistry* 59 (2002) 331.
- [4] K. Abo, F.J. Evans, *Planta Med.* 43 (1981) 392.

HETEROGENEOUS PHOTOCATALYSIS OF IMIDACLOPRID – EFFECT OF REACTION PARAMETERS, MINERALIZATION AND MATRICES

Tamás Hlogvik, Máté Náfrádi, Tünde Alapi

*Department of Inorganic and Analytical Chemistry, University of Szeged, H-6720 Szeged,
Dóm tér 7, Hungary
e-mail: tamas.hlogvik@gmail.com*

Abstract

The photocatalytic removal of imidacloprid, a neonicotinoid insecticide with serious environmental effects, has been investigated. Photocatalytic treatment using TiO_2 photocatalyst was effective at the complete transformation of imidacloprid over 30 minutes. The mineralization was also investigated, and the reduction of total organic carbon and chemical oxygen demand was inhibited after the transformation of imidacloprid, indicating the accumulation of degradation products resistant to $\text{HO}\cdot$. The dechlorination of the organic content was complete, but only 25 % of total nitrogen content was transformed into NO_3^- , indicating that the accumulated products are nitrogen containing organic compounds. The effect of two light matrices, drinking water and purified industrial wastewater was also investigated. The low organic content of the wastewater only slightly reduced the transformation rate of imidacloprid, but the high ionic content of drinking water significantly reduced the effectiveness by increasing the aggregation of TiO_2 .

Introduction

Pesticides are one of the most widespread pollutants of agricultural wastewaters, and they have been detected in trace amounts in natural and drinking water too. Neonicotinoid pesticides have been investigated in the last decade due to their harmful effect on pollinators and aquatic life, especially imidacloprid, which has the highest toxicity to honeybees (LD_{50} 5-70 ng). [1] It has been banned in open-field use by the European Union in 2018, and several researches have been conducted for their removal from water and wastewater. Advanced Oxidation Processes (AOPs) have been investigated for the removal of imidacloprid, and heterogeneous photocatalysis is a promising method for its degradation. [2,3]

The most widespread photocatalyst is TiO_2 . When it absorbs photons with an energy higher than its band gap, a separation of charges occur, forming a conduction band electron (e_{cb}^-), and a valence band hole (h_{vb}^+). [4] These charge carriers may react with O_2 and $\text{H}_2\text{O}/\text{HO}^-$ and through a series of reactions, hydroxyl radical ($\text{HO}\cdot$) form. The photogenerated charges may also react with adsorbed organic compounds in direct charge transfer reactions. [5] Heterogeneous photocatalysis is well known for the high mineralization rates, as the degradation of the target compounds and its intermediates happens at the same time due to the reactions with non-selective $\text{HO}\cdot$.

The aim of this study was to investigate the transformation and mineralization of imidacloprid using commercial TiO_2 photocatalyst. The transformation and mineralization were characterized by the change of the concentration of chemical oxygen demand (COD), total organic carbon (TOC) content, concentration of adsorbable organic halogen content (AOX), NO_3^- concentration and the concentration of H_2O_2 . For the practical reasons, the effect of two light matrices (drinking water from Szeged, and a purified industrial wastewater) were investigated on the effectiveness of the degradation process at two pesticide concentrations.

Experimental

All experiments were performed in a thermostated (at 25 °C) glass reactor. 1.0 g dm⁻³ TiO₂ Aeroxide P25[®] (Acros Organics) suspensions were recirculated, bubbled with air, and stirred during the experiment. 250 cm³ imidacloprid (0.1 and 0.025 mM) was dissolved in either Milli-Q (MQ) water, drinking water or purified wastewater. The samples were centrifuged and filtered with 0.22 µm PVDF-L syringe filters before analysis. The concentration of imidacloprid was measured using HPLC-DAD, using an Agilent 1100 with a Licrosphere 100 RP-18 column. The eluent contained 40 % methanol and 60 % water, its flow rate was 1.0 ml min⁻¹. The detection wavelength was 270 nm. The TOC content was measured using an Analytik Jena N/C 3100. The COD measurements were performed using LCK1414 (Hach) colorimetric cuvette test with a 5.0-60.0 mg dm⁻³ measuring range. The digestion was performed in a HT200S thermostate, the COD values were measured using a DR2800 spectrophotometer. The concentration of H₂O₂ was measured with a cuvette test by Merck, with a 0.015-6.00 mg dm⁻³ measuring range. The NO₃⁻ concentration was also measured with a cuvette test provided by Merck, with a 0.4-111 mg dm⁻³ measuring range. The H₂O₂ and NO₃⁻ tests were measured using a Spectroquant Multy (Merck) spectrophotometer. The AOX measurements were performed using an Analytik Jena Multi X 2500 instrument. Before the measurements 15 cm³ sample was adsorbed on 100 mg high purity activated carbon adsorbent. Drinking water from Szeged (Hungary), and industrial wastewater (purified with reverse osmosis) were used to investigate the matrix effect. The main analytical parameters for both matrices are presented in Table 1.

Table 1. Parameters of the matrices

Parameters	Drinking water	Purified wastewater
pH	7.3	5.5
Conductivity (µS cm⁻¹)	482	21.9
COD (mg dm⁻³)	0.69	< 15
NH₄-N (mg dm⁻³)	< 0.4	< 0.4
NO₃⁻ (mg dm⁻³)	< 0.7	1.5
Cl⁻ (mg dm⁻³)	8.75	-
TOC (mg dm⁻³)	8	-

Results and discussion

First, the transformation and mineralisation of 0.1 mM imidacloprid dissolved in MQ water was investigated. Imidacloprid was completely transformed after 30 minutes, but still a high amount of organic matter remained in the suspension. The TOC and COD values were significantly reduced in the first 30 minutes (to 46 and 70 % respectively), but after the complete transformation of imidacloprid, their reduction rate significantly reduced. After 120 minutes of treatment 25 % TOC and 40 % COD content was still measured. This suggest, that after the transformation of imidacloprid and its main aromatic intermediates, certain products form, that do not react with HO•, or their reaction are very slow, thus they cannot be removed effectively using heterogeneous photocatalysis. The H₂O₂ concentration is increasing at a high rate during the first 20 minutes of the experiment, but it decreases after the transformation of imidacloprid. This also confirms that, the transformation of some interemediates are very

slow or negligible, as H_2O_2 forms primarily during the degradation of organic compounds, due to the HO_2^\bullet elimination from organic peroxy radicals.

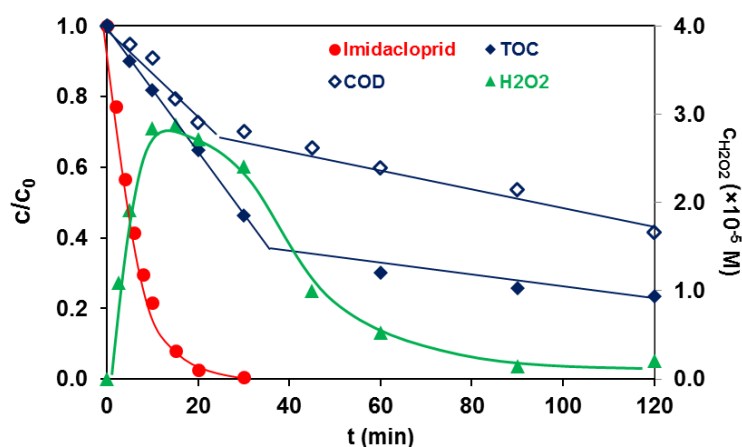


Figure 1. The relative concentration of imidacloprid, TOC, and COD content, and the concentration of H_2O_2 as a function of time

The AOX content was also measured, to investigate the dehalogenation of imidacloprid and its intermediates. The AOX content reduced at a similar rate as imidacloprid, thus no chlorinated intermediates can be observed after 40 minutes of photocatalytic treatment. The NO_3^- content was also measured to investigate the mineralization of the nitrogen-containing organic compounds. After 120 minutes treatment only 25 % of the total nitrogen content was transformed into NO_3^- , indicating that nitrogen containing organic products are highly resistant to photocatalytic treatment.

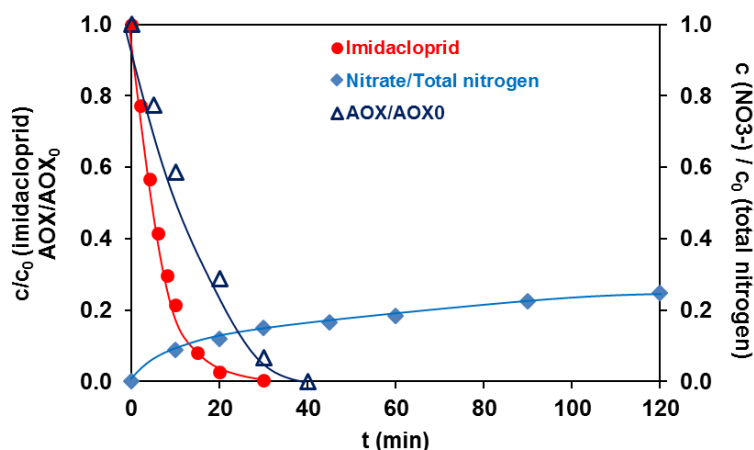


Figure 2. The relative concentration of imidacloprid, the reduction of AOX content and the conversion of total organic nitrogen to NO_3^- as a function of time

For investigation the practical applicability of the method for the removal of imidacloprid, two milde matrices (purified wastewater and tap water) were employed, with two different initial concentrations (0.10 mM and 0.025 mM).

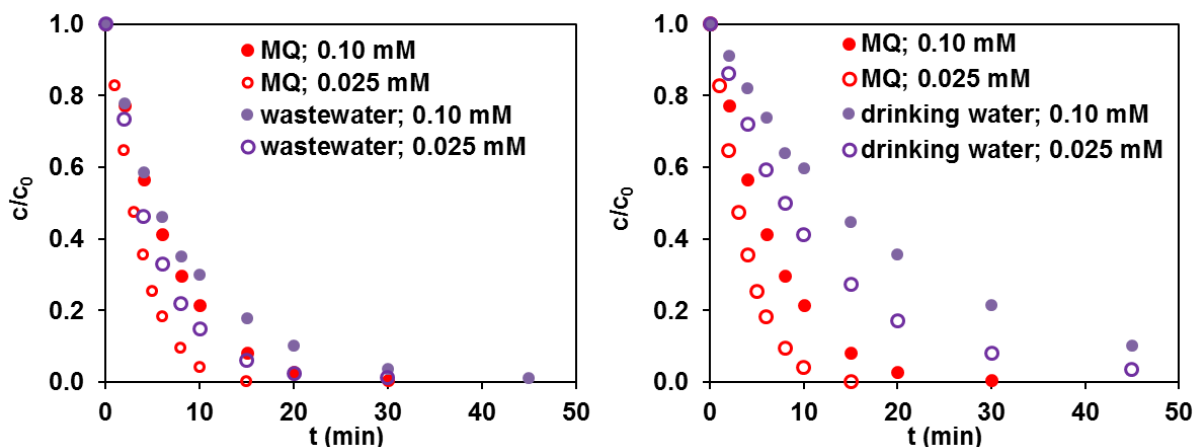


Figure 3. The relative concentration of imidacloprid versus time of irradiation in different matrices

In the case of the purified wastewater, only a slight reduction of reaction rate was observed, most likely due to the organic content of the matrix, as it could compete with imidacloprid for $\text{HO}\cdot$. In the case of drinking water a much more significant negative effect was found, which is most probably caused by the high ionic content. In drinking water the initial reaction rates were reduced by 56 and 60 % for 0.1 and 0.025 mM imidacloprid respectively. The high ionic strength can initiate the aggregation of TiO_2 particles, reducing the effective surface available for light, thus reducing the formation rate of $\text{HO}\cdot$ and transformation rate of organic substrate.

Table 2. Initial reaction rates and relative reaction rates of imidacloprid transformation in matrices, compared to measurement taken in MQ water

	$c_0 (\times 10^{-4} \text{ M})$	$r_0 (\times 10^8 \text{ M s}^{-1})$	r_0/r_0^{ref}
Milli-Q (ref.)	1.00	16.7	-
	0.25	7.3	-
Purified wastewater	1.00	17.3	1.04
	0.25	5.6	0.76
Drinking water	1.00	7.3	0.44
	0.25	2.9	0.40

Conclusion

- The heterogeneous photocatalysis of imidacloprid, a neonicotinoid pesticide that causes serious environmental problems, has been investigated
- 0.1 mM imidacloprid completely transforms during 30 minutes photocatalytic treatment
- Dechlorination is effective, but only 54 % of imidacloprid can be mineralized
- Nitrogen-containing products having low reactivity towards $\text{HO}\cdot$ forms.
- Purified wastewater having low organic content had no significant effect on the transformation rate of imidacloprid, but tap water having high ionic content strongly inhibited the transformation due to the aggregation of TiO_2 particles

Acknowledgements

This publication was supported by the János Bolyai Research Scholarship of the Hungarian Academy of Sciences, ÚNKP-19-3-SZTE-207 and UNKP-19-4-SZTE-115, new national excellence programs of the Ministry for Innovation and Technology.

References

- [1] S. Suchail, D. Guez, L. P. Belzunces (2001) *Environmental Toxicology and Chemistry*, 20(11), 2482–2486
- [2] V. Kitsiou, N. Filippidis, D. Mantzavinos, I. Poulios *Applied Catalysis B: Environmental*, 86 (2009) 27–35
- [3] U. Cernigoj, U. L. Stangar, P. Trebse *Applied Catalysis B: Environmental*, 75 (2007) 229–238
- [4] A. Dombi, I. Ilisz, *Nagyhatékonyságú oxidációs eljárások a környezeti kémiában, A kémia újabb eredményei*, Akadémiai Kiadó, Budapest (2000)
- [5] H. Christensen, K. Sehested, T. Logager, *Radiation Physics and Chemistry*, 43(1994) 527-531

USE OF LASER-INDUCED BREAKDOWN SPECTROSCOPY (LIBS) AS A TOOL FOR THE QUANTITATIVE DETERMINATION OF LITHIUM IN GRANITE ROCK-FORMING MINERALS

Krisztián Jancsek¹, Patrick Janovszky², Judit Kopniczky³,
Gábor Galbács², Tivadar M.-Tóth^{*1}

¹Department of Mineralogy, Geochemistry and Petrology, University of Szeged, 6722 Szeged, Egyetem street 2., Hungary

²Department of Inorganic and Analytical Chemistry, University of Szeged, 6720 Szeged, Dóm square 7., Hungary

³Department of Optics and Quantum Electronics, University of Szeged, 6720 Szeged, Dóm square 9., Hungary
e-mail: mtoth@geo.u-szeged.hu

Introduction

There is a high global demand for lithium resources. From a geochemical perspective, the lithium-bearing minerals such as spodumene, lepidolite or petalite crystallize in the late-magmatic/pegmatitic period, producing granitic pegmatites. One such granitoid massif, about 1 km below the present surface in SE Hungary is located in the Battonya Unit. Here, the granitoids typically contain quartz, feldspar and micas, like biotite and muscovite. All these phases can incorporate a significant amount of lithium, thus may become a potential target of lithium mining.

Drill samples, taken from different locations in the Battonya region, containing different minerals (e.g. feldspar, muscovite, quartz, biotite, chlorite) were used as samples during the study. The ablation behavior of the NIST glass standards were examined and these standards were tested for calibration due to their similarity in matrix composition (silicate).

Experimental

In this work, the LIBS spectra were taken by using the J200 LA-LIBS tandem spectrometer (Applied Spectra Inc., USA). The minerals were presented to the instrument in the form of micro-polished sections. For the examination of the ablation behavior of the NIST standards and the samples profilometry measurements were performed on a Veeco, Dektak 8 Advanced Development Profiler.

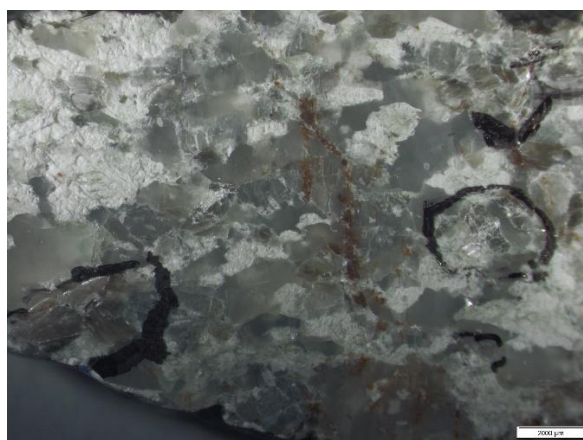


Figure 1.: Optical microscope view of one of the samples

Results and discussion

The comparison of the ablation behavior of NIST glass standards and the samples shows that the ablation craters for the NIST standards look quite similar. At the same time, the crater profiles for the sample minerals are different from each other, but generally also from the NIST standards. Biotite and quartz, both crater shapes and volumes are reasonably similar to those of the standards. For muscovite and feldspar, the matrix effect is remarkable, which may significantly influence quantitative analytical results. Normalization to the crater volume is suggested.

During the determination of Li concentration in the grains we measured all four minerals in and eight drill samples. During the measurements, at least four grains of each minerals were analyzed. Spectra were recorded from two different location in every identified mineral grains. We found that biotite, chlorite, muscovite and feldspar contain a high amount of Li (in some cases reaching 1 mg/g), whereas quartz is generally quite free from Li. An advantage of using LIBS in such prospection studies is that it can also provide a quick estimate for the average useful concentration of Li in rock samples without the need to remove the mineral grains from the rock.

Acknowledgements

Financial support of the project was provided by the National Development, Research and Innovation Office of Hungary under No. K_129063.

INVESTIGATION OF ANTIOXIDANT CAPACITY AND MINERAL CONTENT OF DIFFERENT TEA SAMPLES

Márta Üveges¹, Viktória Kósa¹, Éva Stefanovits-Bányai¹, Anna Mária Nagy²,
Zsuzsa Jókai¹

¹Szent István University, Faculty of Food Science, Department of Applied Chemistry,
H-1118 Budapest, Villányi út 29-43, Hungary

²Holi-Medic Kft. Budapest, Hungary
e-mail: jokaine.szatura.zsuzsanna@etk.szie.hu

Abstract

The consumption of various teas and herbal teas is undergoing a renaissance. They are used for the prevention and cure of various diseases and for pleasure. The herbal parts of teas all have valuable nutritional values, which have excellent antioxidant effect, free radical scavenging properties. The beneficial health effect is due to the polyphenols and the rich mineral element content. During the experiment the polyphenol content and antioxidant capacity of the infusions made from green tea, cranberry, rooibos, honey bush, lemongrass, milfoil and nettle tea, were investigated. The mineral content of the plant parts and teas was also measured. A close correlation was found between polyphenol content and antioxidant capacity indicating the protective role of polyphenols. The antioxidant capacity and polyphenol content of lemongrass and green tea is outstanding compared to the other teas studied, honey bush and nettle showed the smallest content. For magnesium and calcium supplements the cranberry tea is best proposed, For manganese complement it is worth drinking green tea. Lemon grass, cranberry and green tea are the most important phosphorus source. In case of iron deficiency, cranberry tea is recommended, while lemongrass and honey bush tea are the most suitable for zinc supplementation. The results may also have been influenced by the preparation habits, such as the temperature of water or soaking time.

Introduction

Tea has been known since ancient times, it spread in China, thanks to Emperor Sen-nung b.C in 2727. The first teas were the extract of dried leaves of *Camellia sinensis* (L.) Today the naming of tea covers up, traditional teas, green, black, rooibos, while mate teas include different herbal teas, as chamomile, lemongrass, milfoil, nettle etc.

The valuable ingredients of tea - for example flavonoids - are suitable for the prevention and cure of diseases [1, 2, 3]. Free radicals are in the background of many diseases [3, 4, 5, 6, 7] which are formed under biotic and abiotic stress effects [8,9]. In the protection against free radicals play an important role a multitude of low molecular weight molecules, such as vitamins, carotenoids, flavonoids. [10,11,12]. Above all, the rich mineral element content of teas should also be mentioned, hereby teas have a positive effect indirectly [13,14,15,16].

Materials and Methods

Samples

Extracts were made from commercially available samples, they were as follows: green tea (*Camellia sinensis* L.), cranberry (*Vaccinium oxycoccos* L.), rooibos, (*Aspalathus linearis* L.), honeybush (*Cyclopia intermedia* L.), lemongrass (*Melissa Officinalis* L.), milfoil (*Achillea millefolium* L.) and nettle (*Urtica dioica* L.).

The sample preparation was performed according to instructions in *Table 1.*, and the results were converted to 1 g.

Table 1. Preparation of tea samples

Samples	Preparation	Cooking time (min)
green tea (filters)	1 filter + 200 ml 100°C water	3
cranberry (filters)	1 filter + 200 ml 100°C water	5
rooibos (bag)	teaspoon + 300 ml 100°C water	10
honeybush (bag)	teaspoon + 300 ml 100°C water	10
lemongrass (bag)	1 g + 100 ml 100°C water	10
milfoil (bag)	1 g + 100 ml 100°C water	10
nettle (bag)	1 g + 100 ml 100°C water	10

Cooled extracts were centrifuged at 13000 rpm for 10 min at room temperature. The analytical measurements were carried out from pure supernatant.

Determination of antioxidant capacities by FRAP (Ferric Reducing Antioxidant Power) method

Measurement of ferric reducing antioxidant power of the fruit extracts was carried out based on the procedure of Benzie and Strain [17], at 593 nm. (Spectronic Helios Gamma UV Visible Spectrophotometer Thermo Fisher Scientific.) Ascorbic acid (AA) was used as a standard to prepare the calibration solutions. Results were expressed as $\mu\text{MAA/g}$ of dry plant material.

Determination of total phenolic contents by Folin-Ciocalteu method

The Folin - Ciocalteu method is an electron transfer based assay and gives reducing capacity which is expressed as phenolic content. Total phenolic content of the fruit extracts was determined with the Folin-Ciocalteu reagent according to a procedure described by Singleton and Rossi [18], at 760 nm.

Gallic acid (GA) was used as a reference standard to prepare the calibration solutions. The results were expressed as mMGA/g of dry plant material.

Mineral content analysis using ICP-OES

The presence of the following minerals: Ca, Mg, K, Na, Fe, Cu, Zn, Mn and P was investigated by inductively coupled plasma optical emission spectrometry (ICP-OES).

All the previously freeze-dried samples were prepared for the analysis via microwave digestion method by using concentrated nitric acid and hydrogen peroxide.

After mineralization, the resulting solutions were cooled to room temperature, then they were transferred to autosampler tubes and diluted to a final volume of 25 mL with Milli-Q water. The determination of mineral contents in this clear solution was carried out by ICP-OES (Perkin Elmer Optima 8000). The concentrations of the calibration solutions were in the range from 1 to 100 mg/kg (1, 5, 10, 100 mg/kg, respectively) to match the amount of the elements possibly present in the samples.

Results and discussion

In the experiment the polyphenol content and antioxidant capacity of the infusions made from green tea, cranberry, rooibos, honey bush, lemongrass, milfoil and nettle tea, were investigated. As a results show, the polyphenol content of the samples are directly proportional to the antioxidant capacity, which proves that the polyphenols play an important role in the antioxidant protection system of the organism. The antioxidant capacity and the polyphenol content of lemongrass and green tea are extremely high, these parameters of

honeybush and nettle are relatively low. The rooibos-, cranberry- and milfoil teas have an average antioxidant capacity. (Fig 1,2).

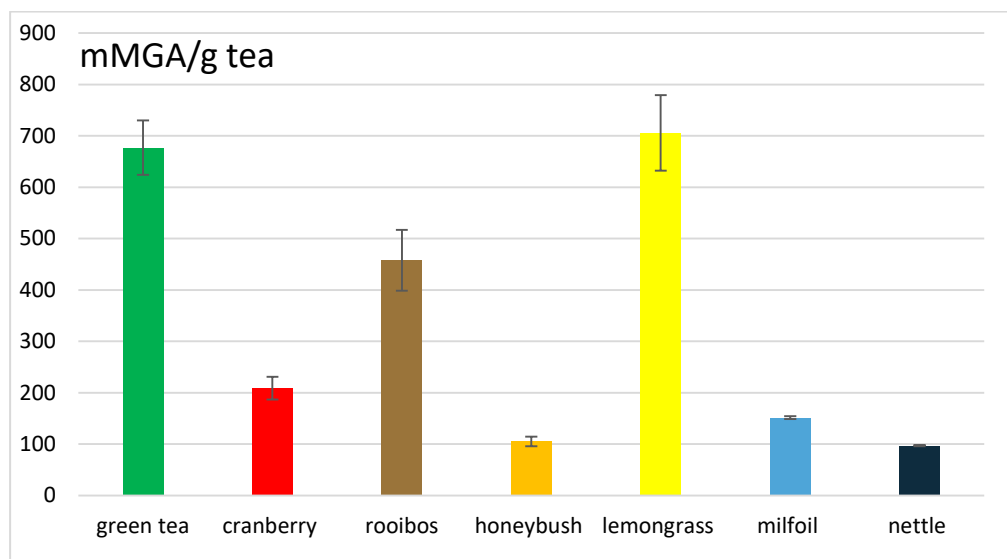


Figure 1. Polyphenolic content in the different teas (mMGA/g dry tea)

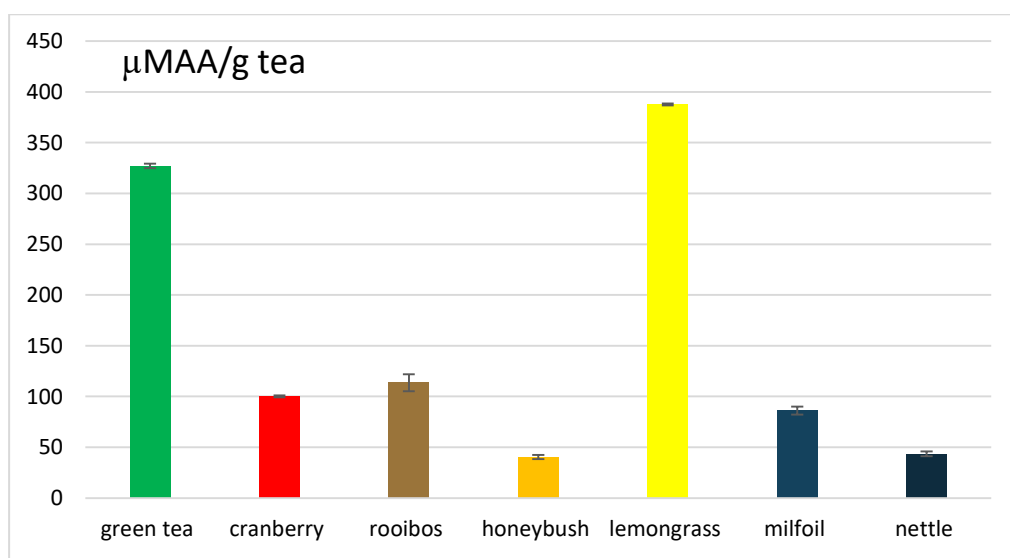


Figure 2. Antioxidant capacity in the different teas (μMAA/g dry tea)

The rooibos and honeybush have a relatively high sodium and low potassium content as a result of soil content of South Africa. Consumption of these kind of influences is undedicated for person with kidney disease, because of their not optimal sodium-potassium rate. As a result of our experiments can be stated, that for manganese complement it is worth drinking green tea. Lemon grass, cranberry and green tea are the most important phosphorus sources. In case of iron deficiency, cranberry tea is recommended, while lemongrass and honey bush teas are the most suitable for zinc supplementation.

Table 2. Element content of different dry teas (mg/kg)

	Ba	Ca	Fe	K	Mg	Mn	Mo	Na	P	Sr	Zn
Lemongrass	36	13300	190	27000	5050	29	2	800	2400	46	25
Cranberry	69	7400	290	13000	1900	180	<0.5	75	1150	44	20
Green tea	58	6300	170	15000	1900	1300	<0.5	18	1900	24	30
Rooibos	8	2600	150	5200	1800	72	<0.5	6000	450	20	65
Honeybush	17	2500	110	3800	930	40	<0.5	2400	260	37	50

Table 3. Element content of different infusion of teas (mg/L)

	Ba	Ca	Fe	K	Mg	Mn	Mo	Na	P	Sr	Zn
Lemongrass	0.01	<0.1	0.02	160	1.2	0.02	<0.1	8.2	5.1	<0.01	0.3
Cranberry	0.2	22	0.2	100	3.4	0.8	<0.1	<0.1	4.6	0.05	0.2
Green tea	0.01	<0.1	0.03	102	1.6	2.2	<0.1	<0.1	4.2	<0.01	0.1
Rooibos	<0.01	<0.1	0.04	17	<0.02	0.06	<0.1	27	0.3	<0.01	0.2
Honeybush	0.01	<0.1	0.05	16	<0.02	0.03	<0.1	15	0.2	<0.01	0.3

Conclusion

The teas have a positive physiological effect thanks to their extremely high antioxidant capacity. However the results may also have been influenced by the preparation habits, such as the temperature of water or soaking time.

Acknowledgement

The Project is supported by the European Union and co-financed by the European Social Fund (grant agreement no. EFOP-3.6.3-VEKOP-16-2017-00005).

The Project is also supported by the Doctoral School of Food Science SZIU.

References

- [1] J.D. Lambert, R.J. Elias, Arch. Biochem. Biophys. 501(1) (2010) 65–72.
- [2] N. Khan, H. Mukhtar, Cancer Lett. 269(2) (2008) 269–280.
- [3] V. Lobo, A. Patil, A. Phatak, N. Chandra, Pharmacogn. Rev. 8 (4) (2010) 118-127.
- [4] S. R. J. Maxwell, Drugs 49(3) (1995) 345-361.
- [5] K. Briegera, S. Schiavonea, F.J. Miller Jr.b, K.H. Krausea, Swiss Med Wkly. 142 (2012) 1-14.
- [6] O.I. Aruoma, JAOCS, 75 (2) (1998) 199-212.
- [7] A.A.Alfadda, R.M.Sallam, J. Biomed. Biotechn. (2012) 14 p.
- [8] S.S. Gill, N. Tuteja, Plant Phys. Biochem. 48 (2010) 909-930.
- [9] S. Bhattacharjee, Current Sci. 89(7) (2005) 1113-1121.
- [10] G.E. Pantelidis, M. Vasilakakis, G.A. Manganaris, Gr. Diamantidis, Food Chem. 102 (2007) 777-783.
- [11] P.T. Gardner, T.A.C. White, D.B. McPhail, G.G. Duthie, Food Chem. 68(2000) 471-474.

- [12] G. Agati, E. Azzarello, S. Pollastri, M. Tattini, *Plant. Sci.* 196 (2012) 67-76.
- [13] K. Pytlakowska, A. Kita, P. Janoska, M. Połowniak, V. Kozik, *Food Chem.* 135 (2012) 494-501.
- [14] K. Szentmihályi, M. Hajdú, J. Fodor, A. Blázovics, A. Somogyi, M. Then, *Biol. Trace Elem.* 114 (2006) 143-150.
- [15] J.L. Marnewick, F.H. van der Westhuizen, E. Joubert, S. Swanevelder, P. Swart, W.C.A. Gelderblom, *Food Chem. Tox.* 47 (2008) 220–229.
- [16] A.M. de Nysschen, B.E. van Wyk, F.R. van Heerden, A.L. Schutte, *Biochem. System. Ecol.* 24 (3) (2006) 243-246.
- [17] I.F.F. Benzie, J.J. Strain, *Anal. Biochem.* 239 (1) (1996) 70-76.
- [18] V.L. Singleton, J. A. Rossi, *Am. J. Enol. Viticult.* 16 (3) (1965) 144-158.

INVESTIGATION OF SIZE DISTRIBUTION AND SPECTRAL RESPONSES OF DIESEL ENGINE EMITTED CARBONACEOUS PARTICULATE USING MULTI WAVELENGTH PHOTOACOUSTIC SPECTROSCOPY (4 λ -PAS) AND SINGLE MOBILITY PARTICLE SIZER (SMPS)

Gergely Kiss-Albert¹, Tibor Ajtai¹, Noémi Utry¹, Máté Pintér¹, Gábor Szabó^{1,2}, Zoltán Bozóki^{1,2}

¹*Department of Optics and Quantum Electronics, University of Szeged, H-6720 Szeged, Dóm tér 9, Hungary*

²*Interdisciplinary Excellence Centre, Department of Optics and Quantum Electronics, University of Szeged, Hungary
e-mail: gergely.kissalbert@hilase.hu*

Abstract

This work discusses some results of the extended measurement campaign focussing the in-situ microphysical characterisation of the emitted diesel particulates of different fuel types at different operational conditions of diesel engine. For measurement of the spectral responses and the size distribution of the diesel emission customised multi wavelength photoacoustic spectrometer and single commercially single mobility particle sizer were used. Based on the size distribution data we experimentally demonstrate that at idle the emitted aerosol assembly has bimodal distribution in all type of fuel and working point of engine. We also demonstrate that the spectral responses of the diesel aerosol are characteristic for the type of fuel and the operational condition of engine. Using posterior temperature treatment we manifest that especially at idle the volatile fraction of the emitted aerosol can be dominantly removed above 150°C temperature. Finally, we also experimentally demonstrated that the biodiesel content of the diesel fuel even in its relatively small blending even in a relatively small (<7%) mixing ratio can significantly modify the climate and health relevant microphysical features of the diesel emission.

Introduction

Due to their adverse health and climate impact the diesel particulate matter (DPM) have been of great scientific concern today. The diesel emitted particulates are one of the dominant sources of light absorbing carbonaceous particulate matter (LAC), which is the second most important climate relevant atmospheric constituent [1]. Through its small size with high number-concentration, high surface area per unit volume and adsorption ability to toxic substances DPM is one of the most harmful air pollutants too. Despite its importance, both the climatic and the health effect of DPM is quite uncertain. Therefore, the diesel engine emission is under prestigious scrutiny in versatile perspectives recently starting from further understanding the fundamentals and causality in scientific sides, through the better characterisation of DPM in methodological and instrumental side, ended by reduction of tailpipe emission in engineering side.

The diesel soot is a complete mixture of organic and inorganic carbonaceous composites which show high versatility in size, and in chemico-physical properties. Moreover, since the particulate dispersed in air continuously interacts with its local ambient some ambient factors such as vapour-particle inter-conversion and photochemical activities can strongly modify the actual features of the investigated particulates. Due to the dynamically changing vapour-particles ratio in the highly reactive and turbulent active zone of engine exhaust, the representative and reproducible sampling and the precise as well as accurate measurements of

the emitted carbonaceous particulate assembly is one of the major challenges in this field presently

The new emission standards can be complied solely by modern diesel engines equipped with complicated after treatment system. However, further restriction in emission in this way it is limited by its durability and maintenance. One of the alternatives for further restriction of emission is the development of fuel.

In this study, some results of the extended measurement campaign focussing on the size distribution and spectral responses of diesel emission of different fuel and biofuel using customizes multi-wavelength photoacoustic spectrometer (4 λ -PAS) and single mobility particle sizer are presented. We experimentally demonstrated that the size distribution of diesel engine is dynamically changed with engine operational parameters. We also demonstrated that the absorption responses quantified by the AAE (Aerosol Angström Exponent) can also shows differences at different engine operational condition.

Experimental

During the measurements direct engine out emission of the test engine (four cylinder EURO 4 PC diesel engine, 2 litres turbo charged, common rail injection system) was measured directly after the turbocharger. The exhaust gas was sampled before the after treatment equipment (catalyst, DPF) meaning that we investigated the raw engine emission which describes the combustion process not considering the effectiveness of the exhaust gas after treatment system.

The engine was powered by commercial diesel fuels according to EN 590 standard in biofree version (B0) and with FAME (B7). The engine was operated at three carefully chosen conditions. Idle mode (820 rpm, 0 Nm torque) and medium and high engine loads (3000 rpm at 100 and 280 Nm torque, respectively). The optical absorption coefficient were measured with our self-developed multi-wavelength photoacoustic spectrometer (4 λ -PAS) at 1064, 532, 355 and 266nm wavelengths [2]. The absorption spectra were quantified by the AAE (the slope of the absorption spectra in log-log representation) value deduced from the measured absorption values. The number sizedistribution was determined by a Scanning Mobility Particle Sizer (SMPS equipped with a Vienna-type DMA+CPC, Grimm Aerosol Technik GmbH & CO., with a size range of 10,1-1093 nm). Butcher type low-flow thermodenuder units were applied for posterior temperature treatment of the exhaust particulates. The thermodenuder units were operated at three temperatures (40°C, 150°C and 300°C). The temperature aftertreatment units were stationed after the extended exhaust pipe of the engine (Fig.1)

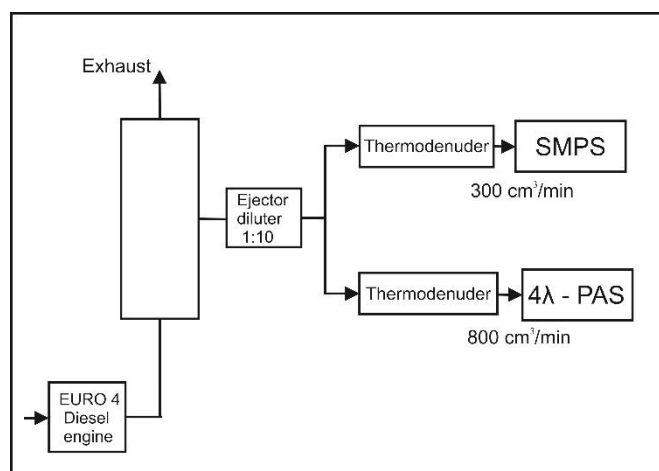


Fig.1: The schematic figure of the experimental set up including diesel engine, mixing chamber, dilution system, thermodenuders, multi wavelength photoacoustic instrument and single mobility particle sizer.

Results and discussion

The measured number size distribution data was analyzed using a simple lognormal multi peak fitting algorithm. Based on the measured data we confirm experimentally that regardless of the operational conditions of the engines the emitted total number concentration of B7 is always higher than that of B0. We also demonstrated that at 0 torque the size distribution shows bimodal distribution in both type of fuels, while at higher torque it shows a simple monodisperse size distribution (Fig.2).

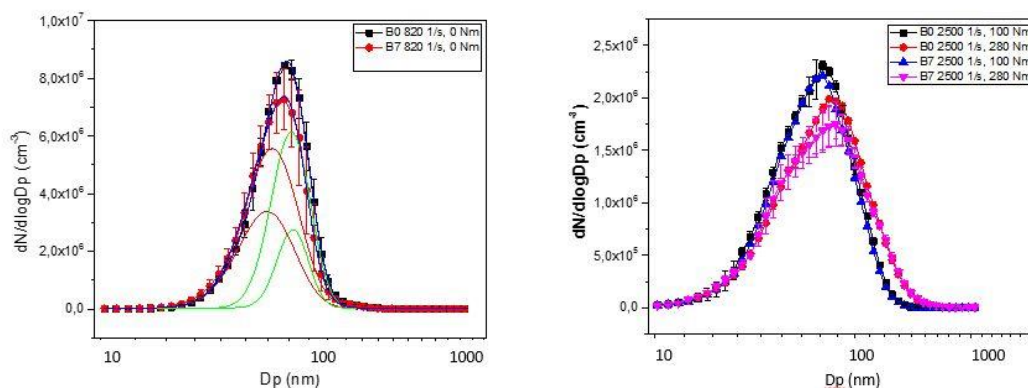


Figure 2. The number size distribution of diesel emission measured at idle (left) and at higher torques (right) at three different engine working point.

Moreover, transforming the number size distribution to volume size distribution the authors also realized that while the total number concentration is decreased towards the higher torques, the total volume concentration behaves reversely. It is a simple consequence about the increasing relative weight of bigger particulates in the spectrum towards the higher torques. The measured data also shown that increasing the temperature in posterior sample treatment procedure the count median diameter and the size concentration is become smaller simple because of the removal of the volatile pieces of the investigated particulate.

The AAE deduced from the measured optical absorption coefficients at the operational wavelengths of the photoacoustic instrument shows that increasing the torque of the engine resulted in decreasing AAE values regardless of the fuel type and temperature of the posterior sample treatment. The decreasing AAE value means that at higher torque the weight of the elemental or black carbon fraction increased in the organic and inorganic mixture of the emitted aerosol (Fig.3).

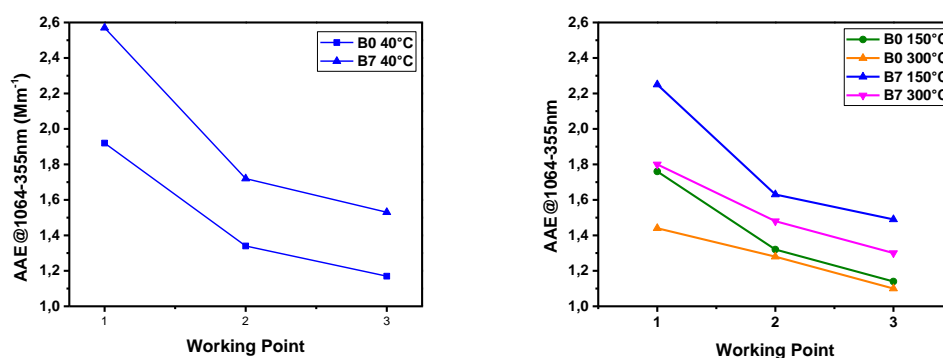


Fig.3. The AAE value of the emitted aerosol assembly measured at reference temperature (left) and higher temperatures (right) of B0 and B7 fuels at three different working points.

Another message of Fig.3 is that B7 fuel has always higher AAE value regardless of the operational condition of engine or temperature of the posterior treatments. This simple means that blending even small amount of biofuel to BO resulted in remarkable higher inorganic organic ratio of the emitted particulate. Finally, Fig.4 also shows that at any working point of engine most of the volatile fraction of the particulate can only be removed at higher temperature ($>150^{\circ}\text{C}$).

Conclusion

This study discuss some results of the intensive measurement campaign focusing on the microphysical characterization of diesel emitted carbonaceous particulate matter using different type of fuel and operational condition of engine. We also demonstrate some results regarding the thermal evolution of emitted particulate using posterior sample treatment.

Through this study we experimentally demonstrated that multi wavelength photoacoustic responses can serve climatic and chemically relevant information. Combining the multi wavelength photoacoustic instruments with commercially used single mobility particle sizer opens up novel and powerful methodologies for in-situ characterization of diesel engine emission.

Acknowledgements

This work was supported by the project GINOP-2.3.2-15-2016-00036 and EFOP-3.6.1-16-2016-00014. This paper was supported by the János Bolyai Research Scholarship of the Hungarian Academy of Sciences. Ministry of Human Capacities, Hungary grant 20391-3/2018/FEKUSTRAT is acknowledged.

References

- [1] Bond, T.C., Doherty, S.J., Fahey, D.W., Forster, P.M., Berntsen, T., DeAngelo, B.J., Flanner, M.G., Ghan, S., Kärcher, B., Koch, D., Kinne, S., Kondo, Y., Quinn, P.K., Sarofim, M.C., Schultz, M.G., Schulz, M., Venkataraman, C., Zhang, H., Zhang, S., Bellouin, N., Guttikunda, S.K., Hopke, P.K., Jacobson, M.Z., Kaiser, J.W., Klimont, Z., Lohmann, U., Schwarz, J.P., Shindell, D., Storelvmo, T., Warren, S.G. and Zender, C.S. (2013). Bounding the role of black carbon in the climate system: A scientific assessment. *J. Geophys. Res.* 118: 5380–5552.
- [2] Ajtai, T., Filep, Á., Schnaiter, M., Linke, C., Vragel, C., Bozóki, Z., Szabó, G. and Leisner, T. (2010a). A novel multi-wavelength photoacoustic spectrometer for the measurement of the UV-vis-NIR spectral absorption coefficient of atmospheric aerosols. *J. Aerosol Sci.* 41: 1020–1029.

DETERMINATION OF DIMETHYLTRYPTAMINE IN RAT PLASMA USING 2D-LC-MS/MS METHOD

**Noémi Kmettykó¹, Tímea Körmöczi¹, Írisz Szabó², Eszter Farkas², Tamás Janáky³,
István Ilisz¹, Róbert Berkecz¹**

¹*Institute of Pharmaceutical Analysis, University of Szeged, H-6720 Szeged, Somogyi street 4, Hungary*

²*Department of Medical Physics and Informatics, University of Szeged, H-6720 Szeged, Korányi alley 9, Hungary*

³*Department of Medical Chemistry, University of Szeged, H-6720 Szeged, Dóm square 8 Hungary,*

e-mail: berkecz.robert@pharm.u-szeged.hu

Abstract

Dimethyltryptamine (DMT) is a natural psychoactive compound which plays a role in oxidative stress-included changes at the endoplasmic reticulum-mitochondria interface. This makes the protective effect of DMT to be significant in hypoxic-anoxic cases.

Online two-dimensional liquid chromatography coupled to tandem mass spectrometry (2D-LC-MS/MS) can provide higher peak capacity, selectivity, resolution and sensitivity than one-dimensional approach. Generally, it is an orthogonal method with combination of different LC techniques such as hydrophilic interaction liquid chromatography (HILIC), reversed-phase (RP) and normal-phase (NP) separation.

Heart-cutting 2D-LC-MS/MS breaks the link between sampling time and the 2D-cycle with taking only the given fraction of the effluent - containing the target compounds - from the first dimension separation.

In this pilot study, heart-cutting 2D-LC-MS/MS method with combination of HILIC and RP separation was fully developed and applied for analysis of exogenous DMT in rat plasma samples. The effluent of first dimension containing DMT and α -methyltryptamine as internal were trapped before second dimensional separation by using RP trap column.

Acknowledgements

This research was supported by the EU-funded Hungarian grant EFOP 3.6.1-16-2016-00008.

CHITOSAN, A NATURAL LIGAND FOR SUSTAINABLE AND ENVIRONMENTALLY BENIGN ASYMMETRIC TRANSFER HYDROGENATIONS

Vanessza Judit Kolcsár,^{1,*} György Szöllősi²

¹*Department of Organic Chemistry, University of Szeged, Dóm tér 8, Szeged, 6720, Hungary*

²*MTA-SZTE Stereochemistry Research Group, Dóm tér 8, Szeged, 6720, Hungary*

**Corresponding author: kolcsar.vanessza@chem.u-szeged.hu*

Abstract

The transfer hydrogenations are convenient methods of obtaining chiral alcohols by enantioselective catalytic reactions. Catalytic methods suit most of the environmental requirements, though most of the chiral catalysts are made of synthetic ligands and are used in organic solvent. Natural ligands have a great potential to meet more requirements particularly if the solvent could be changed to water-based mixtures.

We have studied the transfer hydrogenation of prochiral ketones catalyzed by an *in situ* prepared Ru-chitosan complex in aqueous media. The reaction of acetophenone and its substituted derivatives resulted in good enantioselectivities. Furthermore, to our delight in the reduction of several cyclic ketones over 90%, enantiomeric excesses were obtained, reaching up to 97% in the transfer hydrogenation of heterocyclic 4-chromanone or 4-thiochromanone derivatives. Based on these experiments, several N containing ketones were reduced in the above catalytic system. The results show that the position of the N atom and the number of its substituents influences the reached conversion and ee. Some of the N containing derivatives with the proper structure was transformed with high enantioselectivity (88-95%).

The pre-prepared Ru-chitosan complex provided identical results even after several months' storage without special precautions. With the comparison of the characterisation of the complex and the results of the transfer hydrogenations, we determined a possible complex and transition state structure. In conclusion the chiral catalyst prepared from a natural, inexpensive, readily available chiral ligand is a convenient alternative of the synthetic ligands and may be applied in environmentally friendly and sustainable processes for preparing optically pure chiral alcohols.

Introduction and aims

During the last few decades, the increased demand for optically pure fine chemicals accelerated the development of asymmetric catalytic procedures. Enantioselective transfer hydrogenations are among the most convenient methods for the preparation of optically pure compounds used as intermediates in the production of pharmaceuticals, agrochemicals, flavours and fragrances. For the transfer hydrogenation of various prochiral unsaturated compounds, a large variety of chiral complexes have been developed. Recent trends require environmentally friendly, sustainable processes, so the use of chiral ligands from natural sources became essential. With the deacetylation of chitin, chitosan can be obtained, which has multiple advantages. The biocompatible, biodegradable chitosan may replace the expensive chiral ligands. Due to the presence of the free amino groups in this biopolymer, it may be able to form complexes with metal cations [1]. Furthermore as a result of its hydrophilic character may be used in aqueous media. However, only few studies have been published attempting the use of chitosan complexes in asymmetric transfer hydrogenations and the results obtained until now are far behind the values produced using synthetic chiral ligands. With the use of chitosan derivatives, satisfactory results were obtained [2,3], however functionalization of the chiral polymer decreased the practical value of these procedures.

Our aim was to investigate the transfer hydrogenation of prochiral ketones catalyzed by a chiral Ru-chitosan complex prepared from unmodified, commercially available chitosan in aqueous solvents and to explore the applicability of this chiral complex. We also wanted to determine the structural requirements of the ketones, which are necessary to obtain high optical purities. Examinations of the complex structure and that of the transition state during the reaction were also our primary tasks. As a final goal, we intended to develop a highly enantioselective, economic, environmentally friendly procedure for the convenient transfer hydrogenation of prochiral ketones.

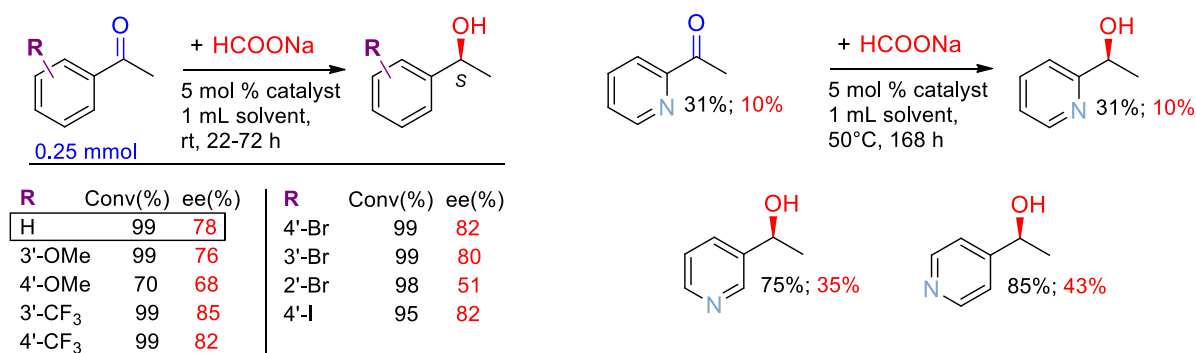
Experimental

The prochiral ketones, the hydrogen donors, the metal precursor and the chitosan were obtained from commercial sources and were used as received. Transfer hydrogenations were carried out in closed glass reactors. In a typical run, the metal precursor and chitosan were stirred in the solvent 30 min followed by addition of the hydrogen donor (HCOONa) and the prochiral ketone. The slurry was stirred for the desired time followed by extraction of the product three times with ethyl acetate. These products were analyzed by GC-MSD and GC-FID using chiral capillary column. For the characterization of the Ru-chitosan complex this was prepared *ex situ* and dried at room temperature. The product was used in SEM and IR spectroscopic investigations.

Results and discussion

First, the transfer hydrogenation of a few acetophenone derivatives was carried out in the new catalytic system. Optimization of the reaction conditions and the solvent composition led us to the conclusion that a water-*i*PrOH 4-1 solvent mixture provides the best enantioselectivities at room temperature. Although, acetylpyridine derivatives have similar structure as the acetophenones, the transfer hydrogenations of these compounds have not been examined before with catalyst bearing chitosan as the chiral ligand. Our experiments showed that the presence of the N in the aromatic ring has a detrimental effect on the conversion and the enantioselectivity, probably due to strong attachment of the ketone to the metal. The results of these experiments are summarized in Figure 1.

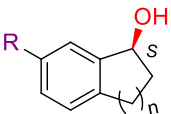
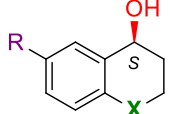
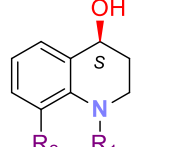
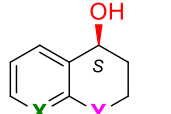
Figure 1. Enantioselective transfer hydrogenation of acetophenone and acetylpyridine derivatives with *in situ* formed Ru-chitosan complex.



Next, we examined the transfer hydrogenation of a large library of prochiral ketones with various structure under conditions found most appropriate in our previous experiments. The reduction of ketones having alicyclic ring connected to the aromatic group gave surprisingly high enantioselectivities, as shown in Figure 2. To our delight, results obtained in our

experiments exceeded the best values reported until now by the use of chitosan derivatives as a ligand. Moreover, the ketones including a heteroatom in the saturated ring, such as 4-chromanones and 4-thiochromanones provided the corresponding alcohols in even better, up to 97%, enantiomer excesses (Figure 2.) Based on these results the transfer hydrogenation of four N-containing ketones with similar structure was carried out. In most of the cases under the right reaction conditions the conversion and the ee approached the values achieved with 4-thiochromanone. As we mentioned before the N atom has a significant influence on the outcome of the reactions. If the N is hindered by a substituent, or by a bulky group in its surroundings the effect of the Ru-N bond will be weaker and the reactions take place faster with better enantioselectivities (Figure 2.). Encouraged by these results, we continued to explore the scope of this catalytic system, by attempting the asymmetric transfer hydrogenations of ketones having pyridyl ring condensed with a heterocyclic moiety. Based on the obtained conversions and ee values we suggest that the nitrogen found in the aromatic ring may strongly interact with the metal and with the chiral ligand as well. We also note that the steric effect of the six-membered cycloaliphatic ring still assured good ee's in these reactions, similarly with transformations of 4-(thio)chromanones.

Figure 2. Results of transfer hydrogenation of cyclic ketones with the Ru-chitosan catalyst.

															
n	Conv(%)	ee(%)		X	R	Conv(%)	ee(%)	R ₁	R ₂	Conv(%)	ee(%)	X	Y	Conv(%)	ee(%)
3	77	65		O	H	98	96	H	H	78	72	N	S	99	94
2	61	93		O	Cl	99	96	Boc	H	96	95	N	N-CH ₃	92	88
1	80	88		S	H	99	97	Br	H	97	88				
1	91	92 (R: CF ₃)		S	Cl	99	97								
				S	Me	91	96								

Further, we prepared the Ru-chitosan complex, which after slow evaporation of the solvent gave a dark orange film-like material (Figure 3.). This catalyst was equally efficient in the transfer hydrogenations as the *in situ* formed catalyst. The FT-IR spectrum of this material indicated the coordination of the Ru to the chitosan.

Based on the IR spectrums and the effect of the ketone structure on the conversion and enantioselectivity we suggested a plausible structure for the complex (Figure 3.). It is assumed that the amino groups of different glucosamine units are involved in the coordination of the Ru(II) ion. An outer-sphere mechanism is suggested, during which the ketones' six-membered ring assures the necessary rigidity to the molecule, whereas hydrogen-bond acceptor heteroatoms in the ring are able to interact with the hydroxyl groups of the chitosan improving the orientation of the ketone. Based on the above results we suggested the possible structure of the complex and the obtained high enantioselectivities were interpreted by stereospecific interactions of the prochiral compounds with the chitosan ligand.

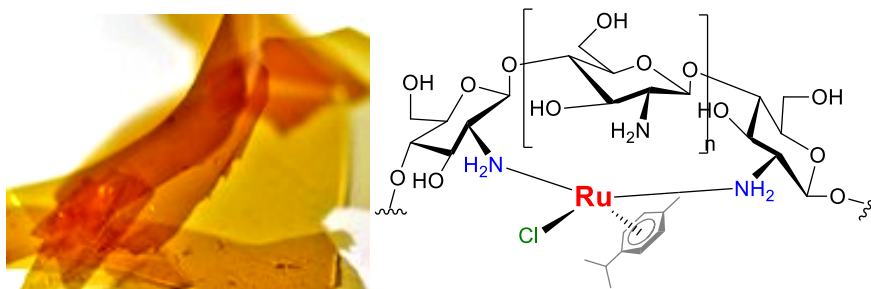


Figure 3. Photo and the probable structure of the *ex situ* prepared Ru-chitosan complex

Conclusions

In summary, we developed a sustainable and green method, using the biopolymer chitosan as a chiral ligand for the *in situ* formation of a Ru complex in aqueous catalytic system, in which high enantioselectivities were obtained in the asymmetric transfer hydrogenation of prochiral ketones. The enantiomeric excess values surpassed those reported in the literature obtained with chitosan derivatives. Acetophenone derivatives were reduced to the corresponding 1-arylethanol in up to 86% ee. The reactions of acetylpyridine derivatives were slower and gave lower ee values due to the strong bonding of the pyridyl N to the Ru. We obtained over 90% ee in the reaction of cyclic ketones, reaching up to 97% in the reduction of compounds having heteroatoms in the alicyclic ring. In the transfer hydrogenation of quinolinone derivatives high enantioselectivities were reached in case the amino group was protected or shielded by a nearby substituent. Further, we prepared *ex situ* the Ru-chitosan complex, which was equally efficient in transfer hydrogenations as the *in situ* formed catalyst. The FT-FIR spectrum of this material indicated the bonds established between the Ru cation and chitosan. Based on the above results we suggested the possible structure of the complex and the obtained high enantioselectivities were interpreted by stereospecific interactions of the prochiral compounds with the chitosan ligand. Finally, we mention that the highly selective chiral Ru complex was prepared using a cheap, natural material as chirality source, thus the developed method is a green, environmentally friendly and sustainable way to obtain optically enriched chiral alcohols.

Acknowledgements

Financial support by the UNKP-19-3-SZTE-153. New National Excellence Program of the Ministry of Human Capacities (V.J. Kolcsár) is appreciated.

References

- [1] A. El Kadib, ChemSusChem, 8 (2015) 217.
- [2] M. Babin, R. Clément, J. Gagnon, F.-G. Fontaine, New J. Chem. 36 (2012) 1548.
- [3] B. Liu, H. Zhou, Y. Li, J. Wang, Chin. J. Org. Chem. 34 (2014) 2554.

ASYMMETRIC MICHAEL-ADDITIONS CATALYZED BY ENVIRONMENTALLY BENIGN HETEROGENEOUS CHIRAL 1,2-DIAMINE DERIVATIVES

Viktória Kozma¹, György Szöllősi²

¹*Department of Organic Chemistry, University of Szeged, 6720 Szeged, Dóm tér 8, Hungary*

²*MTA-SZTE Stereochemistry Research Group, 6720 Szeged, Dóm tér 8, Hungary*

e-mail: kozma.viktoria@chem.u-szeged.hu

Abstract

Asymmetric Michael additions of isobutyraldehyde to maleimides catalyzed by optically pure diamines and their sulfonamides were investigated to develop heterogeneous chiral catalysts for these reactions. Chiral solid materials were prepared by covalent bonding of the diamines on different functionalized organic and inorganic supports. The heterogeneous catalyst prepared by bonding optically pure 1,2-diphenylethane-1,2-diamine to polystyrene support was highly enantioselective, giving results approaching those obtained using soluble sulfonamide derivatives. The catalysts could be recycled a few times, retaining their activity followed by a small decrease in conversion, while still producing high – up to 97% – enantiomeric excess. These materials are the first efficient recyclable catalysts used in the enantioselective Michael-addition of aldehydes to maleimides.

Introduction

Asymmetric Michael-additions are among the most often-used stereospecific reactions for coupling organic molecules, widely applied for preparing optically pure fine chemicals. Succinimide derivatives may be obtained by the enantioselective addition of nucleophiles, such as aldehydes, to maleimides [1]. These reactions are efficiently catalyzed by chiral diamines and their derivatives, among which cyclohexane-1,2-diamines, 1,2-diphenylethane-1,2-diamines, their sulfonamides and thiocarbamides are well-functioning chiral catalysts [2-4].

Until now heterogeneous chiral catalysts have not been used in these reactions, although these environmentally friendly, recyclable materials can serve as good alternatives for their soluble counterparts. A detailed study is of paramount importance for selecting the proper support, catalyst structure and the linker for the immobilization of these organocatalysts in order to obtain heterogeneous, recyclable catalysts. In our previous study, the Michael-additions of aldehydes to maleimides were carried out with commercial chiral catalysts in homogeneous media. Based on the results of this study we aimed to attempt the immobilization of the selected chiral 1,2-diamine catalyst using an appropriate linker over various inorganic and organic supports. Our goal was to develop a highly efficient, reusable heterogeneous chiral catalyst for the asymmetric Michael-addition of isobutyraldehyde to *N*-benzylmaleimide.

Experimental

The heterogeneous catalysts are prepared by coupling reactions in Merrifield flasks. The success of the immobilization process of the chiral compound was checked by FT-IR spectroscopy. We have immobilized optically pure cyclohexane-1,2-diamines or 1,2-diphenylethane-1,2-diamines using linkers having acidic, H-bond donor character, such as sulfonamide, thiocarbamide or squaramide groups over silica or polystyrene resin supports. In a typical reaction, the given amount of catalyst was introduced into a glass vial followed by the addition of the solvent and the reactants. The slurry was stirred magnetically or agitated in a shaker for the given reaction time, diluted with the solvent and the product solution was separated. Products resulted in the Michael-additions were analyzed by GC-MSD and GC-

FID using a chiral capillary column. Larger scale experiments were also carried out, the resulted products were purified by column chromatography for determination of the yields. The pure compounds were characterized by ^1H - and ^{13}C -NMR spectroscopy.

Results and discussion

Immobilization of chiral organocatalysts on insoluble supports is a convenient method to prepare enantioselective heterogeneous chiral catalysts. According to results obtained in homogeneously catalyzed reactions using optically pure 1,2-diamine-derived sulfonamides, anchoring 1,2-diamines by sulfonamide linkers on solid materials may results in efficient chiral catalysts. As has been shown in our previous research, the presence of the formed hydrogen donor group improves the orientation of the molecule in the transition state.

The addition of isobutanal to *N*-benzylmaleimide was selected as a test reaction for studying the influence of the chiral catalyst structure. Several inorganic and organic materials are available commercially, which may be used as supports. Applying such materials we have prepared chiral solids both from optically pure cyclohexane-1,2-diamines and 1,2-diphenylethane-1,2-diamines, respectively. The success of the immobilization process of the chiral compounds was checked by FT-IR spectroscopy.

The method used in the preparation of one of the heterogeneous catalyst is shown in Figure 1. Selected results obtained by reusing this catalyst are also shown in Figure 1. The recyclability of the enantioselective catalysts obtained using the polymeric support was also examined.

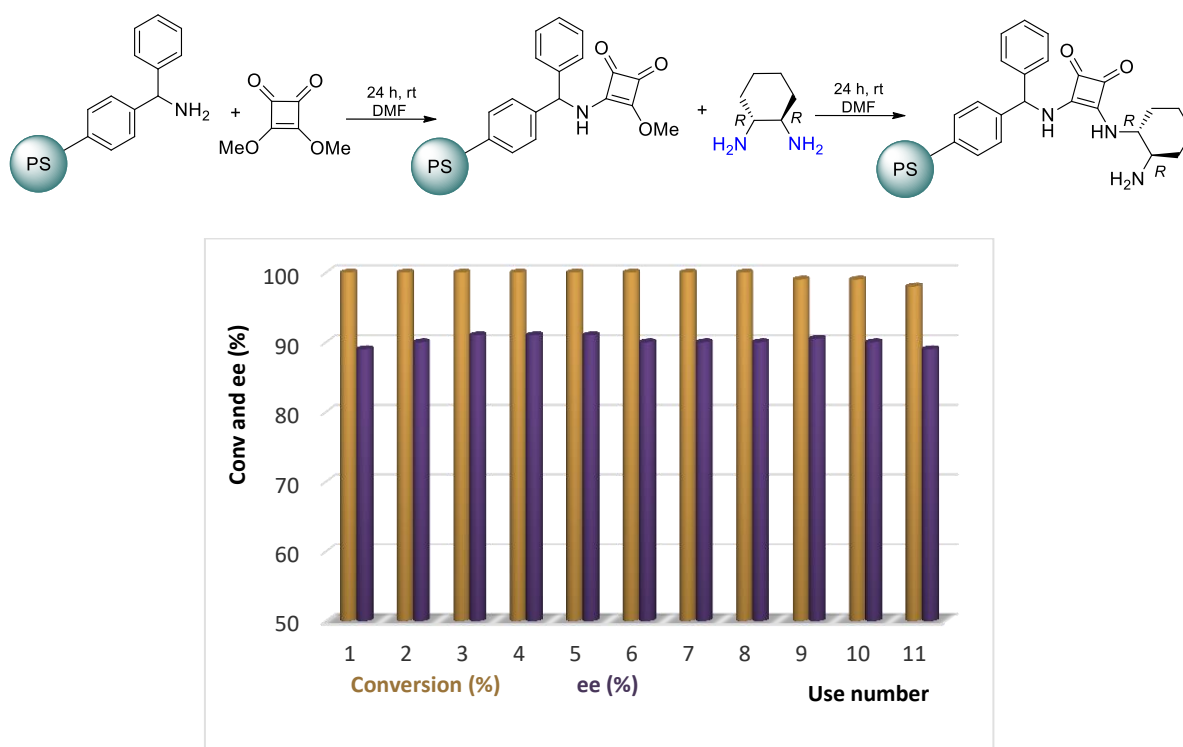


Figure 1. Chiral solid catalysts prepared by immobilization of optically pure 1,2-cyclohexanediamine through squaramide linker and its recyclability.

As shown in Figure 2, the silica-supported catalysts gave lower enantioselectivities and partially lost their activity upon reuse, which we ascribed to the unfavorable effect of the support's surface acidic sites. On the contrary, the chiral catalysts immobilized on polystyrene resins approached the performances of the soluble catalysts, affording the same conversion and only a slight decrease in the enantioselectivity. Moreover, the enantiodiscrimination

ability of the catalyst was kept in a 2nd run. The small decrease in conversion may be attributed to the small amount of catalyst lost during manipulations. Good results were also obtained with catalysts immobilized on polystyrene resins via thiocarbamides groups (not shown in the figure).

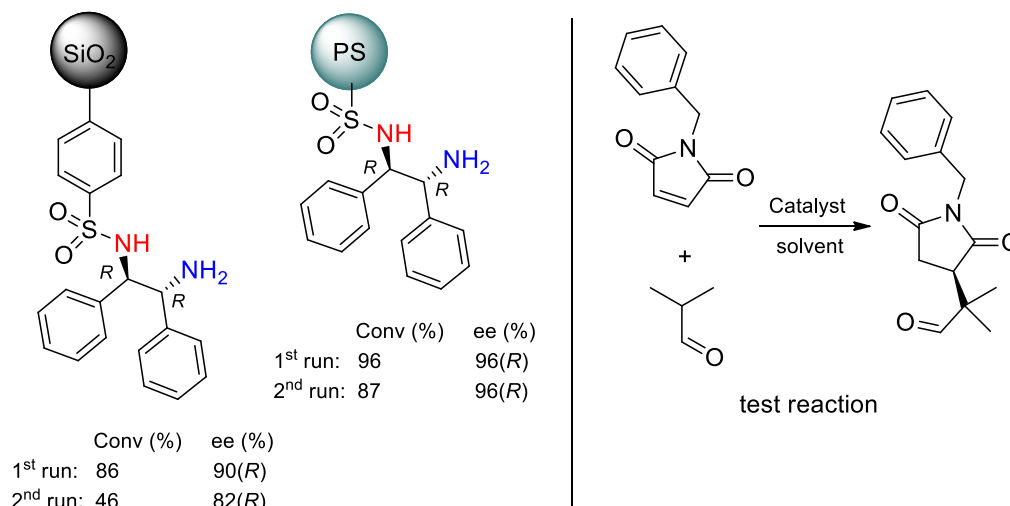


Figure 2. Selected heterogenized chiral catalysts and results obtained in the test reaction.

Conclusion

In our previous studies we have investigated in detail the effect of variations in the structure of the catalysts in homogeneous media. Based on these results we selected the proper catalyst, support and linker for the immobilization of the chiral catalyst to obtain heterogeneous chiral catalysts. These heterogeneous catalysts approached the performances of their soluble counterparts. The proper choice of the support allowed the reuse of the solid catalysts without enantioselectivity decrease. Finally, we note that the prepared heterogeneous catalysts are the first, which were designed for the asymmetric Michael-addition of aldehydes to maleimides. Results presented in this work are also promising starting-points of further efforts devoted to applying heterogeneous, environmentally friendly catalysts in the preparation of practically relevant chiral succinimide derivatives.

References

- [1] P. Chauchan, J. Kaur, S.S. Chimni, *Chem. Asian J.* 8 (2013) 328.
- [2] F. Xue, L. Liu, S. Zhang, W. Duan, W. Wang, *Chem. Eur. J.* 16 (2010) 7979.
- [3] F. Yu, Z. Jin, H. Huang, T. Ye, X. Liang, J. Ye, *Org. Biomol. Chem.* 8 (2010) 4767.
- [4] A. Avila, R. Chinchilla, E. Gómez-Bengoa, C. Nájera, *Tetrahedron: Asymmetry* 24 (2013) 1531.

SIZE DISTRIBUTION AND SPECTRAL RESPONSES OF ATMOSPHERIC AEROSOL MEASURED BY SINGLE MOBILITY PARTICLE SIZER (SMPS) AND MULTI WAVELENGTH PHOTOACOUSTIC SPECTROMETER (4 λ -PAS)

Fruzsina Kun-Szabó¹, Máté Pintér¹, Tibor Ajtai^{1,2}, Zoltán Bozóki^{1,2}, Gábor Szabó^{1,2}

¹ *Department of Optics and Quantum Electronics, University of Szeged, H-6720 Szeged, Dóm tér 9, Hungary*

² *Interdisciplinary Excellence Centre, Department of Optics and Quantum Electronics, University of Szeged, Hungary
e-mail: kszfruzsina@titan.physx.u-szeged.hu*

Abstract

This campaign was made under wintry urban meteorological conditions from late winter until early spring of 2015, in Budapest, the capital of Hungary. Optical absorption coefficient (OAC) is generally measured by two different methodologies. One was the most commonly used Aethalometer [1]. The other was the recently developed multi wavelength photoacoustic instrument (4- λ -PAS) [2]. The size distribution and number concentration of ambient aerosol was measured by a single mobility particle sizer (SMPS). The measurement period could be classified normal days and nucleation days. The correction factor of filter based transmission measurement was experimentally determined using photoacoustic instrument as reference. Both the correction factor and the spectral responses were found to be characteristic for normal and nucleation days.

Introduction

Nowadays you can hear a lot about atmospheric aerosol and its effects on the environment (climate and air quality) and health. In urban air, aerosol has many health effects. May be mild respiratory disease, allergies, impaired respiratory function, lung cancer, etc. The effect of aerosol on climate is very complex; it has direct and indirect parts as soon as cooling and warming climatic impact. The light absorbing carbonaceous aerosol is responsible for the major fraction of uncertainty in climate forcing calculation and one of the most adverse atmospheric component too. It also shows that a precise definition of this is essential. The photoacoustic spectroscopy is one of the most powerful methodology for precise and exact determination of light absorption of aerosol.

Experimental

The measurements were between 15 February 2015-12 March 2015 at the György Marcell Observatory of the Hungarian Meteorological Service in Budapest, the capital of Hungary (47,430009° N, 19,181225° E).

Optical Absorption Coefficient (OAC) was parallel measured by a 7-wavelength Aethalometer (AE42-7, Magee Scientific, Berkley USA) at 370, 470, 520, 590, 660, 880, 950 nm and by our self-developed multi-wavelength photoacoustic spectrometer (4 λ -PAS) at 1064, 532, 355, 266 nm.

Size distribution was determined by a Scanning Mobility Particle Sizer (SMPS equipped with a Vienna-type DMA+CPC, Grimm Aerosol Technik GmbH & CO. Austria, with a size range of 10,1-1093 nm) combined with Portable Aerosol Spectrometer (Model 1.109, Grimm Aerosol Technik GmbH & CO. Austria with a size range of 0,25-32 μ m).

Results and discussion

We analysed the measured size distribution by using lognormal multi peak fitting algorithm. Based on the data evaluation of size distribution, the measurement period can be classified into two categories such as normal and nucleation days. On 5 measurement days clear nucleation events were observed. So there are 2 categories, one for nucleation days (days with particle growth) and the other for normal days (days without particle growth) (Fig.1.).

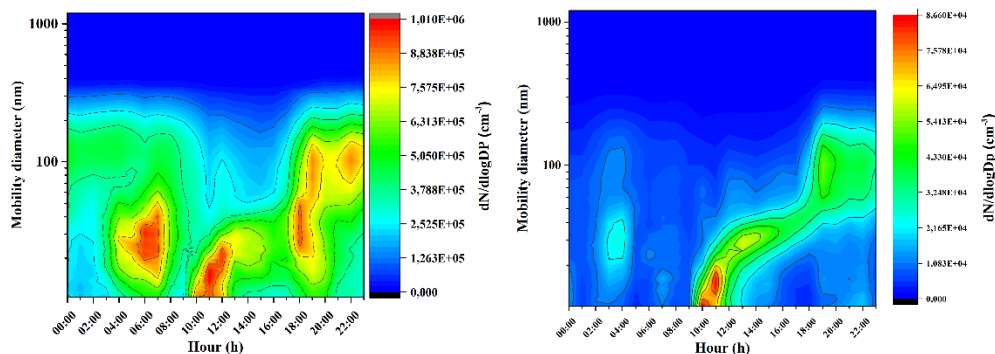


Figure 1.: a) size distribution in normal days b) the banana curve demonstrating a nucleation event

We identified three characteristic size modes both normal and nucleation days, which were Mode 0 (average count median diameter (CMD): 14.89 ± 3.97 on normal and 14.81 ± 3.79 on nucleation days), Mode 1 (average CMD: 25.80 ± 1.60 on normal and 24.23 ± 0.67 on nucleation days) and Mode 2 (average CMD: 115.76 ± 19.17 on normal and 115.60 ± 24.14 on nucleation days). Further these mode structure we found that we can divide the days into 3 parts: namely heating, traffic and nucleation hours. (Table 1)

Part of day	Time period	
	Normal days	Nucleation days
Heating hours	21:00-04:00	22:00-03:00
	12:00-15:00	
Traffic hours	04:00-10:00	03:00-10:00
	15:00-21:00	19:00-21:00
Nucleation hours	10:00-12:00	10:00-19:00

Table 1.: Parts of the day

The diurnal variation of OAC were measured by the 4λ -PAS and the 7λ -Aethalometer. The highest OACs were measured from late afternoon to early morning, while lower values were measured during the morning and the afternoon and the lowest OACs were between the middle of the day and the very early afternoon. We measured Absorption Angström Exponent (AAE) by two instruments (4λ -PAS and the 7λ -Aethalometer) respectively and OAC and AAE data's trends were found to be similar. The highest AAE values were measured during the late afternoon and during the night, lower values during the morning and the early afternoon, while AAE had its diurnal minimum during the midday.

Conclusion

This study discusses the results of a 1-month field measurement campaign during the late winter and the early spring of 2015, in Budapest, the capital of Hungary.

Based on the data evaluation of size distribution, in the measurement period we can characterised two categories. These two class are normal and nucleation days. Both normal and nucleation days could be further categorized to three parts of day, namely heating, traffic and nucleation hours in time series.

Highest OAC and AAE values were measured during heating hours, lower during traffic hours and the lowest values in the nucleation period.

Examining the correlations between the photoacoustic and size distribution data we quantified relationship between the mode structure and the AAE. With this measurement we also identified characteristic spectral responses of nucleation events first and we experimentally demonstrated, uncompleted nucleation events with characteristic AAE values in normal days (which measured by photoacoustic spectroscopy).

We measured parallel OAC by the 7 λ -Aethalometer and a 4 λ -Photoacoustic Spectrometer as reference instrument, wavelength dependent correction factors (f and C) was defined in weingartner posterior correction schemes. [3] The result shows that the correction factor of C has source specific diurnal variations, while correction factor of f no clear trend could be observed during the measurement period.

Acknowledgements

This work was supported by the project GINOP-2.3.2-15-2016-00036 and EFOP-3.6.1-16-2016-00014. This paper was supported by the János Bolyai Research Scholarship of the Hungarian Academy of Sciences. Ministry of Human Capacities, Hungary grant 20391-3/2018/FEKUSTRAT is acknowledged.

References

- [1] Hansen, J. E., & Takahashi, T. (1984). Climate processes and climate sensitivity. Washington DC American Geophysical Union Geophysical Monograph Series, 29.
- [2] Ajtai, T., Filep, Á., Kecskeméti, G., Hopp, B., Bozóki, Z., & Szabó, G. (2011). Wavelength dependent mass-specific optical absorption coefficients of laser generated coal aerosols determined from multi-wavelength photoacoustic measurements. Applied Physics A, 103(4), 1165-1172.
- [3] Weingartner, E., Saathoff, H., Schnaiter, M., Streit, N., Bitnar, B., & Baltensperger, U. (2003). Absorption of light by soot particles: determination of the absorption coefficient by means of aethalometers. Journal of Aerosol Science, 34(10), 1445-1463.

MONITORING OF DROUGHT AND INLAND EXCESS WATER IN THE SERBIAN-HUNGARIAN CROSS-BORDER REGION IN THE FIRST HALF-YEAR OF 2019

Zsuzsanna Ladányi*, Boudewijn van Leeuwen, Viktória Blanka, Zsolt Tobak, Kovács Ferenc, Gábor Mezősi

Department of Physical Geography and Geoinformatics, University of Szeged, H-6720

Szeged, Egyetem u. 2-6, Hungary

**e-mail: ladanyi@geo.u-szeged.hu*

Abstract

Due to climate change and its natural geographic conditions, the water supply of the Hungarian-Serbian cross-border region shows extreme variation. The area suffers from both droughts and inland excess water, thus research and geographical observation of the problems is very important. This study demonstrates the development of a monitoring system of the two phenomena by the help of satellite images supplemented by field data using crowdsourcing elements within the framework of the Drought and Excess Water Research and Monitoring Centre, furthermore, evaluates the monitoring results for the first half-year in 2019.

Introduction

One of the most important environmental problems nowadays is global climate change, and its regional and local effects. In the last 100 years the average temperature of the Earth increased by +0.7°C and undesirable changes occurred also in case of precipitation, as long periods without rainfall and extreme precipitation events became more frequent in large parts of the temperate zones on both hemispheres [1]. Climate change has a considerable impact on the lowland areas of the Carpatian Basin. Due to climate change and the natural geographic conditions, the water supply of the region is showing extreme variation, the area suffers from both drought [2] and inland excess water [3] – these can take turns, and occur in consecutive years or even in the same year.

It was also observed that the frequency of extreme weather conditions' occurrence has also changed. Years drier than the average have become more frequent, and the distribution of the rainfall is turning less and less favourable, as beside the long dry periods, extreme precipitation events occur especially in the summer causing an increase in runoff of the valuable water resources. For this research and geographical observation of the problems related to climate change and hydrological extremes is very important in the region [5] [6] [7]. This study presents the results of the Drought and Excess Water Research and Monitoring Centre (DERMC) to set up a monitoring system of the two phenomenon by the help of satellite images supplemented by field data using crowdsourcing elements in the Hungarian-Serbian cross-border region, furthermore evaluates its operation for the first half-year in 2019.

Study area

The developed monitoring system covers Southeast Hungary (Csongrád and Bács-Kiskun counties) and Vojvodina (Fig. 1a). The majority of the area is lowland, where the mean annual temperature is around 11°C and the annual precipitation is 500-600 mm. The highest mean temperature occurs in July, typically between 21°C and 23°C, while the rainfall is around 300 mm in the summer half of the year [8] [1]. Examining the climate change trends of the last decades reveals that the temperature has been rising and the precipitation level has slightly decreased [9] [10], resulting in a 20-30 mm yearly precipitation shortage in the area. The most important rivers are the Danube, the Tisza/Tisa River, the Maros River, and the Tamiš River; besides these, most of the surface waterflows are artificial canals. The study

area is diverse in terms of soil type, physical properties and soil moisture regime of the soils (Fig. 1b). Chernozem soil and its different variations dominate the area; sandy soils and meadow soils are also common in the region. The land cover and land use of the area is dominated by agricultural land (Fig. 1/c). In the last 200 years large areas of land became used for farming purposes, therefore the proportion of agricultural land is high, and the natural vegetation remained only in relatively small areas. Even in these areas, where the natural vegetation survived, unfavourable processes can be observed, because the climate change of the last few decades and human activities resulted in natural wetland habitats starting to dry out, and this process is accompanied by the degradation and transformation of the vegetation [11].

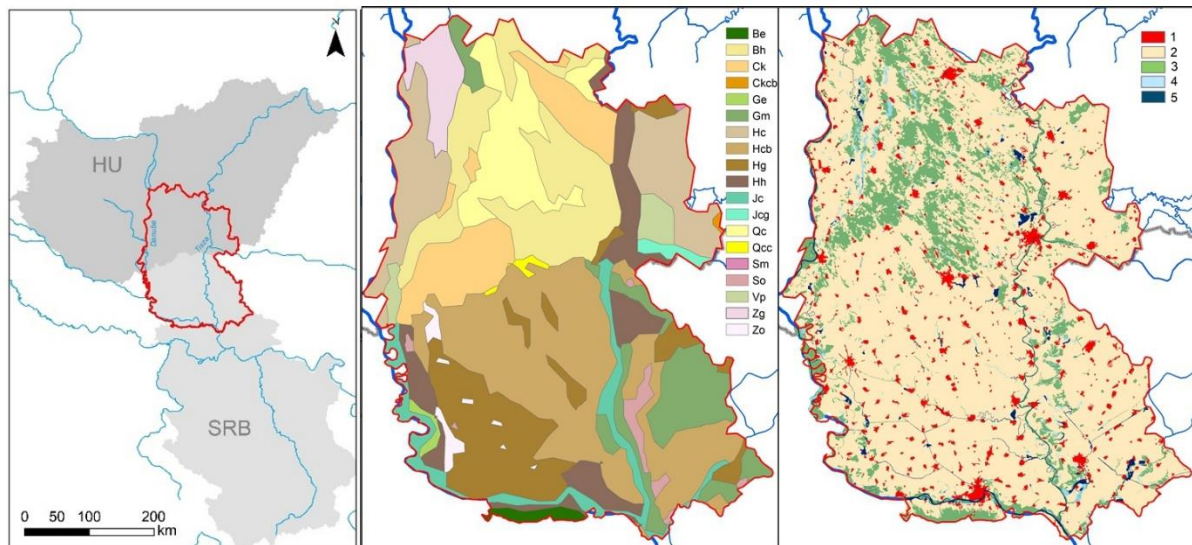


Figure 1. Location of the study area, furthermore its soil types (FAO 1985) and land cover (Corine 2018) (1: Artificial surfaces; 2: Agricultural areas; 3: Forests and semi natural areas; 4: Water bodies; 5: Wetlands)

Methods

The methods for drought and excess water monitoring were based on selected parameters like surface moisture, vegetation and water abundance using medium and low-resolution satellite data and crowdsourcing methods. The main goal was to estimate the spatial and temporal changes of the two hydrological extremes under study. The developed monitoring system collects and processes remotely sensed (drone, Sentinel 1 and MODIS satellite) and in situ surveyed datasets (soil moisture and meteorological data and inland excess water patches). The data is stored in a geodatabase and published online using web mapping technologies.

Inland excess water, vegetation anomaly and surface moisture monitoring using medium and low-resolution satellite images

The work process that was developed for inland excess water monitoring utilises a combination of satellite images from Sentinel 1 radar data and Sentinel 2 multispectral data to produce regional scale inland excess water maps in an operative way, on a weekly basis. The radar and optical data-based processing phases use imagery from Sentinel 1A, 1B, 2A and 2B. These satellites provide a full coverage of the sampling area approximately every third day. Thanks to the C-band active remote sensing technology, data can be acquired regardless the part of the day or weather conditions. The workflow combines radar thresholding, and optical image classification and index based thresholding to generate weekly inland excess water maps (see methods in more details in [12]).

The vegetation assessment uses MOD09A1 surface reflectance images and MOD13A1.006 vegetation index products and data were processed using the Google Earth Engine cloud computing platform (see methods in more details in [13]). For the demonstration of the current condition of vegetation anomalies compared to the long-term average (2000-2017), the NDDI drought index was applied where a positive deviation indicates drought conditions:

$$NDWI = (NIR - SWIR) / (NIR + SWIR)$$

$$NDDI = (NDVI - NDWI) / (NDVI + NDWI)$$

$$NDDI_{\text{standardised}} = (NDDI - NDDI_{\text{average}}) / NDDI_{\text{deviation}}$$

where NIR and SWIR are respectively the near infrared and the short-wave infrared bands of the MODIS instrument. NDVI is Normalized Difference Vegetation Index, NDWI is Normalized Difference Water Index.

Based on the standardised anomaly the water shortage of the studied period can be identified, which reduces the biomass production or delays its temporal dynamics.

Surface moisture monitoring is based on the normalized difference moisture index (NDMI) calculation using Google Earth Engine:

$$NDMI = (NIR - SWIR) / (NIR + SWIR)$$

where NIR is the narrow near infrared band 8a and SWIR is the short-wave infrared band 11 of atmospherically and geometrically corrected Sentinel 2 level 2 data.

To reduce the missing data due to cloud cover, composites were created for the median pixel value of 10 days. This ensures that the pixels of at least 2 images per composite were considered.

GeoApp and crowdsourcing contributing to inland excess water inundation mapping

The location-based data collecting application for Android and iOS devices enables the monitoring of inland excess water patches. The application has an editable layer, during data collection, the features of the inland excess water patches can be provided according to a predefined categorical system, and the location of the observed phenomenon can be specified on the map by manually or using the GPS position. A photograph can be attached to the observation using the camera of the device. The collected data are automatically transferred to the interactive maps of the project. The app can be downloaded for free, but registration is required.

Results and discussion

All data collected and processed in the framework of the project is made available via the public project website (<https://aszaly.geo.u-szeged.hu/wateratrisk/>) and maps or diagrams. Data can be downloaded for further analysis.

Due to the low amount of precipitation between October 2018 and March 2019, drought formed in winter/early spring in 2019, which can be considered extraordinary. There was hardly any water stored in the upper soil layer, resulting in reduced crop growth during the autumn-winter period. At the end of April, a more humid period began, and the soil moisture deficit was recharged, resulting in favourable condition for agriculture e.g. autumn wheat. In May, however, a lot of precipitation fell (more than two times more than the long-term average), causing rather unfavourable impacts (e.g. plant infections) and water management challenges (Fig 2). As a result, also minor inland excess water inundations could form between the end of May and mid-June, which is uncommon in normal years.

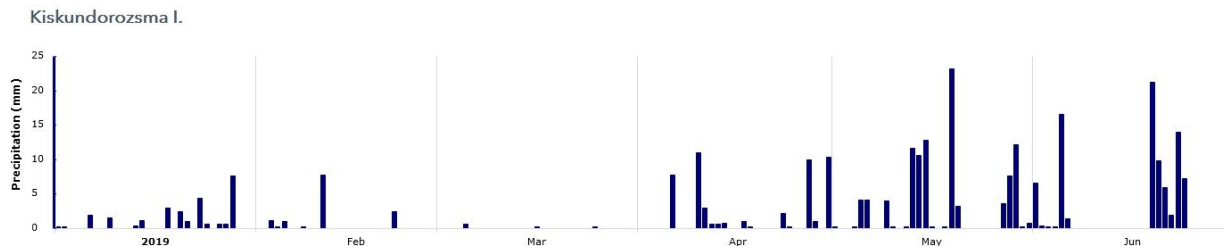


Figure 2. Precipitation conditions in the first half-year in 2019 based on the meteorological station of the DERM (Source: <https://aszaly.geo.u-szeged.hu/wateratrisk/>)

Figure 3 represents the DERM monitoring results in the between March and June 2019. As very limited precipitation fell until April 2019, a significant drought developed, which is well observable on surface wetness maps. Vegetation showed negative anomalies in the first month of the vegetation period only on sand covered areas and along the rivers. Here, differences in soil structure and water household could mitigate the impact of the formed drought on the vegetation (e.g. on Chernozems average conditions can be observed in the upper part of Vojvodina). For the end of April, moisture conditions changed due to rainfall, and the water conditions improved along the rivers according to the surface moisture maps, but still dry conditions can be observed on higher parts of the sandland. Due to the high amount of precipitation in May, the surface moisture conditions were almost 'wet' except for the Chernozems in Vojvodina and South Hungary. In those areas, the vegetation still showed negative anomalies due to the drought conditions. In June, the surface moisture maps showed that the whole area is under wet conditions and vegetation index shows similar conditions compared to the long-term average. In 2019, there were no significant inland excess water floods during the late-winter/early spring period, just some relatively small inundations between the end of May and mid-June. The developed GeoApp will be used in the future to validate the satellite derived inundation patches with field observation.

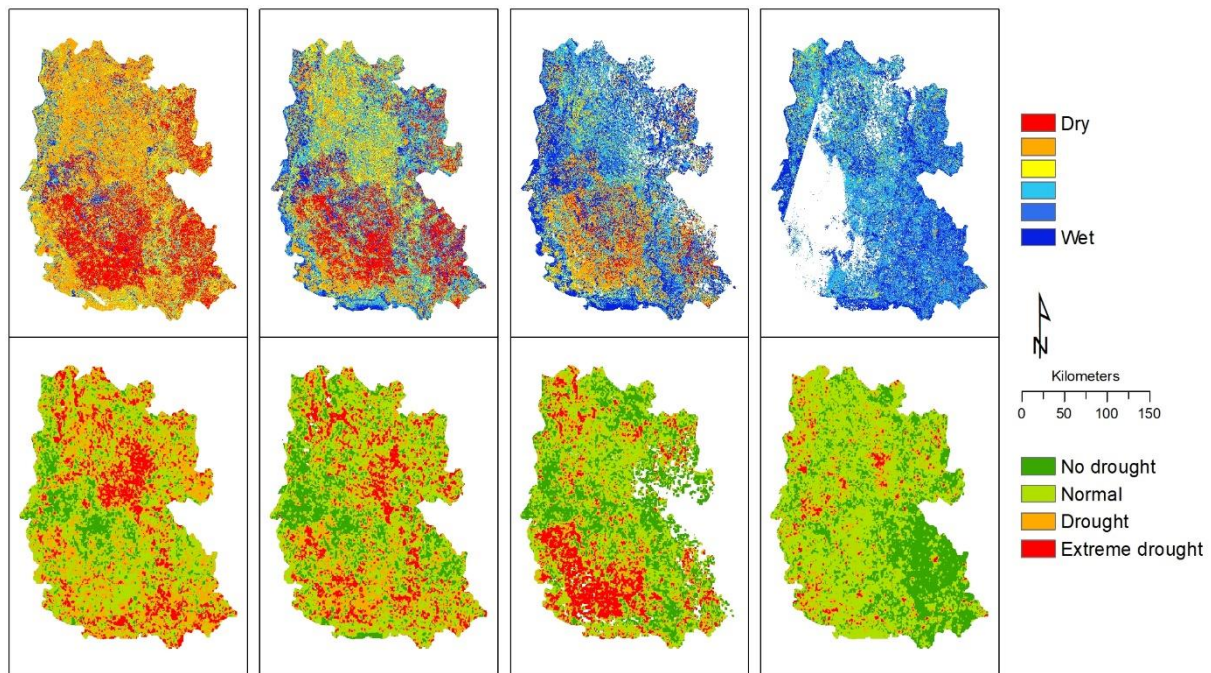


Figure 3. Surface moisture (top) and vegetation anomaly (bottom) maps at the end of March, April, May and June (Source: <https://aszaly.geo.u-szeged.hu/wateratrisk/>)

Conclusion

This study presented the satellite image based and in situ monitoring results of the Drought and Excess Water Research and Monitoring Centre for the HU-SRB cross-border area for the first half-year of 2019. It was shown that substantial drought occurred in the winter-early spring period, which had significant impact on agriculture. Due to the humid May, the situation was balanced, however, the extraordinary amount of precipitation in May and June, resulted in small inland excess water inundations in the study area. The developed methods and the applied used indices for monitoring proved to be useful to demonstrate the drought and excess water conditions in the studied region.

Acknowledgements

The research was funded by the WATERatRISK project (HUSRB/1602/11/0057).

References

- [1] OMSZ. https://www.met.hu/eghajlat/eghajlatvaltozas/megfigyelt_valtozasok/ (2019)
- [2] K. Fiala, V. Blanka, Zs. Ladányi, P. Szilassi, B. Benyhe, D. Dolinaj, I. Pálfa. Drought severity and its effect on agricultural production in the Hungarian-Serbian cross-border area. *Journal of Environmental Geography* 7 (3–4), 43-51. (2014)
- [3] Cs. Bozán, J. Körösparti, L. Pásztor, I. Pálfa. Excess water hazard mapping on the South Great Hungarian Plain. Proceedings of the 13th International Conference on Environmental Science and Technology Athens, Greece, 5-7 September 2013, 8. p. (2013)
- [4] G. Mezősi, V. Blanka, Zs. Ladányi, T. Bata, P. Urdea, A. Frank, B. Meyer. Expected mid- and long-term changes in drought hazard for the South-Eastern Carpathian Basin. *Carpathian Journal of Earth and Environmental Sciences* 11 (2), 355-366. (2016)
- [5] F. Kovács, F. Assessment of regional variations in biomass production using satellite image analysis between 1992 and 2004. *Transactions in GIS* 11/6, 911–926. (2007)
- [6] Zs. Ladányi, J. Rakonczai, Á.J. Deák. A Hungarian landscape under strong natural and human impact in the last century. *Carpathian Journal of Earth and Environmental Sciences* 6 (2), 35-44. (2011).
- [7] J. Rakonczai. Effects and consequences of global climate change in the Carpathian Basin. In: Blanco J., Kheradmand H. (eds.): Climate Change - Geophysical Foundations and Ecological Effects. Rijeka: InTech, 2011, 297-322. (2011)
- [8] J. Smailagic, A. Savovic, D. Markovic, D. Nesic. Climate characteristics of Serbia. Republic Hydrometeorological Service of Serbia. (2013)
- [9] V. Blanka, G. Mezősi, B. Meyer. Projected changes in the drought hazard in Hungary due to climate change. *Időjárás / Quarterly Journal of the Hungarian Meteorological Service* 117(2), 219-237 (2013).
- [10] J. Spinoni, T. Antofie, P. Barbosa, Z. Bihari, M. Lakatos, S. Szalai, T. Szentimrey, J. Vogt. An overview of drought events in the Carpathian Region in 1961–2010. *Advances in Science and Research*, 10, 21-32. DOI: 10.5194/asr-10-21-2013 (2013)
- [11] J. Rakonczai, K. Fiala, M. Mesaroš, A. Frank, S. Popov. Water management conflicts. In: Blanka, V., Ladányi Zs. (eds) Drought and Water Management in South Hungary and Vojvodina. University of Szeged, Szeged, 78-80. (2014)
- [12] B. van Leeuwen, Z. Tobak, F. Kovács, Gy. Sipos. Towards a continuous inland excess water flood monitoring system based on remote sensing data, *Journal of Environmental Geography*, 10(3-4), 9-15. DOI: 10.1515/jengeo-2017-0008 (2017)
- [13] A. Gulácsi, F. Kovács. Drought monitoring of forest vegetation using MODIS-based normalized difference drought index in Hungary. *Hungarian Geographical Bulletin* 67 (1), 29-42. (2018)

INVESTIGATION OF ANTIOXIDANT CAPACITY OF BROWN CAPPED BUTTON MUSHROOM CANDIDATE VARIETIES

Erika Mikola¹, András Geösel², Marietta Fodor¹, Éva Stefanovits-Bányai¹

¹*Department of Applied Chemistry, Szent István University, H-1118 Budapest, Villányi Str. 29-43. Hungary*

²*Department of Vegetable and Mushroom Growing, Szent István University, H-1118 Budapest, Ménesi Str. 44. Hungary*
e-mail: Mikola.Erika@etk.szie.hu

Abstract

The button mushroom (*Agaricus bisporus*) is one of the most widely cultivated mushrooms in the world thanks to its high endogen components. Ingredients of the mushroom with ferric reducing capacity in brown button mushroom can stop or delay the effects of oxidative damage, therefore they play an important role in maintaining health care. During the research process, was used the activity of enzymes participating in antioxidant defense (peroxidase, polyphenol oxidase) and polyphenol content known from non-enzyme defense to describe the reducing properties of brown capped button mushroom candidate varieties, along with the FRAP method based on ferric reducing capacity. Our goal is to compare the number of bioactive substances and substances with significant reducing capacity based on the examined parameters of the button mushroom candidate varieties and, based on the compounds with significant reducing properties to identify the best candidate varieties. According to our results it can be concluded, that there is a strong connection between the measured parameters and the individual candidate varieties, based on which we can choose the candidate variety deemed best.

Introduction

Consuming harvested mushrooms, due to their valuable high endogenous compound content, contributes to proper nutrition and health protection. Mushrooms contain vitamins, vitamin precursors, minerals, trace elements and additionally endogenous materials with specific antioxidant effects, primarily compounds containing phenol [1].

The most widely cultivated mushroom within Europe is *Agaricus bisporus*, which can be found in nature but cultivation technology also highly commercialized. Similar to fruits and vegetables, mushrooms contain valuable substances that play a role in the defense against free radicals and maintaining human health. It is known that an increased number of free radicals can be linked to several diseases [2]. Different enzymes and valuable consumed endogenous components play a role in defense against these free radicals [3, 4]. There have been multiple findings of strong antioxidant effect in the extract of several mushroom varieties, proving that for example, the polyphenols in them have a positive physiological effect [5].

In contrast with crops harvested for hundreds if not thousands of years, during the cultivation of mushrooms, the lack of knowledge about the biology and growing technique of harvested mushrooms is a big challenge. The physiological properties of harvested mushrooms are affected by environmental stresses, therefore the knowledge of their sections of the defense system is crucial. The differences in the activity levels of the peroxidase and polyphenol oxidase enzymes are a great indicator of the different responses given to the reaction to stresses [6] and are an excellent tool to describe resistance [7].

Mushroom reacts to oxidative stresses by preventive and neutralizing activities, which are partially based on the difference between the levels of activity of the enzymes. The examination of endogenous reducing compounds is a proper way of describing the stress-sensitivity and health-protective effect of mushrooms [8, 9].

Materials and methods

The chemicals used during the examination were acquired from Sigma-Aldrich.

The mushroom samples (button mushroom – *Agaricus bisporus*) were cultivated at the Department of Vegetable and Mushroom Growing, Szent István University. The mushrooms were cultivated using the same substrate and cultivation technology, therefore their biophysical parameters are linked with their genetical background. They examined 7 candidate varieties mushrooms were coded B1-B7 and were triturated in a mortar while fresh, with a known amount of extractor, then they were centrifuged and the clear supernatant was stored at -32° C until measurements.

Peroxidase (POD) and polyphenol oxidase (PFO) enzyme activities were measured spectrophotometric method of Shannon [10] and of Flurkey [11] and at $\lambda = 460$ nm and at $\lambda = 420$ nm. The results were given in U/100 g (POD) and U/g (PFO) with respect to dry matter. Total polyphenol content (TPC) was determined by the method of Singleton and Rossi [12] with Folin-Ciocalteu reagent. Color change during the reaction was detected by a spectrophotometric method ($\lambda=760$ nm). The results were expressed in gallic acid equivalent (mM GAE/g dry matter).

The total antioxidant capacity of the different extracts was measured by the FRAP method of Benzie and Strain [13]. The reaction causes a blue color change, which can be detected spectrophotometrically at $\lambda=593$ nm. The results were expressed in ascorbic acid equivalent (μ M AAE/g dry matter).

Results and discussion

The measured enzyme activities in the stipes and caps were different (Figure 1.). The polyphenol oxidase enzyme activity is higher in the stipes in the majority of the cases. The opposite is also true in the case of peroxidase enzyme activity measurements, where the values are higher in the cap of the examined mushrooms. The candidate variety marked B6 showed extraordinarily high values, so presumably, this variety has the most peroxidase and polyphenol oxidase enzyme activity which points to the mushroom's better readiness to stress. The polyphenol oxidase enzyme activity is far greater than that of the peroxidase enzyme activity. The result supports the theory of high polyphenol compound levels in mushrooms.

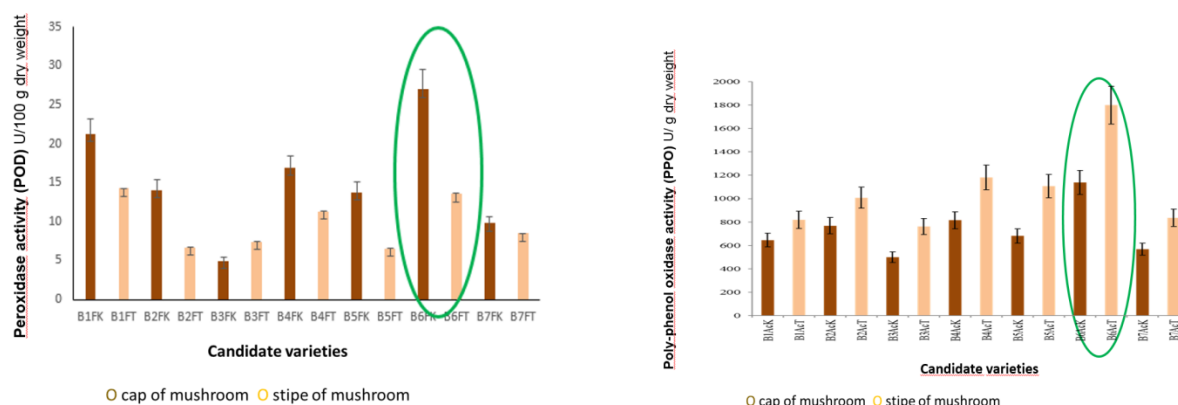


Figure 1. Peroxidase (POD) and Polyphenol oxidase (PFO) enzyme activity of the mushrooms

The total polyphenol content and the antioxidant capacity measurements were made on the separated stipe and cap of the mushroom. Comparing the polyphenol content and antioxidant capacity measured in the cap and stipe of the button mushroom, similar to the previous findings, the values were higher in the cap than in the stipe (Figure 2.). The majority of materials with reducing properties in mushrooms are made of polyphenol-like ingredients, this is supported by the similarity between the illustrations displaying polyphenol content and

antioxidant capacity. Presumably, the differences with candidate variety B6 are caused by another polyphenol based component. The similarity between the diagram displaying the total polyphenol oxidase content and the pictures displaying the number of materials with polyphenol-like properties is proof of the relationship between polyphenol and the enzyme breaking it down. In all cases, especially with candidate variety B6, the accumulated polyphenol content serves the protection of a more resistant candidate variety.

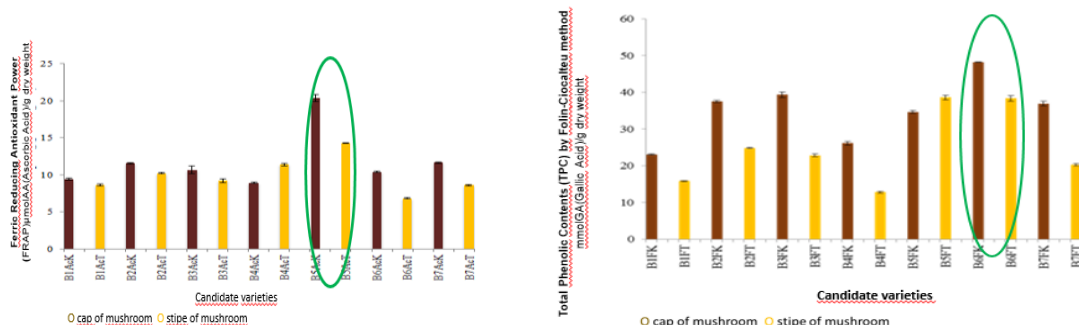


Figure 2. Total polyphenol content (TPC) and Ferric reducing antioxidant capacity (FRAP) of the mushrooms

Conclusion

During the research done on brown button mushroom candidate varieties, comparing antioxidant capacity and total polyphenol content, it can be concluded that polyphenol-based molecules are responsible for the majority of compounds with an antioxidant effect in mushrooms. There are significant differences in the amount of endogenous components measured in the caps and stipes of the different candidate varieties. Based on my research it can be concluded that the components we measured can be isolated, based on which it is possible to choose the candidate variety with the most appealing properties, in this case, candidate variety B6, however, these measurements should, of course, be supported by measuring methods valuable for harvest.

Acknowledgements

The Project is supported by the European Union and co-financed by the European Social Fund (grant agreement no. EFOP-3.6.3-VEKOP-16-2017-00005).

The Project is also supported by the Doctoral School of Food Science SZIU.

References

- [1] N. Kalogeropoulos, A.E. Koutrotsios, M. Aloupi, Food Chem. Toxicol. Greece. 55 (2013) 378-385.
- [2] M. Belury, L.S. Adams, D. Williams, J. Cancer Research and Clinical Oncology. 66 (2006) 12026– 12034.
- [3] A. Garcia-Lafuente, C. Moro, A. Villares, E. Guillaumon, M.A. Rostagno, D.M. Arrigo. Med. Chem. 9 (2010) 125-141.
- [4] H. Ghahremani-Majd, F. Dashti, Horticult. Environ. Biotechn. 56 (3) (2015) 376–382.
- [5] L. Barros, M.J. Ferreira, B. Queiros, I.C.F.R. Ferreira, P.Baptista, Food Chem. 103 (2007) 2:413-419.
- [6] A. Hegedűs, É. Stefanovitsné-Bányai, University of Debrecen, Institutes for Agricultural Research and Educational Farm. Debrecen, 2012.
- [7] A.C. Ramírez-Anguiano, S. Santoyo, G. Reglero, C. Soler-Rivas, J. S. Food and Agricult. 87 (2007) 2983 .
- [8] W. Larcher, Springer-Verlag, Berlin, 1995, 506p.

- [9] M. Kozarski, A. Klaus, D. Jakovljevic, N. Todorovic, J. Vunduk, P. Petrovic, *Molecules*. 20 (2015) 19489-19525.
- [10] L.M. Shannon, E. Kay and J.Y. Lew, *J. Biol. Chem.* 241 (1966) 9:2166-2172.
- [11] W.H. Flurkey, J.J. Jen, *J. Food Sci.* 43 (1978) 1826-1829.
- [12] V.L. Singleton, J.A. Rossi, *American J. Enology and Viticulture*. 16 (1965). 144-158.
- [13] I.F.F. Benzie, J.J. Strain, *Analytical Biochemistry*. 239 (1966) 70-76.

MANAGEMENT OPTIONS OF GLASS AS WASTE

**Zorica Mirosavljević¹, Miodrag Živančev¹, Dušan Milovanović¹, Dragana Štrbac¹,
Milana Ilić Mićunović²**

¹ *Department of Environmental Engineering, University of Novi Sad, 21000 Novi Sad, Trg
Dositeja Obradovića 6, Serbia*

² *Department of Production Engineering, University of Novi Sad, 21000 Novi Sad, Trg
Dositeja Obradovića 6, Serbia
e-mail: zoricavojnovic@uns.ac.rs*

Abstract

One of the most desirable waste management options, of course, is reuse of glass or glass packaging as returnable packaging. However, in this case, glass is not classified as waste. Glass, as waste generated after use, instead of landfilling or incinerator can be used as a resource in the recycling process, with a view to obtaining a new same product or other useful product.

In theory, glass can be fully recycled and can be recycled indefinitely, without loss of quality, however, in order to ultimately obtain the best quality product, the material used for recycling must be of high quality [1]. Therefore, large quantities of waste glass originate from demolished buildings, municipal, industrial and medical waste, which mostly ends up in landfills. Packaging glass production accounts for about 82% of total glass production at glass factories in Europe [2, 3]. For this reason, the options for waste glass packaging management will be considered in the paper.

There are two basic options for waste glass packaging management: Recycling waste glass packaging in order to obtain new glass packaging (Closed Loop Recycling) and Recycling waste glass packaging that does not require re-melting. Of all types of glass, glass packaging is the most important during solid waste management and only glass packaging can be recycled by re-melting to obtain a new glass packaging [3]. Other types of glass have different physical properties and because of this, they cannot be used in this type of glass packaging recycling, as glass recycling could not mix well and melting temperatures vary depending on the type of glass, which would cause defects on the glass newly produced material [4]. Waste glass packaging can be mixed with raw materials or, theoretically, it may be the only raw material used to produce new glass packaging, but in practice, crushed glass, at a rate of 80%, is usually used as input material in the production of new glass packaging [5]. However, crushed glass (cullet), before being included in the production process, must be sorted according to the color of the glass and with a certain degree of purity so as not to degrade the production process of the new glass packaging. The color mix of glass recycling fractions must be less than 2% for the production of transparent glass and less than 5% for the production of colored glass [3]. Unfortunately, so far, Serbia has not provided a system for collecting glass packaging from the municipal solid waste stream, nor is glass packaging recycled in order to obtain new glass packaging. Therefore, it would be useful for Serbia to apply the use of the second waste glass packaging management option. The recycling of waste glass packaging that does not require the re-melting of glass, which is necessary in the production of new glass packaging, has been successfully applied worldwide, and some examples are the use of crushed glass recycling as: additives in the production of bricks, blocks and other ceramics, purification filters water, aggregates in construction, abrasive sanding materials, raw materials for the production of glass beads used in reflective paint for highways, for the manufacture of fiberglass and as fractions for lightening ammunition, and others [6, 7].

When waste glass is not recycled, it is stored or disposed of. The most common disposal options for waste glass packaging are disposal or incineration. However, if this is added to the fact that glass, practically does not break down over time, finding a solution for this type of waste is of great importance from the point of view of environmental protection and preservation.

References

- [1] FEVE. "The European Container Glass Federation - Recycling." 2010. <https://www.britglass.org.uk/our-work/recycling> (accessed Maj 2015).
- [2] IPPC. Intergrated Pollution Prevention and Control-Best available techniques in glass manufacturing industry. IPPC reference document, European Commission (2001).
- [3] Christensen, Thomas H. Solid Waste Technology & Management Volume 1. WILEY, A John Wiley and Sons, Ltd., Publication (2011).
- [4] Vellini, M., Saviola, M. "Energy and environmental analysis of glass container production and recycling." *Energy* 34 (2009): 2137-2143.
- [5] EPA. "Environmental Protection Agency - Glass Production." 2011. <https://www.epa.gov/sites/production/files/2015-02/documents/infosheetn-glassproduction.pdf> (accessed Novembar 2015).
- [6] Park S.B., Lee B.C., Kim J.H. "Studies on Mechanical Properties of Concrete Containing Waste Glass Aggregate." *Cement and Concrete Research* 34 (2004): 2181-2189.
- [7] Vieitez E. R., Eder P., Villanueva A., Saveyn H. End-of-Waste Criteria for Glass Cullet. JRC Technical Proposals, Seville (Spain): Luxembourg: Publications Office of the European Union, European Commission, Joint Research Centre, Institute for Prospective Technological Studies (2011).

SURFACE MORPHOLOGY AND RAMAN STUDY OF GRAPHENE/CuGaO₂ AEROGELS

Cristina Mosoarca¹, Radu Banica¹, Florina Stefania Rus¹, Petrica-Andrei Linul^{1,2}, Daniel Ursu¹, Cosmin Pascariu¹

¹National Institute of Research and Development for Electrochemistry and Condensed Matter, 144 Aurel Paunescu-Podeanu, RO-300569 Timisoara, Romania

²Politehnica University Timisoara, 2 Piata Victoriei Sq., RO-300006 Timisoara, Romania
e-mail: radu.banica@yahoo.com, mosoarca.c@gmail.com

Introduction

Graphene aerogel [1], obtained after a series of steps of cooling and heating under high pressure (supercritical drying) or vacuum (lyophilization), is considered to be the least dense solid in existence, possessing very good elasticity and thus preserving its original form after compression. Due to its low density it also exhibits good absorption properties, finding applications in oil spills and other environmental clean-ups. Hybrid materials like CuGaO₂/graphene aerogels [2] could find applications for a wide range of technologies, from storage and transfer of energy [3] to advanced electrodes and dye-sensitized solar cells.

This paper reports the synthesis of graphene and graphene/CuGaO₂ materials. The samples underwent lyophilization, followed by thermal treatment in vacuum. An aerogel containing a homogenous distribution of CuGaO₂ was obtained by mixing the aqueous solution of graphene oxide and reduced graphene with CuGaO₂, followed by freezing.

The resulting samples were characterized by Scanning Electron Microscopy (SEM), 3D Laser Measuring Microscopy (LSCM) and Raman spectroscopy.

Experimental

The graphene aerogel was obtained from a mixture of graphene oxide (conc. 0.9 mg/mL), prepared by using a modified Hummers method, and graphene Quattro-Type (conc. 1.4 mg/mL) purchased from NanoIntegris. Additionally, the suspension was freeze dried and thermally treated in a GSL-1500X Vacuum furnace (MTI Corporation) at a pressure < 1 Torr and a temperature rise rate of -5 °C/minute, resulting in graphene aerogel samples.

CuGaO₂ was obtained using metal nitrates as precursors under hydrothermal conditions at 250 °C. CuGaO₂ was added to graphene aqueous solution, following the protocol described above, resulting in CuGaO₂/graphene aerogel samples.

Results and discussion

The morphological investigations of topographic surfaces were performed on LEXT OLS4000 3D Laser Measuring Microscope designed for 3D measurement, nanometer level imaging and roughness analysis. The imaging generates a 3D representation of the surface height using LEXT software, by setting the lower and upper limits on the size of the features that are being characterized.

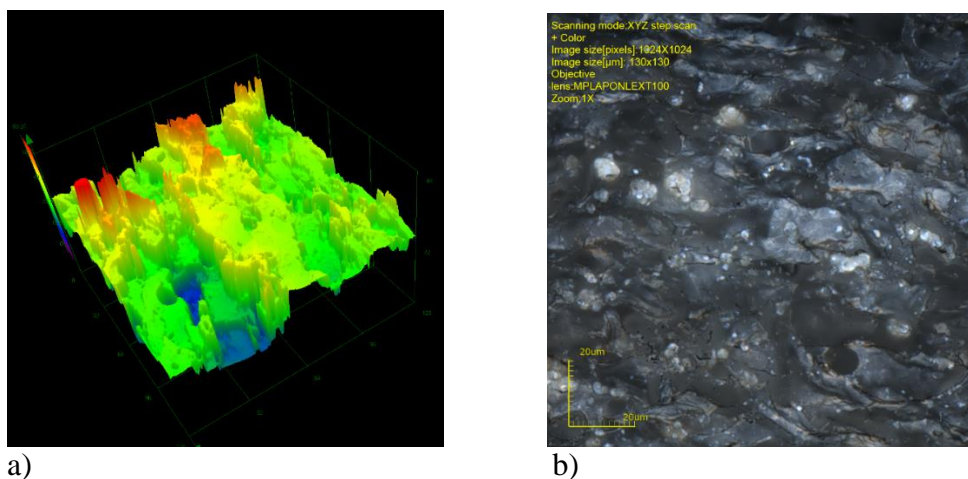


Figure 1. Three-dimensional image taken with an LSCM of CuGaO₂/graphene aerogel, with 100x magnification: (a) in color, (b) black and white.

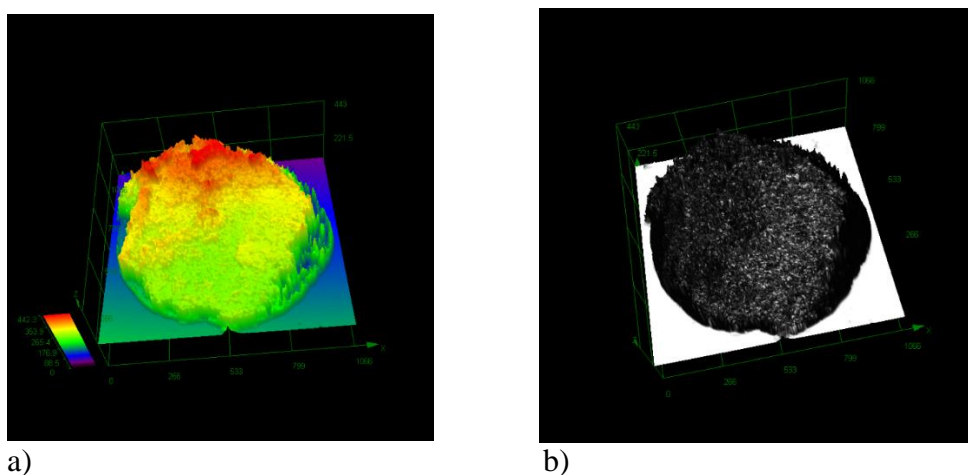


Figure 2. Three-dimensional image taken with an LSCM of CuGaO₂/graphene aerogel, with 10x magnification: (a) in color, (b) black and white.

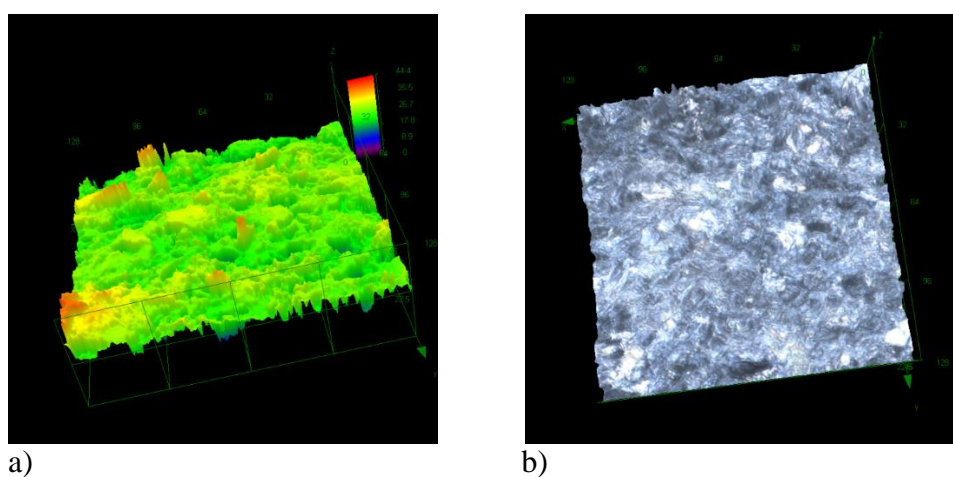


Figure 3. Three-dimensional image taken with an LSCM of graphene aerogel, with 100x magnification: (a) in color, (b) black and white.

The SEM images of CuGaO₂ show that the material is uniformly distributed in the volume of the graphene aerogel (Fig. 4a and 4b), confirming the relative homogenous

dispersion of the inorganic compound in the aerogel matrix. The aerogels have both high electrical conductivity and high polar molecule absorption capacity, the former being due to the reduced graphene, while the latter being due to the functional groups attached to the graphene oxide.

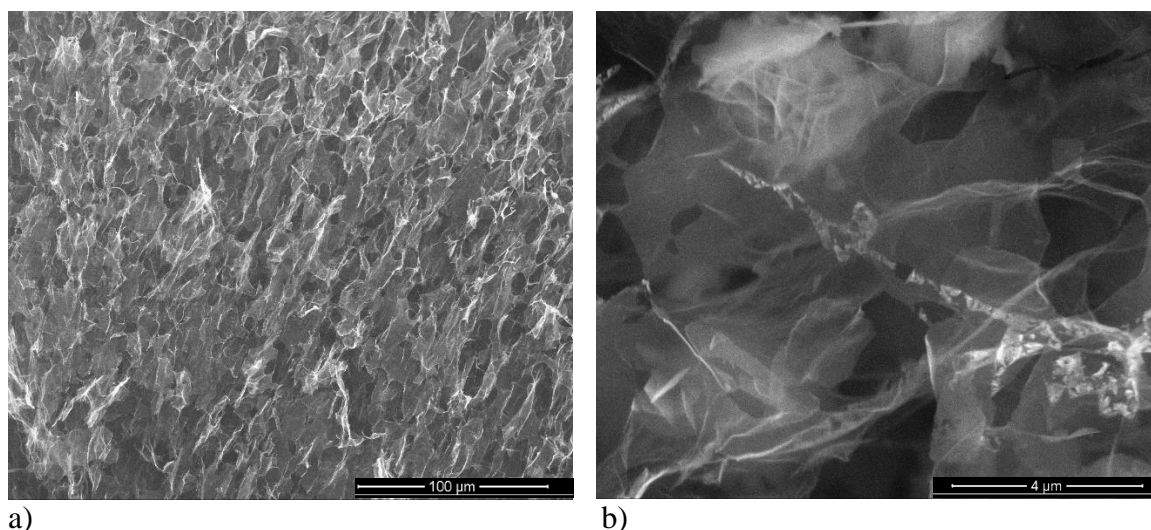


Figure 4. SEM images of CuGaO₂/graphene aerogel: (a) 100 μm, (b) 4 μm magnification.

Raman spectroscopy represents a nondestructive and ambient probing tool which is very sensitive to the microstructure of nanocrystalline materials [4]. Graphene aerogels exhibit common features in the 800–3.250 cm⁻¹ domain. The Raman spectrum, which was recorded using a Nanonics Imaging (Israel) - MultiProbe Imaging - MultiView 1000™ Platform (SPM), equipped with a 532 nm laser, was used in order to identify the vibrational states of the graphene aerogel and is being shown in Fig. 5.

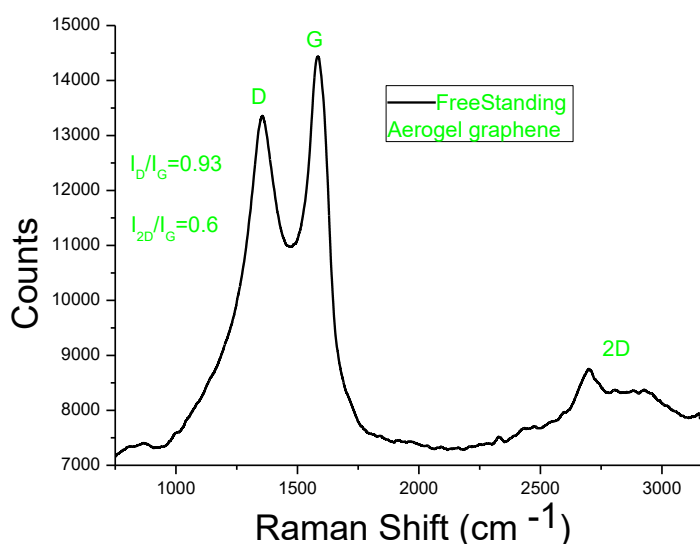


Figure 5. Raman spectrum of graphene aerogel.

Three major peaks are found at 1596, 1353, and 2702 cm⁻¹, representing the G, D, and 2D bands, respectively. The obtained sample exhibits intense G and D bands, which

confirms the presence of defects in the graphene aerogel. The D-mode is caused by a disordered structure of graphene known as an attractive measure of quality. The G peak arises from the stretching of the C-C bonds in graphitic materials, and is common to all sp^2 carbon systems, while the 2D-band (corresponding to an overtone of the D band) is related to the stacking order of graphene layers [5]. Graphene aerogel spectrum exhibits intense D and G bands and a flat 2D region (2400 to 3250 cm^{-1}), with the D band being less intense than the G band ($I_D/I_G = 0.93$). Raman spectrum of a pristine graphene oxide normally shows an intensity ratio between the D and G bands around 0.9 [6], indicating the presence of defects in the crystal lattice which is comparable with as obtained aerogel intensity ratio. We can conclude that the quality of freestanding graphene aerogel is high with low disordered structure.

Conclusion

Graphene and graphene/CuGaO₂ based aerogels, with various possible nanotechnology applications, were obtained by lyophilization followed by thermal treatment in vacuum. The graphene oxide obtained from precursors is partially reduced, during the thermal treatment, while due to condensation and decarboxylation reactions some hydrophilic bonds are lost, leading to a change in the pore sizes after water adsorption. An aerogel with a homogenous distribution of the semiconductor within it was obtained by mixing the aqueous solution containing reduced graphene and graphene oxide with the CuGaO₂ semiconductor, prior to freezing.

Acknowledgements

This work was supported by a grant of the Romanian Ministry of Research and Innovation, CCCDI-UEFISCDI, project number PN-III-P1-1.2-PCCDI-2017-0619/Contract 42/2018 “Nanostructured carbon materials for advanced industrial applications”, within PNCDI III national research program.

References

- [1] G. Gorgolis, C. Galiotis, 2D Materials 7 (2017) 032001.
- [2] D. Ursu, M. Miclau, R. Banica, N. Vaszilcsin, Mat. Lett. 143 (2015) 91-93.
- [3] C. Zamfirescu, I. Dincer, G.F. Naterer, R. Banica, Chem. Eng. Sci. 97 (2013) 235-255.
- [4] E. D. Dikio, F. T. Thema, A. M. Farah, et al., Mater Sci-Pol 31 (2013) 59.
- [5] M. A. Pimenta, G. Dresselhaus, M. S. Dresselhaus, L. G. Cancado, A. Jorio, R. Saito, Phys. Chem. Chem. Phys. 9 (2007) 1276–1291.
- [6] C. Cavallo, M. Agostini, J. P. Genders, M. E. Abdelhamid, A. Matic, J. of Power Sources, 416 (2019) 111-117.

ELECTROCHEMICAL BEHAVIOUR OF LaMnO₃-MODIFIED GRAPHITE ELECTRODES

Bogdan-Ovidiu Taranu*, Iuliana Sebarchievici, Paulina Vlazan, Maria Poienar, Paula Sfirloaga

*National Institute of Research & Development for Electrochemistry and Condensed Matter,
144 Dr. Aurel Păunescu-Podeanu, RO-300569 Timișoara, Romania*

**e-mail: b.taranu84@gmail.com*

Abstract

The electrochemical behaviour of LaMnO₃-modified graphite electrodes was studied using cyclic voltammetry. Potassium ferricyanide was employed as a probe to determine the electroactive surface area of LaMnO₃ modified electrodes and their diffusion coefficient. The electroactive surface area and the diffusion coefficient were calculated using the Randles-Sevcik equation.

Introduction

Perovskites are mixed-metal oxides of great interest for scientific researchers due to their optical, magnetic, catalytic, and electrical properties and not least because of their low price, high oxidation activity and thermal stability [1]. Perovskite ceramics are widely commercialized materials and have found numerous applications, including in automobile exhaust purification, fuel cells, solar cells and sensors [2,3,4,5].

In this paper the electrochemical behaviour of LaMnO₃-modified graphite electrodes is investigated as a preliminary stage in the identification of a suitable application.

Experimental

The electrochemical behaviour of the LaMnO₃ powder was investigated in a conventional three-electrode glass cell equipped with a Pt wire counter electrode, an Ag/AgCl (sat. KCl) reference electrode and a graphite (G) disk electrode ($S = 0.28 \text{ cm}^2$) that served as substrate for a drop-casted thin layer of LaMnO₃. Prior to deposition the G electrode surface was polished and rinsed with double distilled water in an ultrasonic bath. The perovskite suspension was prepared by adding 10 mg LaMnO₃ powder in 500 μL DMF. After 30 min ultrasonication a volume of 15 μL suspension was carefully applied on the graphite electrode and allowed to air dry at room temperature. The modified G electrode was the working electrode and is denoted G_LMO.

Electrochemical experiments were carried out using the PGZ402 Voltalab potentiostat (Radiometer Analytical). Cyclic voltammograms were recorded on the unmodified G electrode as well as on the LaMnO₃-modified G electrode in 0.1 M KNO₃ electrolyte solution containing 4 mM potassium ferricyanide. The voltammograms obtained for the modified electrode were used to calculate its electroactive surface area and the diffusion coefficient (D), using the Randles-Sevcik equation [6,7]:

$$i_p = (2,69 \times 10^5) \times n^{3/2} \times A \times D^{1/2} \times C \times \nu^{1/2}$$

Where: i_p = the peak current; n = the number of electrons involved in the redox process; A = the surface area of the working electrode; D = the diffusion coefficient of the electroactive species; C = the bulk concentration of the electroactive species and ν = the scan rate.

All reagents were of analytical grade and were used as received without further purification. All potentials are referenced to the Ag/AgCl (sat. KCl) reference electrode.

Results and discussion

The voltammetry signals of $\text{Fe}(\text{CN})_6^{3-/4-}$ at the modified graphite electrode were compared to the signals of the bare graphite electrode (Figure 1). The G_LMO response is the most intense and it can be associated with the large electroactive surface area (0.36 vs. 0.09 cm^2) calculated using the Randles–Sevcik equation. The perovskite deposition enhances the electron transfer rate due to the reaction sites it provides.

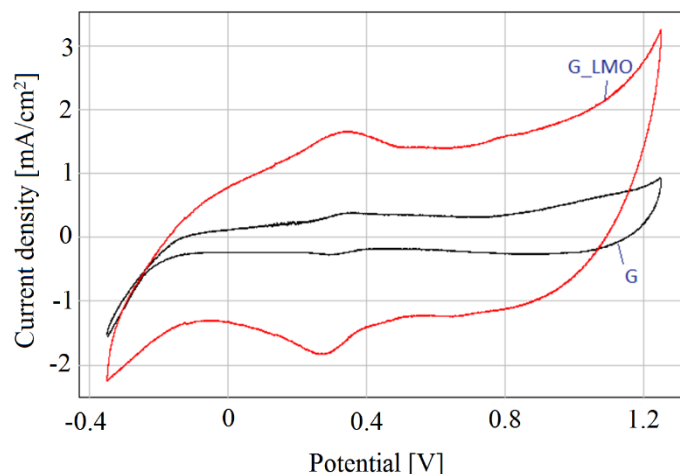


Figure 1. Cyclic voltammograms obtained in 1 M KNO_3 solution supporting electrolyte containing 4 mM $\text{K}_3\text{Fe}(\text{CN})_6$, at 25 mVs^{-1} , for perovskite-modified graphite electrode (G_LMO) compared with the bare graphite electrode (G)

The diffusion coefficients for the two electrodes, in case of the ferrous/ferric redox couple at 298 K, were calculated based on the slope of the plot of the current density vs. the square root of the scan rate. Figure 2 shows the plot of the current density vs. the square root of scan rate obtained for the G_LMO electrode. The redox peak currents are proportional to the square root of the scan rate indicating a diffusion controlled electron-transfer process. The diffusion coefficients for the two electrodes were: $1.127 \cdot 10^{-5} \text{ cm}^2\text{s}^{-1}$ for the G_LMO electrode and $8.342 \cdot 10^{-7} \text{ cm}^2\text{s}^{-1}$ for the bare G electrode. These results show an increase in the apparent diffusivity of the ferricyanide ions in case of the G_LMO electrode by comparison with the bare G electrode.

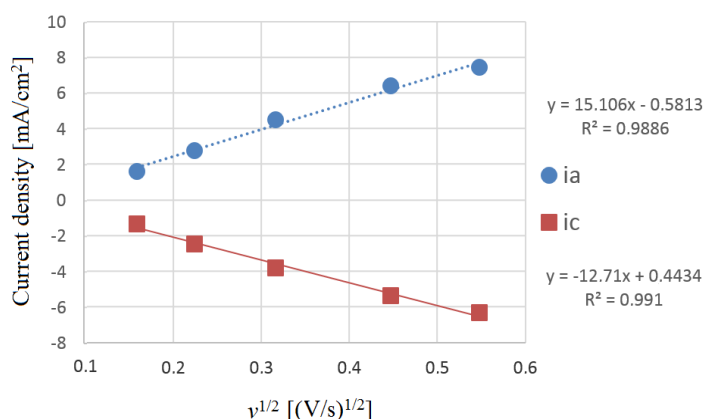


Figure 2. The plot of the current density vs. the square root of scan rate obtained for the G_LMO electrode. ia = anodic current density; ic = cathodic current density

Conclusion

LaMnO₃ was applied on the surface of a graphite electrode. The perovskite acted as an electrode modifier that enhanced the graphite electrode's electroactive surface area, which was calculated using the Randles–Sevcik equation. Furthermore, the perovskite material led to an increase in the apparent diffusivity of the ferricyanide ions.

Acknowledgements

The authors are acknowledging INCEMC Timisoara for financial support as part of the PN 19 22 02 01, 40N/2019, NUCLEU project.

References

- [1] N. Labhasetwar, G. Saravanan, S.K. Megarajan, N. Manwar, R. Khobragade, P. Doggali, F. Grasset, *Sci. Technol. Adv. Mater.* 16 (2015) 1-13.
- [2] F.E. Lopez-Suarez, A. Bueno-López, M.J. Illan-Gomez, J. Trawczynski, *Appl. Catal. A.* 485 (2014) 214-221.
- [3] L. Guangchuan, L. Shuguang, L. Changlong, O. Xiuqin, *J. Rare Earth.* 25 (2007) 264-267.
- [4] J. Cui, H. Yuan, J. Li, X. Xu, Y. Shen, H. Lin, M. Wang, *Sci. Technol. Adv. Mater.* 16 (2015) 1-14.
- [5] J.W. Fergus, *Sens. Actuator B-Chem.* 123 (2007) 1169-1179.
- [6] A.J. Bard, L.R. Faulkner, *Electrochemical Methods: Fundamentals and Applications*, John Wiley & Sons: Hoboken, NJ, USA, 2001.
- [7] A. Baciú, A. Remes, E. Ilinoiu, F. Manea, S.J. Picken, J. Schoonman, *Environ. Eng. Manag. J.* 11 (2012) 239-246.

MEASUREMENT OF AEROSOL FROM EXHAUST EMISSION OF MOTOR VEHICLES USING PHOTOACOUSTIC SPECTROSCOPY

Ouma E. Awuor, Anna Szabó, Zoltan Bozóki

*Department of Optics and Quantum Electronics, University of Szeged, H-6720 Szeged,
Hungary*

E-mail: mlawuor252@gmail.com

Abstract

There is an international concern about the adverse health effects of motor vehicles generated air pollutants in many towns and cities. To investigate the importance and effects of exhaust emissions from both diesel and gasoline motor vehicles to the human population, it is required to effectively measure the aerosol levels emitted into the atmosphere. This work aimed to measure emitted exhaust gases from diesel and gasoline light duty vehicles during controlled laboratory experiments using photoacoustic spectroscopy (PAS) method and a commercially available soot sensor (Opacimeter) as a control set up. Diesel and gasoline light duty vehicles were tested with altering engine speed without load (without dynamometer brake). From the experiments it was established that the response of the PAS system in aerosol measurements agreed well with the well-established and commercially available Opacimeter.

Introduction

Aerosol emission from anthropogenic sources e.g. automotive industry has become an environmental concern on both global and regional scales, mostly because of the emitted chemicals harmful to both animals and humans [1]. Of major interest are the gaseous pollutants present in the vehicles exhaust emissions whose measurement has previously been done using several documented methods which largely depended on the sampling technique and instrument used [2]. Hence there is need to use instruments with great sensitivity that are capable of real time measurement e.g. Photoacoustic Spectroscopy (PAS). PAS is the measurement of the effect of absorbed light on matter (gas, liquid and solid) by means of acoustic detection and has been labelled as highly sensitive and selective method under laboratory and field conditions. Absorption of amplitude-modulated light periodically heats light-absorbing particles in the sample aerosol. Conduction of this heat to the surrounding gas generates pressure waves (acoustic), which are recorded by a microphone. Therefore, the microphone signal is proportional to the volume concentration of the measured aerosol [3].

Experimental

In the experimental set up, two test vehicles were used: Volvo (diesel engine) and Skoda (gasoline engine). Measuring instrumentation was attached to the exhaust pipe of each vehicle using PTFE pipes as shown in Fig. 1. The inlets of the two instruments were placed as close as possible to each other and to the exhaust end to ensure homogeneity in sampling time and points. Gaseous aerosol from the exhausts was then sampled using both PAS and Opacimeter in a time scale of 20 to 40 minutes each. For the PAS, a diode laser at an emission wavelength of 1064 nm was carefully chosen to be the light source. Measurement was then done under altering engine speed without load (without dynamometer brake). The signal generated was then recorded and analysed using electronics (manufactured by Videoton Holding Zrt.), which was connected to a computer.



Figure 1: Picture showing connection of the pipes to the car exhaust

Results and discussion

The longitudinal chamber used was first calibrated and tested with reference to the Soot sensor (opacimeter) and the results are as shown below.

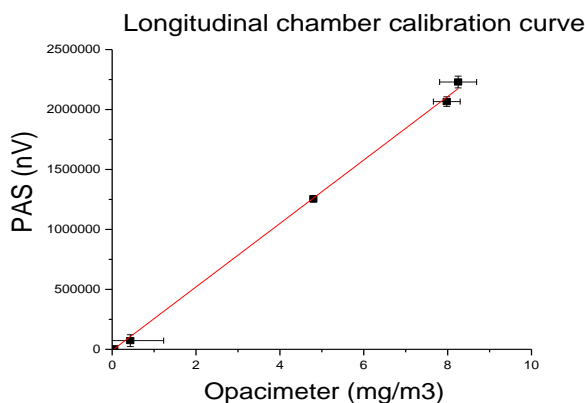


Figure 2: Calibration results

The two instruments were then operated simultaneously. Figure 3. shows the recorded photoacoustic signal and the aerosol concentration measured by the opacimeter.

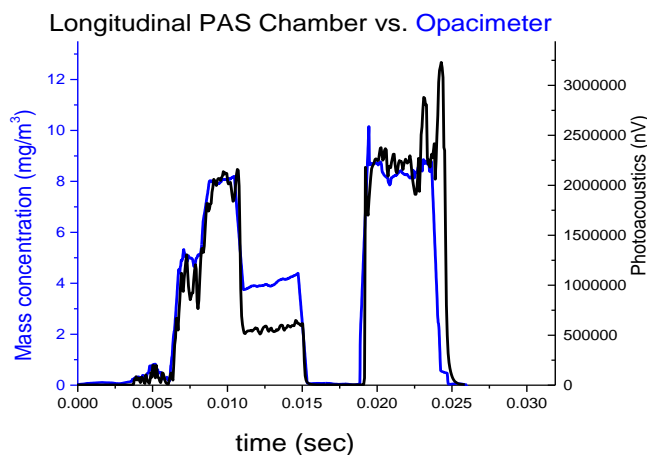


Figure 3: Performance comparison between PAS and the commercial Opacimeter

The Pearson's correlation coefficient between PAS (longitudinal chamber) and the commercial Opacimeter was also calculated and found to be 0.95845. This shows that the two equipment have a positive linear dependence i.e., an increase in one corresponds to an increase in the other.

Conclusion

It has been demonstrated that PAS of laser wavelength 1064 nm, can be used to quantitatively measure the concentration of gaseous aerosol emission in both diesel and gasoline vehicle exhaust. From the experiments it was established that the response of the PAS system in aerosol measurements agreed well with the well-established and commercially available

Opacimeter. The signal delay observed in the results was mainly due to the use of different pipe lengths and flow rates during aerosol sampling.

Acknowledgements

This work was supported by GINOP-2.2.1-15-2017-00036, by the European Union. The author would like to thank Nóra Füle-Ducsay and Hoang Le Minh Tien for their technical assistance.

References

- [1] J. E. Penner, M. O. Andreae, H. Annegarn, L. Barrie, J. Feichter, and D. Hegg, "Aerosols, their Direct and Indirect Effects," in *Climate Change 2001: The Scientific Basis. Contribution of Working Group I to the Third Assessment Report of the Intergovernmental Panel on Climate Change*, Cambridge, UK, and New York, NY, USA: Cambridge University Press., 2001, pp. 289–348.
- [2] M. Peter H, "A review of atmospheric aerosol measurements," *Atmos. Environ.*, vol. 34, no. 12–14, pp. 1959–1999, 2000.
- [3] K. András *et al.*, "Accuracy assessment of aerosol source apportionment by dual wavelength photoacoustic measurements," *J. Aerosol Sci.*, vol. 104, no. April 2016, pp. 10–15, 2017.

LONG BONDS IN RADICAL CATIONS OF SORBITOL AND MANNITOL

Mihai-Cosmin Pascariu^{1,2}, Radu Bănică¹, Eugen Sisu³

¹*Renewable Energies – Photovoltaic Laboratory, National Institute of Research & Development for Electrochemistry and Condensed Matter – INCEMC Timișoara, 144 Aurel Păunescu-Podeanu, RO-300569 Timișoara, Romania*

²*Faculty of Pharmacy, “Vasile Goldiș” Western University of Arad, 86 Liviu Rebreanu, RO-310414 Arad, Romania*

³*“Victor Babeș” University of Medicine and Pharmacy of Timișoara, Faculty of Medicine, 2 Eftimie Murgu Sq., RO-300041 Timișoara, Romania
e-mail: mihai.cosmin.pascariu@gmail.com*

Abstract

The quantum chemical analysis (RM1 semiempirical method) of sorbitol and mannitol in their radical cation states reveals C-C long bonds with lengths around 2.1 or 2.2 Å. In some cases, the stabilities of these long bonds appear to be related with the intensities of the corresponding peaks found in the mass spectra of these hexitols.

Introduction

Sorbitol and mannitol belong to the chemical family of sugar alcohols, or the broader category of polyols (particularly hexitols). Polyols are polyhydric alcohols derived through chemical reduction (hydrogenation) of reducing sugars. Most of the commercially important polyols are produced by chemical hydrogenation of their corresponding reducing sugars. For example, sorbitol is produced by hydrogenation of dextrose (glucose), while mannitol is derived through fructose hydrogenation [1].

Alongside monosaccharide sugars, polyols are carbohydrate materials of considerable commercial value and interest to the commercial food sector. Besides their role of food nutrients and sweeteners, they also provide specific functional properties in manufactured food products [1].

Sorbitol belongs to the group of naturally occurring hexitols. In fruit and leaves, sorbitol is formed as a biochemical intermediate in the synthesis of starch, cellulose, sorbose, or vitamin C. In animals, sorbitol can be detected as an intermediate in the absorption of glucose or the formation of fructose via glucose. Sorbitol is produced on a large scale by means of the catalytic hydrogenation of D-glucose (dextrose) [2].

D-Mannitol is a hexitol derived from D-mannose. D-Mannitol is widely distributed in nature, occurring in olive trees, plane trees, and fruit and vegetables. It is also naturally found in some edible fungi and Laminaria species seaweed (marine algae, especially brown algae, containing 10–20% mannitol, depending on the time of harvest). Furthermore, a large number of fungi and bacteria can produce this polyol from glucose, fructose, or sucrose [2].

In this paper we investigate, using computational methods, the presence of C-C long bonds in the radical cations of sorbitol and mannitol and the possibility of a relation between the intrinsic stability of such long bonds and the intensity of some peaks found in the mass spectra of the two compounds.

Experimental

The molecules of sorbitol and mannitol were initially modelled using the *HyperChem* software [3]. After the “Add H & Model Build” command, the starting neutral molecules were pre-optimized using the MM+ force field and then optimized with the RM1 semiempirical method [4]. The radical cations (formal charge “+1”, spin multiplicity “2”)

were obtained from these structures and were finally optimized with the RM1 semiempirical method. As for “Spin Pairing”, RHF operators were used for neutral molecules, while UHF operators were employed for radical cations. The SCF “Convergence limit” was set at 10^{-5} , without using the “Accelerate convergence” feature. For geometry optimization and $\Delta_f H$ calculation, the “Polak-Ribière (Conjugate gradient)” algorithm was selected with a RMS gradient of 0.01 kcal/(Å mol), the molecules being considered in vacuum (conditions similar to those found in the EI-MS detectors). The radical cation molecular graphs showing the total spin density were plotted using the “Wire mesh” rendering (carbon – cyan, hydrogen – white, oxygen – red, positive spin density – green wire mesh, and negative spin density – violet wire mesh).

The EI-MS spectral data for sorbitol and mannitol were downloaded from the *NIST Chemistry WebBook* site [5] and visualized using the *ACD/Labs 6.00* software, while the exact masses, the molecular weights and the m/z values given under the chemical formulas are those predicted by the *ChemBioDraw Ultra* (v. 12.0) program (included in the *ChemBioOffice 2010* software).

Results and discussion

The EI-MS spectra of sorbitol and mannitol are shown in Fig. 1, while their chemical structure and five possible fragmentations, which are responsible for some of the EI-MS peaks, are shown in Figs. 2 and 3. The intensity of these peaks are shown in Tables 1 and 2.

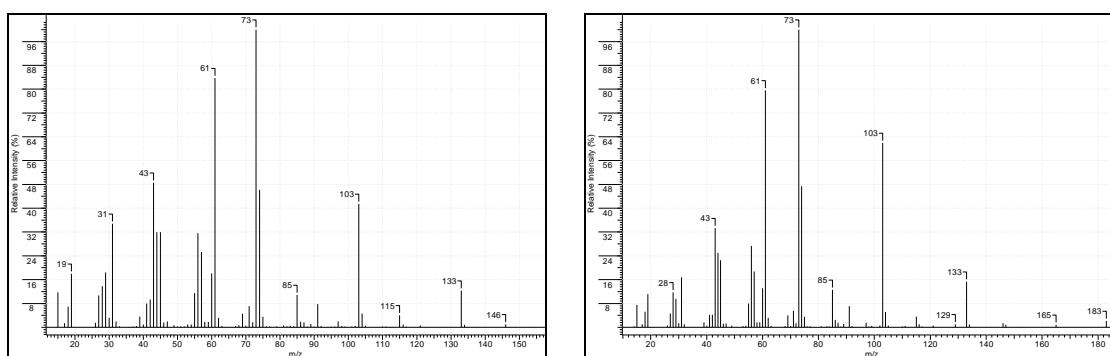


Figure 1. EI-MS spectrum of sorbitol (left) and mannitol (right)

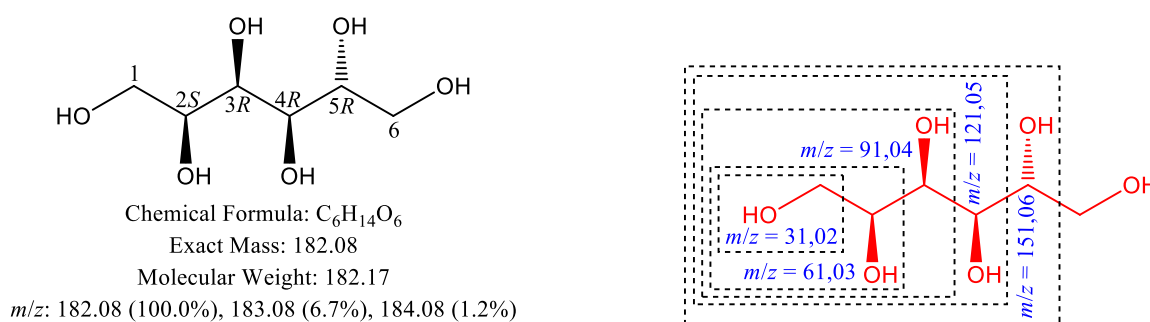


Figure 2. Left: chemical structure of sorbitol (with carbon chain numbering and optical configurations); right: five possible EI-MS fragmentations

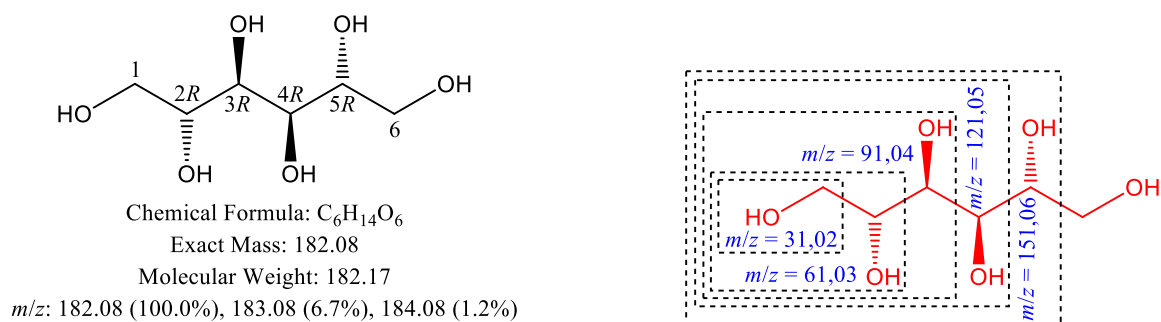


Figure 3. Left: chemical structure of mannitol (with carbon chain numbering and optical configurations); right: five possible EI-MS fragmentations

Table 1. Intensity of target peaks for sorbitol

m/z	RI (%)	TIC (%)
31	34.793	4.937
61	83.698	11.877
91	7.791	1.105
121	0.600	0.085
151	0	0

Table 2. Intensity of target peaks for mannitol

m/z	RI (%)	TIC (%)
31	16.792	2.754
61	79.598	13.055
91	7.091	1.163
121	0.600	0.098
151	0.100	0.016

The ball-and-stick model of different variants of radical cations, obtained by using the RM1 semiempirical method, are shown in Figs. 4 (sorbitol) and 5 (mannitol). The position of the long bonds is clearly established using the green wire mesh, which shows the total spin density. The C-C bond lengths, together with heat of formation values for the neutral species and the various forms of radical cations, are presented in Tables 3 and 4.

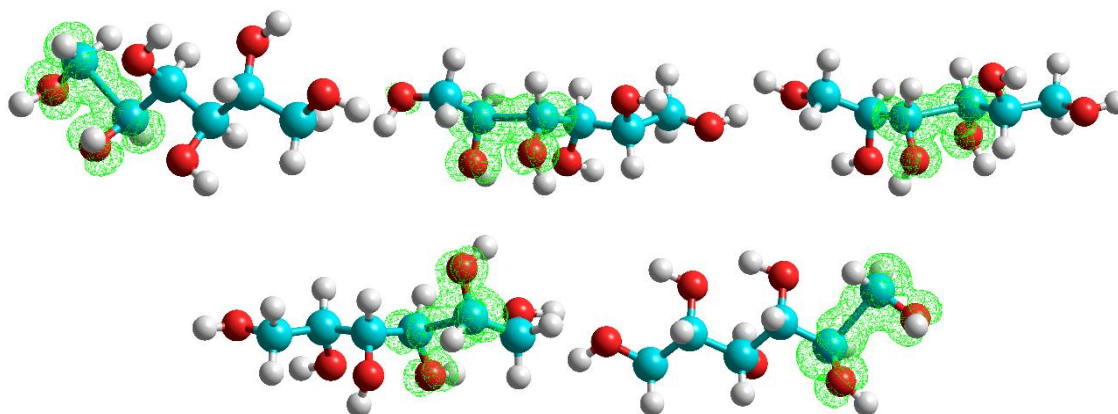


Figure 4. Ball-and-stick model of different variants of radical cations of sorbitol (numbering of carbon atoms starts from left)

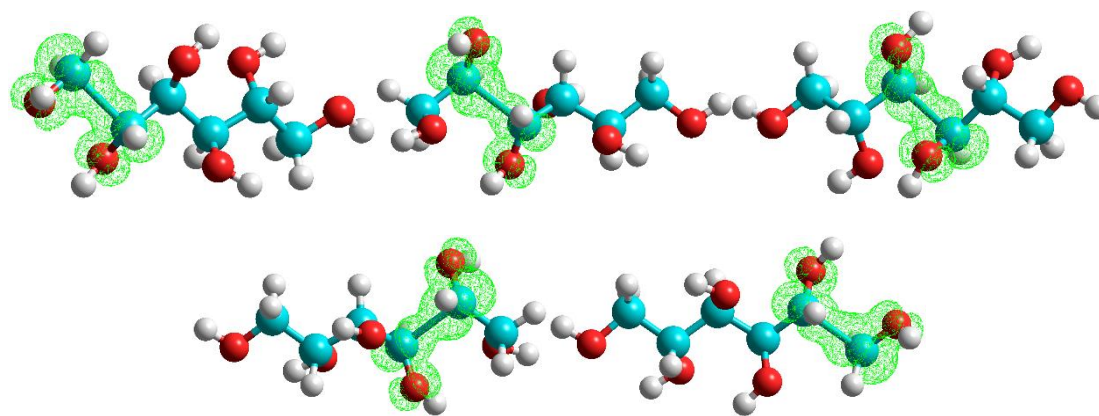


Figure 5. Ball-and-stick model of different variants of radical cations of mannitol (numbering of carbon atoms starts from left)

Table 3. Sorbitol: C-C bond lengths and heats of formation for the neutral molecule and for the radical cation (the most stable form is shown in red)

Bond	Neutral molecule		Radical cation	
	Length (Å)	$\Delta_f H$ (kcal/mol)	Length (Å)	$\Delta_f H$ (kcal/mol)
C1-C2	1.538	446.909	2.100	650.946
C2-C3	1.539		2.084	652.723
C3-C4	1.542		2.122*	651.854*
C4-C5	1.543		2.167	648.572
C5-C6	1.538		2.101	652.330

*MM+ pre-optimization of radical cation

Table 4. Mannitol: C-C bond lengths and heats of formation for the neutral molecule and for the radical cation (the most stable form is shown in red)

Bond	Neutral molecule		Radical cation	
	Length (Å)	$\Delta_f H$ (kcal/mol)	Length (Å)	$\Delta_f H$ (kcal/mol)
C1-C2	1.536	450.572	2.110	656.222
C2-C3	1.543		2.179	651.038
C3-C4	1.543		2.145	651.544
C4-C5	1.543		2.180	651.038
C5-C6	1.536		2.110	656.222

For both hexitols it can be seen that, among the five considered EI-MS peaks, the one from m/z 61 shows the highest intensity, in relation to the preferred long bond position at C4-C5 (or, with the same heat of formation value, at C2-C3 for mannitol), which gives for the radical cation the lowest heat of formation.

In the case of sorbitol, this is followed by m/z 31, corresponding to the breaking at C1-C2, while the breaking at C3-C4 shows the lowest probability, according to the higher heat of formation value for the corresponding radical cation.

For mannitol, the reverse was found for the cleavages at C1-C2 or C5-C6 and, respectively, C3-C4. However, the particularly high value for the heat of formation in the case of C1-C2 or C5-C6 fragmentations could indicate that these might not be the ground states of these radical cations, and more work would be required in order to geometrically optimize these structures.

Conclusion

The present computational study has proved the existence of C-C long bonds (around 2.1 or 2.2 Å) in radical cations of sorbitol and mannitol. Also, a relation with the intensity of some mass spectrometric peaks for the two compounds was established.

Acknowledgements

Part of the research was performed at *The Center of Genomic Medicine* from the ‘Victor Babes’ University of Medicine and Pharmacy of Timisoara, POSCCE 185/48749, contract 677/09.04.2015.

References

- [1] R.B. Friedman, in: B.O. Fraser-Reid, K. Tatsuta, J. Thiem (Eds.), *Glycoscience*, Springer, Berlin, Heidelberg, 2008, pp. 841-856, DOI: 10.1007/978-3-540-30429-6_19.
- [2] H. Schiweck et al., in: *Ullmann's Encyclopedia of Industrial Chemistry*, 2012, DOI: 10.1002/14356007.a25_413.pub3.
- [3] HyperChem™ Professional, Hypercube, Inc., 1115 NW 4th Street, Gainesville, Florida 32601, USA.
- [4] G.B. Rocha, R.O. Freire, A.M. Simas, J.J.P. Stewart, *J. Comput. Chem.* 27 (2006) 1101, DOI: 10.1002/jcc.20425.
- [5] William E. Wallace (director), “Mass Spectra” by NIST Mass Spectrometry Data Center in NIST Chemistry WebBook, NIST Standard Reference Database Number 69, Eds. P.J. Linstrom and W.G. Mallard, National Institute of Standards and Technology, Gaithersburg MD, 20899, <https://doi.org/10.18434/T4D303> (retrieved September 20, 2019).

THE USE OF INVASIVE SPECIES AS WATER CONTAMINATION BIOINDICATORS: *SINANODONTA WOODIANA* CASE

Aleksandra Petrović¹, Vojislava Bursić¹, Gorica Vuković², Dušan Marinković¹, Ivana Ivanović¹, Bojan Konstantinović¹, Nikola Puvača³

¹Department for Environmental and Plant Protection, Faculty of Agriculture, University of Novi Sad, 21000 Novi Sad, Trg Dositeja Obradovića 8, Serbia

²Institute of Public Health of Belgrade, 11000 Belgrade, Bulevar despota Stefana 54A, Serbia

³Faculty of Economics and Engineering Management, University Business Academy, 21000 Novi Sad, Cvečarska 2, Serbia
e-mail: petra@polj.uns.ac.rs

Abstract

Freshwater mussels are considered as the suitable bioindicators of ecosystems health, both, aquatic and surrounding terrestrial. These species have high filtration rates, providing an important link between the water column and the benthic zone, and also playing an important role in the nutrient cycling, substrate stability, bioturbation, and controlling the levels of suspended solids. The aim of this study is to obtain preliminary results of *Sinanodonta woodiana* use, as a potential bioindicator for pesticide residues detection in the river Danube. LC-MS/MS method indicated the qualitative and quantitative presence of six pesticide residues: chlorotoluron, diuron, linuron, metolahlor, terbuthylazine and acetamiprid in *S. woodiana* soft tissue. Biomonitoring with mussels has several potential applications. It may be used to complement or supplement the traditional water and sediment monitoring programs.

Introduction

The freshwater bodies, lakes and rivers in Europe, are under heavy contamination pressure by different organic and inorganic pollutants and contaminants. In order to preserve these aquatic habitats, the use of bioindicators and biomonitors is more than obligatory in monitoring programmes. Almost any organism could indicate the processes of the environment degradation, but some organisms perform this function much better than the others. The high-quality bioindicators should be sensible but tolerant, capable for bioaccumulation, widely distributed, easy to sample, identify and analyze.

Freshwater mussels are usually considered as the suitable bioindicators and biomonitors of ecosystems health, both, aquatic and surrounding terrestrial. These species have high filtration rates, providing an important link between the water column and the benthic zone, and also playing an important role in nutrient cycling, substrate stability, bioturbation, and controlling the levels of suspended solids. The abundance, diversity and species richness of freshwater mussels are severely decreasing worldwide, where nearly half of the species are thought to be currently threatened. Consequently, the logic question has arisen: if the mussels are excellent bioindicators, but most species are currently endangered, is it justify and economically effective to use invasive mussels, such as *Sinandonta (Anodonta) woodiana* (Lea, 1834) as the water contamination bioindicator?

S. woodiana, Chinese pond mussel, is a native species of East Asia and lives in a large area from the River Amur, through China to Cambodia. In the early 1970s, different species of carp fish, infested with glochidia, have been excessively imported to European countries for biological control of organic debris, freshwater plants and mosquitos. In this way, *S. woodiana* spread out and established stabile populations in almost all European countries, including some Indonesian islands, Dominican Republic, Costa Rica and recently USA [1]

[2]. In some countries, for example Italy, Chinese pond mussel was introduced intentionally, related to some commercial activity, such as the production of artificial pearls in Tuscany [3] and as a “bio filter” for garden ponds, commercially sold in some garden centers [4].

More than 140 billion kilograms of fertilizers and large quantities of pesticides are used and disposed annually in the agricultural sector, creating huge sources of diffuse pollution in freshwater ecosystems. The presence of these contaminants and pollutants in aquatic and terrestrial ecosystems has become a globally important issue. The river ecosystem is a subject to increased stress associated with diverse human activities. Modern agriculture contributes to the soil and water pollution, as it often involves the use of different pesticides, which results in a gradual increase of their residues and metabolites in the aquatic environment and consequently in aquatic organisms.

According to [5], the mussels may cumulate, without any distinct physiological effects, significant amounts of pollutants in both, soft tissues and shells. The amounts of the actual accumulation may not be indicative of real pollutant emissions only, but they also may indicate the mobilization and transfer within the trophic webs of the long-term pollutant accumulations that are contained in the aquatic ecosystems bottom sediments.

The aim of this study is to obtain preliminary results of *S. woodiana* use, as a potential bioindicator for pesticide residues detection in the river Danube.

Experimental

Mussel collection

The mussels were collected from two localities on the river Danube: Petrovaradin and Sremski Karlovci. The transect method was used for mussel sampling, along the 200 m of the coast and 5 m from the coast, at a depth of 0.10 to 1.5 m. The mussels were collected by hand or by sieving the sediment using a 1 m² mesh (diameter 25x25 mm). Individuals longer than 7 cm were separated and only *S. woodiana*, which is an invasive and allochthonous species. The mussels were washed in tap and distilled water, the shells were removed, and complete soft tissues were prepared for further analyses.

Pesticide residues detection

A validated LC-MS/MS method was used for qualitative and quantitative determination of pesticide content in the mussel soft tissue. The validation was done in accordance to SANTE/11813/2017 by triple quadrupole mass spectrometer (Agilent 6410B Triple Quad Mass Spectrometer, USA) in positive electrospray ionization using multiple reaction monitoring mode (MRM). The method was validated for accuracy, precision, linearity, limits of detection and limits of quantification (LODs and LOQs). The extracts were obtained using the acetonitrile-based QuEChERS preparation technique. The calibration was performed in MMC. The calibration range was from 0.01 to 0.5 µg/ml. The obtained R² was higher than 0.99 for all the studied pesticides. The LODs were below 0.005 mg/kg and the LOQs were set on 0.01 mg/kg. For the recovery, the samples were spiked with the analytes at three concentration levels (0.05, 0.1 and 0.2 mg/kg).

Results and discussion

The average recoveries for all analytes were in the range from 70.1 to 91.3% (RSDs 3.77 – 10.12%) (Table 1.). The obtained mean values of the responds were with RSD <20%. An efficient, sensitive and reliable LC–MS/MS(ESI), has been developed and applied for the detection of 26 pesticides in mussel soft tissue.

Table 1. Average recoveries

Pesticides	R ²	Average recoveries ± RSD (%)
Carbendazim	0.9941	80.7±3.77
Metribuzin	0.9990	91.2±6.42
Chloridazon	0.9998	89.4±5.71
Chlortoluron	0.9936	81.5±6.91
Chloroxuron	0.9995	90.8±5.17
Desethyl atrazine	0.9994	86.4±4.87
Sebutilazin	0.9990	87.2±10.12
Dimefuron	0.9993	80.4±8.26
Diuron	0.9998	72.5±5.83
Etidimuron	0.9998	98.8±7.13
Isoproturon	0.9997	70.1±9.11
Metobromuron	0.9996	72.4±6.47
Metamitron	0.9989	71.3±5.63
Metazachlor	0.9999	91.3±6.53
Methabenzthiazuron	0.9997	83.5±7.91
Metolachlor	0.9997	70.7±6.42
Propazine	0.9998	80.1±7.70
Simazine	0.9974	82.4±6.47
Terbuthylazine	0.9988	73.4±7.61
Terbuthylazine-desethyl	0.9996	82.7±5.17
Acetamiprid	0.9918	81.4±5.88
Imidacloprid	0.9997	82.2±4.90
Clothianidin	0.9926	89.1±8.26
Thiamethoxam	0.9990	86.7±5.51
Thiacloprid	0.9967	81.4±5.72
6-Chloronicotinic acid	0.9948	80.7±6.24

QuEChERS method indicated the qualitative and quantitative presence of six pesticide residues: chlorotoluron, diuron, linuron, metolachlor, terbuthylazine and acetamiprid in *S. woodiana* soft tissue (Table 2.).

Table 2. Pesticide residues in mussel soft tissues (mg/kg)

Pesticide residues	Locality	
	Petrovaradin	Sremski Karlovci
Chlorotoluron	0.013	0.016
Diuron	0.006	0.003
Linuron	0.002	0.002
Metolachlor	0.010	0.005
Terbuthylazine	0.003	0.003
Acetamiprid	0.003	-

Similarly to pesticide residues, the mussels' ability to accumulate heavy metals appears to be a taxonomic feature that depends on both, individual requirements for bio-elements and behavior, as well as on the related metabolic processes in a given environment [6]. Recorded differences in the pollutant concentrations of specific mussel species living in the same

environment are the result of the selective elements uptake with food and the variable regulation of their concentration levels in soft tissues and shells [7].

S. woodiana represent an excellent bioindicator species, as it is easy for handling regarding the size (it could grow up to 30 cm) [8], short juvenile stage, as this species reproduces already in the first year of life, having reached the shell length of 3-4 cm [9] and long life span, as the individuals can live between 12 – 14 years [10]. The species is a habitat generalist found in heavily modified and artificial habitats, tolerant to high siltation rates [1] and prefers habitats with higher temperatures (the optimal thermal conditions vary within 10 and 35°C) [11]. Larvae, glochidia are released from May to August (mainly in June and July), and this species can develop 2 – 3 larval stages per year, compared to the native species which reproduce once a year. Parasitic period lasts between 5 and 15 days, depending on the water temperature [10].

As spatial bioindicators and biomonitors, mussels are superior to fish, which are very mobile and in some cases migratory. Furthermore, as a monitoring medium, mussels are also superior to the sediment, because they can be more easily standardized. While the sources of biological variability in mussel samples can be controlled, the factors, such as particle size distribution and organic content, which strongly affect the contaminant adsorption to the sediments, cannot [12].

Biomonitoring with invasive mussel species has several potential applications. They may be used to complement or supplement the traditional water and sediment monitoring programs, principally to provide information on bioavailability, simultaneously preserving the native mussel species populations. Residues in mussels can also be used to define the impact zone of potential point source pollution and can serve as a feedback mechanism for determining the effectiveness of pollution control measures as they are implemented. These organisms constitute the major portion of the benthic biomass in many areas and they significantly modify the sediment by burrowing, respiratory and excretory activities, thus altering the profiles of contaminants in bottom sediment and contributing to their transformation [12].

Conclusion

European rivers are contaminated with pesticides and in almost half of the river basins, the levels of chemicals that can harm fish, invertebrates and algae have been measured. A significant improvement in water quality has been declared a goal for all EU Member States and provided by the provisions of the Water Framework Directive. However, new scientific research has shown that this goal was not achieved due to the high level of the toxic substances in the water. The Danube, with its fascinating ecosystems that provide from recreation and fishing to river drinking water for millions of people, are polluted by chemicals from cities, agriculture and industry. Such a chemical "cocktail" seriously damages aquatic organisms, but also poses a potential risk to humans, other animals and environment.

Acknowledgements

The authors acknowledge the financial support of the Ministry of Education and Science, Republic of Serbia, Project Ref. III43005 and TR31084.

References

- [1] M. Paunovic, B. Csányi, V. Simic, B. Stojanovic, P. Cakic, *Aquat. Invasions*. 1(3) (2006) 154-160.
- [2] J. Lajtner, P. Crnčan, *Aquat. Invasions*. 6(1) (2011) 119-124.
- [3] P. Berni, S. Bitossi, M. Salvato, M. Orlandi, J. Salviati, M. Silvestri, P. Megale, P. Orlandi, R. Billiard, International Workshop "Tinca e acquacoltura nelle acque interne", Italy (2004) 179-185.

- [4] J. Packet, T. Van den Neucker, R. Sablon. Research Institute for Nature and Forest, Brussels, Belgium (2009) available:
http://ias.biodiversity.be/meetings/200905_science_facing_alien/poster_21.pdf.
- [5] E. Królak, B. Zdanowski, Arch. Pol. Fish. 9(2) (2001) 229-237.
- [6] E. Jurkiewicz-Karnkowska, Wiad. ekol. 40(3) (1994) 127-141.
- [7] T.R. Parsons, C.A. Bawden, W.A. Heath, J. Fish. Res. Board Can. 30 (1973) 1014-1016.
- [8] A. J. Benson, USGS Nonindigenous Aquatic Species Database (2015), available:
<http://nas.er.usgs.gov/queries/FactSheet.aspx?speciesID=2824>.
- [9] J. Domagała, A.M. Łabęcka, B. Migdalska, M. Pilecka-Rapacz, Pol J Nat Sci, 22(4) (2007) 679-690.
- [10] O.P. Popa, L.O. Popa, Travaux du Muséum National d'Histoire Naturelle, 49 (2006) 7-12.
- [11] C.G. Demayo, K.M.C. Cabacaba, M.A.J. Torres, Adv. Environ. Biol., 6 (2012) 1468-1473.
- [12] J.L. Metcalfe, M.N. Charlton, Sci Total Environ, 97/98 (1990) 595-615.

**THE CHANGES IN BASIC SOIL CHARACTERISTICS
AND ACCUMULATION OF HEAVY METALS UNDER IMPACTS OF
VITICULTURE IN ACIDIC VINEYARD SOIL AT TÁLLYA, TOKAJ-HEGYALJA**

Nhung Thi-Ha Pham^{*}, Izabella Babcsányi and Andrea Farsang

*Doctoral School of Environmental Science;
Department of Physical Geography and Geoinformatic, University of Szeged,
Egyetem u. 2-6, Szeged, HU-6722
^{*}e-mail: hanhung@geo.u-szeged.hu*

Abstract

Since the XVI-XVII centuries, Tállya, which was one of the most significant regions of the Tokaj-Hegyalja, had become famous for its vine-growing. However, the soil erosion and tillage process, as well as toxic compounds from chemical fertilizer, Cu-fungicides had transformed the basic soil parameters of the topsoils and brought environmental risks from soil pollution especially from trace elements. Research results at Tállya indicated that grape cultivation had influenced on the soil environment, particularly the 0-10 cm soil layer via the alkalization process. The average soil pH of the topsoil in Halastó vineyard was 6.36 at the slightly acid level, while the soil pH at the control area (the forest) was 4.66 classified in the strongly acid category. Besides, the difference between the humus content of the topsoil in the control area (4.00%) and in the vineyard (1.48%) illustrated the decline in soil humus and the potential from soil nutrient erosion after viticulture was applied. Viticulture and soil erosion according to the terrain impacted on soil texture, from there, topsoil in the vineyard had a lighter texture than this in the control area. Analysis results showed that all of studied heavy metal elements (Zn, Pb, Co, Ni, Cr) had lower total content compared with background concentration, except for Cu. There was remarkable high Cu content at the soil surface (87.13 mg/kg on average) which exceeded pollution limit "B". Enrichment factor analysis (Sc as reference element) reflected that Zn (EF = 0.80), Pb (EF = 1.26), Co (EF = 1.52), Ni (EF = 0.75), and Cr (EF = 1.03) have not enriched in the topsoil, in contrast, EF of Cu was 10.69 at significant enrichment level. The high enrichment factor of Cu also indicated that Cu mainly originated from anthropogenic sources.

Keywords: Heavy metal accumulation, soil erosion, enrichment factor, vineyard soil, Tokaj

Acknowledgments: The study was carried out with the support of OTKA 1K 116981 and by the 'Thematic Network for the Sustainable Use of Resources – RING2017' project (program code: EFOP-3.6.2-16-201700010).

THE CONCENTRATION OF NITRATES IN CAULIFLOWER AND BROCCOLI UNDER DIFFERENT FERTILITY REGIMES

Marina Putnik-Delić¹, Ivana Maksimović¹, Milan Mirosavljević², Žarko Ilin¹, Rudolf Kastori¹, Milena Rajić¹, Boris Adamović¹

¹*University of Novi Sad, Faculty of Agriculture, Trg D. Obradovića 8, Novi Sad, 21000, SERBIA*

²*Institute of field and vegetable crops, Maksima Gorkog 30, 21000 Novi Sad, SERBIA
e-mail: putnikdelic@polj.uns.ac.rs*

Abstract

Cauliflower and broccoli are the vegetables that are grown and consumed around the world. The concentration of nitrate largely determines the quality of the vegetables. As the elevated content of consumed nitrates can significantly affect the health of humans and especially children, it is necessary to examine the influence of different organic and mineral fertilizers on nitrate content in these vegetables as well as the influence of the presence or absence of mulch. In the present study nine types of organic, mineral and combined fertilizers have been applied to cauliflower and broccoli with and without the presence of mulch. The content of nitrates, depending on the applied fertilizer, differed significantly, up to 4.4 times in cauliflower with mulch, or up to 3 times in broccoli without mulch. Proper fertilization and use of mulch can make a significant contribution to making vegetables a health-safe food.

Introduction

Although vegetables are considered as healthy food, their inadequate quality can greatly affect human health in terms of increasing the risk of chronic illness, cancer, cardiovascular diseases, and many others (Nerdy and Putra, 2018). The concentration of nitrates is a parameter that can largely determine the quality of vegetables and, depending on concentration, places it in potentially dangerous food for human health. Nitrates have been linked to diseases like ovarian, colon, rectal, bladder, stomach, esophageal, pancreatic, gastrointestinal and thyroid cancer, leukemia and non-Hodgkin lymphoma (Afzaly and Elahi, 2014).

In addition to the fact that fertilization plays an important role in achieving high yields, it plays a very significant role in achieving a good quality. Taking this into account, it is necessary to examine effect of different concentrations and types of fertilizers, as well as application of mulch, on the nitrate content in broccoli and cauliflower.

Experimental

Broccoli (variety Corvet) and cauliflower (variety Snezna grudva) were grown under 9 fertilization schemes (Table 1), each of which was conducted in two variants - unmulched and mulched with plastic foil.

Before the onset of the experiment, agrochemical properties of soil and chemical composition of applied manure were analyzed (Table 2 and Table 3).

The concentration of nitrate was assessed by spectrophotometric method (Giné et al, 1983).

Table 1. Fertilization treatments of broccoli and cauliflower

No	Fertilizer	Applied dose (t/ha)	Fertilizer (mineral)	Applied dose (kg/ha)
1.	Control	-	-	-
2.	Beef manure	20	-	-
3.	Pig manure	20	-	-
4.	Beef manure	20	NPK	300
5.	Pig manure	20	NPK	300
6.	Beef manure	20	NPK	500
7.	Pig manure	20	NPK	500
8.	-	-	NPK	300
9.	-	-	NPK	500

Table 2. Agrochemical properties of soil before experiment setting (Bogdanović et al., 2011)

Depth (cm)	pH		%	%	% N	mg P ₂ O ₅ 100g ⁻¹	mg K ₂ O 100g ⁻¹	NH ₄ -N kg ha ⁻¹	NO ₃ -N kg ha ⁻¹
	H ₂ O	KCl	CaCO ₃	humus					
0-30	7.6	7.0	4.59	3.12	0.16	21.9	22.1	28.0	36.1
30-60	7.8	7.0	5.42	2.96	0.15	14.3	21.0	23.4	41.6

Table 3. Chemical composition of applied manure (Bogdanović et al., 2011)

Manure type	pH		%N	%P	%K
	H ₂ O	KCl			
Well-rotted beef manure	6.9	6.6	1.2	1.82	0.33
Composted pig manure	7.9	7.7	1.3	3.58	1.68

Statistical analysis was performed using STATISTICA 13.3 [StatSoft, University Licence, University of Novi Sad, 2019]. Means of replicates and evaluation of the significance of differences between means were determined by descriptive statistics and ANOVA analysis, followed by LSD *post hoc* test ($\alpha=0.05$).

Results and discussion

Different doses of mineral and organic fertilizers significantly influenced the nitrate content in broccoli and cauliflower (Table 4. and Figure 1. and 2.)

Table 4. Descriptive statistics for the concentration of nitrates ($\mu\text{gNO}_3^-/\text{g DM}$) in broccoli and cauliflower

Variable	Descriptive Statistics								
	Valid N	Mean	Sum	Min	Max	Variance	Std. dev	Coef. var	Std. Error
Broccoli	36	1132.4	40766.8	598.0	1792.2	116638.3	341.5	30.1	56.9
Cauliflower	36	616.7	22201.3	192.0	1398.7	75703.1	275.1	44.6	45.8

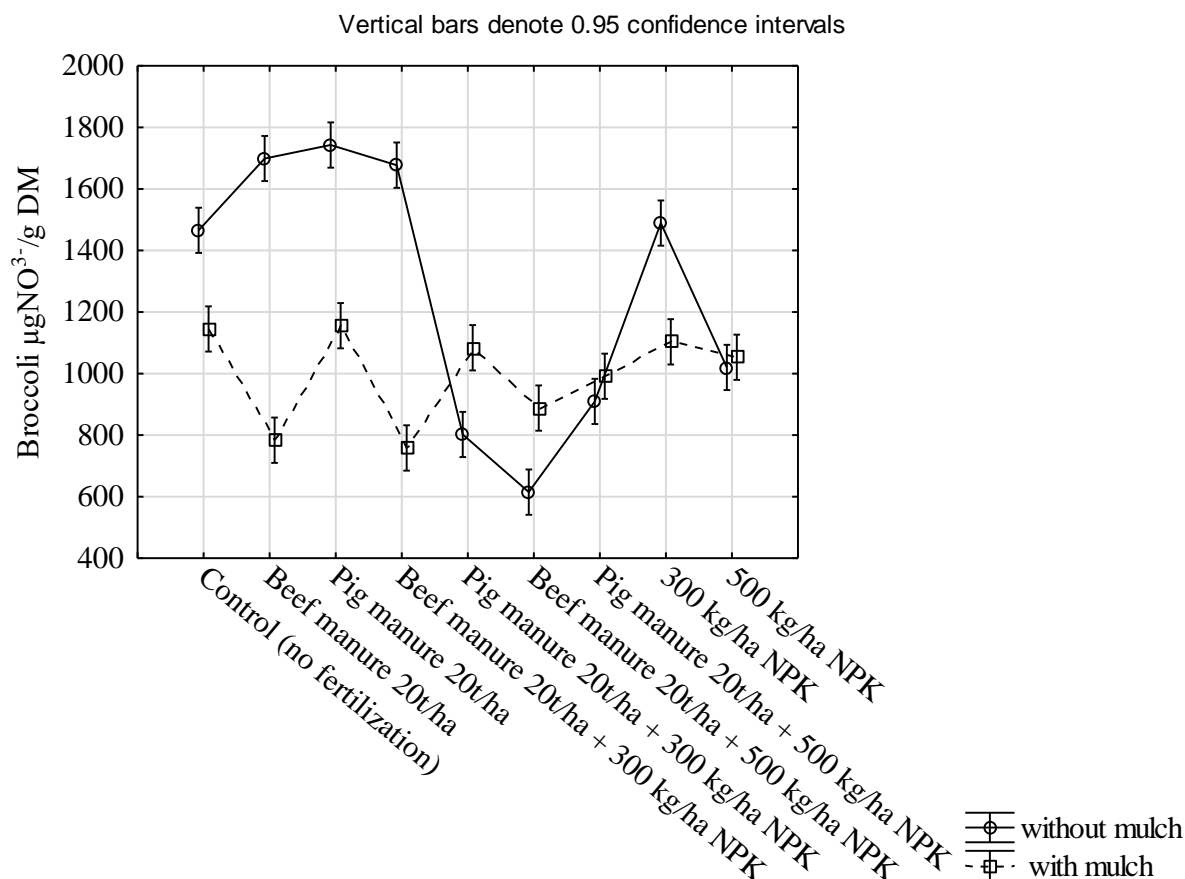


Figure 1. The concentration of nitrates in broccoli exposed to different fertilization schemes in the presence or absence of mulch

In 67% of broccoli fertilization treatments, the use of mulch had a positive effect as nitrate concentrations were significantly lower (Figure 1). The combination of organic and mineral fertilizers gave the best result in broccoli without mulch, because concentration of nitrates decreased. The use of mulch and beef manure alone and in combination with 300 kg of NPK also showed good results in terms of a better quality of broccoli. In cauliflower were found larger differences in nitrate content depending on the type of fertilizer with mulch (Figure 2). In broccoli, nitrate concentrations varied by as much as 2.9 times. In the presence of mulch, concentrations were lower and less variable in the nitrate content of plants in the presence of different fertilizers, unlike cauliflower. For cauliflower, there is as much as 4.3 times the difference between the highest and the lowest concentration of nitrate (Pig manure 20 t⁻¹ ha + 500 kg/ha NPK and 300 kg/ha NPK, respectively).

The European Food Safety Authority recommended the acceptable daily intake of nitrate in the human body and for an adult it amounts to 3.7 mg/kg body weight/day, i.e. for a person with bodyweight of 60 kg, it is 222.0 mg/day (Brkić et al, 2017). Therefore, if people consume the recommended amount of vegetables (up to 150 g/day), all these variations in nitrates (2,59-24,19 mg/150 g portion of vegetable/day) do not pose the risk for health.

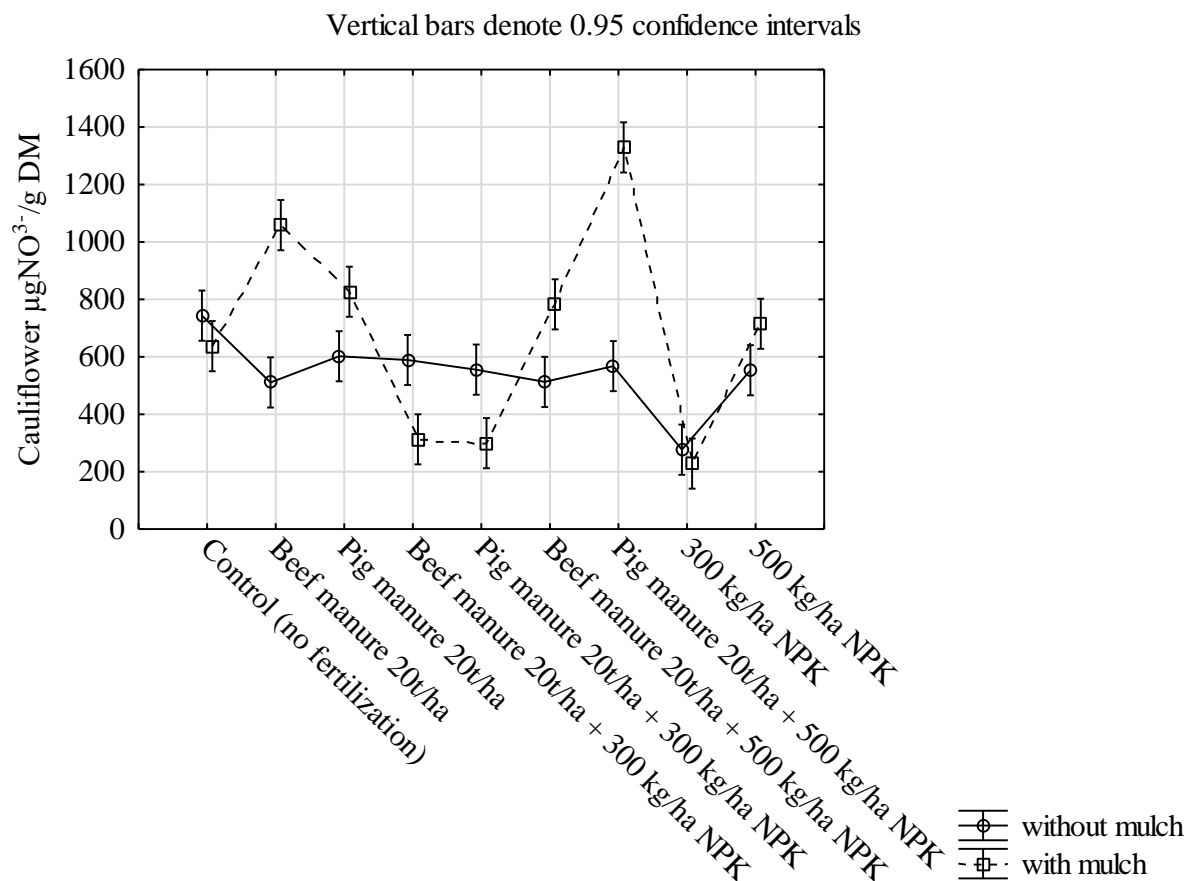


Figure 2. The concentration of nitrates in cauliflower exposed to different fertilization schemes in the presence or absence of mulch

Conclusion

The promotion of healthy diet is in focus nowadays, which imposes the need for production of vegetables that contain as little nitrate as possible, which is under high influence of fertilization. In the present paper the combination of mineral and organic fertilizers gives the best result in the sense of quality of broccoli and cauliflower. The mulch with plastic foil also significantly affected the nitrate concentration in the investigated vegetables. Besides the concentration of nitrates, it would be useful to examine the effect of the other types of fertilizers and mulching materials on the accumulation of active biomolecules such as antioxidants, which are also important features of quality.

Acknowledgments

We thank Ministry of Education, Science and Technological Development of the Republic of Serbia, TR 31036, for financial support.

References

- [1] S. F. Afzali, R. Elahi, J. Appl. Sci. Environ. Manage. 18 (2014) 451-457.
- [2] D. Bogdanović, Ž. Ilin, R. Čabilovski, D. Marinković, Letopis naučnih radova 35, 1, (2011) 57-66.
- [3] D. Brkić, J. Bošnjir, M. Bevardi, A. Gross Bošković, S. Miloš, D. Lasić, A. Krivohlavek, A. Racz, A. Mojsović-Čujić, N. Uršulin Trstenjak, Afr. J. Tradit. Complement Altern. Med. 14 (2017) 31-41.

- [4] M.F. Giné, B.F. Reis, E.A.G. Zaatto, F.J. Krug, A.O. Jacintho, *Anal. Chim. Acta*, 155 (1983) 131-138.
- [5] N. Nerdy, E de Lux Putra, *Orijent J. Chem.* 34 (2018) 2983-2991.

TUNABLE HIERARCHICAL POROUS POLYMERS WITH SUPPORTED CONTROLLED SIZE NANOPARTICLES IN HETEROGENEOUS CATALYTIC REACTIONS

**Viktória Rácz¹, Juan Gómez-Pérez¹, Gábor Varga^{1,2}, Fanni Czirok¹, Zita Sándor¹,
András Sági^{1*}, Eszter Szentpéteri¹, Ákos Kukovecz¹, Zoltán Kónya¹**

¹ *Department of Applied and Environmental Chemistry, University of Szeged, Rerrich Béla tér 1, H-6720 Szeged, Hungary*

² *Department of Organic Chemistry, University of Szeged, Dóm tér 8, H-6720 Szeged, Hungary*

³ *MTA-SZTE Reaction Kinetics and Surface Chemistry Research Group, Rerrich Béla tér 1, H-6720 Szeged, Hungary*

* *Corresponding author: sapia@chem.u-szeged.hu*

Abstract

Hierarchically porous polymers (HPPs) with different meso- and microstructures were decorated with controlled size platinum nanoparticles in the range of 1-12 nm. In this project, we have tested the HPPs+Pt composites as novel catalysts in the gas and liquid phase for CO oxidation and Suzuki coupling reactions, respectively. In the Suzuki coupling reactions, the catalysts made of HPP and Pt nanoparticles have shown better catalytic performance and recyclability in different solvents, in comparison with SBA+Pt catalysts. Furthermore, the samples were examined by different characterization methods such as Raman spectroscopy, SAXS, BET, TEM, TGA, ICP-MS to identify their surface properties, thermal stability, and the accurate percentage of Pt nanoparticles in the composites. Our results revealed that the tuning of the HPP pore structure is the key for high activity and selectivity reactions.

Keywords: HPP, Pt nanoparticles, CO oxidation, Suzuki coupling reaction

THE EFFECT OF ORGANIC MATTER TYPE OF HUNGARIAN OIL SHALE IN SORPTION OF ACETOCHLOR

Renáta Rauch¹, Rita Földényi²

¹ *Research Institute of Bio-nanotechnology and Chemical Engineering, University of Pannonia, Egyetem Str. 10., 8200-Veszprém, Hungary
e-mail: rauch@mukki.richem.hu*

² *Soós Ernő Water Technology Research and Development Center, University of Pannonia, Egyetem Str. 10., 8200-Veszprém, Hungary*

Abstract

The development of efficient methods for the removal of different type of organic contaminates of natural waters is an ever challenging task in the modern environmental technology. The paper reports the physical characterization and adsorption properties of a Hungarian oil shale (OSR). Static equilibrium experiments were carried out to study the adsorption of acetochlor from aqueous solution. The obtained equilibrium data were satisfactorily fitted by a multistep adsorption isotherm within the concentration range of 0 to 100 mg/l. More than 90 % of the added acetochlor was adsorbed by the studied oil shale. The contaminants are bound strongly by the sorbent therefore they cannot be washed out by the groundwater flow which, in turn, favors to the natural bacterial decomposition process of the polluting compound. This is considered as a significant advantage of the adsorbent because no chemical regeneration of the inexpensive oil shale is required. The reported results indicate that the oil shale can be used efficiently for the treatment of natural waters to remove their organic contaminants.

Keywords: oil shale, adsorption, acetochlor

Introduction

Water pollution problems caused by organic contaminants emitted by the chemical industry and agricultural activity are especially severe because they threaten both soil and aquatic life too. They are present in surface and subsurface waters as a result of natural degradation of different pollutants released by the agriculture and by various industrial plants [1]. Chloroacetanilide are persistent in the environment [2] and can cause toxicity especially by bioaccumulation in animals and plants whereby threatening human health too [3]. The removal of these compounds from contaminated raw water is a difficult task.

The studied oil shale adsorbent contains considerable amounts of clay minerals as well as organic matter too which is finely dispersed in the macro- and micropores of the inorganic matrix. Oil shale sources are located at several places of the Carpathian Basin, and especially large amounts can be found in the Hungarian mines. It is an algae based biomass fossil fine-grained sedimentary rock containing large amounts of organic matter, clay volcanic ash and calcium carbonate. The shale originates from the biomass of yellow green algae – genus *Botryococcus braunii* – accumulated in the volcanic craters over 4 to 5 million years [3]. The organic matter (OM) in oil shale is composed of bitumen and large amount of kerogen [4].

The aim of our work is to investigate the sorption properties of Hungarian oil shale as an adsorbent for the removal of acetochlor from model water samples, under laboratory conditions. The effect of organic material content and type of the oil shale were examined.

Materials and methods

Analytical grade sodium chloride, sodium dihydrogen phosphate and disodium hydrogen phosphate were obtained from Reanal Chemical Co. (Hungary). The HPLC grade solvent

(acetonitrile) was provided by VWR Ltd. (Hungary). The acetochlor standard reference material (>99%) was the product of Sigma Aldrich.

Hungarian oil shale sample was first air-dried, then milled for 1 hour and sieved (particle size below 360 μm was used). Particle size distribution of OSR was measured using Mastersizer 2000 laser diffraction system (Malvern Instruments Ltd). Total organic carbon content (TOC) of adsorbents were determined by Apollo 9000 (TEKMAR DOHRMAN) TOC Analyzer. Nitrogen gas adsorption isotherms (BET surface) and pore size were obtained with ASAP 2000 apparatus.

The main mineral fraction of adsorbents was analyzed using the PHILIPS PW3710 X-ray diffractometer (K filter, Cu radiation (50 kV, 40 mA)). The crystalline phases were identified using the X'Pert Highscore Plus software. Scanning electron microscopy for oil shale samples was conducted using Thermo Fischer APREO SEM attached with EDX units, with accelerating voltage 20 kV. The pH of OSR were measured by a Radelkis pH meter (OP-211) using a combined glass electrode (Radelkis, OP-0808P).

The measured physical and chemical properties of the studied OSR are summarized in Table 1.

Table 1. Characterization of the oil shale (OSR) sorbent

<i>Properties</i>	<i>OSR</i>
pH (1 mol/L KCl)	7.21
BET*, m ² /g	31.87
Typical pore size, nm	3.4
Main fraction, %	80.8
Particle size, μm	50-150
Organic content, %	9.79
Carbonate content, %	41.2
Main mineral phases, %	
	23.0
Calcite	7.3
Quartz	1.6
Siderite	6.2
Dolomite	2.5
Albite	1.8
Caolinite	0.6
Montmorillonite	38.7
Illite	0.7
Amorphous material	17.7

*Specific surface obtained by BET nitrogen adsorption method

Samples having different amounts of organic matter were used in order to investigate the effect of OM on adsorption of acetochlor on oil shale. Therefore humic substances (HS) were removed from OSR according to the Kézdi's method [5]: the oil shale was treated with hydrogen-peroxide (30 % w/w) solution, then dried and milled.

Since montmorillonite is the main mineral in OSR, bentonite from Egyházaskesző (Hungary) containing 81 % clay mineral (mostly montmorillonite) was used as an adsorbent too.

Adsorption studies

The adsorption isotherms were obtained in a series of batch experiments. The procedure is summarized in the scheme shown in Fig. 1. Static equilibrium experiments were carried out in a solution containing 0.1 mol/l NaCl and 0.01 mol/l phosphate buffer (pH=7). 5-5 g of adsorbent were left to swell in 5 ml distilled water for 24 h at room temperature, then 65 ml of acetochlor (solute) in appropriate buffer solutions (0-100 mg/l) was added. The suspension

was shaken for 1 hour in an orbital shaker then separated by centrifuge at 6000 rpm for 20 min. The supernatant was filtered then analyzed by HPLC.

In the supernatant, the concentration of acetochlor was determined by a MERCK LaChrom HPLC system equipped with a LiChospher 100 column filled with 5 μ m RP-18 packing material (125 mm x 4 mm) and with programmable UV detector. Samples of 10 μ l injected by an autosampler were isocratically eluted by a hydro-organic eluent containing 65 % acetonitrile and 35 % water; flow rate: 0.7 ml/min; λ =218 nm.

Results and discussion

The adsorption isotherms are important to describe the solute-adsorbent interaction. A multi-step isotherm model [6] was employed for the numerical fitting of the isotherm data to Equ. (1) by the Microcal TM, Origin 6.0 software.

$$q = \sum_{i=1}^s \left\{ \frac{q_{Ti} K_i (c - b_i + |c - b_i|)^{n_i}}{2^{n_i} + K_i (c - b_i + |c - b_i|)^{n_i}} \right\} \quad (1)$$

where

c is the equilibrium concentration of solution, [μ mol/l],

s is the number of steps of the isotherm ($i = 1 \dots s$),

q_{Ti} is the adsorption capacity, [μ mol/g],

K_i is the equilibrium constant, [$(l/\mu\text{mol})^{n_i}$],

b_i is the critical concentration limit, [μ mol/l],

n_i is the average degree of association assigned to the i -th step of the adsorption curve.

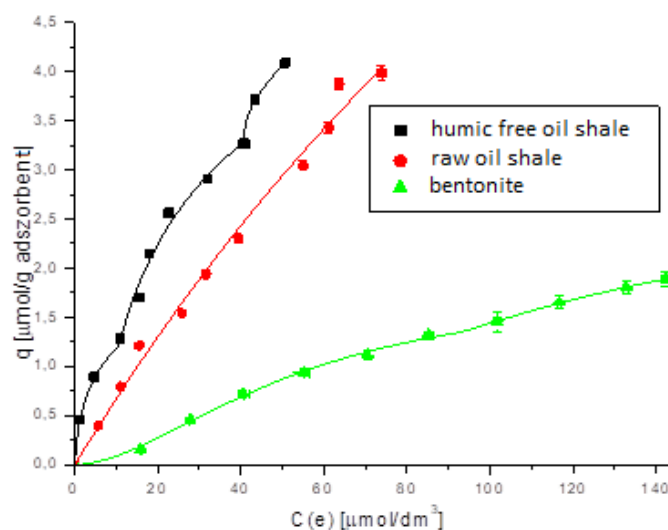


Figure 1. Effect of organic matter content of oil shale on sorption of acetochlor

Adsorption isotherms for the acetochlor on oil shale (OSR) at different organic matter content values of the solution are shown in Fig. 1.

Effect of organic material type of sorbent

In this work the adsorption capacity of three samples containing different amount and type of organic phase was compared. Several studies confirmed that the high organic matter content of the adsorbent significantly increases the adsorption of organic compounds [6]. In this study the organic matter values were as follows: bentonite < humic free oil shale < OSR (see Table 2).

Table 2. Organic material content of adsorbents

	OSR	humic free oil shale	bentonite
TOC (solid), %	14.4	10.5	0.09
HS, (%)	3.81	0.00	0.05
Kerogen (%)	10.5	10.5	0.04
DOC* (mgC/l)	78.1	93.0	11.7

DOC: dissolved organic carbon

The Fig. 1 shows the adsorption isotherms of acetochlor on bentonite, humic free oil shale and raw oil shale. It can be seen that acetochlor was bound better by the humic free sample than by the HS containing sample. It seems that the higher organic content of OSR resulted in lower adsorbed amount of acetochlor. In this untreated sample the surface is covered by HS (Fig. 2), therefore it is just partially accessible for contaminants. The presence of humic substances increased the solubility of acetochlor, thus HS decreased its adsorbed amounts compared to the treated oil shale.

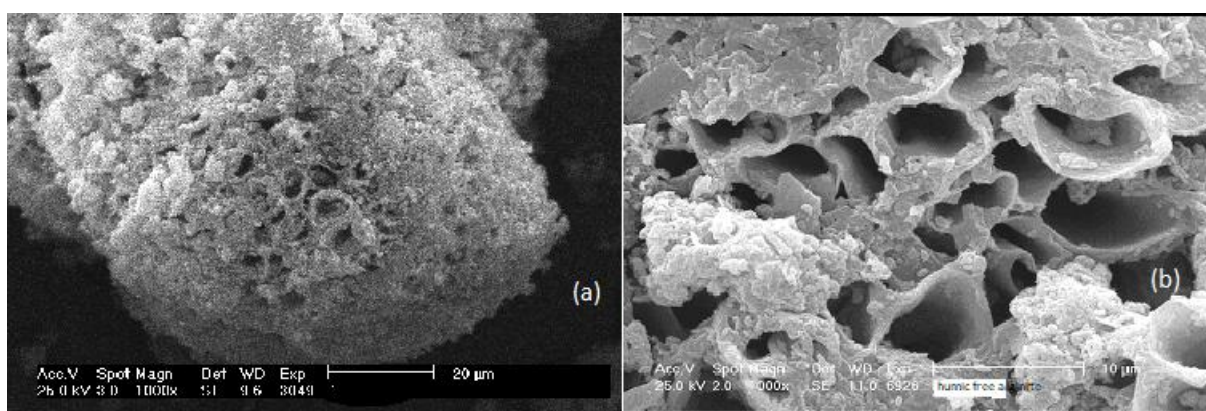


Fig. 2 SEM images of raw oil shale (a) and humic free oil shale (b)

When HS was removed from the oil shale with hydrogen peroxide the kerogen and bitumen fraction remained unchanged on the surface [8]. Making a comparison among the adsorption isotherms in Fig. 1 proves that bitumen and kerogen are responsible for the relatively high solid TOC (see Table 2) and sorption capacity. The absence of organic matter (bentonite) resulted in the lowest adsorbed amount of acetochlor. This compound is better bound by the organic matter content of the adsorbent, while clay minerals do not play an important role in this adsorption process.

Conclusion

Laboratory scale study of adsorption properties of the Hungarian oil shale revealed that it can be used as a low-cost adsorbent for the efficient removal of acetochlor and similar organic contaminants from polluted raw waters. The results of static equilibrium studies were fitted by a multi-step isotherm equation. The adsorption is favored by the special organic matter content (bitumen, kerogen) of the adsorbent (raw oil shale) but lower values of HS (H_2O_2 treated oil shale, bentonite).

References

- [1] Radhika M, Palanivelu K., J. Hazard Mater. (2006) 138(1):116-24.
- [2] M. D. Baker, C. I. Mayfield, Water, Air, and Soil Pollution, 1980, 13(4):411-424.
- [3] Dionýz Vass, Michal Elečko, Vlastimil Konečný, Geology Today (1997) 13(4):149 – 153.
- [4] Sameer Al-Asheh, Fawzi Banat, Asmahan Masad, Env. Geol., (2004) 45(8):1109-1117.

- [5] Kézdi, Á., “Talajmechanika”, (Soil Mechanics Manual) Tankönyvkiadó, Budapest, Hungary, (1976) pp. 170., (in Hungarian)
- [6] Imre Czinkota, Rita Földényi, Zsófia Lengyel, Aurél Marton, Chemosphere, (2002) 48(7):725-731.
- [7] Sadegh-Zadeh, F., Abd Wahid, S., Jalili, B., Advances in Environmental Technology, (2017) 3(2):119-132.
- [8] Szabó, L. P., Desalination, (2004) 163(1-3):85-91.

ISOLATION OF BEAUVERIOLIDES FROM *CORDYCEPS MILITARIS* MYCELIUM

**András Sárközy¹, Zoltán Béni², Miklós Dékányi², Nikolett Sipos¹, Norbert Kúsz¹,
Solomon Wasser³, Judit Hohmann^{1,4}, Attila Ványolós¹**

¹Department of Pharmacognosy, University of Szeged, Szeged, Hungary

²Spectroscopic Research, Gedeon Richter Plc., Budapest, Hungary

³Department of Evolutionary and Environmental Biology, University of Haifa, Haifa, Israel

⁴Interdisciplinary Centre for Natural Products, University of Szeged, Szeged, Hungary

The first author's e-mail address: sarkozy@pharmacognosy.hu

The corresponding author's e-mail address: vanyolosa@pharmacognosy.hu

Cordyceps militaris and its close relative, *Cordyceps sinensis* are well-known medicinal mushrooms in the oriental traditional medicine. Mostly due to its atypical, butterfly pupa-parasitic lifestyle and rarity, it is considered as the key of longevity in China, Japan and Korea. *C. sinensis* is also native to Hungary.

The aim of our work was the mycochemical analysis of the mycelium samples of *Cordyceps militaris* originated from Israel. The procession of the sample started with an extraction with methanol by percolation, followed by solvent-solvent extraction, applying *n*-hexane, chloroform and ethyl-acetate, respectively.

The chloroform and ethyl-acetate fractions were subjected to NP-flash chromatography on silica gel using a gradient system of *n*-hexane : acetone and chloroform : methanol mixtures in multiple steps. This separation afforded two fractions, which were identified as mixture of two rarely occurring cyclodepsipeptides, beauveriolide I and III, on the basis of NMR and MS investigations. The beauveriolides consisting of three amino acids and a β -hydroxylic acid. The cyclodepsipeptide mixture could be separated using NP-HPLC applying cyclohexane: isopropyl alcohol gradient system, with detection at 215 nm.

Beauveriolide III was identified in *Cordyceps militaris* for the first time, while beauveriolide I however was previously isolated from this species [1]. Both compounds together with semi-synthetic beauveriolides are under pharmacological investigation in order to gain detailed information about their anti-inflammatory potential.

References:

[1] Shigeru Nakaya, Saki Mizuno, Hiroki Ishigami, Yasuhiro Yamakawa, Hirokazu Kawagishi, Takashi Ushimaru: New Rapid Screening Method for Anti-Aging Compounds Using Budding Yeast and Identification of Beauveriolide I as a Potent Active Compound; Bioscience, Biotechnology, and Biochemistry (2012); 76:6; 1226-1228

SYNTHESIS OF NEW FLUORINE-CONTAINING β -AMINO ACID ENANTIOMERS THROUGH LIPASE CATALYZED HYDROLYSIS

Sayeh Shahmohammadi, Enikő Forró, and Ferenc Fülöp

*Institute of Pharmaceutical Chemistry, University of Szeged, H-6720 Szeged, Eötvös u. 6, Hungary
e-mail: sayeh.s@pharm.u-szeged.hu*

Abstract

An efficient and novel enzymatic method was developed for the synthesis of β -aryl-fluorine-containing β -amino acid enantiomers through lipase PS IM (*Burkholderia cepasia*) catalyzed hydrolysis in *i*-Pr₂O at 45 °C in the presence of Et₃N. In order to follow the enzymatic reactions, an adequate analytical method was devised for the enantioseparation of racemic β -amino esters and β -amino acids.

Introduction

In recent years, enantiomerically pure β -aryl-substituted β -amino acids have been intensively investigated due to their unique and remarkable biological properties [1] and their utility in drug research [2]. In particular, incorporation of fluorine into the structure of β -amino acids has become the core of interest of scientists in the last decades, because of unique properties of fluorine atom and its importance for the synthesis of pharmaceuticals [3]. Enzymatic hydrolysis of both cyclic [4] and acyclic [5] β -amino esters is known in the literature. Herein, our aim was to devise an enzymatic protocol for the preparation of new enantiomeric β -aryl-fluorine-containing β -amino acids, important from both pharmaceutical and chemical aspects.

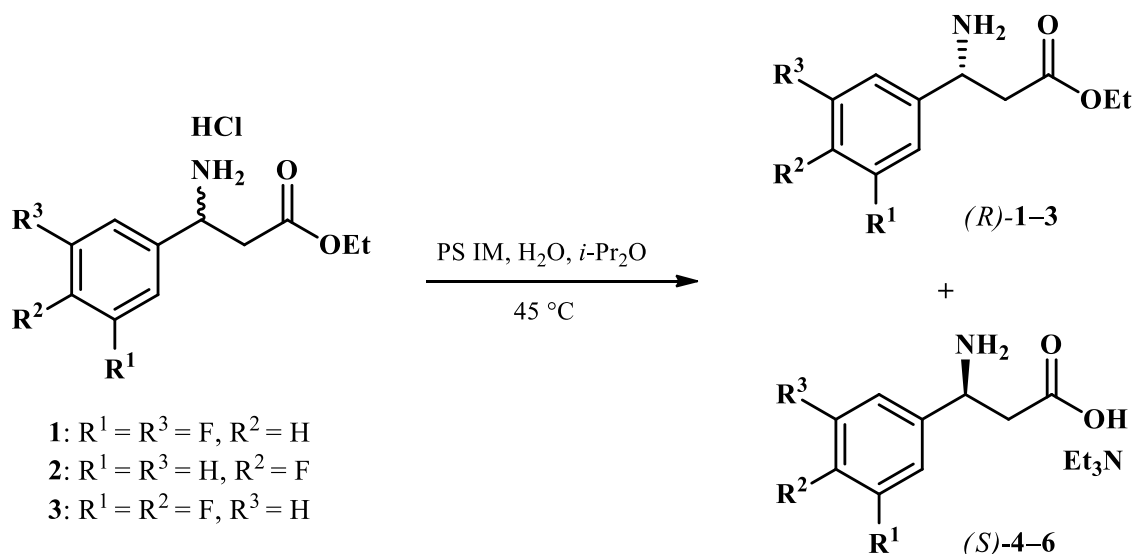
Experimental

Lipase PS IM was from Amano Pharmaceuticals. Substituted benzaldehydes were from Sigma-Aldrich. Triethylamine was from Merck. The solvents were of the highest analytical grade and from Sigma-Aldrich. Optical rotations were measured with a Perkin-Elmer 341 Polarimeter. ¹H NMR and ¹³C NMR spectra were recorded on a Bruker Avance DRX 400 spectrometer. Melting points were determined on a Kofler apparatus. The enantiomeric excess *ee* values for the unreacted β -amino ester and the β -amino acid enantiomers produced were determined by GC equipped with a Chirasil-L-Val column after double derivatization [6] with (i) diazomethane [**Caution!** the derivatization with diazomethane should be performed under a well-working hood]; (ii) acetic anhydride in the presence of 4-dimethylaminopyridine and pyridine [90 °C for 10 min → 170 °C (temperature rise 20 °C min⁻¹), 10 psi].

Results and discussion

Racemic β -amino acids were synthesized with good yields (42-75%) by Rodionov synthesis [7] through the reactions of aldehydes with malonic acid in the presence of NH₄OAc in EtOH at reflux. Subsequently, the β -amino esters were prepared with yields ranging from 76 to 87% by the esterification of corresponding β -amino acids in the presence of SOCl₂ in EtOH.

Preparative scale resolution of (\pm)-**1-3** were performed under the optimized conditions [lipase PS IM, H₂O, *i*-Pr₂O, Et₃N,], and the reaction mixture was shaken in an incubator shaker at 45 °C, 200 rpm. The progress of reaction was followed by taking samples from the reaction mixture at intervals and analyzing them by gas chromatography. The reaction was stopped by filtering off the enzyme at 50% conversion. The products were separated by column chromatography. Unreacted amino esters (*R*)-**1-3** and the product amino acids (*S*)-**4-6** were obtained with high *ee* ($\geq 99\%$), and good yields ($\geq 48\%$).



Conclusion

Novel fluorine-containing amino acid enantiomers have been prepared through PS IM lipase catalyzed hydrolysis of racemic amino esters **1-3**. Excellent enantioselectivities ($E > 200$) were obtained when the reactions were performed with H_2O as a nucleophile in $i\text{-Pr}_2\text{O}$ at $45\text{ }^\circ\text{C}$, in the presence of Et_3N . Both the unreacted amino esters (R)-**1-3** and product amino acids (S)-**4-6** were isolated with high *ee* ($\geq 99\%$), and promising yields ($\geq 48\%$). To follow the enzymatic reactions and calculate the enantiomeric excess, conversion and enantioselectivities suitable analytical methods were optimized.

Acknowledgements

The authors thank to the Hungarian Scientific Research Council (OTKA, K129049) and the Ministry of National Economy, National Research, Development and Innovation Office (GINOP, 2.3.2-15-2016-00014) for financial support.

References

- [1] a) H. H. Wasserman, G. D. Berger, *Tetrahedron* **1983**, 39, 2459-2464 b) H. H. Wasserman, H. Matsuyama, R. P. Robinson, *Tetrahedron* **2002**, 58, 7177-7190.
- [2] E. Juaristi, V. A. Soloshonok, Enantioselective synthesis of β -amino acids, 2nd edn. (Eds.: E. Juaristi, V. A. Soloshonok), Wiley-Interscience, Hoboken, NJ, **2005**.
- [3] D. L. Steer, R. A. Lew, P. Perlmutter, A. I. Smith, M. I. Aguilar, *Curr. Med. Chem.* **2002**, 9, 811-822.
- [4] E. Forró, F. Fülöp, Recent lipase-catalysed hydrolytic approaches to pharmacologically important β - and γ -amino acid enantiomers, *Curr. Med. Chem.* **2012**, 19, 6178-6187.
- [5] M. R. Mata, E. G. Urdiales, V. G. Fernandez, V. Gotor, Stereoselective Chemoenzymatic Preparation of β -Amino Esters: Molecular Modelling Considerations in Lipase-Mediated Processes and Application to the Synthesis of (S)-Dapoxetine, *Adv. Synth. Catal.* **2010**, 352, 395-406.
- [6] E. Forró, New gas chromatographic method for the enantioseparation of β -amino acids by a rapid double derivatization technique, *J. Chromatogr. A*, **2009**, 1216, 1025-1029.
- [7] G. Tasnádi, E. Forró, F. Fülöp, *Burkholderia cepacia* lipase is an excellent enzyme for the enantioselective hydrolysis of β -heteroaryl- β -amino esters, *Tetrahedron: Asymmetry*, **2009**, 20, 1771-1777.

EFFECT OF *CANNABIS SATIVA* L. EXTRACT TO OXIDATIVE STRESS OF *Sorghum halepense* L.

Konstantinović Bojan¹, Šućur Jovana¹, Kojić Mirjana⁴, Samardžić Nataša¹, Vidović Senka², Koren Anamarija³, Vladić Jelena², Gavarić Aleksandra², Popov Milena¹

1 University of Novi Sad, Faculty of Agriculture, Department of Environmental and Plant Protection, Trg Dositeja Obradovića 8, 21000 Novi Sad, Serbia

2 University of Novi Sad, Faculty of Technology, Bulevar cara Lazara 1, 21000 Novi sad, Serbia

3 Institute of field and vegetable crops, Maksima Gorkog 30, 21000 Novi Sad, Serbia

*4 PhD grant student of Ministry of education science and technological development
e-mail: bojank@polj.uns.ac.rs*

Abstract

The growing desire to find new biopesticides has put allelopathy at center of research interest. Aim of this study was to investigate allelopathic effect of *Cannabis sativa* L. extract on activity of antioxidant enzymes superoxide dismutase (SOD) and catalase (CAT) in leaves of treated plants of *Sorghum halepense* L. Extract was obtained by classical extraction process and applied concentrations were 100%, 50%, 25% and 10%, until control variant was not treated. Plant of *S. halepense* L. was treated under field conditions in initial growth stages. After 6h and 24h from treatment leaves of treated plants were sampled. The samples were monitored for activity of antioxidant enzymes superoxide dismutase (SOD) and catalase (CAT). Results indicate increased activity of monitored enzymes after 6h only in variant treated with the highest concentration of extract. After 24h enzyme activity was significantly lower compared to the untreated sample. An increase in activity of antioxidant enzymes after 6h is a response to stress caused by applied extract of *C. sativa* L., respectively an allelopathic effect was observed.

Keywords: *Cannabis sativa* L., *Sorghum halepense* L., allelopathy, superoxide dismutase (SOD), catalase (CAT)

Introduction

Invasive plant species have been subject of numerous studies. Finding methods of controlling invasive plant species, with good efficiency and minimizing environmental impact, becoming a goal of today's agricultural production. Allelopathy has great potential for finding new biopesticides. Allelopathy is a relationship in which plants release chemical substances by affecting growth of other plants, inhibiting or stimulating it [1]. Allelopathy is very important in weed control since it does not involve the use of synthetic compounds [2]. Numerous growth inhibitors have been identified in plants that are responsible for allelopathic properties of certain plant species and provide potential for their use in the development of bioherbicides [3]. Some of plant species with proven allelopathic properties are: *Ambrosia artemisiifolia* L., *Avena* sp., *Amaranthus retroflexus* L., *Cyperus esculents* L., *Chenopodium album* L., *Helianthus tuberosus* L., *Rumex crispus* L., *Xanthium strumarium* L. [4]. McPartland [5] indicates a repellent and pesticidal properties of *C. sativa* L. Allelopathic effect of extract is highly dependent on applied concentration and length of exposure of treated plant [6]. Barnes & Putnam [7] point to fact that lower concentrations of applied extract may also have higher allelopathic activity in sterile soils as opposed to their activity in non-sterile soils. Allelochemicals in certain plant species can cause oxidative stress, which is manifested as activation of an antioxidant mechanism [8]. Plants with their enzymatic activity respond to adverse environmental influences [9]. Since enzymes such as superoxide dismutase (SOD) and catalase (CAT) are very important in process of protecting cells from reactive oxygen

species, their activity can be used as an indicator of plant oxidative stress [10]. Aim of this study was to investigate effect of *C. sativa* L. extract on activity of antioxidant enzymes superoxide dismutase (SOD) and catalase (CAT) in treated *S. halepense* L. plants.

Material and method

Cannabis sativa L. plant material used is of Helena variety, collected at ripening stage in Bački Petrovac during 2018. Dry plant material was crushed and 400g was added to 4l of distilled water. Classical extraction for 24h at 25°C gave extract used, which was filtered through filter paper. Field sprayer treated field with *Sorghum halepense* L. in initial growth stages. After 6h and 24h from treatment, leaves of treated plants were sampled for biochemical analyzes. Each 2g of fresh leaves sampled was homogenized in 10ml of phosphate buffer (0.1M, pH 7.0). Samples were then centrifuged for 20min at 10000 x g (Boeco, Germany) and filtered. Samples thus obtained were used for further biochemical analyzes. Activity of antioxidant dismutase (SOD) and catalase (CAT) was examined. Readings were performed using a Thermo Scientific Evolution 220 (USA) UV/VIS spectrophotometer. Activity of SOD was determined based on photochemical reduction of nitroblutetrazolium (NBT) in which formazan was produced. A sample of 10μL was added to a 1.2ml solution (50mM phosphate buffer (pH 7.8), 13mM L-methionine, 75μM NBT, 0.1mM EDTA) and then 600 μL riboflavin was added. Prepared solution was stirred and placed in front of light source for 20min. The SOD activity unit is amount of enzyme that inhibits NBT reduction by 50% at 25°C and 560nm. CAT activity was determined based on a decrease in H₂O₂ absorption in presence of enzyme extract at 240nm. Unit of catalase activity is amount of enzyme that causes degradation of 1μmol H₂O₂ over a period of 1min at 25°C, expressed per miligram of protein. An enzyme extract obtained from leaves of *S. halepense* L. of 40μL was added to a 2ml solution consisting of 50mM potassium phosphate buffer (pH 7.0) and 10mM H₂O₂. Obtained values of monitored parameters are shown as mean values with standard error. Values were processed by one-way analysis of variance (ANOVA) and comparison test used was Duncan's test in Statistica for Windows. Values indicated by same letters are of same statistical significance at confidence level P<0.05.

Results and discussion

Applied concentrations of *Cannabis sativa* L. extract indicate a change in activity of monitored enzymes superoxide dismutase (SOD) and catalase (CAT) relative to control. After 6h of plants treatment with extract only concentration of 100% gave higher activity while other applied concentrations decreased activity of SOD. After 24h of treatment, decreased SOD activity was observed in treated samples except variant with application of a minimum extract concentration of 10%. Obtained values of activity of superoxide dismutase (SOD) enzyme with standard error and statistical significance are shown in Table 1. After 6h of treatment, CAT values increased significantly relative to control. Concentration of 100% gave the highest activity. Unlike 24h post-treatment period where treated samples indicate significantly less CAT activity than control variant. Obtained values of catalase enzyme (CAT) activity with standard error and statistical significance are shown in Table 1.

Table 1. Superoxide dismutase (SOD) and catalase (CAT) activities in leaves of *Sorghum halepense* L. after 6h and 24h after treatment with *Cannabis sativa* L. extract

Enzyme	Concentration	100%	50%	25%	10%	0%
SOD	Activity after 6h	782,61±8,78 ^{bcd}	650,72±26,52 ^{ae}	660,14±1,92 ^a	686,95±27,18 ^a	720,29±24,22 ^b
	Activiti after 24h	688,40±16,85 ^{bde}	634,06±15,34 ^{acde}	725,36±12,32 ^{bd}	784,78±8,76 ^{abc}	761,59±14,97 ^{ab}
CAT	Activiti after 6h	102,66±36,39 ^{bcdde}	26,75±14,69 ^a	19,93±7,36 ^a	32,42±12,84 ^a	20,55±3,09 ^a
	Activiti after 24h	27,07±9,58 ^d	15,15±6,13 ^d	39,77±5,98	9,43±3,87 ^d	72,75±25,93 ^{abc}

*values with same letter are at same level of significance (p<0,05)

Allelopathic property of *C. sativa* L. is also proven by Mahmoodzadeh et al [11], Akhter et al. [12], Rueda-Ayala et al. [13] using bioassays, examining effect of applied extract on germination and initial growth of *Lactuca sativa* L. plants.

Conclusion

Our results indicate an increased activity of monitored SOD and CAT enzymes in samples of treated plants *Sorghum halepense* L. only after 6h at the highest concentration of *Cannabis sativa* L. extract. After 24h, there was a decrease in activity of SOD and CAT enzymes in samples treated with extract used. Changes in enzyme activity have been reported to indicate stress in treated plants. Plants treated with the highest concentration of extract exhibit the greatest stress after 6h from time of treatment.

References

- [1]Gella, D., Ashagre, H., Negewo, T. 2013: Allelopathic effect of aqueous extracts of major weed species plant parts on germination and growth of wheat. *Journal of Agricultural and Crop Research*, 1(3): 30–35.
- [2]Sharma, M., Satsangi, G.P. 2013: Potential Allelopathic Influence of Sunflower (*Helianthus Annuus* L.) on Germination and Growth behavior of Two Weeds in-vitro Condition. *International Journal of Biotechnology and Bioengineering Research*, 4(5):421–426.
- [3]Xuan, T.D., Shinkichi, T., Khanh, D.T., Min, C.I. 2005: Biological control of weeds and plant pathogens in paddy rice by exploiting plant allelopathy: an overview. *Crop Protection*, 24: 197–206.
- [4]Šćepanović M., Novak N., Barić K., Ostojić Z., Galzina N., Goršić M. (2007) Alelopatski utjecaj korovnih vrsta *Abutilon theophrasti* Med. i *Datura stramonium* L. na početni razvoj kukuruza, *Agronomski glasnik* 6/2017, str. 459-472.
- [5]McPartland J. (1997), *Cannabis* as repellent and pesticide, *Journal of the International Hemp Association* 4(2): 87-92.
- [6]Hisna, Shah, M., Sayyed, A., Shabeena, Aziz, L., Ismail, Gul., H. 2016: Allelopathic effect of *Salvia plebia* R. Brown on germination and growth of *Zea mays* var. 30-25 Hybrid, *Triticum astivum* var. Pirsabak-04 and *Sorghum bicolor* L. *Journal of Applied Environmental and Biological Sciences*, 6(4): 93–104.
- [7]Barnes, J.P., Putnam, A.R. 1986: Evidence for Allelopathy by Residues and Aqueous Extracts of Rye (*Secale cereale*). *Weed Science*, 34(3): 384–390.
- [8]Cruz-Ortega R., Lara-Nunez L., Luisa Anaya A. 2007: Allelochemical stress can trigger oxidative damage in receptor plants: mode of action of phytotoxicity, *Plant signaling & behavior* 2(4), 269-270.
- [9]Sunmonu TO, Van Staden J. 2014: Phytotoxicity evaluation of six fast-growing tree species in South Africa, *South African Journal of Botany* 90, 101-106.
- [10]Kuthan H., Haussmann H.J., Werringloer J. 1986: A spectrophotometric assay for superoxid dismutase activities in crude tissue fractions, *Biochemical Journal* 237(1), 175-180.
- [11]Mahmoodzadeh H., Ghasemi M., Zanganeh H. 2015: Allelopathic effect of medicinal plant *Cannabis sativa* L. on *Lactuca sativa* L. seed germination, *Acta agriculturae Slovenica*, 105-2, 233-239.
- [12]Akhtar, S, Bangash, N, Asghar, R, Khalid, N. 2014: Allelopathic assessment of selective invasive species of Pakistan, *Pakistan Journal of Botany* 46(5): 1709-1713.
- [13]Rueda-Ayala, V, Jacck, O, Gerhards, R. 2015: Investigation of biochemical and competitive effects of cover crops on crops and weeds, *Crop Protection* 71, 79-87.

ISOLATION OF PHENANTHRENES FROM *JUNCUS MARITIMUS*

Dóra Stefkó¹, Anita Barta¹, Norbert Kúsz¹, László Bakacsy², Judit Hohmann^{1,3}, Andrea Vasas¹

¹ Department of Pharmacognosy, University of Szeged, Eötvös u. 6, H-6720 Szeged, Hungary

² Department of Plant Biology, University of Szeged, Közép fasor 52, H-6726 Szeged, Hungary

³ Interdisciplinary Centre of Natural Products, University of Szeged, Eötvös u. 6, H-6720 Szeged, Hungary

e-mail: stefkodora@pharmacognosy.hu

Introduction: *Juncus maritimus* Lam. belongs to the genus *Juncus*. *Juncus* is one of the biggest genera of Juncaceae plant family and by far the most important one from phytochemical and pharmacological points of view. Juncaceae species accumulate different secondary metabolites, among them flavonoids, phenanthrenes, coumarins, triterpenes, steroids and phenolic acid derivatives. However, the major bioactive components of Juncaceae species are phenanthrenes. Phenanthrenes compose a small group of aromatic secondary metabolites. They are divided into three major groups: mono-, di-, and triphenanthrenes. Several isolated compounds possessed different biological activities [antiproliferative, antimicrobial, anti-inflammatory, antioxidant, spasmolytic, anxiolytic, antialgal effects] [1].

In continuation of our work dealing with the isolation of biologically active secondary metabolites from Juncaceae species, *Juncus maritimus* was investigated.

Results and discussion: The dried plant material was extracted with methanol. After evaporation, the extract was dissolved in 50% methanol and then subjected to solvent–solvent partition with *n*-hexane, CHCl₃ and finally ethyl acetate. The CHCl₃ fraction contained phenanthrenes; therefore, it was separated by a combination of different chromatographic methods, including VLC, MPLC, gel filtration, preparative TLC, and HPLC. The structure elucidation of the compounds was carried out by extensive NMR spectroscopic analysis, and HRMS experiments. As a result of the preparative work, seven phenanthrenes (maritins A and B, juncusol, effusol, jinflexin A, 2,7-dihydroxy-5-formyl-1-methyl-9,10-dihydrophenanthrene, and effususin A) and two flavonoids (apigenin and luteolin) were identified from the aerial part of the plant.

Conclusion: With a combination of different chromatographic techniques, altogether nine compounds (seven phenanthrenes and two flavonoids) were isolated from *J. maritimus*. Maritins A and B are new natural products. All compounds were isolated for the first time from the plant, with the exception of effusol [2].

Acknowledgement:

This work was supported by the ÚNKP-19-3 New National Excellence Program of the Ministry for Innovation and Technology, National Research, Development and Innovation Office, Hungary (NKFIH; K128963), and GINOP-2.3.2-15-2016-00012.

References:

- [1] C. Bús, B. Tóth, D. Stefkó, J. Hohmann, A. Vasas, *Phytochem. Rev.* 17 (2018) 833–851.
- [2] R. Sahli, C. Rivière, A. Siah, A. Smaoui, J. Samaillie, T. Hennebelle, V. Roumy, R. Ksouri, P. Halama, S. Sahpaz, *Environ. Sci. Pollut. Res. Int.* 25 (2018) 29775–29783.

GC-MS ANALYSIS OF THE *EUCALYPTUS OBLIQUA* L'HÉR. (MYRTACEAE)
CHEMICAL COMPOSITION

Tijana Stojanović^{1*}, Vojislava Bursić¹, Gorica Vuković², Nikola Puvača³, Bojan Konstantinović¹, Boris Kuzmanović¹, Milena Đorđević¹

¹University of Novi Sad, Faculty of Agriculture, Trg Dositeja Obradovića 8, Novi Sad, Serbia

²Institute of Public Health, Bulevar Despota Stefana 54a, Belgrade, Serbia

³Department of Engineering Management in Biotechnology, Faculty of Economics and Engineering Management, University Business Academy, Cvečarska, 2, Novi Sad, Serbia
e-mail: tijana.stojanovic@polj.edu.rs

Abstract

Since there are few studies regarding *Eucalyptus obliqua* and that it is just starting to receive the attention in terms of many potential effects and properties, the aim of this study was to analyse its essential oil by GC-MS. The major detected compound in the studied essential oil was 1,8-cineole (eucalyptol) with 64.7% in content, followed by α -pinene (12.6% in content), γ -terpinene (7.4% in content), limonene (3.9% in content) and *p*-cymene (3.2% in content). Considering the fact that *Eucalyptus* species in great extent owe their medicinal value to the main constituent of their essential oil \rightarrow 1,8-cineole (eucalyptol) it was expected that eucalyptol would be the most abundant component. Beside the mentioned components there were 20 constituents which in total make less than 10.00% of the studied essential oil.

Introduction

Due to their biologically active components essential oils are gathering remarkable attention which is undeniably growing from year to year. As the by-products of plant metabolism they are regarded as evaporable secondary metabolites of plants which are the mixture of mono and sesquiterpenes [1]. A large number of isolated allelochemicals show their bioactivity in low (10^{-5} – 10^{-6} mol/dm³) or extremely low concentrations (10^{-10} mol/dm³) [2].

Genus *Eucalyptus* has been described by a French botanist L' Heritier. Until now circa 800 species have been described all over the world. Originary *Eucalyptus sp.* come from Australia and Tasmania, but now they can be found in almost all tropical and subtropical areas, while being cultivated in many other climates. *Eucalyptus* species have been known for long time in terms of their antimicrobial, antiseptic, antioxidant, anti-inflammatory, astringent and anticancer effects, as well as for their wound healing, disinfectant and expectorant properties, but *Eucalyptus obliqua* is just starting to receive the attention in this regard. *Eucalyptus sp.* have been traditionally used as a treatment for various health conditions, such as: respiratory diseases, common cold, influenza and sinus congestion. Aborigines used many *Eucalyptus* species in order to deal with gastrointestinal symptoms, open wounds, muscles and joints pains, toothache, fever, enteric infections such as diarrhea and dysentery, constipation among other stomach problems, asthma, bronchitis and athletes foot [3]. *Eucalyptus sp.* also show great antidiabetic and hypoglycemic potentials [4]. In great extent *Eucalyptus* species owe their medicinal value to the main constituent of their essential oil \rightarrow 1,8-cineole (eucalyptol). Essential oil of eucalyptus has been marked as safe and non-toxic by the United States Food and Drug Administration (FDA). However, that comes with the substantial risk whenever the essential oil is used pure or in high concentrations, with allergic contact dermatitis as the most common observed adverse effect. Considering that the more detailed risk assessment of potential toxicity is of great importance [3].

The main source of eucalyptus oil in the world is *E. globulus*, also known as the Blue Gum. Except for the essential oil, *Eucalyptus* species have been used in the production of timber,

fuel, paper pulp, as well as like water and wind erosion control measure in environmental plantings [3].

Eucalyptus obliqua is a tall fast growing evergreen tree, with the species name derived from the feature of bearing oblique leaves. It is known for being used to drain swamps, while from its leaves the potent antimalarial bioactive components have been extracted [4].

Experimental

The eucalyptus essential oil has been extracted from commercially available dried plant material by supercritical fluid extraction (SFE).

Conventional semi-continuous method was applied, using supercritical CO₂. The CO₂ with increased purity was heated through preheating coil. Forty grams of sample together with glass beads were put into the extraction cell with volume of 100 mL. As to prevent solid samples to enter the system, cotton wool was placed at the end of the cell. Heated CO₂ was injected into the extraction cell, after which it was allowed to dissolve the essential oil by constant static extraction time. The essential oil left the cell by the constant flow rate of the CO₂, while being captured and harvested with 10 mL of ethanol solvent. Essential oil was kept in the refrigerator until the GC and GC-MS analysis.

Gas chromatography (GC) and gas chromatography-mass spectrometry (GC-MS) analysis, as well as identification of essential oil components, were done as described in our previous researches [5,6].

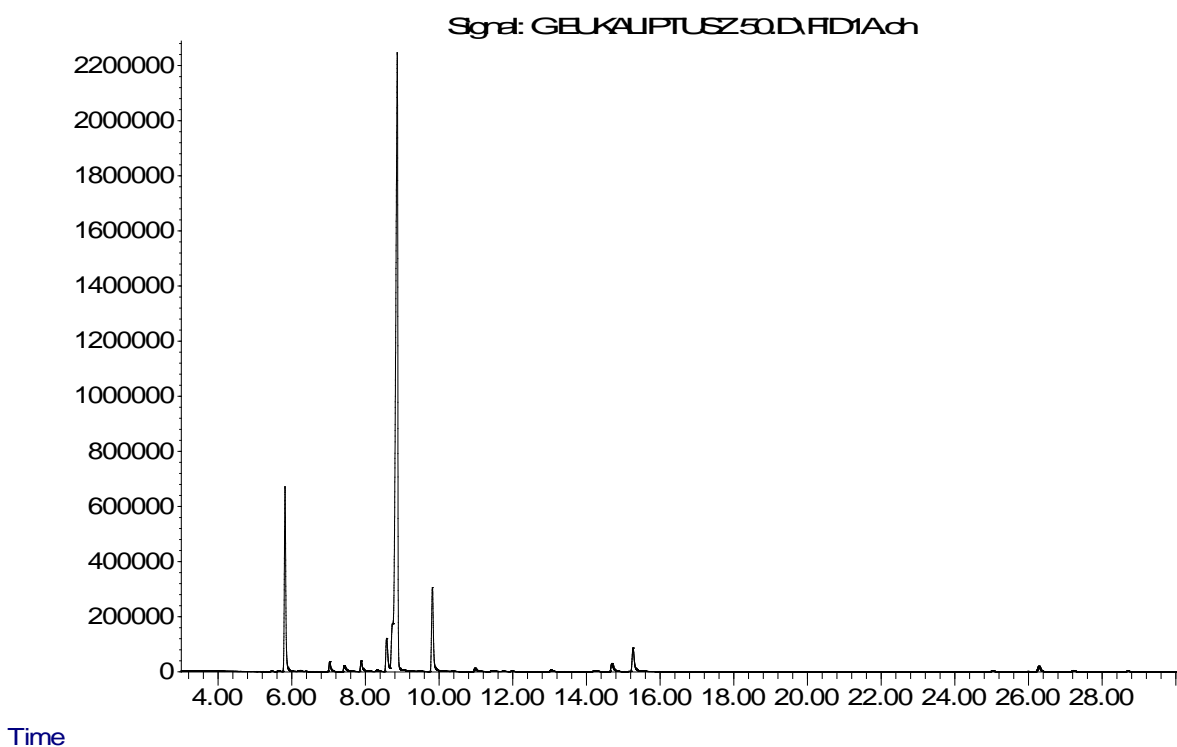
Gas chromatography (GC) and gas chromatography-mass spectrometry (GC-MS) analyses were performed using an Agilent 7890A GC equipped with an inert 5975C XL EI/CI mass spectrometer detector (MSD) and flame ionisation detector (FID) connected by capillary flow technology 2-way splitter with make-up. The HP-5MS capillary column (30 m × 0.25 mm × 0.25 µm) was used. The GC oven temperature was programmed from 60 to 300 °C at a rate of 3 °C min⁻¹ and held for 15 min. Helium was used as the carrier gas at 16.255 psi (constant pressure mode). An auto-injection system (Agilent 7683B Series Injector) was employed to inject 1 µL of sample. The sample was analysed in the splitless mode. The injector temperature was 300 °C, while the detector temperature was 300 °C. MS data were acquired in the EI mode with scan range of 30–550 m/z, source temperature of 230 °C and quadrupole temperature of 150 °C; the solvent delay was 3 min.

Identification of all compounds in the analyses was matched by comparison of their linear retention indices (relative to C8-C36 *n*-alkanes on the HP-5MSI column) and MS spectra with those of authentic standards from NIST (2011) and homemade MS library databases.

Results and discussion

The chromatogram obtained by the GC-MS analysis of the studied essential oil can be seen in Figure 1.

Response_

Figure 1. Chromatogram of the *E. obliqua* essential oil

From the obtained results it could be concluded that the main constituent of the *E. obliqua* essential oil is 1,8-cineole (eucalyptol) with 64.7% in content. Other constituents detected in the significant amount were α -pinene (12.6% in content), γ -terpinene (7.4% in content), limonene (3.9% in content) and *p*-cymene (3.2% in content). Beside the mentioned components there were 20 constituents which in total make less than 10.00% of the studied essential oil (Table 1).

Table 1. Constituents of the *E. obliqua* essential oil

peak #		RI	RI NIST	R.T. min	Start min	peak area	% max.
---				----	-----	-----	-----
1	Thujene<alpha->	923	924	5.632	5.586	88640	0.1%
2	Pinene<alpha->	930	932	5.817	5.74	17974244	12.6%
3	Camphene	944	946	6.228	6.137	147857	0.1%
4	Thuja-2,4(10)-diene	950	952	6.378	6.334	20228	0.0%
5	Pinene<beta->	974	974	7.031	6.984	1200970	0.8%
6	Myrcene	988	988	7.421	7.385	829040	0.6%
7	Phellandrene<alpha->	1004	1002	7.884	7.84	1347632	0.9%
8	Carene<delta-3->	1009	1008	8.09	8.038	70844	0.0%
9	Terpinene<alpha->	1015	1014	8.309	8.254	217585	0.2%
10	Cymene<para->	1022	1020	8.574	8.525	4617134	3.2%
11	Limonene	1027	1024	8.75	8.665	5523423	3.9%
12	Cineole<1,8->	1033	1026	8.864	8.753	92303398	64.7%
13	Ocimene<(Z)-beta->	1035	1032	9.035	8.994	400005	0.3%
14	Ocimene<(E)-beta->	1046		9.45	9.427	27069	0.0%

15	Terpinene<gamma->	1057	1054	9.819	9.759	10511232	7.4%
16	Terpinolene	1088	1086	10.973	10.922	501673	0.4%
17	Linalool	1099	1095	11.423	11.372	135751	0.1%
18	Sabinol<trans-> (trans for OH vs. IPP)	1137	1137	13.036	12.986	203070	0.1%
19	NI	1165		14.257	14.21	96761	0.1%
20	Terpinen-4-ol	1175	1174	14.688	14.639	1360864	1.0%
21	Terpineol<alpha->	1189	1186	15.264	15.2	3566940	2.5%
22	Gurjunene<alpha->	1409	1409	25.023	24.963	166526	0.1%
23	Aromadendrene	1439	1439	26.282	26.179	984478	0.7%
24	Caryophyllene<9-epi-(E)->	1462	1464	27.225	27.054	238351	0.2%
25	Viridiflorene	1497	1496	28.693	28.62	103837	0.1%

Similar results were obtained by [4] who identified 1,8-cineole and α -pinene as being in the top five components in terms of their content in the studied essential oil of *E. obliqua*.

Conclusion

The major detected compound in the studied essential oil of *E. oblique* was 1,8-cineole (eucalyptol) with 64.7% in content, followed by α -pinene (12.6% in content), γ -terpinene (7.4% in content), limonene (3.9% in content) and *p*-cymene (3.2% in content). Considering the fact that *Eucalyptus* species in great extent owe their medicinal value to the main constituent of their essential oil \rightarrow 1,8-cineole (eucalyptol) it was expected that eucalyptol would be the most abundant component. Beside the mentioned components there were 20 constituents which in total make less than 10.00% of the studied essential oil.

Acknowledgements

The authors would like to thank the Ministry of Education, Science and Technological Development for the financial support (Projects TR 31027 and TR 31038).

References

- [1] T. Stojanović, V. Tešević, V. Bursić, G. Vuković, J. Šućur, A. Popović, M. Petrović, The chromatographic analysis of caraway essential oil as the potential biopesticide, Proceedings of the 23rd International Symposium on Analytical and Environmental Problems October 9-10, Szeged, Hungary, Publisher: University of Szeged, Department of Inorganic and Analytical Chemistry, p. 15.
- [2] T. Stojanović, A. Popović, M. Petrović, J. Šućur, M. Mezei, V. Bursić, M. Aćimović, Biological activity of essential oil of dill on *Tenebrio molitor* adults, 10th European Conference on pesticides and related micropollutants in the environment & 16th Symposium on chemistry and fate of modern pesticides join to 10th MGPR, September 12-14, Bologna, Italy, Book of abstracts, p. 67.
- [3] B. Salehi, J. Sharifi-Rad, C. Quispe, H. Llaque, M. Villalobos, A. Smeriglio, D. Trombetta, S.M. Ezzat, M.A. Salem, A.M. Zayed, C.M. Salgado Castillo, S.E. Yazdi, S. Sen, K. Acharya, F. Sharopov, N. Martins, Insights into *Eucalyptus* genus chemical constituents, biological activities and health-promoting effects, Trends in Food Science & Technology 91 (2019), pp. 609-624.
- [4] S. Sabiu, A.O.T. Ashafa, Membrane stabilization and kinetics of carbohydrate metabolizing enzymes (α -amylase and α -glucosidase) inhibitory potentials of *Eucalyptus obliqua* L.Her. (Myrtaceae) Blakely ethanolic leaf extract: An in vitro assessment, South African Journal of Botany 105 (2016), pp. 264, 265, 268.

- [5] T. Stojanović, V. Bursić, G. Vuković, J. Šućur, A. Popović, M. Zmijanac, B. Kuzmanović, A. Petrović, The chromatographic analysis of the star anise essential oil as the potential biopesticide, *Journal of Agronomy, Technology and Engineering Management* 1 (1) (2018), pp. 66, 67.
- [6] M. Petrović, A. Popović, D. Kojić, J. Šućur, V. Bursić, M. Aćimović, Đ. Malenčić, T. Stojanović, G. Vuković, Assessment of toxicity and biochemical response of *Tenebrio molitor* and *Tribolium confusum* exposed to *Carum carvi* essential oil, *Entomologia Generalis*, 38 (4) (2019), p. 336.

GROWTH OF CNT FORESTS ON TITANIUM SUBSTRATES: EFFECT OF CATALYST RATION AND HYDROGEN ON THE INCORPORATION OF NITROGEN INTO CARBON NANOTUBE STRUCTURE

Anna Szabó¹, Zsuzsanna Pápa², Tamás Gyulavári¹, Krisztián Németh¹, Diána Nagy¹, Klára Hernádi¹

¹*Department of Applied and Environmental Chemistry, University of Szeged, H-6720 Szeged, Rerrich Béla tér 1, Hungary*

²*Department of Optics and Quantum Electronics, University of Szeged, H-6720 Szeged, Dóm tér 9, Hungary*

e-mail: szabo.anna@chem.u-szeged.hu

Abstract

For better electrical contacts of potential devices, growth of vertically aligned carbon nanotubes (CNT forests) directly onto conductive substrates is an emerging challenge. Here, we report a systematic study on the CCVD synthesis of carbon nanotube forests on titanium-based substrates. As a crucial issue, the effect of the presence of an insulating layer (alumina) on the growing forest was investigated. Other important parameters, such as the influence of water vapor or the Fe-Co catalyst ratio, and the incorporation of nitrogen into carbon nanotube were also studied during the synthesis. As-prepared CNT forests were characterized by various techniques: scanning and transmission electron microscopies, Raman spectroscopy, energy-dispersive X-ray spectroscopy, spectroscopic ellipsometry.

Introduction

In the past two decades, in the field of carbon nanotube (CNT) research important results have been achieved, which revealed that carbon nanotubes have extremely good electrical and mechanical properties. Vertically aligned carbon nanotubes (VACNT) which are often referred to as carbon nanotube forests in the literature (CNT forest), were synthesized for the first time in 1996 [1]. Their synthesis is a key issue therefore many efforts have been done to improve quality. Growing well-aligned carbon nanotube forests is a promising tool in order to finely tune features required [2]. Although, there is a growing understanding about the molecular-level mechanism of this so called “super-growth” method, still studying the influence of the synthesis conditions on the physicochemical properties of CNTs is still crucial, in order to reveal and tune the parameter space of the properties such as the orientation, the height, the density, and degree of graphitization. The catalyst layer can be deposited *via* various techniques. In 2007, Noda et al. [3] studied the effect of the presence of aluminum oxide on silicon substrate in relation to the synthesis of carbon nanotube forests. They have found that the intermediate oxide support on the silicon substrate was crucial to provide a strong interaction between the oxide layer and the catalyst layer. Here, we investigate the effect of aluminum oxide support on the growth of carbon nanotube forests over metallic titanium substrates as well as few parameters that influence the growth of carbon nanotube forests (ratio of catalyst, the effect of hydrogen, the incorporation of nitrogen).

Experimental

Catalyst Layer Production

Catalyst and oxide layers were prepared by PLD method. Catalyst and oxide target were made of metal oxides' powder (Fe_2O_3 , CoO and Al_2O_3) with a total weight of 1 g shaped into a 1 cm diameter pellet. The mechanical resistance was improved by heat treatment, which in this

case lasted 4 h at 500°C in air. In order to provide reproducible adhering conditions onto the substrate, the titanium substrate was sequentially washed with distilled water, absolute ethanol, and acetone prior to catalyst layer deposition. For the layer deposition, laser pulses of a LLG TWINAMP ArF excimer laser ($\lambda = 193$ nm, pulse length: 18 ns, repetition rate: 10 Hz) with average fluence of 13 J/cm² were focused on the target pellets placed in front of the titanium substrate where the layer was formed. The target substrate distance was 3 cm. According to a previous thickness optimization [4], the catalyst layer thickness was set to be 5 nm proven by spectroscopic ellipsometry measurements (Woollam M-2000F).

CCVD Synthesis

For the carbon nanotube forest production, the CCVD synthesis method was used. The titanium sheets including the catalyst layers were cut into 4×4 mm small sheets, in order to fit the quartz boat, (diameter 20 mm). Experiments were carried out at 700°C and the reaction time was 30 min. During the synthesis, the carrier gas was nitrogen with a flow rate of 50 cm³/min, the carbon source was ethylene with a flow rate of 70 cm³/min, the reducing agent was hydrogen with a flow rate of 50 cm³/min, while the system contained water vapor with a flow rate of 30 cm³/min, which contributed to the growth of carbon nanotube forests, and the N-containing compound (TPA- tripropylamine) had a flow rate of 45 cm³/min in some cases. In the first step of the synthesis, the reactor was purged with nitrogen to exclude oxygen from the system (2 min). Then hydrogen gas was introduced into the reactor, to reduce the catalysts (5 min). Subsequently, ethylene and water vapor were added to the synthesis. When the reaction was finished, all gas flows were closed, except nitrogen gas, which remained in the system for an additional 5 min. After the reactor was removed from the oven, and it was cooled to room temperature; in the final step as-synthesized samples were removed from the reactor. “Blank” synthesis was also carried out with the elimination of carbon source ethylene (Figure 1.) [5].

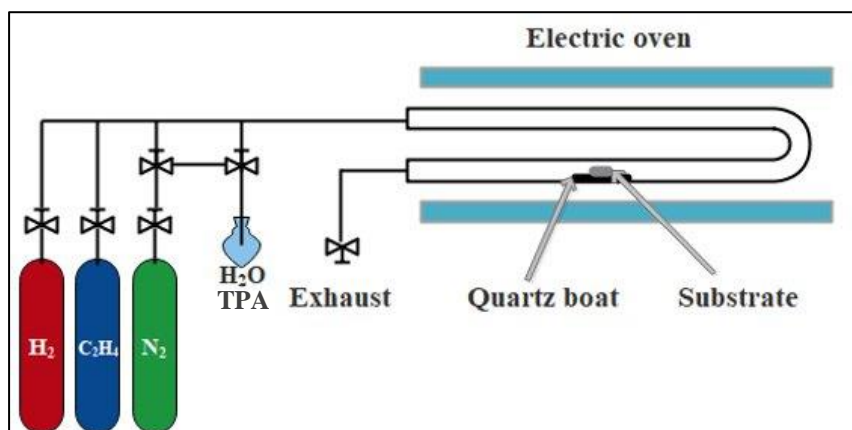


Figure 1. Schematic image of CCVD reactor.

Microscopic and Spectroscopic Investigations

Characterization of CNT Samples The orientation of the CNT forests was investigated by the means of Scanning Electron Microscopy (SEM), which type was Hitachi S-4700 Type II FE-SEM (5–15 keV). The diameters of the carbon nanotubes were examined by Transmission Electron Microscopy (TEM, Philips CM 10, 100 keV). The graphitic properties of CNT were analyzed by Raman Spectroscopy (Thermo Scientific DXR Raman microscope, excitation wavelength 532 nm).

Results and discussion

We successfully prepared carbon nanotube forests on titanium substrate both with and without Al_2O_3 , and investigated the effects of water vapor and the incorporation of nitrogen-containing compounds in carbon nanotubes. Based on SEM images, the height of carbon nanotube forests have an outstanding value with water vapor, especially when the substrate was with Al_2O_3 layer. In those cases when no water vapor was present in the system, the height of the carbon nanotube forests was lower, when without alumina layer on the titanium substrate, the height of the carbon nanotube forests was only 5 μm , which is an extremely low height in therein research. As well as to the effect of hydrogen that the presence of the promoter plays an influential role on the height of carbon nanotube forests and in the incorporation of nitrogen, in the results can be achieved the lower height of carbon nanotube forests in the absence of hydrogen and suppress the incorporation of nitrogen into the carbon nanotubes.

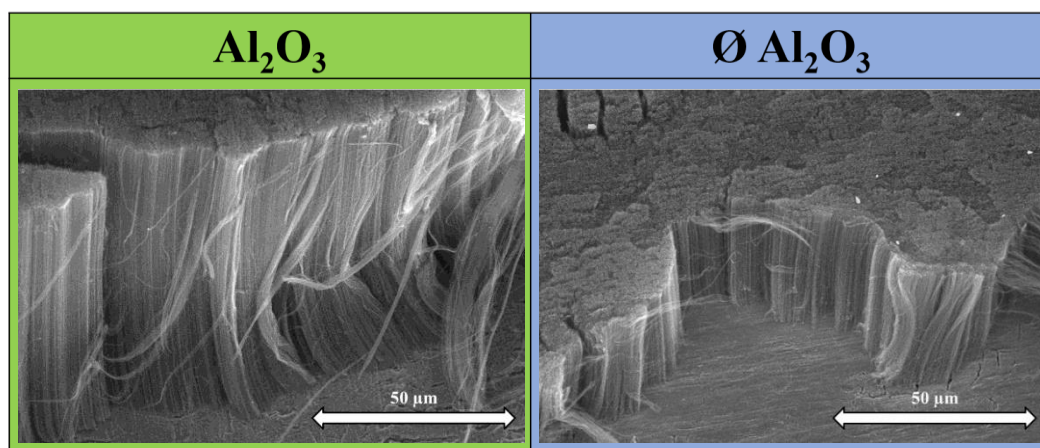


Figure 2. SEM images of CNT forests synthesized with Al_2O_3 oxide support and without Al_2O_3 oxide support

The catalyst morphology, of a sample with a layer thickness of 5 nm, was investigated right after the heat treatment. During this blank synthesis, the carbon source was not allowed into the system. From the SEM images, it can be observed, that the catalyst particles are separated when the oxide layer is deposited in advance onto the surface of the substrate and their average diameter is 27.5 ± 5.7 nm. However, when there was no aluminum oxide layer on the substrate, the catalyst particles were aggregated probably as a result of the different wetting properties of the oxide and the metal and their average diameter was 50.4 ± 11.6 nm.

TEM analysis was carried out to verify the quality of individual carbon nanotubes. TEM investigations revealed that fewer defects can be detected in the CNT walls when an oxide layer is also deposited on the titanium substrate. HR-TEM images revealed that the CNTs were typically consisted of 8–9 walls in average. The CNT with an increased number of walls showed much less graphitic features. The outer diameter of carbon nanotubes was between 12–13 nm for both samples. Based on the Raman spectra, only a small difference was observed, however, in the presence of Al_2O_3 the value of the I_G/I_D peaks fraction was: $I_G/I_D = 1.18$, while in the absence of Al_2O_3 it was $I_G/I_D = 1.33$.

We investigated the composition of different catalyst ratios to influence the height of carbon nanotube forests with and without Al_2O_3 layer.

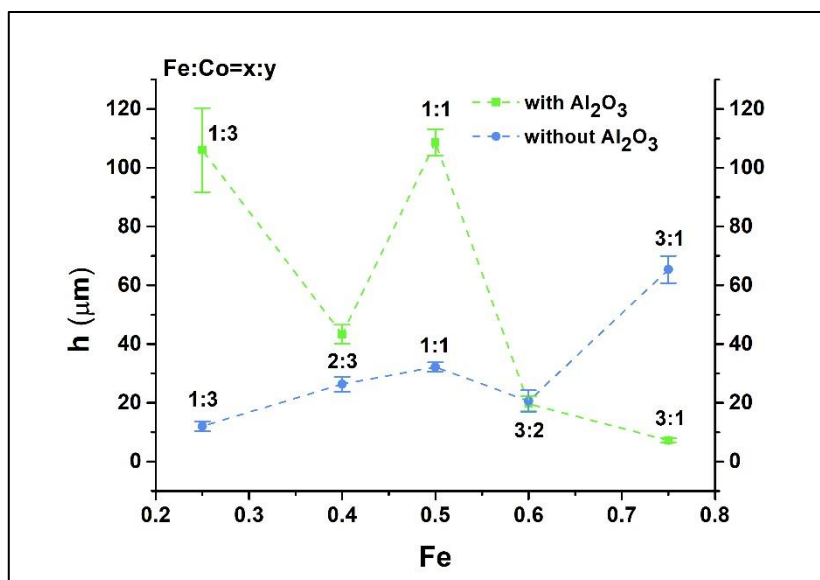


Figure 3. Heights of CNT forests with Al_2O_3 oxide support and without Al_2O_3 oxide support.

From the results of the two series, it was observed that in the presence of an insulating oxide layer on the surface of titanium substrate higher CNT forests were obtained. Interestingly, when the catalyst ratio was 2:3 or 3:2, the height of the CNT forests was relatively close in both cases, independently of the presence of the alumina layer. In our case when there was Al_2O_3 oxide support on the substrate, the highest CNT forest grew over the layers with 1:1 and 1:3 ratio as shown in Figure 3. In the second case when the substrate was applied without Al_2O_3 oxide layer, the maximum height of carbon nanotube forests was observed at the ratio of 3:1 as shown in Figure 3 and practically the height increases linearly with iron content.

Conclusion

In conclusion, certain parameters during both catalyst preparation procedure and CCVD synthesis can strongly affect the growth of vertically aligned carbon nanotubes. Applying titanium plates as a substrate it was found that the presence of an alumina layer on the surface significantly modifies the morphology of the catalyst layer (before reaction), thus influencing the CNT forest growth. One could expect that titanium as a metallic substrate dissolves reduced Fe-Co nanoparticles during preliminary hydrogenation and in this way completely inhibits carbon deposition. However, in this study, titanium proved to show a different feature. Nevertheless, it was attested that the insulating layer plays a significant role in CNT forest formation: both the height and the quality of CNT forest depended on the initial structure of the catalyst layer. It was also pointed out that water vapor in the gas feed during CCVD considerably affects the same parameters of the final product and that the presence of hydrogen in the system affects the incorporation of nitrogen into the carbon nanotubes. Structural characterization revealed important differences in CNT forests grown with or without alumina layer. These minor differences can be a result of many parameters such as graphitization of the CNTs, presence of alumina layer, density of CNT forest, fabrication conditions, etc. Therefore, we could postulate that the alumina layer does not play an important role as a current blocking layer.

Acknowledgements

This work was supported by the OTKA NN114463 and GINOP-2.3.2-15-2016-00013 project. SUPPORTED BY THE ÚNKP-19-3-SZTE-264 NEW NATIONAL EXCELLENCE PROGRAM OF THE MINISTRY FOR INNO-VATION AND TECHNOLOGY.

References

- [1] Li, W. Z., Xie, S. S., Qian, L. X., Chang, B. H., Zou, B. S., Zhou, W. Y., et al. Sci. (1996), 274, 1701–1703.
- [2] Hata, K., Futaba, D. N., Mizuno, K., Namai, T., Yumura, M., and Iijima, S. Sci. (2004), 306, 1362–1364.
- [3] Noda, S., Hasegawa, K., Sugime, H., Kakehi, K., Zhang, Z., Maruyama, S., et al. J. Appl. Phys. Part 2 Lett. (2007), 46:3.
- [4] Pápa, Z., Kecsenovity, E., Fejes, D., Budai, J., Toth, Z., and Hernadi, K. Appl. Surface Sci. (2018), 428, 885–894.
- [5] A. Szabó, P. Andricević, Z. Pápa, T. Gyulavári, K. Németh, E. Horvath, L. Forró, K. Hernadi. Front. Chem. (2018), 6, 1–9.

PREPARATION AND EVALUATION OF POLYANILINE-BASED PT CATALYSTS FOR SUZUKI COUPLING REACTIONS

Eszter Szentpéteri¹, Gábor Varga¹, Juan Gómez-Pérez¹, Fanni Czirok¹, Zita Sándor¹, Zoltán Kónya^{1,2}, András Sapi^{1*}

¹ *Department of Applied and Environmental Chemistry, University of Szeged, H-6720 Szeged, Rerrich Béla tér 1, Hungary*

² *MTA-SZTE Reaction Kinetics and Surface Chemistry Research Group, H-6720 Szeged, Rerrich Béla tér 1, Hungary*

** Corresponding author: sapia@chem.u-szeged.hu*

Abstract

Composites made of polyaniline (PANI) and platinum nanoparticles were prepared in order to evaluate their catalytic performance in Suzuki coupling reactions. The differences on the oxidation state of the PANI, the temperature of the reaction conditions, the role of the solvent and the synergetic effect of the PANI with different sized Pt nanoparticles were investigated. The obtained materials were examined with a battery of characterization techniques including BET, SEM, TEM, TGA, XPS, and Raman spectroscopy in order to determine their surface properties, morphology, thermal stability, and oxidation degree, respectively. In comparison with equivalent composites made of SBA and Pt nanoparticles, our PANI-based catalysts exhibit better catalytic performance and recyclability even in the case of greener solvents.

Keywords: Pt nanoparticles, PANI, Suzuki coupling reaction, green solvent

HETEROGENEOUS ASYMMETRIC MICHAEL ADDITIONS USING ENVIRONMENTALLY FRIENDLY CATALYSIS: APPLICATION OF CHIRAL INORGANIC-ORGANIC HYBRID MATERIALS

György Szöllősi^{1*}, Vanessza Judit Kolcsár², Viktória Kozma²,
Brigitta Fancsal², Attila Zsolt Mogyorós², Dániel Gombkötő³, Gabriella Köhl²

¹MTA-SZTE Stereochemistry Research Group, Dóm tér 8, Szeged, 6720, Hungary

²Department of Organic Chemistry, University of Szeged, Dóm tér 8, Szeged, 6720, Hungary

³Institute of Pharmaceutical Chemistry, University of Szeged, H-6720 Szeged, Eötvös u. 6,
Hungary

*e-mail: szollosi@chem.u-szeged.hu

Abstract

In the last few decades, the development of environmentally benign, sustainable processes for the preparation of optically pure intermediates used in the pharmaceutical, food and agrochemical industries received increasing attention. Processes applying recyclable, chiral heterogeneous catalysts based on readily available, natural, optically pure compounds may be convenient alternatives of the classical asymmetric synthetic methods. During our studies, we have attempted the development of novel heterogeneous catalysts by adsorption of natural amino acids on the surface of inorganic oxides. These materials formed either *in-situ* during reactions or prepared *ex-situ* were tested in various asymmetric Michael additions. Amino acids adsorbed on laponite were found the most efficient in catalyzing the addition of aldehydes or ketones to nitrostyrene derivatives. In these reactions occurring via enamine catalysis, the material obtained by adsorption of proline was found to be a highly active and stereoselective catalyst, although proline afforded low enantioselectivities. In the Michael addition of nitroalkanes or β -keto esters to unsaturated ketones, both laponite and alumina were efficient in increasing the enantioselectivities. In these reactions, which take place through iminium catalysis, only moderate enantioselectivities could be reached. The chiral inorganic-organic hybrid materials were characterized by infrared spectroscopy and powder X-ray diffractometry, evidencing bonding of the amino acids on the surface of the oxides. Our results demonstrated that an inorganic surface on which a chiral organocatalyst is immobilized by simple adsorption may have beneficial effect on the asymmetric reaction catalyzed by the chiral material, due to surface improved asymmetric induction. In conclusion, these hybrid materials are promising candidates for future application in environmentally friendly processes.

Introduction and aims

Asymmetric catalytic methods are convenient procedures for preparing optically pure organic chemicals [1]. Recent requirements to decrease the environmental impact and improve the sustainability of fine chemicals production motivated the use of heterogeneous, easily separable, recyclable chiral catalysts in these processes. From practical reasons is advantageous the attachment of chiral soluble catalysts to solid supports by noncovalent bonding. Noncovalent immobilizations of optically pure organocatalysts were seldom reported [2,3]. Natural amino acids are cheap, readily available chiral organocatalysts. However, only few catalytic systems are known in which these catalysts were immobilized on supports by simple adsorption or hydrogen bonding and provided improved activity and/or stereoselectivity [4,5]. It is also important that anchoring of organocatalysts on supports by simple adsorption may be carried out *in-situ*, without pre-preparation of the solid catalyst.

Michael additions are among the most studied C–C bond-forming organocatalytic asymmetric reactions, due to the easy preparation of complex organic molecules via these transformations [6]. In our previous studies we have observed the remarkable effect of inorganic oxide additives on the proline catalyzed asymmetric aldol reactions [5] and the Michael addition of aldehydes on β -nitrostyrene derivatives [7]. In the present work, our aim was to study the applicability of the proline-inorganic oxide hybrid catalyst in various asymmetric Michael additions. The effect of addition of oxide additives on the asymmetric addition of aldehydes or ketones to nitrostyrene will be compared with that obtained in other Michael additions. Among the reactions studied using proline catalyst both without and with inorganic additives are reactions of α,β -unsaturated ketones with nitroalkanes or β -ketoesters.

Experimental

Inorganic oxides used in this study were commercially available materials. Amino acids used as catalysts and reactants: *trans*- β -nitrostyrene, aldehydes, ketones, α,β -unsaturated ketones, nitroalkanes, β -ketoesters and solvents were of analytical grade and used as provided by suppliers.

In a typical reaction, the given amount of amino acid and inorganic oxide were introduced into a glass vial followed by the addition of the solvent and the reactants. The slurry was stirred magnetically for the given reaction time, diluted with the solvent and centrifuged. The supernatant solution was analysed by GC-MSD for identification of the products and by GC-FID to determine the conversions and stereoselectivities. The addition products were purified by flash chromatography for determination of the yields. The purity of the products was checked by ^1H and ^{13}C NMR spectroscopy. The inorganic-organic hybrid materials were examined by infrared spectroscopy, powder X-ray diffractometry and scanning electron microscopy.

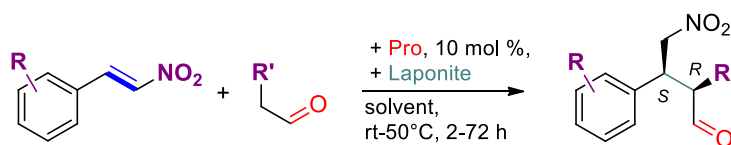
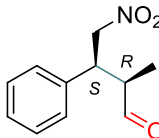
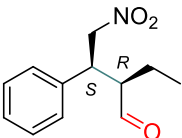
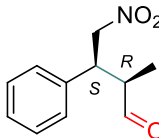
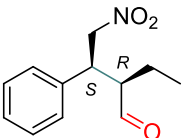
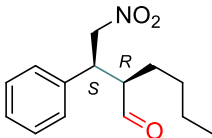
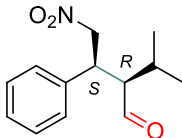
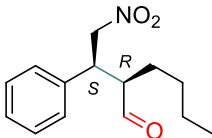
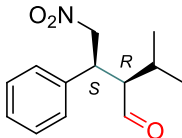
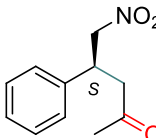
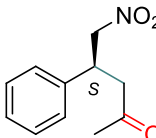
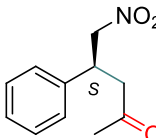
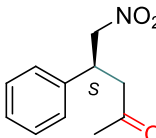
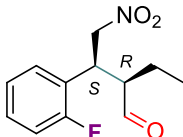
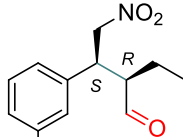
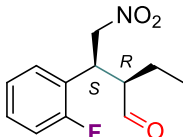
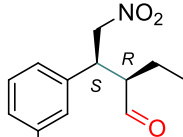
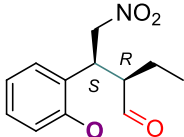
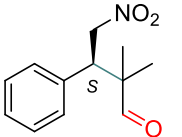
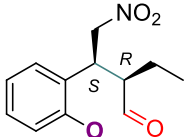
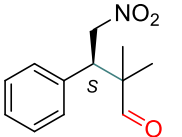
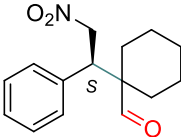
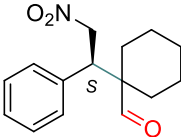
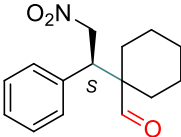
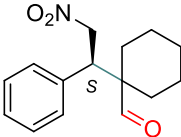
Results and discussion

In our initial investigation, we examined the scope of the proline catalyzed Michael addition of aldehydes to β -nitrostyrenes, a reaction occurring through enamine activation, similarly as the organocatalytic asymmetric aldol addition of ketones to aldehydes. In the latter reactions, inversion of the sense of the enantioselectivity was observed by addition of γ -alumina, explained by the involvement of the solid surface in the stereoselective step [5]. During an initial screening, various oxide additives were tested. As compared with the reaction using solely the L-proline (Pro) as catalyst, the enantioselectivity of the reaction increased significantly in the presence of $\gamma\text{-Al}_2\text{O}_3$, montmorillonite, bentonite and laponite (Lap). The latter material gave the best values in the addition of butanal to β -nitrostyrene. The scope of the reaction was found to be broad; in the reaction of several linear aldehydes high enantiomeric excesses (ee) were obtained (Figure 1). Substituents on the phenyl ring had small effects on the enantioselectivities. In the addition of α -branched aldehydes also increased both the conversions and the enantiomeric excesses in the presence of laponite, however lower values were obtained as compared with reactions of the linear aldehydes. The reactions of ketones was also accelerated and improved enantioselectivities were obtained, although, in these reactions the ee values remained low.

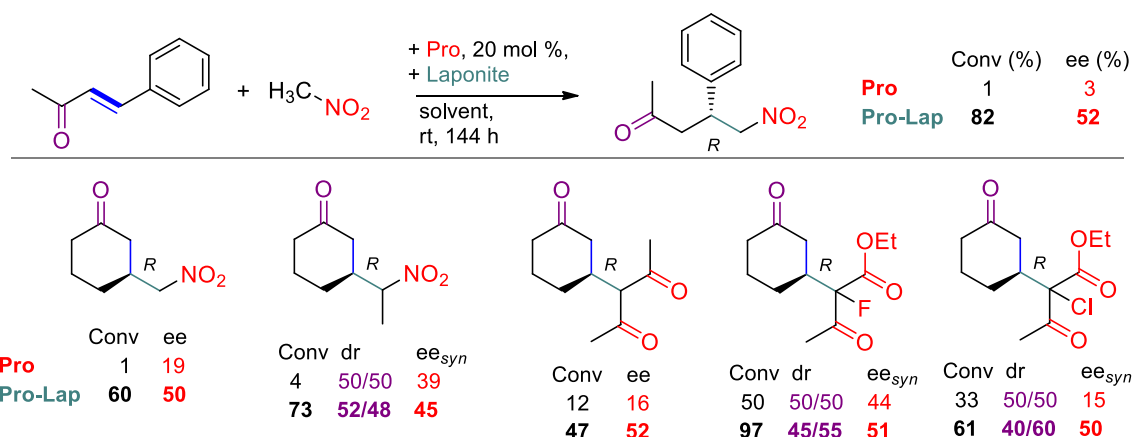
The adsorption of Pro on laponite with the involvement of the surface silanol groups, i.e. by hydrogen-bonding, was demonstrated by infrared spectroscopy. To determine the location of the amino acid attached to the Lap particles X-ray diffractometric investigations were carried out, which indicated the adsorption of Pro on the surface of Lap particles. This may explain the relatively easy partial desorption of the amino acid during reaction upon recycling. However, the recovered solid hybrid material could be recycled several times with only a small decrease in its activity. Results obtained with pyrrolidine derivatives used instead of

Pro, showed that the carboxylic acid group play role in anchoring the amino acid on the surface. Acceleration of the reaction may be attributed to the presence of the acidic surface silanol groups. As in homogeneous reactions acid additives influenced only the diastereoselectivity of the reaction, while the ee was not affected, the ee increase observed in the surface reactions may be ascribed mostly to steric effects.

Figure 1. Results of the asymmetric Michael addition of carbonyl compounds to β -nitrostyrene derivatives catalyzed by Pro or Pro-Lap hybrid material.

		Conv (%); ds _{syn} (%); ee _{syn} (%)							
Pro		Conv	ds _{syn}	ee _{syn}	Pro-Lap		Conv	ds _{syn}	ee _{syn}
	65	93	43	98		94	39		
Pro-Lap		99	92	86	Pro-Lap		99	95	88
Pro		Conv	ds _{syn}	ee _{syn}	Pro-Lap		Conv	ds _{syn}	ee _{syn}
	95	93	26	99		93	94		
Pro-Lap		99	93	26	Pro-Lap		91	95	86
Pro		Conv		ee	Pro-Lap		Conv		ee
	30		3	84			30		
Pro-Lap					Pro-Lap				
Pro		Conv	ds _{syn}	ee _{syn}	Pro-Lap		Conv	ds _{syn}	ee _{syn}
	99	94	35	99		91	40		
Pro-Lap		99	94	89	Pro-Lap		93	93	91
Pro		Conv	ds _{syn}	ee _{syn}	Pro-Lap		Conv	ds _{syn}	ee _{syn}
	83	95	3	97		94	92		
Pro-Lap		99	95	3	Pro-Lap		99	95	92
Pro		Conv		ee	Pro-Lap		Conv		ee
	18		33	17			25		
Pro-Lap		89		74	Pro-Lap		31		77

According to the above-described results obtained in Michael additions occurring via enamine mechanism, Pro adsorbed on the surface of an inorganic oxide may increase the activity of the organocatalyst accompanied by a significant increase of the stereoselectivity, if steric constraints allow the approach of the reactants to the chiral centre situated on the surface. Our next goal was to test other Michael additions, which proceed through iminium salt formation in order to attempt further extension of the scope of the developed inorganic-organic chiral hybrid catalyst. Results obtained in the additions of nitromethane or nitroethane to 4-phenyl-3-buten-2-one or 2-cyclohexen-1-one are presented in Figure 2. Minor conversions and low enantioselectivities were obtained when Pro was used as catalyst. The presence of laponite increased significantly the conversions, thus, the corresponding products were obtained in good yields.

Figure 2. Results of the Michael addition of various nucleophiles to α,β -unsaturated ketones using Pro or Pro-Lap catalysts.

The enantiomeric excesses also increased, however, in all three reactions only around 50% ee could be reached. Similarly, in reactions of acetylacetone or α -substituted acetoacetates with 2-cyclohexen-1-one, both the conversions and the ee values increased with Pro-Lap, as compared with Pro. Interestingly, in these transformations also enantiomeric excess values around 50% were reached, although the structure of the Michael donor differed significantly in comparison with the nitroalkanes. However, these results showed without any doubt that in presence of Lap the reactions occur on the surface of the *in-situ* formed chiral hybrid material. According to the above results, we reached to the conclusion that in asymmetric reactions proceeding through iminium activation the structure of the surface species formed by participation of the adsorbed amino acid and the unsaturated ketone will determine the stereochemical outcome of the reactions, whereas the structure of the donor has only marginal effect. Moreover, the similar results obtained with the two unsaturated ketones indicated that the stereochemistry of the surface reaction is influenced mostly by the adsorbed organocatalyst, thus we may anticipate a large substrate scope of this chiral heterogeneous catalytic system.

Conclusions

In summary, during our studies, we have attempted the development of novel heterogeneous catalysts by adsorption of natural amino acids on the surface of inorganic oxides. These materials formed either *in-situ* during reactions or prepared *ex-situ*, were tested in various asymmetric Michael additions occurring both through enamine and iminium activation. Amino acids adsorbed on laponite were found the most efficient in catalyzing the addition of aldehydes or ketones to nitrostyrene. The material obtained by adsorption of proline was found to be a highly active and stereoselective catalyst, comparable with the laboriously prepared synthetic chiral organocatalysts. In the Michael addition of nitroalkanes or β -ketoesters to unsaturated ketones also increased conversions and enantioselectivities were obtained in the presence of oxide additives. In the latter reactions the similar enantiomeric excesses showed that the stereochemical outcome of the additions is influenced mostly by the structure of the oxide and the amino acid, thus a generally applicable asymmetric heterogeneous catalytic system was developed. Our results demonstrated that an inorganic oxide may have beneficial effect on the asymmetric reaction catalyzed by a chiral organocatalyst immobilized on its surface by simple adsorption, due to a surface improved

asymmetric catalytic process. Accordingly, these hybrid materials are promising candidates for future application in environmentally friendly processes.

Acknowledgements

Financial support by the UNKP-19-3-SZTE-153 New National Excellence Program of the Ministry of Human Capacities (V. J. Kolcsár) is appreciated.

References

- [1] I. Ojima (Ed.), *Catalytic Asymmetric Synthesis*, 3rd ed., John Wiley & Sons, Hoboken, New Jersey, 2010.
- [2] M. Benaglia, *Recoverable and Recyclable Catalysts*, John Wiley & Sons, Chichester, 2009.
- [3] Gy. Szöllősi, L. Kovács, V. Kozma, V.J. Kolcsár, *React. Kinet. Mech. Catal.* 121, 2017, 293.
- [4] S. Vijaikumar, A. Dhakshinamoorthy, K. Pitchumani, *Appl. Catal. A: Gen.* 340, 2008, 25.
- [5] Gy. Szöllősi, M. Fekete, A.A. Gurka, M. Bartók, *Catal. Lett.* 144, 2014, 478.
- [6] U. Scheffler, R. Mahrwald, *Chem. Eur. J.* 19, 2013, 14346.
- [7] Gy. Szöllősi, D. Gombkötő, A.Zs. Mogyorós, F. Fülöp, *Adv. Synth. Catal.* 360, 2018, 1992.

BIOGAS PRODUCTION FROM AGROINDUSTRIAL WASTE PRE-TREATED WITH LIGNOLYTIC FUNGI

Csilla Szűcs¹, Etelka Kovács¹, Zoltán Bagi¹, Gábor Rákhely^{1,2,3}, Kornél L. Kovács^{1,4,5}

¹Department of Biotechnology, University of Szeged, Szeged, Hungary

²Institute of Environmental and Technological Sciences, University of Szeged, Hungary

³Institute of Biophysics, BRC, Szeged, Hungary

⁴Department of Oral Biology and Experimental Dentistry, University of Szeged, Szeged, Hungary

⁵Hungarian Biogas Association

Abstract

Renewable energy was never more important than in a century when energy consumption is unprecedented. Biogas is considered to be one of the most important natural energy sources. We aim to enhance biogas production through the pre-treatment of substrates, that are normally hard to digest because of their high content of cellulose, hemi- and lignocellulose. As part of fungal pre-treatment we used *Aspergillus nidulans* and *Trichoderma reesei*. Both of these filamentous fungi are well known for their ability to synthesise various enzymes – including cellulases. During our experiments *A. nidulans* and *T. reesei* filamentous fungi's endoglucanase activities were measured by spectrophotometer and methane-producing was monitored by gas chromatography.

Introduction

Our society's hunger for energy is growing rapidly. Solving the situation should include environmentally friendly energy sources, such as plant biomass, which is produced in large amounts every day – in both natural and artificial ways. [1] Agroindustry generates unbelievable quantities of corn stalk and wheat straw each year, and they cannot be used in further processes. Organic waste and by-products are processed and valuable energy (biogas) is gained by anaerobic digestion. [2] Filamentous fungi are known as inhabitant of lignocellulose-rich plant tissues and also as unique enzyme producers. [3,4] Combining these two properties suggests that filamentous fungi can successfully enhance biogas production.

Experimental

Filamentous fungi *A. nidulans* was isolated from cattle rumen previously. *T. reesei* was used from our strain collection. (Department of Biotechnology, University of Szeged, Szeged, Hungary) The fungal colonies were maintained on Czapek-Dox-agar plates. [5] Plates contained 3 g/l NaNO₃, 1 g/l K₂HPO₄, 0.5 g/l MgSO₄, 0.5 g/l KCl, 0.5 g/l FeSO₄, 15 g/l agar and either corn stalk or wheat straw as source of carbohydrate. Corn stalk and wheat straw were inoculated with the filamentous fungi as pre-treatment. The sterilized substrates were added 20 ml of sterile distilled water and 10⁷ spores of either *A. nidulans* or *T. reesei* in the different samples.

Endo-(1,4)-β-D-glucanase activity was measured in every three day during the pre-treatment using 3,5-dinitrosalicylic acid (DNSA) method [6]. The absorbance of the samples were measured spectrophotometrically at 550 nm using a GENESYS UV-Visible scanning Spectrophotometer (ThermoFisher Scientific, Wilmington, DE, USA). After 10 days of fungal pre-treatment the samples were inoculated with sludge. (Zöldforrás Biogas Plant, Szeged, Hungary)

The negative controls contained only sludge, the positive controls contained only α-cellulose as substrate. All anaerobic digestion experiments were carried out under mesophilic conditions. Methane-concentration of the produced biogas was measured daily via gas chromatography (Agilent 6890N Gas Chromatograph, Agilent Technologies, Santa Clara, CA, USA).

Results and discussion

Scanning electron microscopy pictures (SEM) were taken of the plant tissues during pre-treatment. *A. nidulans* filamentous fungus obviously inhabited the substrate wheat straw (Fig. 1-2.).

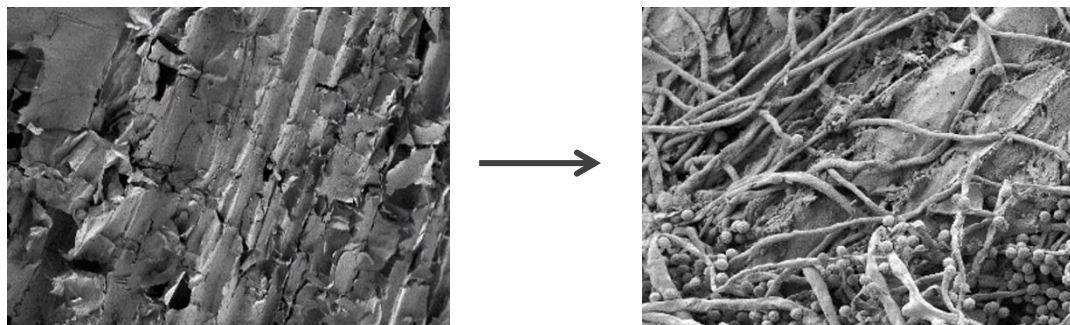


Figure 1. and 2.

Endoglucanase activity

It was observed that endo-(1,4)- β -D-glucanase activity depends mostly on the applied substrate and fungus. As it was expected *A. nidulans* proved to be a stunning enzyme producer. It preferred corn stalk as a substrate rather than wheat straw. Figure 3. shows that endoglucanase activity was outstanding when corn stalk was applied as a source of carbohydrate for *A. nidulans*.

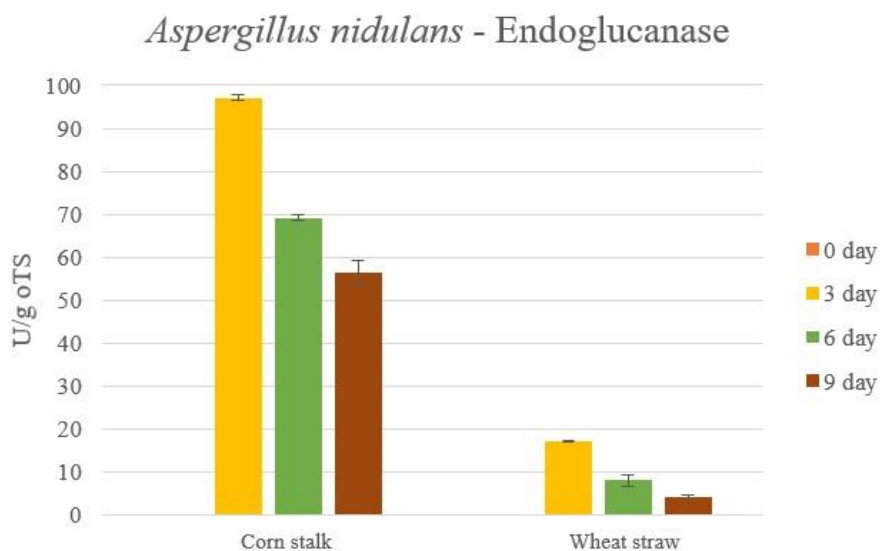
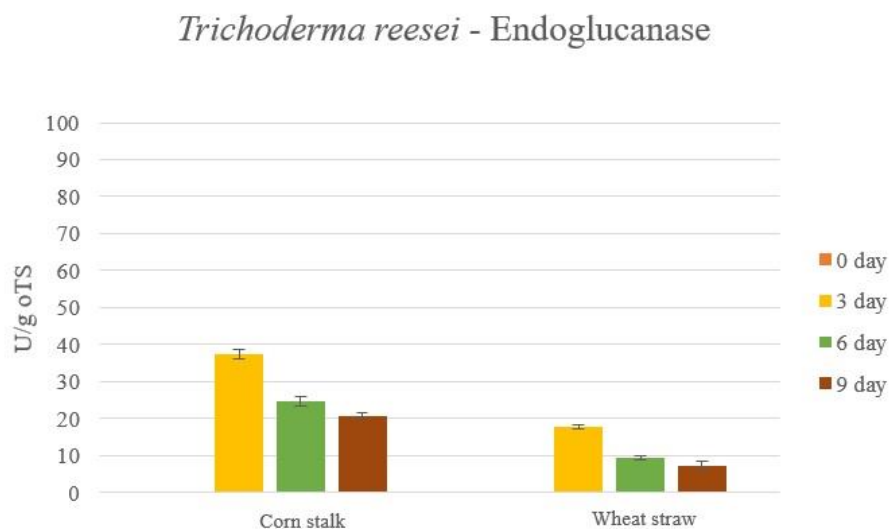
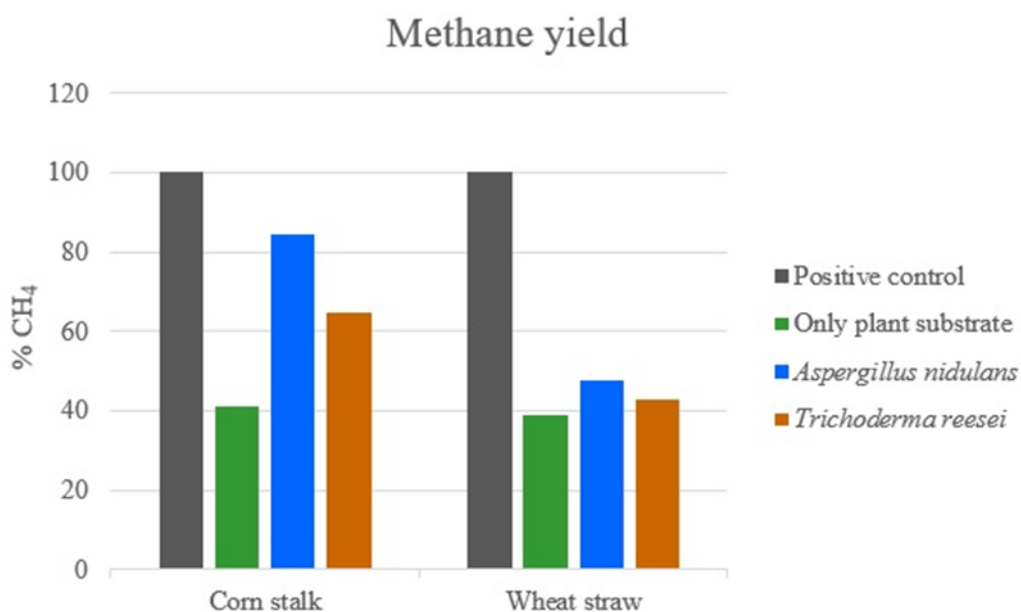


Figure 3.

The endoglucanase activity of *T. reesei* was lower on both substrates, however this fungus was also more successful on corn stalk. (Fig. 4.) A descending activity was observed in every sample, which refers to the diminishing of nutrients in the solutions.

Methane production**Figure 4.**

On Fig. 5. it is shown that fungal pretreatment increased methane yield. The results of methane production is expressed as percentage of the non pre-treated substrates. As it was expected after the enzyme activity assays, corn stalk combined with *A. nidulans* had the highest methane yield, pre-treatment of substrate with *T. reesei* also enhanced biogas production.

**Figure 5.**

Conclusion

As demonstrated above both *A. nidulans* and *T. reesei* have significant enzyme producing capability in cellulose-rich environment. Therefore, it is understandable that pre-treatment of plant substrate before anaerobic digestion positively affected biogas production. Furthermore, it is not only beneficial as renewable energy source, but with this method we could decrease the amount of organic waste in a more profitable way.

Acknowledgements

This work was supported by the Hungarian National Research, Development and Innovation Fund (grant number NKFI-PD 128345), the domestic grant GINOP-2.2.1-15-2017-00081 and the EU Horizon 2020 research and innovation programme, BIOSURF project (contract number 646533).

We owe special thanks to Dr. Gergő Maróti and Attila Farkas (Biological Research Centre) for taking fantastic SEM photos of our samples.

References

- [1] Plazonić, I., Barbarić-Mikočević, Ž., Antonović, A. (2016). Chemical composition of straw as an alternative material to wood raw material in fibre isolation. *Drvna industrija*, 67(2), p. 119–125. <https://doi.org/10.5552/drind.2016.1446>
- [2] Bolzonella D., Battistoni P., Mata-Alvarez J., Cecchi F. (2003). Anaerobic digestion of organic solid wastes: process behaviour in transient conditions. *Water Sci Technol* 48(4): p1–8
- [3] Akin, D. E., Rigsby, L. L. (1987). Mixed fungal populations and lignocellulosic tissue degradation in the bovine rumen. *Applied and Environmental Microbiology*, 53(9)
- [4] Gupta, V. K. (2016). *Aspergillus* System Properties and Applications. *New and Future Developments in Microbial Biotechnology and Bioengineering: Microbial Cellulase System Properties and Applications*. <https://doi.org/10.1016/B978-0-444-63507-5.00008-3> ISBN: 978-0-444-63507-5
- [5] https://www.dsmz.de/microorganisms/medium/pdf/DSMZ_Medium130.pdf
- [6] Ahmed I., Zia M. A., Iqbal H. M. N. (2010). Bioprocessing of proximally analyzed wheat straw for enhanced cellulase production through process optimization with *Trichoderma viridae* under SSF. *Int. J. Biol. Life Sci.* 6:3.

REMODELLING OF LCA COMPATIBLE ENVIRONMENT LOADING

Ildikó Trója, István Varga, Anna Gutási, Péter Hausinger, Zsolt Molnár, Andrea Serester, Márta Gálfi, Marianna Radács

*Institute of Applied Natural Science, Faculty of Education, University of Szeged Hungary,
Department of Environmental Biology and Education, Juhász Gyula Faculty of Education,
University of Szeged
e-mail: trildi92@gmail.com*

Abstract

Organizations that maintain the modern economy (companies, business organizations, social units) have the basic purpose of operating in order to make the highest profits, which is why they are looking for the key positions of production with which they can significantly reduce their expenses. A standardized method for tracking environmental pressures resulting from social activities is required, so our research team introduces the use of 1,4-dichlorobenzene as a model compound in its research protocols following the LCA standard.

Introduction

The system with the highest complexity known under terrestrial conditions is the human society, in which actors are able to transform the environment according to their particular needs, through cooperative action patterns. Thus, environmentally conscious social and organizational management has become a key and several methods of its implementation are known the Environmental Management System (KIR) [1]. KIR has made it possible to link the organization's objectives, which interpret the pursuit of economic efficiency with the need to maintain ever-increasing environmental safety [2]. The assessment of environmental problems characteristically addresses the economic aspects by which, in the current state of knowledge, it constantly iterates the methods of implementing the mandatory principle of continuity. In line with this logic, the need to optimize increasing use of the environment in a corporate environment is essential. In this context, society has created a set of standards that can be used for life cycle analysis (LCA), the International Standard 14040. The standard does not interpret the environmental emissions and environmental impacts and risks associated with a particular product as such, but it integrates them into environmental problems. Several methods of analysis are known, including acidification potential, ozone depletion potential, eutrophication potential, human toxicity potential [3]. Because of the variety of methods involved in presenting the results, our research team uses 1,4-dichlorobenzene (dCIB) as a reference compound linked to the LCA standard, as this agent may be useful in detecting the ecotoxic potential of substances. During the environmental cycle, chlorobenzenes can accumulate in plant and animal organisms. Exposure to chlorobenzene in the human population may occur during the production and use of chlorinated organic compounds. Their neurotoxic endocrine disruptor activity has been reported in numerous literatures [4, 5].

Aims

The aim of this present work is to develop a test model that conforms to the LCA standard so that the results obtained are comparable and reliable.

Methods

Prolactinomas adenohypophysis (AdH) was induced by subcutaneously administered estrone acetate (CAS registration number 901-93-9, Sigma, Germany; 150 µg / bw kg / week) for 6 months. Following pentobarbital anesthesia (4.5 mg / kg Nembutal, Abbott, USA), the animals were decapitated and the transformed AdHs were sterile removed under a preparative

microscope. Subsequently, primary monolayer cell cultures were prepared from the preparations. Cell cultures were treated with: Corticosterone (B): 1 μg / ml; AVP (arginine-vasopressin) 10^{-6} M; + B + AVP: in combination, B was pretreated with AVP 20 minutes before treatment, 1,4-dichlorobenzene (dCIB): 0.1 ng / ml; chlorobenzene mix (mCIB): 0.1 ng / ml; fenuron (PU) 10^{-6} M; monuron (MU): 10^{-6} M; diuron (DU) with 10^{-6} M agents.

Results and discussion

The human toxicity potential for dCIB effects is standardized by ISO 14040. Accordingly, we have introduced impact studies that underpin this standardization in our research. Data suggest that dCIB modulates ACTH secretion in the adenohypophysis and its prolactinomic transformation.

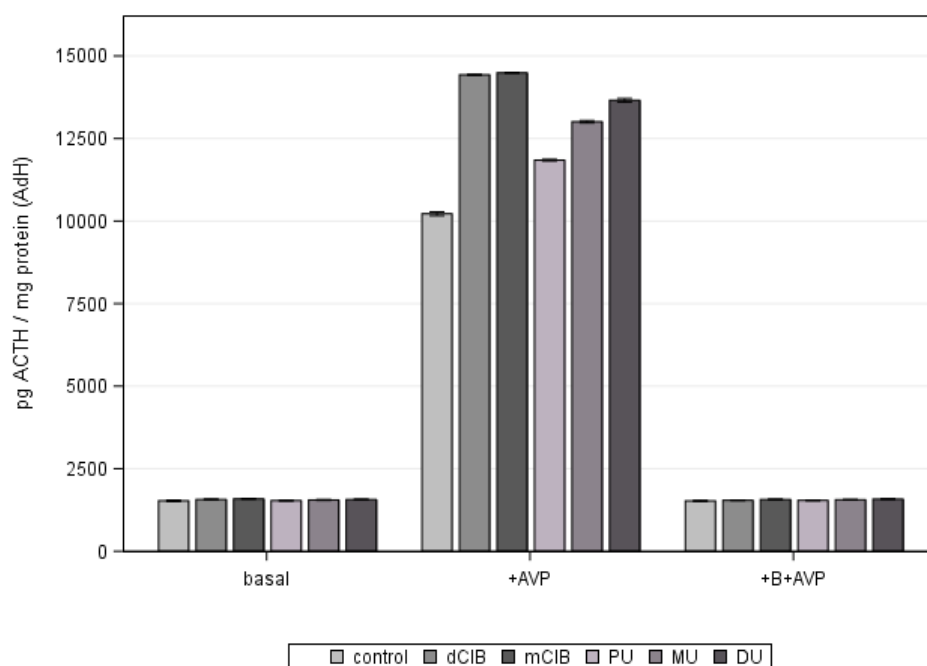


Figure 1. Effect of chlorobenzene and phenylurea treatments on ACTH secretion in normal adenohypophyseal cell cultures (mean \pm SEM, n = 6)

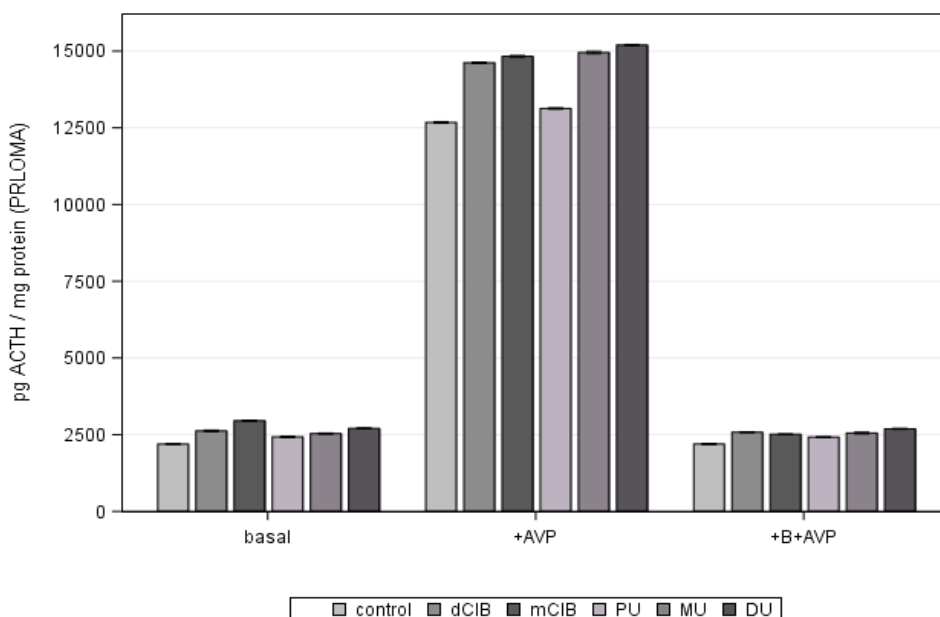


Figure 2. Effect of chlorobenzene and phenylurea treatments on ACTH secretion in prolactinoma adenohypophysis (PRLOMA) cell cultures (mean \pm SEM, n = 6)

Conclusion

It has been shown that both adenohypophysis and prolactinoma adenohypophysis in cultured cell cultures have primary endocrine disruptors in ACTH secretion. The human toxicity potential for dCIB effects is standardized by ISO 14040. Accordingly, we have introduced in our research the so-called standardization effect assays that characterize the endocrine disruptor compounds we study, so that the data become internationally comparable.

Acknowledgement

EFOP-3.4.3-16-2016-00014, EFOP-3.6.1-16-2016-00008, TÁMOP-4.2.4.A/2-11/1-2012-0001

References

- [1] H. C. Guo, L. Liu, G. H. Huang, G. A. Fuller, R. Zou, Y. Y. Yin. A system dynamics approach for regional environmental planning and management: A study for the Lake Erhai Basin, *Journal of Environmental Management*, 2001, 61, 93-111.
- [2] R. J. Barro, X. S. Martin. *Economic Growth*, Second Edition, The MIT Press, 2003, ISBN 978-0262025539.
- [3] J. F. Henry. *The Making of Neoclassical Economics*, Routledge, 1990, ISBN 978-0415618731.
- [4] M. Weselak, T. E. Arbuckle, W. Foster. Pesticide exposures and developmental outcomes: the epidemiological evidence. *J Toxicol Environ Health B Crit Rev*, 2007, 10, 41-80.
- [5] T. Colborn, F. S. vom Saal, A. M. Soto. Developmental effects of endocrine-disrupting chemicals in wildlife and humans. *Environ Health Perspect*, 1993, 101, 378-384.

THE INVESTIGATION OF SUGAR SUBSTITUTE COMPOUNDS ON NEUROENDOCRINE FUNCTIONS - IN ENVIRONMENTAL LOAD MODEL

István Varga, Zsolt Molnár, Anna Gutási, Ildikó Trója, Péter Hausinger, Marianna Radács, Márta Gálfi

*Institute of Applied Natural Science, Faculty of Education, University of Szeged Hungary
Department of Environmental Biology and Education, JuhászGyula Faculty of Education,
University of Szeged
e-mail: vargaistvan551@gmail.com*

Abstract

Nowadays in the society sugar substitutes are gaining high importance. These substitutes can enter the human body through nutrition and may alter metabolic pathways through potential related mechanisms. The neuroendocrine system plays a key role in maintaining homeostasis, including sugar balance. The aim of this present work was to develop a model system in which the effects of certain sugar substitutes on endocrine function can be traced and presented with a well-understood data system.

Introduction

Psycho-immuno-neuroendocrine activity is essential in the homeostasis, which enables human potential to maintain social, biological equilibrium. The viability of psychogenic activity (e.g. learning, cognitive function, behaviour, etc.) is embedded in the complex biogenic activity (neuroendocrine immune functions). It is a very interesting question how much the psychic activity elements of social life (e.g. cognition) can change when neuroendocrine communication is interrupted when it is necessarily altered by chemical environmental influences (e.g. nutritional biological agents) through actual technosphere exposures [1, 2]. Nowadays, sugar substitutes are widely used, are nutritionally important, and can thus act as potential external agents to activate internal biological metabolic pathways; e.g. modulating sugar metabolism. Adaptation is achieved in human activities (such as social, learning, emotional, intellectual, etc.) through social engagement. We investigated this by studying regulation of the hypothalamic-pituitary axis by *in vivo* and *in vitro* model systems as neuroendocrine regulation, in which the neurohypophysis (NH) hormones oxytocin (OT) and arginine-vasopressin (AVP) were prominent [3, 4]. Due to its antidiuretic role, AVP is essential in osmoregulation, volume regulation, and is also known as an effector neuropeptide of behavior, learning (implicit), memory functions, attachment, trust, cognitive function, properties) mediation (creative) element [5, 6]. These endocrine hormones are involved in neuronal processes via monoamine (MA) signalling [7], which is confirmed by the mechanisms of action of dopamine (DA), norepinephrine (NE), and serotonin (5-HT). Events regulated through the cellular energy cascade will be detected, which can be strongly modulated by the presence of nutritional biological conditions (sugar substitutes).

Aims

Our aim is to investigate the effects of changes in environmental conditions in cognitive processes mediated by neuroendocrine communication, in which we study the (chemical) changes in the environmental conditions of neuroendocrine cycles in a standardized model system; and how they may affect homeostatic complexity (which we also want to follow through cognitive function, learning).

Methods

In our experimental model, male Wistar rats were used to prepare primary neurohypophysis cell cultures. The rats were treated in vivo with sugar replacement compounds for 16 weeks: erythriol 4 g / day, saccharin 0.2 mg / day, xylitol 40 mg / day and stevia at 40 mg / day. After anesthesia with pentobarbital (4.5 mg / kg, Nembutal, Abbott, USA), the rats were decapitated and then subjected to a preparative microscope to separate the neurohypophysis and adenohypophysis. Primary, monolayer neurohypophysis cell cultures were prepared by enzymatic and mechanical dissociation. The tissues were digested enzymatically (trypsin: 0.2 % /Sigma, Germany/ for 30 min; collagenase /Sigma, Germany/: 30 µg/ml for 40 min; dispase /Sigma, Germany/: 50 µg/ml for 40 min in phosphate-buffered saline /PBS-A/; temperature: 37°C). After viability and functional standardization, the starting cell density was $2 \times 10^5/\text{cm}^2$. cell cultures were treated with 10^{-6}M of NA. The AVP content of supernatant media was determined by RIA method.

Results and discussion

According to our results, discrete modulation has occurred as a result of the effects of these sugar-substituting compounds on cell cultures, it is demonstrated that the discrete differences in the sugar substitutes used were modulated in the activation-driven model system. The assay protocol shown may be suitable for environmental exposures, in particular for nutritional biologically important sugar substitutes.

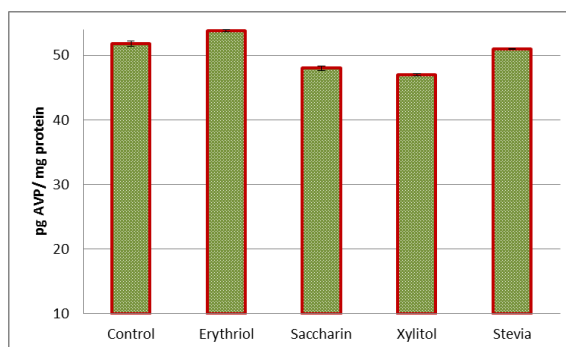


Figure 1. Effect of sugar substitutes on AVP secretion of NH cell cultures (means \pm SEM, n=6)

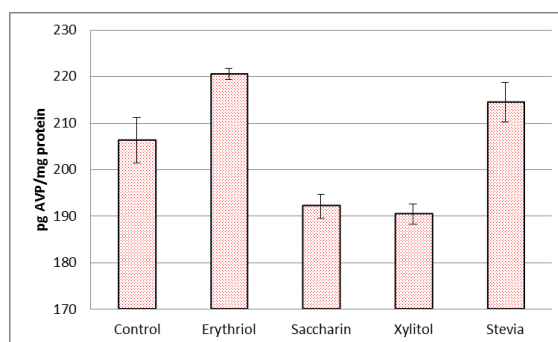


Figure 2. Effect of NA activated and sugar replacement compounds on AVP secretion in NH cell cultures (means \pm SEM, n=6)

Conclusion

In order to meet basic needs in society, many substances which have a significant effect on the endocrine system and / or its system of contacts are warranted, and therefore endocrine-related compounds of nutritional importance should be investigated.

Acknowledgements

EFOP-3.4.3-16-2016-00014, EFOP-3.6.1-16-2016-00008, TÁMOP-4.2.4.A/2-11/1-2012-0001

References

- [1] S. D. Anton, C. K. Martin, H. Han, S. Coulon, W.T. Cefalu, P. Geiselman, D. A. Williamson, Effects of stevia, aspartame, and sucrose on food intake, satiety, and postprandial glucose and insulin levels. *Appetite*, 2010, 55, 37-43.
- [2] Z. Molnár, R. Pálföldi, A. László, M. Radács, K. Sepp, P. Hausinger, L. Tiszlavicz, Z. Valkusz, M. Gálfi, Effects of chronic and subtoxic chlorobenzenes on adrenocorticotrophic hormone release. *Journal of Environmental Sciences*, 2015, 34, 165-70.
- [3] Gálfi, M., Radács, M., Molnár, Z., Budai, I., Tóth, G., Pósa, A., Kupai, K., Szalai, Z., Szabó, R., Molnár, H.A. 2016. Ghrelin-induced enhancement of vasopressin and oxytocin secretion in rat neurohypophyseal cell cultures. *Journal of Molecular Neuroscience* 60 ,525-530.
- [4] H. F. Clarke, S. C. Walker, H. S. Crofts, J. W. Dalley, T. W. Robbins, A. C Roberts., Prefrontal serotonin depletion affects recersasl learning but not attentional set shifting. *The Journal of Neuroscience*, 2005, 25, 532-538.
- [5] R. Hurlemann, A. Patin, O. A. Onur, M. X. Cohen, T. Baumgartner, S. Metzler, I. Dziobek, J. Gallinat, M. Wagner, W. Maire, K. M. Kendrick, Oxytocin enhances amygdala-dependent, socially reinforced learning and emotional empathy in humans. *Journal of Neuroscience*, 2010, 30, 4999-5007.
- [6] C. W. Harley, Norepinephrine and dopamine as learning signals. *Neural Plasticity*, 2004, 11, 191-204.
- [7] de D. Wied, Neuropeptides in learning and memory processes. *Behavioural Brain Research*, 1997, 83, 83-90.
- [8] B. Alescio-Lautier, B. Soumireu-Mourat, Role of vasopressin in learning and memory in the hippocampus. *Prog. Brain. Res.*, 1998, 119, 501-521.

MICROPLASTICS AS ENVIRONMENTAL THREAT

Vesna Vasic, Dragana Kukic, Marina Šciban, Nevena Blagojev, Jelena Prodanović

University of Novi Sad, Faculty of Technology Novi Sad, Bul.cara Lazara 1, 21000 Novi Sad, Serbia

e-mail: vesnavasic@tf.uns.ac.rs

Abstract

The reason for initiating this topic is the fact that the presence of microplastic in surface waters has become an alarming global problem. Except in water, microplastics can be found in sediment and soil, but also in groundwaters, bottled waters, sea salt, food from the sea, other foods (for example, honey) and drinks (for example, beer), air, etc. Both national and European regulations do not prescribe determination of microplastics in wastewaters discharged into the environment, as well as in drinking water, food and beverages. Considering the prevalence of the problem it can be expect this item to be entered into the relevant regulations. In addition, the European Marine Strategy Directive requires EU Member States to ensure that by 2020 "the characteristics and quantities of waste in the sea do not harm the coastal and marine environment". Preventive action and shared responsibility in combating damage would result in the preservation of biological balance. Regardless the regulations, it is desirable to know the extent of load of sea water and surface waters by microplastic. The production of plastic in the world has increased about 20 times, in the last few decades. Although the most of the used plastic is trying to recycle, a significant part gets to the environment, intentionally or accidentally. World production of plastic surpassed the 320 million tons mark in the 2016. Also, it is estimated that between 5 and 13 million tons of plastic waste leaks into the World's oceans every year as a result of inappropriately dumped and mismanaged [1]. Sources of microplastics are widespread. It originates from diverse sources and can be broadly classified into land- and sea-based sources. They include: agricultural runoff, urban runoff, stormwater, aquaculture, textiles, tyres, paints, cruise ships, ocean dumping, etc. Terrestrial emissions are the dominant source of microplastics. Microplastics originate predominantly from automobile tire wear, household and laundry dust, industrial processes (e.g., blasting and deflashing of plastics), and through deterioration of surfaces made of or coated with plastic, for example, artificial turf and polymeric paint, etc. Most of these emissions occur in urban and residential areas [2]. Sea-based sources of microplastics are attributed to the fishing, shipping, and offshore industry sectors. Among mentioned sources, wastewater treatment plants are one of the dominant sources of microplastics. In his work Li et al. [3] lists the key results from the microplastics studies on several wastewater treatment plants.

Plastic products are produced to be long lasting and therefore pose a long lasting environmental hazard. When they get into the water, due to a different effects (wind, rain, UV light, mechanical action), the plastic objects are braking to the micro sizes of so-called microplastics (secondary microplastics). In addition, plastic origins from personal hygiene products (toothpastes, washing agents, roll-on deodorants, exfoliating body washes, facial scrubs etc.) gets into the wastewaters as micro-size balls of plastic so-called microbeads (primary microplastics). Microbeads are tiny polyethylene spheres which, contrary to microplastics, do not come from the degradation of large pieces of plastic. Instead, they are manufactured on purpose to be put into consumer products. These tiny plastic microbeads are usually less than 1 millimetre at their largest [4]. Due to their small size as well as small density, they can pass through the wastewater treatment plant and end up in the water in nature. Therefore, their use in the United States, Canada and the United Kingdom is already

prohibited, and a ban is also expected in the European Union. However, the risk of microplastic originating from larger plastic objects is and will remain a big problem for a long time.

Recent researches suggest that plastics can accumulate different pollutants. Based on the literature data, it is believed that the remains of plastics can attract and concentrate up to one million times more pollutants compared to their amount in seawater. Variety of animals living in the water adopt microplastic as food. Ingestion of microplastics by water organisms in most cases is accidental because the particle is often mistaken for food [5]. Microplastics ingested by water organisms can cause chemical and physical harm (hindering mobility and clogging of the digestive tract, inflammation, hepatic stress, decreased growth). The consumption of microplastics is common to a wide range of water organisms, such as invertebrates, mussels, barnacle, sea cucumbers, zooplankton and fishes. Also, turtles, fish-eating birds and mammals can consume microplastics, which can interfere with the food chain as microplastics ingested by organisms in the lower trophic level could pass up the food chain when lower trophic organisms are fed upon by organisms in the higher trophic level [6]. The presence of microplastics in water could lead to contamination of water products that humans use as food. One of such product is sea salt. These particles have also been reported in drinking water. Eerkes-Medrano et al. [7] reviewed studies about findings of microplastics in drinking water (bottled water and drinking water treatment plants). Presence of microplastics in food for human consumption and in air samples has been reported. Thus, microplastics exposure via diet or inhalation could occur, and cause the effects on human health.

Therefore, it is clear that it is necessary to take all measures to minimize damaging impact of microplastics on the environment, human and animal health. What are the solutions? Education and raising awareness about harmful effects of microplastics on the environment, good management of plastic waste (e.g. recycling), reduce the use of plastic packaging, improve wastewater treatment processes and developing and improving of methods for microplastics detection and analysis

These are things to think about when it comes to the use of plastic and its impact on the environment. First of all, this refers to education, primarily children and young people, in order to raise awareness about the importance of this problem.

Acknowledgement

This research was supported by the grant number III 43005 from the Ministry of Education and Science of the Republic of Serbia.

References

- [1] A.B.Silva, A.S. Bastos, C.I.L. Justino, J.P. da Costa, A.C. Duarte, T.A.P. Rocha-Santos, Microplastics in the environment: Challenges in analytical chemistry – A review. *Analytica Chimica Acta* 1017 (2018), 1-9.
- [2] L. Nizzetto, M. Futter, S. Langaas, Are Agricultural Soils Dumps for Microplastics of Urban Origin? *Environmental Science and Technology* 50 (2016), 10777–10779.
- [3] J. Li, H. Liu, J.P. Chen, Microplastics in freshwater systems: A review on occurrence, environmental effects and methods for microplastics detection. *Water Research* 137 (2018), 362-374.
- [4] <https://get-green-now.com/how-do-microplastics-affect-the-environment/>
- [5] O.M. Lönnstedt, P. Eklöv, Environmentally relevant concentrations of microplastic particles influence larval fish ecology. *Science* 352 (2016), 1213-1216.
- [6] H.S. Auta, C.U. Emenike, S.H. Fauziah, Distribution and importance of the microplastics in the marine environment: A review of the sources, fate, effects, and potential solutions. *Environment International* 102 (2017), 165-176.

[7]D. Eerkes-Madrano, H.A. Leslie, B. Quinn, Microplastics in drinking water: A review and assessment. *Current Opinion in Environmental Science & Health* 7 (2019), 69-75.

DETERMINATION OF GLUTAMATE AND GABA FROM RAT CENTRAL NERVOUS SYSTEM SAMPLES WITH HPLC UTILIZING FLUORESCENT DETECTION

Gábor Veres^{1,2}, Andrea Tellér³, Diána Martos¹, István Szatmári⁴, Lóránd Kiss⁴, László Vécsei^{1,2}, Dénes Zádori²

¹*Department of Neurology, Faculty of Medicine, Albert Szent-Györgyi Clinical Center, University of Szeged, H6725, Szeged, Semmelweis str. 6., Hungary*

²*MTA-SZTE Neuroscience Research Group, H6725, Szeged, Tisza Lajos krt. 113., Hungary*

³*Department of Physiology, Anatomy and Neuroscience, University of Szeged, H6726, Szeged, Közép fasor 52., Hungary*

⁴*Institute of Pharmaceutical Chemistry, University of Szeged, H6725, Szeged, Zrínyi str. 9., Hungary*

e-mail: veres.gabor@med.u-szeged.hu

Abstract

The research of neurological diseases has great importance and the determination of neurotransmitter concentrations is essential during these investigations. The levels of main excitatory (glutamate) and inhibitory (γ -amino-butyric acid (GABA)) neurotransmitters often change as a result of pathological alterations. For example, in case of migraine, elevated glutamate release is suggested to be a part of the pathomechanism, causing hypersensitivity to pain. Our goal in this study was to optimize a liquid chromatography method to measure glutamate and GABA from the trigeminal nucleus pars caudalis (TNC) of rats, which is responsible for pain processing. As a result, we were able to validate our method according to international guidelines where the investigated parameters were LOD, LOQ, precision and recovery. Furthermore, we applied a new internal standard which has not been published so far. This method will be utilized in the investigation of migraine animal models to evaluate potential new therapeutic approaches.

Introduction

Headache, one of the most common disorders of the nervous system, is a major health problem worldwide. The global prevalence of active headache disorders for the adult population is 46% for headache in general, 11% for migraine, 42% for tension-type headache and 3% for chronic daily headache [1]. The treatment of primary headache disorders is challenging and requires both acute and preventive therapeutic strategies [2]. The efficacy of these treatments is not always satisfactory and the contraindications and side-effects often limit the options of the physician [3, 4]. There is, therefore, a constant need for the study and development of new therapeutic approaches.

Animal and human studies suggest that glutamate receptors are present in various parts of the trigeminal system [5] which is the system responsible for processing most of the pain originating from the head area [6]. The stimulation of the trigeminal nerve results in elevated glutamate levels in the spinal trigeminal nucleus pars caudalis (TNC, [7]). The peripheral application of glutamate to deep craniofacial tissue proved to activate and sensitize nociceptive afferents and neurons in the upper cervical cord [8]. These findings suggest that excitatory amino acid receptors (particularly N-methyl-D-aspartate receptors (NMDAR)) play an important role in pain processing and the sensitization process as well [9].

Based on these findings, our aim in this study was to optimize an HPLC method to measure the excitatory amino acid glutamate and its inhibitory counterpart γ -amino-butyric acid

(GABA) in rat TNC samples for the future evaluation of these neurotransmitters in preclinical investigations of migraine.

Sample acquisition and preparation

For this study we used male Sprague-Dawley rats weighing 250-300 g. The animals were housed in cages under standard conditions with a 12-12-h light-dark cycle and free access to food and water. To acquire the TNC, rats were anesthetized with 4 w/w% chloral hydrate intraperitoneally then they were transcardially perfused with artificial cerebrospinal fluid (pH = 7.4, concentrations in mM: 122 NaCl, 3 KCl, 1 Na₂SO₄, 1.25 KH₂PO₄, 10 D-glucose monohydrate, 1 MgCl₂ x 6 H₂O, 2 CaCl₂ x 2 H₂O, 6 NaHCO₃). The samples containing the medullary segment of TNC were then removed and stored at -80°C until measurement.

Before measurement, the tissue samples were sonicated in ice cold 85% methanol (10 µl/mg tissue) then they were centrifuged (12 000 RPM, 10 min, 4°C) and the supernatants were collected. Then 100 µl sample was derivatized with 100 µl freshly prepared solution (2 ml o-phthalaldehyde, 7.94 ml 0.2 M borate buffer (pH = 9.9), 60 µl 3-mercaptopropionic acid) and 50 µl distilled water containing the internal standards homoserine and (1R,2S)-2-amino cyclopent-3-ene-1-carboxylic acid (ACK).

HPLC method

For the determination of glutamate and GABA, we used an Agilent 1100/1260 system (Agilent Technologies, Santa Clara, CA, USA) equipped with a fluorescence detector (FLD). Chromatographic separations were performed on a Kinetex C18 150x4.6 i.d. 5 µm particle size column (Phenomenex Inc., Torrance, CA, USA) after passage through a SecurityGuard pre-column C18, 4x3 mm i.d., 5 µm particle size (Phenomenex Inc., Torrance, CA, USA) applying gradient elution. Mobile phase A was 95:5 V/V% 0.05 M sodium acetate (pH = 5.5):methanol, while mobile phase B was 45:45:10 V/V% methanol:acetonitrile:water. The elution started with 95% A decreasing linearly to 50% then staying there for 2 min and reequilibrating to 95% in 1 min for a total 16 min runtime. The flow rate was 1 ml/min, injection volume was 10 µl and the fluorescent detector was set to 230/440 nm for excitation/emission wavelengths.

Results and discussion

The first step of our method optimization was to determine the optimal excitation and emission wavelengths for the fluorescent detector. The acquired spectrum can be seen in Figure 1. and 2. and based on these spectrums the wavelengths were set to 230/440 nm for excitation/emission.

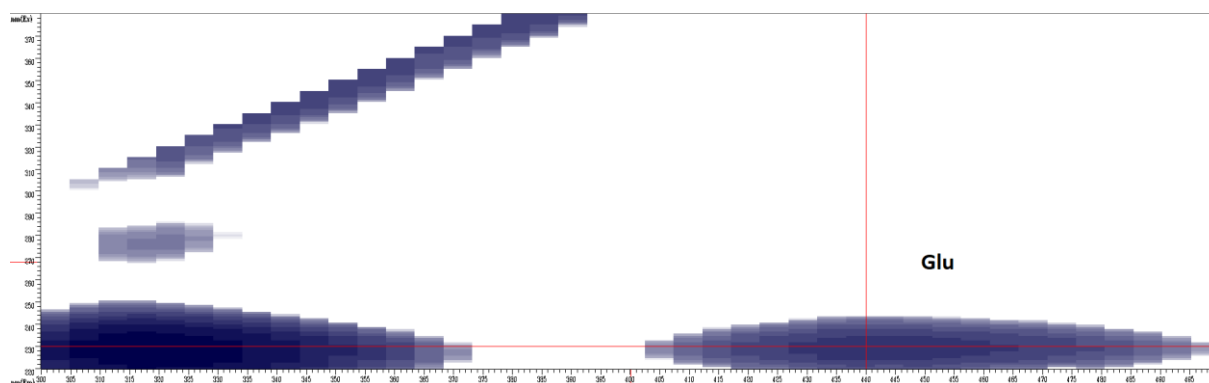


Figure 1. The fluorescent spectrum of glutamate

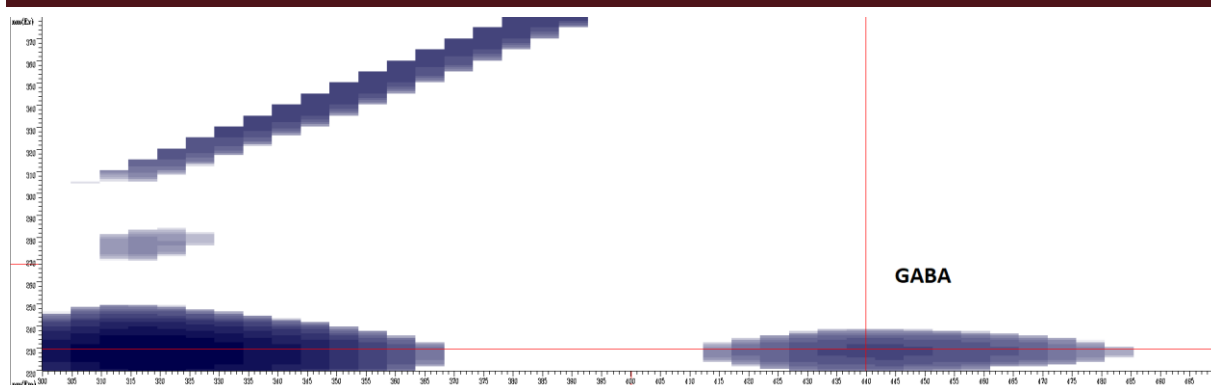


Figure 2. The fluorescent spectrum of GABA

During our measurements we used standard solutions in 6 different concentrations for external calibration. The calculated calibration curve was linear in the investigated concentration range and its details can be seen in Table 1.

Table 1. Main characteristics of calibration

	Glu	GABA	Homoserine	ACK
Calibration range (μG/ML)	0.08–4	0.008–0.4	0.4	0.4
Calibration line slope	0.591	3.581	-	-
Calibration line	0.0013	0.0081	-	-
Intercept linearity (R^2)	0.999	0.999	-	-
Retention time (min)	5.348	10.713	7.036	12.627

The selectivity of the method was checked by comparing the chromatograms of glutamate, GABA, homoserine and ACK for a blank TNC sample and those for a spiked sample. All compounds could be detected in their own selected chromatograms without any significant interference. A sample chromatogram of a TNC sample can be seen on Figure 3.

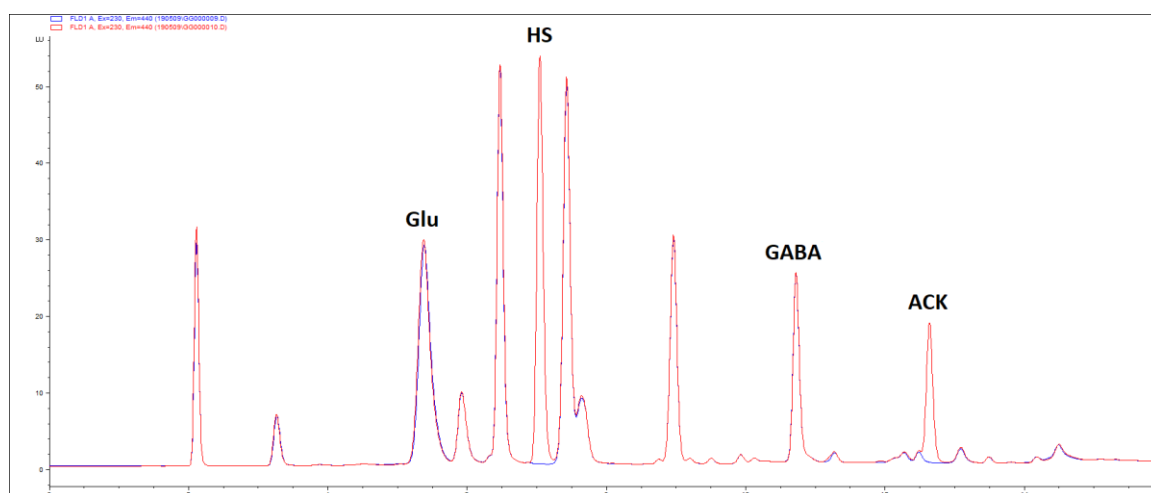


Figure 3. Representative chromatogram of a TNC sample with (red) and without (blue) internal standards. *Glu* glutamate; *HS* homoserine; *GABA* γ-amino-butyric acid; *ACK* (1R,2S)-2-amino cyclopent-3-ene-1-carboxylic acid

In the current study, LOD and LOQ were calculated as shown in Equation 1. The LOD values for glutamate and GABA were 0.03 and 0.006 µg/ml, respectively. The LOQ values for glutamate and GABA were 0.09 és 0.019 µg/ml, respectively

$$\text{LOD} = 3.3 * \frac{\text{Df}}{\text{S}'} \text{ and } \text{LOQ} = 10 * \frac{\text{Df}}{\text{S}'}$$

Equation 1.

The calculation of LOD and LOQ values by formula, where σ is the standard error of the intercept and S' is the slope of the calibration curve of the analyte. *LOD* limit of detection; *LOQ* limit of quantification.

With regard to the within-run precision, after 6 consecutive injections the coefficients of variation of the concentrations were 1.3% and 0.35% for glutamate and GABA, respectively. The relative recoveries were estimated by measuring spiked samples of glutamate and GABA at two different concentration levels with three replicates of each. No significant differences were observed for the lower and higher concentrations. The recoveries for the TNC samples ranged from 88 to 100% for glutamate and 104 to 122% for GABA. These results are in line with Food and Drug Administration recommendations [10].

Conclusion

As a result of our method optimization, we were able to measure glutamate and GABA from rat TNC samples with a robust, reliable method. This region of the central nervous system was not investigated before with similar applications. Furthermore, we also applied a new internal standard for amino acid determination, which was not described before. In the future, this method will be applied in animal models of migraine to investigate potential protective therapies and we plan to extend this method to other biological matrices too, especially for cerebrospinal fluid and microdialysate samples.

Acknowledgements

The research was supported by GINOP-2.3.2-15- 2016-00034 ('Molecular Biological Fundamentals of Neurodegenerative and Immune Diseases: Therapeutic Trials with Kynurenines') and EFOP-3.6.1-16-2016-00008 ('Development of intelligent life science technologies, methods, applications and development of innovative processes and services based on the knowledge base of Szeged').

References

- [1] Stovner, L., Hagen, K., Jensen, R., Katsarava, Z., Lipton, R., Scher, A., Steiner, T., and Zwart, J.-A. 2007. The global burden of headache: A documentation of headache prevalence and disability worldwide. *Cephalalgia* 27(3): 193–210. doi:10.1111/j.1468-2982.2007.01288.x.
- [2] Weatherall, M.W. 2015. Drug therapy in headache. *Clin. Med.* 15(3): 273–279. doi:10.7861/clinmedicine.15-3-273.
- [3] Obermann, M., Holle, D., Naegel, S., Burmeister, J., and Diener, H.-C. 2015. Pharmacotherapy options for cluster headache. *Expert Opin. Pharmacother.* 16(8): 1177–1184. doi:10.1517/14656566.2015.1040392.
- [4] Diener, H.-C., Charles, A., Goadsby, P.J., and Holle, D. 2015. New therapeutic approaches for the prevention and treatment of migraine. *Lancet Neurol.* 14(10): 1010–1022. doi:10.1016/S1474-4422(15)00198-2.
- [5] Tallaksen-Greene, S.J., Young, A.B., Penney, J.B., and Beitz, A.J. 1992. Excitatory amino acid binding sites in the trigeminal principal sensory and spinal trigeminal nuclei of the rat. *Neurosci. Lett.* 141(1): 79–83. doi:10.1016/0304-3940(92)90339-9
- [6] Carpenter, M.B., and Sutin, J. 1983. Human neuroanatomy. Williams & Wilkins, Baltimore.
- [7] Oshinsky, M.L., and Luo, J. 2006. Neurochemistry of trigeminal activation in an animal model of migraine. *Headache* 46 Suppl 1: S39-44.
- [8] Lam, D.K., Sessle, B.J., and Hu, J.W. 2009a. Glutamate and capsaicin effects on trigeminal nociception I: Activation and peripheral sensitization of deep craniofacial nociceptive afferents. *Brain Res.* 1251: 130–139. doi:10.1016/j.brainres.2008.11.029.
- [9] Vikelis, M., and Mitsikostas, D.D. 2007. The role of glutamate and its receptors in migraine. *CNS Neurol. Disord. Drug Targets* 6(4): 251–257.
- [10] ICH. 1995. ICH harmonised tripartite guideline, validation of analytical procedures. Fed Regist: 60:11260.

ESTIMATE OF CONTROL MEASURES FOR AQUATIC MACROPHYTES IN BEČEJ-BOGOJEVO CHANNEL (SERBIA)

Maja Meseldžija¹, Milica Dudić¹, Radovan Begović², Marko Džigurski¹

¹University of Novi Sad, Faculty of Agriculture, Trg Dositeja Obradovića 8, Novi Sad, Serbia

²Chemical Agrosava, Palmira Toljatića 5/IV, Novi Beograd, Serbia

e-mail: maja@polj.uns.ac.rs

Abstract

From June to August 2016, a field survey of the distribution of aquatic macrophytes was performed along Bečej-Bogojevo channel, survey mark 0+250-1+600km. In this research taxonomy and vegetation of macrophytes are given. Dominant aquatic macrophytes were identified as well as their morphological and biological characteristics. Based on results at 10 locations of the Bečej-Bogojevo channel 16 weed species were determined. The main aquatic macrophytes occurring in study area are *Ceratophyllum demersum* L., *Trapa natans* L., and *Salvinia natans* L. All. Mechanical control measures were effective on all identified species except *Salvinia natans* (L). All. which is restores from fragments, while from biological measures in our country only the introduction of the grass carp species is applied (*Ctenopharyngodon idella* Valenciennes in Cuvier & Valenciennes, 1844).

Introduction

Aquatic macrophyte species are important parts of natural aquatic systems because they produce oxygen and perform a water-purification function by binding heavy metals and removing nutrient loads [1]. Macrophytes serve as habitats for a wide diversity of organisms, they promote sediment deposition, increase water clarity and quality and have an influence on fish productivity [2]. Problems with aquatic plants have increased in the last two centuries, so they disturb the flow of water in irrigation canals and drainage channels. Deep-rooted submerged weeds cause a reduction in oxygen levels and present gas exchange with water resulting in unfavorable fish production, and provide ideal habitat for the mosquito development, and serve as vectors for disease [3]. The most widespread macrophytes in the Danube-Tisa-Danube channel are *Ceratophyllum demersum* L., *Trapa natans* L., *Typha latifolia* L., *Salvinia natans* L. All., *Hydrocharis morsus ranae* L., *Potamogeton lucens* L., *Lemna minor* L., *Nymphaea alba* L. [4]. The Danube-Tisa-Danube (DTD) hydro-system is a multivalent water system connecting waters of Bačka and Banat regions in Serbia. The Bečej-Bogojevo canal is 90km long and it starts from the Tisa river at Bečej lock. The canal weed control is a complex task demanding knowledge of aquatic plants. Mechanical control is expensive and requires access to waterways, while chemical control is easier, quick and usually cheaper when compared to mechanical methods [5], but herbicides are often toxic that the water cannot be used often for fish culture or human consumption. The species which has been most widely used in biological control is the grass carp, *Ctenopharyngodon idella*. The aim of this paper was to review the most frequent aquatic weeds of the canal DTD and to provide recommendations for their mechanical, chemical and biological control.

Experimental

In this paper, during the vegetation period in 2016, the presence of aquatic weed species was examined on the Bečej-Bogojevo channel (survey mark 0+250-1+600km) in Serbia. Collected plant material was identified by „Flora of SR Serbia I-IX, [6], „Flora of Serbia X, [7], „Flora of Serbia I, [8], „Flora Europae I-V, [9] i Iconographie der Flora des Sudostlichen Mitteleuropa, [10]. The standard phytocenological methods of the Swiss-French school were

used to record vegetation [11]. Biological and morphological properties of aquatic macrophytes are also shown. The assessment of measures has been compared with the literature data, where both the advantages and disadvantages for all measures individually by species suppressed are given.

Results and discussion

Phytocenological analysis was performed on the Bečej-Bogojevo channel at 10 localities by Braun-Blanquet method. The results and available weeds in the selected area are given in Table 1-3 with their scientific names. During the floristic research different types of species were found in the study area on the Bečej-Bogojevo channel. In that area, 16 weed species were identified.

Analyzing higher taxonomic categories, of the 16 constant species, 4 species belong to the class Magnoliopsida (*Ceratophyllum demersum* L., *Trapa natans* L. (agg.), *Rumex lapatifolium* L., *Rumex hydrolaphatum* (Huds), 11 species to the class Liliopsida (*Typha latifolia* L., *Hydrocharis morsus-ranae* L., *Typha angustifolia* L., *Phragmites communis* L. Trin., *Lemna minor* L., *Potamogeton pectinatus* L., *Glyceria maxima* (Hartm) Holm, *Potamogeton crispus* L., *Butomus umbellatus* L., *Vallisneria spiralis* L., *Najas marina* L.) and 1 species belong to the classes Polypodiopsida (*Salvinia natans* L. All.). The flora is divided into 11 families, of which the representatives of the families *Poaceae*, *Polygonaceae*, *Hydrochariaceae*, *Typhaceae*, *Potamogetonaceae* are presented with 2 representatives for each family, while the families *Lemnaceae*, *Najadaceae*, *Ceratophyllaceae*, *Salviniaceae*, *Trapaceae*, *Butomaceae* are presented with only one.

Table 1. Phytocenological recordings, June 2016

Surface size (m ²)	25	25	25	25	25	25	25	25	25	25	The level of presence	Cover value
General coverage	70	80	95	70	100	95	95	100	100	100		
Number of plant species	3	4	9	7	6	3	6	5	3	5		
Plant species	1	2	3	4	5	6	7	8	9	10		
<i>Ceratophyllum demersum</i> L.	1.1	2.2	3.3	4.4	3.3	3.3	2.2	1.1	3.3	1.1	V	2625
<i>Trapa natans</i> L.(agg.)	-	1.1	-	2.2	3.3	-	-	+1	+1	3.3	IV	985
<i>Typha latifolia</i> L.	-	-	2.2	-	-	-	-	3.3	-	4.4	II	1175
<i>Salvinia natans</i> L. Alli.	-	-	-	-	-	-	-	-	-	-	-	-
<i>Hydrocharis morsus-ranae</i> L.	-	-	-	-	-	-	-	-	-	-	-	-
<i>Typha angustifolia</i> L.	-	-	-	-	3.3	-	-	-	3.3	-	I	750
<i>Phragmites communis</i> Trin.	-	4.4	-	-	2.2	-	-	4.4	-	-	II	1425
<i>Lemna minor</i> L.	-	-	-	-	-	-	-	-	-	-	-	-
<i>Rumex lapatifolium</i> L.	-	-	1.1	1.1	-	-	1.1	-	-	-	II	150
<i>Potamogeton pectinatus</i> L.	-	-	+1	+1	-	-	-	+1	-	+1	II	20
<i>Glyceria maxime</i> (Hartm) Holm	1.1	-	2.2	-	1.1	-	1.1	-	-	1.1	III	375

<i>Potamogeton crispus</i> L.	-	-	+1	+1	+1	-	-	-	-	-	I	15
<i>Butomus umbellatus</i> L.	-	-	+1	+1	-	+1	+1	-	-	-	II	20
<i>Vallisneria spiralis</i> L.	2.2	+1	+1	-	-	-	+1	-	-	-	II	190
<i>Rumex hydrolaphatum</i> (Huds)	-	-	+1	+1	-	+1	+1	-	-	-	II	20
<i>Najas marina</i> L.	-	-	-	-	-	-	-	-	-	-	-	-

During June 2016, at the tested localities, dominant species were *Ceratophyllum demersum* L., *Phragmites communis* Trin., and *Typha latifolia* L., of which *C. demersum* had the highest cover value, with the level of presence V. *Ceratophyllum demersum* is a submerged, perennial plant with no roots, attached to the lake bottom by modified leaves. Mechanical measures had good effects in some more temperate areas. Engel (1990) [12] states that the best results were obtained if suppression was carried out during July. In Serbia, herbicides diquat and 2,4-D have been registered for this species. It is successfully suppressed using the fish *Ctenopharyngodon idella*, as a biological control measure.

Table 2. Phytocoenological recordings, July 2016

Surface size (m ²)	25	25	25	25	25	25	25	25	25	25	The level of presence	Cover value
General coverage	70	80	95	70	100	95	95	100	100	100		
Number of plant species	5	8	12	9	5	3	8	4	4	6		
Plant species	1	2	3	4	5	6	7	8	9	10		
<i>Ceratophyllum demersum</i> L.	1.1	2.2	3.3	4.4	3.3	2.2	2.2	1.1	3.3	1.1	V	2425
<i>Trapa natans</i> L.(agg.)	1.1	1.1	2.2	2.2	2.2	-	1.1	-	2.2	2.2	IV	1025
<i>Typha latifolia</i> L.	-	-	2.2	-	-	-	-	3.3	-	4.4	I	1175
<i>Salvinia natans</i> L. Alli.	-	-	-	-	-	-	-	-	-	-	-	-
<i>Hydrocharis morsus-ranae</i> L.	-	2.2	2.2	+1	-	-	+1	-	1.1	2.2	III	585
<i>Typha angustifolia</i> L.	-	-	-	-	3.3	-	-	-	3.3	-	I	750
<i>Phragmites communis</i> L. Trin.	-	4.4	-	-	2.2	-	-	4.4	-	-	II	1425
<i>Lemna minor</i> L.	1.1	1.1	2.2	2.2	-	-	1.1	-	-	1.1	III	550
<i>Rumex lapatifolium</i> L.	-	-	1.1	1.1	-	-	1.1	-	-	-	II	150
<i>Potamogeton pectinatus</i> L.	-	-	1.1	1.1	-	-	-	+1	-	+1	II	110
<i>Glyceria maxime</i> (Hartm) Holm	+1	-	+1	-	+1	-	+1	-	-	-	II	20
<i>Potamogeton crispus</i> L.	-	+1	+1	+1	-	-	-	-	-	-	I	15
<i>Butomus umbellatus</i> L.	-	+1	+1	-	-	-	-	-	-	-	I	10

<i>Vallisneria spiralis</i> L.	+1	+1	+1	+1	-	-	+1	-	-	-	III	25
<i>Rumex hydrolaphatum</i> (Huds)	-	-	+1	+1	-	+1	+1	-	-	-	II	20
<i>Najas marina</i> L.	-	-	-	-	-	+1	-	-	-	-	I	5

In submerged vegetation during the July, the dominant role had the species *Ceratophyllum demersum* L., whose level of presence was V. When it comes to flotant plants, *Trapa natans* L. was most dominant, with a cover value of 1025 and the level of presence IV. In addition to these two species, *Phragmites communis* L. Trin and *Typha latifolia* were also dominant. *Trapa natans* L. is a floating herb, that colonizes areas of freshwater lakes and ponds where it forms floating vegetation, causing problems for boaters and swimmers. Early detection of introductions and rapid control response are key to preventing high impact infestations. Herbicides that are effective on *T. natans* are glyphosate, triclopyr, and 2,4-D. The most promising biocontrol species appears to be the leaf beetle *Galerucella birmanica*.

Table 3. Phytocoenological recordings, August 2016

Surface size (m ²)	25	25	25	25	25	25	25	25	25	25	The level of presence	Cover value
General coverage	70	95	95	80	100	90	95	100	100	100		
Number of plant species	5	7	9	5	6	5	8	5	5	6		
Plant species	1	2	3	4	5	6	7	8	9	10		
<i>Ceratophyllum demersum</i> L.	2.2	2.2	2.2	3.3	2.2	2.2	2.2	1.1	2.2	1.1	V	1700
<i>Trapa natans</i> L.(agg.)	+1	+1	1.1	1.1	2.2	-	1.1	-	1.1	+1	IV	390
<i>Typha latifolia</i> L.	-	-	4.4	-	-	-	-	3.3	-	4.4	II	1625
<i>Salvinia natans</i> L. Alli.	1.1	2.2	3.3	2.2	2.2	1.1	-	3.3	3.3	3.3	IV	1950
<i>Hydrocharis morsus-ranae</i> L.	-	3.3	2.2	2.2	+1	1.1	+1	-	1.1	-	IV	835
<i>Typha angustifolia</i> L.	-	-	-	-	-	-	-	-	3.3	-	I	375
<i>Phragmites communis</i> L. Trin.	-	3.3	-	-	3.3	-	-	3.3	-	-	II	1125
<i>Lemna minor</i> L.	-	-	+1	-	-	-	1.1	-	-	+1	II	60
<i>Rumex lapatifolium</i> L.	-	-	-	-	-	-	1.1	-	-	-	I	50
<i>Potamogeton pectinatus</i> L.	-	-	+1	1.1	+1	-	-	+1	-	+1	III	70
<i>Glyceria maxime</i> (Hartm) Holm	+1	-	+1	-	-	-	+1	-	-	-	II	15
<i>Potamogeton crispus</i> L.	-	+1	+1	-	-	-	-	-	-	-	I	10
<i>Butomus umbellatus</i> L.	-	+1	-	-	-	-	-	-	-	-	I	5
<i>Vallisneria spiralis</i> L.	3.3	-	-	-	-	+1	+1	-	-	-	I	375
<i>Rumex hydrolaphatum</i>	-	-	-	-	-	-	+1	-	-	-	I	5

(Huds)												
<i>Najas marina</i> L.	-	-	-	-	-	+1	-	-	-	-	I	5

The dominant aquatic macrophytes in August 2016, were *Salvinia natans*, with the level of presence IV, then *Ceratophyllum demersum* L., and *Typha latifolia* L. Many endangered plant species are found in aquatic ecosystems. Some of these species are *Najas marina* L., *Hydrocharis morsus-ranae* L., *Ceratophyllum demersum* L., *Trapa natans* L., *Butomus umbellatus* L., *Vallisneria spiralis* L., which deserves special attention because their protection contributes to the conservation of ecosystem diversity.

Conclusion

Based on the number and coverage, 16 aquatic weeds species were identified at 10 localities of the Bečej-Bogojevo canal in the period June-August 2016. The most common are the representatives of the family *Poaceae*, *Polygonaceae*, *Hydrochariaceae*, *Typhaceae*, *Potamogetonaceae*. The predominant aquatic macrophytes at the investigated localities in June was *Ceratophyllum demersum* L., in July *Trapa natans* L. and in August month *Salvinia natans* L. All. During the vegetation period, in June and July 2016, it is recommended that mechanical suppression need to be repeated based on the dominant aquatic flora. In the case of the introduction of grass carp into the Bečej-Bogojevo canal, as a form of biological control, the application of mechanical suppression would be reduced.

References

- [1] L. Moeller, A. Bauer, H. Wedwitschka, W. Stinner, A. Zehnsdorf, Crop Characteristics of Aquatic Macrophytes for Use as a Substrate in Anaerobic Digestion Plants—A Study from Germany. *Energies*, (2018), 11, p. 3016.
- [2] H. Yu, W. Qi, C. Liu, L. Yang, L. Wang, T. Lv, J. Peng, Different Stages of Aquatic Vegetation Succession Driven by Environmental Disturbance in the Last 38 Years. *Water*, 11(7), (2019), p.1412.
- [3] M. Salwa Abou El Ellaand, A. Tarek El Samman. Review: Egyptian Experience in Controlling Aquatic Weeds. *J Am Sci*, (2016), pp. 104-115.
- [4] B. Konstantinović, M. Meseldžija, S. Maletin, Mogućnost primene herbicida i biljovedih riba u uklanjanju korovske vegetacije iz kanalske mreže. U: *Održive melioracije*, Belić, S. (ed.), Univerzitet u Novom Sadu Poljoprivredni, Novi Sad, (2007).
- [5] S. Datta, Aquatic Weeds and Their Management for Fisheries, *Aquatic Weeds and Their Management for Fisheries*, (2009), pp. 1-22.
- [6] M. Josifović, (ed.). *Flora SR Serbia*, I-IX, SANU, Belgrade, (1970-1977).
- [7] Sarić, M. (ed.). *Flora of Serbia X*, SANU, Belgrade, (1986).
- [8] Sarić, M. (ed.). *Flora of Serbia I*. SANU, Belgrade, (1992).
- [9] G. Tutin, V.H. Heywood, N.A. Burges, D.H. Valentine, S.M. Walters, D.A. Webb, (ed.) *Flora Europaea I*, Cambridge University press, Cambridge, England, (1964).
- [10] S. Jávorka, V. Csapody, Icanographie der Flora des Südostlichen Mitteleuropa. *Akademiai Kiado*, Budapest, (1975).
- [11] J. Braun-Blanquet, *Pflanzesociologie, Grundzuge der Vegetations Kunde*. 3rd ed. Springer Verlag, Wien-New York, (1964).
- [12] S. Engel, Ecological impacts of harvesting macrophytes in Halverson lake, Wisconsin. *Journal of Aquatic Plant Management*, (1990), pp. 41-45.

NEW WAY TO GREEN BIOLOGICAL ASSAYS FLUORESCENT STEROIDS REPLACE RADIOISOTOPES

Vivien Szabó¹, Boglárka Anna Orosz¹, Réka Rigó², Csilla Özvegy-Laczka², Erzsébet Mernyák¹

¹Department of Organic Chemistry, University of Szeged, H-6720 Szeged, Dóm tér 8;

²Hungary Membrane protein research group, Institute of Enzymology, Research Centre for Natural Sciences, Hungarian Academy of Sciences, Magyar tudósok körútja 2, H-1117 Budapest, Hungary;

e-mail: viviens@chem.u-szeged.hu

Abstract

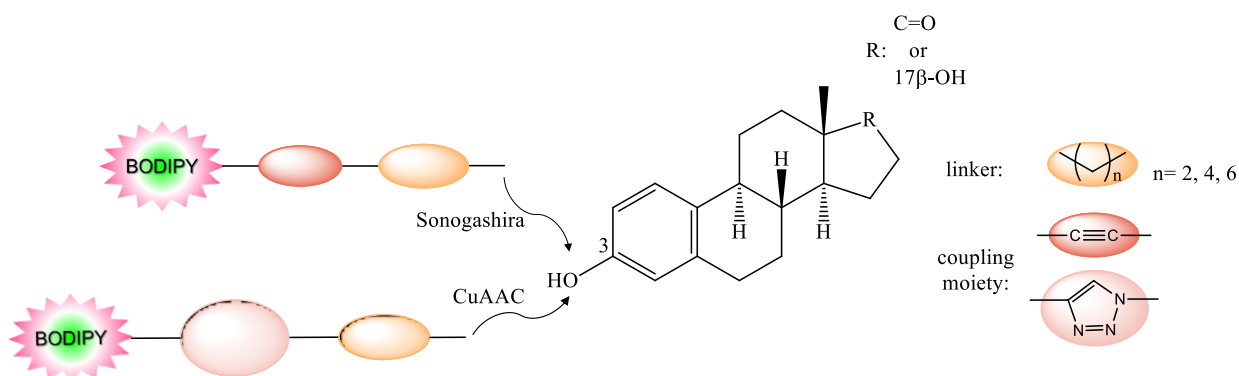
Novel BODIPY–estrone and BODIPY–estradiol conjugates have been synthesized via Cu(I)-catalyzed azide-alkyne click (CuAAC) and/or Sonogashira reactions by selecting position C-3-O for labeling. The steroidal azides and/or bromides were reacted with BODIPY-based fluorescent dye bearing alkyne function. The new fluorescent estrone conjugates might replace radiolabeled compounds in certain biochemical assays.

Introduction

One of the primary goals of modern drug research is the use of environmentally friendly biochemical techniques that are based on the principles of green chemistry. Nowadays, methods based on the use of fluorescently labeled compounds are gaining prominence. There are only a few literature reports about the pharmacological effects of fluorescently labeled estrone derivatives.

Experimental

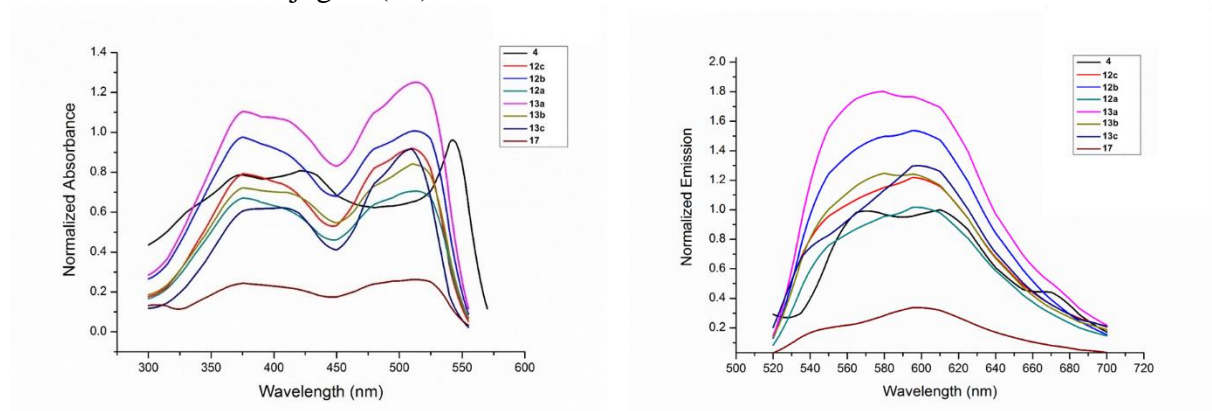
The labeling was planned with a BODIPY derivative as a fluorescent moiety containing a terminal alkyne function, because it is stable under physiological conditions and offers many possibilities for its synthesis and functionalization. Conjugation of E1 and E2 via the chemically important C-3-O position was accomplished by 1,3-dipolar cycloaddition² (CuAAC) via triazole ring incorporation or Sonogashira coupling³ (Figure 1). We aimed to synthesize the conjugates via inserting C₄–C₈ long linkers between the steroid and the dye.



3. Figure Synthesis of estrone-BODIPY and estradiol-BODIPY conjugates

Results and discussion

The synthesis of BODIPY alkyne was performed via our recently established efficient methodology¹. Figure 2. shows the absorption and the fluorescence emission spectra of the non-conjugated BODIPY dye (4), the estradiol-BODIPY conjugates (12a–c, 13a–c), and the estrone–BODIPY conjugate (17).



4. Figure Normalized absorbance and emission spectra of the dye (4) and the conjugates (12a-c, 13a-c,17)

According to these data, these BODIPY-conjugated steroids have spectral characteristics similar to those of the non-conjugated BODIPY dye and may facilitate observations in living cells and tissues.

Conclusion

We have synthesized 6 new estrone-BODIPY and 6 new estradiol-BODIPY derivatives – conjugated with different chain length linkers – via CuAAC and/or Sonogashira reactions. The newly synthesized fluorescent estrone derivatives may serve as good candidates for the development of “green” biological assays. Additionally, thanks to the “visibility” of fluorescent estrogens, new important biological actions might also be identified.

Acknowledgements

This research was supported by OTKA SNN 124329. The work of Erzsébet Mernyák and Csilla Özvegy-Laczka in this project was supported by the János Bolyai Research Scholarship of the Hungarian Academy of Sciences.

References

- [1] I. Bacsa, E. Mernyák, *Molecules* **2018**, *23*, 821.
- [2] E. J. Moses, A. D. Moorhouse, *Chem. Soc. Rev.* **2007**, *36*, 1249.
- [3.] R. Chinchilla, C. Nájera, *Chem. Soc. Rev.* **2011**, *40*, 5084.

DETERMINATION OF ANTIOXIDANT CAPACITY IN SOME FRUIT CONCENTRATES AND POWDERS BY DIFFERENT METHODS

Csaba Miski¹, Éva Stefanovits- Bányai², Noémi Koczka³, Anna Mária Nagy⁴

¹GPS Kft, Hungary,

²Szent István University, Faculty of Food Science, Department of Applied Chemistry,
H-1118 Budapest, Villányi street 29-43, Hungary,

³Szent István University, Faculty of Agricultural and Environmental Sciences, Institute of
Horticulture, H-2100 Gödöllő, Páter K. street 1, Hungary

⁴Holi-Medic Kft, Hungary
e-mail: holimedic@gmail.com

Abstract

There is a great demand on consumption of natural and healthy foods, which includes also fresh fruits and food products made by different technological processes. In our experiment, fruit concentrates and powders of elderberry (*Sambucus nigra* L.) and blackcurrant (*Ribes nigrum* L.) were studied. For evaluating their health protective effect, the antioxidant/reducing properties of both fruits were obtained. The total phenolic content (TPC) and the antioxidant capacity determined by the FRAP, TEAC, and DPPH methods were analysed. Results are expressed on a dry matter basis for better comparison. TPC and antioxidant activity detected by different methods were higher in elderberry (*Sambucus nigra* L.) for both concentrates and powders than in blackcurrant (*Ribes nigrum* L.). Dry powders made from fruit concentrates showed in almost all cases a lower antioxidant activity than the concentrates. The results clearly show that it is recommended to characterize the antioxidant properties in as many ways as possible in order to evaluate the beneficial effects of fruits and their processed goods on the human organism.

Introduction

One way to increase your fruit and vegetable consumption is to produce a food that is easy to prepare, does not require a lengthy preparation, is of good quality and is available at all times of the year. Vacuum drying is one of the methods developed to meet these needs to the fullest. The low drying temperature and the short drying time used in the technology enable the production of long-lasting goods with favourable nutritional and organoleptic properties.

By choosing the right diet, we can prevent certain diseases. Eating vegetables and fruits rich in vitamins and antioxidants can reduce the risk of their occurrence because free radical reactions responsible for the onset of diseases can be delayed or inhibited by antioxidants [1,2,3,4].

The antioxidant or reducing capacity is the combined effect of all the antioxidant compounds in a system. Several methods have been developed for evaluation of antioxidant power, the number of them exceeds one hundred [5].

Methods for measuring antioxidant capacity are commonly classified into two groups, as hydrogen atom transfer (HAT)- and electron transfer (ET)-based assays [6]. Of course, all methods have their strengths and weaknesses, the processes in the body cannot be exactly tracked, only an approximate characterization and comparison of the tested samples is possible. For example, the FRAP and TPC assays work on a non-physiological pH (pH 3.6 and pH 10, respectively) [7], and the DPPH and TEAC methods use free radicals that do not occur in the body [8,9].

Experimental

All chemicals for the experiments were purchased from Sigma Aldrich.

Sample preparation

Samples were taken from filtered frozen (-18°C) concentrates of elderberry (*Sambucus nigra* L.) and blackcurrant (*Ribes nigrum* L.).

The powders of both fruits were produced in a tray-type LMIM LP-405 vacuum oven with three parallel tray drying (temperature detection per tray) at a pressure range of 20 mbar to atmospheric pressure, at 10 °C to 60 °C for 240 minutes after a short warm-up time.

The dry material was crushed using a coffee grinder (Delonghi KG49), and samples were stored in sealed polyethylene bags at -32 °C until measurement.

Both fruit concentrates and lyophilized samples (diluted with distilled water) were analysed for analytical measurements. The diluted aqueous solutions were placed in a cooled ultrasonic water bath for 30 minutes. The samples were then centrifuged at 13,500 rpm at 10 °C for 15 minutes. In all cases, the analytical tests were carried out on the supernatants.

Electron transfer methods detect the reducing capacity of solutions. The reactions are followed by colour changes, which can be monitored spectrophotometrically (Thermo Scientific –Evolution 300 UV-VIS spectrophotometer).

Analytical methods

Determination of total phenolic contents (TPC) by Folin-Ciocalteu method: The Folin-Ciocalteu spectrophotometric method by Singleton and Rossi [10], at 760 nm is an electron transfer based assay and shows the reducing capacity, which is expressed as phenolic content. Gallic acid (GA) was used to prepare the standard curve. The results were expressed as mM GA/g of dry matter (DM).

Determination of antioxidant capacities by FRAP (Ferric Reducing Antioxidant Power) method: Measurement of ferric reducing antioxidant power of the fruit extracts was carried out based on the procedure of Benzie and Strain [11], at 593 nm. Ascorbic acid (AA) was used as a standard to prepare the calibration solutions. Results were expressed as μ MAA/g DM.

Determination of antioxidant capacities by TEAC (Trolox Equivalent Antioxidant Capacity) method: Miller and coworkers [12] described the Trolox equivalent antioxidant capacity (TEAC) method. The assay is based on formation of the ABTS \bullet + cation [2,2'-azinobis (3-ethylbenzothiazoline-6-sulfonic acid)] and its scavenging by antioxidant sample constituents measured by spectrophotometry at 743 nm (decay of green/blue chromophore absorbance is inversely associated with antioxidant sample content). Trolox, a hydrophilic vitamin E analog, was used as a standard and values were expressed as mM TE (Trolox equivalent)/g DM.

Determination of antioxidant capacities by DPPH (2,2-Diphenyl-1-picrylhydrazyl) radical-scavenging activity method: The spectrophotometric method (517 nm) of DPPH radical-scavenging activity was carried out according to the method of Blois [13] and modifications by Hatano and others [14]. The results were expressed as mM of TE (Trolox equivalent)/g DM.

In the last two methods, artificial radicals were used that do not occur in the living organism [6], and in the case of the DPPH method the anthocyanins interfere in the measurement [7].

Results and discussion

Figure 1.A represents data for the total polyphenolic content of elderberry and blackcurrant samples. It can be clearly seen that the TPC of the elderberry concentrate was extremely high (708.0 mM GA/g DM). For the blackcurrant concentrate, 415.7 mM GA/g DM was measured. Comparing the obtained results with literature data [9,15] it can be said that they are almost identical. Vacuum drying resulted in a decrease in the TPC, the loss of phenolics was 7.5% for elderberry and 18.0% for blackcurrant.

The antioxidant capacity measured by the FRAP method (Fig. 1.B) showed similar correlations. The elderberry concentrate had an outstanding antioxidant power (522.8 μ MAA/ g DM), followed by blackcurrant concentrate (369.6 μ MAA/ g DM). The decrease on antioxidant capacity after vacuum drying was 9.7% in the case of elderberry, while very high in blackcurrant (32.4%).

The antioxidant activity determined by the TEAC method (Fig. 1.C), was significant higher for elderberry concentrate and powder than for blackcurrant samples. Vacuum drying resulted in an increase in radical scavenging properties for both product types, which may be explained by a possible change in the endogenous components.

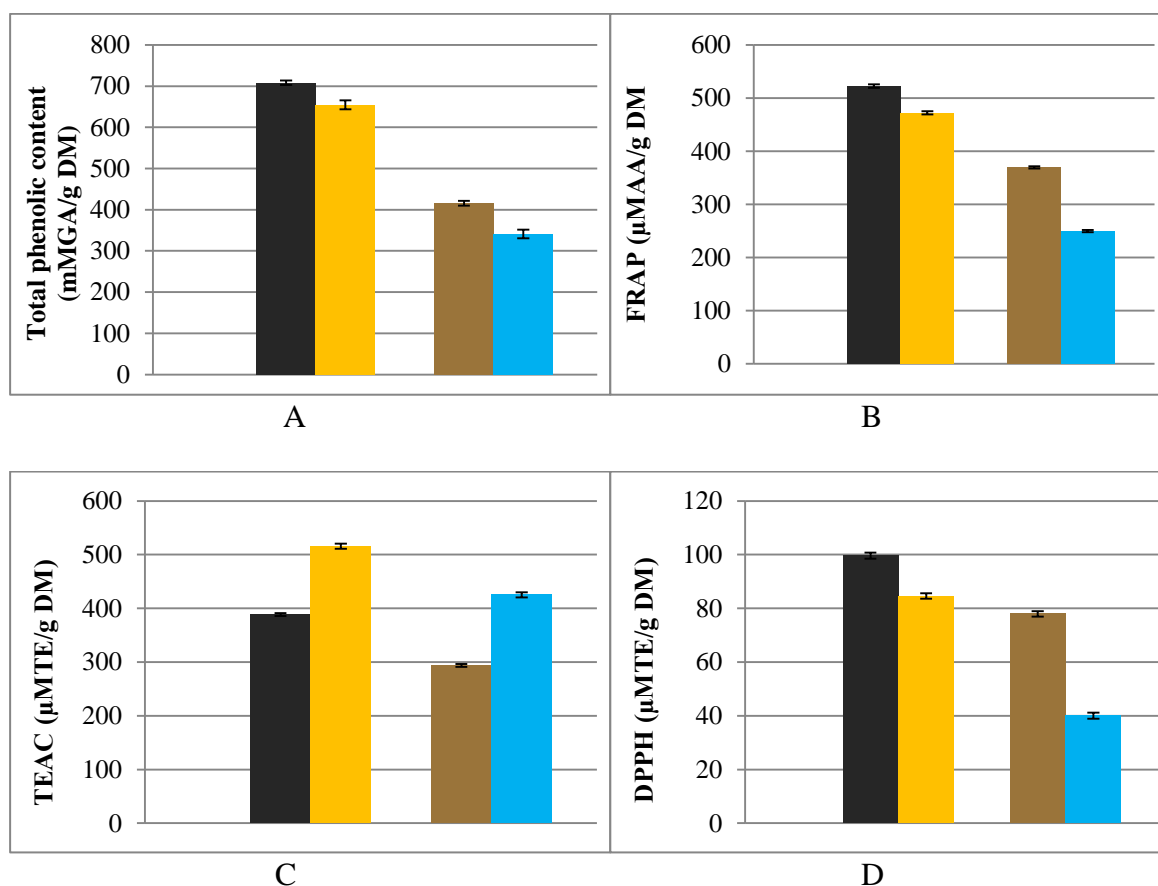


Figure 1. The antioxidant capacity measured by different methods
A) total phenol content, B) FRAP, C) TEAC and D) DPPH

legend:

elderberry concentrate elderberry powder black currant concentrate
black currant powder

In the case of DPPH method (Fig. 1.D), the elderberry concentrate showed the highest antioxidant capacity (99.6 μ M TE/ g DM), followed by blackcurrant concentrate (78.0 μ M

TE/ g DM). Vacuum drying caused a significant decrease of the antioxidant power, a decline of 15.1% was found for elderberry and 48.6% for blackcurrant.

Conclusion

Total phenolic content and antioxidant capacity determined by different methods (FRAP, TEAC, DPPH) were higher in elderberry (*Sambucus nigra* L.) than in blackcurrant (*Ribes nigrum* L.). Comparing fruit concentrates to powders made from them, significant differences could be found. The concentrates had a higher TPC and antioxidant activity measured by FRAP and DPPH methods than the powders, however, using the TEAC assay just the opposite was obtained for both fruits. These results clearly show that more methods are needed to determinate the antioxidant status of the fruit samples, and to characterize the health protective effect of different food products.

References

- [1] G. Block, B. Patterson, A. Subar, Nutr. Cancer Int. J. 18 (1992)1-29.
- [2] H.C. Hung, K.J. Joshipura, R. Jiang, F. Hu, D. Hunter, S.A. Smith-Warner, G.A. Colditz, B. Rosner, D. Spiegelman, W.C. Willett, J. National Cancer Ins. 96 (2004) 1577-1584.
- [3] V. Lobo, A. Patil, A. Phatak, N. Chandra, Pharmacog. Rev. 4 (2010) 118-126.
- [4] S.H. Nile, S.W. Park, Nutr. 30 (2014) 2.134-144.
- [5] U. Cornetti, Clinics Dermatol. 27 (2009) 175-194.
- [6] E.N. Frankel, A.S. Meyer, J. Sci.Food Agr. 80 (2000) 13, 1925-1941.
- [7] R. Apak, K. Güclü, B. Demirata, M. Özyürek, S.E. Celik, B. Bektasoglu, K.I. Berker, D. Özyurt, Molecul. 12 (7) (2007) 1496-1547.
- [8] R.L. Prior, G. Cao, Free Rad. Biol.Med. 27 (11-12) (1999) 1173-1181.
- [9] E. Balogh, A. Hegedüs, É. Stefanovits-Bányai, Scientia Hort. 125 (3) (2010) 332-336.
- [10] V.L. Singleton, J. A. Rossi, Am. J.Enol. Viticult. 16 (3) (1965) 144-158.
- [11] I.F.F. Benzie, J.J. Strain, Anal.Biochem. 239 (1) (1996) 70-76.
- [12] N.J. Miller, C. Rice-Evans, M.J. Davies, V. Gopinathan, A. Milner, Clinic.Sci. 84 (1993) 407-412.
- [13] M.S. Blois, Nature 4617(1958)1198-1200.
- [14] T. Hatano, H. Kagawa, T. Yasuhara, T. Okuda, Chem. Pharm. Bull. 36. (1988) 2090-2097.
- [15] B. Bazaria, P. Kumar J. Food Proces. Preserv. 6 (2016) 1215-1222.

Acknowledgements

This research was supported by the Higher Education Institutional Excellence Program (1783-3/2018/FEKUTSTRAT) awarded by the Ministry of Human Capacities within the framework of plant breeding and plant protection researches of Szent István University, and by the European Structural and Investment Funds (grant agreement no. VEKOP-2.3.3-15-2017-00022).

LABORATORY MICROCOSM STUDY OF A POLLUTED GROUNDWATER ZONE

Ingrid Zsilinszky¹, István Kiss¹, Sándor Mészáros¹, Balázs Fehér¹¹Bay Zoltán Nonprofit Ltd. for Applied Research, H-6726 Szeged, Derkovits fasor 2, Hungary
e-mail: ingrid.zsilinszky@bayzoltan.hu**Abstract**

Microcosm studies were set up to predict and evaluate the most effective conditions for the bioremediation of a chlorobenzene contaminated groundwater zone. In the literature there are only few studies for chlorobenzene degradation under nitrate reducing circumstances. In most of our microcosms the indigenous groundwater bacteria were able to degrade this widespread recalcitrant compound under the new conditions. We have isolated a chlorobenzene degrading bacterium, *Pseudomonas* sp. EM1 which is capable of the mineralisation under aerobic and anaerobic conditions.

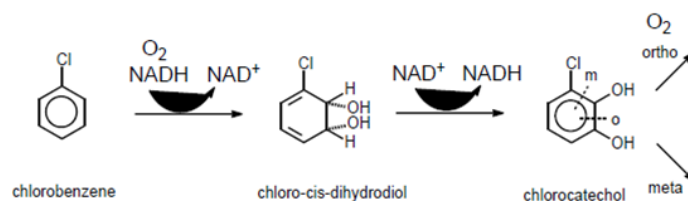
Introduction

Chlorobenzene is primarily used as a solvent for paints and pharmaceutical products, as a heat transfer medium, and in the production of phenol, aniline and silicone. The production and usage of this organic compound has been declining due to the availability of more environmentally friendly replacements [1,2].

Chlorobenzene has a greater density than water and only slightly soluble in water (500 mg/l), it belongs to the DNAPLs (Dense Non-Aqueous Phase Liquids). It can be slightly accumulated at the bottom of an aquifer as a DNAPL pool which can serve as a continuous source of groundwater pollution [3,4]. Different methods have been developed to transform chlorobenzene into less toxic by-products, including adsorption [5], ozone oxidation [3], Fenton's reaction [6] and catalytic hydrodechlorination [7,8]. Biodegradation also can be an effective method. Even though chlorobenzene is a recalcitrant chemical, it can be mineralised with microorganisms under aerobic and anaerobic conditions.

Aerobic degradation

There are a couple of aerobic microbes that can use chlorobenzene as the sole energy and carbon source. The activation of the C-Cl bond requires high activation energy and a strong attacking nucleophile [9]. *Figure 1.* shows that the initial aerobic attack of chlorobenzene is catalysed by dioxygenases resulting in the formation of 3-chlorocatechol as an intermediate [10].

**Figure 1: The aerobic initial attack of chlorobenzene**

After the first step of the aerobic chlorobenzene degradation, there are two pathways: ortho and meta cleavage. The intermediates are metabolized further compounds of the citric acid cycle (CAC)[9].

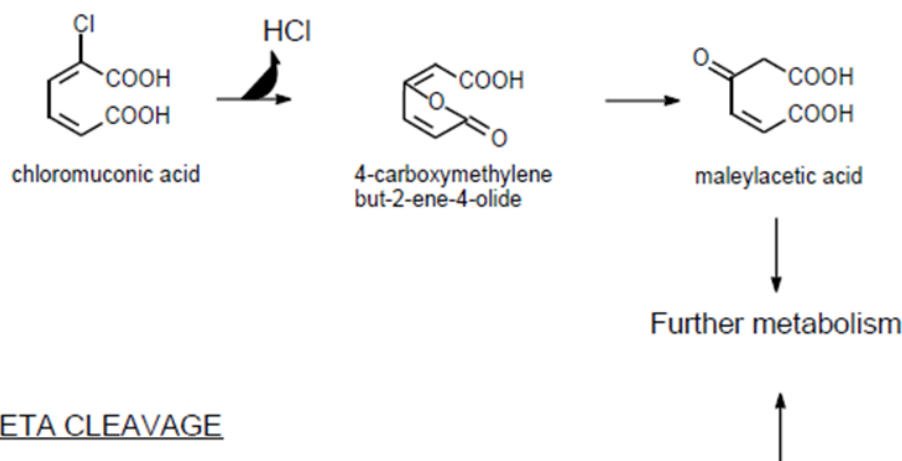
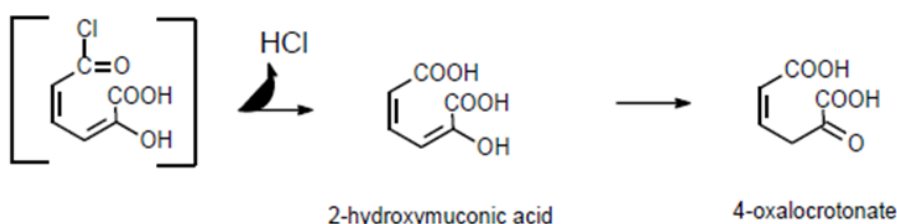
ORTHO CLEAVAGEMETA CLEAVAGE

Figure 2: The ortho and meta cleavage of aerobic chlorobenzene degradation (9)

Anaerobic reductive dechlorination

The reduction of chlorobenzene under anaerobic conditions generates benzene and HCl. In this pathway the microorganisms use hydrogen as an electron donor and use the chlorobenzene as an electron acceptor [11]. This pathway requires the presence of an electron donor and it can result in the accumulation of benzene [10].

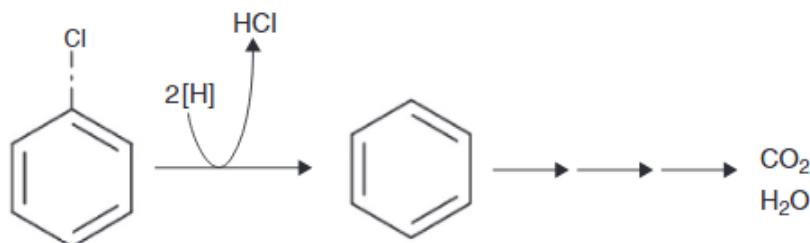


Figure 3: Pathway of anaerobic reductive dechlorination of chlorobenzene (12)

Anaerobic nitrate reducing degradation of chlorobenzene

There are quite a few experimental studies about chlorobenzene degradation under nitrate reducing circumstances [12–14]. In the contaminated area the pollution is combined, it contains BTEX compounds, *cis*-1,2-dichloroethylene, vinyl chloride and *tert*-butyl alcohol. Some studies showed that at low dissolved oxygen concentrations there is an enhanced biodegradation of BTEX in the presence of nitrate [15,16].

Experimental

In the contaminated area the primary contamination is chlorobenzene (> 25,000 µg/l), the secondary is BTEX (> 3,000 µg/l), and the tertiary is *cis*-1,2-dichloroethylene, vinyl chloride and *tert*-butyl alcohol. The polluted groundwater also contains acetic acid and ethanol which can serve as carbon and energy sources for the microbes. The pollution was originated from a drug company. The unique character of the area and the nature of DNAPLs, the most effective

chlorobenzene degradation way, the aerobic degradation was unaccomplishable, hence we tested the nitrate reducing circumstances.

First of all we made some microcosm studies to know more about the groundwater. Microcosm is like a tiny, simplified ecosystem which can simulate the behaviour of natural ecosystems under different conditions. It is an excellent method to predict whether the indigenous microflora is capable of the degradation of the pollution and if it is which the best circumstances for the bioremediation are.

The microcosms were set up using 8 groundwater samples from 8 monitoring wells from the contaminated area. Three different types of microcosms were set up from every groundwater sample. There was an abiotic microcosm supplemented with mercury (II) sulphate, to evaluate abiotic degradation and volatilization. There was a biotic microcosm which contained only the untreated groundwater, it was used for modelling the natural conditions in the

lūarea. The third type of the microcosms, the biostimulated microcosm, was supplemented with nitrate, phosphate and microelements. Microcosms were incubated at 13-15 °C which is characteristic of the natural area. Every fourth week samples were taken to analyse the concentration of VOCs, nitrate, nitrite, phosphate, chloride, organic acids and ethanol. Nitrate or phosphate was spiked when it was necessary to maintain the appropriated circumstances in the microcosms.

Results and discussion

Microcosms studies

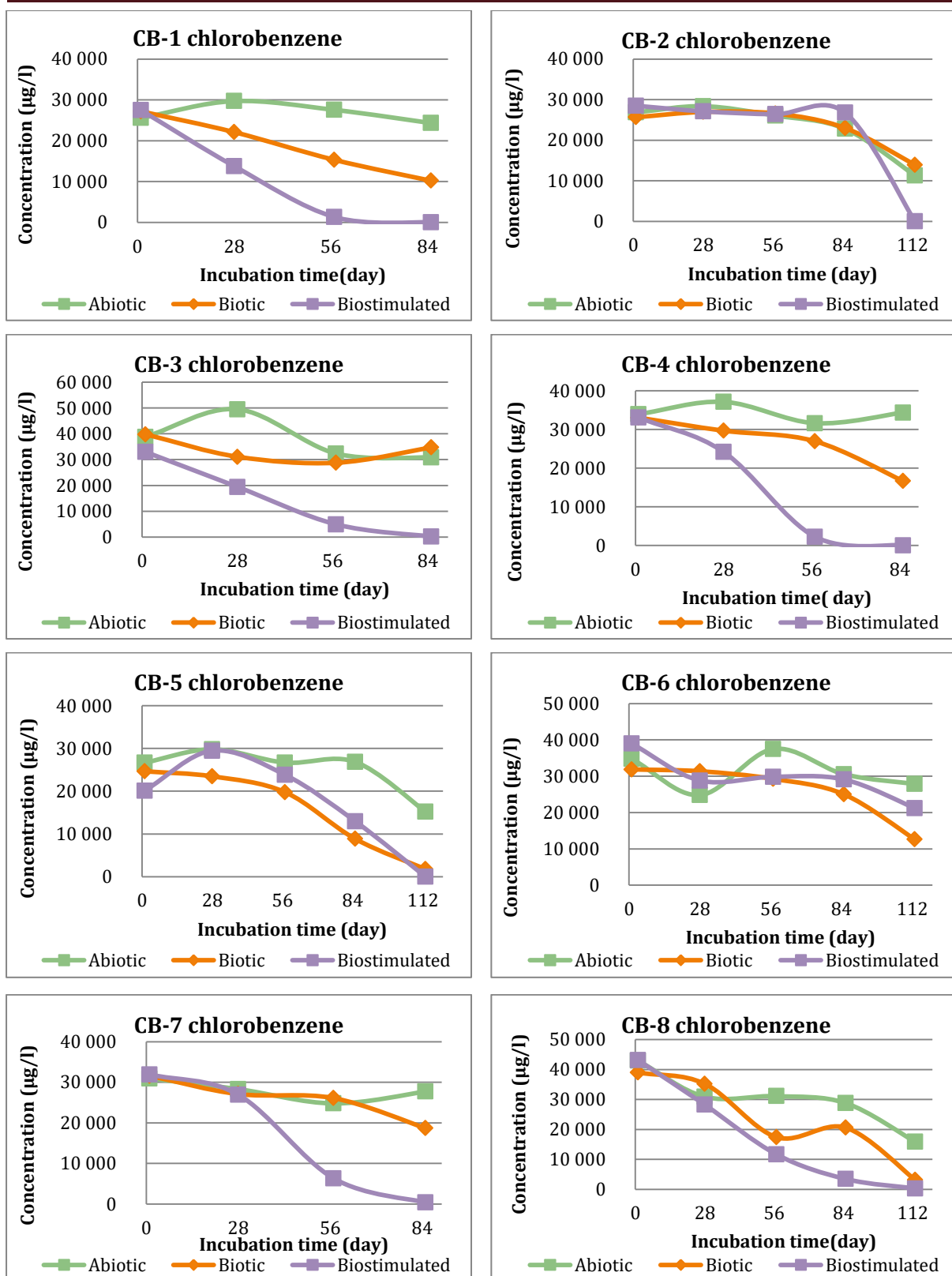
Figure 4. shows the overall results of the various chlorobenzene degradation experiments. In the groundwater samples from CB-1, CB-2, CB-3, CB-4, CB-7 and CB-8 monitoring wells the nitrate reducing circumstances promoted the chlorobenzene degradation. Additional microbiological activity (increased acetic acid degradation) was noticed in the biostimulated microcosm from CB-5 well, but the biostimulation did not have any positive effects on VOC degradation. The nitrate reducing conditions had no additional impact on the groundwater from CB-6 monitoring well. Increased BTEX degradation was observed in the microcosms from CB-1, CB-2, CB-3, CB-4 and CB-7 monitoring wells. The injection of nitrate, sulphate, phosphate and microelements to the contaminated area is recommended due to their positive effect on the degradation of chlorobenzene and BTEX compounds.

Isolation of chlorobenzene degrading bacteria

We have managed to isolate a novel microorganism (*Pseudomonas* sp. EM1) which is capable of chlorobenzene mineralisation under aerobic and anaerobic (nitrate reducing) circumstances. Now this microbe is under licensing procedures. In the future we intend to inject *Pseudomonas* sp. EM1 to the contaminated area.

Conclusion

Our goal was to determine the most effective conditions for chlorobenzene biodegradation in the contaminated aquifer. Microcosm studies were set up to evaluate and predict the effect of nitrate reducing circumstances in the polluted samples. In 6 out of 8 cases the biostimulation had really positive results and the recalcitrant chlorobenzene was biodegraded by the indigenous microflora. BTEX degradation was also contributed thanks to the nitrate reducing medium. *Pseudomonas* sp. EM1 was isolated from the groundwater. This microorganism is capable of the degradation of chlorobenzene both in aerobic and anaerobic conditions.



5. Figure: The change of chlorobenzene concentrations (µg/l) in the microcosm studies

References

- [1] Pravasi SD. Chlorobenzene. *Encycl. Toxicol.*, Elsevier; 2014, p. 870–3. doi:10.1016/B978-0-12-386454-3.00279-7.
- [2] WHO, IPCS INCHEM. Chlorobenzenes other than hexachlorobenzene (EHC 128, 1991) 1991.
- [3] Power C, Gerhard JJ, Karaoulis M, Tsourlos P, Giannopoulos A. Evaluating four-dimensional time-lapse electrical resistivity tomography for monitoring DNAPL source zone remediation. *J Contam Hydrol* 2014;162–163:27–46. doi:10.1016/j.jconhyd.2014.04.004.
- [4] Lin K-S, Mdlovu NV, Chen C-Y, Chiang C-L, Dehvari K. Degradation of TCE, PCE, and 1,2-DCE DNAPLs in contaminated groundwater using polyethylenimine-modified zero-valent iron nanoparticles. *J Clean Prod* 2018;175:456–66. doi:10.1016/j.jclepro.2017.12.074.
- [5] Liu Q, Chen Y, Wang J, Yu J, Chen J, Zhou G. Electrochemical Oxidation of 1,4-Dichlorobenzene on Platinum Electrodes in Acetonitrile-Water Solution: Evidence for Direct and Indirect Electrochemical Oxidation Pathways. *Int J Electrochem Sci* 2011;6:19.
- [6] Wang J, Mei Y, Liu C, Chen J. Chlorobenzene degradation by electro-heterogeneous catalysis in aqueous solution: intermediates and reaction mechanism. *J Environ Sci* 2008;20:1306–11. doi:10.1016/S1001-0742(08)62226-3.
- [7] Pagano M, Volpe A, Lopez A, Mascolo G, Ciannarella R. Degradation of chlorobenzene by Fenton-like processes using zero-valent iron in the presence of Fe³⁺ and Cu²⁺. *Environ Technol* 2011;32:155–65. doi:10.1080/09593330.2010.490855.
- [8] Immobilized palladium-catalyzed electro-Fenton's degradation of chlorobenzene in groundwater | Elsevier Enhanced Reader n.d. doi:10.1016/j.chemosphere.2018.10.143.
- [9] Field JA, Sierra-Alvarez R. Biodegradability of chlorinated aromatic compounds 2007:124.
- [10] Liang X, Devine CE, Nelson J, Sherwood Lollar B, Zinder S, Edwards EA. Anaerobic conversion of chlorobenzene and benzene to CH₄ and CO₂ in bioaugmented microcosms. *Environ Sci Technol* 2013;47:2378–85. doi:10.1021/es3043092.
- [11] Adrian L, Görisch H. Microbial transformation of chlorinated benzenes under anaerobic conditions. *Res Microbiol* 2002;153:131–7. doi:10.1016/S0923-2508(02)01298-6.
- [12] Vogt C, Alfreider A, Lorbeer H, Hoffmann D, Wuensche L, Babel W. Bioremediation of chlorobenzene-contaminated ground water in an in situ reactor mediated by hydrogen peroxide. *J Contam Hydrol* 2004;68:121–41. doi:10.1016/S0169-7722(03)00092-5.
- [13] Wise DL. *Bioremediation of Contaminated Soils*. 1st edition. CRC Press; 2000.
- [14] Nestler H, Kiesel B, Kaschabek SR, Mau M, Schlömann M, Balcke GU. Biodegradation of chlorobenzene under hypoxic and mixed hypoxic-denitrifying conditions. *Biodegradation* 2007;18:755–67. doi:10.1007/s10532-007-9104-z.
- [15] Durant LPW, P.C. D'Adamo, E.J. Bouwer. Aromatic Hydrocarbon Biodegradation with Mixtures of O₂ and NO₃[–] as Electron Acceptors. *Environ Eng Sci* 2009;6. doi:http://doi.org/10.1089/ees.1999.16.487.
- [16] Ma Guihua, Love Nancy G. BTX Biodegradation in Activated Sludge under Multiple Redox Conditions. *J Environ Eng* 2001;127:509–16. doi:10.1061/(ASCE)0733-9372(2001)127:6(509).

UV AND UV/VUV PHOTOLYSIS OF SULFAMETHAZINE

Ilaria Minzini¹, Máté Náfrádi², Luca, Farkas², Dalma Fuderer², Tünde Alapi²

¹*University of Padova, Department of Chemical Sciences, Via Marzolo, 1-35131, Padova, Italy*

²*Department of Inorganic and Analytical Chemistry, University of Szeged, H-6720 Szeged, Dóm tér 7, Hungary
e-mail: alapi@chem.u-szeged.hu*

Abstract

In this work, UV and UV/VUV photolysis of sulfamethazine was investigated. Sulfamethazine is one of the most often used antibioticum, wich can be detected in soils and surface water. The applied light sources were low-pressure mercury vapour lamps having identical geometry and electric parameters. One of the light sources amitts only 254 nm UV light, while the other one emitts both 254 nm UV and 185 nm VUV light.

Both UV and UV/VUV photolysis were found to be effective in the transformation of sulfamethazine, but COD decrease was observed only in the presence of VUV light. In parallel with the transformation of sulfamethazine, H₂O₂ formation was detected. Its concentration reached higher value in the case of UV/VUV than in UV radiation.

Spectrophotometric measurements suggested that dissolved oxygen has effect on the formed interemdiates in both UV and UV/VUV photolysis.

Transformation rates were determined in purified wastewater and tap water and compared to the values determined in Milli-Q water. Results showed that these mild matrices decreased the transformation rates in both cases. The inhibition effect in more pronounced in the case of UV photolysis.

Introduction

Antibiotics are a main and essential resource for the treatment of multiple types of infectious diseases, both in humans and animals. However, in recent years its widespread use, both to treat diseases and to promote growth the efficiency of food has generated serious concerns, mainly due to the increase in the diversity and dispersion of organisms resistant to these compounds. The amount of antibiotics sold for animals destined to food is approximately four times greater than for human use, whereas the world consumption of antibiotics is estimated an increase of 67% for the year 2030. Among antibiotics, sulfonamides are one of the most widely used in veterinary medicine. In 2014, sulfonamides were the third group of veterinary antibiotics most used in Europe, reaching 11% of the total sale of antibiotics. Its extensive use is due to their broad spectrum against most Gram-positive organisms and many Gram-negative organisms. [1,2]

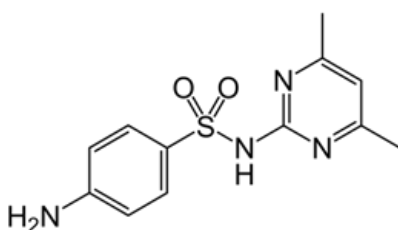


Figure 1: Chemical structure of sulfamethazine

Sulfonamides are poorly absorbed on soils. In the specific case of sulfonamides, they are considered the most mobile antibiotics, and easily transported to water bodies. In fact, these compounds are frequently detected in surface waters, groundwater and in different types of crops. Therefore, the study of the degradation of sulfonamides, both chemical and biological, is crucial to establish the environmental impact of these compounds.

Experimental

Two low-pressure mercury vapour (LP) lamps (GCL307T5/CELL and GCL307T5VH/CELL, 227 mm arc length, both produced by LightTech) were used for UV (254 nm) and UV/VUV185 nm (254 nm/185 nm) irradiations. The parameters (electrical power 15 W and UVC-flux power 4.3 W) of both lamps were the same. The envelope of the UV lamp emitting at 254 nm was made of commercial quartz, while the UV/VUV185 nm lamp's envelope was made of synthetic quartz to be able to transmit the VUV185 nm photons. The flux of 254 nm photons ($5.97 \times 10^{-6} \text{ mol}_{\text{photon}} \text{ s}^{-1}$) of both lamps (UV and UV/VUV185 nm) was determined by ferrioxalate actinometry and found to be the same. The relative radiant power efficiency of the 185 nm VUV light is about 6 - 8% compared to the 254 nm emission.

The reactor geometrical parameters were adapted to the lamp's parameters: 30 mm internal diameter and 320 mm long. Thus the optical path length was 10 mm. The total volume of the treated solution was 500 mL. The aqueous solution was continuously bubbled with oxygen, air or nitrogen to set various dissolved oxygen concentration. The gas was bubbled through the solution using a gas dispersing system. Gas bubbling was started 20 min before the measurement.

Sulfamethazine (Sigma-Aldrich, 99.9%) solutions (500 mL) with initial concentration $1.0 \times 10^{-4} \text{ mol L}^{-1}$ was made in ultrapure MILLI-Q water (MILLIPORE Milli-Q Direct 8/16).

Separation of the aromatic components in the treated solutions was performed by Agilent 1100 type HPLC equipped with diode array detector (DAD) using LiChroCart® (250-4, RP-18, 5 μm) reverse-phase column.

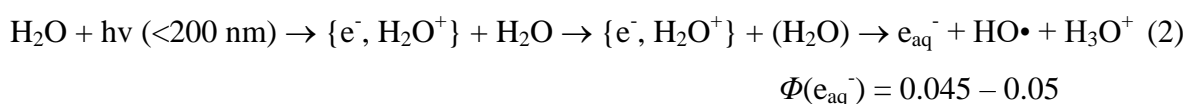
The COD measurements were performed using LCK1414 (Hach) colorimetric cuvette test with a 5.0-60.0 mg dm^{-3} measuring range and a DR2800 spectrophotometer. The concentration of H_2O_2 was measured with a cuvette test by Merck, with a 0.015 - 6.00 mg dm^{-3} measuring range. The NO_3^- concentration was determined by using colorimetric cuvette test provided by Merck, with a 0.4-111 mg dm^{-3} range. For the experiments in various matrices, drinking water from Szeged (Hungary), and industrial wastewater (purified with reverse osmosis) has been chosen. The main analytical parameters available for both matrices are compared in Table 1.

Table 1. Typical parameters of the used matrices that could affects water treatment

Parameters	Drinking water	Purified wastewater
pH	7.3	5.5
Conductivity ($\mu\text{S cm}^{-1}$)	482	21.9
COD (mg dm^{-3})	0.69	< 15
$\text{NH}_4\text{-N}$ (mg dm^{-3})	< 0.4	< 0.4
NO_3^- (mg dm^{-3})	< 0.7	1.5
Cl (mg dm^{-3})	8.75	-
TOC (mg dm^{-3})	8	-

Results and discussion

Comparing the transformation rate of sulfamethazine in UV and UV/VUV radiated solutions, we could observed that the presence of VUV strongly enhanced the transformation rate opposite that it has a quite low intensity comparing to the UV light intensity. In UV radiated solution the direct photolysis of sulfamethazine takes place, its efficiency depends on the molar absorbance of the target substance at 254 nm and quantum yield of its transformation. In VUV radiated aqueous solution, the 185 nm VUV light is absorbed by water and results in the formation of reactive species, namely hydrogen radical ($\text{H}\bullet$), hydroxyl radical ($\text{HO}\bullet$) and with lower yield hydrated electron (e_{aq}^-) [3-6].



Thus, the transformation of sulfamethazine in UV/VUV irradiated solution can take place by two different ways: direct UV photolysis and radical based reactions. The relative contribution of the radical based reaction seems to be similar to that of direct UV photolysis, since the transformation rate determined in UV/VUV irradiated solution is about two times higher than that determined in UV radiated one.

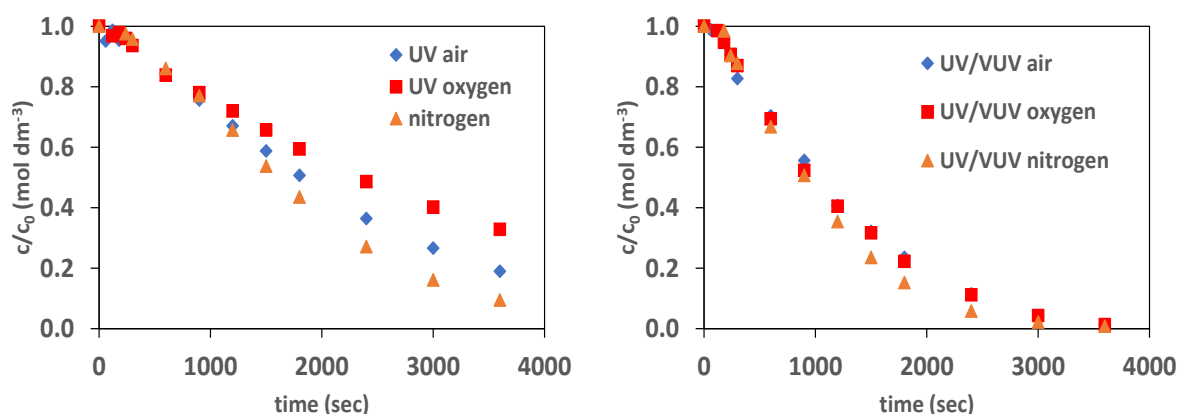


Figure 1. Relative concentration of sulfamethazine versus time of irradiation in the case of UV and UV/VUV photolysis

The effect of dissolved oxygen concentration on the transformation rate was investigated at 1.0×10^{-4} M initial concentration. The $\text{H}\bullet$ and e_{aq}^- reacts with dissolved oxygen and produce by this way a less reactive $\text{HO}_2\bullet$ and $\text{O}_2^{\bullet-}$ radicals. Opposite that, highly reactive species are eliminated by this way, oxygen generally has a positive effect on the transformation of organic substances because of the formation of peroxy type radicals [4-8]. Although, a positive effect of oxygen was expected in both cases, using UV photolysis, the transformation rate was slightly decreased with increase of the dissolved oxygen concentration after the first period. This can be explained by the formation of various intermediates, having different absorption at 254 nm and able to compete for 254 nm photons with sulfamethazine. At the same time, the effect of dissolved oxygen in UV/VUV irradiated solution was found to be negligible. Probably the negative effect (elimination of $\text{H}\bullet$) and the positive effect (formation of peroxy radical) compensates each other's.

The changing of the absorbance of the solutions was followed by taking spectra of the samples. There was no difference between the spectra series taken in air and nitrogen saturated UV irradiated solutions, while both of the shape of spectra and the changing of absorbance at characteristic wavelengths showed significant difference in the case of UV/VUV photolysis, and depended on the dissolved oxygen concentration. The observed effect of dissolved oxygen is most probably can be explained by the possibility of peroxy radical formation.

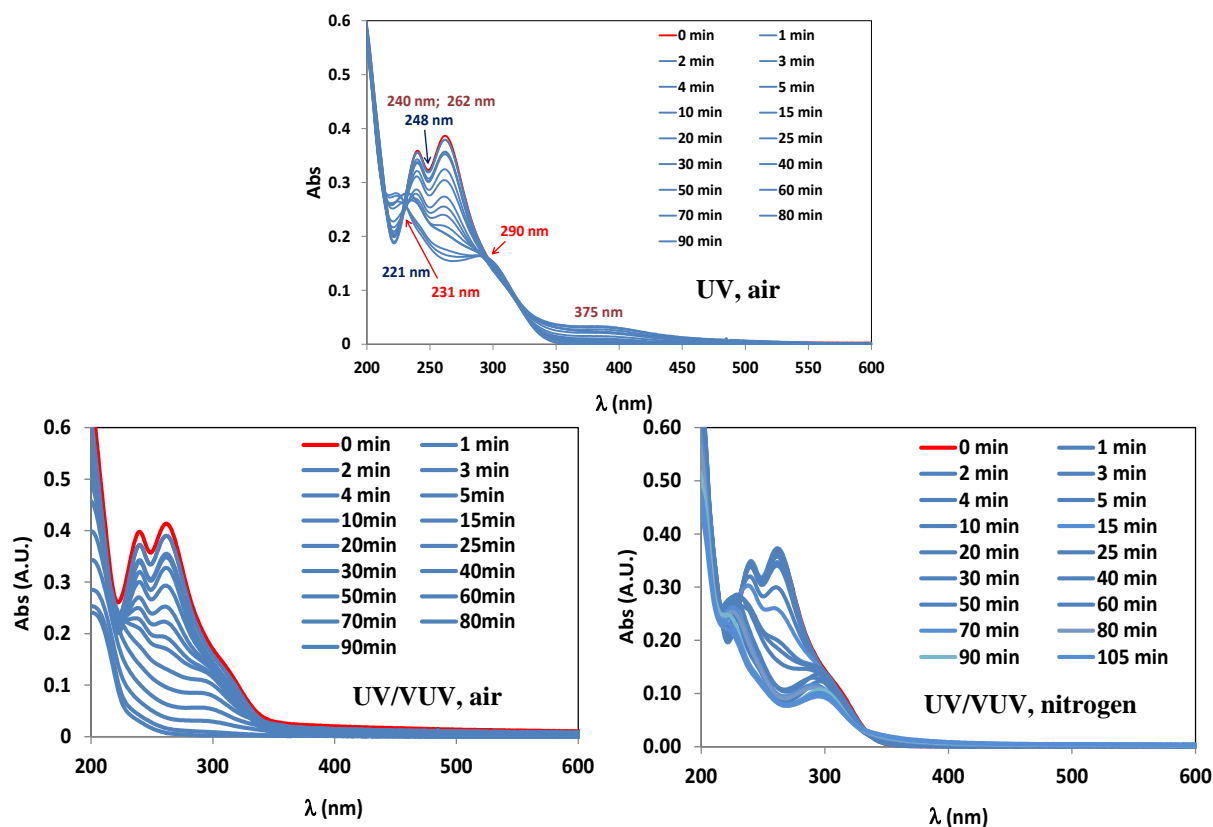


Figure 2. Spectra of sulfamethazine solutions radiated with UV and UV/VUV light

The pH decreased during both treatments, probably because of the formation of organic acids due to the fragmentation and oxidation processes. Although oxygen has no effect on the initial transformation rates, it has significant effect on the COD decrease and H_2O_2 formation. Using UV photolysis the decrease of the COD value is negligible, which suggests that hardly oxidizable intermediates form in this case. Using UV/VUV photolysis the COD decrease is no more than 25% during the time required for the transformation of sulfamethazine. After this period the COD decrease became faster and reached almost 70% by the end of treatment (120 min). Without dissolved oxygen there is no COD decrease proving the essential role of oxygen in the mineralization.

H_2O_2 forms only in the presence of dissolved oxygen. After a slight increase, the H_2O_2 concentration became constant in UV radiated solution. In the presence of VUV light the H_2O_2 concentration is higher and its formation is faster. H_2O_2 concentration reaches highest value, when sulfamethazine decomposed completely. After that decrease slowly and getting be closer to the value detected in pure Milli-Q water.

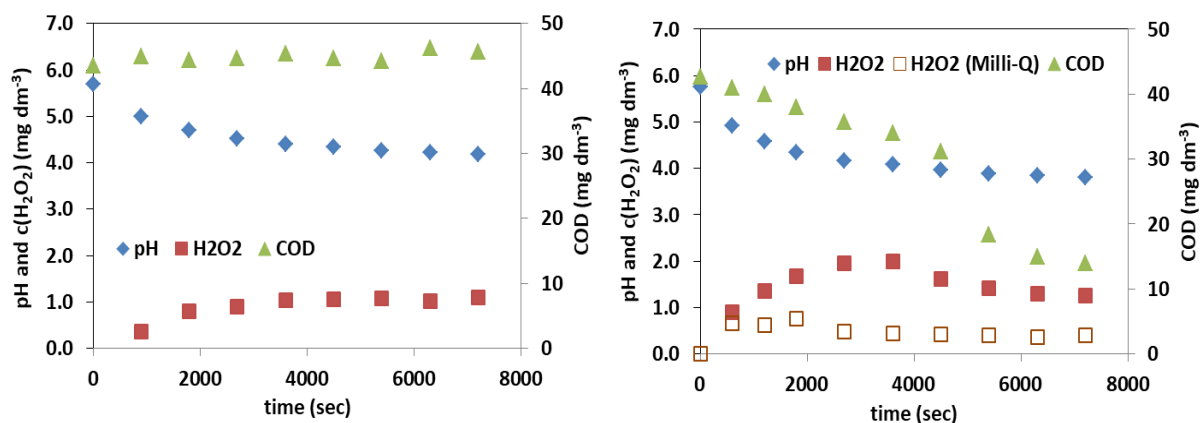


Figure 3. pH, COD and H₂O₂ concentration versus time of irradiation in aerated UV (A) and UV/VUV (B) radiated solutions

Transformation rates were determined in purified wastewater and tap water and compared to the values determined in Milli-Q water. Results showed that these mild matrices decreased the transformation rates in both cases. The inhibition effect is more pronounced in the case of UV photolysis.

Conclusion

- Both UV and UV/VUV photolysis effective for the elimination of sulfamethazine from aqueous solutions
- Dissolved oxygen has no significant effect on the transformation rate
- VUV light having low intensity highly increase the transformation rate
- COD decrease can be observed only in the case of combination UV and VUV photolysis

Acknowledgements

This publication was supported by the János Bolyai Research Scholarship of the Hungarian Academy of Sciences, and ÚNKP-19-3-SZTE-207 and UNKP-19-4-SZTE-115, new national excellence programs of the Ministry for Innovation and Technology.

References

- [1] I.T. Carvalho, L. Santos, *Environ. Int.* 2016. 94, 736–757.
- [2] M. Biošić, M. Mitrevski, S. Babić, *Environ. Sci. Pollut. Res.* 2017. 24, 9802–9812.
- [3] M.C. Gonzalez, E. Oliveros, M. Worner and A. Braun *J Photochem and Photobiol C*: 5 (3), 225–246. (2004)
- [4] T. Oppenländer: Vacuum-UV Oxidation, The H₂O-VUV AOP, in book *Photochemical Purification of water and air*, Wiley-VCH, 2003
- [5] T. Alapi, K. Schrantz, E. Arany, Zs. Kozméri; Ed.: Mihaela I. Stefan, *Advanced oxidation processes for water treatment : fundamentals and applications*. IWA, 2018
- [6] G. Heit, A. Neuner, P.-Y. Saugy, A. M. Braun; *J. Phys. Chem. A* 1998, 102, 5551–5561
- [7] E. J. Hart, M. Anbar; *Journal of Molecular Structure*, 1970, 9, p. 486–486
- [8] S. Al-Gharabli, P. Engeßer, D. Gera, S. Klein, T. Oppenlander, *Chemosphere*, 2016, 144, 811–5

CHARACTERIZATION OF THE ORGANIC LOAD OF THE WASTE FOUNTAIN SOLUTION

**Savka Adamović¹, Vladimir Rajs¹, Aleksandra Mihailović¹, Robert Lakatoš¹,
Dragan Adamović¹**

¹*University of Novi Sad, Faculty of Technical Sciences, Trg Dositeja Obradovića 6,
21000 Novi Sad, Serbia*

e-mail: adamovicsavka@uns.ac.rs

Abstract

The qualitative analysis of the organic loads of waste fountain solution (WFS) was investigated in the paper. Two liquid/liquid (L/L) extraction methods were used for WFS sample preparation: L/L extraction with methylene chloride and sequential L/L extraction with n-pentane, methylene chloride and methylene chloride at pH 2. Qualitative characterization of the organic load profile of offset effluent was performed using a gas chromatographic/mass spectrometric method.

Introduction

The sheet-fed offset printing process is based on the interaction of printing ink and fountain solution with the process materials. The fountain solution is expected to keep the printing ink off the non-printing areas of the printing plate with a liquid film, to maintain the hydrophilic nature of the non-printing areas, to promote fast spreading over the plate, to lubricate the plate and the rubber blanket, and to control the emulsification of ink and water. The fountain solution usually contains plate preservative agents, wetting agents, isopropyl alcohol or glycol-based surfactants, buffer substances, and antimicrobial additives [1]. WFS is generated as a reaction between printing plate, an initial fountain solution, printing inks and printing substrate. Therefore, the offset printing sites should apply measures that would be focused on monitoring, prevention and then on preparation for re-use of the WFS before being discharged into water and soil recipients.

Due to the dynamic markets and the competitive forces that govern it, most manufacturers do not define the exact chemical composition of the developer [2] or other offset materials such as WFS. Unique publish information about the composition of a chemical in the printing process is available in Material Safety Data Sheet (MSDS), patent holders, or a scientific publication setting the chemical definition of analytical methods.

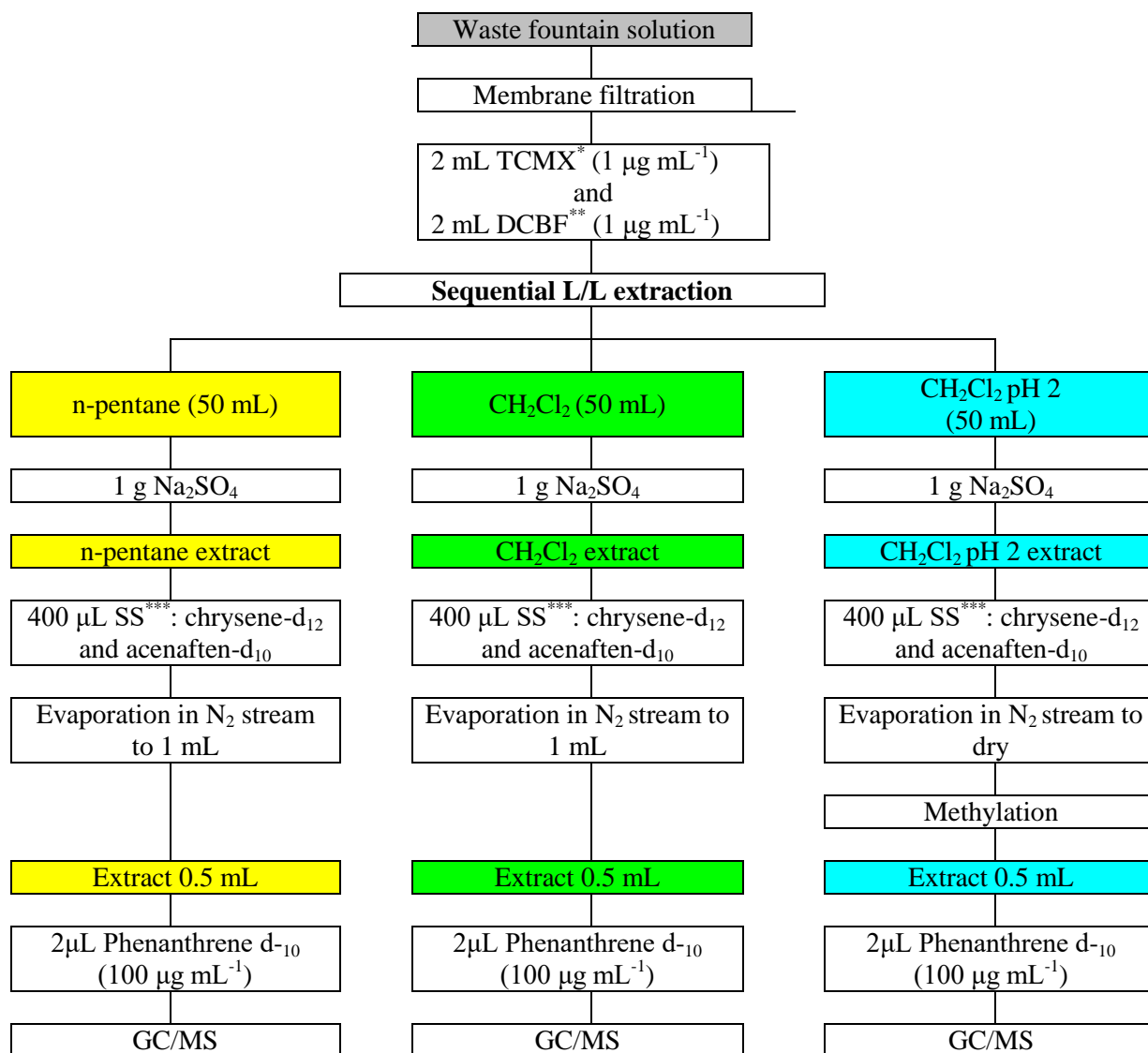
The paper aims are to characterize the WFS and to validate the extraction methods for the future selection of adequate effluent treatment for its safe disposal in a printing environment.

Experimental

The qualitative organic load profile of WFS was analysed by gas chromatographic/mass spectrometric (GC/MS) method. The analysis was performed using a gas chromatograph with a mass detector (Agilent 7890A GC with 5975C MSD, USA) and with an Agilent J&W Scientific DB-5MS chromatographic column of appropriate dimensions (30 m x 0.25 mm ID x 0.25 µm). Helium was used for the gas carrier. The samples were injected at an injector temperature of 270°C, while the detector temperature was 150°C. WFS sample was prepared with L/L extraction with methylene chloride and sequential L/L extraction with n-pentane, methylene chloride and methylene chloride at pH 2.

In L/L extraction with methylene chloride (I method), 1 L of WFS sample in a separation funnel was extracted with 30 ml of methylene chloride (CH₂Cl₂, J.T. Baker, USA). The extract was first collected in a laboratory beaker with three tablespoons of anhydrous sodium

sulfate (Na_2SO_4 , p.a., Sigma-Aldrich, Germany) due to high contamination of WFS. The extract was then transferred to a separation funnel. The extraction was repeated once more with another 30 ml of methylene chloride. The cumulative extract is evaporated to dryness and reconstituted with 2 ml of phenanthrene d_{10} (concentration of $0.4 \mu\text{g/mL}$) in a mixture of hexane and methylene chloride (1:1). After L/L extraction with methylene chloride at the actual pH of WFS (pH 8.0), the pH of WFS was adjusted to 2 additions of concentrated hydrochloric acid (HCl , 35%, p.a., Merck, Germany). As the pH values of the compounds change their shape, adjust the pH of WFS to 2, the invisible ionized compounds at pH 8.0 become visible at pH 2. The L/L extraction process with methylene chloride at pH 2 was repeated according to the same procedure described above.



*TCMX = 2,4,5,6-tetrachloro-m-xylene, **DCBF = decachlorobiphenyl, ***SS = surogat standarda

Figure 1. Scheme of WFS preparation procedures by sequential L/L extraction

Sequential L/L extraction (II method) of WFS was performed according to the procedure presented in the study of Dsikowitzky et al. [3] with increasing concentrations of individual chemicals due to the multicomponent and contamination of offset effluent. Figure 1 schematically shows the WFS preparation procedures by sequential L/L extraction. To

remove suspended solids from WFS, before sequential L/L extraction, 1L WFS was filtered through a membrane filtration set with a cellulose nitrate membrane filter (Sartorius Stedim Biotech GmbH, Germany) and a vacuum pump (MILIPORE, Germany). The third fraction with CH_2Cl_2 in an acidic medium was subjected to a methylation procedure. Methylation was performed according to the procedure of Santos-Delgado et al. [4] as follows: the evaporated extract was dissolved in 1 mL of methanol. 250 μL of concentrated sulfuric acid (H_2SO_4 p.a., Merck, Germany) was slowly added to the extract, after which the extract was left in the ultrasonic bath for 1 minute. The extract was then heated in a water bath for 12 minutes at 59°C . 6 mL of 2% potassium chloride solution was added to the cooled extract. The esters were extracted with 1 mL of hexane, and then 0.5 mL of the extract was separated for GC/MS analysis.

A blank sample (1 L of distilled water) was prepared for each fraction to the same procedure as WFS. The dishes were washed with acetone: hexane in a 1: 1 ratio before use.

Deconvolution Reporting Software (DRS) was used to create the GC/MS organic profile of WFS. The Automated Mass Spectral Deconvolution and Identification System (AMDIS) software was used to identify organic substances. For more accurate identification, all mass spectra obtained with the AMDIS software were compared with the NIST (National Institute of Standards and Technology) reference spectra of the database. The presence of an organic compound in a WFS sample has been proved if the probability of presence, obtained by using AMDIS software and the NIST database, is more than 70%.

Results and discussion

To obtain profiles with more detected organic substances, a cumulative GC/MS profile of both L/L extraction methods with the probability of organic substances presence more than 70% was determined (Table 1). The cumulative qualitative GC/MS profile of organic substances in the WFS indicates that the effluent contains 73 organic substances with a probability of presence more than 70% by using AMDIS software and the NIST database.

Table 1. Cumulative GC/MS profile of organic substances in the WFS

Organic compounds	I method	II method	AMDIS >70%	NIST >70%
Hydrocarbons				
Tridecen		+	+	+
1-heksadecene		+	+	+
Eikosan		+	+	+
Heneikosane		+	+	+
Tetrakosane		+	+	+
Heksakosane		+	+	+
Heptakosane		+	+	+
Oktakosane		+	+	+
Skvalene		+	+	+
Triakontane		+	+	+
Polycyclic Aromatic Hydrocarbons (PAH)				
1-Naphthalenol	+		+	+
2-Naphthalenol	+		+	+
Phenanthrene	+		+	+
Anthracene	+		+	+
Alcohols				
Phenylmethanol		+	+	+
2-ethyl-1-hexanol	+	+	+	+

1-undecanol	+		+	+
1-dodecanol		+	+	+
1-tetradecanol	+	+	+	+
Ethers				
bis (chloromethyl) ether	+		+	+
2-Butoxy-ethanol	+	+	+	+
2-(hexyloxy)-ethanol		+	+	+
2-phenoxy-ethanol	+	+	+	+
2-(2-methoxyethoxy)-ethanol	+		+	+
2-(2-Ethoxyethoxy)-ethanol	+	+	+	+
2-(2-Butoxyethoxy)-ethanol	+	+	+	+
2-[2-(2-Butoxyethoxy) ethoxy]-ethanol	+	+	+	+
1-[2-(2-methoxy-1-methoxyethoxy)-1-methoxyethoxy]-2-propanol		+	+	+
Ketones				
1-(2,4,6-trimethylphenyl)-ethanone	+	+	+	+
1-Phenyl-1-propanone		+	+	+
4-Methyl-3-penten-2-one		+	+	+
Phenols				
Phenol		+	+	+
2-methoxy-phenol		+	+	+
2,6-Diisopropyl-phenol	+	+	+	+
m-tert-butyl-phenol		+	+	+
2,4-di-tert-butyl-phenol		+	+	+
o-phenyl-phenol	+		+	+
Substituted benzenes and benzene derivatives				
1,3,5-trimethyl-benzene		+	+	+
1,2,3,5-Tetramethyl-benzene		+	+	+
1,3-dimethyl-5-(1-methylethyl)-benzene	+	+	+	+
1,3-bis(1-methylethyl)-benzene		+	+	+
1,4-bis(1-methylethyl)-benzene		+	+	+
Benzoic acid	+		+	+
p-aminotoluene	+	+	+	+
Vanillin		+	+	+
Benzoic acid methyl ester		+	+	+
Benzoic acid 4-methyl methyl ester		+	+	+
Organic acids				
Dodecanoic acid		+	+	+
Tertridecanoic acid	+	+	+	+
Hexadecanoic acid	+	+	+	+
Octadecanoic acid	+	+	+	+
Fumaric acid	+		+	+
Terephthalic acid	+		+	+
Esters				
Octane acid methyl ester		+	+	+
Decanoic acid methyl ester		+	+	+
Tetradecanoic acid methyl ester		+	+	+
Hexadecanoic acid methyl ester		+	+	+
Linoleic acid methyl ester		+	+	+
9-(Z)-Octadecanoic acid methyl ester	+	+	+	+
Octadecanoic acid methyl ester		+	+	+
Phthalic acid dionyl ester	+		+	+

Amides				
1-methyl-1-nitrosourea	+		+	+
N-(4-ethoxyphenyl)-acetamide		+	+	+
N-butylbenzensulfonamid		+	+	+
Organic compounds with nitrogen				
Diazomethane		+	+	+
2-ethylpyridine		+	+	+
N-butylbenzenesulfonamide	+		+	+
Organic compounds with nitrogen and oxygen				
5-chloro-2-methyl-2H-isothiazol-3-one		+	+	+
1,3-benzothiazole		+	+	+
2-methylthiobenzothiazole		+	+	+
Organic compounds with phosphorus				
Tributyl phosphate		+	+	+
Amines				
Phenylamine	+		+	+
2,6-dimethyl-benzenamine		+	+	+

Comparison of GC/MS profiles obtained by L/L extraction with one solvent (I method) and with three solvents (II method) it was found that sequential L/L extraction (with 58 organic compounds) detected 48% more organic substances compared to L/L excretion with methylene chloride (with 30 organic compounds). Also, PAH compounds were detected only by L/L extraction with methylene chloride, while hydrocarbons and organic compounds with nitrogen and oxygen were detected only in sequential L/L extraction. It is concluded that the nature of the solvent determines a number and classes of extracted organic compounds.

Conclusion

The obtained GC/MS profiles show that 48% more organic substances are detected by sequential L/L extraction compared to L/L extraction with methylene chloride. Thus, the extraction solvent determines the class of organic compounds that will be extracted from the WFS.

When we have a complex effluent such as WFS to obtain a profile with more detected organic substances, it is best to determine the cumulative GC/MS profile of both L/L extraction methods.

Acknowledgements

The authors acknowledge the financial support of the Ministry of Education, Science and Technological Development, Republic of Serbia (Grant No. III43008).

References

- [1] M. Prica, S. Adamovic, B. Dalmacija, Lj. Rajic, J. Trickovic, S. Rapajic, M. Becelic-Tomin, *Process Saf. Environ. Prot.* 94 (2015) 262.
- [2] T. Vengris, R. Binkienė, R. Butkienė, O. Nivinskienė, V. Melvydas, L. Manusadžianas, *J. Hazard. Mater.* 113 (2004) 181.
- [3] L. Dsikowitzky, J. Schwarzbauer, R. Littke, *Org. Geochem.* 33 (2002) 1747.
- [4] M.J. Santos-Delgado, E. Crespo-Corral, L.M. Polo-Díez, *Talanta*. 53 (2000) 367.

METHOD FOR THE DETERMINATION OF TRICLOPYR RESIDUES IN SOIL

Sanja Lazić, Dragana Šunjka, Maja Meseldžija, Milica Dudić, Slavica Vuković,
Dragana Bošković

¹*Faculty of Agriculture, University of Novi Sad, Novi Sad, Trg Dositeja Obradovića 8,
SERBIA*

e-mail: draganas@polj.uns.ac.rs

Abstract

In this study, a method for the determination of triclopyr in soil samples has been developed. The analyte was extracted with acidified acetonitrile, while the determination and quantification of triclopyr were performed by high-performance liquid chromatography (HPLC) with a diode array detection. Optimal HPLC-DAD conditions were: mobile phase acetonitrile and 0.1% H₃PO₄ (50:50), the flow rate of 0.9 ml/min, and 220 nm of wavelength. In terms of method validation, accuracy (expressed as recovery), linearity, precision (RSD) and LOQ were determined. Obtained results for the recovery using this method, at the three spiking levels, were 81-93%. Precision, expressed as RSD, was 9.1%, while the LOQ was 0.01 mg/kg. Therefore, it can be concluded that the proposed method could be applied for the analysis of triclopyr residues in the soil samples.

Introduction

Triclopyr (3,5, 6-trichloro-2-pyridyloxyacetic acid) [1] is an auxin-type, post-emergent herbicide, widely used for weed control in pastures, rangelands and non-crop areas (Figure 1). After application, it is rapidly absorbed by the foliage and roots and translocated throughout the plant, inducing an auxin-type response in susceptible plant species, causing epinastic bending and twisting of the stems that result in growth inhibition [2, 3]. Triclopyr has shown high efficacy for a wide variety of annual and perennial broadleaf weeds.

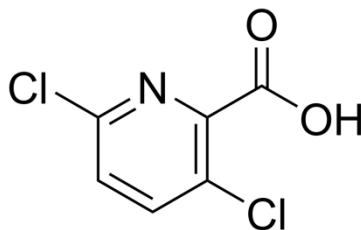


Figure 1. Triclopyr – structural formula

However, with their widespread use in agriculture, the potential adverse effects of their residues becoming evident. Due to their intensive use, herbicides fate and their presence in the environment become a great concern.

Due to agricultural activities, residual activity in the soil can result in damage to succeeding crops, contamination of water sources by leaching, and toxicity to non-target organism. Triclopyr concentrations remain in the soil after application, are of great concern. Residual herbicide may affect the growth of succeeding vegetation and can reach groundwater. The trace determination of herbicide residues, generally in environmental samples, presents a challenging analytical problem [4].

In order to evaluate the presence of triclopyr residues in the soil, it is necessary to apply the appropriate method. Aim of this study was to develop and validate the method for the determination of triclopyr residues in soil.

Experimental

Analytical standard of triclopyr (purity 95%) was purchased from Dr. Ehrenstorfer (Augsburg, Germany). Acetonitrile (HPLC grade) and phosphoric acid were provided by J.T. Baker (Deventer, The Netherlands), while water was purified by Milli-Q (Millipore, Billerica, MA, USA) system. For the extraction, QuEChERS sorbent kits and pouches of salts were purchased from the Agilent Technologies (Cat. No. 5982-5650).

For the method validation blank soil samples were used. Previously, soil samples were homogenized, sieved (2 mm) and air-dried at room temperature before their use.

Triclopyr was extracted from soil by modified QuEChERS method. Ten grams of homogenized soil sample in a 50 mL polypropylene tube was enriched with the appropriate amount of triclopyr analytical standard. Afterward, 10 mL of acetonitrile was added and hand-shaken for 1 min. A mixture of buffered salts (4 g MgSO_4 , 1 g NaCl, 1 g trisodium citrate dihydrate and 0.5 g disodium hydrogen citrate sesquihydrate) was added, hand-shaken for 1 min, vortexed for 1 min, centrifugation at 3000 rpm during 5 minutes.

A separated acetonitrile layer was filtered through a 0.45 μm nylon filter to an autosampler vial and analyzed using HPLC/DAD.

Validation of the method was performed through the following parameters: linearity, accuracy, precision, and limit of quantification (LOQ).

Results and discussion

For the chromatographic analysis, an Agilent 1100 Series system with DAD detector and Zorbax Eclipse XDB-C18 (50 mm \times 4.6 mm, 1.8 μm) were used. The mobile phases, composed of acetonitrile and 0.1% phosphoric acid (50/50, V/V) were pumped at a flow rate of 0.9 ml/min, while wavelength was 220 nm (Figure 2 and 3).

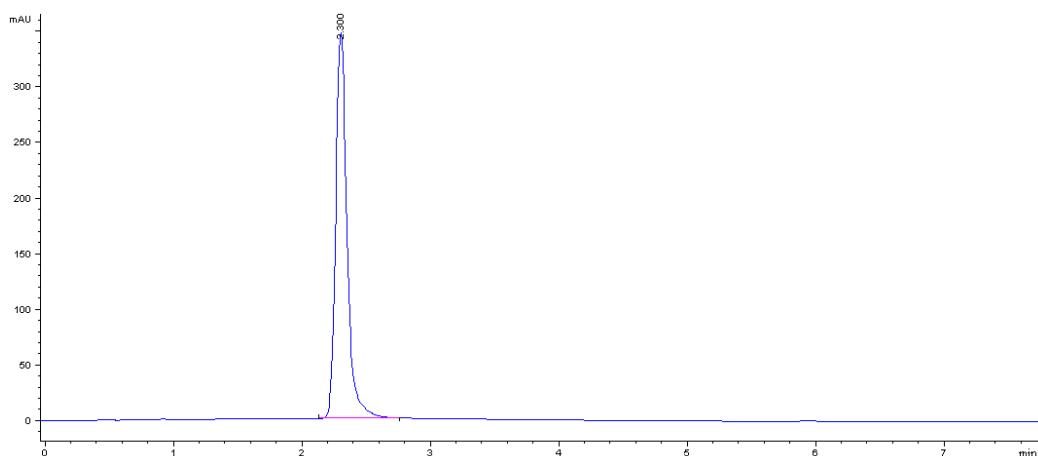


Figure 2. HPLC/DAD chromatogram of triclopyr in acetonitrile

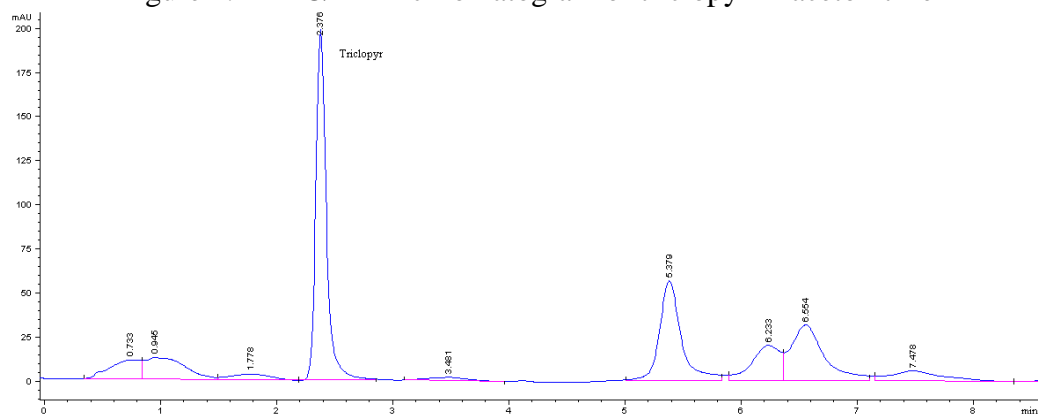


Figure 3. HPLC/DAD chromatogram of triclopyr in soil matrix

Method for the determination of pesticide residues in soil samples has been validated in accordance with SANCO/3029/99 rev.4 11/07/00 [5]. The achieved values completely fulfilled the required criteria (Table 1).

Table 2. Analytical parameters for HPLC/DAD determination of triclopyr

Parameter	Concentration interval (µg/ml)	Slope ^a	Correlation coefficient ^a	Recovery (%)	LOQ (mg/kg)
Triclopyr	0.01-120	3.29	0.999	81-93	0.01

$$^aY = ax + b$$

The QuEChERS method, without purification step, was applied to estimate the effectiveness of the method. Obtained results for the recovery using this method, at the three spiking levels, was 81-93%. Precision, expressed as relative standard deviation, was 9.1%, while the limit of quantification was 0.01 mg/kg.

All of these parameters meet the SANCO criteria that prescribe yield extraction of 70-110%, precision reported as repeatability less than 20%, and quantification limit of at least 0.05 mg/kg.

Conclusions

In this study, methods based on reversed-phase liquid chromatography and modified QuEChERS method was validated. The proposed procedure, without cleanup, is more practical due to the consumption of less solvent in comparison with the method including purification step. According to SANCO criteria, results of all analyzed parameters were satisfied, recommending this method for use on real soil samples.

Acknowledgement

This research is a part of project III43005 financed by Ministry of Education, Science and Technological Development, Republic of Serbia.

References

- [1] C. Tomlin, (ed) The Pesticide Manual: Eleventh Edition. Crop Protection Publications, British Crop Protection Council and the Royal Society of Chemistry, United Kingdom, 1997.
- [2] A. Cessna, R. Grover, D.T. Waite, Reviews of environmental contamination and toxicology 174 (2002) 19.
- [3] S.A. Senseman, (Ed.), Herbicide handbook, ninth ed. Weed Science Society of America, Lawrence, KS, USA, 2007.
- [4] S. Lazić, D. Šunjka, R. Čabrilovski, S. Vuković, M. Manojlović Determination of sulfonylurea herbicide residues in agricultural soil. Proceedings of the 15th International Conference on Environmental Science and Technology Rhodes, Greece, 31 August to 2 September 2017 Rhodes Greece, p. 1-3. CEST2017_01277.
- [5] SANCO/3029/99 rev.4, 11/07/00. Guidance for generating and reporting methods of analysis support of pre-registration data requirements for Annex II (part A, Section 4) and Annex III (part A, Section 5) of Directive 91/414.

DEVELOPMENT OF NOVEL EXPERIMENTAL METHODS AND CALCULATIONS FOR THE DETERMINATION AND OPTIMIZATION OF THE RESPONSE TIME OF A PHOTOACOUSTIC GAS ANALYSER

Diána Kiss¹, Anna Szabó¹, Attila Czirják², Gábor Szabó¹, Zoltán Bozóki¹

1. Department of Optics and Quantum Electronics, University of Szeged, H-6720 Szeged, Dóm tér 9, Hungary

2. Department of Theoretical Physics, University of Szeged, H-6720 Szeged, Tisza L. krt. 84 - 86., Hungary

e-mail: kissdiana@titan.physx.u-szeged.hu

Abstract

Monitoring and controlling of short-term physico-chemical processes frequently require gas analyzers with high time resolution. The scope of the present study was to shorten the response time of the longitudinal-differential cell-based photoacoustic systems. Finite element analysis and visual investigation of the gas flow were used to improve the purge of the gas sample through the photoacoustic cell. A diffuser providing quick purging was attached to the first buffer of the cell. The optimization of the measurement parameters (including temperature, tube materials, flow rate) and the use of the diffuser resulted in a reduced response time, which was found to be around 1 second. In addition, response time characteristics was determined by measurement of instantaneous injection of analyte.

Introduction

In-situ and real time gas measurements are essential to detect rapid changes and allow continuous optimization of industrial processes. Photoacoustic (PA) spectroscopy-based gas measuring systems meet the requirements of process analysis due to their high sensitivity, wide dynamic range, robust construction, automatic operation and short response time. The typical response time of a PA system is around 2-3 seconds, it is expected that the scope of applications can be extended by improving response time of the analyzers [1-2].

Experimental

Response time measurement

NO, NO₂ and N₂ gases were used for the measurement of response time. Figure 1. shows the experimental setup. The gas flows were continuously 3 l/min. A four-way switching valve generated Heaviside function like concentration changes (NO-N₂ and NO₂-N₂). The materials, length and temperature of the pipe between the four-way switching valve and the photoacoustic chamber were changed to measure their effect on the response time. The PA chamber with and without diffuser were measured. The needle valve was set to maintain 1 l/min gas flow. The gas was drawn by a membrane pump. The NO gas was measured with the addition of water vapor. The NO gas was measured with QCL and NO₂ gas was measured with diode lasers.

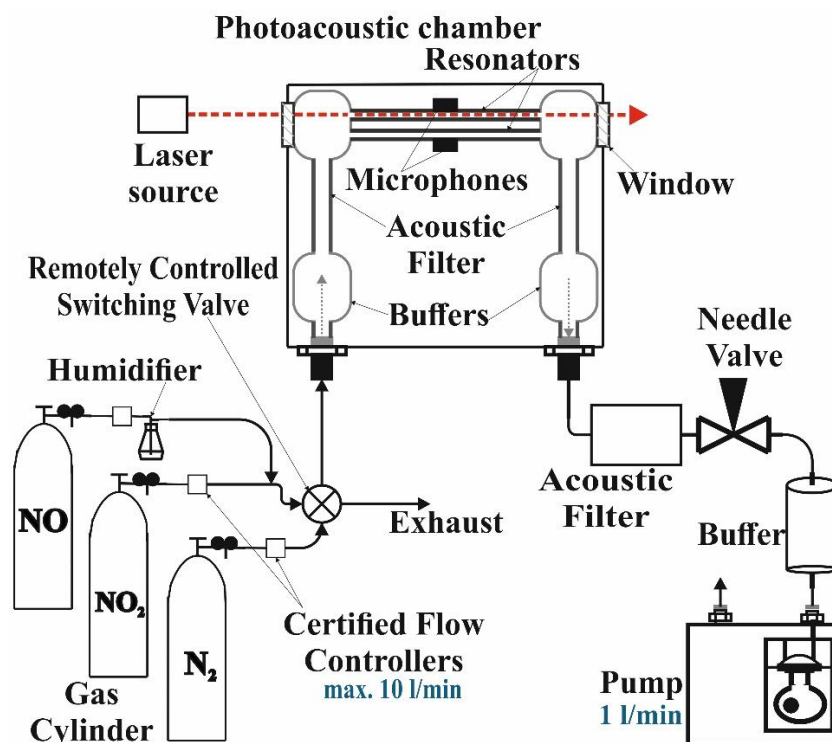


Figure. 1. Response time measurement system

Transfer function measurement

NO and N₂ gases were used for the measurement the transfer function. The gas flows were continuously 2 l/min. 0.5 ml and then 0.25 ml NO (157 ppm in N₂) gas were injected in the N₂ flow through a membrane with a Hamilton syringe (Figure 2.). The needle valve was set to maintain 1 l/min gas flow. The gas was drawn by a membrane pump. The NO gas was measured with the addition of water vapor. The NO gas was measured with QCL lasers.

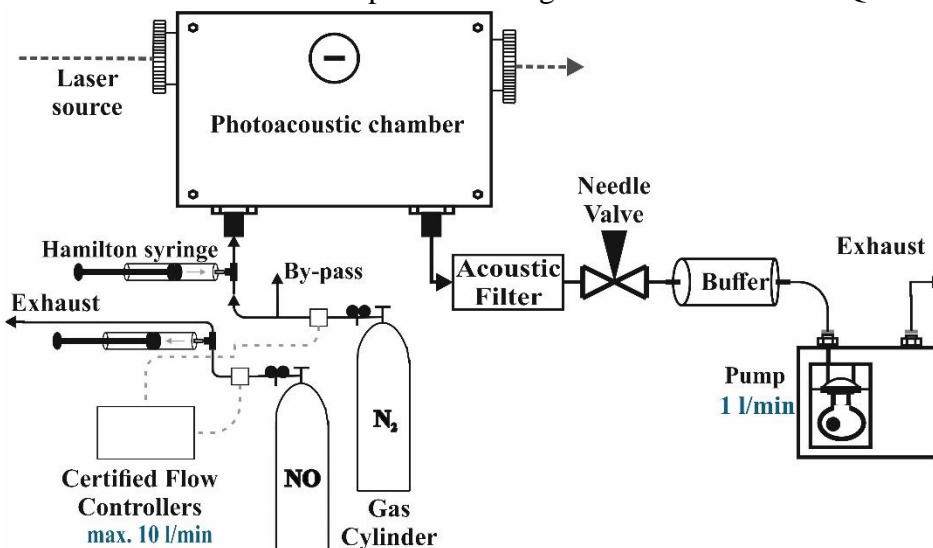


Figure. 2. Measurement system for determination of the transfer function

Results and discussion

Finite element analysis and visual investigation of the gas flow indicated that in the longitudinal-differential PA cell the purge of the gas sample is limited. Therefore, a diffuser allowing quicker purging was attached to the first buffer of the cell. Response time measurements of a PA system with longitudinal-differential cell (with and without diffuser)

were performed with nitrogen monoxide (NO) and nitrogen dioxide (NO₂). Results showed that the diffuser reduces the response time on average by 35%. Furthermore, several factors influencing the response time were investigated (e.g. material of the cell and pipes, temperature, flow rate etc.). For NO and NO₂ measurement, heated polytetrafluoroethylene (PTFE) pipe was found to have the lowest response time. In case of NO and NO₂ measurement it is also important to operate the PA cell at elevated temperature, the optimal temperature was found to be 80°C. Moreover, the most important parameter is the flow rate of the gas sampling, which is highly limited by the PA cell, because above a certain flow rate the flow becomes turbulent resulting in rapidly decreasing signal-to-noise-ratio. It was found that the present system can be operated with a flow rate up to 1 liter/min, which in combination with the low volume of the cell results in short rinse time [3]. The optimization of these parameters and the use of the diffuser resulted in a reduced response time, which was found to be around 1 second. The efficiency of the diffuser was investigated by a finite element modelling performed in COMSOL Multiphysics 5.3. The results of the model proved efficiency of the diffuser. Figure 3. shows the streamlines of a PA cell without diffuser (a) and with diffuser (b).

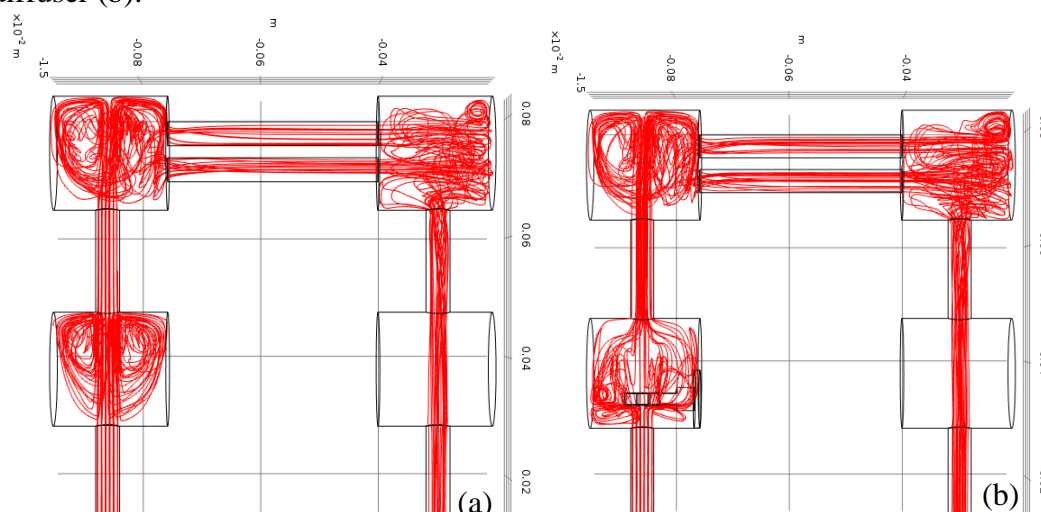


Figure. 3. Streamlines (a) PA cell without diffuser (b) PA cell with diffuser

In addition, the transfer function of the system can be calculated based on response time characteristics. If the transfer function of the system is known and the response of the system is measured, then convolution based analysis can be used to study real-time physico-chemical processes affecting the response time (e.g. adsorption-desorption).

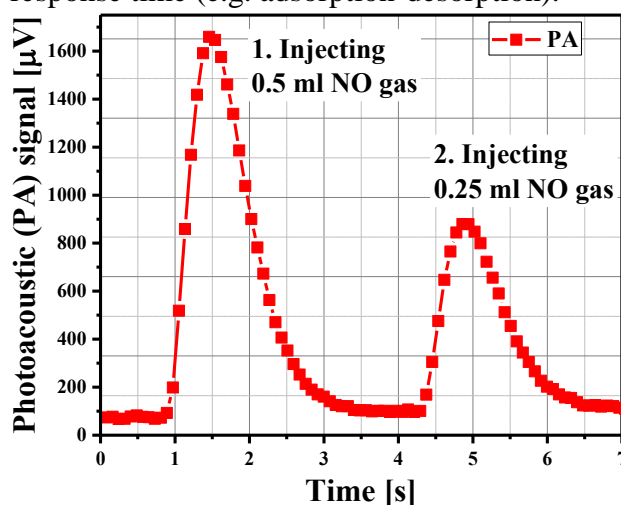


Figure. 4. Response time characteristics of the PA system

Response time characteristics was determined by measurement of instantaneous injection of analyte. The results (Fig. 4.) clearly show that the response of the system extended. Our further aim is to develop a system theory based method that allows the calculation of the concentration changes occurring at the inlet of the PA system with a time resolution below the response time of the system.

Conclusion

The PA system response time was reduced to 1 second. The influencing factors of response time were defined. A method was designed to determine the transfer function of the system and the first measurement was made.

Acknowledgements

Our project was supported by „SUPPORTED BY THE ÚNKP-19-2-SZTE-69 NEW NATIONAL EXCELLENCE PROGRAM OF THE MINISTRY FOR INNOVATION AND TECHNOLOGY”.



References

1. D. Tátrai, Z. Bozóki, H. Smit, C. Rolf, N. Spelten, M. Kramer, A. Filegs, C. Gerbig, G. Gulyás, G. Szabó *Atmos. Meas. Tech. Discuss.*, 7, 6359-6384, (2014) doi:10.5194/amtd-7-6359-2014
2. A. Miklós, P. Hess, Z. Bozóki, *AIP Review of Scientific Instruments*, 72, 4, (2001) doi:10.1063/1.1353198
3. A. Schmohl, A. Miklos, P. Hess, *Applied Optics*, 40, 15, (2001) doi:10.1364/AO.40.002571